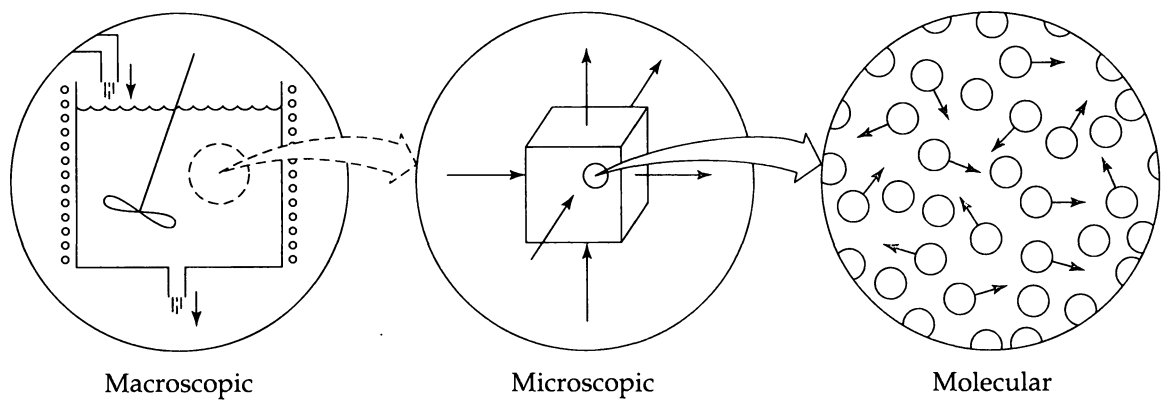
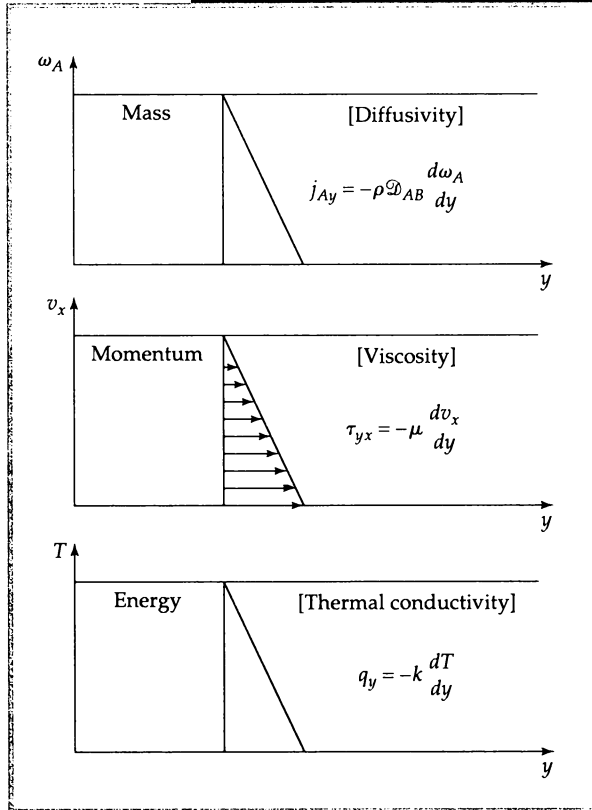


Transport Phenomena

Second Edition



R. Byron Bird • Warren E. Stewart
Edwin N. Lightfoot



JOHN WILEY & SONS, INC.
 New York Chichester Weinheim
 Brisbane Singapore Toronto

<http://www.wiley.com/college/bird>

ISBN 0-471-41077-2



Transport Phenomena

Second Edition

R. Byron Bird
Warren E. Stewart
Edwin N. Lightfoot

*Chemical Engineering Department
University of Wisconsin-Madison*



John Wiley & Sons, Inc.
New York / Chichester / Weinheim / Brisbane / Singapore / Toronto

Acquisitions Editor *Wayne Anderson*
Marketing Manager *Katherine Hepburn*
Senior Production Editor *Petrina Kulek*
Director Design *Madelyn Lesure*
Illustration Coordinator *Gene Aiello*

This book was set in Palatino by UG / GGS Information Services, Inc. and printed and bound by Hamilton Printing. The cover was printed by Phoenix.

This book is printed on acid free paper. ∞

Copyright © 2002 John Wiley & Sons, Inc. All rights reserved.

No part of this publication may be reproduced, stored in a retrieval system or transmitted in any form or by any means, electronic, mechanical, photocopying, recording, scanning or otherwise, except as permitted under Sections 107 or 108 of the 1976 United States Copyright Act, without either the prior written permission of the Publisher, or authorization through payment of the appropriate per-copy fee to the Copyright Clearance Center, 222 Rosewood Drive, Danvers, MA 01923, (508)750-8400, fax (508)750-4470. Requests to the Publisher for permission should be addressed to the Permissions Department, John Wiley & Sons, Inc., 605 Third Avenue, New York, NY 10158-0012, (212)850-6011, fax (212)850-6008, E-Mail: PERMREQ@WILEY.COM. To order books or for customer service please call 1-800-CALL WILEY (225-5945).

Library of Congress Cataloging-in-Publication Data

Bird, R. Byron (Robert Byron), 1924-

Transport phenomena / R. Byron Bird, Warren E. Stewart, Edwin N. Lightfoot.—2nd ed.

p. cm.

Includes indexes.

ISBN 0-471-41077-2 (cloth : alk. paper)

1. Fluid dynamics. 2. Transport theory. I. Stewart, Warren E., 1924- II. Lightfoot, Edwin N., 1925- III. Title.

QA929.B5 2001
530.13'8—dc21

2001023739

ISBN 0-471-41077-2

Printed in the United States of America

10 9 8 7 6 5 4 3 2 1

Preface

While momentum, heat, and mass transfer developed independently as branches of classical physics long ago, their unified study has found its place as one of the fundamental engineering sciences. This development, in turn, less than half a century old, continues to grow and to find applications in new fields such as biotechnology, microelectronics, nanotechnology, and polymer science.

Evolution of transport phenomena has been so rapid and extensive that complete coverage is not possible. While we have included many representative examples, our main emphasis has, of necessity, been on the fundamental aspects of this field. Moreover, we have found in discussions with colleagues that transport phenomena is taught in a variety of ways and at several different levels. Enough material has been included for two courses, one introductory and one advanced. The elementary course, in turn, can be divided into one course on momentum transfer, and another on heat and mass transfer, thus providing more opportunity to demonstrate the utility of this material in practical applications. Designation of some sections as optional (○) and other as advanced (●) may be helpful to students and instructors.

Long regarded as a rather mathematical subject, transport phenomena is most important for its physical significance. The essence of this subject is the careful and compact statement of the conservation principles, along with the flux expressions, with emphasis on the similarities and differences among the three transport processes considered. Often, specialization to the boundary conditions and the physical properties in a specific problem can provide useful insight with minimal effort. Nevertheless, the language of transport phenomena is mathematics, and in this textbook we have assumed familiarity with ordinary differential equations and elementary vector analysis. We introduce the use of partial differential equations with sufficient explanation that the interested student can master the material presented. Numerical techniques are deferred, in spite of their obvious importance, in order to concentrate on fundamental understanding.

Citations to the published literature are emphasized throughout, both to place transport phenomena in its proper historical context and to lead the reader into further extensions of fundamentals and to applications. We have been particularly anxious to introduce the pioneers to whom we owe so much, and from whom we can still draw useful inspiration. These were human beings not so different from ourselves, and perhaps some of our readers will be inspired to make similar contributions.

Obviously both the needs of our readers and the tools available to them have changed greatly since the first edition was written over forty years ago. We have made a serious effort to bring our text up to date, within the limits of space and our abilities, and we have tried to anticipate further developments. Major changes from the first edition include:

- transport properties of two-phase systems
- use of “combined fluxes” to set up shell balances and equations of change
- angular momentum conservation and its consequences
- complete derivation of the mechanical energy balance
- expanded treatment of boundary-layer theory
- Taylor dispersion
- improved discussions of turbulent transport

- Fourier analysis of turbulent transport at high Pr or Sc
- more on heat and mass transfer coefficients
- enlarged discussions of dimensional analysis and scaling
- matrix methods for multicomponent mass transfer
- ionic systems, membrane separations, and porous media
- the relation between the Boltzmann equation and the continuum equations
- use of the “Q+W” convention in energy discussions, in conformity with the leading textbooks in physics and physical chemistry

However, it is always the youngest generation of professionals who see the future most clearly, and who must build on their imperfect inheritance.

Much remains to be done, but the utility of transport phenomena can be expected to increase rather than diminish. Each of the exciting new technologies blossoming around us is governed, at the detailed level of interest, by the conservation laws and flux expressions, together with information on the transport coefficients. Adapting the problem formulations and solution techniques for these new areas will undoubtedly keep engineers busy for a long time, and we can only hope that we have provided a useful base from which to start.

Each new book depends for its success on many more individuals than those whose names appear on the title page. The most obvious debt is certainly to the hard-working and gifted students who have collectively taught us much more than we have taught them. In addition, the professors who reviewed the manuscript deserve special thanks for their numerous corrections and insightful comments: Yu-Ling Cheng (University of Toronto), Michael D. Graham (University of Wisconsin), Susan J. Muller (University of California-Berkeley), William B. Russel (Princeton University), Jay D. Schieber (Illinois Institute of Technology), and John F. Wendt (Von Kármán Institute for Fluid Dynamics). However, at a deeper level, we have benefited from the departmental structure and traditions provided by our elders here in Madison. Foremost among these was Olaf Andreas Hougen, and it is to his memory that this edition is dedicated.

Madison, Wisconsin

R. B. B.
W. E. S.
E. N. L.

Contents

Preface

Chapter 0 The Subject of Transport Phenomena 1

Part I Momentum Transport

Chapter 1 Viscosity and the Mechanisms of Momentum Transport 11

§1.1	Newton's Law of Viscosity (Molecular Momentum Transport)	11
	Ex. 1.1-1 Calculation of Momentum Flux	15
§1.2	Generalization of Newton's Law of Viscosity	16
§1.3	Pressure and Temperature Dependence of Viscosity	21
	Ex. 1.3-1 Estimation of Viscosity from Critical Properties	23
§1.4 ^O	Molecular Theory of the Viscosity of Gases at Low Density	23
	Ex. 1.4-1 Computation of the Viscosity of a Gas Mixture at Low Density	28
	Ex. 1.4-2 Prediction of the Viscosity of a Gas Mixture at Low Density	28
§1.5 ^O	Molecular Theory of the Viscosity of Liquids	29
	Ex. 1.5-1 Estimation of the Viscosity of a Pure Liquid	31
§1.6 ^O	Viscosity of Suspensions and Emulsions	31
§1.7	Convective Momentum Transport	34
Questions for Discussion		37
Problems		37

Chapter 2 Shell Momentum Balances and Velocity Distributions in Laminar Flow 40

§2.1	Shell Momentum Balances and Boundary Conditions	41
§2.2	Flow of a Falling Film	42
	Ex. 2.2-1 Calculation of Film Velocity	47
	Ex. 2.2-2 Falling Film with Variable Viscosity	47
§2.3	Flow Through a Circular Tube	48
	Ex. 2.3-1 Determination of Viscosity from Capillary Flow Data	52
	Ex. 2.3-2 Compressible Flow in a Horizontal Circular Tube	53

§2.4	Flow through an Annulus	53
§2.5	Flow of Two Adjacent Immiscible Fluids	56
§2.6	Creeping Flow around a Sphere	58
	Ex. 2.6-1 Determination of Viscosity from the Terminal Velocity of a Falling Sphere	61
Questions for Discussion		61
Problems		62

Chapter 3 The Equations of Change for Isothermal Systems 75

§3.1	The Equation of Continuity	77
	Ex. 3.1-1 Normal Stresses at Solid Surfaces for Incompressible Newtonian Fluids	78
§3.2	The Equation of Motion	78
§3.3	The Equation of Mechanical Energy	81
§3.4 ^O	The Equation of Angular Momentum	82
§3.5	The Equations of Change in Terms of the Substantial Derivative	83
	Ex. 3.5-1 The Bernoulli Equation for the Steady Flow of Inviscid Fluids	86
§3.6	Use of the Equations of Change to Solve Flow Problems	86
	Ex. 3.6-1 Steady Flow in a Long Circular Tube	88
	Ex. 3.6-2 Falling Film with Variable Viscosity	89
	Ex. 3.6-3 Operation of a Couette Viscometer	89
	Ex. 3.6-4 Shape of the Surface of a Rotating Liquid	93
	Ex. 3.6-5 Flow near a Slowly Rotating Sphere	95
§3.7	Dimensional Analysis of the Equations of Change	97
	Ex. 3.7-1 Transverse Flow around a Circular Cylinder	98
	Ex. 3.7-2 Steady Flow in an Agitated Tank	101
	Ex. 3.7-3 Pressure Drop for Creeping Flow in a Packed Tube	103
Questions for Discussion		104
Problems		104

Chapter 4 Velocity Distributions with More than One Independent Variable 114

§4.1	Time-Dependent Flow of Newtonian Fluids	114
	Ex. 4.1-1 Flow near a Wall Suddenly Set in Motion	115

<p>Ex. 4.1-2 Unsteady Laminar Flow between Two Parallel Plates 117</p> <p>Ex. 4.1-3 Unsteady Laminar Flow near an Oscillating Plate 120</p> <p>§4.2^o Solving Flow Problems Using a Stream Function 121</p> <p>Ex. 4.2-1 Creeping Flow around a Sphere 122</p> <p>§4.3^o Flow of Inviscid Fluids by Use of the Velocity Potential 126</p> <p>Ex. 4.3-1 Potential Flow around a Cylinder 128</p> <p>Ex. 4.3-2 Flow into a Rectangular Channel 130</p> <p>Ex. 4.3-3 Flow near a Corner 131</p> <p>§4.4^o Flow near Solid Surfaces by Boundary-Layer Theory 133</p> <p>Ex. 4.4-1 Laminar Flow along a Flat Plate (Approximate Solution) 136</p> <p>Ex. 4.4-2 Laminar Flow along a Flat Plate (Exact Solution) 137</p> <p>Ex. 4.4-3 Flow near a Corner 139</p> <p>Questions for Discussion 140</p> <p>Problems 141</p>	<p>Ex. 6.2-2 Flow Rate for a Given Pressure Drop 183</p> <p>§6.3 Friction Factors for Flow around Spheres 185</p> <p>Ex. 6.3-1 Determination of the Diameter of a Falling Sphere 187</p> <p>§6.4^o Friction Factors for Packed Columns 188</p> <p>Questions for Discussion 192</p> <p>Problems 193</p>
Chapter 7 Macroscopic Balances for Isothermal Flow Systems 197	
<p>§5.1 Comparisons of Laminar and Turbulent Flows 154</p> <p>§5.2 Time-Smoothed Equations of Change for Incompressible Fluids 156</p> <p>§5.3 The Time-Smoothed Velocity Profile near a Wall 159</p> <p>§5.4 Empirical Expressions for the Turbulent Momentum Flux 162</p> <p>Ex. 5.4-1 Development of the Reynolds Stress Expression in the Vicinity of the Wall 164</p> <p>§5.5 Turbulent Flow in Ducts 165</p> <p>Ex. 5.5-1 Estimation of the Average Velocity in a Circular Tube 166</p> <p>Ex. 5.5-2 Application of Prandtl's Mixing Length Formula to Turbulent Flow in a Circular Tube 167</p> <p>Ex. 5.5-3 Relative Magnitude of Viscosity and Eddy Viscosity 167</p> <p>§5.6^o Turbulent Flow in Jets 168</p> <p>Ex. 5.6-1 Time-Smoothed Velocity Distribution in a Circular Wall Jet 168</p> <p>Questions for Discussion 172</p> <p>Problems 172</p>	<p>§7.1 The Macroscopic Mass Balance 198</p> <p>Ex. 7.1-1 Draining of a Spherical Tank 199</p> <p>§7.2 The Macroscopic Momentum Balance 200</p> <p>Ex. 7.2-1 Force Exerted by a Jet (Part a) 201</p> <p>§7.3 The Macroscopic Angular Momentum Balance 202</p> <p>Ex. 7.3-1 Torque on a Mixing Vessel 202</p> <p>§7.4 The Macroscopic Mechanical Energy Balance 203</p> <p>Ex. 7.4-1 Force Exerted by a Jet (Part b) 205</p> <p>§7.5 Estimation of the Viscous Loss 205</p> <p>Ex. 7.5-1 Power Requirement for Pipeline Flow 207</p> <p>§7.6 Use of the Macroscopic Balances for Steady-State Problems 209</p> <p>Ex. 7.6-1 Pressure Rise and Friction Loss in a Sudden Enlargement 209</p> <p>Ex. 7.6-2 Performance of a Liquid–Liquid Ejector 210</p> <p>Ex. 7.6-3 Thrust on a Pipe Bend 212</p> <p>Ex. 7.6-4 The Impinging Jet 214</p> <p>Ex. 7.6-5 Isothermal Flow of a Liquid through an Orifice 215</p> <p>§7.7^o Use of the Macroscopic Balances for Unsteady-State Problems 216</p> <p>Ex. 7.7-1 Acceleration Effects in Unsteady Flow from a Cylindrical Tank 217</p> <p>Ex. 7.7-2 Manometer Oscillations 219</p> <p>§7.8• Derivation of the Macroscopic Mechanical Energy Balance 221</p> <p>Questions for Discussion 223</p> <p>Problems 224</p>
Chapter 8 Polymeric Liquids 231	
<p>§6.1 Definition of Friction Factors 178</p> <p>§6.2 Friction Factors for Flow in Tubes 179</p> <p>Ex. 6.2-1 Pressure Drop Required for a Given Flow Rate 183</p>	<p>§8.1 Examples of the Behavior of Polymeric Liquids 232</p> <p>§8.2 Rheometry and Material Functions 236</p> <p>§8.3 Non-Newtonian Viscosity and the Generalized Newtonian Models 240</p> <p>Ex. 8.3-1 Laminar Flow of an Incompressible Power-Law Fluid in a Circular Tube 242</p> <p>Ex. 8.3-2 Flow of a Power-Law Fluid in a Narrow Slit 243</p>

<p><i>Ex. 8.3-3 Tangential Annular Flow of a Power-Law Fluid</i> 244</p> <p>§8.4^O Elasticity and the Linear Viscoelastic Models 244</p> <ul style="list-style-type: none"> <i>Ex. 8.4-1 Small-Amplitude Oscillatory Motion</i> 247 <i>Ex. 8.4-2 Unsteady Viscoelastic Flow near an Oscillating Plate</i> 248 <p>§8.5• The Corotational Derivatives and the Nonlinear Viscoelastic Models 249</p> <ul style="list-style-type: none"> <i>Ex. 8.5-1 Material Functions for the Oldroyd 6-Constant Model</i> 251 <p>§8.6• Molecular Theories for Polymeric Liquids 253</p> <ul style="list-style-type: none"> <i>Ex. 8.6-1 Material Functions for the FENE-P Model</i> 255 <p>Questions for Discussion 258</p> <p>Problems 258</p>

Part II Energy Transport

Chapter 9 Thermal Conductivity and the Mechanisms of Energy Transport 263

<p>§9.1 Fourier's Law of Heat Conduction (Molecular Energy Transport) 266</p> <ul style="list-style-type: none"> <i>Ex. 9.1-1 Measurement of Thermal Conductivity</i> 270 <p>§9.2 Temperature and Pressure Dependence of Thermal Conductivity 272</p> <ul style="list-style-type: none"> <i>Ex. 9.2-1 Effect of Pressure on Thermal Conductivity</i> 273 <p>§9.3^O Theory of Thermal Conductivity of Gases at Low Density 274</p> <ul style="list-style-type: none"> <i>Ex. 9.3-1 Computation of the Thermal Conductivity of a Monatomic Gas at Low Density</i> 277 <i>Ex. 9.3-2 Estimation of the Thermal Conductivity of a Polyatomic Gas at Low Density</i> 278 <i>Ex. 9.3-3 Prediction of the Thermal Conductivity of a Gas Mixture at Low Density</i> 278 <p>§9.4^O Theory of Thermal Conductivity of Liquids 279</p> <ul style="list-style-type: none"> <i>Ex. 9.4-1 Prediction of the Thermal Conductivity of a Liquid</i> 280 <p>§9.5^O Thermal Conductivity of Solids 280</p> <p>§9.6^O Effective Thermal Conductivity of Composite Solids 281</p> <p>§9.7 Convective Transport of Energy 283</p> <p>§9.8 Work Associated with Molecular Motions 284</p> <p>Questions for Discussion 286</p> <p>Problems 287</p>

Chapter 10 Shell Energy Balances and Temperature Distributions in Solids and Laminar Flow 290

<p>§10.1 Shell Energy Balances; Boundary Conditions 291</p> <p>§10.2 Heat Conduction with an Electrical Heat Source 292</p> <ul style="list-style-type: none"> <i>Ex. 10.2-1 Voltage Required for a Given Temperature Rise in a Wire Heated by an Electric Current</i> 295 <i>Ex. 10.2-2 Heated Wire with Specified Heat Transfer Coefficient and Ambient Air Temperature</i> 295 <p>§10.3 Heat Conduction with a Nuclear Heat Source 296</p> <p>§10.4 Heat Conduction with a Viscous Heat Source 298</p> <p>§10.5 Heat Conduction with a Chemical Heat Source 300</p> <p>§10.6 Heat Conduction through Composite Walls 303</p> <ul style="list-style-type: none"> <i>Ex. 10.6-1 Composite Cylindrical Walls</i> 305 <p>§10.7 Heat Conduction in a Cooling Fin 307</p> <ul style="list-style-type: none"> <i>Ex. 10.7-1 Error in Thermocouple Measurement</i> 309 <p>§10.8 Forced Convection 310</p> <p>§10.9 Free Convection 316</p> <p>Questions for Discussion 319</p> <p>Problems 320</p>

Chapter 11 The Equations of Change for Nonisothermal Systems 333

<p>§11.1 The Energy Equation 333</p> <p>§11.2 Special Forms of the Energy Equation 336</p> <p>§11.3 The Boussinesq Equation of Motion for Forced and Free Convection 338</p> <p>§11.4 Use of the Equations of Change to Solve Steady-State Problems 339</p> <ul style="list-style-type: none"> <i>Ex. 11.4-1 Steady-State Forced-Convection Heat Transfer in Laminar Flow in a Circular Tube</i> 342 <i>Ex. 11.4-2 Tangential Flow in an Annulus with Viscous Heat Generation</i> 342 <i>Ex. 11.4-3 Steady Flow in a Nonisothermal Film</i> 343 <i>Ex. 11.4-4 Transpiration Cooling</i> 344 <i>Ex. 11.4-5 Free Convection Heat Transfer from a Vertical Plate</i> 346 <i>Ex. 11.4-6 Adiabatic Frictionless Processes in an Ideal Gas</i> 349 <i>Ex. 11.4-7 One-Dimensional Compressible Flow: Velocity, Temperature, and Pressure Profiles in a Stationary Shock Wave</i> 350
--

§11.5 Dimensional Analysis of the Equations of Change for Nonisothermal Systems	353	§13.4° Temperature Distribution for Turbulent Flow in Tubes	411	
<i>Ex. 11.5-1 Temperature Distribution about a Long Cylinder</i>	356	§13.5° Temperature Distribution for Turbulent Flow in Jets	415	
<i>Ex. 11.5-2 Free Convection in a Horizontal Fluid Layer; Formation of Bénard Cells</i>	358	§13.6• Fourier Analysis of Energy Transport in Tube Flow at Large Prandtl Numbers	416	
<i>Ex. 11.5-3 Surface Temperature of an Electrical Heating Coil</i>	360	Questions for Discussion	421	
Questions for Discussion	361	Problems	421	
Problems	361	<hr/>		
Chapter 12 Temperature Distributions with More than One Independent Variable	374	Chapter 14 Interphase Transport in Nonisothermal Systems	422	
§12.1 Unsteady Heat Conduction in Solids	374	§14.1 Definitions of Heat Transfer Coefficients	423	
<i>Ex. 12.1-1 Heating of a Semi-Infinite Slab</i>	375	<i>Ex. 14.1-1 Calculation of Heat Transfer Coefficients from Experimental Data</i>	426	
<i>Ex. 12.1-2 Heating of a Finite Slab</i>	376	§14.2 Analytical Calculations of Heat Transfer Coefficients for Forced Convection through Tubes and Slits	428	
<i>Ex. 12.1-3 Unsteady Heat Conduction near a Wall with Sinusoidal Heat Flux</i>	379	§14.3 Heat Transfer Coefficients for Forced Convection in Tubes	433	
<i>Ex. 12.1-4 Cooling of a Sphere in Contact with a Well-Stirred Fluid</i>	379	<i>Ex. 14.3-1 Design of a Tubular Heater</i>	437	
§12.2° Steady Heat Conduction in Laminar, Incompressible Flow	381	§14.4 Heat Transfer Coefficients for Forced Convection around Submerged Objects	438	
<i>Ex. 12.2-1 Laminar Tube Flow with Constant Heat Flux at the Wall</i>	383	§14.5 Heat Transfer Coefficients for Forced Convection through Packed Beds	441	
<i>Ex. 12.2-2 Laminar Tube Flow with Constant Heat Flux at the Wall: Asymptotic Solution for the Entrance Region</i>	384	§14.6° Heat Transfer Coefficients for Free and Mixed Convection	442	
§12.3° Steady Potential Flow of Heat in Solids	385	<i>Ex. 14.6-1 Heat Loss by Free Convection from a Horizontal Pipe</i>	445	
<i>Ex. 12.3-1 Temperature Distribution in a Wall</i>	386	§14.7° Heat Transfer Coefficients for Condensation of Pure Vapors on Solid Surfaces	446	
§12.4° Boundary Layer Theory for Nonisothermal Flow	387	<i>Ex. 14.7-1 Condensation of Steam on a Vertical Surface</i>	449	
<i>Ex. 12.4-1 Heat Transfer in Laminar Forced Convection along a Heated Flat Plate (the von Kármán Integral Method)</i>	388	Questions for Discussion	449	
<i>Ex. 12.4-2 Heat Transfer in Laminar Forced Convection along a Heated Flat Plate (Asymptotic Solution for Large Prandtl Numbers)</i>	391	Problems	450	
<i>Ex. 12.4-3 Forced Convection in Steady Three-Dimensional Flow at High Prandtl Numbers</i>	392	<hr/>		
Questions for Discussion	394	Chapter 15 Macroscopic Balances for Nonisothermal Systems	454	
Problems	395	§15.1 The Macroscopic Energy Balance	455	
Chapter 13 Temperature Distributions in Turbulent Flow	407	§15.2 The Macroscopic Mechanical Energy Balance	456	
§13.1 Time-Smoothed Equations of Change for Incompressible Nonisothermal Flow	407	§15.3 Use of the Macroscopic Balances to Solve Steady-State Problems with Flat Velocity Profiles	458	
§13.2 The Time-Smoothed Temperature Profile near a Wall	409	<i>Ex. 15.3-1 The Cooling of an Ideal Gas</i>	459	
§13.3 Empirical Expressions for the Turbulent Heat Flux	410	<i>Ex. 15.3-2 Mixing of Two Ideal Gas Streams</i>	460	
<i>Ex. 13.3-1 An Approximate Relation for the Wall Heat Flux for Turbulent Flow in a Tube</i>	411	§15.4 The <i>d</i> -Forms of the Macroscopic Balances	461	
		<i>Ex. 15.4-1 Parallel- or Counter-Flow Heat Exchangers</i>	462	
		<i>Ex. 15.4-2 Power Requirement for Pumping a Compressible Fluid through a Long Pipe</i>	464	
		§15.5° Use of the Macroscopic Balances to Solve Unsteady-State Problems and Problems with Nonflat Velocity Profiles	465	

<i>Ex. 15.5-1 Heating of a Liquid in an Agitated Tank</i>	466	<i>Ex. 17.2-3 Estimation of Binary Diffusivity at High Density</i>	524
<i>Ex. 15.5-2 Operation of a Simple Temperature Controller</i>	468	§17.3 ^o Theory of Diffusion in Gases at Low Density	525
<i>Ex. 15.5-3 Flow of Compressible Fluids through Heat Meters</i>	471	<i>Ex. 17.3-1 Computation of Mass Diffusivity for Low-Density Monatomic Gases</i>	528
<i>Ex. 15.5-4 Free Batch Expansion of a Compressible Fluid</i>	472	§17.4 ^o Theory of Diffusion in Binary Liquids	528
Questions for Discussion	474	<i>Ex. 17.4-1 Estimation of Liquid Diffusivity</i>	530
Problems	474	§17.5 ^o Theory of Diffusion in Colloidal Suspensions	531
Chapter 16 Energy Transport by Radiation 487		§17.6 ^o Theory of Diffusion in Polymers	532
§16.1 The Spectrum of Electromagnetic Radiation	488	§17.7 Mass and Molar Transport by Convection	533
§16.2 Absorption and Emission at Solid Surfaces	490	§17.8 Summary of Mass and Molar Fluxes	536
§16.3 Planck's Distribution Law, Wien's Displacement Law, and the Stefan-Boltzmann Law	493	§17.9 ^o The Maxwell-Stefan Equations for Multicomponent Diffusion in Gases at Low Density	538
<i>Ex. 16.3-1 Temperature and Radiation-Energy Emission of the Sun</i>	496	Questions for Discussion	538
§16.4 Direct Radiation between Black Bodies in Vacuo at Different Temperatures	497	Problems	539
<i>Ex. 16.4-1 Estimation of the Solar Constant</i>	501	Chapter 18 Concentration Distributions in Solids and Laminar Flow 543	
<i>Ex. 16.4-2 Radiant Heat Transfer between Disks</i>	501	§18.1 Shell Mass Balances; Boundary Conditions	545
§16.5 ^o Radiation between Nonblack Bodies at Different Temperatures	502	§18.2 Diffusion through a Stagnant Gas Film	545
<i>Ex. 16.5-1 Radiation Shields</i>	503	<i>Ex. 18.2-1 Diffusion with a Moving Interface</i>	549
<i>Ex. 16.5-2 Radiation and Free-Convection Heat Losses from a Horizontal Pipe</i>	504	<i>Ex. 18.2-2 Determination of Diffusivity</i>	549
<i>Ex. 16.5-3 Combined Radiation and Convection</i>	505	<i>Ex. 18.2-3 Diffusion through a Nonisothermal Spherical Film</i>	550
§16.6 ^o Radian Energy Transport in Absorbing Media	506	§18.3 Diffusion with a Heterogeneous Chemical Reaction	551
<i>Ex. 16.6-1 Absorption of a Monochromatic Radiant Beam</i>	507	<i>Ex. 18.3-1 Diffusion with a Slow Heterogeneous Reaction</i>	553
Questions for Discussion	508	§18.4 Diffusion with a Homogeneous Chemical Reaction	554
Problems	508	<i>Ex. 18.4-1 Gas Absorption with Chemical Reaction in an Agitated Tank</i>	555
Part III Mass Transport		§18.5 Diffusion into a Falling Liquid Film (Gas Absorption)	558
Chapter 17 Diffusivity and the Mechanisms of Mass Transport 513		<i>Ex. 18.5-1 Gas Absorption from Rising Bubbles</i>	560
§17.1 Fick's Law of Binary Diffusion (Molecular Mass Transport)	514	§18.6 Diffusion into a Falling Liquid Film (Solid Dissolution)	562
<i>Ex. 17.1-1. Diffusion of Helium through Pyrex Glass</i>	519	§18.7 Diffusion and Chemical Reaction inside a Porous Catalyst	563
<i>Ex. 17.1-2 The Equivalence of D_{AB} and D_{BA}</i>	520	§18.8 ^o Diffusion in a Three-Component Gas System	567
§17.2 Temperature and Pressure Dependence of Diffusivities	521	Questions for Discussion	568
<i>Ex. 17.2-1 Estimation of Diffusivity at Low Density</i>	523	Problems	568
<i>Ex. 17.2-2 Estimation of Self-Diffusivity at High Density</i>	523	Chapter 19 Equations of Change for Multicomponent Systems 582	
§19.1 The Equations of Continuity for a Multicomponent Mixture	582	<i>Ex. 19.1-1 Diffusion, Convection, and Chemical Reaction</i>	585

§19.2	Summary of the Multicomponent Equations of Change	586	§20.5• "Taylor Dispersion" in Laminar Tube Flow	643			
§19.3	Summary of the Multicomponent Fluxes	590	Questions for Discussion	647			
	<i>Ex. 19.3-1 The Partial Molar Enthalpy</i>	591	Problems	648			
§19.4	Use of the Equations of Change for Mixtures	592	Chapter 21 Concentration Distributions in Turbulent Flow 657				
	<i>Ex. 19.4-1 Simultaneous Heat and Mass Transport</i>	592	§21.1	Concentration Fluctuations and the Time-Smoothed Concentration	657		
	<i>Ex. 19.4-2 Concentration Profile in a Tubular Reactor</i>	595	§21.2	Time-Smoothing of the Equation of Continuity of <i>A</i>	658		
	<i>Ex. 19.4-3 Catalytic Oxidation of Carbon Monoxide</i>	596	§21.3	Semi-Empirical Expressions for the Turbulent Mass Flux	659		
	<i>Ex. 19.4-4 Thermal Conductivity of a Polyatomic Gas</i>	598	§21.4 ^O	Enhancement of Mass Transfer by a First-Order Reaction in Turbulent Flow	659		
§19.5	Dimensional Analysis of the Equations of Change for Nonreacting Binary Mixtures	599	§21.5•	Turbulent Mixing and Turbulent Flow with Second-Order Reaction	663		
	<i>Ex. 19.5-1 Concentration Distribution about a Long Cylinder</i>	601	Questions for Discussion	667			
	<i>Ex. 19.5-2 Fog Formation during Dehumidification</i>	602	Problems	668			
	<i>Ex. 19.5-3 Blending of Miscible Fluids</i>	604					
Questions for Discussion				605			
Problems				606			

Chapter 20 Concentration Distributions with More than One Independent Variable 612

§20.1	Time-Dependent Diffusion	613	§22.1	Definition of Transfer Coefficients in One Phase	672
	<i>Ex. 20.1-1 Unsteady-State Evaporation of a Liquid (the "Arnold Problem")</i>	613	§22.2	Analytical Expressions for Mass Transfer Coefficients	676
	<i>Ex. 20.1-2 Gas Absorption with Rapid Reaction</i>	617	§22.3	Correlation of Binary Transfer Coefficients in One Phase	679
	<i>Ex. 20.1-3 Unsteady Diffusion with First-Order Homogeneous Reaction</i>	619		<i>Ex. 22.3-1 Evaporation from a Freely Falling Drop</i>	682
	<i>Ex. 20.1-4 Influence of Changing Interfacial Area on Mass Transfer at an Interface</i>	621		<i>Ex. 22.3-2 The Wet and Dry Bulb Psychrometer</i>	683
§20.2 ^O	Steady-State Transport in Binary Boundary Layers	623		<i>Ex. 22.3-3 Mass Transfer in Creeping Flow through Packed Beds</i>	685
	<i>Ex. 20.2-1 Diffusion and Chemical Reaction in Isothermal Laminar Flow along a Soluble Flat Plate</i>	625		<i>Ex. 22.3-4 Mass Transfer to Drops and Bubbles</i>	687
	<i>Ex. 20.2-2 Forced Convection from a Flat Plate at High Mass-Transfer Rates</i>	627	§22.4	Definition of Transfer Coefficients in Two Phases	687
	<i>Ex. 20.2-3 Approximate Analogies for the Flat Plate at Low Mass-Transfer Rates</i>	632		<i>Ex. 22.4-1 Determination of the Controlling Resistance</i>	690
§20.3•	Steady-State Boundary-Layer Theory for Flow around Objects	633		<i>Ex. 22.4-2 Interaction of Phase Resistances</i>	691
	<i>Ex. 20.3-1 Mass Transfer for Creeping Flow around a Gas Bubble</i>	636		<i>Ex. 22.4-3 Area Averaging</i>	693
§20.4•	Boundary Layer Mass Transport with Complex Interfacial Motion	637	§22.5 ^O	Mass Transfer and Chemical Reactions	694
	<i>Ex. 20.4-1 Mass Transfer with Nonuniform Interfacial Deformation</i>	641		<i>Ex. 22.5-1 Estimation of the Interfacial Area in a Packed Column</i>	694
	<i>Ex. 20.4-2 Gas Absorption with Rapid Reaction and Interfacial Deformation</i>	642		<i>Ex. 22.5-2 Estimation of Volumetric Mass Transfer Coefficients</i>	695

§20.5•	"Taylor Dispersion" in Laminar Tube Flow	643
Questions for Discussion	647	
Problems	648	

Chapter 21 Concentration Distributions in Turbulent Flow 657

§21.1	Concentration Fluctuations and the Time-Smoothed Concentration	657
§21.2	Time-Smoothing of the Equation of Continuity of <i>A</i>	658
§21.3	Semi-Empirical Expressions for the Turbulent Mass Flux	659
§21.4 ^O	Enhancement of Mass Transfer by a First-Order Reaction in Turbulent Flow	659
§21.5•	Turbulent Mixing and Turbulent Flow with Second-Order Reaction	663
Questions for Discussion	667	
Problems	668	

Chapter 22 Interphase Transport in Nonisothermal Mixtures 671

§22.1	Definition of Transfer Coefficients in One Phase	672
§22.2	Analytical Expressions for Mass Transfer Coefficients	676
§22.3	Correlation of Binary Transfer Coefficients in One Phase	679
	<i>Ex. 22.3-1 Evaporation from a Freely Falling Drop</i>	682
	<i>Ex. 22.3-2 The Wet and Dry Bulb Psychrometer</i>	683
	<i>Ex. 22.3-3 Mass Transfer in Creeping Flow through Packed Beds</i>	685
	<i>Ex. 22.3-4 Mass Transfer to Drops and Bubbles</i>	687
§22.4	Definition of Transfer Coefficients in Two Phases	687
	<i>Ex. 22.4-1 Determination of the Controlling Resistance</i>	690
	<i>Ex. 22.4-2 Interaction of Phase Resistances</i>	691
	<i>Ex. 22.4-3 Area Averaging</i>	693
§22.5 ^O	Mass Transfer and Chemical Reactions	694
	<i>Ex. 22.5-1 Estimation of the Interfacial Area in a Packed Column</i>	694
	<i>Ex. 22.5-2 Estimation of Volumetric Mass Transfer Coefficients</i>	695
	<i>Ex. 22.5-3 Model-Insensitive Correlations for Absorption with Rapid Reaction</i>	696
§22.6 ^O	Combined Heat and Mass Transfer by Free Convection	698
	<i>Ex. 22.6-1 Additivity of Grashof Numbers</i>	698
	<i>Ex. 22.6-2 Free-Convection Heat Transfer as a Source of Forced-Convection Mass Transfer</i>	698

§22.7 ^o	Effects of Interfacial Forces on Heat and Mass Transfer	699
	Ex. 22.7-1 Elimination of Circulation in a Rising Gas Bubble	701
	Ex. 22.7-2 Marangoni Instability in a Falling Film	702
§22.8 ^o	Transfer Coefficients at High Net Mass Transfer Rates	703
	Ex. 22.8-1 Rapid Evaporation of a Liquid from a Plane Surface	710
	Ex. 22.8-2 Correction Factors in Droplet Evaporation	711
	Ex. 22.8-3 Wet-Bulb Performance Corrected for Mass-Transfer Rate	711
	Ex. 22.8-4 Comparison of Film and Penetration Models for Unsteady Evaporation in a Long Tube	712
	Ex. 22.8-5 Concentration Polarization in Ultrafiltration	713
§22.9 ^o	Matrix Approximations for Multicomponent Mass Transport	716
	Questions for Discussion	721
	Problems	722
Chapter 23 Macroscopic Balances for Multicomponent Systems 726		
§23.1	The Macroscopic Mass Balances	727
	Ex. 23.1-1 Disposal of an Unstable Waste Product	728
	Ex. 23.1-2 Binary Splitters	730
	Ex. 23.1-3 The Macroscopic Balances and Dirac's "Separative Capacity" and "Value Function"	731
	Ex. 23.1-4 Compartmental Analysis	733
	Ex. 23.1-5 Time Constants and Model Insensitivity	736
§23.2 ^o	The Macroscopic Momentum and Angular Momentum Balances	738
§23.3	The Macroscopic Energy Balance	738
§23.4	The Macroscopic Mechanical Energy Balance	739
§23.5	Use of the Macroscopic Balances to Solve Steady-State Problems	739
	Ex. 23.5-1 Energy Balances for a Sulfur Dioxide Converter	739
	Ex. 23.5-2 Height of a Packed-Tower Absorber	742
	Ex. 23.5-3 Linear Cascades	746
	Ex. 23.5-4 Expansion of a Reactive Gas Mixture through a Frictionless Adiabatic Nozzle	749
§23.6 ^o	Use of the Macroscopic Balances to Solve Unsteady-State Problems	752
	Ex. 23.6-1 Start-Up of a Chemical Reactor	752

Ex. 23.6-2 Unsteady Operation of a Packed Column 753

Ex. 23.6-3 The Utility of Low-Order Moments 756

Questions for Discussion 758
Problems 759

Chapter 24 Other Mechanisms for Mass Transport 764

§24.1	• The Equation of Change for Entropy	765
§24.2	• The Flux Expressions for Heat and Mass	767
	Ex. 24.2-1 Thermal Diffusion and the Clusius-Dickel Column	770
	Ex. 24.2-2 Pressure Diffusion and the Ultracentrifuge	772
§24.3 ^o	Concentration Diffusion and Driving Forces	774
§24.4 ^o	Applications of the Generalized Maxwell-Stefan Equations	775
	Ex. 24.4-1 Centrifugation of Proteins	776
	Ex. 24.4-2 Proteins as Hydrodynamic Particles	779
	Ex. 24.4-3 Diffusion of Salts in an Aqueous Solution	780
	Ex. 24.4-4 Departures from Local Electroneutrality: Electro-Osmosis	782
	Ex. 24.4-5 Additional Mass-Transfer Driving Forces	784
§24.5 ^o	Mass Transport across Selectively Permeable Membranes	785
	Ex. 24.5-1 Concentration Diffusion between Preexisting Bulk Phases	788
	Ex. 24.5-2 Ultrafiltration and Reverse Osmosis	789
	Ex. 24.5-3 Charged Membranes and Donnan Exclusion	791
§24.6 ^o	Mass Transport in Porous Media	793
	Ex. 24.6-1 Knudsen Diffusion	795
	Ex. 24.6-2 Transport from a Binary External Solution	797
	Questions for Discussion	798
	Problems	799
Postface 805		
Appendices		
Appendix A Vector and Tensor Notation 807		
§A.1	Vector Operations from a Geometrical Viewpoint	808
§A.2	Vector Operations in Terms of Components	810
	Ex. A.2-1 Proof of a Vector Identity	814

§A.3	Tensor Operations in Terms of Components	815	§C.2	Expansions of Functions in Taylor Series	853
§A.4	Vector and Tensor Differential Operations <i>Ex. A.4-1 Proof of a Tensor Identity</i>	819	§C.3	Differentiation of Integrals (the Leibniz Formula)	854
§A.5	Vector and Tensor Integral Theorems	824	§C.4	The Gamma Function	855
§A.6	Vector and Tensor Algebra in Curvilinear Coordinates	825	§C.5	The Hyperbolic Functions	856
§A.7	Differential Operations in Curvilinear Coordinates <i>Ex. A.7-1 Differential Operations in Cylindrical Coordinates</i> <i>Ex. A.7-2 Differential Operations in Spherical Coordinates</i>	829	§C.6	The Error Function	857
§A.8	Integral Operations in Curvilinear Coordinates	839	Appendix D The Kinetic Theory of Gases 858		
§A.9	Further Comments on Vector–Tensor Notation	841	SD.1	The Boltzmann Equation	858
Appendix B Fluxes and the Equations of Change 843			SD.2	The Equations of Change	859
SB.1	Newton's Law of Viscosity	843	SD.3	The Molecular Expressions for the Fluxes	859
SB.2	Fourier's Law of Heat Conduction	845	SD.4	The Solution to the Boltzmann Equation	860
SB.3	Fick's (First) Law of Binary Diffusion	846	SD.5	The Fluxes in Terms of the Transport Properties	860
SB.4	The Equation of Continuity	846	SD.6	The Transport Properties in Terms of the Intermolecular Forces	861
SB.5	The Equation of Motion in Terms of τ	847	SD.7	Concluding Comments	861
SB.6	The Equation of Motion for a Newtonian Fluid with Constant ρ and μ	848	Appendix E Tables for Prediction of Transport Properties 863		
SB.7	The Dissipation Function Φ_v for Newtonian Fluids	849	SE.1	Intermolecular Force Parameters and Critical Properties	864
SB.8	The Equation of Energy in Terms of q	849	SE.2	Functions for Prediction of Transport Properties of Gases at Low Densities	866
SB.9	The Equation of Energy for Pure Newtonian Fluids with Constant ρ and k	850	Appendix F Constants and Conversion Factors 867		
SB.10	The Equation of Continuity for Species α in Terms of j_α	850	SF.1	Mathematical Constants	867
SB.11	The Equation of Continuity for Species A in Terms of ω_A for Constant $\rho \mathcal{D}_{AB}$	851	SF.2	Physical Constants	867
Appendix C Mathematical Topics 852			SF.3	Conversion Factors	868
SC.1	Some Ordinary Differential Equations and Their Solutions	852	Notation 872		
			Author Index 877		
			Subject Index 885		

Chapter 0

The Subject of Transport Phenomena

§0.1 What are the transport phenomena?

§0.2 Three levels at which transport phenomena can be studied

§0.3 The conservation laws: an example

§0.4 Concluding comments

The purpose of this introductory chapter is to describe the scope, aims, and methods of the subject of transport phenomena. It is important to have some idea about the structure of the field before plunging into the details; without this perspective it is not possible to appreciate the unifying principles of the subject and the interrelation of the various individual topics. A good grasp of transport phenomena is essential for understanding many processes in engineering, agriculture, meteorology, physiology, biology, analytical chemistry, materials science, pharmacy, and other areas. Transport phenomena is a well-developed and eminently useful branch of physics that pervades many areas of applied science.

§0.1 WHAT ARE THE TRANSPORT PHENOMENA?

The subject of transport phenomena includes three closely related topics: fluid dynamics, heat transfer, and mass transfer. Fluid dynamics involves the transport of *momentum*, heat transfer deals with the transport of *energy*, and mass transfer is concerned with the transport of *mass* of various chemical species. These three transport phenomena should, at the introductory level, be studied together for the following reasons:

- They frequently occur simultaneously in industrial, biological, agricultural, and meteorological problems; in fact, the occurrence of any one transport process by itself is the exception rather than the rule.
- The basic equations that describe the three transport phenomena are closely related. The similarity of the equations under simple conditions is the basis for solving problems “by analogy.”
- The mathematical tools needed for describing these phenomena are very similar. Although it is not the aim of this book to teach mathematics, the student will be required to review various mathematical topics as the development unfolds. Learning how to use mathematics may be a very valuable by-product of studying transport phenomena.
- The molecular mechanisms underlying the various transport phenomena are very closely related. All materials are made up of molecules, and the same molecular

motions and interactions are responsible for viscosity, thermal conductivity, and diffusion.

The main aim of this book is to give a balanced overview of the field of transport phenomena, present the fundamental equations of the subject, and illustrate how to use them to solve problems.

There are many excellent treatises on fluid dynamics, heat transfer, and mass transfer. In addition, there are many research and review journals devoted to these individual subjects and even to specialized subfields. The reader who has mastered the contents of this book should find it possible to consult the treatises and journals and go more deeply into other aspects of the theory, experimental techniques, empirical correlations, design methods, and applications. That is, this book should not be regarded as the complete presentation of the subject, but rather as a stepping stone to a wealth of knowledge that lies beyond.

§0.2 THREE LEVELS AT WHICH TRANSPORT PHENOMENA CAN BE STUDIED

In Fig. 0.2-1 we show a schematic diagram of a large system—for example, a large piece of equipment through which a fluid mixture is flowing. We can describe the transport of mass, momentum, energy, and angular momentum at three different levels.

At the *macroscopic level* (Fig. 0.2-1a) we write down a set of equations called the “macroscopic balances,” which describe how the mass, momentum, energy, and angular momentum in the system change because of the introduction and removal of these entities via the entering and leaving streams, and because of various other inputs to the system from the surroundings. No attempt is made to understand all the details of the system. In studying an engineering or biological system it is a good idea to start with this macroscopic description in order to make a global assessment of the problem; in some instances it is only this overall view that is needed.

At the *microscopic level* (Fig. 0.2-1b) we examine what is happening to the fluid mixture in a small region within the equipment. We write down a set of equations called the “equations of change,” which describe how the mass, momentum, energy, and angular momentum change within this small region. The aim here is to get information about velocity, temperature, pressure, and concentration profiles within the system. This more detailed information may be required for the understanding of some processes.

At the *molecular level* (Fig. 0.2-1c) we seek a fundamental understanding of the mechanisms of mass, momentum, energy, and angular momentum transport in terms of mol-

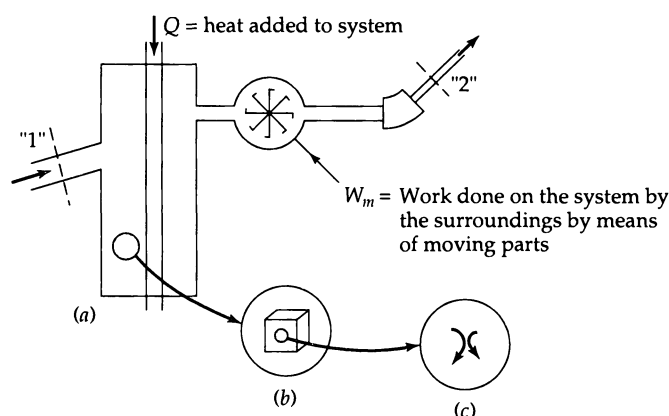


Fig. 0.2-1 (a) A macroscopic flow system containing N_2 and O_2 ; (b) a microscopic region within the macroscopic system containing N_2 and O_2 , which are in a state of flow; (c) a collision between a molecule of N_2 and a molecule of O_2 .

ecular structure and intermolecular forces. Generally this is the realm of the theoretical physicist or physical chemist, but occasionally engineers and applied scientists have to get involved at this level. This is particularly true if the processes being studied involve complex molecules, extreme ranges of temperature and pressure, or chemically reacting systems.

It should be evident that these three levels of description involve different “length scales”: for example, in a typical industrial problem, at the macroscopic level the dimensions of the flow systems may be of the order of centimeters or meters; the microscopic level involves what is happening in the micron to the centimeter range; and molecular-level problems involve ranges of about 1 to 1000 nanometers.

This book is divided into three parts dealing with

- Flow of pure fluids at constant temperature (with emphasis on viscous and convective momentum transport)—Chapters 1–8
- Flow of pure fluids with varying temperature (with emphasis on conductive, convective, and radiative energy transport)—Chapters 9–16
- Flow of fluid mixtures with varying composition (with emphasis on diffusive and convective mass transport)—Chapters 17–24

That is, we build from the simpler to the more difficult problems. Within each of these parts, we start with an initial chapter dealing with some results of the molecular theory of the transport properties (viscosity, thermal conductivity, and diffusivity). Then we proceed to the microscopic level and learn how to determine the velocity, temperature, and concentration profiles in various kinds of systems. The discussion concludes with the macroscopic level and the description of large systems.

As the discussion unfolds, the reader will appreciate that there are many connections between the levels of description. The transport properties that are described by molecular theory are used at the microscopic level. Furthermore, the equations developed at the microscopic level are needed in order to provide some input into problem solving at the macroscopic level.

There are also many connections between the three areas of momentum, energy, and mass transport. By learning how to solve problems in one area, one also learns the techniques for solving problems in another area. The similarities of the equations in the three areas mean that in many instances one can solve a problem “by analogy”—that is, by taking over a solution directly from one area and, then changing the symbols in the equations, write down the solution to a problem in another area.

The student will find that these connections—among levels, and among the various transport phenomena—reinforce the learning process. As one goes from the first part of the book (momentum transport) to the second part (energy transport) and then on to the third part (mass transport) the story will be very similar but the “names of the players” will change.

Table 0.2-1 shows the arrangement of the chapters in the form of a 3×8 “matrix.” Just a brief glance at the matrix will make it abundantly clear what kinds of interconnections can be expected in the course of the study of the book. We recommend that the book be studied by columns, particularly in undergraduate courses. For graduate students, on the other hand, studying the topics by rows may provide a chance to reinforce the connections between the three areas of transport phenomena.

At all three levels of description—molecular, microscopic, and macroscopic—the *conservation laws* play a key role. The derivation of the conservation laws for molecular systems is straightforward and instructive. With elementary physics and a minimum of mathematics we can illustrate the main concepts and review key physical quantities that will be encountered throughout this book. That is the topic of the next section.

Table 0.2-1 Organization of the Topics in This Book

Type of transport	Momentum	Energy	Mass
Transport by molecular motion	1 Viscosity and the stress (momentum flux) tensor	9 Thermal conductivity and the heat-flux vector	17 Diffusivity and the mass-flux vectors
Transport in one dimension (shell-balance methods)	2 Shell momentum balances and velocity distributions	10 Shell energy balances and temperature distributions	18 Shell mass balances and concentration distributions
Transport in arbitrary continua (use of general transport equations)	3 Equations of change and their use [isothermal]	11 Equations of change and their use [nonisothermal]	19 Equations of change and their use [mixtures]
Transport with two independent variables (special methods)	4 Momentum transport with two independent variables	12 Energy transport with two independent variables	20 Mass transport with two independent variables
Transport in turbulent flow, and eddy transport properties	5 Turbulent momentum transport; eddy viscosity	13 Turbulent energy transport; eddy thermal conductivity	21 Turbulent mass transport; eddy diffusivity
Transport across phase boundaries	6 Friction factors; use of empirical correlations	14 Heat-transfer coefficients; use of empirical correlations	22 Mass-transfer coefficients; use of empirical correlations
Transport in large systems, such as pieces of equipment or parts thereof	7 Macroscopic balances [isothermal]	15 Macroscopic balances [nonisothermal]	22 Macroscopic balances [mixtures]
Transport by other mechanisms	8 Momentum transport in polymeric liquids	16 Energy transport by radiation	24 Mass transport in multi-component systems; cross effects

§0.3 THE CONSERVATION LAWS: AN EXAMPLE

The system we consider is that of two colliding diatomic molecules. For simplicity we assume that the molecules do not interact chemically and that each molecule is homonuclear—that is, that its atomic nuclei are identical. The molecules are in a low-density gas, so that we need not consider interactions with other molecules in the neighborhood. In Fig. 0.3-1 we show the collision between the two homonuclear diatomic molecules, A and B, and in Fig. 0.3-2 we show the notation for specifying the locations of the two atoms of one molecule by means of position vectors drawn from an arbitrary origin.

Actually the description of events at the atomic and molecular level should be made by using quantum mechanics. However, except for the lightest molecules (H_2 and He) at

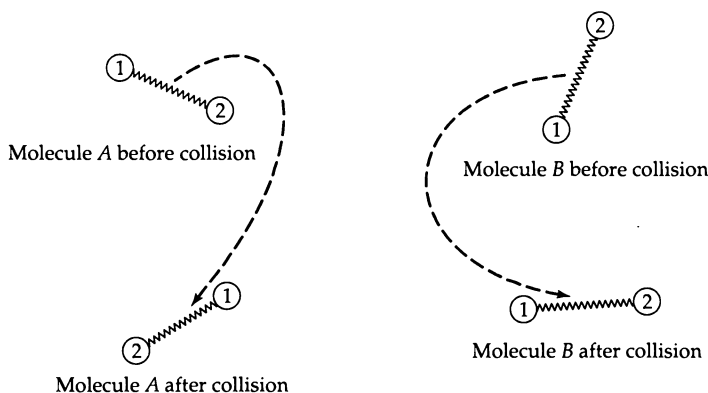


Fig. 0.3-1 A collision between homonuclear diatomic molecules, such as N_2 and O_2 . Molecule A is made up of two atoms A_1 and A_2 . Molecule B is made up of two atoms B_1 and B_2 .

temperatures lower than 50 K, the kinetic theory of gases can be developed quite satisfactorily by use of classical mechanics.

Several relations must hold between quantities before and after a collision. Both before and after the collision the molecules are presumed to be sufficiently far apart that the two molecules cannot “feel” the intermolecular force between them; beyond a distance of about 5 molecular diameters the intermolecular force is known to be negligible. Quantities after the collision are indicated with primes.

(a) According to the *law of conservation of mass*, the total mass of the molecules entering and leaving the collision must be equal:

$$m_A + m_B = m'_A + m'_B \quad (0.3-1)$$

Here m_A and m_B are the masses of molecules A and B. Since there are no chemical reactions, the masses of the individual species will also be conserved, so that

$$m_A = m'_A \quad \text{and} \quad m_B = m'_B \quad (0.3-2)$$

(b) According to the *law of conservation of momentum* the sum of the momenta of all the atoms before the collision must equal that after the collision, so that

$$m_{A1}\dot{\mathbf{r}}_{A1} + m_{A2}\dot{\mathbf{r}}_{A2} + m_{B1}\dot{\mathbf{r}}_{B1} + m_{B2}\dot{\mathbf{r}}_{B2} = m'_{A1}\dot{\mathbf{r}}'_{A1} + m'_{A2}\dot{\mathbf{r}}'_{A2} + m'_{B1}\dot{\mathbf{r}}'_{B1} + m'_{B2}\dot{\mathbf{r}}'_{B2} \quad (0.3-3)$$

in which \mathbf{r}_{A1} is the position vector for atom 1 of molecule A, and $\dot{\mathbf{r}}_{A1}$ is its velocity. We now write $\mathbf{r}_{A1} = \mathbf{r}_A + \mathbf{R}_{A1}$ so that \mathbf{r}_{A1} is written as the sum of the position vector for the

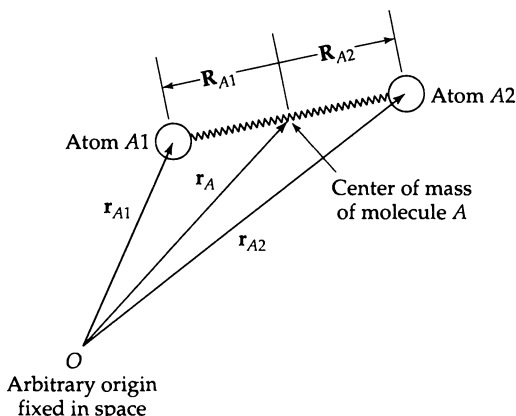


Fig. 0.3-2 Position vectors for the atoms A_1 and A_2 in molecule A.

center of mass and the position vector of the atom with respect to the center of mass, and we recognize that $\mathbf{R}_{A2} = -\mathbf{R}_{A1}$; we also write the same relations for the velocity vectors. Then we can rewrite Eq. 0.3-3 as

$$m_A \dot{\mathbf{r}}_A + m_B \dot{\mathbf{r}}_B = m_A \dot{\mathbf{r}}'_A + m_B \dot{\mathbf{r}}'_B \quad (0.3-4)$$

That is, the conservation statement can be written in terms of the molecular masses and velocities, and the corresponding atomic quantities have been eliminated. In getting Eq. 0.3-4 we have used Eq. 0.3-2 and the fact that for homonuclear diatomic molecules $m_{A1} = m_{A2} = \frac{1}{2} m_A$.

(c) According to the *law of conservation of energy*, the energy of the colliding pair of molecules must be the same before and after the collision. The energy of an isolated molecule is the sum of the kinetic energies of the two atoms and the interatomic potential energy, ϕ_A , which describes the force of the chemical bond joining the two atoms 1 and 2 of molecule A, and is a function of the interatomic distance $|\mathbf{r}_{A2} - \mathbf{r}_{A1}|$. Therefore, energy conservation leads to

$$\begin{aligned} & \left(\frac{1}{2} m_{A1} \dot{\mathbf{r}}_{A1}^2 + \frac{1}{2} m_{A2} \dot{\mathbf{r}}_{A2}^2 + \phi_A \right) + \left(\frac{1}{2} m_{B1} \dot{\mathbf{r}}_{B1}^2 + \frac{1}{2} m_{B2} \dot{\mathbf{r}}_{B2}^2 + \phi_B \right) = \\ & \left(\frac{1}{2} m'_{A1} \dot{\mathbf{r}}'_{A1}^2 + \frac{1}{2} m'_{A2} \dot{\mathbf{r}}'_{A2}^2 + \phi'_A \right) + \left(\frac{1}{2} m'_{B1} \dot{\mathbf{r}}'_{B1}^2 + \frac{1}{2} m'_{B2} \dot{\mathbf{r}}'_{B2}^2 + \phi'_B \right) \end{aligned} \quad (0.3-5)$$

Note that we use the standard abbreviated notation that $\dot{\mathbf{r}}_{A1}^2 = (\dot{\mathbf{r}}_{A1} \cdot \dot{\mathbf{r}}_{A1})$. We now write the velocity of atom 1 of molecule A as the sum of the velocity of the center of mass of A and the velocity of 1 with respect to the center of mass; that is, $\dot{\mathbf{r}}_{A1} = \dot{\mathbf{r}}_A + \dot{\mathbf{R}}_{A1}$. Then Eq. 0.3-5 becomes

$$\left(\frac{1}{2} m_A \dot{\mathbf{r}}_A^2 + u_A \right) + \left(\frac{1}{2} m_B \dot{\mathbf{r}}_B^2 + u_B \right) = \left(\frac{1}{2} m'_{A1} \dot{\mathbf{r}}'_{A1}^2 + u'_A \right) + \left(\frac{1}{2} m'_{B1} \dot{\mathbf{r}}'_{B1}^2 + u'_B \right) \quad (0.3-6)$$

in which $u_A = \frac{1}{2} m_{A1} \dot{\mathbf{R}}_{A1}^2 + \frac{1}{2} m_{A2} \dot{\mathbf{R}}_{A2}^2 + \phi_A$ is the sum of the kinetic energies of the atoms, referred to the center of mass of molecule A, and the interatomic potential of molecule A. That is, we split up the energy of each molecule into its kinetic energy with respect to fixed coordinates, and the internal energy of the molecule (which includes its vibrational, rotational, and potential energies). Equation 0.3-6 makes it clear that the kinetic energies of the colliding molecules can be converted into internal energy or vice versa. This idea of an interchange between kinetic and internal energy will arise again when we discuss the energy relations at the microscopic and macroscopic levels.

(d) Finally, the *law of conservation of angular momentum* can be applied to a collision to give

$$\begin{aligned} & ([\mathbf{r}_{A1} \times m_{A1} \dot{\mathbf{r}}_{A1}] + [\mathbf{r}_{A2} \times m_{A2} \dot{\mathbf{r}}_{A2}]) + ([\mathbf{r}_{B1} \times m_{B1} \dot{\mathbf{r}}_{B1}] + [\mathbf{r}_{B2} \times m_{B2} \dot{\mathbf{r}}_{B2}]) = \\ & ([\mathbf{r}'_{A1} \times m'_{A1} \dot{\mathbf{r}}'_{A1}] + [\mathbf{r}'_{A2} \times m'_{A2} \dot{\mathbf{r}}'_{A2}]) + ([\mathbf{r}'_{B1} \times m'_{B1} \dot{\mathbf{r}}'_{B1}] + [\mathbf{r}'_{B2} \times m'_{B2} \dot{\mathbf{r}}'_{B2}]) \end{aligned} \quad (0.3-7)$$

in which \times is used to indicate the cross product of two vectors. Next we introduce the center-of-mass and relative position vectors and velocity vectors as before and obtain

$$\begin{aligned} & ([\mathbf{r}_A \times m_A \dot{\mathbf{r}}_A] + \mathbf{l}_A) + ([\mathbf{r}_B \times m_B \dot{\mathbf{r}}_B] + \mathbf{l}_B) = \\ & ([\mathbf{r}'_A \times m_A \dot{\mathbf{r}}'_A] + \mathbf{l}'_A) + ([\mathbf{r}'_B \times m_B \dot{\mathbf{r}}'_B] + \mathbf{l}'_B) \end{aligned} \quad (0.3-8)$$

in which $\mathbf{l}_A = [\mathbf{R}_{A1} \times m_{A1} \dot{\mathbf{R}}_{A1}] + [\mathbf{R}_{A2} \times m_{A2} \dot{\mathbf{R}}_{A2}]$ is the sum of the angular momenta of the atoms referred to an origin of coordinates at the center of mass of the molecule—that is, the “internal angular momentum.” The important point is that there is the possibility for interchange between the angular momentum of the molecules (with respect to the origin of coordinates) and their internal angular momentum (with respect to the center of mass of the molecule). This will be referred to later in connection with the equation of change for angular momentum.

The conservation laws as applied to collisions of monatomic molecules can be obtained from the results above as follows: Eqs. 0.3-1, 0.3-2, and 0.3-4 are directly applicable; Eq. 0.3-6 is applicable if the internal energy contributions are omitted; and Eq. 0.3-8 may be used if the internal angular momentum terms are discarded.

Much of this book will be concerned with setting up the conservation laws at the microscopic and macroscopic levels and applying them to problems of interest in engineering and science. The above discussion should provide a good background for this adventure. For a glimpse of the conservation laws for species mass, momentum, and energy at the microscopic and macroscopic levels, see Tables 19.2-1 and 23.5-1.

§0.4 CONCLUDING COMMENTS

To use the macroscopic balances intelligently, it is necessary to use information about interphase transport that comes from the equations of change. To use the equations of change, we need the transport properties, which are described by various molecular theories. Therefore, from a teaching point of view, it seems best to start at the molecular level and work upward toward the larger systems.

All the discussions of theory are accompanied by examples to illustrate how the theory is applied to problem solving. Then at the end of each chapter there are problems to provide extra experience in using the ideas given in the chapter. The problems are grouped into four classes:

- Class A: Numerical problems, which are designed to highlight important equations in the text and to give a feeling for the orders of magnitude.
- Class B: Analytical problems that require doing elementary derivations using ideas mainly from the chapter.
- Class C: More advanced analytical problems that may bring ideas from other chapters or from other books.
- Class D: Problems in which intermediate mathematical skills are required.

Many of the problems and illustrative examples are rather elementary in that they involve oversimplified systems or very idealized models. It is, however, necessary to start with these elementary problems in order to understand how the theory works and to develop confidence in using it. In addition, some of these elementary examples can be very useful in making order-of-magnitude estimates in complex problems.

Here are a few suggestions for studying the subject of transport phenomena:

- Always read the text with pencil and paper in hand; work through the details of the mathematical developments and supply any missing steps.
- Whenever necessary, go back to the mathematics textbooks to brush up on calculus, differential equations, vectors, etc. This is an excellent time to review the mathematics that was learned earlier (but possibly not as carefully as it should have been).
- Make it a point to give a physical interpretation of key results; that is, get in the habit of relating the physical ideas to the equations.
- Always ask whether the results seem reasonable. If the results do not agree with intuition, it is important to find out which is incorrect.
- Make it a habit to check the dimensions of all results. This is one very good way of locating errors in derivations.

We hope that the reader will share our enthusiasm for the subject of transport phenomena. It will take some effort to learn the material, but the rewards will be worth the time and energy required.

QUESTIONS FOR DISCUSSION

1. What are the definitions of momentum, angular momentum, and kinetic energy for a single particle? What are the dimensions of these quantities?
2. What are the dimensions of velocity, angular velocity, pressure, density, force, work, and torque? What are some common units used for these quantities?
3. Verify that it is possible to go from Eq. 0.3-3 to Eq. 0.3-4.
4. Go through all the details needed to get Eq. 0.3-6 from Eq. 0.3-5.
5. Suppose that the origin of coordinates is shifted to a new position. What effect would that have on Eq. 0.3-7? Is the equation changed?
6. Compare and contrast angular velocity and angular momentum.
7. What is meant by internal energy? Potential energy?
8. Is the law of conservation of mass always valid? What are the limitations?

Part One

Momentum Transport

Viscosity and the Mechanisms of Momentum Transport

- §1.1 **Newton's law of viscosity (molecular momentum transport)**
- §1.2 **Generalization of Newton's law of viscosity**
- §1.3 **Pressure and temperature dependence of viscosity**
- §1.4^o **Molecular theory of the viscosity of gases at low density**
- §1.5^o **Molecular theory of the viscosity of liquids**
- §1.6^o **Viscosity of suspensions and emulsions**
- §1.7 **Convective momentum transport**

The first part of this book deals with the flow of viscous fluids. For fluids of low molecular weight, the physical property that characterizes the resistance to flow is the *viscosity*. Anyone who has bought motor oil is aware of the fact that some oils are more "viscous" than others and that viscosity is a function of the temperature.

We begin in §1.1 with the simple shear flow between parallel plates and discuss how momentum is transferred through the fluid by viscous action. This is an elementary example of *molecular momentum transport* and it serves to introduce "Newton's law of viscosity" along with the definition of viscosity μ . Next in §1.2 we show how Newton's law can be generalized for arbitrary flow patterns. The effects of temperature and pressure on the viscosities of gases and liquids are summarized in §1.3 by means of a dimensionless plot. Then §1.4 tells how the viscosities of gases can be calculated from the kinetic theory of gases, and in §1.5 a similar discussion is given for liquids. In §1.6 we make a few comments about the viscosity of suspensions and emulsions.

Finally, we show in §1.7 that momentum can also be transferred by the bulk fluid motion and that such *convective momentum transport* is proportional to the fluid density ρ .

§1.1 NEWTON'S LAW OF VISCOSITY (MOLECULAR TRANSPORT OF MOMENTUM)

In Fig. 1.1-1 we show a pair of large parallel plates, each one with area A , separated by a distance Y . In the space between them is a fluid—either a gas or a liquid. This system is initially at rest, but at time $t = 0$ the lower plate is set in motion in the positive x direction at a constant velocity V . As time proceeds, the fluid gains momentum, and ultimately the linear steady-state velocity profile shown in the figure is established. We require that the flow be laminar ("laminar" flow is the orderly type of flow that one usually observes when syrup is poured, in contrast to "turbulent" flow, which is the irregular, chaotic flow one sees in a high-speed mixer). When the final state of steady motion

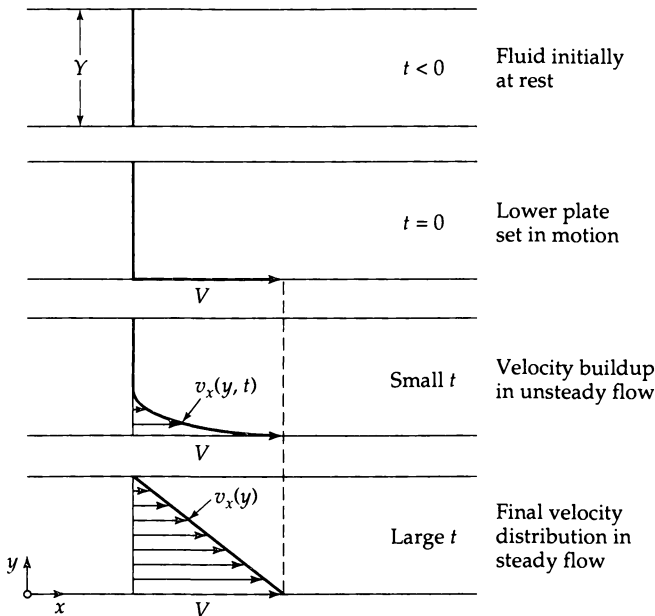


Fig. 1.1-1 The buildup to the steady, laminar velocity profile for a fluid contained between two plates. The flow is called “laminar” because the adjacent layers of fluid (“laminae”) slide past one another in an orderly fashion.

has been attained, a constant force F is required to maintain the motion of the lower plate. Common sense suggests that this force may be expressed as follows:

$$\frac{F}{A} = \mu \frac{V}{Y} \quad (1.1-1)$$

That is, the force should be proportional to the area and to the velocity, and inversely proportional to the distance between the plates. The constant of proportionality μ is a property of the fluid, defined to be the *viscosity*.

We now switch to the notation that will be used throughout the book. First we replace F/A by the symbol τ_{yx} , which is the force in the x direction on a unit area perpendicular to the y direction. It is understood that this is the force exerted by the fluid of lesser y on the fluid of greater y . Furthermore, we replace V/Y by $-dv_x/dy$. Then, in terms of these symbols, Eq. 1.1-1 becomes

$$\tau_{yx} = -\mu \frac{dv_x}{dy} \quad (1.1-2)^1$$

This equation, which states that the shearing force per unit area is proportional to the negative of the velocity gradient, is often called *Newton's law of viscosity*.² Actually we

¹ Some authors write Eq. 1.1-2 in the form

$$g_c \tau_{yx} = -\mu \frac{dv_x}{dy} \quad (1.1-2a)$$

in which τ_{yx} [=] lb_f/ft², v_x [=] ft/s, y [=] ft, and μ [=] lb_m/ft · s; the quantity g_c is the “gravitational conversion factor” with the value of 32.174 poundals/lb_f. In this book we will always use Eq. 1.1-2 rather than Eq. 1.1-2a.

² Sir Isaac Newton (1643–1727), a professor at Cambridge University and later Master of the Mint, was the founder of classical mechanics and contributed to other fields of physics as well. Actually Eq. 1.1-2 does not appear in Sir Isaac Newton's *Philosophiae Naturalis Principia Mathematica*, but the germ of the idea is there. For illuminating comments, see D. J. Acheson, *Elementary Fluid Dynamics*, Oxford University Press, 1990, §6.1.

should not refer to Eq. 1.1-2 as a "law," since Newton suggested it as an empiricism³—the simplest proposal that could be made for relating the stress and the velocity gradient. However, it has been found that the resistance to flow of all gases and all liquids with molecular weight of less than about 5000 is described by Eq. 1.1-2, and such fluids are referred to as *Newtonian fluids*. Polymeric liquids, suspensions, pastes, slurries, and other complex fluids are not described by Eq. 1.1-2 and are referred to as *non-Newtonian fluids*. Polymeric liquids are discussed in Chapter 8.

Equation 1.1-2 may be interpreted in another fashion. In the neighborhood of the moving solid surface at $y = 0$ the fluid acquires a certain amount of x -momentum. This fluid, in turn, imparts momentum to the adjacent layer of liquid, causing it to remain in motion in the x direction. Hence x -momentum is being transmitted through the fluid in the positive y direction. Therefore τ_{yx} may also be interpreted as the *flux of x-momentum in the positive y direction*, where the term "flux" means "flow per unit area." This interpretation is consistent with the molecular picture of momentum transport and the kinetic theories of gases and liquids. It also is in harmony with the analogous treatment given later for heat and mass transport.

The idea in the preceding paragraph may be paraphrased by saying that momentum goes "downhill" from a region of high velocity to a region of low velocity—just as a sled goes downhill from a region of high elevation to a region of low elevation, or the way heat flows from a region of high temperature to a region of low temperature. The velocity gradient can therefore be thought of as a "driving force" for momentum transport.

In what follows we shall sometimes refer to Newton's law in Eq. 1.1-2 in terms of forces (which emphasizes the mechanical nature of the subject) and sometimes in terms of momentum transport (which emphasizes the analogies with heat and mass transport). This dual viewpoint should prove helpful in physical interpretations.

Often fluid dynamicists use the symbol ν to represent the viscosity divided by the density (mass per unit volume) of the fluid, thus:

$$\nu = \mu / \rho \quad (1.1-3)$$

This quantity is called the *kinematic viscosity*.

Next we make a few comments about the units of the quantities we have defined. If we use the symbol [=] to mean "has units of," then in the SI system τ_{yx} [=] N/m² = Pa, v_x [=] m/s, and y [=] m, so that

$$\mu = -\tau_{yx} \left(\frac{dv_x}{dy} \right)^{-1} [=] (\text{Pa})[(\text{m/s})(\text{m}^{-1})]^{-1} = \text{Pa} \cdot \text{s} \quad (1.1-4)$$

since the units on both sides of Eq. 1.1-2 must agree. We summarize the above and also give the units for the c.g.s. system and the British system in Table 1.1-1. The conversion tables in Appendix F will prove to be very useful for solving numerical problems involving diverse systems of units.

The viscosities of fluids vary over many orders of magnitude, with the viscosity of air at 20°C being 1.8×10^{-5} Pa · s and that of glycerol being about 1 Pa · s, with some silicone oils being even more viscous. In Tables 1.1-2, 1.1-3, and 1.1-4 experimental data⁴ are

³ A relation of the form of Eq. 1.1-2 does come out of the simple kinetic theory of gases (Eq. 1.4-7). However, a rigorous theory for gases sketched in Appendix D makes it clear that Eq. 1.1-2 arises as the first term in an expansion, and that additional (higher-order) terms are to be expected. Also, even an elementary kinetic theory of liquids predicts non-Newtonian behavior (Eq. 1.5-6).

⁴ A comprehensive presentation of experimental techniques for measuring transport properties can be found in W. A. Wakeham, A. Nagashima, and J. V. Sengers, *Measurement of the Transport Properties of Fluids*, CRC Press, Boca Raton, Fla. (1991). Sources for experimental data are: Landolt-Börnstein, *Zahlenwerte und Funktionen*, Vol. II, 5, Springer (1968–1969); *International Critical Tables*, McGraw-Hill, New York (1926); Y. S. Touloukian, P. E. Liley, and S. C. Saxena, *Thermophysical Properties of Matter*, Plenum Press, New York (1970); and also numerous handbooks of chemistry, physics, fluid dynamics, and heat transfer.

Table 1.1-1 Summary of Units for Quantities Related to Eq. 1.1-2

	SI	c.g.s.	British
τ_{yx}	Pa	dyn/cm ²	poundals/ft ²
v_x	m/s	cm/s	ft/s
y	m	cm	ft
μ	Pa · s	gm/cm · s = poise	lb _m /ft · s
ν	m ² /s	cm ² /s	ft ² /s

Note: The pascal, Pa, is the same as N/m², and the newton, N, is the same as kg · m/s². The abbreviation for "centipoise" is "cp."

Table 1.1-2 Viscosity of Water and Air at 1 atm Pressure

Temperature T (°C)	Water (liq.) ^a		Air ^b	
	Viscosity μ (mPa · s)	Kinematic viscosity ν (cm ² /s)	Viscosity μ (mPa · s)	Kinematic viscosity ν (cm ² /s)
0	1.787	1.787	0.01716	13.27
20	1.0019	1.0037	0.01813	15.05
40	0.6530	0.6581	0.01908	16.92
60	0.4665	0.4744	0.01999	18.86
80	0.3548	0.3651	0.02087	20.88
100	0.2821	0.2944	0.02173	22.98

^a Calculated from the results of R. C. Hardy and R. L. Cottington, *J. Research Natl. Bur. Standards*, **42**, 573–578 (1949); and J. F. Swidells, J. R. Coe, Jr., and T. B. Godfrey, *J. Research Natl. Bur. Standards*, **48**, 1–31 (1952).

^b Calculated from "Tables of Thermal Properties of Gases," *National Bureau of Standards Circular 464* (1955), Chapter 2.

Table 1.1-3 Viscosities of Some Gases and Liquids at Atmospheric Pressure^a

Gases	Temperature T (°C)	Viscosity μ (mPa · s)	Liquids	Temperature T (°C)	Viscosity μ (mPa · s)
i-C ₄ H ₁₀	23	0.0076 ^c	(C ₂ H ₅) ₂ O	0	0.283
SF ₆	23	0.0153		25	0.224
CH ₄	20	0.0109 ^b	C ₆ H ₆	20	0.649
H ₂ O	100	0.01211 ^d	Br ₂	25	0.744
CO ₂	20	0.0146 ^b	Hg	20	1.552
N ₂	20	0.0175 ^b	C ₂ H ₅ OH	0	1.786
O ₂	20	0.0204		25	1.074
Hg	380	0.0654 ^d		50	0.694
			H ₂ SO ₄	25	25.54
			Glycerol	25	934.

^a Values taken from N. A. Lange, *Handbook of Chemistry*, McGraw-Hill, New York, 15th edition (1999), Tables 5.16 and 5.18.

^b H. L. Johnston and K. E. McKloskey, *J. Phys. Chem.*, **44**, 1038–1058 (1940).

^c CRC Handbook of Chemistry and Physics, CRC Press, Boca Raton, Fla. (1999).

^d Landolt-Börnstein Zahlenwerte und Funktionen, Springer (1969).

Table 1.1-4 Viscosities of Some Liquid Metals

Metal	Temperature T (°C)	Viscosity μ (mPa · s)
Li	183.4	0.5918
	216.0	0.5406
	285.5	0.4548
Na	103.7	0.686
	250	0.381
	700	0.182
K	69.6	0.515
	250	0.258
	700	0.136
Hg	-20	1.85
	20	1.55
	100	1.21
	200	1.01
Pb	441	2.116
	551	1.700
	844	1.185

Data taken from *The Reactor Handbook*, Vol. 2, Atomic Energy Commission AECD-3646, U.S. Government Printing Office, Washington, D.C. (May 1955), pp. 258 *et seq.*

given for pure fluids at 1 atm pressure. Note that for gases at low density, the viscosity *increases* with increasing temperature, whereas for liquids the viscosity usually *decreases* with increasing temperature. In gases the momentum is transported by the molecules in free flight between collisions, but in liquids the transport takes place predominantly by virtue of the intermolecular forces that pairs of molecules experience as they wind their way around among their neighbors. In §§1.4 and 1.5 we give some elementary kinetic theory arguments to explain the temperature dependence of viscosity.

EXAMPLE 1.1-1

Calculation of Momentum Flux

Compute the steady-state momentum flux τ_{yx} in lb_f/ft² when the lower plate velocity V in Fig. 1.1-1 is 1 ft/s in the positive x direction, the plate separation Y is 0.001 ft, and the fluid viscosity μ is 0.7 cp.

SOLUTION

Since τ_{yx} is desired in British units, we should convert the viscosity into that system of units. Thus, making use of Appendix F, we find $\mu = (0.7 \text{ cp})(2.0886 \times 10^{-5}) = 1.46 \times 10^{-5} \text{ lb}_f \cdot \text{s}/\text{ft}^2$. The velocity profile is linear so that

$$\frac{dv_x}{dy} = \frac{\Delta v_x}{\Delta y} = \frac{-1.0 \text{ ft/s}}{0.001 \text{ ft}} = -1000 \text{ s}^{-1} \quad (1.1-5)$$

Substitution into Eq. 1.1-2 gives

$$\tau_{yx} = -\mu \frac{dv_x}{dy} = -(1.46 \times 10^{-5})(-1000) = 1.46 \times 10^{-2} \text{ lb}_f/\text{ft}^2 \quad (1.1-6)$$

§1.2 GENERALIZATION OF NEWTON'S LAW OF VISCOSITY

In the previous section the viscosity was defined by Eq. 1.1-2, in terms of a simple steady-state shearing flow in which v_x is a function of y alone, and v_y and v_z are zero. Usually we are interested in more complicated flows in which the three velocity components may depend on all three coordinates and possibly on time. Therefore we must have an expression more general than Eq. 1.1-2, but it must simplify to Eq. 1.1-2 for steady-state shearing flow.

This generalization is not simple; in fact, it took mathematicians about a century and a half to do this. It is not appropriate for us to give all the details of this development here, since they can be found in many fluid dynamics books.¹ Instead we explain briefly the main ideas that led to the discovery of the required generalization of Newton's law of viscosity.

To do this we consider a very general flow pattern, in which the fluid velocity may be in various directions at various places and may depend on the time t . The velocity components are then given by

$$v_x = v_x(x, y, z, t); \quad v_y = v_y(x, y, z, t); \quad v_z = v_z(x, y, z, t) \quad (1.2-1)$$

In such a situation, there will be nine stress components τ_{ij} (where i and j may take on the designations x , y , and z), instead of the component τ_{yx} that appears in Eq. 1.1-2. We therefore must begin by defining these stress components.

In Fig. 1.2-1 is shown a small cube-shaped volume element within the flow field, each face having unit area. The center of the volume element is at the position x, y, z . At

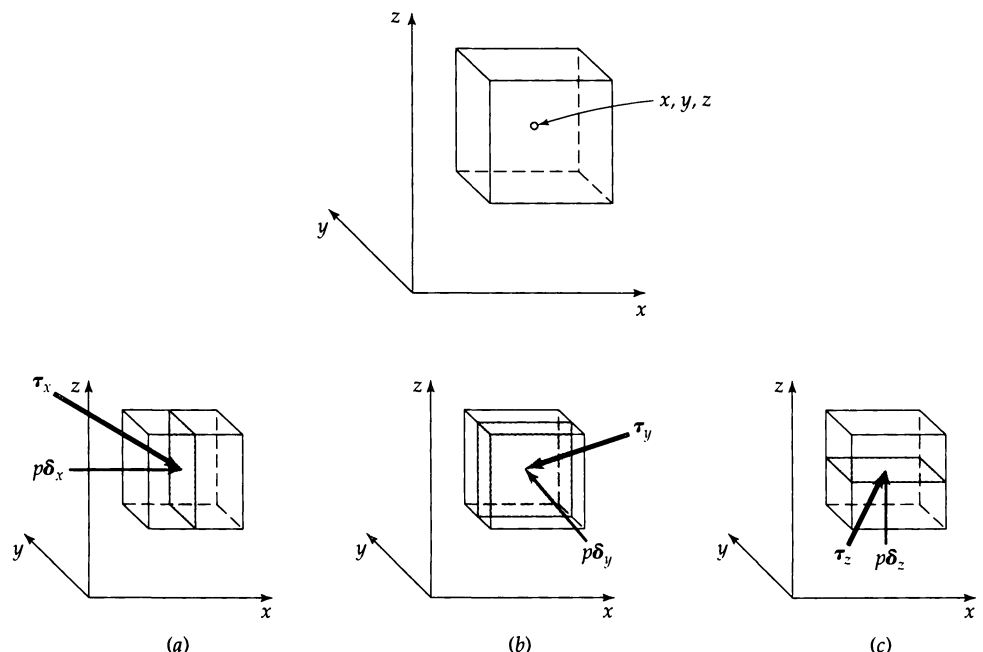


Fig. 1.2-1 Pressure and viscous forces acting on planes in the fluid perpendicular to the three coordinate systems. The shaded planes have unit area.

¹ W. Prager, *Introduction to Mechanics of Continua*, Ginn, Boston (1961), pp. 89–91; R. Aris, *Vectors, Tensors, and the Basic Equations of Fluid Mechanics*, Prentice-Hall, Englewood Cliffs, N.J. (1962), pp. 30–34, 99–112; L. Landau and E. M. Lifshitz, *Fluid Mechanics*, Pergamon, London, 2nd edition (1987), pp. 44–45. Lev Davyдович Ландау (1908–1968) received the Nobel prize in 1962 for his work on liquid helium and superfluid dynamics.

any instant of time we can slice the volume element in such a way as to remove half the fluid within it. As shown in the figure, we can cut the volume perpendicular to each of the three coordinate directions in turn. We can then ask what force has to be applied on the free (shaded) surface in order to replace the force that had been exerted on that surface by the fluid that was removed. There will be two contributions to the force: that associated with the pressure, and that associated with the viscous forces.

The pressure force will always be perpendicular to the exposed surface. Hence in (a) the force per unit area on the shaded surface will be a vector $p\delta_x$ —that is, the pressure (a scalar) multiplied by the unit vector δ_x in the x direction. Similarly, the force on the shaded surface in (b) will be $p\delta_y$, and in (c) the force will be $p\delta_z$. The pressure forces will be exerted when the fluid is stationary as well as when it is in motion.

The viscous forces come into play only when there are velocity gradients within the fluid. In general they are neither perpendicular to the surface element nor parallel to it, but rather at some angle to the surface (see Fig. 1.2-1). In (a) we see a force per unit area τ_x exerted on the shaded area, and in (b) and (c) we see forces per unit area τ_y and τ_z . Each of these forces (which are vectors) has components (scalars); for example, τ_x has components τ_{xx} , τ_{xy} , and τ_{xz} . Hence we can now summarize the forces acting on the three shaded areas in Fig. 1.2-1 in Table 1.2-1. This tabulation is a summary of the forces per unit area (*stresses*) exerted within a fluid, both by the thermodynamic pressure and the *viscous stresses*. Sometimes we will find it convenient to have a symbol that includes both types of stresses, and so we define the *molecular stresses* as follows:

$$\pi_{ij} = p\delta_{ij} + \tau_{ij} \quad \text{where } i \text{ and } j \text{ may be } x, y, \text{ or } z \quad (1.2-2)$$

Here δ_{ij} is the *Kronecker delta*, which is 1 if $i = j$ and zero if $i \neq j$.

Just as in the previous section, the τ_{ij} (and also the π_{ij}) may be interpreted in two ways:

$\pi_{ij} = p\delta_{ij} + \tau_{ij}$ = force in the j direction on a unit area perpendicular to the i direction,
where it is understood that the fluid in the region of lesser x_i is exerting
the force on the fluid of greater x_i ,

$\pi_{ij} = p\delta_{ij} + \tau_{ij}$ = flux of j -momentum in the positive i direction—that is, from the region
of lesser x_i to that of greater x_i

Both interpretations are used in this book; the first one is particularly useful in describing the forces exerted by the fluid on solid surfaces. The stresses $\pi_{xx} = p + \tau_{xx}$, $\pi_{yy} = p + \tau_{yy}$, $\pi_{zz} = p + \tau_{zz}$ are called *normal stresses*, whereas the remaining quantities, $\pi_{xy} = \tau_{xy}$, $\pi_{yz} = \tau_{yz}$, \dots are called *shear stresses*. These quantities, which have two subscripts associated with the coordinate directions, are referred to as “tensors,” just as quantities (such as velocity) that have one subscript associated with the coordinate directions are called

Table 1.2-1 Summary of the Components of the Molecular Stress Tensor (or Molecular Momentum-Flux Tensor)^a

Direction normal to the shaded face	Vector force per unit area on the shaded face (momentum flux through shaded face)	Components of the forces (per unit area) acting on the shaded face (components of the momentum flux through the shaded face)		
		<i>x</i> -component	<i>y</i> -component	<i>z</i> -component
<i>x</i>	$\pi_x = p\delta_x + \tau_x$	$\pi_{xx} = p + \tau_{xx}$	$\pi_{xy} = \tau_{xy}$	$\pi_{xz} = \tau_{xz}$
<i>y</i>	$\pi_y = p\delta_y + \tau_y$	$\pi_{yx} = \tau_{yx}$	$\pi_{yy} = p + \tau_{yy}$	$\pi_{yz} = \tau_{yz}$
<i>z</i>	$\pi_z = p\delta_z + \tau_z$	$\pi_{zx} = \tau_{zx}$	$\pi_{zy} = \tau_{zy}$	$\pi_{zz} = p + \tau_{zz}$

^a These are referred to as components of the “molecular momentum flux tensor” because they are associated with the molecular motions, as discussed in §1.4 and Appendix D. The additional “convective momentum flux tensor” components, associated with bulk movement of the fluid, are discussed in §1.7.

“vectors.” Therefore we will refer to τ as the *viscous stress tensor* (with components τ_{ij}) and π as the *molecular stress tensor* (with components π_{ij}). When there is no chance for confusion, the modifiers “viscous” and “molecular” may be omitted. A discussion of vectors and tensors can be found in Appendix A.

The question now is: How are these stresses τ_{ij} related to the velocity gradients in the fluid? In generalizing Eq. 1.1-2, we put several restrictions on the stresses, as follows:

- The viscous stresses may be linear combinations of all the velocity gradients:

$$\tau_{ij} = -\sum_k \sum_l \mu_{ijkl} \frac{\partial v_k}{\partial x_l} \quad \text{where } i, j, k, \text{ and } l \text{ may be } 1, 2, 3 \quad (1.2-3)$$

Here the 81 quantities μ_{ijkl} are “viscosity coefficients.” The quantities x_1, x_2, x_3 in the derivatives denote the Cartesian coordinates x, y, z , and v_1, v_2, v_3 are the same as v_x, v_y, v_z .

- We assert that time derivatives or time integrals should not appear in the expression. (For viscoelastic fluids, as discussed in Chapter 8, time derivatives or time integrals are needed to describe the elastic responses.)
- We do not expect any viscous forces to be present, if the fluid is in a state of pure rotation. This requirement leads to the necessity that τ_{ij} be a symmetric combination of the velocity gradients. By this we mean that if i and j are interchanged, the combination of velocity gradients remains unchanged. It can be shown that the only symmetric linear combinations of velocity gradients are

$$\left(\frac{\partial v_j}{\partial x_i} + \frac{\partial v_i}{\partial x_j} \right) \quad \text{and} \quad \left(\frac{\partial v_x}{\partial x} + \frac{\partial v_y}{\partial y} + \frac{\partial v_z}{\partial z} \right) \delta_{ij} \quad (1.2-4)$$

- If the fluid is isotropic—that is, it has no preferred direction—then the coefficients in front of the two expressions in Eq. 1.2-4 must be scalars so that

$$\tau_{ij} = A \left(\frac{\partial v_j}{\partial x_i} + \frac{\partial v_i}{\partial x_j} \right) + B \left(\frac{\partial v_x}{\partial x} + \frac{\partial v_y}{\partial y} + \frac{\partial v_z}{\partial z} \right) \delta_{ij} \quad (1.2-5)$$

We have thus reduced the number of “viscosity coefficients” from 81 to 2!

- Of course, we want Eq. 1.2-5 to simplify to Eq. 1.1-2 for the flow situation in Fig. 1.1-1. For that elementary flow Eq. 1.2-5 simplifies to $\tau_{yx} = A dv_x/dy$, and hence the scalar constant A must be the same as the negative of the *viscosity* μ .
- Finally, by common agreement among most fluid dynamicists the scalar constant B is set equal to $\frac{2}{3}\mu - \kappa$, where κ is called the *dilatational viscosity*. The reason for writing B in this way is that it is known from kinetic theory that κ is identically zero for monatomic gases at low density.

Thus the required generalization for Newton’s law of viscosity in Eq. 1.1-2 is then the set of nine relations (six being independent):

$$\tau_{ij} = -\mu \left(\frac{\partial v_j}{\partial x_i} + \frac{\partial v_i}{\partial x_j} \right) + (\frac{2}{3}\mu - \kappa) \left(\frac{\partial v_x}{\partial x} + \frac{\partial v_y}{\partial y} + \frac{\partial v_z}{\partial z} \right) \delta_{ij} \quad (1.2-6)$$

Here $\tau_{ij} = \tau_{ji}$, and i and j can take on the values 1, 2, 3. These relations for the stresses in a Newtonian fluid are associated with the names of Navier, Poisson, and Stokes.² If de-

² C.-L.-M.-H. Navier, *Ann. Chimie*, **19**, 244–260 (1821); S.-D. Poisson, *J. École Polytech.*, **13**, Cahier 20, 1–174 (1831); G. G. Stokes, *Trans. Camb. Phil. Soc.*, **8**, 287–305 (1845). Claude-Louis-Marie-Henri Navier (1785–1836) (pronounced “Nah-vyay,” with the second syllable accented) was a civil engineer whose specialty was road and bridge building; George Gabriel Stokes (1819–1903) taught at Cambridge University and was president of the Royal Society. Navier and Stokes are well known because of the Navier–Stokes equations (see Chapter 3). See also D. J. Acheson, *Elementary Fluid Mechanics*, Oxford University Press (1990), pp. 209–212, 218.

sired, this set of relations can be written more concisely in the vector-tensor notation of Appendix A as

$$\tau = -\mu(\nabla \mathbf{v} + (\nabla \mathbf{v})^\dagger) + (\frac{2}{3}\mu - \kappa)(\nabla \cdot \mathbf{v})\delta \quad (1.2-7)$$

in which δ is the *unit tensor* with components δ_{ij} , $\nabla \mathbf{v}$ is the *velocity gradient tensor* with components $(\partial/\partial x_i)v_j$, $(\nabla \mathbf{v})^\dagger$ is the "transpose" of the velocity gradient tensor with components $(\partial/\partial x_j)v_i$, and $(\nabla \cdot \mathbf{v})$ is the *divergence* of the velocity vector.

The important conclusion is that we have a generalization of Eq. 1.1-2, and this generalization involves not one but two coefficients³ characterizing the fluid: the viscosity μ and the dilatational viscosity κ . Usually, in solving fluid dynamics problems, it is not necessary to know κ . If the fluid is a gas, we often assume it to act as an ideal monoatomic gas, for which κ is identically zero. If the fluid is a liquid, we often assume that it is incompressible, and in Chapter 3 we show that for incompressible liquids $(\nabla \cdot \mathbf{v}) = 0$, and therefore the term containing κ is discarded anyway. The dilatational viscosity is important in describing sound absorption in polyatomic gases⁴ and in describing the fluid dynamics of liquids containing gas bubbles.⁵

Equation 1.2-7 (or 1.2-6) is an important equation and one that we shall use often. Therefore it is written out in full in Cartesian (x, y, z), cylindrical (r, θ, z), and spherical (r, θ, ϕ) coordinates in Table B.1. The entries in this table for curvilinear coordinates are obtained by the methods outlined in §§A.6 and A.7. It is suggested that beginning students not concern themselves with the details of such derivations, but rather concentrate on using the tabulated results. Chapters 2 and 3 will give ample practice in doing this.

In curvilinear coordinates the stress components have the same meaning as in Cartesian coordinates. For example, τ_{rz} in cylindrical coordinates, which will be encountered in Chapter 2, can be interpreted as: (i) the viscous force in the z direction on a unit area perpendicular to the r direction, or (ii) the viscous flux of z -momentum in the positive r direction. Figure 1.2-2 illustrates some typical surface elements and stress-tensor components that arise in fluid dynamics.

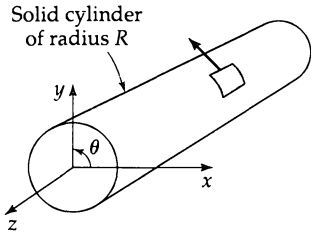
The shear stresses are usually easy to visualize, but the normal stresses may cause conceptual problems. For example, τ_{zz} is a force per unit area in the z direction on a plane perpendicular to the z direction. For the flow of an incompressible fluid in the convergent channel of Fig. 1.2-3, we know intuitively that v_z increases with decreasing z ; hence, according to Eq. 1.2-6, there is a nonzero stress $\tau_{zz} = -2\mu(\partial v_z / \partial z)$ acting in the fluid.

Note on the Sign Convention for the Stress Tensor We have emphasized in connection with Eq. 1.1-2 (and in the generalization in this section) that τ_{yx} is the force in the positive x direction on a plane perpendicular to the y direction, and that this is the force exerted by the fluid in the region of the *lesser* y on the fluid of *greater* y . In most fluid dynamics and elasticity books, the words "lesser" and "greater" are interchanged and Eq. 1.1-2 is written as $\tau_{yx} = +\mu(dv_x/dy)$. The advantages of the sign convention used in this book are: (a) the sign convention used in Newton's law of viscosity is consistent with that used in Fourier's law of heat conduction and Fick's law of diffusion; (b) the sign convention for τ_{ij} is the same as that for the convective momentum flux $\rho \mathbf{v} \mathbf{v}$ (see

³ Some writers refer to μ as the "shear viscosity," but this is inappropriate nomenclature inasmuch as μ can arise in nonshearing flows as well as shearing flows. The term "dynamic viscosity" is also occasionally seen, but this term has a very specific meaning in the field of viscoelasticity and is an inappropriate term for μ .

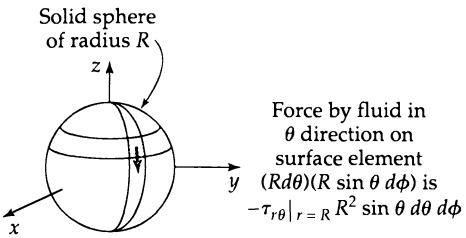
⁴ L. Landau and E. M. Lifshitz, *op. cit.*, Ch. VIII.

⁵ G. K. Batchelor, *An Introduction to Fluid Dynamics*, Cambridge University Press (1967), pp. 253–255.



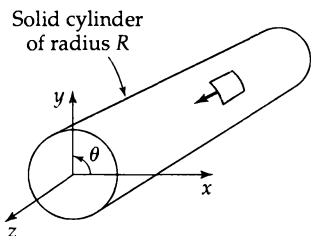
Solid cylinder
of radius R

Force by fluid in
 $+\theta$ direction on
surface element
($Rd\theta)(dz)$ is
 $-\tau_{r\theta}|_{r=R} R d\theta dz$



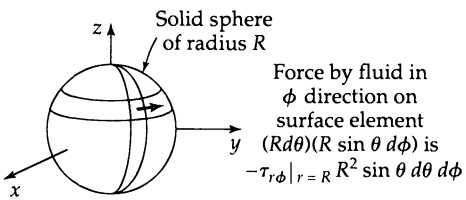
Solid sphere
of radius R

Force by fluid in
 θ direction on
surface element
($Rd\theta)(R \sin \theta d\phi)$ is
 $-\tau_{r\theta}|_{r=R} R^2 \sin \theta d\theta d\phi$



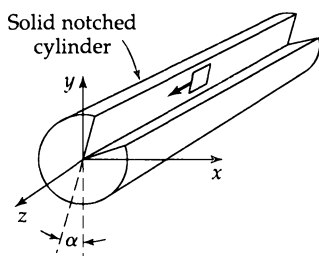
Solid cylinder
of radius R

Force by fluid in
 $+z$ direction on
surface element
($Rd\theta)(dz)$ is
 $-\tau_{rz}|_{r=R} R d\theta dz$



Solid sphere
of radius R

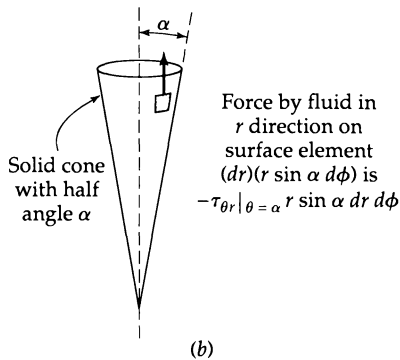
Force by fluid in
 ϕ direction on
surface element
($Rd\theta)(R \sin \theta d\phi)$ is
 $-\tau_{r\phi}|_{r=R} R^2 \sin \theta d\theta d\phi$



Solid notched
cylinder

Force by fluid in
 z direction on
surface element
($dr)(dz)$ is
 $+\tau_{\theta z}|_{\theta=(\pi/2)-\alpha} dr dz$

(a)



Force by fluid in
 r direction on
surface element
($dr)(r \sin \alpha d\phi)$ is
 $-\tau_{\theta r}|_{\theta=\alpha} r \sin \alpha dr d\phi$

(b)

Fig. 1.2-2 (a) Some typical surface elements and shear stresses in the cylindrical coordinate system.
(b) Some typical surface elements and shear stresses in the spherical coordinate system.

§1.7 and Table 19.2-2); (c) in Eq. 1.2-2, the terms $p\delta_{ij}$ and τ_{ij} have the same sign affixed, and the terms p and τ_{ii} are both positive in compression (in accordance with common usage in thermodynamics); (d) all terms in the entropy production in Eq. 24.1-5 have the same sign. Clearly the sign convention in Eqs. 1.1-2 and 1.2-6 is arbitrary, and either sign convention can be used, provided that the physical meaning of the sign convention is clearly understood.

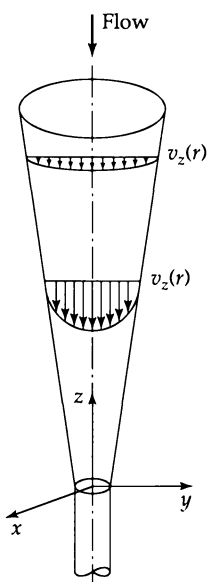


Fig. 1.2-3 The flow in a converging duct is an example of a situation in which the normal stresses are not zero. Since v_z is a function of r and z , the normal-stress component $\tau_{zz} = -2\mu(\partial v_z / \partial z)$ is nonzero. Also, since v_r depends on r and z , the normal-stress component $\tau_{rr} = -2\mu(\partial v_r / \partial r)$ is not equal to zero. At the wall, however, the normal stresses all vanish for fluids described by Eq. 1.2-7 provided that the density is constant (see Example 3.1-1 and Problem 3C.2).

§1.3 PRESSURE AND TEMPERATURE DEPENDENCE OF VISCOSITY

Extensive data on viscosities of pure gases and liquids are available in various science and engineering handbooks.¹ When experimental data are lacking and there is not time to obtain them, the viscosity can be estimated by empirical methods, making use of other data on the given substance. We present here a *corresponding-states correlation*, which facilitates such estimates and illustrates general trends of viscosity with temperature and pressure for ordinary fluids. The principle of corresponding states, which has a sound scientific basis,² is widely used for correlating equation-of-state and thermodynamic data. Discussions of this principle can be found in textbooks on physical chemistry and thermodynamics.

The plot in Fig. 1.3-1 gives a global view of the pressure and temperature dependence of viscosity. The reduced viscosity $\mu_r = \mu / \mu_c$ is plotted versus the reduced temperature $T_r = T/T_c$ for various values of the reduced pressure $p_r = p/p_c$. A “reduced” quantity is one that has been made dimensionless by dividing by the corresponding quantity at the critical point. The chart shows that the viscosity of a gas approaches a limit (the low-density limit) as the pressure becomes smaller; for most gases, this limit is nearly attained at 1 atm pressure. The viscosity of a gas at low density *increases* with increasing temperature, whereas the viscosity of a liquid *decreases* with increasing temperature.

Experimental values of the critical viscosity μ_c are seldom available. However, μ_c may be estimated in one of the following ways: (i) if a value of viscosity is known at a given reduced pressure and temperature, preferably at conditions near to those of

¹ J. A. Schetz and A. E. Fuhs (eds.), *Handbook of Fluid Dynamics and Fluid Machinery*, Wiley-Interscience, New York (1996), Vol. 1, Chapter 2; W. M. Rohsenow, J. P. Hartnett, and Y. I. Cho, *Handbook of Heat Transfer*, McGraw-Hill, New York, 3rd edition (1998), Chapter 2. Other sources are mentioned in fn. 4 of §1.1.

² J. Millat, J. H. Dymond, and C. A. Nieto de Castro (eds.), *Transport Properties of Fluids*, Cambridge University Press (1996), Chapter 11, by E. A. Mason and F. J. Uribe, and Chapter 12, by M. L. Huber and H. M. M. Hanley.

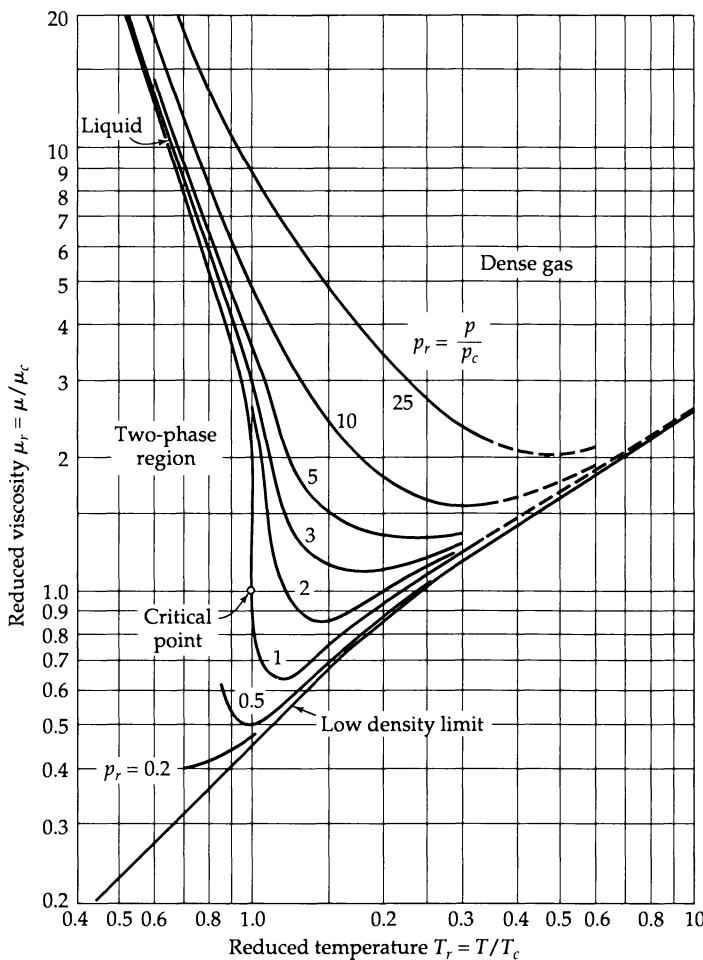


Fig. 1.3-1 Reduced viscosity $\mu_r = \mu/\mu_c$ as a function of reduced temperature for several values of the reduced pressure. [O. A. Uyehara and K. M. Watson, *Nat. Petroleum News, Tech. Section*, 36, 764 (Oct. 4, 1944); revised by K. M. Watson (1960). A large-scale version of this graph is available in O. A. Hougen, K. M. Watson, and R. A. Ragatz, *C. P. P. Charts*, Wiley, New York, 2nd edition (1960)].

interest, then μ_c can be calculated from $\mu_c = \mu/\mu_r$; or (ii) if critical p - V - T data are available, then μ_c may be estimated from these empirical relations:

$$\mu_c = 61.6(MT_c)^{1/2}(\tilde{V}_c)^{-2/3} \quad \text{and} \quad \mu_c = 7.70M^{1/2}p_c^{2/3}T_c^{-1/6} \quad (1.3-1a, b)$$

Here μ_c is in micropoises, p_c in atm, T_c in K, and \tilde{V}_c in $\text{cm}^3/\text{g-mole}$. A tabulation of critical viscosities³ computed by method (i) is given in Appendix E.

Figure 1.3-1 can also be used for rough estimation of viscosities of mixtures. For an N -component mixture, use is made of "pseudocritical" properties⁴ defined as

$$p'_c = \sum_{\alpha=1}^N x_\alpha p_{c\alpha} \quad T'_c = \sum_{\alpha=1}^N x_\alpha T_{c\alpha} \quad \mu'_c = \sum_{\alpha=1}^N x_\alpha \mu_{c\alpha} \quad (1.3-2a, b, c)$$

That is, one uses the chart exactly as for pure fluids, but with the pseudocritical properties instead of the critical properties. This empirical procedure works reasonably well

³ O. A. Hougen and K. M. Watson, *Chemical Process Principles*, Part III, Wiley, New York (1947), p. 873. **Olaf Andreas Hougen** (pronounced "How-gen") (1893–1986) was a leader in the development of chemical engineering for four decades; together with K. M. Watson and R. A. Ragatz, he wrote influential books on thermodynamics and kinetics.

⁴ O. A. Hougen and K. M. Watson, *Chemical Process Principles*, Part II, Wiley, New York (1947), p. 604.

unless there are chemically dissimilar substances in the mixture or the critical properties of the components differ greatly.

There are many variants on the above method, as well as a number of other empiricisms. These can be found in the extensive compilation of Reid, Prausnitz, and Poling.⁵

EXAMPLE 1.3-1

Estimation of Viscosity from Critical Properties

Estimate the viscosity of N₂ at 50°C and 854 atm, given $M = 28.0 \text{ g/g-mole}$, $p_c = 33.5 \text{ atm}$, and $T_c = 126.2 \text{ K}$.

SOLUTION

Using Eq. 1.3-1b, we get

$$\begin{aligned}\mu_c &= 7.70(2.80)^{1/2}(33.5)^{2/3}(126.2)^{-1/6} \\ &= 189 \text{ micropoises} = 189 \times 10^{-6} \text{ poise}\end{aligned}\quad (1.3-3)$$

The reduced temperature and pressure are

$$T_r = \frac{273.2 + 50}{126.2} = 2.56; \quad p_r = \frac{854}{33.5} = 25.5 \quad (1.3-4a, b)$$

From Fig. 1.3-1, we obtain $\mu_r = \mu/\mu_c = 2.39$. Hence, the predicted value of the viscosity is

$$\mu = \mu_c(\mu_r) = (189 \times 10^{-6})(2.39) = 452 \times 10^{-6} \text{ poise} \quad (1.3-5)$$

The measured value⁶ is 455×10^{-6} poise. This is unusually good agreement.

§1.4 MOLECULAR THEORY OF THE VISCOSITY OF GASES AT LOW DENSITY

To get a better appreciation of the concept of molecular momentum transport, we examine this transport mechanism from the point of view of an elementary kinetic theory of gases.

We consider a pure gas composed of rigid, nonattracting spherical molecules of diameter d and mass m , and the number density (number of molecules per unit volume) is taken to be n . The concentration of gas molecules is presumed to be sufficiently small that the average distance between molecules is many times their diameter d . In such a gas it is known¹ that, at equilibrium, the molecular velocities are randomly directed and have an average magnitude given by (see Problem 1C.1)

$$\bar{u} = \sqrt{\frac{8kT}{\pi m}} \quad (1.4-1)$$

in which k is the Boltzmann constant (see Appendix F). The frequency of molecular bombardment per unit area on one side of any stationary surface exposed to the gas is

$$Z = \frac{1}{4}n\bar{u} \quad (1.4-2)$$

⁵ R. C. Reid, J. M. Prausnitz, and B. E. Poling, *The Properties of Gases and Liquids*, McGraw-Hill, New York, 4th edition (1987), Chapter 9.

⁶ A. M. J. F. Michels and R. E. Gibson, *Proc. Roy. Soc. (London)*, **A134**, 288–307 (1931).

¹ The first four equations in this section are given without proof. Detailed justifications are given in books on kinetic energy—for example, E. H. Kennard, *Kinetic Theory of Gases*, McGraw-Hill, New York (1938), Chapters II and III. Also E. A. Guggenheim, *Elements of the Kinetic Theory of Gases*, Pergamon Press, New York (1960), Chapter 7, has given a short account of the elementary theory of viscosity. For readable summaries of the kinetic theory of gases, see R. J. Silbey and R. A. Alberty, *Physical Chemistry*, Wiley, New York, 3rd edition (2001), Chapter 17, or R. S. Berry, S. A. Rice, and J. Ross, *Physical Chemistry*, Oxford University Press, 2nd edition (2000), Chapter 28.

The average distance traveled by a molecule between successive collisions is the *mean free path* λ , given by

$$\lambda = \frac{1}{\sqrt{2}\pi d^2 n} \quad (1.4-3)$$

On the average, the molecules reaching a plane will have experienced their last collision at a distance a from the plane, where a is given very roughly by

$$a = \frac{2}{3}\lambda \quad (1.4-4)$$

The concept of the mean free path is intuitively appealing, but it is meaningful only when λ is large compared to the range of intermolecular forces. The concept is appropriate for the rigid-sphere molecular model considered here.

To determine the viscosity of a gas in terms of the molecular model parameters, we consider the behavior of the gas when it flows parallel to the xz -plane with a velocity gradient dv_x/dy (see Fig. 1.4-1). We assume that Eqs. 1.4-1 to 4 remain valid in this non-equilibrium situation, provided that all molecular velocities are calculated relative to the average velocity \bar{v} in the region in which the given molecule had its last collision. The flux of x -momentum across any plane of constant y is found by assuming the x -momenta of the molecules that cross in the positive y direction and subtracting the x -momenta of those that cross in the opposite direction, as follows:

$$\tau_{yx} = Zmv_x|_{y-a} - Zmv_x|_{y+a} \quad (1.4-5)$$

In writing this equation, we have assumed that all molecules have velocities representative of the region in which they last collided and that the velocity profile $v_x(y)$ is essentially linear for a distance of several mean free paths. In view of the latter assumption, we may further write

$$v_x|_{y\pm a} = v_x|_y \pm \frac{2}{3}\lambda \frac{dv_x}{dy} \quad (1.4-6)$$

By combining Eqs. 1.4-2, 5, and 6 we get for the net flux of x -momentum in the positive y direction

$$\tau_{yx} = -\frac{1}{3}nm\bar{\mu}\lambda \frac{dv_x}{dy} \quad (1.4-7)$$

This has the same form as Newton's law of viscosity given in Eq. 1.1-2. Comparing the two equations gives an equation for the viscosity

$$\mu = \frac{1}{3}nm\bar{\mu}\lambda = \frac{1}{3}\rho\bar{\mu}\lambda \quad (1.4-8)$$

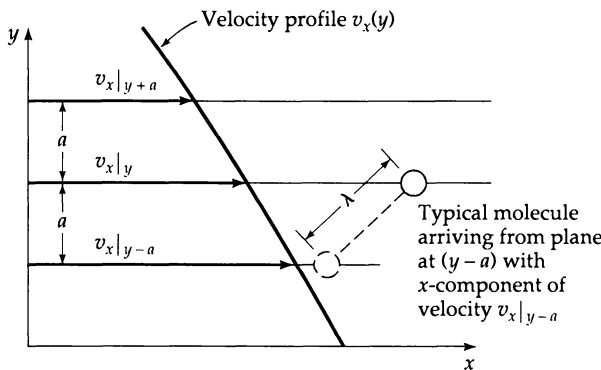


Fig. 1.4-1 Molecular transport of x -momentum from the plane at $(y - a)$ to the plane at y .

or, by combining Eqs. 1.4-1, 3, and 8

$$\mu = \frac{2}{3} \frac{\sqrt{mKT/\pi}}{\pi d^2} = \frac{2}{3\pi} \frac{\sqrt{\pi mKT}}{\pi d^2} \quad (1.4-9)$$

This expression for the viscosity was obtained by Maxwell² in 1860. The quantity πd^2 is called the *collision cross section* (see Fig. 1.4-2).

The above derivation, which gives a qualitatively correct picture of momentum transfer in a gas at low density, makes it clear why we wished to introduce the term "momentum flux" for τ_{yx} in §1.1.

The prediction of Eq. 1.4-9 that μ is independent of pressure agrees with experimental data up to about 10 atm at temperatures above the critical temperature (see Fig. 1.3-1). The predicted temperature dependence is less satisfactory; data for various gases indicate that μ increases more rapidly than \sqrt{T} . To better describe the temperature dependence of μ , it is necessary to replace the rigid-sphere model by one that portrays the attractive and repulsive forces more accurately. It is also necessary to abandon the mean free path theories and use the Boltzmann equation to obtain the molecular velocity distribution in nonequilibrium systems more accurately. Relegating the details to Appendix D, we present here the main results.^{3,4,5}

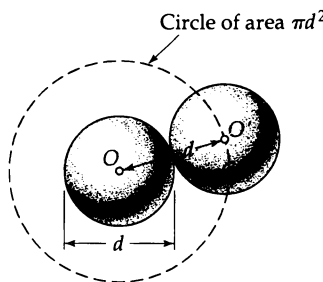


Fig. 1.4-2 When two rigid spheres of diameter d approach each other, the center of one sphere (at O') "sees" a circle of area πd^2 about the center of the other sphere (at O), on which a collision can occur. The area πd^2 is referred to as the "collision cross section."

² James Clerk Maxwell (1831–1879) was one of the greatest physicists of all time; he is particularly famous for his development of the field of electromagnetism and his contributions to the kinetic theory of gases. In connection with the latter, see J. C. Maxwell, *Phil. Mag.*, **19**, 19, Prop. XIII (1860); S. G. Brush, *Am. J. Phys.*, **30**, 269–281 (1962). There is some controversy concerning Eqs. 1.4-4 and 1.4-9 (see S. Chapman and T. G. Cowling, *The Mathematical Theory of Non-Uniform Gases*, Cambridge University Press, 3rd edition 1970), p. 98; R. E. Cunningham and R. J. J. Williams, *Diffusion in Gases and Porous Media*, Plenum Press, New York (1980), §6.4.

³ Sydney Chapman (1888–1970) taught at Imperial College in London, and thereafter was at the High Altitude Observatory in Boulder, Colorado; in addition to his seminal work on gas kinetic theory, he contributed to kinetic theory of plasmas and the theory of flames and detonations. David Enskog (1884–1947) (pronounced, roughly, "Ayn-skohg") is famous for his work on kinetic theories of low- and high-density gases. The standard reference on the Chapman–Enskog kinetic theory of dilute gases is S. Chapman and T. G. Cowling, *The Mathematical Theory of Non-Uniform Gases*, Cambridge University Press, 3rd edition (1970); pp. 407–409 give a historical summary of the kinetic theory. See also D. Enskog, *Inaugural Dissertation*, Uppsala (1917). In addition J. H. Ferziger and H. G. Kaper, *Mathematical Theory of Transport Processes in Gases*, North-Holland, Amsterdam (1972), is a very readable account of molecular theory.

⁴ The Curtiss–Hirschfelder⁵ extension of the Chapman–Enskog theory to multicomponent gas mixtures, as well as the development of useful tables for computation, can be found in J. O. Hirschfelder, C. F. Curtiss, and R. B. Bird, *Molecular Theory of Gases and Liquids*, Wiley, New York, 2nd corrected printing (1964). See also C. F. Curtiss, *J. Chem. Phys.*, **49**, 2917–2919 (1968), as well as references given in Appendix E. Joseph Oakland Hirschfelder (1911–1990), founding director of the Theoretical Chemistry Institute at the University of Wisconsin, specialized in intermolecular forces and applications of kinetic theory.

⁵ C. F. Curtiss and J. O. Hirschfelder, *J. Chem. Phys.*, **17**, 550–555 (1949).

A rigorous kinetic theory of monatomic gases at low density was developed early in the twentieth century by Chapman in England and independently by Enskog in Sweden. The Chapman–Enskog theory gives expressions for the transport properties in terms of the *intermolecular potential energy* $\varphi(r)$, where r is the distance between a pair of molecules undergoing a collision. The intermolecular force is then given by $F(r) = -d\varphi/dr$. The exact functional form of $\varphi(r)$ is not known; however, for nonpolar molecules a satisfactory empirical expression is the *Lennard-Jones (6-12) potential*⁶ given by

$$\varphi(r) = 4\epsilon \left[\left(\frac{\sigma}{r} \right)^{12} - \left(\frac{\sigma}{r} \right)^6 \right] \quad (1.4-10)$$

in which σ is a characteristic diameter of the molecules, often called the *collision diameter* and ϵ is a characteristic energy, actually the maximum energy of attraction between a pair of molecules. This function, shown in Fig. 1.4-3, exhibits the characteristic features of intermolecular forces: weak attractions at large separations and strong repulsions at small separations. Values of the parameters σ and ϵ are known for many substances; a partial list is given in Table E.1, and a more extensive list is available elsewhere.⁴ When σ and ϵ are not known, they may be estimated from properties of the fluid at the critical point (c), the liquid at the normal boiling point (b), or the solid at the melting point (m), by means of the following empirical relations:⁴

$$\epsilon/k = 0.77T_c \quad \sigma = 0.841\tilde{V}_c^{1/3} \quad \text{or} \quad \sigma = 2.44(T_c/p_c)^{1/3} \quad (1.4-11a, b, c)$$

$$\epsilon/k = 1.15T_b \quad \sigma = 1.166\tilde{V}_{b,\text{liq}}^{1/3} \quad (1.4-12a, b)$$

$$\epsilon/k = 1.92T_m \quad \sigma = 1.222\tilde{V}_{m,\text{sol}}^{1/3} \quad (1.4-13a, b)$$

Here ϵ/k and T are in K, σ is in Ångström units ($1 \text{ \AA} = 10^{-10} \text{ m}$), \tilde{V} is in $\text{cm}^3/\text{g-mole}$, and p_c is in atmospheres.

The viscosity of a pure monatomic gas of molecular weight M may be written in terms of the Lennard-Jones parameters as

$$\mu = \frac{5}{16} \frac{\sqrt{\pi mkT}}{\pi \sigma^2 \Omega_\mu} \quad \text{or} \quad \mu = 2.6693 \times 10^{-5} \frac{\sqrt{MT}}{\sigma^2 \Omega_\mu} \quad (1.4-14)$$

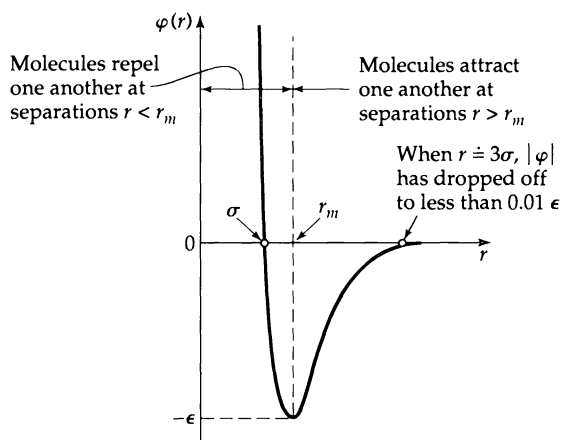


Fig. 1.4-3 Potential energy function $\varphi(r)$ describing the interaction of two spherical, nonpolar molecules. The Lennard-Jones (6-12) potential, given in Eq. 1.4-10, is one of the many empirical equations proposed for fitting this curve. For $r < r_m$ the molecules repel one another, whereas for $r > r_m$ the molecules attract one another.

⁶ J. E. (Lennard-)Jones, *Proc. Roy. Soc.*, **A106**, 441–462, 463–477 (1924). See also R. J. Silbey and R. A. Alberty, *Physical Chemistry*, Wiley, 2nd edition (2001), §§11.10, 16.14, and 17.9; and R. S. Berry, S. A. Rice, and J. Ross, *Physical Chemistry*, Oxford University Press, 2nd edition (2000), §10.2.

In the second form of this equation, if $T [=] \text{K}$ and $\sigma [=] \text{\AA}$, then $\mu [=] \text{g/cm} \cdot \text{s}$. The dimensionless quantity Ω_μ is a slowly varying function of the dimensionless temperature $\kappa T/\epsilon$, of the order of magnitude of unity, given in Table E.2. It is called the "collision integral for viscosity," because it accounts for the details of the paths that the molecules take during a binary collision. If the gas were made up of rigid spheres of diameter σ (instead of real molecules with attractive and repulsive forces), then Ω_μ would be exactly unity. Hence the function Ω_μ may be interpreted as describing the deviation from rigid-sphere behavior.

Although Eq. 1.4-14 is a result of the kinetic theory of monatomic gases, it has been found to be remarkably good for polyatomic gases as well. The reason for this is that, in the equation of conservation of momentum for a collision between polyatomic molecules, the center of mass coordinates are more important than the internal coordinates [see §0.3(b)]. The temperature dependence predicted by Eq. 1.4-14 is in good agreement with that found from the low-density line in the empirical correlation of Fig. 1.3-1. The viscosity of gases at low density increases with temperature, roughly as the 0.6 to 1.0 power of the absolute temperature, and is independent of the pressure.

To calculate the viscosity of a gas mixture, the multicomponent extension of the Chapman-Enskog theory can be used.^{4,5} Alternatively, one can use the following very satisfactory semiempirical formula:⁷

$$\mu_{\text{mix}} = \sum_{\alpha=1}^N \frac{x_\alpha \mu_\alpha}{\sum_\beta x_\beta \Phi_{\alpha\beta}} \quad (1.4-15)$$

in which the dimensionless quantities $\Phi_{\alpha\beta}$ are

$$\Phi_{\alpha\beta} = \frac{1}{\sqrt{8}} \left(1 + \frac{M_\alpha}{M_\beta} \right)^{-1/2} \left[1 + \left(\frac{\mu_\alpha}{\mu_\beta} \right)^{1/2} \left(\frac{M_\beta}{M_\alpha} \right)^{1/4} \right]^2 \quad (1.4-16)$$

Here N is the number of chemical species in the mixture, x_α is the mole fraction of species α , μ_α is the viscosity of pure species α at the system temperature and pressure, and M_α is the molecular weight of species α . Equation 1.4-16 has been shown to reproduce measured values of the viscosities of mixtures within an average deviation of about 2%. The dependence of mixture viscosity on composition is extremely nonlinear for some mixtures, particularly mixtures of light and heavy gases (see Problem 1A.2).

To summarize, Eqs. 1.4-14, 15, and 16 are useful formulas for computing viscosities of nonpolar gases and gas mixtures at low density from tabulated values of the intermolecular force parameters σ and ϵ/κ . They will not give reliable results for gases consisting of polar or highly elongated molecules because of the angle-dependent force fields that exist between such molecules. For polar vapors, such as H_2O , NH_3 , CHOH , and NOCl , an angle-dependent modification of Eq. 1.4-10 has given good results.⁸ For the light gases H_2 and He below about 100K, quantum effects have to be taken into account.⁹

Many additional empiricisms are available for estimating viscosities of gases and gas mixtures. A standard reference is that of Reid, Prausnitz, and Poling.¹⁰

⁷ C. R. Wilke, *J. Chem. Phys.*, **18**, 517–519 (1950); see also J. W. Buddenberg and C. R. Wilke, *Ind. Eng. Chem.*, **41**, 1345–1347 (1949).

⁸ E. A. Mason and L. Monchick, *J. Chem. Phys.*, **35**, 1676–1697 (1961) and **36**, 1622–1639, 2746–2757 (1962).

⁹ J. O. Hirschfelder, C. F. Curtiss, and R. B. Bird, *op. cit.*, Chapter 10; H. T. Wood and C. F. Curtiss, *J. Chem. Phys.*, **41**, 1167–1173 (1964); R. J. Munn, F. J. Smith, and E. A. Mason, *J. Chem. Phys.*, **42**, 537–539 (1965); S. Imam-Rahajoe, C. F. Curtiss, and R. B. Bernstein, *J. Chem. Phys.*, **42**, 530–536 (1965).

¹⁰ R. C. Reid, J. M. Prausnitz, and B. E. Poling, *The Properties of Gases and Liquids*, McGraw-Hill, New York, 4th edition (1987).

EXAMPLE 1.4-1

Compute the viscosity of CO₂ at 200, 300, and 800K and 1 atm.

Computation of the Viscosity of a Pure Gas at Low Density

SOLUTION

Use Eq. 1.4-14. From Table E.1, we find the Lennard-Jones parameters for CO₂ to be $\varepsilon/k = 190$ K and $\sigma = 3.996$ Å. The molecular weight of CO₂ is 44.01. Substitution of M and σ into Eq. 1.4-14 gives

$$\mu = 2.6693 \times 10^{-5} \frac{\sqrt{44.01T}}{(3.996)^2 \Omega_\mu} = 1.109 \times 10^{-5} \frac{\sqrt{T}}{\Omega_\mu} \quad (1.4-17)$$

in which $\mu [=] \text{ g/cm} \cdot \text{s}$ and $T [=] \text{ K}$. The remaining calculations may be displayed in a table.

Viscosity (g/cm · s)					
T (K)	kT/ε	Ω_μ	\sqrt{T}	Predicted	Observed ¹¹
200	1.053	1.548	14.14	1.013×10^{-4}	1.015×10^{-4}
300	1.58	1.286	17.32	1.494×10^{-4}	1.495×10^{-4}
800	4.21	0.9595	28.28	3.269×10^{-4}	...

Experimental data are shown in the last column for comparison. The good agreement is to be expected, since the Lennard-Jones parameters of Table E.1 were derived from viscosity data.

EXAMPLE 1.4-2

Prediction of the Viscosity of a Gas Mixture at Low Density

Estimate the viscosity of the following gas mixture at 1 atm and 293K from the given data on the pure components at the same pressure and temperature:

Species α	Mole fraction, x_α	Molecular weight, M_α	Viscosity, μ_α (g/cm · s)
1. CO ₂	0.133	44.01	1462×10^{-7}
2. O ₂	0.039	32.00	2031×10^{-7}
3. N ₂	0.828	28.02	1754×10^{-7}

SOLUTION

Use Eqs. 1.4-16 and 15 (in that order). The calculations can be systematized in tabular form, thus:

α	β	M_α/M_β	μ_α/μ_β	$\Phi_{\alpha\beta}$	$\sum_{\beta=1}^3 x_\alpha \Phi_{\alpha\beta}$
1.	1	1.000	1.000	1.000	0.763
	2	1.375	0.720	0.730	
	3	1.571	0.834	0.727	
2.	1	0.727	1.389	1.394	1.057
	2	1.000	1.000	1.000	
	3	1.142	1.158	1.006	
3.	1	0.637	1.200	1.370	1.049
	2	0.876	0.864	0.993	
	3	1.000	1.000	1.000	

¹¹ H. L. Johnston and K. E. McCloskey, *J. Phys. Chem.*, **44**, 1038–1058 (1940).

Eq. 1.4-15 then gives

$$\begin{aligned}\mu &= \frac{(0.1333)(1462)(10^{-7})}{0.763} + \frac{(0.039)(2031)(10^{-7})}{1.057} + \frac{(0.828)(1754)(10^{-7})}{1.049} \\ &= 1714 \times 10^{-7} \text{ g/cm} \cdot \text{s}\end{aligned}$$

The observed value¹² is $1793 \times 10^{-7} \text{ g/cm} \cdot \text{s}$.

§1.5 MOLECULAR THEORY OF THE VISCOSITY OF LIQUIDS

A rigorous kinetic theory of the transport properties of monatomic liquids was developed by Kirkwood and coworkers.¹ However this theory does not lead to easy-to-use results. An older theory, developed by Eyring² and coworkers, although less well grounded theoretically, does give a qualitative picture of the mechanism of momentum transport in liquids and permits rough estimation of the viscosity from other physical properties. We discuss this theory briefly.

In a pure liquid at rest the individual molecules are constantly in motion. However, because of the close packing, the motion is largely confined to a vibration of each molecule within a “cage” formed by its nearest neighbors. This cage is represented by an energy barrier of height $\Delta\tilde{G}_0^+/\tilde{N}$, in which $\Delta\tilde{G}_0^+$ is the molar free energy of activation for escape from the cage in the stationary fluid (see Fig. 1.5-1). According to Eyring, a liquid at rest continually undergoes rearrangements, in which one molecule at a time escapes from its “cage” into an adjoining “hole,” and that the molecules thus move in each of the

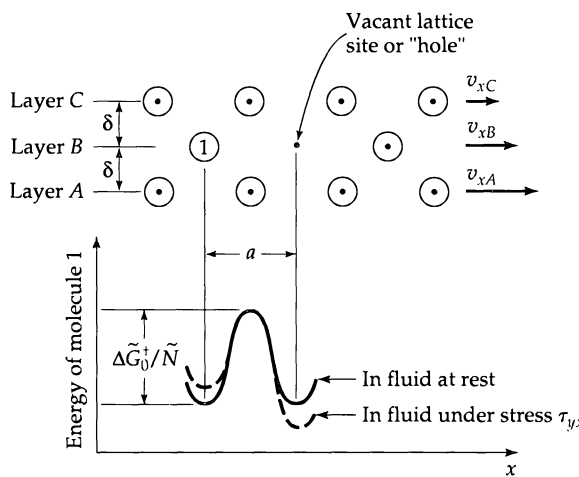


Fig. 1.5-1 Illustration of an escape process in the flow of a liquid. Molecule 1 must pass through a “bottleneck” to reach the vacant site.

¹² F. Herning and L. Zipperer, *Gas- und Wasserfach*, **79**, 49–54, 69–73 (1936).

¹ J. H. Irving and J. G. Kirkwood, *J. Chem. Phys.*, **18**, 817–823 (1950); R. J. Bearman and J. G. Kirkwood, *J. Chem. Phys.*, **28**, 136–146 (1958). For additional publications, see John Gamble Kirkwood, *Collected Works*, Gordon and Breach, New York (1967). **John Gamble Kirkwood** (1907–1959) contributed much to the kinetic theory of liquids, properties of polymer solutions, theory of electrolytes, and thermodynamics of irreversible processes.

² S. Glasstone, K. J. Laidler, and H. Eyring, *Theory of Rate Processes*, McGraw-Hill, New York (1941), Chapter 9; H. Eyring, D. Henderson, B. J. Stover, and E. M. Eyring, *Statistical Mechanics*, Wiley, New York (1964), Chapter 16. See also R. J. Silbey and R. A. Alberty, *Physical Chemistry*, Wiley, 3rd edition (2001), §20.1; and R. S. Berry, S. A. Rice, and J. Ross, *Physical Chemistry*, Oxford University Press, 2nd edition (2000), Ch. 29. **Henry Eyring** (1901–1981) developed theories for the transport properties based on simple physical models; he also developed the theory of absolute reaction rates.

coordinate directions in jumps of length a at a frequency ν per molecule. The frequency is given by the rate equation

$$\nu = \frac{kT}{h} \exp(-\Delta\tilde{G}_0^+/RT) \quad (1.5-1)$$

In which k and h are the Boltzmann and Planck constants, \tilde{N} is the Avogadro number, and $R = \tilde{N}k$ is the gas constant (see Appendix F).

In a fluid that is flowing in the x direction with a velocity gradient dv_x/dy , the frequency of molecular rearrangements is increased. The effect can be explained by considering the potential energy barrier as distorted under the applied stress τ_{yx} (see Fig. 1.5-1), so that

$$-\Delta\tilde{G}^\pm = -\Delta\tilde{G}_0^\pm \pm \left(\frac{a}{\delta}\right)\left(\frac{\tau_{yx}\tilde{V}}{2}\right) \quad (1.5-2)$$

where \tilde{V} is the volume of a mole of liquid, and $\pm(a/\delta)(\tau_{yx}\tilde{V}/2)$ is an approximation to the work done on the molecules as they move to the top of the energy barrier, moving *with* the applied shear stress (plus sign) or *against* the applied shear stress (minus sign). We now define ν_+ as the frequency of forward jumps and ν_- as the frequency of backward jumps. Then from Eqs. 1.5-1 and 1.5-2 we find that

$$\nu_\pm = \frac{kT}{h} \exp(-\Delta\tilde{G}_0^\pm/RT) \exp(\pm a\tau_{yx}\tilde{V}/2\delta RT) \quad (1.5-3)$$

The net velocity with which molecules in layer A slip ahead of those in layer B (Fig. 1.5-1) is just the distance traveled per jump (a) times the *net* frequency of forward jumps ($\nu_+ - \nu_-$); this gives

$$v_{xA} - v_{xB} = a(\nu_+ - \nu_-) \quad (1.5-4)$$

The velocity profile can be considered to be linear over the very small distance δ between the layers A and B , so that

$$-\frac{dv_x}{dy} = \left(\frac{a}{\delta}\right)(\nu_+ - \nu_-) \quad (1.5-5)$$

By combining Eqs. 1.5-3 and 5, we obtain finally

$$\begin{aligned} -\frac{dv_x}{dy} &= \left(\frac{a}{\delta}\right)\left(\frac{kT}{h} \exp(-\Delta\tilde{G}_0^+/RT)\right)\left(\exp(+a\tau_{yx}\tilde{V}/2\delta RT) - \exp(-a\tau_{yx}\tilde{V}/2\delta RT)\right) \\ &= \left(\frac{a}{\delta}\right)\left(\frac{kT}{h} \exp(-\Delta\tilde{G}_0^+/RT)\right)\left(2 \sinh \frac{a\tau_{yx}\tilde{V}}{2\delta RT}\right) \end{aligned} \quad (1.5-6)$$

This predicts a nonlinear relation between the shear stress (momentum flux) and the velocity gradient—that is, *non-Newtonian flow*. Such nonlinear behavior is discussed further in Chapter 8.

The usual situation, however, is that $a\tau_{yx}\tilde{V}/2\delta RT \ll 1$. Then we can use the Taylor series (see §C.2) $\sinh x = x + (1/3!)x^3 + (1/5!)x^5 + \dots$ and retain only one term. Equation 1.5-6 is then of the form of Eq. 1.1-2, with the viscosity being given by

$$\mu = \left(\frac{\delta}{a}\right)^2 \frac{\tilde{N}h}{\tilde{V}} \exp(\Delta\tilde{G}_0^+/RT) \quad (1.5-7)$$

The factor δ/a can be taken to be unity; this simplification involves no loss of accuracy, since $\Delta\tilde{G}_0^+$ is usually determined empirically to make the equation agree with experimental viscosity data.

It has been found that free energies of activation, $\Delta\tilde{G}_0^+$, determined by fitting Eq. 1.5-7 to experimental data on viscosity versus temperature, are almost constant for a given

fluid and are simply related to the internal energy of vaporization at the normal boiling point, as follows:³

$$\Delta\tilde{G}_0^{\ddagger} \approx 0.408 \Delta\tilde{U}_{\text{vap}} \quad (1.5-8)$$

By using this empiricism and setting $\delta/a = 1$, Eq. 1.5-7 becomes

$$\mu = \frac{\tilde{N}h}{\tilde{V}} \exp(0.408 \Delta\tilde{U}_{\text{vap}}/RT) \quad (1.5-9)$$

The energy of vaporization at the normal boiling point can be estimated roughly from Trouton's rule

$$\Delta\tilde{U}_{\text{vap}} \approx \Delta\tilde{H}_{\text{vap}} - RT_b \cong 9.4RT_b \quad (1.5-10)$$

With this further approximation, Eq. 1.5-9 becomes

$$\mu = \frac{\tilde{N}h}{\tilde{V}} \exp(3.8T_b/T) \quad (1.5-11)$$

Equations 1.5-9 and 11 are in agreement with the long-used and apparently successful empiricism $\mu = A \exp(B/T)$. The theory, although only approximate in nature, does give the observed decrease of viscosity with temperature, but errors of as much as 30% are common when Eqs. 1.5-9 and 11 are used. They should not be used for very long slender molecules, such as n-C₂₀H₄₂.

There are, in addition, many empirical formulas available for predicting the viscosity of liquids and liquid mixtures. For these, physical chemistry and chemical engineering textbooks should be consulted.⁴

EXAMPLE 1.5-1

Estimate the viscosity of liquid benzene, C₆H₆, at 20°C (293.2 K).

SOLUTION

Use Eq. 1.5-11 with the following information:

$$\begin{aligned}\tilde{V} &= 89.0 \text{ cm}^3/\text{g-mole} \\ T_b &= 80.1^\circ\text{C}\end{aligned}$$

Since this information is given in c.g.s. units, we use the values of Avogadro's number and Planck's constant in the same set of units. Substituting into Eq. 1.5-11 gives:

$$\begin{aligned}\mu &= \frac{(6.023 \times 10^{23})(6.624 \times 10^{-27})}{(89.0)} \exp\left(\frac{3.8 \times (273.2 + 80.1)}{293.2}\right) \\ &= 4.5 \times 10^{-3} \text{ g/cm} \cdot \text{s} \quad \text{or} \quad 4.5 \times 10^{-4} \text{ Pa} \cdot \text{s} \quad \text{or} \quad 0.45 \text{ mPa} \cdot \text{s}\end{aligned}$$

§1.6 VISCOSITY OF SUSPENSIONS AND EMULSIONS

Up to this point we have been discussing fluids that consist of a single homogeneous phase. We now turn our attention briefly to two-phase systems. The complete description of such systems is, of course, quite complex, but it is often useful to replace the suspension or emulsion by a hypothetical one-phase system, which we then describe by

³ J. F. Kincaid, H. Eyring, and A. E. Stearn, *Chem. Revs.*, **28**, 301–365 (1941).

⁴ See, for example, J. R. Partington, *Treatise on Physical Chemistry*, Longmans, Green (1949); or R. C. Reid, J. M. Prausnitz, and B. E. Poling, *The Properties of Gases and Liquids*, McGraw-Hill, New York, 4th edition (1987). See also P. A. Egelstaff, *An Introduction to the Liquid State*, Oxford University Press, 2nd edition (1994), Chapter 13; and J. P. Hansen and I. R. McDonald, *Theory of Simple Liquids*, Academic Press, London (1986), Chapter 8.

Newton's law of viscosity (Eq. 1.1-2 or 1.2-7) with two modifications: (i) the viscosity μ is replaced by an *effective viscosity* μ_{eff} , and (ii) the velocity and stress components are then redefined (with no change of symbol) as the analogous quantities averaged over a volume large with respect to the interparticle distances and small with respect to the dimensions of the flow system. This kind of theory is satisfactory as long as the flow involved is steady; in time-dependent flows, it has been shown that Newton's law of viscosity is inappropriate, and the two-phase systems have to be regarded as viscoelastic materials.¹

The first major contribution to the theory of the *viscosity of suspensions of spheres* was that of Einstein.² He considered a suspension of rigid spheres, so dilute that the movement of one sphere does not influence the fluid flow in the neighborhood of any other sphere. Then it suffices to analyze only the motion of the fluid around a single sphere, and the effects of the individual spheres are additive. The *Einstein equation* is

$$\frac{\mu_{\text{eff}}}{\mu_0} = 1 + \frac{5}{2} \phi \quad (1.6-1)$$

in which μ_0 is the viscosity of the suspending medium, and ϕ is the volume fraction of the spheres. Einstein's pioneering result has been modified in many ways, a few of which we now describe.

For *dilute suspensions of particles of various shapes* the constant $\frac{5}{2}$ has to be replaced by a different coefficient depending on the particular shape. Suspensions of elongated or flexible particles exhibit non-Newtonian viscosity.^{3,4,5,6}

For *concentrated suspensions of spheres* (that is, ϕ greater than about 0.05) particle interactions become appreciable. Numerous semiempirical expressions have been developed, one of the simplest of which is the *Mooney equation*⁷

$$\frac{\mu_{\text{eff}}}{\mu_0} = \exp\left(\frac{\frac{5}{2}\phi}{1 - (\phi/\phi_0)}\right) \quad (1.6-2)$$

in which ϕ_0 is an empirical constant between about 0.74 and 0.52, these values corresponding to the values of ϕ for closest packing and cubic packing, respectively.

¹ For dilute suspensions of rigid spheres, the linear viscoelastic behavior has been studied by H. Fröhlich and R. Sack, *Proc. Roy. Soc., A185*, 415–430 (1946), and for dilute emulsions, the analogous derivation has been given by J. G. Oldroyd, *Proc. Roy. Soc., A218*, 122–132 (1953). In both of these publications the fluid is described by the Jeffreys model (see Eq. 8.4-4), and the authors found the relations between the three parameters in the Jeffreys model and the constants describing the structure of the two-phase system (the volume fraction of suspended material and the viscosities of the two phases). For further comments concerning suspensions and rheology, see R. B. Bird and J. M. Wiest, Chapter 3 in *Handbook of Fluid Dynamics and Fluid Machinery*, J. A. Schetz and A. E. Fuhs (eds.), Wiley, New York (1996).

² Albert Einstein (1879–1955) received the Nobel prize for his explanation of the photoelectric effect, not for his development of the theory of special relativity. His seminal work on suspensions appeared in A. Einstein, *Ann. Phys. (Leipzig)*, **19**, 289–306 (1906); erratum, *ibid.*, **24**, 591–592 (1911). In the original publication, Einstein made an error in the derivation and got ϕ instead of $\frac{5}{2}\phi$. After experiments showed that his equation did not agree with the experimental data, he recalculated the coefficient. Einstein's original derivation is quite lengthy; for a more compact development, see L. D. Landau and E. M. Lifshitz, *Fluid Mechanics*, Pergamon Press, Oxford, 2nd edition (1987), pp. 73–75. The mathematical formulation of multiphase fluid behavior can be found in D. A. Drew and S. L. Passman, *Theory of Multicomponent Fluids*, Springer, Berlin (1999).

³ H. L. Frisch and R. Simha, Chapter 14 in *Rheology*, Vol. 1, (F. R. Eirich, ed.), Academic Press, New York (1956), Sections II and III.

⁴ E. W. Merrill, Chapter 4 in *Modern Chemical Engineering*, Vol. 1, (A. Acritos, ed.), Reinhold, New York (1963), p. 165.

⁵ E. J. Hinch and L. G. Leal, *J. Fluid Mech.*, **52**, 683–712 (1972); **76**, 187–208 (1976).

⁶ W. R. Schowalter, *Mechanics of Non-Newtonian Fluids*, Pergamon, Oxford (1978), Chapter 13.

⁷ M. Mooney, *J. Coll. Sci.*, **6**, 162–170 (1951).

Another approach for concentrated suspensions of spheres is the “cell theory,” in which one examines the dissipation energy in the “squeezing flow” between the spheres. As an example of this kind of theory we cite the *Graham equation*⁸

$$\frac{\mu_{\text{eff}}}{\mu_0} = 1 + \frac{5}{2}\phi + \frac{9}{4}\left(\frac{1}{\psi(1 + \frac{1}{2}\psi)(1 + \psi)^2}\right) \quad (1.6-3)$$

in which $\psi = 2[1 - \sqrt[3]{\phi/\phi_{\text{max}}}/\sqrt[3]{\phi/\phi_{\text{max}}}]$, where ϕ_{max} is the volume fraction corresponding to the experimentally determined closest packing of the spheres. This expression simplifies to Einstein’s equation for $\phi \rightarrow 0$ and the Frankel–Acrivos equation⁹ when $\phi \rightarrow \phi_{\text{max}}$.

For concentrated suspensions of nonspherical particles, the Krieger–Dougherty equation¹⁰ can be used:

$$\frac{\mu_{\text{eff}}}{\mu_0} = \left(1 - \frac{\phi}{\phi_{\text{max}}}\right)^{-A\phi_{\text{max}}} \quad (1.6-4)$$

The parameters A and ϕ_{max} to be used in this equation are tabulated¹¹ in Table 1.6-1 for suspensions of several materials.

Non-Newtonian behavior is observed for concentrated suspensions, even when the suspended particles are spherical.¹¹ This means that the viscosity depends on the velocity gradient and may be different in a shear than it is in an elongational flow. Therefore, equations such as Eq. 1.6-2 must be used with some caution.

Table 1.6-1 Dimensionless Constants for Use in Eq. 1.6-4

System	A	ϕ_{max}	Reference
Spheres (submicron)	2.7	0.71	a
Spheres ($40 \mu\text{m}$)	3.28	0.61	b
Ground gypsum	3.25	0.69	c
Titanium dioxide	5.0	0.55	c
Laterite	9.0	0.35	c
Glass rods ($30 \times 700 \mu\text{m}$)	9.25	0.268	d
Glass plates ($100 \times 400 \mu\text{m}$)	9.87	0.382	d
Quartz grains (53–76 μm)	5.8	0.371	d
Glass fibers (axial ratio 7)	3.8	0.374	b
Glass fibers (axial ratio 14)	5.03	0.26	b
Glass fibers (axial ratio 21)	6.0	0.233	b

^a C. G. de Kruif, E. M. F. van Ievsel, A. Vrij, and W. B. Russel, in *Viscoelasticity and Rheology* (A. S. Lodge, M. Renardy, J. A. Nohel, eds.), Academic Press, New York (1985).

^b H. Giesekus, in *Physical Properties of Foods* (J. Jowitt et al., eds.), Applied Science Publishers (1983), Chapter 13.

^c R. M. Turian and T.-F. Yuan, *AIChE Journal*, **23**, 232–243 (1977).

^d B. Clarke, *Trans. Inst. Chem. Eng.*, **45**, 251–256 (1966).

⁸ A. L. Graham, *Appl. Sci. Res.*, **37**, 275–286 (1981).

⁹ N. A. Frankel and A. Acrivos, *Chem. Engr. Sci.*, **22**, 847–853 (1967).

¹⁰ I. M. Krieger and T. J. Dougherty, *Trans. Soc. Rheol.*, **3**, 137–152 (1959).

¹¹ H. A. Barnes, J. F. Hutton, and K. Walters, *An Introduction to Rheology*, Elsevier, Amsterdam (1989), p. 125.

For *emulsions or suspensions of tiny droplets*, in which the suspended material may undergo internal circulation but still retain a spherical shape, the effective viscosity can be considerably less than that for suspensions of solid spheres. The viscosity of dilute emulsions is then described by the *Taylor equation*:¹²

$$\frac{\mu_{\text{eff}}}{\mu_0} = 1 + \left(\frac{\mu_0 + \frac{5}{2}\mu_1}{\mu_0 + \mu_1} \right) \phi \quad (1.6-5)$$

in which μ_1 is the viscosity of the disperse phase. It should, however, be noted that surface-active contaminants, frequently present even in carefully purified liquids, can effectively stop the internal circulation;¹³ the droplets then behave as rigid spheres.

For *dilute suspensions of charged spheres*, Eq. 1.6-1 may be replaced by the *Smoluchowski equation*¹⁴

$$\frac{\mu_{\text{eff}}}{\mu_0} = 1 + \frac{5}{2} \phi \left(1 + \frac{(D\zeta/2\pi R)^2}{\mu_0 k_e} \right) \quad (1.6-6)$$

in which D is the dielectric constant of the suspending fluid, k_e the specific electrical conductivity of the suspension, ζ the electrokinetic potential of the particles, and R the particle radius. Surface charges are not uncommon in stable suspensions. Other, less well understood, surface forces are also important and frequently cause the particles to form loose aggregates.⁴ Here again, non-Newtonian behavior is encountered.¹⁵

§1.7 CONVECTIVE MOMENTUM TRANSPORT

Thus far we have discussed the *molecular transport* of momentum, and this led to a set of quantities π_{ij} , which give the flux of j -momentum across a surface perpendicular to the i direction. We then related the π_{ij} to the velocity gradients and the pressure, and we found that this relation involved two material parameters μ and κ . We have seen in §§1.4 and 1.5 how the viscosity arises from a consideration of the random motion of the molecules in the fluid—that is, the random molecular motion with respect to the bulk motion of the fluid. Furthermore, in Problem 1C.3 we show how the pressure contribution to π_{ij} arises from the random molecular motions.

Momentum can, in addition, be transported by the bulk flow of the fluid, and this process is called *convective transport*. To discuss this we use Fig. 1.7-1 and focus our attention on a cube-shaped region in space through which the fluid is flowing. At the center of the cube (located at x, y, z) the fluid velocity vector is \mathbf{v} . Just as in §1.2 we consider three mutually perpendicular planes (the shaded planes) through the point x, y, z , and we ask how much momentum is flowing through each of them. Each of the planes is taken to have unit area.

The volume rate of flow across the shaded unit area in (a) is v_x . This fluid carries with it momentum ρv per unit volume. Hence the momentum flux across the shaded area is $v_x \rho v$; note that this is the momentum flux from the region of lesser x to the region

¹² G. I. Taylor, *Proc. Roy. Soc.*, A138, 41–48 (1932). Geoffrey Ingram Taylor (1886–1975) is famous for Taylor dispersion, Taylor vortices, and his work on the statistical theory of turbulence; he attacked many complex problems in ingenious ways that made maximum use of the physical processes involved.

¹³ V. G. Levich, *Physicochemical Hydrodynamics*, Prentice-Hall, Englewood Cliffs, N.J. (1962), Chapter 8. Veniamin Grigorevich Levich (1917–1987), physicist and electrochemist, made many contributions to the solution of important problems in diffusion and mass transfer.

¹⁴ M. von Smoluchowski, *Kolloid Zeits.*, 18, 190–195 (1916).

¹⁵ W. B. Russel, *The Dynamics of Colloidal Systems*, U. of Wisconsin Press, Madison (1987), Chapter 4; W. B. Russel, D. A. Saville, and W. R. Schowalter, *Colloidal Dispersions*, Cambridge University Press (1989); R. G. Larson, *The Structure and Rheology of Complex Fluids*, Oxford University Press (1998).

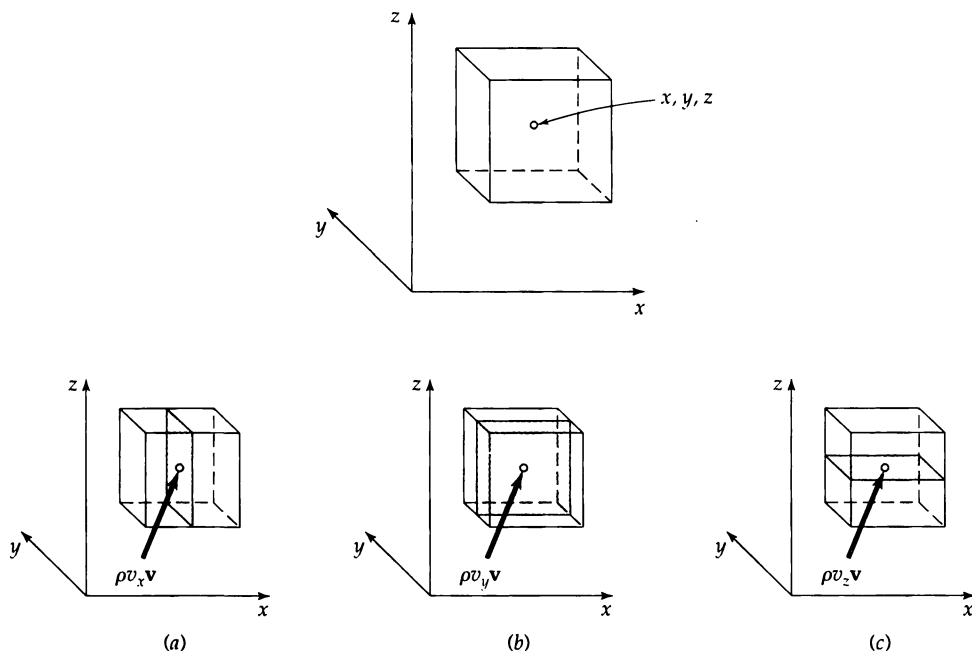


Fig. 1.7-1 The convective momentum fluxes through planes of unit area perpendicular to the coordinate directions.

of greater x . Similarly the momentum flux across the shaded area in (b) is $v_y \rho v$, and the momentum flux across the shaded area in (c) is $v_z \rho v$.

These three vectors— $\rho v_x v$, $\rho v_y v$, and $\rho v_z v$ —describe the momentum flux across the three areas perpendicular to the respective axes. Each of these vectors has an x -, y -, and z -component. These components can be arranged as shown in Table 1.7-1. The quantity $\rho v_x v_y$ is the convective flux of y -momentum across a surface perpendicular to the x direction. This should be compared with the quantity τ_{xy} , which is the molecular flux of y -momentum across a surface perpendicular to the x direction. The sign convention for both modes of transport is the same.

The collection of nine scalar components given in Table 1.7-1 can be represented as

$$\begin{aligned} \rho v v &= (\Sigma_i \delta_i \rho v_i) v = (\Sigma_i \delta_i \rho v_i) (\Sigma_j \delta_j v_j) \\ &= \Sigma_i \Sigma_j \delta_i \delta_j \rho v_i v_j \end{aligned} \quad (1.7-1)$$

Since each component of $\rho v v$ has two subscripts, each associated with a coordinate direction, $\rho v v$ is a (second-order) tensor; it is called the *convective momentum-flux tensor*. Table 1.7-1 for the convective momentum flux tensor components should be compared with Table 1.2-1 for the molecular momentum flux tensor components.

Table 1.7-1 Summary of the Convective Momentum Flux Components

Direction normal to the shaded surface	Flux of momentum through the shaded surface	Convective momentum flux components		
		x -component	y -component	z -component
x	$\rho v_x v$	$\rho v_x v_x$	$\rho v_x v_y$	$\rho v_x v_z$
y	$\rho v_y v$	$\rho v_y v_x$	$\rho v_y v_y$	$\rho v_y v_z$
z	$\rho v_z v$	$\rho v_z v_x$	$\rho v_z v_y$	$\rho v_z v_z$

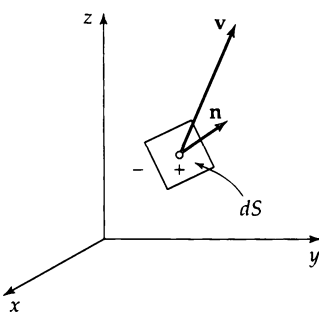


Fig. 1.7-2 The convective momentum flux through a plane of arbitrary orientation \mathbf{n} is $(\mathbf{n} \cdot \mathbf{v})\rho\mathbf{v} = [\mathbf{n} \cdot \rho\mathbf{v}\mathbf{v}]$.

Next we ask what the convective momentum flux would be through a surface element whose orientation is given by a unit normal vector \mathbf{n} (see Fig. 1.7-2). If a fluid is flowing through the surface dS with a velocity \mathbf{v} , then the volume rate of flow through the surface, from the minus side to the plus side, is $(\mathbf{n} \cdot \mathbf{v})dS$. Hence the rate of flow of momentum across the surface is $(\mathbf{n} \cdot \mathbf{v})\rho v dS$, and the convective momentum flux is $(\mathbf{n} \cdot \mathbf{v})\rho\mathbf{v}$. According to the rules for vector-tensor notation given in Appendix A, this can also be written as $[\mathbf{n} \cdot \rho\mathbf{v}\mathbf{v}]$ —that is, the dot product of the unit normal vector \mathbf{n} with the convective momentum flux tensor $\rho\mathbf{v}\mathbf{v}$. If we let \mathbf{n} be successively the unit vectors pointing in the x , y , and z directions (i.e., δ_x , δ_y , and δ_z), we obtain the entries in the second column of Table 1.7-1.

Similarly, the *total molecular momentum flux* through a surface of orientation \mathbf{n} is given by $[\mathbf{n} \cdot \boldsymbol{\pi}] = p\mathbf{n} + [\mathbf{n} \cdot \boldsymbol{\tau}]$. It is understood that this is the flux from the minus side to the plus side of the surface. This quantity can also be interpreted as the force per unit area exerted by the minus material on the plus material across the surface. A geometric interpretation of $[\mathbf{n} \cdot \boldsymbol{\pi}]$ is given in Problem 1D.2.

In this chapter we defined the *molecular transport* of momentum in §1.2, and in this section we have described the *convective transport* of momentum. In setting up shell momentum balances in Chapter 2 and in setting up the general momentum balance in Chapter 3, we shall find it useful to define the *combined momentum flux*, which is the sum of the molecular momentum flux and the convective momentum flux:

$$\Phi = \boldsymbol{\pi} + \rho\mathbf{v}\mathbf{v} = p\boldsymbol{\delta} + \boldsymbol{\tau} + \rho\mathbf{v}\mathbf{v} \quad (1.7-2)$$

Keep in mind that the contribution $p\boldsymbol{\delta}$ contains no velocity, only the pressure; the combination $\rho\mathbf{v}\mathbf{v}$ contains the density and products of the velocity components; and the contribution $\boldsymbol{\tau}$ contains the viscosity and, for a Newtonian fluid, is linear in the velocity gradients. All these quantities are second-order tensors.

Most of the time we will be dealing with components of these quantities. For example the components of Φ are

$$\phi_{xx} = \pi_{xx} + \rho v_x v_x = p + \tau_{xx} + \rho v_x v_x \quad (1.7-3a)$$

$$\phi_{xy} = \pi_{xy} + \rho v_x v_y = \tau_{xy} + \rho v_x v_y \quad (1.7-3b)$$

and so on, paralleling the entries in Tables 1.2-1 and 1.7-1. The important thing to remember is that

ϕ_{xy} = the combined flux of y -momentum across a surface perpendicular to the x direction by molecular and convective mechanisms.

The second index gives the component of momentum being transported and the first index gives the direction of transport.

The various symbols and nomenclature that are used for momentum fluxes are given in Table 1.7-2. The same sign convention is used for all fluxes.

Table 1.7-2 Summary of Notation for Momentum Fluxes

Symbol	Meaning	Reference
ρvv	Convective momentum-flux tensor	Table 1.7-1
τ	Viscous momentum-flux tensor ^a	Table 1.2-1
$\pi = p\delta + \tau$	Molecular momentum-flux tensor ^b	Table 1.2-1
$\phi = \pi + \rho vv$	Combined momentum-flux tensor	Eq. 1.7-2

^a For viscoelastic fluids (see Chapter 8), this should be called the viscoelastic momentum-flux tensor or the viscoelastic stress tensor.

^b This may be referred to as the molecular stress tensor.

QUESTIONS FOR DISCUSSION

1. Compare Newton's law of viscosity and Hooke's law of elasticity. What is the origin of these "laws"?
2. Verify that "momentum per unit area per unit time" has the same dimensions as "force per unit area."
3. Compare and contrast the molecular and convective mechanisms for momentum transport.
4. What are the physical meanings of the Lennard-Jones parameters and how can they be determined from viscosity data? Is the determination unique?
5. How do the viscosities of liquids and low-density gases depend on the temperature and pressure?
6. The Lennard-Jones potential depends only on the intermolecular separation. For what kinds of molecules would you expect that this kind of potential would be inappropriate?
7. Sketch the potential energy function $\varphi(r)$ for rigid, nonattracting spheres.
8. Molecules differing only in their atomic isotopes have the same values of the Lennard-Jones potential parameters. Would you expect the viscosity of CD_4 to be larger or smaller than that of CH_4 at the same temperature and pressure?
9. Fluid A has a viscosity twice that of fluid B; which fluid would you expect to flow more rapidly through a horizontal tube of length L and radius R when the same pressure difference is imposed?
10. Draw a sketch of the intermolecular force $F(r)$ obtained from the Lennard-Jones function for $\varphi(r)$. Also, determine the value of r_m in Fig. 1.4-2 in terms of the Lennard-Jones parameters.
11. What main ideas are used when one goes from Newton's law of viscosity in Eq. 1.1-2 to the generalization in Eq. 1.2-6?
12. What reference works can be consulted to find out more about kinetic theory of gases and liquids, and also for obtaining useful empiricisms for calculating viscosity?

PROBLEMS

1A.1 Estimation of dense-gas viscosity. Estimate the viscosity of nitrogen at 68°F and 1000 psig by means of Fig. 1.3-1, using the critical viscosity from Table E.1. Give the result in units of $lb_m/ft \cdot s$. For the meaning of "psig," see Table F.3-2.

Answer: $1300 \times 10^{-7} lb_m/ft \cdot s$

1A.2 Estimation of the viscosity of methyl fluoride. Use Fig. 1.3-1 to find the viscosity in $Pa \cdot s$ of CH_3F at 370°C and 120 atm. Use the following values¹ for the critical constants: $T_c = 4.55^\circ C$, $p_c = 58.0$ atm, $\rho_c = 0.300$ g/cm³.

¹ K. A. Kobe and R. E. Lynn, Jr., *Chem. Revs.* **52**, 117–236 (1953), see p. 202.

1A.3 Computation of the viscosities of gases at low density. Predict the viscosities of molecular oxygen, nitrogen, and methane at 20°C and atmospheric pressure, and express the results in mPa · s. Compare the results with experimental data given in this chapter.

Answers: 0.0203, 0.0175, 0.0109 mPa · s

1A.4 Gas-mixture viscosities at low density. The following data² are available for the viscosities of mixtures of hydrogen and Freon-12 (dichlorodifluoromethane) at 25°C and 1 atm:

Mole fraction of H ₂ :	0.00	0.25	0.50	0.75	1.00
$\mu \times 10^6$ (poise):	124.0	128.1	131.9	135.1	88.4

Use the viscosities of the pure components to calculate the viscosities at the three intermediate compositions by means of Eqs. 1.4-15 and 16.

Sample answer: At 0.5, $\mu = 0.013515$ cp

1A.5 Viscosities of chlorine-air mixtures at low density. Predict the viscosities (in cp) of chlorine-air mixtures at 75°F and 1 atm, for the following mole fractions of chlorine: 0.00, 0.25, 0.50, 0.75, 1.00. Consider air as a single component and use Eqs. 1.4-14 to 16.

Answers: 0.0183, 0.0164, 0.0150, 0.0139, 0.0131 cp

1A.6 Estimation of liquid viscosity. Estimate the viscosity of saturated liquid water at 0°C and at 100°C by means of (a) Eq. 1.5-9, with $\Delta\bar{U}_{\text{vap}} = 897.5$ Btu/lb_m at 100°C, and (b) Eq. 1.5-11. Compare the results with the values in Table 1.1-1.

Answer: (b) 4.0 cp, 0.95 cp

1A.7 Molecular velocity and mean free path. Compute the mean molecular velocity \bar{u} (in cm/s) and the mean free path λ (in cm) for oxygen at 1 atm and 273.2 K. A reasonable value for d is 3 Å. What is the ratio of the mean free path to the molecular diameter under these conditions? What would be the order of magnitude of the corresponding ratio in the liquid state?

Answers: $\bar{u} = 4.25 \times 10^4$ cm/s, $\lambda = 9.3 \times 10^{-6}$ cm

1B.1 Velocity profiles and the stress components τ_{ij} . For each of the following velocity distributions, draw a meaningful sketch showing the flow pattern. Then find all the components of τ and $\rho v v$ for the Newtonian fluid. The parameter b is a constant.

- (a) $v_x = by, v_y = 0, v_z = 0$
- (b) $v_x = by, v_y = bx, v_z = 0$
- (c) $v_x = -by, v_y = bx, v_z = 0$
- (d) $v_x = -\frac{1}{2}bx, v_y = -\frac{1}{2}by, v_z = bz$

1B.2 A fluid in a state of rigid rotation.

(a) Verify that the velocity distribution (c) in Problem 1B.1 describes a fluid in a state of pure rotation; that is, the fluid

is rotating like a rigid body. What is the angular velocity of rotation?

(b) For that flow pattern evaluate the symmetric and anti-symmetric combinations of velocity derivatives:

- (i) $(\partial v_y / \partial x) + (\partial v_x / \partial y)$
- (ii) $(\partial v_y / \partial x) - (\partial v_x / \partial y)$

(c) Discuss the results of (b) in connection with the development in §1.2.

1B.3 Viscosity of suspensions. Data of Vand³ for suspensions of small glass spheres in aqueous glycerol solutions of ZnI₂ can be represented up to about $\phi = 0.5$ by the semiempirical expression

$$\frac{\mu_{\text{eff}}}{\mu_0} = 1 + 2.5\phi + 7.17\phi^2 + 16.2\phi^3 + \dots \quad (1B.3-1)$$

Compare this result with the Mooney equation.

Answer: The Mooney equation gives a good fit of Vand's data if ϕ_0 is assigned the very reasonable value of 0.70.

1C.1 Some consequences of the Maxwell-Boltzmann distribution. In the simplified kinetic theory in §1.4, several statements concerning the equilibrium behavior of a gas were made without proof. In this problem and the next, some of these statements are shown to be exact consequences of the Maxwell-Boltzmann velocity distribution.

The Maxwell-Boltzmann distribution of molecular velocities in an ideal gas at rest is

$$f(u_x, u_y, u_z) = n(m/2\pi kT)^{3/2} \exp(-mu^2/2kT) \quad (1C.1-1)$$

in which \mathbf{u} is the molecular velocity, n is the number density, and $f(u_x, u_y, u_z) du_x du_y du_z$ is the number of molecules per unit volume that is expected to have velocities between u_x and $u_x + du_x$, u_y and $u_y + du_y$, u_z and $u_z + du_z$. It follows from this equation that the distribution of the molecular speed u is

$$f(u) = 4\pi n u^2 (m/2\pi kT)^{3/2} \exp(-mu^2/2kT) \quad (1C.1-2)$$

(a) Verify Eq. 1.4-1 by obtaining the expression for the mean speed \bar{u} from

$$\bar{u} = \frac{\int_0^\infty u f(u) du}{\int_0^\infty f(u) du} \quad (1C.1-3)$$

(b) Obtain the mean values of the velocity components \bar{u}_x , \bar{u}_y , and \bar{u}_z . The first of these is obtained from

$$\bar{u}_x = \frac{\int_{-\infty}^{+\infty} \int_{-\infty}^{+\infty} \int_{-\infty}^{+\infty} u_x f(u_x, u_y, u_z) du_x du_y du_z}{\int_{-\infty}^{+\infty} \int_{-\infty}^{+\infty} \int_{-\infty}^{+\infty} f(u_x, u_y, u_z) du_x du_y du_z} \quad (1C.1-4)$$

What can one conclude from the results?

² J. W. Buddenberg and C. R. Wilke, *Ind. Eng. Chem.*, **41**, 1345–1347 (1949).

³ V. Vand, *J. Phys. Colloid Chem.*, **52**, 277–299, 300–314, 314–321 (1948).

(c) Obtain the mean kinetic energy per molecule by

$$\frac{1}{2}m\bar{u}^2 = \frac{\int_0^\infty \frac{1}{2}mu^2 f(u) du}{\int_0^\infty f(u) du} \quad (1C.1-5)$$

The correct result is $\frac{1}{2}m\bar{u}^2 = \frac{3}{2}kT$.

1C.2 The wall collision frequency. It is desired to find the frequency Z with which the molecules in an ideal gas strike a unit area of a wall from one side only. The gas is at rest and at equilibrium with a temperature T and the number density of the molecules is n . All molecules have a mass m . All molecules in the region $x < 0$ with $u_x > 0$ will hit an area S in the yz -plane in a short time Δt if they are in the volume $Su_x \Delta t$. The number of wall collisions per unit area per unit time will be

$$Z = \frac{\int_{-\infty}^{+\infty} \int_{-\infty}^{+\infty} \int_0^{+\infty} (Su_x \Delta t) f(u_x, u_y, u_z) du_x du_y du_z}{S \Delta t}$$

$$= n \left(\frac{m}{2\pi kT} \right)^{3/2} \left(\int_0^{+\infty} u_x \exp(-mu^2/2kT) du_x \right)$$

$$\left(\int_{-\infty}^{+\infty} \exp(-mu^2/2kT) du_y \right) \left(\int_{-\infty}^{+\infty} \exp(-mu^2/2kT) du_z \right)$$

$$= n \sqrt{\frac{kT}{2\pi m}} = \frac{1}{4}n\bar{u} \quad (1C.2-1)$$

Verify the above development.

1C.3 Pressure of an ideal gas.⁴ It is desired to get the pressure exerted by an ideal gas on a wall by accounting for the rate of momentum transfer from the molecules to the wall.

(a) When a molecule traveling with a velocity \mathbf{v} collides with a wall, its incoming velocity components are u_x, u_y, u_z , and after a specular reflection at the wall, its components are $-u_x, u_y, u_z$. Thus the net momentum transmitted to the wall by a molecule is $2mu_x$. The molecules that have an x -component of the velocity equal to u_x , and that will collide with the wall during a small time interval Δt , must be within the volume $Su_x \Delta t$. How many molecules with velocity components in the range from u_x, u_y, u_z to $u_x + \Delta u_x, u_y + \Delta u_y, u_z + \Delta u_z$ will hit an area S of the wall with a velocity u_x within a time interval Δt ? It will be $f(u_x, u_y, u_z)du_x du_y du_z$ times $Su_x \Delta t$. Then the pressure exerted on the wall by the gas will be

$$p = \frac{\int_{-\infty}^{+\infty} \int_{-\infty}^{+\infty} \int_{-\infty}^{+\infty} (Su_x \Delta t)(2mu_x) f(u_x, u_y, u_z) du_x du_y du_z}{S \Delta t} \quad (1C.3-1)$$

Explain carefully how this expression is constructed. Verify that this relation is dimensionally correct.

(b) Insert Eq. 1C.1-1 for the Maxwell-Boltzmann equilibrium distribution into Eq. 1C.3-1 and perform the integration. Verify that this procedure leads to $p = nkT$, the ideal gas law.

1D.1 Uniform rotation of a fluid.

(a) Verify that the velocity distribution in a fluid in a state of pure rotation (i.e., rotating as a rigid body) is $\mathbf{v} = [\mathbf{w} \times \mathbf{r}]$, where \mathbf{w} is the angular velocity (a constant) and \mathbf{r} is the position vector, with components x, y, z .

(b) What are $\nabla \mathbf{v} + (\nabla \mathbf{v})^\dagger$ and $(\nabla \cdot \mathbf{v})$ for the flow field in (a)?

(c) Interpret Eq. 1.2-7 in terms of the results in (b).

1D.2 Force on a surface of arbitrary orientation.⁵ (Fig. 1D.2) Consider the material within an element of volume $OABC$ that is in a state of equilibrium, so that the sum of the forces acting on the triangular faces $\triangle OBC$, $\triangle OCA$, $\triangle OAB$, and $\triangle ABC$ must be zero. Let the area of $\triangle ABC$ be dS , and the force per unit area acting from the minus to the plus side of dS be the vector $\boldsymbol{\pi}_n$. Show that $\boldsymbol{\pi}_n = [\mathbf{n} \cdot \boldsymbol{\pi}]$.

(a) Show that the area of $\triangle OBC$ is the same as the area of the projection $\triangle ABC$ on the yz -plane; this is $(\mathbf{n} \cdot \boldsymbol{\delta}_x)dS$. Write similar expressions for the areas of $\triangle OCA$ and $\triangle OAB$.

(b) Show that according to Table 1.2-1 the force per unit area on $\triangle OBC$ is $\boldsymbol{\delta}_x \boldsymbol{\pi}_{xx} + \boldsymbol{\delta}_y \boldsymbol{\pi}_{xy} + \boldsymbol{\delta}_z \boldsymbol{\pi}_{xz}$. Write similar force expressions for $\triangle OCA$ and $\triangle OAB$.

(c) Show that the force balance for the volume element $OABC$ gives

$$\boldsymbol{\pi}_n = \sum_i \sum_j (\mathbf{n} \cdot \boldsymbol{\delta}_i)(\boldsymbol{\delta}_j \boldsymbol{\pi}_{ij}) = [\mathbf{n} \cdot \sum_i \sum_j \boldsymbol{\delta}_i \boldsymbol{\delta}_j \boldsymbol{\pi}_{ij}] \quad (1D.2-1)$$

in which the indices i, j take on the values x, y, z . The double sum in the last expression is the stress tensor $\boldsymbol{\pi}$ written as a sum of products of unit dyads and components.

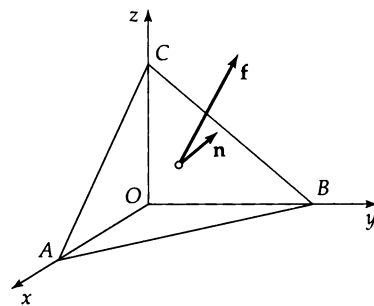


Fig. 1D.2 Element of volume $OABC$ over which a force balance is made. The vector $\boldsymbol{\pi}_n = [\mathbf{n} \cdot \boldsymbol{\pi}]$ is the force per unit area exerted by the minus material (material inside $OABC$) on the plus material (material outside $OABC$). The vector \mathbf{n} is the outwardly directed unit normal vector on face ABC .

⁴ R. J. Silbey and R. A. Alberty, *Physical Chemistry*, Wiley, New York, 3rd edition (2001), pp. 639–640.

⁵ M. Abraham and R. Becker, *The Classical Theory of Electricity and Magnetism*, Blackie and Sons, London (1952), pp. 44–45.

Shell Momentum Balances and Velocity Distributions in Laminar Flow

§2.1 Shell momentum balances and boundary conditions

§2.2 Flow of a falling film

§2.3 Flow through a circular tube

§2.4 Flow through an annulus

§2.5 Flow of two adjacent immiscible fluids

§2.6 Creeping flow around a sphere

In this chapter we show how to obtain the velocity profiles for laminar flows of fluids in simple flow systems. These derivations make use of the definition of viscosity, the expressions for the molecular and convective momentum fluxes, and the concept of a momentum balance. Once the velocity profiles have been obtained, we can then get other quantities such as the maximum velocity, the average velocity, or the shear stress at a surface. Often it is these latter quantities that are of interest in engineering problems.

In the first section we make a few general remarks about how to set up differential momentum balances. In the sections that follow we work out in detail several classical examples of viscous flow patterns. These examples should be thoroughly understood, since we shall have frequent occasions to refer to them in subsequent chapters. Although these problems are rather simple and involve idealized systems, they are nonetheless often used in solving practical problems.

The systems studied in this chapter are so arranged that the reader is gradually introduced to a variety of factors that arise in the solution of viscous flow problems. In §2.2 the falling film problem illustrates the role of gravity forces and the use of Cartesian coordinates; it also shows how to solve the problem when viscosity may be a function of position. In §2.3 the flow in a circular tube illustrates the role of pressure and gravity forces and the use of cylindrical coordinates; an approximate extension to compressible flow is given. In §2.4 the flow in a cylindrical annulus emphasizes the role played by the boundary conditions. Then in §2.5 the question of boundary conditions is pursued further in the discussion of the flow of two adjacent immiscible liquids. Finally, in §2.6 the flow around a sphere is discussed briefly to illustrate a problem in spherical coordinates and also to point out how both tangential and normal forces are handled.

The methods and problems in this chapter apply only to *steady flow*. By “steady” we mean that the pressure, density, and velocity components at each point in the stream do not change with time. The general equations for unsteady flow are given in Chapter 3.

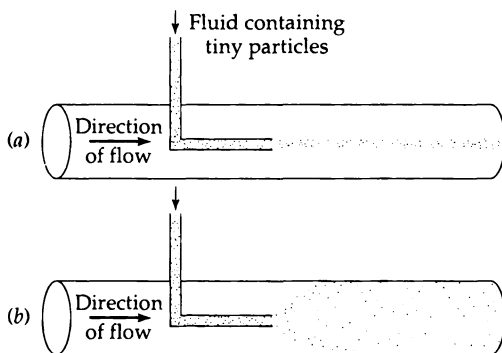


Fig. 2.0-1 (a) Laminar flow, in which fluid layers move smoothly over one another in the direction of flow, and (b) turbulent flow, in which the flow pattern is complex and time-dependent, with considerable motion perpendicular to the principal flow direction.

This chapter is concerned only with *laminar flow*. “Laminar flow” is the orderly flow that is observed, for example, in tube flow at velocities sufficiently low that tiny particles injected into the tube move along in a thin line. This is in sharp contrast with the wildly chaotic “turbulent flow” at sufficiently high velocities that the particles are flung apart and dispersed throughout the entire cross section of the tube. Turbulent flow is the subject of Chapter 5. The sketches in Fig. 2.0-1 illustrate the difference between the two flow regimes.

§2.1 SHELL MOMENTUM BALANCES AND BOUNDARY CONDITIONS

The problems discussed in §2.2 through §2.5 are approached by setting up momentum balances over a thin “shell” of the fluid. For *steady flow*, the momentum balance is

$$\left\{ \begin{array}{l} \text{rate of} \\ \text{momentum in} \\ \text{by convective} \\ \text{transport} \end{array} \right\} - \left\{ \begin{array}{l} \text{rate of} \\ \text{momentum out} \\ \text{by convective} \\ \text{transport} \end{array} \right\} + \left\{ \begin{array}{l} \text{rate of} \\ \text{momentum in} \\ \text{by molecular} \\ \text{transport} \end{array} \right\} - \left\{ \begin{array}{l} \text{rate of} \\ \text{momentum out} \\ \text{by molecular} \\ \text{transport} \end{array} \right\} + \left\{ \begin{array}{l} \text{force of gravity} \\ \text{acting on system} \end{array} \right\} = 0 \quad (2.1-1)$$

This is a restricted statement of the law of conservation of momentum. In this chapter we apply this statement only to one component of the momentum—namely, the component in the direction of flow. To write the momentum balance we need the expressions for the convective momentum fluxes given in Table 1.7-1 and the molecular momentum fluxes given in Table 1.2-1; keep in mind that the molecular momentum flux includes both the pressure and the viscous contributions.

In this chapter the momentum balance is applied only to systems in which there is just one velocity component, which depends on only one spatial variable; in addition, the flow must be rectilinear. In the next chapter the momentum balance concept is extended to unsteady-state systems with curvilinear motion and more than one velocity component.

The procedure in this chapter for setting up and solving viscous flow problems is as follows:

- Identify the nonvanishing velocity component and the spatial variable on which it depends.
- Write a momentum balance of the form of Eq. 2.1-1 over a thin shell perpendicular to the relevant spatial variable.
- Let the thickness of the shell approach zero and make use of the definition of the first derivative to obtain the corresponding differential equation for the momentum flux.

- Integrate this equation to get the momentum-flux distribution.
- Insert Newton's law of viscosity and obtain a differential equation for the velocity.
- Integrate this equation to get the velocity distribution.
- Use the velocity distribution to get other quantities, such as the maximum velocity, average velocity, or force on solid surfaces.

In the integrations mentioned above, several constants of integration appear, and these are evaluated by using "boundary conditions"—that is, statements about the velocity or stress at the boundaries of the system. The most commonly used boundary conditions are as follows:

- a. At *solid–fluid* interfaces the fluid velocity equals the velocity with which the solid surface is moving; this statement is applied to both the tangential and the normal component of the velocity vector. The equality of the tangential components is referred to as the "no-slip condition."
- b. At a *liquid–liquid* interfacial plane of constant x , the tangential velocity components v_y and v_z are continuous through the interface (the "no-slip condition") as are also the molecular stress-tensor components $p + \tau_{xx}$, τ_{xy} , and τ_{xz} .
- c. At a *liquid–gas* interfacial plane of constant x , the stress-tensor components τ_{xy} and τ_{xz} are taken to be zero, provided that the gas-side velocity gradient is not too large. This is reasonable, since the viscosities of gases are much less than those of liquids.

In all of these boundary conditions it is presumed that there is no material passing through the interface; that is, there is no adsorption, absorption, dissolution, evaporation, melting, or chemical reaction at the surface between the two phases. Boundary conditions incorporating such phenomena appear in Problems 3C.5 and 11C.6, and §18.1.

In this section we have presented some guidelines for solving simple viscous flow problems. For some problems slight variations on these guidelines may prove to be appropriate.

§2.2 FLOW OF A FALLING FILM

The first example we discuss is that of the flow of a liquid down an inclined flat plate of length L and width W , as shown in Fig. 2.2-1. Such films have been studied in connection with wetted-wall towers, evaporation and gas-absorption experiments, and applications of coatings. We consider the viscosity and density of the fluid to be constant.

A complete description of the liquid flow is difficult because of the disturbances at the edges of the system ($z = 0, z = L, y = 0, y = W$). An adequate description can often be

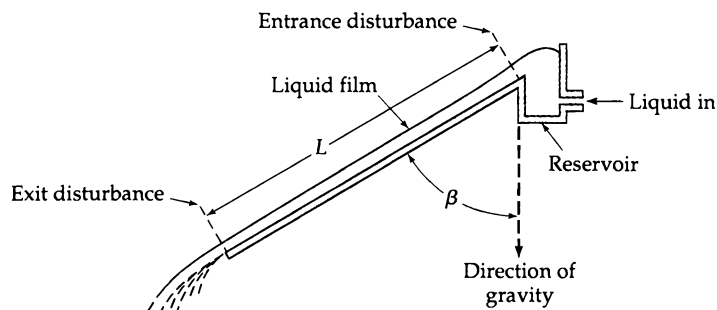


Fig. 2.2-1 Schematic diagram of the falling film experiment, showing end effects.

obtained by neglecting such disturbances, particularly if W and L are large compared to the film thickness δ . For small flow rates we expect that the viscous forces will prevent continued acceleration of the liquid down the wall, so that v_z will become independent of z in a short distance down the plate. Therefore it seems reasonable to postulate that $v_z = v_z(x)$, $v_x = 0$, and $v_y = 0$, and further that $p = p(x)$. From Table B.1 it is seen that the only nonvanishing components of τ are then $\tau_{xz} = \tau_{zx} = -\mu(dv_z/dx)$.

We now select as the "system" a thin shell perpendicular to the x direction (see Fig. 2.2-2). Then we set up a z -momentum balance over this shell, which is a region of thickness Δx , bounded by the planes $z = 0$ and $z = L$, and extending a distance W in the y direction. The various contributions to the momentum balance are then obtained with the help of the quantities in the "z-component" columns of Tables 1.2-1 and 1.7-1. By using the components of the "combined momentum-flux tensor" ϕ defined in 1.7-1 to 3, we can include all the possible mechanisms for momentum transport at once:

$$\text{rate of } z\text{-momentum in across surface at } z = 0 \quad (W\Delta x)\phi_{zz}|_{z=0} \quad (2.2-1)$$

$$\text{rate of } z\text{-momentum out across surface at } z = L \quad (W\Delta x)\phi_{zz}|_{z=L} \quad (2.2-2)$$

$$\text{rate of } z\text{-momentum in across surface at } x \quad (LW)(\phi_{xz})|_x \quad (2.2-3)$$

$$\text{rate of } z\text{-momentum out across surface at } x + \Delta x \quad (LW)(\phi_{xz})|_{x+\Delta x} \quad (2.2-4)$$

$$\text{gravity force acting on fluid in the } z \text{ direction} \quad (LW\Delta x)(\rho g \cos \beta) \quad (2.2-5)$$

By using the quantities ϕ_{xz} and ϕ_{zz} we account for the z -momentum transport by all mechanisms, convective and molecular. Note that we take the "in" and "out" directions in the direction of the positive x - and z -axes (in this problem these happen to coincide with the directions of z -momentum transport). The notation $|_{x+\Delta x}$ means "evaluated at $x + \Delta x$," and g is the gravitational acceleration.

When these terms are substituted into the z -momentum balance of Eq. 2.1-1, we get

$$LW(\phi_{xz}|_x - \phi_{xz}|_{x+\Delta x}) + W\Delta x(\phi_{zz}|_{z=0} - \phi_{zz}|_{z=L}) + (LW\Delta x)(\rho g \cos \beta) = 0 \quad (2.2-6)$$

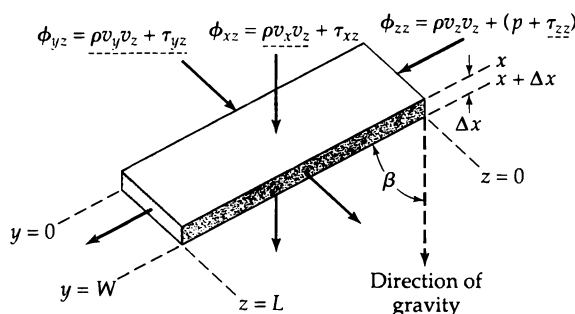


Fig. 2.2-2 Shell of thickness Δx over which a z -momentum balance is made. Arrows show the momentum fluxes associated with the surfaces of the shell. Since v_x and v_y are both zero, $\rho v_x v_z$ and $\rho v_y v_z$ are zero. Since v_z does not depend on y and z , it follows from Table B.1 that $\tau_{yz} = 0$ and $\tau_{zz} = 0$. Therefore, the dashed-underlined fluxes do not need to be considered. Both p and $\rho v_z v_z$ are the same at $z = 0$ and $z = L$, and therefore do not appear in the final equation for the balance of z -momentum, Eq. 2.2-10.

When this equation is divided by $LW\Delta x$, and the limit taken as Δx approaches zero, we get

$$\lim_{\Delta x \rightarrow 0} \left(\frac{\phi_{xz}|_{x+\Delta x} - \phi_{xz}|_x}{\Delta x} \right) - \frac{\phi_{zz}|_{z=0} - \phi_{zz}|_{z=L}}{L} = \rho g \cos \beta \quad (2.2-7)$$

The first term on the left side is exactly the definition of the derivative of ϕ_{xz} with respect to x . Therefore Eq. 2.2-7 becomes

$$\frac{\partial \phi_{xz}}{\partial x} - \frac{\phi_{zz}|_{z=0} - \phi_{zz}|_{z=L}}{L} = \rho g \cos \beta \quad (2.2-8)$$

At this point we have to write out explicitly what the components ϕ_{xz} and ϕ_{zz} are, making use of the definition of ϕ in Eqs. 1.7-1 to 3 and the expressions for τ_{xz} and τ_{zz} in Appendix B.1. This ensures that we do not miss out on any of the forms of momentum transport. Hence we get

$$\phi_{xz} = \tau_{xz} + \rho v_x v_z = -\mu \frac{\partial v_z}{\partial x} + \rho v_x v_z \quad (2.2-9a)$$

$$\phi_{zz} = p + \tau_{zz} + \rho v_z v_z = p - 2\mu \frac{\partial v_z}{\partial z} + \rho v_z v_z \quad (2.2-9b)$$

In accordance with the postulates that $v_z = v_z(x)$, $v_x = 0$, $v_y = 0$, and $p = p(x)$, we see that (i) since $v_x = 0$, the $\rho v_x v_z$ term in Eq. 2.2-9a is zero; (ii) since $v_z = v_z(x)$, the term $-2\mu(\partial_z/\partial z)$ in Eq. 2.2-9b is zero; (iii) since $v_z = v_z(x)$, the term $\rho v_z v_z$ is the same at $z = 0$ and $z = L$; and (iv) since $p = p(x)$, the contribution p is the same at $z = 0$ and $z = L$. Hence τ_{xz} depends only on x , and Eq. 2.2-8 simplifies to

$$\boxed{\frac{d\tau_{xz}}{dx} = \rho g \cos \beta} \quad (2.2-10)$$

This is the differential equation for the momentum flux τ_{xz} . It may be integrated to give

$$\tau_{xz} = (\rho g \cos \beta)x + C_1 \quad (2.2-11)$$

The constant of integration may be evaluated by using the boundary condition at the gas–liquid interface (see §2.1):

$$\text{B.C. 1:} \quad \text{at } x = 0, \quad \tau_{xz} = 0 \quad (2.2-12)$$

Substitution of this boundary condition into Eq. 2.2-11 shows that $C_1 = 0$. Therefore the momentum-flux distribution is

$$\tau_{xz} = (\rho g \cos \beta)x \quad (2.2-13)$$

as shown in Fig. 2.2-3.

Next we substitute Newton's law of viscosity

$$\tau_{xz} = -\mu \frac{dv_z}{dx} \quad (2.2-14)$$

into the left side of Eq. 2.2-13 to obtain

$$\frac{dv_z}{dx} = -\left(\frac{\rho g \cos \beta}{\mu}\right)x \quad (2.2-15)$$

which is the differential equation for the velocity distribution. It can be integrated to give

$$v_z = -\left(\frac{\rho g \cos \beta}{2\mu}\right)x^2 + C_2 \quad (2.2-16)$$

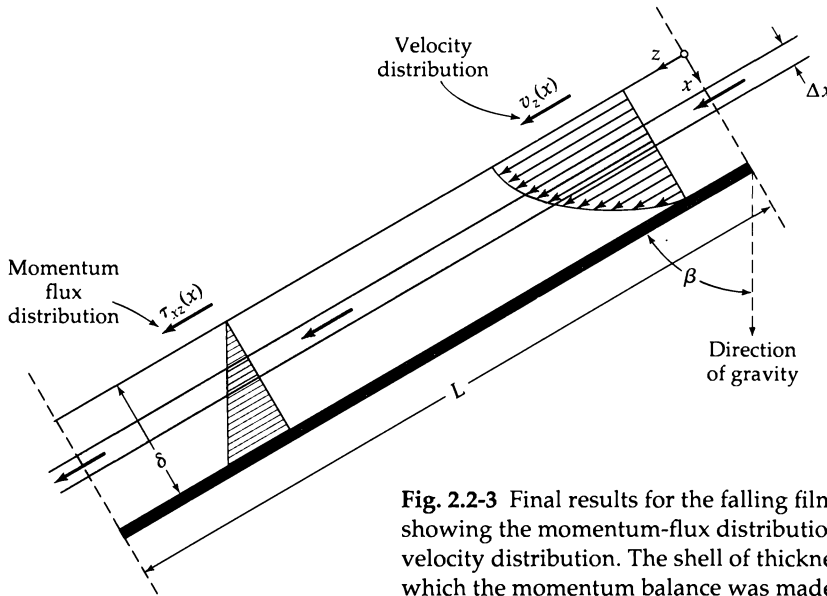


Fig. 2.2-3 Final results for the falling film problem, showing the momentum-flux distribution and the velocity distribution. The shell of thickness Δx , over which the momentum balance was made, is also shown.

The constant of integration is evaluated by using the no-slip boundary condition at the solid surface:

$$\text{B.C. 2} \quad \text{at } x = \delta, \quad v_z = 0 \quad (2.2-17)$$

Substitution of this boundary condition into Eq. 2.2-16 shows that $C_2 = (\rho g \cos \beta / 2\mu)\delta^2$. Consequently, the velocity distribution is

$$v_z = \frac{\rho g \delta^2 \cos \beta}{2\mu} \left[1 - \left(\frac{x}{\delta} \right)^2 \right] \quad (2.2-18)$$

This parabolic velocity distribution is shown in Fig. 2.2-3. It is consistent with the postulates made initially and must therefore be a *possible* solution. Other solutions might be possible, and experiments are normally required to tell whether other flow patterns can actually arise. We return to this point after Eq. 2.2-23.

Once the velocity distribution is known, a number of quantities can be calculated:

(i) The *maximum velocity* $v_{z,\max}$ is clearly the velocity at $x = 0$; that is,

$$v_{z,\max} = \frac{\rho g \delta^2 \cos \beta}{2\mu} \quad (2.2-19)$$

(ii) The *average velocity* $\langle v_z \rangle$ over a cross section of the film is obtained as follows:

$$\begin{aligned} \langle v_z \rangle &= \frac{\int_0^W \int_0^\delta v_z dx dy}{\int_0^W \int_0^\delta dx dy} = \frac{1}{\delta} \int_0^\delta v_z dx \\ &= \frac{\rho g \delta^2 \cos \beta}{2\mu} \int_0^1 \left[1 - \left(\frac{x}{\delta} \right)^2 \right] d\left(\frac{x}{\delta} \right) \\ &= \frac{\rho g \delta^2 \cos \beta}{3\mu} = \frac{2}{3} v_{z,\max} \end{aligned} \quad (2.2-20)$$

The double integral in the denominator of the first line is the cross-sectional area of the film. The double integral in the numerator is the volume flow rate through a differential element of the cross section, $v_z dx dy$, integrated over the entire cross section.

(iii) The *mass rate of flow w* is obtained from the average velocity or by integration of the velocity distribution

$$w = \int_0^W \int_0^\delta \rho v_z dx dy = \rho W \delta \langle v_z \rangle = \frac{\rho^2 g W \delta^3 \cos \beta}{3\mu} \quad (2.2-21)$$

(iv) The *film thickness δ* may be given in terms of the average velocity or the mass rate of flow as follows:

$$\delta = \sqrt{\frac{3\mu \langle v_z \rangle}{\rho g \cos \beta}} = \sqrt[3]{\frac{3\mu w}{\rho^2 g W \cos \beta}} \quad (2.2-22)$$

(v) The force per unit area in the z direction on a surface element perpendicular to the x direction is $+\tau_{xz}$ evaluated at $x = \delta$. This is the force exerted by the fluid (region of lesser x) on the wall (region of greater x). The z -component of the *force F of the fluid on the solid surface* is obtained by integrating the shear stress over the fluid–solid interface:

$$\begin{aligned} F_z &= \int_0^L \int_0^W (\tau_{xz}|_{x=\delta}) dy dz = \int_0^L \int_0^W \left(-\mu \frac{dv_z}{dx} \Big|_{x=\delta} \right) dy dz \\ &= (LW)(-\mu) \left(-\frac{\rho g \delta \cos \beta}{\mu} \right) = \rho g \delta LW \cos \beta \end{aligned} \quad (2.2-23)$$

This is the z -component of the weight of the fluid in the entire film—as we would have expected.

Experimental observations of falling films show that there are actually three “flow regimes,” and that these may be classified according to the *Reynolds number*,¹ Re , for the flow. For falling films the Reynolds number is defined by $Re = 4\delta \langle v_z \rangle \rho / \mu$. The three flow regime are then:

laminar flow with negligible rippling	$Re < 20$
laminar flow with pronounced rippling	$20 < Re < 1500$
turbulent flow	$Re > 1500$

The analysis we have given above is valid only for the first regime, since the analysis was restricted by the postulates made at the outset. Ripples appear on the surface of the fluid at all Reynolds numbers. For Reynolds numbers less than about 20, the ripples are very long and grow rather slowly as they travel down the surface of the liquid; as a result the formulas derived above are useful up to about $Re = 20$ for plates of moderate length. Above that value of Re , the ripple growth increases very rapidly, although the flow remains laminar. At about $Re = 1500$ the flow becomes irregular and chaotic, and the flow is said to be turbulent.^{2,3} At this point it is not clear why the value of the

¹This dimensionless group is named for **Osborne Reynolds** (1842–1912), professor of engineering at the University of Manchester. He studied the laminar-turbulent transition, turbulent heat transfer, and theory of lubrication. We shall see in the next chapter that the Reynolds number is the ratio of the inertial forces to the viscous forces.

²G. D. Fulford, *Adv. Chem. Engr.*, **5**, 151–236 (1964); S. Whitaker, *Ind. Eng. Chem. Fund.*, **3**, 132–142 (1964); V. G. Levich, *Physicochemical Hydrodynamics*, Prentice-Hall, Englewood Cliffs, N.J. (1962), §135.

³H.-C. Chang, *Ann. Rev. Fluid Mech.*, **26**, 103–136 (1994); S.-H. Hwang and H.-C. Chang, *Phys. Fluids*, **30**, 1259–1268 (1987).

Reynolds number should be used to delineate the flow regimes. We shall have more to say about this in §3.7.

This discussion illustrates a very important point: theoretical analysis of flow systems is limited by the postulates that are made in setting up the problem. It is absolutely necessary to do experiments in order to establish the flow regimes so as to know when instabilities (spontaneous oscillations) occur and when the flow becomes turbulent. Some information about the onset of instability and the demarcation of the flow regimes can be obtained by theoretical analysis, but this is an extraordinarily difficult subject. This is a result of the inherent nonlinear nature of the governing equations of fluid dynamics, as will be explained in Chapter 3. Suffice it to say at this point that experiments play a *very* important role in the field of fluid dynamics.

EXAMPLE 2.2-1

Calculation of Film Velocity

An oil has a kinematic viscosity of $2 \times 10^{-4} \text{ m}^2/\text{s}$ and a density of $0.8 \times 10^3 \text{ kg/m}^3$. If we want to have a falling film of thickness of 2.5 mm on a vertical wall, what should the mass rate of flow of the liquid be?

SOLUTION

According to Eq. 2.2-21, the mass rate of flow in kg/s is

$$w = \frac{\rho g \delta^3 W}{3\nu} = \frac{(0.8 \times 10^3)(9.80)(2.5 \times 10^{-3})^3 W}{3(2 \times 10^{-4})} = 0.204 W \quad (2.2-24)$$

To get the mass rate of flow one then needs to insert a value for the width of the wall in meters. This is the desired result provided that the flow is laminar and nonrippling. To determine the flow regime we calculate the Reynolds number, making use of Eqs. 2.2-21 and 24

$$\text{Re} = \frac{4\delta \langle v_z \rangle \rho}{\mu} = \frac{4w/W}{\nu\rho} = \frac{4(0.204)}{(2 \times 10^{-4})(0.8 \times 10^3)} = 5.1 \quad (2.2-25)$$

This Reynolds number is sufficiently low that rippling will not be pronounced, and therefore the expression for the mass rate of flow in Eq. 2.2-24 is reasonable.

EXAMPLE 2.2-2

Falling Film with Variable Viscosity

Rework the falling film problem for a position-dependent viscosity $\mu = \mu_0 e^{-\alpha x/\delta}$, which arises when the film is nonisothermal, as in the condensation of a vapor on a wall. Here μ_0 is the viscosity at the surface of the film and α is a constant that describes how rapidly μ decreases as x increases. Such a variation could arise in the flow of a condensate down a wall with a linear temperature gradient through the film.

SOLUTION

The development proceeds as before up to Eq. 2.2-13. Then substituting Newton's law with variable viscosity into Eq. 2.2-13 gives

$$-\mu_0 e^{-\alpha x/\delta} \frac{dv_z}{dx} = \rho g x \cos \beta \quad (2.2-26)$$

This equation can be integrated, and using the boundary conditions in Eq. 2.2-17 enables us to evaluate the integration constant. The velocity profile is then

$$v_z = \frac{\rho g \delta^2 \cos \beta}{\mu_0} \left[e^\alpha \left(\frac{1}{\alpha} - \frac{1}{\alpha^2} \right) - e^{\alpha x/\delta} \left(\frac{x}{\alpha \delta} - \frac{1}{\alpha^2} \right) \right] \quad (2.2-27)$$

As a check we evaluate the velocity distribution for the constant-viscosity problem (that is, when α is zero). However, setting $\alpha = 0$ gives $\infty - \infty$ in the two expressions within parentheses.

This difficulty can be overcome if we expand the two exponentials in Taylor series (see §C.2), as follows:

$$\begin{aligned}
 (v_z)_{\alpha=0} &= \frac{\rho g \delta^2 \cos \beta}{\mu_0} \lim_{\alpha \rightarrow 0} \left[\left(1 + \alpha + \frac{\alpha^2}{2!} + \frac{\alpha^3}{3!} + \dots \right) \left(\frac{1}{\alpha} - \frac{1}{\alpha^2} \right) \right. \\
 &\quad \left. - \left(1 + \frac{\alpha x}{\delta} + \frac{\alpha^2 x^2}{2! \delta^2} + \frac{\alpha^3 x^3}{3! \delta^3} + \dots \right) \left(\frac{x}{\alpha \delta} - \frac{1}{\alpha^2} \right) \right] \\
 &= \frac{\rho g \delta^2 \cos \beta}{\mu_0} \lim_{\alpha \rightarrow 0} \left[\left(\frac{1}{2} + \frac{1}{3} \alpha + \dots \right) - \left(\frac{1}{2} \frac{x^2}{\delta^2} - \frac{1}{3} \frac{x^3}{\delta^3} \alpha + \dots \right) \right] \\
 &= \frac{\rho g \delta^2 \cos \beta}{2 \mu_0} \left[1 - \left(\frac{x}{\delta} \right)^2 \right]
 \end{aligned} \tag{2.2-28}$$

which is in agreement with Eq. 2.2-18.

From Eq. 2.2-27 it may be shown that the average velocity is

$$\langle v_z \rangle = \frac{\rho g \delta^2 \cos \beta}{\mu_0} \left[e^\alpha \left(\frac{1}{\alpha} - \frac{2}{\alpha^2} + \frac{2}{\alpha^3} \right) - \frac{2}{\alpha^3} \right] \tag{2.2-29}$$

The reader may verify that this result simplifies to Eq. 2.2-20 when α goes to zero.

§2.3 FLOW THROUGH A CIRCULAR TUBE

The flow of fluids in circular tubes is encountered frequently in physics, chemistry, biology, and engineering. The laminar flow of fluids in circular tubes may be analyzed by means of the momentum balance described in §2.1. The only new feature introduced here is the use of cylindrical coordinates, which are the natural coordinates for describing positions in a pipe of circular cross section.

We consider then the steady-state, laminar flow of a fluid of constant density ρ and viscosity μ in a vertical tube of length L and radius R . The liquid flows downward under the influence of a pressure difference and gravity; the coordinate system is that shown in Fig. 2.3-1. We specify that the tube length be very large with respect to the tube radius, so that "end effects" will be unimportant throughout most of the tube; that is, we can ignore the fact that at the tube entrance and exit the flow will not necessarily be parallel to the tube wall.

We postulate that $v_z = v_z(r)$, $v_r = 0$, $v_\theta = 0$, and $p = p(z)$. With these postulates it may be seen from Table B.1 that the only nonvanishing components of τ are $\tau_{rz} = \tau_{zr} = -\mu(dv_z/dr)$.

We select as our system a cylindrical shell of thickness Δr and length L and we begin by listing the various contributions to the z-momentum balance:

$$\text{rate of } z\text{-momentum in} \qquad \qquad \qquad (2\pi r \Delta r)(\phi_{zz})|_{z=0} \tag{2.3-1}$$

across annular surface at $z = 0$

$$\text{rate of } z\text{-momentum out} \qquad \qquad \qquad (2\pi r \Delta r)(\phi_{zz})|_{z=L} \tag{2.3-2}$$

across annular surface at $z = L$

$$\text{rate of } z\text{-momentum in} \qquad \qquad \qquad (2\pi r L)(\phi_{rz})|_r = (2\pi r L \phi_{rz})|_r \tag{2.3-3}$$

across cylindrical surface at r

$$\text{rate of } z\text{-momentum out} \qquad \qquad \qquad (2\pi(r + \Delta r)L)(\phi_{rz})|_{r+\Delta r} = (2\pi r L \phi_{rz})|_{r+\Delta r} \tag{2.3-4}$$

across cylindrical surface at $r + \Delta r$

$$\text{gravity force acting in} \qquad \qquad \qquad (2\pi r \Delta r L) \rho g \tag{2.3-5}$$

z direction on cylindrical shell

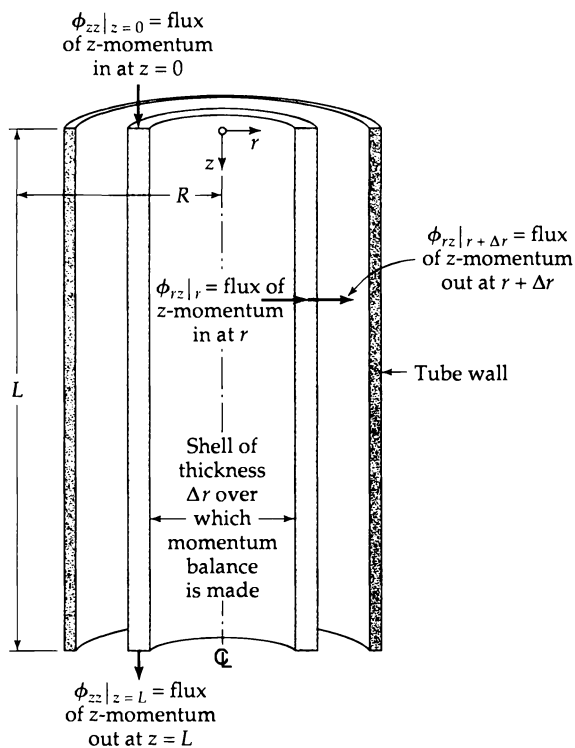


Fig. 2.3-1 Cylindrical shell of fluid over which the z -momentum balance is made for axial flow in a circular tube (see Eqs. 2.3-1 to 5). The z -momentum fluxes ϕ_{rz} and ϕ_{zz} are given in full in Eqs. 2.3-9a and 9b.

The quantities ϕ_{zz} and ϕ_{rz} account for the momentum transport by all possible mechanisms, convective and molecular. In Eq. 2.3-4, $(r + \Delta r)$ and $(r)|_{r+\Delta r}$ are two ways of writing the same thing. Note that we take “in” and “out” to be in the positive directions of the r - and z -axes.

We now add up the contributions to the momentum balance:

$$(2\pi r L \phi_{rz})|_r - (2\pi r L \phi_{rz})|_{r+\Delta r} + (2\pi r \Delta r)(\phi_{zz})|_{z=0} - (2\pi r \Delta r)(\phi_{zz})|_{z=L} + (2\pi r \Delta r L) \rho g = 0 \quad (2.3-6)$$

When we divide Eq. (2.3-8) by $2\pi L \Delta r$ and take the limit as $\Delta r \rightarrow 0$, we get

$$\lim_{\Delta r \rightarrow 0} \left(\frac{(r\phi_{rz})|_{r+\Delta r} - (r\phi_{rz})|_r}{\Delta r} \right) = \left(\frac{\phi_{zz}|_{z=0} - \phi_{zz}|_{z=L}}{L} + \rho g \right) r \quad (2.3-7)$$

The expression on the left side is the definition of the first derivative of $r\tau_{rz}$ with respect to r . Hence Eq. 2.3-7 may be written as

$$\frac{\partial}{\partial r} (r\phi_{rz}) = \left(\frac{\phi_{zz}|_{z=0} - \phi_{zz}|_{z=L}}{L} + \rho g \right) r \quad (2.3-8)$$

Now we have to evaluate the components ϕ_{rz} and ϕ_{zz} from Eq. 1.7-1 and Appendix B.1:

$$\phi_{rz} = \tau_{rz} + \rho v_r v_z = -\mu \frac{\partial v_z}{\partial r} + \rho v_r v_z \quad (2.3-9a)$$

$$\phi_{zz} = p + \tau_{zz} + \rho v_z v_z = p - 2\mu \frac{\partial v_z}{\partial z} + \rho v_z v_z \quad (2.3-9b)$$

Next we take into account the postulates made at the beginning of the problem—namely, that $v_z = v_z(r)$, $v_r = 0$, $v_\theta = 0$, and $p = p(z)$. Then we make the following simplifications:

(i) because $v_r = 0$, we can drop the term $\rho v_r v_z$ in Eq. 2.3-9a; (ii) because $v_z = v_z(r)$, the term $\rho v_z v_z$ will be the same at both ends of the tube; and (iii) because $v_z = v_z(r)$, the term $-2\mu \partial v_z / \partial z$ will be the same at both ends of the tube. Hence Eq. 2.3-8 simplifies to

$$\frac{d}{dr} (r \tau_{rz}) = \left(\frac{(p_0 - \mathcal{P}_0) - (p_L - \mathcal{P}_L)}{L} \right) r \equiv \left(\frac{\mathcal{P}_0 - \mathcal{P}_L}{L} \right) r \quad (2.3-10)$$

in which $\mathcal{P} = p - \rho g z$ is a convenient abbreviation for the sum of the pressure and gravitational terms.¹ Equation 2.3-10 may be integrated to give

$$\tau_{rz} = \left(\frac{\mathcal{P}_0 - \mathcal{P}_L}{2L} \right) r + \frac{C_1}{r} \quad (2.3-11)$$

The constant C_1 is evaluated by using the boundary condition

$$\text{B.C. 1:} \quad \text{at } r = 0, \quad \tau_{rz} = \text{finite} \quad (2.3-12)$$

Consequently C_1 must be zero, for otherwise the momentum flux would be infinite at the axis of the tube. Therefore the momentum flux distribution is

$$\tau_{rz} = \left(\frac{\mathcal{P}_0 - \mathcal{P}_L}{2L} \right) r \quad (2.3-13)$$

This distribution is shown in Fig. 2.3-2.

Newton's law of viscosity for this situation is obtained from Appendix B.2 as follows:

$$\tau_{rz} = -\mu \frac{dv_z}{dr} \quad (2.3-14)$$

Substitution of this expression into Eq. 2.3-13 then gives the following differential equation for the velocity:

$$\frac{dv_z}{dr} = -\left(\frac{\mathcal{P}_0 - \mathcal{P}_L}{2\mu L} \right) r \quad (2.3-15)$$

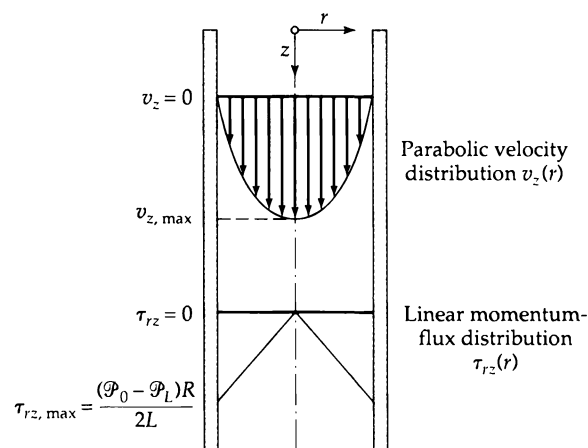


Fig. 2.3-2 The momentum-flux distribution and velocity distribution for the downward flow in a circular tube.

¹ The quantity designated by \mathcal{P} is called the *modified pressure*. In general it is defined by $\mathcal{P} = p + \rho gh$, where h is the distance "upward"—that is, in the direction opposed to gravity from some preselected reference plane. Hence in this problem $h = -z$.

This first-order separable differential equation may be integrated to give

$$v_z = -\left(\frac{\mathcal{P}_0 - \mathcal{P}_L}{4\mu L}\right)r^2 + C_2 \quad (2.3-16)$$

The constant C_2 is evaluated from the boundary condition

$$\text{B.C. 2:} \quad \text{at } r = R, \quad v_z = 0 \quad (2.3-17)$$

From this C_2 is found to be $(\mathcal{P}_0 - \mathcal{P}_L)R^2/4\mu L$. Hence the velocity distribution is

$$v_z = \frac{(\mathcal{P}_0 - \mathcal{P}_L)R^2}{4\mu L} \left[1 - \left(\frac{r}{R} \right)^2 \right] \quad (2.3-18)$$

We see that the velocity distribution for laminar, incompressible flow of a Newtonian fluid in a long tube is parabolic (see Fig. 2.3-2).

Once the velocity profile has been established, various derived quantities can be obtained:

- (i) The *maximum velocity* $v_{z,\max}$ occurs at $r = 0$ and is

$$v_{z,\max} = \frac{(\mathcal{P}_0 - \mathcal{P}_L)R^2}{4\mu L} \quad (2.3-19)$$

- (ii) The *average velocity* $\langle v_z \rangle$ is obtained by dividing the total volumetric flow rate by the cross-sectional area

$$\langle v_z \rangle = \frac{\int_0^{2\pi} \int_0^R v_z r dr d\theta}{\int_0^{2\pi} \int_0^R r dr d\theta} = \frac{(\mathcal{P}_0 - \mathcal{P}_L)R^2}{8\mu L} = \frac{1}{2}v_{z,\max} \quad (2.3-20)$$

- (iii) The *mass rate of flow* w is the product of the cross-sectional area πR^2 , the density ρ , and the average velocity $\langle v_z \rangle$

$$w = \frac{\pi(\mathcal{P}_0 - \mathcal{P}_L)R^4\rho}{8\mu L} \quad (2.3-21)$$

This rather famous result is called the *Hagen–Poiseuille² equation*. It is used, along with experimental data for the rate of flow and the modified pressure difference, to determine the viscosity of fluids (see Example 2.3-1) in a “capillary viscometer.”

- (iv) The *z-component of the force*, F_z , of the fluid on the wetted surface of the pipe is just the shear stress τ_{rz} integrated over the wetted area

$$\begin{aligned} F_z &= (2\pi RL) \left(-\mu \frac{dv_z}{dr} \right) \Big|_{r=R} = \pi R^2 (\mathcal{P}_0 - \mathcal{P}_L) \\ &= \pi R^2 (p_0 - p_L) + \pi R^2 L \rho g \end{aligned} \quad (2.3-22)$$

This result states that the viscous force F_z is counterbalanced by the net pressure force and the gravitational force. This is exactly what one would obtain from making a force balance over the fluid in the tube.

² G. Hagen, *Ann. Phys. Chem.*, **46**, 423–442 (1839); J. L. Poiseuille, *Comptes Rendus*, **11**, 961 and 1041 (1841). Jean Louis Poiseuille (1799–1869) (pronounced “Pwa-zo’-yuh,” with σ is roughly the “oo” in book) was a physician interested in the flow of blood. Although Hagen and Poiseuille established the dependence of the flow rate on the fourth power of the tube radius, Eq. 2.3-21 was first derived by E. Hagenbach, *Pogg. Annalen der Physik u. Chemie*, **108**, 385–426 (1860).

The results of this section are only as good as the postulates introduced at the beginning of the section—namely, that $v_z = v_z(r)$ and $p = p(z)$. Experiments have shown that these postulates are in fact realized for Reynolds numbers up to about 2100; above that value, the flow will be turbulent if there are any appreciable disturbances in the system—that is, wall roughness or vibrations.³ For circular tubes the Reynolds number is defined by $Re = D\langle v_z \rangle \rho / \mu$, where $D = 2R$ is the tube diameter.

We now summarize all the assumptions that were made in obtaining the Hagen–Poiseuille equation.

- (a) The flow is laminar; that is, Re must be less than about 2100.
- (b) The density is constant (“incompressible flow”).
- (c) The flow is “steady” (i.e., it does not change with time).
- (d) The fluid is Newtonian (Eq. 2.3-14 is valid).
- (e) End effects are neglected. Actually an “entrance length,” after the tube entrance, of the order of $L_e = 0.035D Re$, is needed for the buildup to the parabolic profile. If the section of pipe of interest includes the entrance region, a correction must be applied.⁴ The fractional correction in the pressure difference or mass rate of flow never exceeds L_e/L if $L > L_e$.
- (f) The fluid behaves as a continuum—this assumption is valid, except for very dilute gases or very narrow capillary tubes, in which the molecular mean free path is comparable to the tube diameter (the “slip flow region”) or much greater than the tube diameter (the “Knudsen flow” or “free molecule flow” regime).⁵
- (g) There is no slip at the wall, so that B.C. 2 is valid; this is an excellent assumption for pure fluids under the conditions assumed in (f). See Problem 2B.9 for a discussion of wall slip.

EXAMPLE 2.3-1

Determination of Viscosity from Capillary Flow Data

Glycerine ($\text{CH}_2\text{OH} \cdot \text{CHOH} \cdot \text{CH}_2\text{OH}$) at 26.5°C is flowing through a horizontal tube 1 ft long and with 0.1 in. inside diameter. For a pressure drop of 40 psi, the volume flow rate w/ρ is $0.00398 \text{ ft}^3/\text{min}$. The density of glycerine at 26.5°C is 1.261 g/cm^3 . From the flow data, find the viscosity of glycerine in centipoises and in $\text{Pa} \cdot \text{s}$.

SOLUTION

From the Hagen–Poiseuille equation (Eq. 2.3-21), we find

$$\begin{aligned} \mu &= \frac{\pi(p_0 - p_L)R^4}{8(w/\rho)L} \\ &= \frac{\pi \left(40 \frac{\text{lb}_f}{\text{in.}^2} \right) \left(6.8947 \times 10^4 \frac{\text{dyn}/\text{cm}^2}{\text{lb}_f/\text{in.}^2} \right) \left(0.05 \text{ in.} \times \frac{1 \text{ ft}}{12 \text{ in.}} \right)^4}{8 \left(0.00398 \frac{\text{ft}^3}{\text{min}} \times \frac{1 \text{ min}}{60 \text{ s}} \right) (1 \text{ ft})} \\ &= 4.92 \text{ g/cm} \cdot \text{s} = 492 \text{ cp} = 0.492 \text{ Pa} \cdot \text{s} \end{aligned} \quad (2.3-23)$$

³ A. A. Draad [Doctoral Dissertation, Technical University of Delft (1996)] in a carefully controlled experiment, attained laminar flow up to $Re = 60,000$. He also studied the nonparabolic velocity profile induced by the earth’s rotation (through the Coriolis effect). See also A. A. Draad and F. T. M. Nieuwstadt, *J. Fluid. Mech.*, **361**, 207–308 (1998).

⁴ J. H. Perry, *Chemical Engineers Handbook*, McGraw-Hill, New York, 3rd edition (1950), pp. 388–389; W. M. Kays and A. L. London, *Compact Heat Exchangers*, McGraw-Hill, New York (1958), p. 49.

⁵ Martin Hans Christian Knudsen (1871–1949), professor of physics at the University of Copenhagen, did key experiments on the behavior of very dilute gases. The lectures he gave at the University of Glasgow were published as M. Knudsen, *The Kinetic Theory of Gases*, Methuen, London (1934); G. N. Patterson, *Molecular Flow of Gases*, Wiley, New York (1956). See also J. H. Ferziger and H. G. Kaper, *Mathematical Theory of Transport Processes in Gases*, North-Holland, Amsterdam (1972), Chapter 15.

To check whether the flow is laminar, we calculate the Reynolds number

$$\begin{aligned} \text{Re} &= \frac{D\langle v_z \rangle \rho}{\mu} = \frac{4(w/\rho)\rho}{\pi D \mu} \\ &= \frac{4(0.00398 \frac{\text{ft}^3}{\text{min}})(2.54 \frac{\text{cm}}{\text{in.}} \times 12 \frac{\text{in.}}{\text{ft}})^3 \left(\frac{1}{60} \frac{\text{min}}{\text{s}}\right) \left(1.261 \frac{\text{g}}{\text{cm}^3}\right)}{\pi \left(0.1 \text{ in.} \times 2.54 \frac{\text{cm}}{\text{in.}}\right) \left(4.92 \frac{\text{g}}{\text{cm} \cdot \text{s}}\right)} \\ &= 2.41 \text{ (dimensionless)} \end{aligned} \quad (2.3-24)$$

Hence the flow is indeed laminar. Furthermore, the entrance length is

$$L_e = 0.035D \text{ Re} = (0.035)(0.1/12)(2.41) = 0.0007 \text{ ft} \quad (2.3-25)$$

Hence, entrance effects are not important, and the viscosity value given above has been calculated properly.

EXAMPLE 2.3-2

*Compressible Flow in a Horizontal Circular Tube*⁶

Obtain an expression for the mass rate of flow w for an ideal gas in laminar flow in a long circular tube. The flow is presumed to be isothermal. Assume that the pressure change through the tube is not very large, so that the viscosity can be regarded a constant throughout.

SOLUTION

This problem can be solved *approximately* by assuming that the Hagen–Poiseuille equation (Eq. 2.3-21) can be applied over a small length dz of the tube as follows:

$$w = \frac{\pi \rho R^4}{8\mu} \left(-\frac{dp}{dz} \right) \quad (2.3-26)$$

To eliminate ρ in favor of p , we use the ideal gas law in the form $p/\rho = p_0/\rho_0$, where p_0 and ρ_0 are the pressure and density at $z = 0$. This gives

$$w = \frac{\pi R^4}{8\mu} \frac{\rho_0}{p_0} \left(-p \frac{dp}{dz} \right) \quad (2.3-27)$$

The mass rate of flow w is the same for all z . Hence Eq. 2.3-27 can be integrated from $z = 0$ to $z = L$ to give

$$w = \frac{\pi R^4}{16\mu L} \frac{\rho_0}{p_0} (p_0^2 - p_L^2) \quad (2.3-28)$$

Since $p_0^2 - p_L^2 = (p_0 + p_L)(p_0 - p_L)$, we get finally

$$w = \frac{\pi(p_0 - p_L)R^4\rho_{\text{avg}}}{8\mu L} \quad (2.3-29)$$

where $\rho_{\text{avg}} = \frac{1}{2}(\rho_0 + \rho_L)$ is the average density calculated at the average pressure $p_{\text{avg}} = \frac{1}{2}(p_0 + p_L)$.

§2.4 FLOW THROUGH AN ANNULUS

We now solve another viscous flow problem in cylindrical coordinates, namely the steady-state axial flow of an incompressible liquid in an annular region between two coaxial cylinders of radii κR and R as shown in Fig. 2.4-1. The fluid is flowing upward in

⁶ L. Landau and E. M. Lifshitz, *Fluid Mechanics*, Pergamon, 2nd edition (1987), §17, Problem 6. A perturbation solution of this problem was obtained by R. K. Prud'homme, T. W. Chapman, and J. R. Bowen, *Appl. Sci. Res.*, **43**, 67–74 (1986).

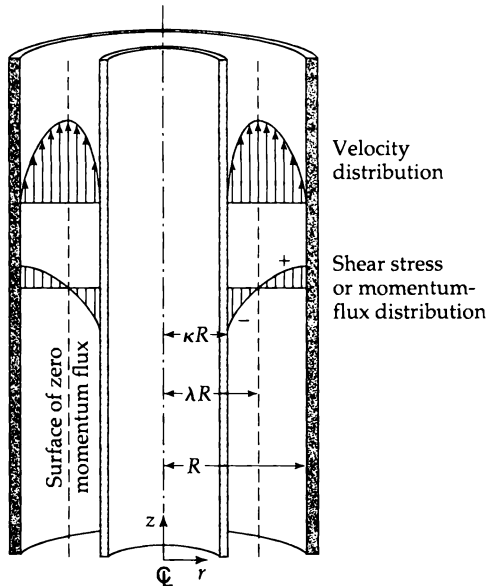


Fig. 2.4-1 The momentum-flux distribution and velocity distribution for the upward flow in a cylindrical annulus. Note that the momentum flux changes sign at the same value of r for which the velocity has a maximum.

the tube—that is, in the direction opposed to gravity. We make the same postulates as in §2.3: $v_z = v_z(r)$, $v_\theta = 0$, $v_r = 0$, and $p = p(z)$. Then when we make a momentum balance over a thin cylindrical shell of liquid, we arrive at the following differential equation:

$$\frac{d}{dr}(r\tau_{rz}) = \left(\frac{(p_0 + \rho g 0) - (p_L + \rho g L)}{L} \right) r \equiv \left(\frac{\mathcal{P}_0 - \mathcal{P}_L}{L} \right) r \quad (2.4-1)$$

This differs from Eq. 2.3-10 only in that $\mathcal{P} = p + \rho g z$ here, since the coordinate z is in the direction opposed to gravity (i.e., z is the same as the h of footnote 1 in §2.3). Integration of Eq. 2.4-1 gives

$$\tau_{rz} = \left(\frac{\mathcal{P}_0 - \mathcal{P}_L}{2L} \right) r + \frac{C_1}{r} \quad (2.4-2)$$

just as in Eq. 2.3-11.

The constant C_1 cannot be determined immediately, since we have no information about the momentum flux at the fixed surfaces $r = \kappa R$ and $r = R$. All we know is that there will be a maximum in the velocity curve at some (as yet unknown) plane $r = \lambda R$ at which the momentum flux will be zero. That is,

$$0 = \left(\frac{\mathcal{P}_0 - \mathcal{P}_L}{2L} \right) \lambda R + \frac{C_1}{\lambda R} \quad (2.4-3)$$

When we solve this equation for C_1 and substitute it into Eq. 2.4-2, we get

$$\tau_{rz} = \frac{(\mathcal{P}_0 - \mathcal{P}_L)R}{2L} \left[\left(\frac{r}{R} \right) - \lambda^2 \left(\frac{R}{r} \right) \right] \quad (2.4-4)$$

The only difference between this equation and Eq. 2.4-2 is that the constant of integration C_1 has been eliminated in favor of a different constant λ . The advantage of this is that we know the geometrical significance of λ .

We now substitute Newton's law of viscosity, $\tau_{rz} = -\mu(dv_z/dr)$, into Eq. 2.4-4 to obtain a differential equation for v_z

$$\frac{dv_z}{dr} = -\frac{(\mathcal{P}_0 - \mathcal{P}_L)R}{2\mu L} \left[\left(\frac{r}{R} \right) - \lambda^2 \left(\frac{R}{r} \right) \right] \quad (2.4-5)$$

Integration of this first-order separable differential equation then gives

$$v_z = -\frac{(\mathcal{P}_0 - \mathcal{P}_L)R^2}{4\mu L} \left[\left(\frac{r}{R} \right)^2 - 2\lambda^2 \ln \left(\frac{r}{R} \right) + C_2 \right] \quad (2.4-6)$$

We now evaluate the two constants of integration, λ and C_2 , by using the no-slip condition on each solid boundary:

$$\text{B.C. 1:} \quad \text{at } r = \kappa R, \quad v_z = 0 \quad (2.4-7)$$

$$\text{B.C. 2:} \quad \text{at } r = R, \quad v_z = 0 \quad (2.4-8)$$

Substitution of these boundary conditions into Eq. 2.4-6 then gives two simultaneous equations:

$$0 = \kappa^2 - 2\lambda^2 \ln \kappa + C_2; \quad 0 = 1 + C_2 \quad (2.4-9, 10)$$

From these the two integration constants λ and C_2 are found to be

$$C_2 = -1; \quad 2\lambda^2 = \frac{1 - \kappa^2}{\ln(1/\kappa)} \quad (2.4-11, 12)$$

These expressions can be inserted into Eqs. 2.4-4 and 2.4-6 to give the momentum-flux distribution and the velocity distribution¹ as follows:

$$\boxed{\tau_{rz} = \frac{(\mathcal{P}_0 - \mathcal{P}_L)R}{2L} \left[\left(\frac{r}{R} \right)^2 - \frac{1 - \kappa^2}{2 \ln(1/\kappa)} \left(\frac{R}{r} \right) \right]} \quad (2.4-13)$$

$$\boxed{v_z = \frac{(\mathcal{P}_0 - \mathcal{P}_L)R^2}{4\mu L} \left[1 - \left(\frac{r}{R} \right)^2 - \frac{1 - \kappa^2}{\ln(1/\kappa)} \ln \left(\frac{R}{r} \right) \right]} \quad (2.4-14)$$

Note that when the annulus becomes very thin (i.e., κ only slightly less than unity), these results simplify to those for a plane slit (see Problem 2B.5). It is always a good idea to check “limiting cases” such as these whenever the opportunity presents itself.

The lower limit of $\kappa \rightarrow 0$ is not so simple, because the ratio $\ln(R/r)/\ln(1/\kappa)$ will always be important in a region close to the inner boundary. Hence Eq. 2.4-14 does not simplify to the parabolic distribution. However, Eq. 2.4-17 for the mass rate of flow does simplify to the Hagen–Poiseuille equation.

Once we have the momentum-flux and velocity distributions, it is straightforward to get other results of interest:

(i) The *maximum velocity* is

$$v_{z,\max} = v_z|_{r=\lambda R} = \frac{(\mathcal{P}_0 - \mathcal{P}_L)R^2}{4\mu L} [1 - \lambda^2(1 - \ln \lambda^2)] \quad (2.4-15)$$

where λ^2 is given in Eq. 2.4-12.

(ii) The *average velocity* is given by

$$\langle v_z \rangle = \frac{\int_0^{2\pi} \int_{\kappa R}^R v_z r dr d\theta}{\int_0^{2\pi} \int_{\kappa R}^R r dr d\theta} = \frac{(\mathcal{P}_0 - \mathcal{P}_L)R^2}{8\mu L} \left[\frac{1 - \kappa^4}{1 - \kappa^2} - \frac{1 - \kappa^2}{\ln(1/\kappa)} \right] \quad (2.4-16)$$

(iii) The *mass rate of flow* is $w = \pi R^2(1 - \kappa^2)\rho\langle v_z \rangle$, or

$$w = \frac{\pi(\mathcal{P}_0 - \mathcal{P}_L)R^4\rho}{8\mu L} \left[(1 - \kappa^4) - \frac{(1 - \kappa^2)^2}{\ln(1/\kappa)} \right] \quad (2.4-17)$$

¹ H. Lamb, *Hydrodynamics*, Cambridge University Press, 2nd edition (1895), p. 522.

- (iv) The force exerted by the fluid on the solid surfaces is obtained by summing the forces acting on the inner and outer cylinders, as follows:

$$\begin{aligned} F_z &= (2\pi\kappa RL)(-\tau_{rz}|_{r=\kappa R}) + (2\pi RL)(+\tau_{rz}|_{r=R}) \\ &= \pi R^2(1 - \kappa^2)(P_0 - P_L) \end{aligned} \quad (2.4-18)$$

The reader should explain the choice of signs in front of the shear stresses above and also give an interpretation of the final result.

The equations derived above are valid only for laminar flow. The laminar-turbulent transition occurs in the neighborhood of $Re = 2000$, with the Reynolds number defined as $Re = 2R(1 - \kappa)\langle v_z \rangle \rho / \mu$.

§2.5 FLOW OF TWO ADJACENT IMMISCIBLE FLUIDS¹

Thus far we have considered flow situations with solid-fluid and liquid-gas boundaries. We now give one example of a flow problem with a liquid-liquid interface (see Fig. 2.5-1).

Two immiscible, incompressible liquids are flowing in the z direction in a horizontal thin slit of length L and width W under the influence of a horizontal pressure gradient $(p_0 - p_L)/L$. The fluid flow rates are adjusted so that the slit is half filled with fluid I (the more dense phase) and half filled with fluid II (the less dense phase). The fluids are flowing sufficiently slowly that no instabilities occur—that is, that the interface remains exactly planar. It is desired to find the momentum-flux and velocity distributions.

A differential momentum balance leads to the following differential equation for the momentum flux:

$$\frac{d\tau_{xz}}{dx} = \frac{p_0 - p_L}{L} \quad (2.5-1)$$

This equation is obtained for both phase I and phase II. Integration of Eq. 2.5-1 for the two regions gives

$$\tau_{xz}^I = \left(\frac{p_0 - p_L}{L} \right) x + C_1 \quad (2.5-2)$$

$$\tau_{xz}^{II} = \left(\frac{p_0 - p_L}{L} \right) x + C_2 \quad (2.5-3)$$

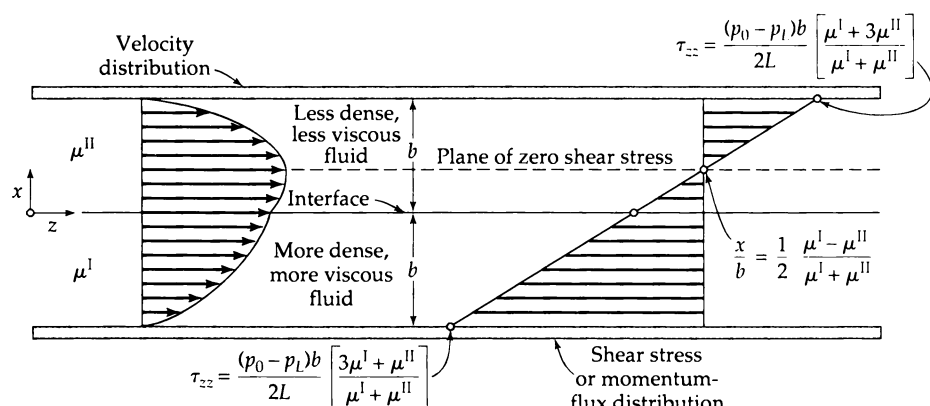


Fig. 2.5-1 Flow of two immiscible fluids between a pair of horizontal plates under the influence of a pressure gradient.

¹ The adjacent flow of gases and liquids in conduits has been reviewed by A. E. Dukler and M. Wicks, III, in Chapter 8 of *Modern Chemical Engineering*, Vol. 1, "Physical Operations," A. Acritovs (ed.), Reinhold, New York (1963).

We may immediately make use of one of the boundary conditions—namely, that the momentum flux τ_{xz} is continuous through the fluid–fluid interface:

$$\text{B.C. 1: at } x = 0, \quad \tau_{xz}^I = \tau_{xz}^{II} \quad (2.5-4)$$

This tells us that $C_1^I = C_1^{II}$; hence we drop the superscript and call both integration constants C_1 .

When Newton's law of viscosity is substituted into Eqs. 2.5-2 and 2.5-3, we get

$$-\mu^I \frac{dv_z^I}{dx} = \left(\frac{p_0 - p_L}{L} \right) x + C_1 \quad (2.5-5)$$

$$-\mu^{II} \frac{dv_z^{II}}{dx} = \left(\frac{p_0 - p_L}{L} \right) x + C_1 \quad (2.5-6)$$

These two equations can be integrated to give

$$v_z^I = -\left(\frac{p_0 - p_L}{2\mu^I L} \right) x^2 - \frac{C_1}{\mu^I} x + C_2^I \quad (2.5-7)$$

$$v_z^{II} = -\left(\frac{p_0 - p_L}{2\mu^{II} L} \right) x^2 - \frac{C_1}{\mu^{II}} x + C_2^{II} \quad (2.5-8)$$

The three integration constants can be determined from the following no-slip boundary conditions:

$$\text{B.C. 2: at } x = 0, \quad v_z^I = v_z^{II} \quad (2.5-9)$$

$$\text{B.C. 3: at } x = -b, \quad v_z^I = 0 \quad (2.5-10)$$

$$\text{B.C. 4: at } x = +b, \quad v_z^{II} = 0 \quad (2.5-11)$$

When these three boundary conditions are applied, we get three simultaneous equations for the integration constants:

$$\text{from B.C. 2: } C_2^I = C_2^{II} \quad (2.5-12)$$

$$\text{from B.C. 3: } 0 = -\left(\frac{p_0 - p_L}{2\mu^I L} \right) b^2 + \frac{C_1}{\mu^I} b + C_2^I \quad (2.5-13)$$

$$\text{from B.C. 4: } 0 = -\left(\frac{p_0 - p_L}{2\mu^{II} L} \right) b^2 - \frac{C_1}{\mu^{II}} b + C_2^{II} \quad (2.5-14)$$

From these three equations we get

$$C_1 = -\frac{(p_0 - p_L)b}{2L} \left(\frac{\mu^I - \mu^{II}}{\mu^I + \mu^{II}} \right) \quad (2.5-15)$$

$$C_2^I = +\frac{(p_0 - p_L)b^2}{2\mu^I L} \left(\frac{2\mu^I}{\mu^I + \mu^{II}} \right) = C_2^{II} \quad (2.5-16)$$

The resulting momentum-flux and velocity profiles are

$$\tau_{xz} = \frac{(p_0 - p_L)b}{L} \left[\left(\frac{x}{b} \right) - \frac{1}{2} \left(\frac{\mu^I - \mu^{II}}{\mu^I + \mu^{II}} \right) \right] \quad (2.5-17)$$

$$v_z^I = \frac{(p_0 - p_L)b^2}{2\mu^I L} \left[\left(\frac{2\mu^I}{\mu^I + \mu^{II}} \right) + \left(\frac{\mu^I - \mu^{II}}{\mu^I + \mu^{II}} \right) \left(\frac{x}{b} \right) - \left(\frac{x}{b} \right)^2 \right] \quad (2.5-18)$$

$$v_z^{II} = \frac{(p_0 - p_L)b^2}{2\mu^{II} L} \left[\left(\frac{2\mu^{II}}{\mu^I + \mu^{II}} \right) + \left(\frac{\mu^I - \mu^{II}}{\mu^I + \mu^{II}} \right) \left(\frac{x}{b} \right) - \left(\frac{x}{b} \right)^2 \right] \quad (2.5-19)$$

These distributions are shown in Fig. 2.5-1. If both viscosities are the same, then the velocity distribution is parabolic, as one would expect for a pure fluid flowing between parallel plates (see Eq. 2B.3-2).

The *average velocity* in each layer can be obtained and the results are

$$\langle v_z^I \rangle = \frac{1}{b} \int_{-b}^0 v_z^I dx = \frac{(p_0 - p_L)b^2}{12\mu^I L} \left(\frac{7\mu^I + \mu^{II}}{\mu^I + \mu^{II}} \right) \quad (2.5-20)$$

$$\langle v_z^{II} \rangle = \frac{1}{b} \int_0^b v_z^{II} dx = \frac{(p_0 - p_L)b^2}{12\mu^{II} L} \left(\frac{\mu^I + 7\mu^{II}}{\mu^I + \mu^{II}} \right) \quad (2.5-21)$$

From the velocity and momentum-flux distributions given above, one can also calculate the maximum velocity, the velocity at the interface, the plane of zero shear stress, and the drag on the walls of the slit.

§2.6 CREEPING FLOW AROUND A SPHERE^{1,2,3,4}

In the preceding sections several elementary viscous flow problems have been solved. These have all dealt with rectilinear flows with only one nonvanishing velocity component. Since the flow around a sphere involves two nonvanishing velocity components, v_r and v_θ , it cannot be conveniently understood by the techniques explained at the beginning of this chapter. Nonetheless, a brief discussion of flow around a sphere is warranted here because of the importance of flow around submerged objects. In Chapter 4 we show how to obtain the velocity and pressure distributions. Here we only cite the results and show how they can be used to derive some important relations that we need in later discussions. The problem treated here, and also in Chapter 4, is concerned with "creeping flow"—that is, very slow flow. This type of flow is also referred to as "Stokes flow."

We consider here the flow of an incompressible fluid about a solid sphere of radius R and diameter D as shown in Fig. 2.6-1. The fluid, with density ρ and viscosity μ , ap-

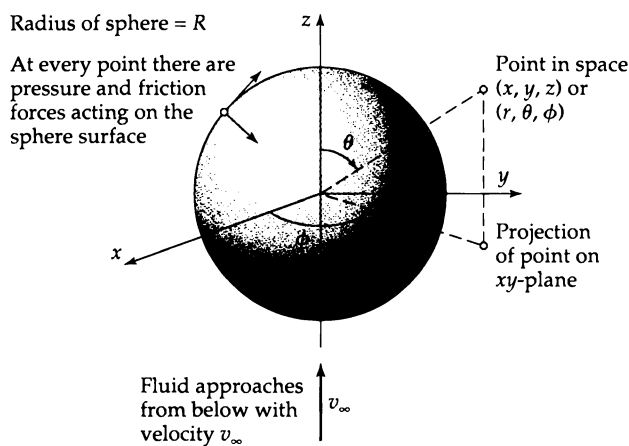


Fig. 2.6-1 Sphere of radius R around which a fluid is flowing. The coordinates r , θ , and ϕ are shown. For more information on spherical coordinates, see Fig. A.8-2.

¹ G. G. Stokes, *Trans. Cambridge Phil. Soc.*, **9**, 8–106 (1851). For creeping flow around an object of arbitrary shape, see H. Brenner, *Chem. Engr. Sci.*, **19**, 703–727 (1964).

² L. D. Landau and E. M. Lifshitz, *Fluid Mechanics*, 2nd edition, Pergamon, London (1987), §20.

³ G. K. Batchelor, *An Introduction to Fluid Dynamics*, Cambridge University Press (1967), §4.9.

⁴ S. Kim and S. J. Karrila, *Microhydrodynamics: Principles and Selected Applications*, Butterworth-Heinemann, Boston (1991), §4.2.3; this book contains a thorough discussion of "creeping flow" problems.

proaches the fixed sphere vertically upward in the z direction with a uniform velocity v_∞ . For this problem, "creeping flow" means that the Reynolds number $\text{Re} = Dv_\infty\rho/\mu$ is less than about 0.1. This flow regime is characterized by the absence of eddy formation downstream from the sphere.

The velocity and pressure distributions for this creeping flow are found in Chapter 4 to be

$$v_r = v_\infty \left[1 - \frac{3}{2} \left(\frac{R}{r} \right) + \frac{1}{2} \left(\frac{R}{r} \right)^3 \right] \cos \theta \quad (2.6-1)$$

$$v_\theta = v_\infty \left[-1 + \frac{3}{4} \left(\frac{R}{r} \right) + \frac{1}{4} \left(\frac{R}{r} \right)^3 \right] \sin \theta \quad (2.6-2)$$

$$v_\phi = 0 \quad (2.6-3)$$

$$p = p_0 - \rho g z - \frac{3}{2} \frac{\mu v_\infty}{R} \left(\frac{R}{r} \right)^2 \cos \theta \quad (2.6-4)$$

In the last equation the quantity p_0 is the pressure in the plane $z = 0$ far away from the sphere. The term $-\rho g z$ is the hydrostatic pressure resulting from the weight of the fluid, and the term containing v_∞ is the contribution of the fluid motion. Equations 2.6-1, 2, and 3 show that the fluid velocity is zero at the surface of the sphere. Furthermore, in the limit as $r \rightarrow \infty$, the fluid velocity is in the z direction with uniform magnitude v_∞ ; this follows from the fact that $v_z = v_r \cos \theta - v_\theta \sin \theta$, which can be derived by using Eq. A.6-33, and $v_x = v_y = 0$, which follows from Eqs. A.6-31 and 32.

The components of the stress tensor τ in spherical coordinates may be obtained from the velocity distribution above by using Table B.1. They are

$$\tau_{rr} = -2\tau_{\theta\theta} = -2\tau_{\phi\phi} = \frac{3\mu v_\infty}{R} \left[-\left(\frac{R}{r} \right)^2 + \left(\frac{R}{r} \right)^4 \right] \quad (2.6-5)$$

$$\tau_{r\theta} = \tau_{\theta r} = \frac{3}{2} \frac{\mu v_\infty}{r} \left(\frac{R}{r} \right)^4 \sin \theta \quad (2.6-6)$$

and all other components are zero. Note that the normal stresses for this flow are nonzero, except at $r = R$.

Let us now determine the force exerted by the flowing fluid on the sphere. Because of the symmetry around the z -axis, the resultant force will be in the z direction. Therefore the force can be obtained by integrating the z -components of the normal and tangential forces over the sphere surface.

Integration of the Normal Force

At each point on the surface of the sphere the fluid exerts a force per unit area $-(p + \tau_{rr})|_{r=R}$ on the solid, acting normal to the surface. Since the fluid is in the region of greater r and the sphere in the region of lesser r , we have to affix a minus sign in accordance with the sign convention established in §1.2. The z -component of the force

is $-(p + \tau_{rr})|_{r=R}(\cos \theta)$. We now multiply this by a differential element of surface $R^2 \sin \theta d\theta d\phi$ to get the force on the surface element (see Fig. A.8-2). Then we integrate over the surface of the sphere to get the resultant normal force in the z direction:

$$F^{(n)} = \int_0^{2\pi} \int_0^\pi (-(p + \tau_{rr})|_{r=R} \cos \theta) R^2 \sin \theta d\theta d\phi \quad (2.6-7)$$

According to Eq. 2.6-5, the normal stress τ_{rr} is zero⁵ at $r = R$ and can be omitted in the integral in Eq. 2.6-7. The pressure distribution at the surface of the sphere is, according to Eq. 2.6-4,

$$p|_{r=R} = p_0 - \rho g R \cos \theta - \frac{3}{2} \frac{\mu v_\infty}{R} \cos \theta \quad (2.6-8)$$

When this is substituted into Eq. 2.6-7 and the integration performed, the term containing p_0 gives zero, the term containing the gravitational acceleration g gives the buoyant force, and the term containing the approach velocity v_∞ gives the "form drag" as shown below:

$$F^{(n)} = \frac{4}{3} \pi R^3 \rho g + 2\pi \mu R v_\infty \quad (2.6-9)$$

The buoyant force is the mass of displaced fluid ($\frac{4}{3}\pi R^3 \rho$) times the gravitational acceleration (g).

Integration of the Tangential Force

At each point on the solid surface there is also a shear stress acting tangentially. The force per unit area exerted in the $-\theta$ direction by the fluid (region of greater r) on the solid (region of lesser r) is $+\tau_{r\theta}|_{r=R}$. The z -component of this force per unit area is $(\tau_{r\theta}|_{r=R}) \sin \theta$. We now multiply this by the surface element $R^2 \sin \theta d\theta d\phi$ and integrate over the entire spherical surface. This gives the resultant force in the z direction:

$$F^{(t)} = \int_0^{2\pi} \int_0^\pi (\tau_{r\theta}|_{r=R} \sin \theta) R^2 \sin \theta d\theta d\phi \quad (2.6-10)$$

The shear stress distribution on the sphere surface, from Eq. 2.6-6, is

$$\tau_{r\theta}|_{r=R} = \frac{3}{2} \frac{\mu v_\infty}{R} \sin \theta \quad (2.6-11)$$

Substitution of this expression into the integral in Eq. 2.6-10 gives the "friction drag"

$$F^{(t)} = 4\pi \mu R v_\infty \quad (2.6-12)$$

Hence the total force F of the fluid on the sphere is given by the sum of Eqs. 2.6-9 and 2.6-12:

$$F = \frac{4}{3} \pi R^3 \rho g + 2\pi \mu R v_\infty + 4\pi \mu R v_\infty \quad (2.6-13)$$

buoyant form friction
force drag drag

or

$$F = F_b + F_k = \frac{4}{3} \pi R^3 \rho g + 6\pi \mu R v_\infty \quad (2.6-14)$$

buoyant kinetic
force force

⁵ In Example 3.1-1 we show that, for incompressible, Newtonian fluids, all three of the normal stresses are zero at fixed solid surfaces in all flows.

The first term is the *buoyant force*, which would be present in a fluid at rest; it is the mass of the displaced fluid multiplied by the gravitational acceleration. The second term, the *kinetic force*, results from the motion of the fluid. The relation

$$F_k = 6\pi\mu Rv_\infty \quad (2.6-15)$$

is known as *Stokes' law*.¹ It is used in describing the motion of colloidal particles under an electric field, in the theory of sedimentation, and in the study of the motion of aerosol particles. Stokes' law is useful only up to a Reynolds number $Re = Dv_\infty\rho/\mu$ of about 0.1. At $Re = 1$, Stokes' law predicts a force that is about 10% too low. The flow behavior for larger Reynolds numbers is discussed in Chapter 6.

This problem, which could not be solved by the shell balance method, emphasizes the need for a more general method for coping with flow problems in which the streamlines are not rectilinear. That is the subject of the following chapter.

EXAMPLE 2.6-1

Determination of Viscosity from the Terminal Velocity of a Falling Sphere

Derive a relation that enables one to get the viscosity of a fluid by measuring the terminal velocity v_t of a small sphere of radius R in the fluid.

SOLUTION

If a small sphere is allowed to fall from rest in a viscous fluid, it will accelerate until it reaches a constant velocity—the *terminal velocity*. When this steady-state condition has been reached the sum of all the forces acting on the sphere must be zero. The force of gravity on the solid acts in the direction of fall, and the buoyant and kinetic forces act in the opposite direction:

$$\frac{4}{3}\pi R^3 \rho_s g = \frac{4}{3}\pi R^3 \rho g + 6\pi\mu Rv_t \quad (2.6-16)$$

Here ρ_s and ρ are the densities of the solid sphere and the fluid. Solving this equation for the terminal velocity gives

$$\mu = \frac{2}{9}R^2(\rho_s - \rho)g/v_t \quad (2.6-17)$$

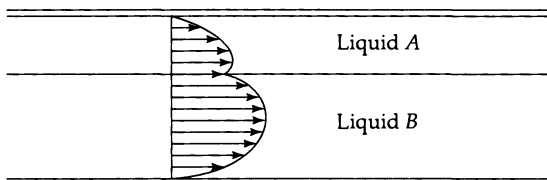
This result may be used only if the Reynolds number is less than about 0.1.

This experiment provides an apparently simple method for determining viscosity. However, it is difficult to keep a homogeneous sphere from rotating during its descent, and if it does rotate, then Eq. 2.6-17 cannot be used. Sometimes weighted spheres are used in order to preclude rotation; then the left side of Eq. 2.6-16 has to be replaced by m , the mass of the sphere, times the gravitational acceleration.

QUESTIONS FOR DISCUSSION

1. Summarize the procedure used in the solution of viscous flow problems by the shell balance method. What kinds of problems can and cannot be solved by this method? How is the definition of the first derivative used in the method?
2. Which of the flow systems in this chapter can be used as a viscometer? List the difficulties that might be encountered in each.
3. How are the Reynolds numbers defined for films, tubes, and spheres? What are the dimensions of Re ?
4. How can one modify the film thickness formula in §2.2 to describe a thin film falling down the interior wall of a cylinder? What restrictions might have to be placed on this modified formula?
5. How can the results in §2.3 be used to estimate the time required for a liquid to drain out of a vertical tube that is open at both ends?
6. Contrast the radial dependence of the shear stress for the laminar flow of a Newtonian liquid in a tube and in an annulus. In the latter, why does the function change sign?

7. Show that the Hagen–Poiseuille formula is dimensionally consistent.
8. What differences are there between the flow in a circular tube of radius R and the flow in the same tube with a thin wire placed along the axis?
9. Under what conditions would you expect the analysis in §2.5 to be inapplicable?
10. Is Stokes' law valid for droplets of oil falling in water? For air bubbles rising in benzene? For tiny particles falling in air, if the particle diameters are of the order of the mean free path of the molecules in the air?
11. Two immiscible liquids, A and B , are flowing in laminar flow between two parallel plates. Is it possible that the velocity profiles would be of the following form? Explain.



12. What is the terminal velocity of a spherical colloidal particle having an electric charge e in an electric field of strength \mathcal{E} ? How is this used in the Millikan oil-drop experiment?

PROBLEMS

- 2A.1 Thickness of a falling film.** Water at 20°C is flowing down a vertical wall with $Re = 10$. Calculate (a) the flow rate, in gallons per hour per foot of wall length, and (b) the film thickness in inches.

Answers: (a) 0.727 gal/hr · ft; (b) 0.00361 in.

- 2A.2 Determination of capillary radius by flow measurement.** One method for determining the radius of a capillary tube is by measuring the rate of flow of a Newtonian liquid through the tube. Find the radius of a capillary from the following flow data:

Length of capillary tube	50.02 cm
Kinematic viscosity of liquid	$4.03 \times 10^{-5} \text{ m}^2/\text{s}$
Density of liquid	$0.9552 \times 10^3 \text{ kg/m}^3$
Pressure drop in the horizontal tube	$4.829 \times 10^5 \text{ Pa}$
Mass rate of flow through tube	$2.997 \times 10^{-3} \text{ kg/s}$

What difficulties may be encountered in this method? Suggest some other methods for determining the radii of capillary tubes.

- 2A.3 Volume flow rate through an annulus.** A horizontal annulus, 27 ft in length, has an inner radius of 0.495 in. and an outer radius of 1.1 in. A 60% aqueous solution of sucrose ($C_{12}H_{22}O_{11}$) is to be pumped through the annulus at 20°C. At this temperature the solution density is 80.3 lb/ft³ and the viscosity is 136.8 lb_m/ft · hr. What is the volume flow rate when the impressed pressure difference is 5.39 psi?

Answer: 0.108 ft³/s

- 2A.4 Loss of catalyst particles in stack gas.**

(a) Estimate the maximum diameter of microspherical catalyst particles that could be lost in the stack gas of a fluid cracking unit under the following conditions:

Gas velocity at axis of stack = 1.0 ft/s (vertically upward)

Gas viscosity = 0.026 cp

Gas density = 0.045 lb/ft³

Density of a catalyst particle = 1.2 g/cm³

Express the result in microns (1 micron = $10^{-6} = 1\mu\text{m}$).

(b) Is it permissible to use Stokes' law in (a)?

Answers: (a) 110 μm ; $Re = 0.93$

- 2B.1 Different choice of coordinates for the falling film problem.** Rederive the velocity profile and the average velocity in §2.2, by replacing x by a coordinate \bar{x} measured away from the wall; that is, $\bar{x} = 0$ is the wall surface, and $\bar{x} = \delta$ is the liquid–gas interface. Show that the velocity distribution is then given by

$$v_z = (\rho g \delta^2 / \mu) [(\bar{x}/\delta) - \frac{1}{2}(\bar{x}/\delta)^2] \cos \beta \quad (2B.1-1)$$

and then use this to get the average velocity. Show how one can get Eq. 2B.1-1 from Eq. 2.2-18 by making a change of variable.

- 2B.2 Alternate procedure for solving flow problems.** In this chapter we have used the following procedure: (i) derive an equation for the momentum flux, (ii) integrate this equation, (iii) insert Newton's law to get a first-order differential equation for the velocity, (iv) integrate the latter to get the velocity distribution. Another method is: (i) derive an equation for the momentum flux, (ii) insert Newton's law to get a second-order differential equation for the velocity profile, (iii) integrate the latter to get the velocity distribution. Apply this second method to the falling film problem by substituting Eq. 2.2-14 into Eq. 2.2-10 and continuing as directed until the velocity distribution has been obtained and the integration constants evaluated.

- 2B.3 Laminar flow in a narrow slit (see Fig. 2B.3).**

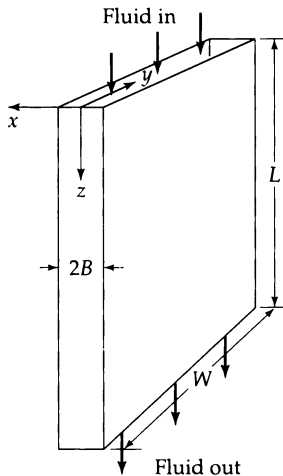


Fig. 2B.3 Flow through a slit, with $B \ll W \ll L$.

- (a) A Newtonian fluid is in laminar flow in a narrow slit formed by two parallel walls a distance $2B$ apart. It is understood that $B \ll W$, so that "edge effects" are unimportant. Make a differential momentum balance, and obtain the following expressions for the momentum-flux and velocity distributions:

$$\tau_{xz} = \left(\frac{\mathcal{P}_0 - \mathcal{P}_L}{L} \right) x \quad (2B.3-1)$$

$$v_z = \frac{(\mathcal{P}_0 - \mathcal{P}_L)B^2}{2\mu L} \left[1 - \left(\frac{x}{B} \right)^2 \right] \quad (2B.3-2)$$

In these expressions $\mathcal{P} = p + \rho gh = p - \rho gz$.

- (b) What is the ratio of the average velocity to the maximum velocity for this flow?
(c) Obtain the slit analog of the Hagen–Poiseuille equation.
(d) Draw a meaningful sketch to show why the above analysis is inapplicable if $B = W$.
(e) How can the result in (b) be obtained from the results of §2.5?

Answers: (b) $\langle v_z \rangle / v_{z,\max} = \frac{2}{3}$

$$(c) w = \frac{2}{3} \frac{(\mathcal{P}_0 - \mathcal{P}_L)B^3 W \rho}{\mu L}$$

- 2B.4 Laminar slit flow with a moving wall ("plane Couette flow").** Extend Problem 2B.3 by allowing the wall at $x = B$ to move in the positive z direction at a steady speed v_0 . Obtain (a) the shear-stress distribution and (b) the velocity distribution. Draw carefully labeled sketches of these functions.

$$\text{Answers: } \tau_{xz} = \left(\frac{\mathcal{P}_0 - \mathcal{P}_L}{L} \right) x - \frac{\mu v_0}{2B}; \quad v_z = \frac{(\mathcal{P}_0 - \mathcal{P}_L)B^2}{2\mu L} \left[1 - \left(\frac{x}{B} \right)^2 \right] + \frac{v_0}{2} \left(1 + \frac{x}{B} \right)$$

- 2B.5 Interrelation of slit and annulus formulas.** When an annulus is very thin, it may, to a good approximation, be considered as a thin slit. Then the results of Problem 2B.3 can be taken over with suitable modifications. For example, the mass rate of flow in an annulus with outer wall of radius R and inner wall of radius $(1 - \epsilon)R$, where ϵ is small, may be obtained from Problem 2B.3 by replacing $2B$ by ϵR , and W by $2\pi(1 - \frac{1}{2}\epsilon)R$. In this way we get for the mass rate of flow:

$$w = \frac{\pi(\mathcal{P}_0 - \mathcal{P}_L)R^4\epsilon^3\rho}{6\mu L} (1 - \frac{1}{2}\epsilon) \quad (2B.5-1)$$

Show that this same result may be obtained from Eq. 2.4-17 by setting κ equal to $1 - \epsilon$ everywhere in the formula and then expanding the expression for w in powers of ϵ . This requires using the Taylor series (see §C.2)

$$\ln(1 - \epsilon) = -\epsilon - \frac{1}{2}\epsilon^2 - \frac{1}{3}\epsilon^3 - \frac{1}{4}\epsilon^4 - \dots \quad (2B.5-2)$$

and then performing a long division. The first term in the resulting series will be Eq. 2B.5-1. *Caveat:* In the derivation it is necessary to use the first four terms of the Taylor series in Eq. 2B.5-2.

- 2B.6 Flow of a film on the outside of a circular tube** (see Fig. 2B.6). In a gas absorption experiment a viscous fluid flows upward through a small circular tube and then downward in laminar flow on the outside. Set up a momentum balance over a shell of thickness Δr in the film,

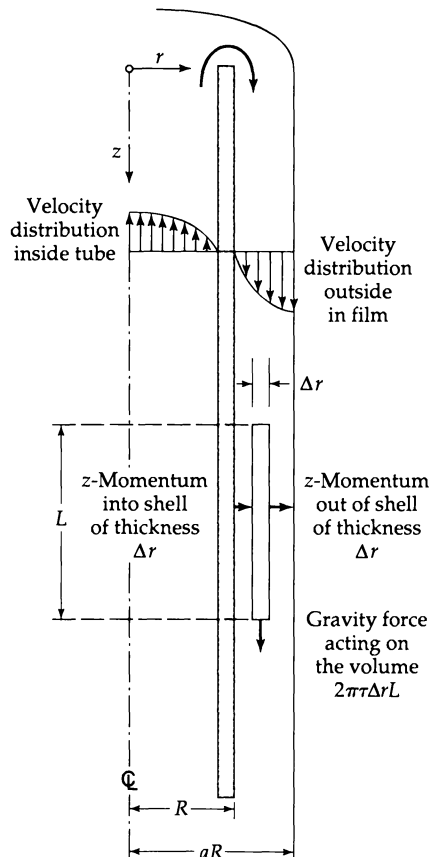


Fig. 2B.6 Velocity distribution and z-momentum balance for the flow of a falling film on the outside of a circular tube.

as shown in Fig. 2B.6. Note that the "momentum in" and "momentum out" arrows are always taken in the positive coordinate direction, even though in this problem the momentum is flowing through the cylindrical surfaces in the negative r direction.

(a) Show that the velocity distribution in the falling film (neglecting end effects) is

$$v_z = \frac{\rho g R^2}{4\mu} \left[1 - \left(\frac{r}{R} \right)^2 + 2a^2 \ln \left(\frac{r}{R} \right) \right] \quad (2B.6-1)$$

(b) Obtain an expression for the mass rate of flow in the film.

(c) Show that the result in (b) simplifies to Eq. 2.2-21 if the film thickness is very small.

- 2B.7 Annular flow with inner cylinder moving axially** (see Fig. 2B.7). A cylindrical rod of diameter κR moves axially with velocity v_0 along the axis of a cylindrical cavity of radius R as seen in the figure. The pressure at both ends of the cavity is the same, so that the fluid moves through the annular region solely because of the rod motion.

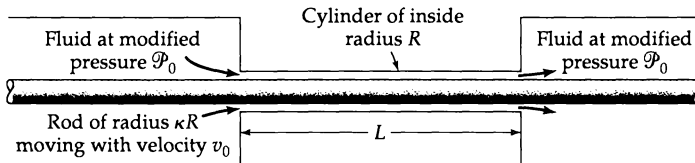


Fig. 2B.7 Annular flow with the inner cylinder moving axially.

- (a) Find the velocity distribution in the narrow annular region.
 (b) Find the mass rate of flow through the annular region.
 (c) Obtain the viscous force acting on the rod over the length L .
 (d) Show that the result in (c) can be written as a "plane slit" formula multiplied by a "curvature correction." Problems of this kind arise in studying the performance of wire-coating dies.¹

Answers: (a) $\frac{v_z}{v_0} = \frac{\ln(r/R)}{\ln\kappa}$

(b) $w = \frac{\pi R^2 v_0 \rho}{2} \left[\frac{(1-\kappa^2)}{\ln(1/\kappa)} - 2\kappa^2 \right]$

(c) $F = 2\pi L \mu v_0 / \ln(1/\kappa)$

(d) $F = \frac{2\pi L \mu v_0}{\varepsilon} (1 - \frac{1}{2}\varepsilon - \frac{1}{12}\varepsilon^2 + \dots)$ where $\varepsilon = 1 - \kappa$ (see Problem 2B.5)

- 2B.8 Analysis of a capillary flowmeter** (see Fig. 2B.8). Determine the rate of flow (in lb/hr) through the capillary flow meter shown in the figure. The fluid flowing in the inclined tube is

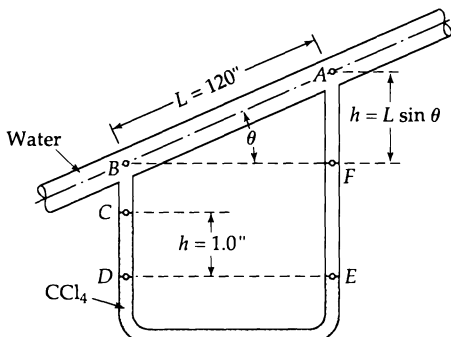


Fig. 2B.8 A capillary flow meter.

¹ J. B. Paton, P. H. Squires, W. H. Darnell, F. M. Cash, and J. F. Carley, *Processing of Thermoplastic Materials*, E. C. Bernhardt (ed.), Reinhold, New York (1959), Chapter 4.

water at 20°C, and the manometer fluid is carbon tetrachloride (CCl_4) with density 1.594 g/cm³. The capillary diameter is 0.010 in. Note: Measurements of H and L are sufficient to calculate the flow rate; θ need not be measured. Why?

- 2B.9 Low-density phenomena in compressible tube flow**^{2,3} (Fig. 2B.9). As the pressure is decreased in the system studied in Example 2.3-2, deviations from Eqs. 2.3-28 and 2.3-29 arise. The gas behaves as if it slips at the tube wall. It is conventional² to replace the customary “no-slip” boundary condition that $v_z = 0$ at the tube wall by

$$v_z = -\zeta \frac{dv_z}{dr}, \quad \text{at } r = R \quad (2B.9-1)$$

in which ζ is the *slip coefficient*. Repeat the derivation in Example 2.3-2 using Eq. 2B.9-1 as the boundary condition. Also make use of the experimental fact that the slip coefficient varies inversely with the pressure $\zeta = \zeta_0/p$, in which ζ_0 is a constant. Show that the mass rate of flow is

$$w = \frac{\pi(p_0 - p_L)R^4\rho_{\text{avg}}}{8\mu L} \left(1 + \frac{4\zeta_0}{Rp_{\text{avg}}}\right) \quad (2B.9-2)$$

in which $p_{\text{avg}} = \frac{1}{2}(p_0 + p_L)$.

When the pressure is decreased further, a flow regime is reached in which the mean free path of the gas molecules is large with respect to the tube radius (*Knudsen flow*). In that regime³

$$w = \sqrt{\frac{2m}{\pi\kappa T}} \left(\frac{4}{3}\pi R^3\right) \left(\frac{p_0 - p_L}{L}\right) \quad (2B.9-3)$$

in which m is the molecular mass and κ is the Boltzmann constant. In the derivation of this result it is assumed that all collisions of the molecules with the solid surfaces are *diffuse* and not *specular*. The results in Eqs. 2.3-29, 2B.9-2, and 2B.9-3 are summarized in Fig. 2B.9.

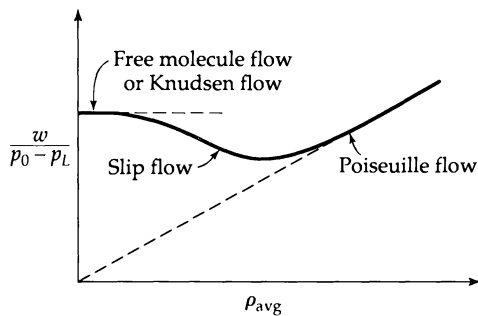


Fig. 2B.9 A comparison of the flow regimes in gas flow through a tube.

- 2B.10 Incompressible flow in a slightly tapered tube.** An incompressible fluid flows through a tube of circular cross section, for which the tube radius changes linearly from R_0 at the tube entrance to a slightly smaller value R_L at the tube exit. Assume that the Hagen–Poiseuille equation is approximately valid over a differential length, dz , of the tube so that the mass flow rate is

$$w = \frac{\pi[R(z)]^4\rho}{8\mu} \left(-\frac{d\mathcal{P}}{dz}\right) \quad (2B.10-1)$$

This is a differential equation for \mathcal{P} as a function of z , but, when the explicit expression for $R(z)$ is inserted, it is not easily solved.

² E. H. Kennard, *Kinetic Theory of Gases*, McGraw-Hill, New York (1938), pp. 292–295, 300–306.

³ M. Knudsen, *The Kinetic Theory of Gases*, Methuen, London, 3rd edition (1950). See also R. J. Silbey and R. A. Alberty, *Physical Chemistry*, Wiley, New York, 3rd edition (2001), §17.6.

- (a) Write down the expression for R as a function of z .
 (b) Change the independent variable in the above equation to R , so that the equation becomes

$$w = \frac{\pi R^4 \rho}{8\mu} \left(-\frac{dP}{dR} \right) \left(\frac{R_L - R_0}{L} \right) \quad (2B.10-2)$$

- (c) Integrate the equation, and then show that the solution can be rearranged to give

$$w = \frac{\pi (\mathcal{P}_0 - \mathcal{P}_L) R_0^4 \rho}{8\mu} \left[1 - \frac{1 + (R_L/R_0) + (R_L/R_0)^2 - 3(R_L/R_0)^3}{1 + (R_L/R_0) + (R_L/R_0)^2} \right] \quad (2B.10-3)$$

Interpret the result. The approximation used here that a flow between nonparallel surfaces can be regarded locally as flow between parallel surfaces is sometimes referred to as the *lubrication approximation* and is widely used in the theory of lubrication. By making a careful order-of-magnitude analysis, it can be shown that, for this problem, the lubrication approximation is valid as long as⁴

$$\frac{R_L}{R_0} \left(1 - \left(\frac{R_L}{R_0} \right)^2 \right) \ll 1 \quad (2B.10-4)$$

- 2B.11 The cone-and-plate viscometer** (see Fig. 2B.11). A cone-and-plate viscometer consists of a stationary flat plate and an inverted cone, whose apex just contacts the plate. The liquid whose viscosity is to be measured is placed in the gap between the cone and plate. The cone is rotated at a known angular velocity Ω , and the torque T_z required to turn the cone is measured. Find an expression for the viscosity of the fluid in terms of Ω , T_z , and the angle ψ_0 between the cone and plate. For commercial instruments ψ_0 is about 1 degree.

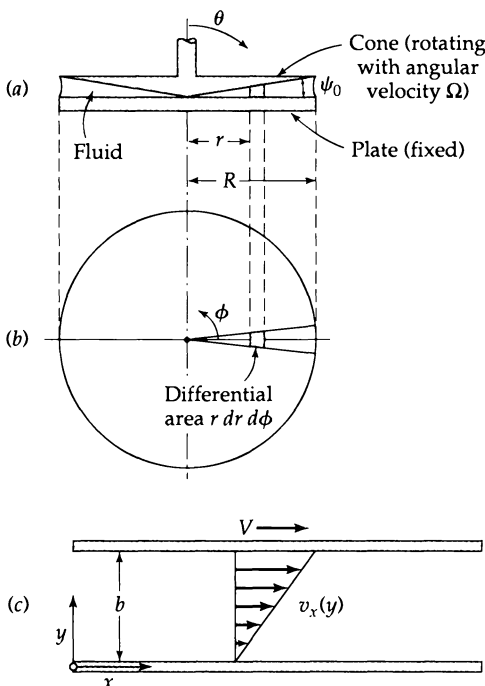


Fig. 2B.11 The cone-and-plate viscometer:
 (a) side view of the instrument; (b) top view of the cone-plate system, showing a differential element $r dr d\phi$; (c) an approximate velocity distribution within the differential region. To equate the systems in (a) and (c), we identify the following equivalences:
 $V = \Omega r$ and $b = r \sin \psi_0 \approx r\psi_0$.

⁴ R. B. Bird, R. C. Armstrong, and O. Hassager, *Dynamics of Polymeric Liquids*, Vol. 1, Wiley-Interscience, New York, 2nd edition (1987), pp. 16–18.

- (a) Assume that locally the velocity distribution in the gap can be very closely approximated by that for flow between parallel plates, the upper one moving with a constant speed. Verify that this leads to the *approximate* velocity distribution (in spherical coordinates)

$$\frac{v_\phi}{r} = \Omega \left(\frac{(\pi/2) - \theta}{\psi_0} \right) \quad (2B.11-1)$$

This approximation should be rather good, because ψ_0 is so small.

- (b) From the velocity distribution in Eq. 2B.11-1 and Appendix B.1, show that a reasonable expression for the shear stress is

$$\tau_{\theta\phi} = \mu(\Omega/\psi_0) \quad (2B.11-2)$$

This result shows that the shear stress is uniform throughout the gap. It is this fact that makes the cone-and-plate viscometer quite attractive. The instrument is widely used, particularly in the polymer industry.

- (c) Show that the torque required to turn the cone is given by

$$T_z = \frac{2}{3}\pi\mu\Omega R^3/\psi_0 \quad (2B.11-3)$$

This is the standard formula for calculating the viscosity from measurements of the torque and angular velocity for a cone-plate assembly with known R and ψ_0 .

- (d) For a cone-and-plate instrument with radius 10 cm and angle ψ_0 equal to 0.5 degree, what torque (in $\text{dyn} \cdot \text{cm}$) is required to turn the cone at an angular velocity of 10 radians per minute if the fluid viscosity is 100 cp?

Answer: (d) 40,000 $\text{dyn} \cdot \text{cm}$

- 2B.12 Flow of a fluid in a network of tubes** (Fig. 2B.12). A fluid is flowing in laminar flow from A to B through a network of tubes, as depicted in the figure. Obtain an expression for the mass flow rate w of the fluid entering at A (or leaving at B) as a function of the modified pressure drop $\mathcal{P}_A - \mathcal{P}_B$. Neglect the disturbances at the various tube junctions.

$$\text{Answer: } w = \frac{3\pi(\mathcal{P}_A - \mathcal{P}_B)R^4\rho}{20\mu L}$$

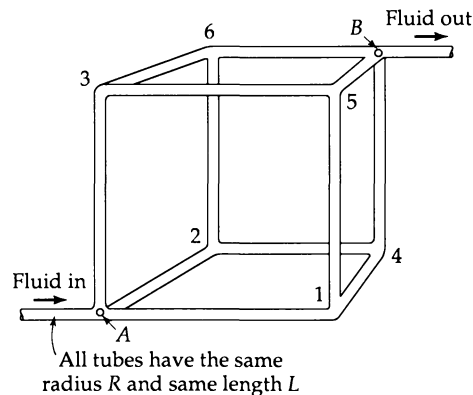


Fig. 2B.12 Flow of a fluid in a network with branching.

- 2C.1 Performance of an electric dust collector** (see Fig. 2C.1)⁵.

- (a) A dust precipitator consists of a pair of oppositely charged plates between which dust-laden gases flow. It is desired to establish a criterion for the minimum length of the precipitator in terms of the charge on the particle e , the electric field strength E , the pressure difference

⁵ The answer given in the first edition of this book was incorrect, as pointed out to us in 1970 by Nau Gab Lee of Seoul National University.

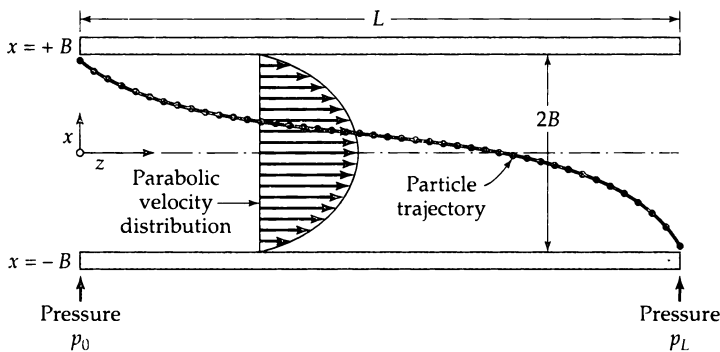


Fig. 2C.1 Particle trajectory in an electric dust collector. The particle that begins at $z = 0$ and ends at $x = +B$ may not necessarily travel the longest distance in the z direction.

($p_0 - p_L$), the particle mass m , and the gas viscosity μ . That is, for what length L will the smallest particle present (mass m) reach the bottom just before it has a chance to be swept out of the channel? Assume that the flow between the plates is laminar so that the velocity distribution is described by Eq. 2B.3-2. Assume also that the particle velocity in the z direction is the same as the fluid velocity in the z direction. Assume further that the Stokes drag on the sphere as well as the gravity force acting on the sphere as it is accelerated in the negative x direction can be neglected.

- (b) Rework the problem neglecting acceleration in the x direction, but including the Stokes drag.
- (c) Compare the usefulness of the solutions in (a) and (b), considering that stable aerosol particles have effective diameters of about 1–10 microns and densities of about 1 g/cm^3 .

Answer: (a) $L_{\min} = [12(p_0 - p_L)^2 B^5 m / 25\mu^2 e \epsilon]^{1/4}$

- 2C.2 Residence time distribution in tube flow.** Define the *residence time function* $F(t)$ to be that fraction of the fluid flowing in a conduit which flows completely through the conduit in a time interval t . Also define the *mean residence time* t_m by the relation

$$t_m = \int_0^1 t dF \quad (2C.2-1)$$

- (a) An incompressible Newtonian liquid is flowing in a circular tube of length L and radius R , and the average flow velocity is $\langle v_z \rangle$. Show that

$$F(t) = 0 \quad \text{for } t \leq (L/2\langle v_z \rangle) \quad (2C.2-2)$$

$$F(t) = 1 - (L/2\langle v_z \rangle)t^2 \quad \text{for } t \geq (L/2\langle v_z \rangle) \quad (2C.2-3)$$

- (b) Show that $t_m = (L/\langle v_z \rangle)$.

- 2C.3 Velocity distribution in a tube.** You have received a manuscript to referee for a technical journal. The paper deals with heat transfer in tube flow. The authors state that, because they are concerned with nonisothermal flow, they must have a “general” expression for the velocity distribution, one that can be used even when the viscosity of the fluid is a function of temperature (and hence position). The authors state that a “general expression for the velocity distribution for flow in a tube” is

$$\frac{v_z}{\langle v_z \rangle} = \frac{\int_y^1 (\bar{y}/\mu) d\bar{y}}{\int_0^1 (\bar{y}^3/\mu) d\bar{y}} \quad (2C.3-1)$$

in which $y = r/R$. The authors give no derivation, nor do they give a literature citation. As the referee you feel obliged to derive the formula and list any restrictions implied.

2C.4 Falling-cylinder viscometer (see Fig. 2C.4).⁶ A falling-cylinder viscometer consists of a long vertical cylindrical container (radius R), capped at both ends, with a solid cylindrical slug (radius κR). The slug is equipped with fins so that its axis is coincident with that of the tube.

One can observe the rate of descent of the slug in the cylindrical container when the latter is filled with fluid. Find an equation that gives the viscosity of the fluid in terms of the terminal velocity v_0 of the slug and the various geometric quantities shown in the figure.

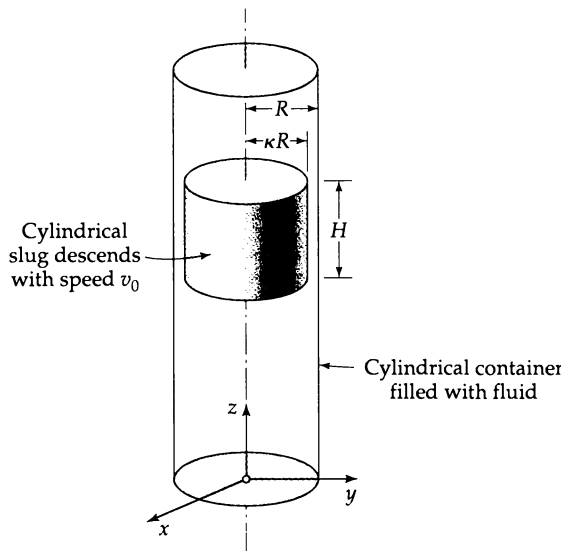


Fig. 2C.4 A falling-cylinder viscometer with a tightly fitting solid cylinder moving vertically. The cylinder is usually equipped with fins to maintain centering within the tube. The fluid completely fills the tube, and the top and bottom are closed.

(a) Show that the velocity distribution in the annular slit is given by

$$\frac{v_z}{v_0} = -\frac{(1 - \xi^2) - (1 + \kappa^2) \ln(1/\xi)}{(1 - \kappa^2) - (1 + \kappa^2) \ln(1/\kappa)} \quad (2C.4-1)$$

in which $\xi = r/R$ is a dimensionless radial coordinate.

(b) Make a force balance on the cylindrical slug and obtain

$$\mu = \frac{(\rho_0 - \rho)g(\kappa R)^2}{2v_0} \left[\left(\ln \frac{1}{\kappa} \right) - \left(\frac{1 - \kappa^2}{1 + \kappa^2} \right) \right] \quad (2C.4-2)$$

in which ρ and ρ_0 are the densities of the fluid and the slug, respectively.

(c) Show that, for small slit widths, the result in (b) may be expanded in powers of $\epsilon = 1 - \kappa$ to give

$$\mu = \frac{(\rho_0 - \rho)gR^2\epsilon^3}{6v_0} (1 - \frac{1}{2}\epsilon - \frac{13}{20}\epsilon^2 + \dots) \quad (2C.4-3)$$

See §C.2 for information on expansions in Taylor series.

2C.5 Falling film on a conical surface (see Fig. 2C.5).⁷ A fluid flows upward through a circular tube and then downward on a conical surface. Find the film thickness as a function of the distance s down the cone.

⁶ J. Lohrenz, G. W. Swift, and F. Kurata, *AICHE Journal*, **6**, 547–550 (1960) and **7**, 6S (1961); E. Ashare, R. B. Bird, and J. A. Lescarboura, *AICHE Journal*, **11**, 910–916 (1965).

⁷ R. B. Bird, in *Selected Topics in Transport Phenomena*, CEP Symposium Series #58, **61**, 1–15 (1965).

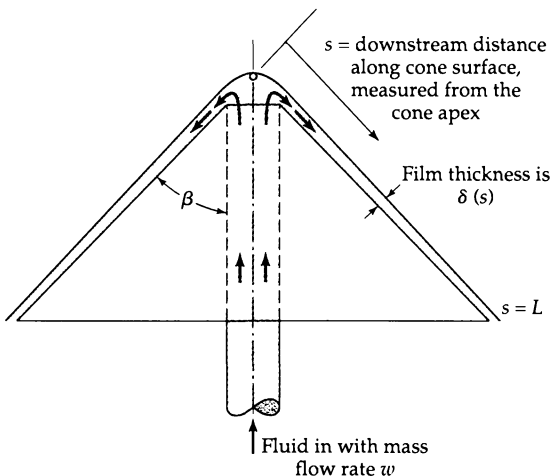


Fig. 2C.5 A falling film on a conical surface.

- (a) Assume that the results of §2.2 apply *approximately* over any small region of the cone surface. Show that a mass balance on a ring of liquid contained between s and $s + \Delta s$ gives:

$$\frac{d}{ds}(s\delta(v)) = 0 \quad \text{or} \quad \frac{d}{ds}(s\delta^3) = 0 \quad (2C.5-1)$$

- (b) Integrate this equation and evaluate the constant of integration by equating the mass rate of flow w up the central tube to that flowing down the conical surface at $s = L$. Obtain the following expression for the film thickness:

$$\delta = \sqrt[3]{\frac{3\mu w}{\pi\rho^2 g L \sin 2\beta}} \left(\frac{L}{s} \right) \quad (2C.5-2)$$

- 2C.6 Rotating cone pump** (see Fig. 2C.6). Find the mass rate of flow through this pump as a function of the gravitational acceleration, the impressed pressure difference, the angular velocity of the cone, the fluid viscosity and density, the cone angle, and other geometrical quantities labeled in the figure.

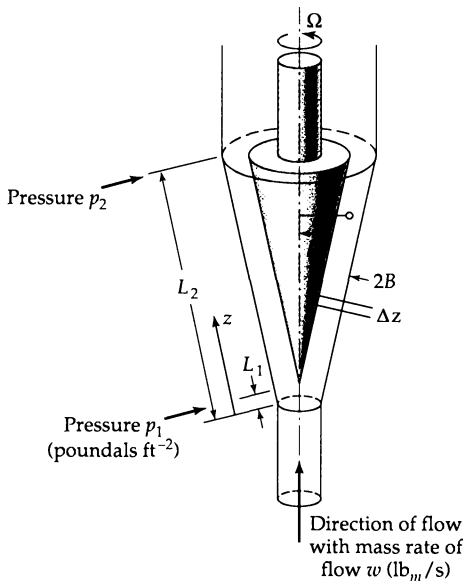


Fig. 2C.6 A rotating-cone pump. The variable r is the distance from the axis of rotation out to the center of the slit.

(a) Begin by analyzing the system without the rotation of the cone. Assume that it is possible to apply the results of Problem 2B.3 locally. That is, adapt the solution for the mass flow rate from that problem by making the following replacements:

$$\begin{aligned} \text{replace } (\mathcal{P}_0 - \mathcal{P}_L)/L &\text{ by } -d\mathcal{P}/dz \\ \text{replace } W &\text{ by } 2\pi r = 2\pi z \sin \beta \end{aligned}$$

thereby obtaining

$$w = \frac{2}{3} \left(-\frac{d\mathcal{P}}{dz} \right) \frac{B^3 \rho \cdot 2\pi z \sin \beta}{\mu} \quad (2C.6-1)$$

The mass flow rate w is a constant over the range of z . Hence this equation can be integrated to give

$$(\mathcal{P}_1 - \mathcal{P}_2) = \frac{3}{4\pi} \frac{\mu w}{B^3 \rho \sin \beta} \ln \frac{L_2}{L_1} \quad (2C.6-2)$$

(b) Next, modify the above result to account for the fact that the cone is rotating with angular velocity Ω . The mean centrifugal force per unit volume acting on the fluid in the slit will have a z -component *approximately* given by

$$(F_{\text{centrif.}})_z = K\rho\Omega^2 z \sin^2 \beta \quad (2C.6-3)$$

What is the value of K ? Incorporate this as an additional force tending to drive the fluid through the channel. Show that this leads to the following expression for the mass rate of flow:

$$w = \frac{4\pi B^3 \rho \sin \beta}{3\mu} \left[\frac{(\mathcal{P}_1 - \mathcal{P}_2) + (\frac{1}{2}K\rho\Omega^2 \sin^2 \beta)(L_2^2 - L_1^2)}{\ln(L_2/L_1)} \right] \quad (2C.6-4)$$

Here $\mathcal{P}_i = p_i + \rho g L_i \cos \beta$.

- 2C.7 A simple rate-of-climb indicator** (see Fig. 2C.7). Under the proper circumstances the simple apparatus shown in the figure can be used to measure the rate of climb of an airplane. The gauge pressure inside the Bourdon element is taken as proportional to the rate of climb. For the purposes of this problem the apparatus may be assumed to have the following properties: (i) the capillary tube (of radius R and length L , with $R \ll L$) is of negligible volume but appreciable flow resistance; (ii) the Bourdon element has a constant volume V and offers negligible resistance to flow; and (iii) flow in the capillary is laminar and incompressible, and the volumetric flow rate depends only on the conditions at the ends of the capillary.

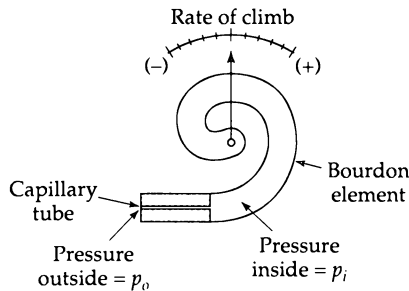


Fig. 2C.7 A rate-of-climb indicator.

- (a) Develop an expression for the change of air pressure with altitude, neglecting temperature changes, and considering air to be an ideal gas of constant composition. (*Hint:* Write a shell balance in which the weight of gas is balanced against the static pressure.)

- (b) By making a mass balance over the gauge, develop an approximate relation between gauge pressure $p_i - p_o$ and rate of climb v_z for a long continued constant-rate climb. Neglect change of air viscosity, and assume changes in air density to be small.
- (c) Develop an approximate expression for the "relaxation time" t_{rel} of the indicator—that is, the time required for the gauge pressure to drop to $1/e$ of its initial value when the external pressure is suddenly changed from zero (relative to the interior of the gauge) to some different constant value, and maintained indefinitely at this new value.
- (d) Discuss the usefulness of this type of indicator for small aircraft.
- (e) Justify the plus and minus signs in the figure.

Answers: (a) $dp/dz = -\rho g = -(pM/RT)g$

(b) $p_i - p_o \approx v_z(8\mu L/\pi R^4)(MgV/R_g T)$, where R_g is the gas constant and M is the molecular weight.

(c) $t_0 = (128/\pi)(\mu VL/\pi D^4 \bar{p})$, where $\bar{p} = \frac{1}{2}(p_i + p_o)$

2D.1 Rolling-ball viscometer. An approximate analysis of the rolling-ball experiment has been given, in which the results of Problem 2B.3 are used.⁸ Read the original paper and verify the results.

2D.2 Drainage of liquids⁹ (see Fig. 2D.2). How much liquid clings to the inside surface of a large vessel when it is drained? As shown in the figure there is a thin film of liquid left behind on the wall as the liquid level in the vessel falls. The local film thickness is a function of both z (the distance down from the initial liquid level) and t (the elapsed time).

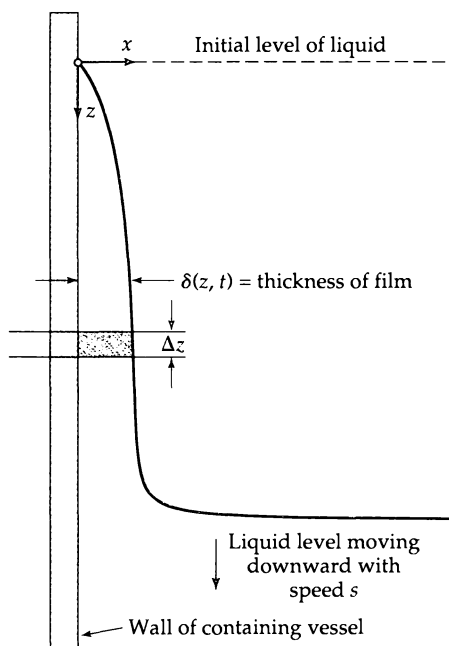


Fig. 2D.2 Clinging of a viscous fluid to wall of vessel during draining.

⁸ H. W. Lewis, *Anal. Chem.*, **25**, 507 (1953); R. B. Bird and R. M. Turian, *Ind. Eng. Chem. Fundamentals*, **3**, 87 (1964); J. Šesták and F. Ambros, *Rheol. Acta*, **12**, 70–76 (1973).

⁹ J. J. van Rossum, *Appl. Sci. Research*, **A7**, 121–144 (1958); see also V. G. Levich, *Physicochemical Hydrodynamics*, Prentice-Hall, Englewood Cliffs, N.J. (1962), Chapter 12.

(a) Make an unsteady-state mass balance on a portion of the film between z and $z + \Delta z$ to get

$$\frac{\partial}{\partial z} \langle v_z \rangle \delta = -\frac{\partial \delta}{\partial t} \quad (2D.2-1)$$

(b) Use Eq. 2.2-18 and a quasi-steady-assumption to obtain the following first-order partial differential equation for $\delta(z, t)$:

$$\frac{\partial \delta}{\partial t} + \frac{\rho g}{\mu} \delta^2 \frac{\partial \delta}{\partial z} = 0 \quad (2D.2-2)$$

(c) Solve this equation to get

$$\delta(z, t) = \sqrt{\frac{\mu}{\rho g} \frac{z}{t}} \quad (2D.2-3)$$

What restrictions have to be placed on this result?

The Equations of Change for Isothermal Systems

- §3.1 The equation of continuity
- §3.2 The equation of motion
- §3.3 The equation of mechanical energy
- §3.4^o The equation of angular momentum
- §3.5 The equations of change in terms of the substantial derivative
- §3.6 Use of the equations of change to solve flow problems
- §3.7 Dimensional analysis of the equations of change

In Chapter 2, velocity distributions were determined for several simple flow systems by the shell momentum balance method. The resulting velocity distributions were then used to get other quantities, such as the average velocity and drag force. The shell balance approach was used to acquaint the novice with the notion of a momentum balance. Even though we made no mention of it in Chapter 2, at several points we tacitly made use of the idea of a mass balance.

It is tedious to set up a shell balance for each problem that one encounters. What we need is a general mass balance and a general momentum balance that can be applied to any problem, including problems with nonrectilinear motion. That is the main point of this chapter. The two equations that we derive are called the *equation of continuity* (for the mass balance) and the *equation of motion* (for the momentum balance). These equations can be used as the starting point for studying all problems involving the isothermal flow of a pure fluid.

In Chapter 11 we enlarge our problem-solving capability by developing the equations needed for nonisothermal pure fluids by adding an equation for the temperature. In Chapter 19 we go even further and add equations of continuity for the concentrations of the individual species. Thus as we go from Chapter 3 to Chapter 11 and on to Chapter 19 we are able to analyze systems of increasing complexity, using the complete set of *equations of change*. It should be evident that Chapter 3 is a very important chapter—perhaps the most important chapter in the book—and it should be mastered thoroughly.

In §3.1 the equation of continuity is developed by making a mass balance over a small element of volume through which the fluid is flowing. Then the size of this element is allowed to go to zero (thereby treating the fluid as a continuum), and the desired partial differential equation is generated.

In §3.2 the equation of motion is developed by making a momentum balance over a small element of volume and letting the volume element become infinitesimally small. Here again a partial differential equation is generated. This equation of motion can be used, along with some help from the equation of continuity, to set up and solve all the problems given in Chapter 2 and many more complicated ones. It is thus a key equation in transport phenomena.

In §3.3 and §3.4 we digress briefly to introduce the equations of change for mechanical energy and angular momentum. These equations are obtained from the equation of motion and hence contain no new physical information. However, they provide a convenient starting point for several applications in this book—particularly the macroscopic balances in Chapter 7.

In §3.5 we introduce the “substantial derivative.” This is the time derivative following the motion of the substance (i.e., the fluid). Because it is widely used in books on fluid dynamics and transport phenomena, we then show how the various equations of change can be rewritten in terms of the substantial derivatives.

In §3.6 we discuss the solution of flow problems by use of the equations of continuity and motion. Although these are partial differential equations, we can solve many problems by postulating the form of the solution and then discarding many terms in these equations. In this way one ends up with a simpler set of equations to solve. In this chapter we solve only problems in which the general equations reduce to one or more ordinary differential equations. In Chapter 4 we examine problems of greater complexity that require some ability to solve partial differential equations. Then in Chapter 5 the equations of continuity and motion are used as the starting point for discussing turbulent flow. Later, in Chapter 8, these same equations are applied to flows of polymeric liquids, which are non-Newtonian fluids.

Finally, §3.7 is devoted to writing the equations of continuity and motion in dimensionless form. This makes clear the origin of the Reynolds number, Re , often mentioned in Chapter 2, and why it plays a key role in fluid dynamics. This discussion lays the groundwork for scale-up and model studies. In Chapter 6 dimensionless numbers arise again in connection with experimental correlations of the drag force in complex systems.

At the end of §2.2, we emphasized the importance of experiments in fluid dynamics. We repeat those words of caution here and point out that photographs and other types of flow visualization have provided us with a much deeper understanding of flow problems than would be possible by theory alone.¹ Keep in mind that when one derives a flow field from the equations of change, it is not necessarily the only physically admissible solution.

Vector and tensor notations are occasionally used in this chapter, primarily for the purpose of abbreviating otherwise lengthy expressions. The beginning student will find that only an elementary knowledge of vector and tensor notation is needed for reading this chapter and for solving flow problems. The advanced student will find Appendix A helpful in getting a better understanding of vector and tensor manipulations. With regard to the notation, it should be kept in mind that we use *lightface italic* symbols for scalars, **boldface Roman** symbols for vectors, and **boldface Greek** symbols for tensors. Also dot-product operations enclosed in () are scalars, and those enclosed in [] are vectors.

¹ We recommend particularly M. Van Dyke, *An Album of Fluid Motion*, Parabolic Press, Stanford (1982); H. Werlé, *Ann. Rev. Fluid Mech.*, **5**, 361–382 (1973); D. V. Boger and K. Walters, *Rheological Phenomena in Focus*, Elsevier, Amsterdam (1993).

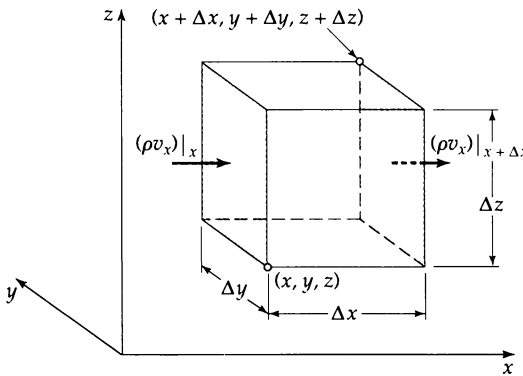


Fig. 3.1-1. Fixed volume element \$\Delta x \Delta y \Delta z\$ through which a fluid is flowing. The arrows indicate the mass flux in and out of the volume at the two shaded faces located at \$x\$ and \$x + \Delta x\$.

§3.1 THE EQUATION OF CONTINUITY

This equation is developed by writing a mass balance over a volume element \$\Delta x \Delta y \Delta z\$, fixed in space, through which a fluid is flowing (see Fig. 3.1-1):

$$\left\{ \begin{array}{l} \text{rate of} \\ \text{increase} \\ \text{of mass} \end{array} \right\} = \left\{ \begin{array}{l} \text{rate of} \\ \text{mass} \\ \text{in} \end{array} \right\} - \left\{ \begin{array}{l} \text{rate of} \\ \text{mass} \\ \text{out} \end{array} \right\} \quad (3.1-1)$$

Now we have to translate this simple physical statement into mathematical language.

We begin by considering the two shaded faces, which are perpendicular to the \$x\$-axis. The rate of mass entering the volume element through the shaded face at \$x\$ is \$(\rho v_x)|_x \Delta y \Delta z\$, and the rate of mass leaving through the shaded face at \$x + \Delta x\$ is \$(\rho v_x)|_{x+\Delta x} \Delta y \Delta z\$. Similar expressions can be written for the other two pairs of faces. The rate of increase of mass within the volume element is \$\Delta x \Delta y \Delta z (\partial \rho / \partial t)\$. The mass balance then becomes

$$\begin{aligned} \Delta x \Delta y \Delta z \frac{\partial \rho}{\partial t} &= \Delta y \Delta z [(\rho v_x)|_x - (\rho v_x)|_{x+\Delta x}] \\ &\quad + \Delta z \Delta x [(\rho v_y)|_y - (\rho v_y)|_{y+\Delta x}] \\ &\quad + \Delta x \Delta y [(\rho v_z)|_z - (\rho v_z)|_{z+\Delta z}] \end{aligned} \quad (3.1-2)$$

By dividing the entire equation by \$\Delta x \Delta y \Delta z\$ and taking the limit as \$\Delta x\$, \$\Delta y\$, and \$\Delta z\$ go to zero, and then using the definitions of the partial derivatives, we get

$$\frac{\partial \rho}{\partial t} = - \left(\frac{\partial}{\partial x} \rho v_x + \frac{\partial}{\partial y} \rho v_y + \frac{\partial}{\partial z} \rho v_z \right) \quad (3.1-3)$$

This is the *equation of continuity*, which describes the time rate of change of the fluid density at a fixed point in space. This equation can be written more concisely by using vector notation as follows:

$\frac{\partial \rho}{\partial t}$ rate of increase of mass per unit volume	$= -(\nabla \cdot \rho \mathbf{v})$ net rate of mass addition per unit volume by convection	(3.1-4)
---	---	---------

Here $(\nabla \cdot \rho \mathbf{v})$ is called the “divergence of $\rho \mathbf{v}$,” sometimes written as “div $\rho \mathbf{v}$.” The vector $\rho \mathbf{v}$ is the mass flux, and its divergence has a simple meaning: it is the net rate of mass efflux per unit volume. The derivation in Problem 3D.1 uses a volume element of arbitrary shape; it is not necessary to use a rectangular volume element as we have done here.

A very important special form of the equation of continuity is that for a fluid of constant density, for which Eq. 3.1-4 assumes the particularly simple form

$$(\text{incompressible fluid}) \quad (\nabla \cdot \mathbf{v}) = 0 \quad (3.1-5)$$

Of course, no fluid is truly incompressible, but frequently in engineering and biological applications, the assumption of constant density results in considerable simplification and very little error.^{1,2}

EXAMPLE 3.1-1

Normal Stresses at Solid Surfaces for Incompressible Newtonian Fluids

Show that for any kind of flow pattern, the normal stresses are zero at fluid–solid boundaries, for Newtonian fluids with constant density. This is an important result that we shall use often.

SOLUTION

We visualize the flow of a fluid near some solid surface, which may or may not be flat. The flow may be quite general, with all three velocity components being functions of all three coordinates and time. At some point P on the surface we erect a Cartesian coordinate system with the origin at P . We now ask what the normal stress τ_{zz} is at P .

According to Table B.1 or Eq. 1.2-6, $\tau_{zz} = -2\mu(\partial v_z / \partial z)$, because $(\nabla \cdot \mathbf{v}) = 0$ for incompressible fluids. Then at point P on the surface of the solid

$$\tau_{zz}|_{z=0} = -2\mu \frac{\partial v_z}{\partial z} \Big|_{z=0} = +2\mu \left(\frac{\partial v_x}{\partial x} + \frac{\partial v_y}{\partial y} \right) \Big|_{z=0} = 0 \quad (3.1-6)$$

First we replaced the derivative $\partial v_z / \partial z$ by using Eq. 3.1-3 with ρ constant. However, on the solid surface at $z = 0$, the velocity v_x is zero by the no-slip condition (see §2.1), and therefore the derivative $\partial v_x / \partial x$ on the surface must be zero. The same is true of $\partial v_y / \partial y$ on the surface. Therefore τ_{zz} is zero. It is also true that τ_{xx} and τ_{yy} are zero at the surface because of the vanishing of the derivatives at $z = 0$. (Note: The vanishing of the normal stresses on solid surfaces does not apply to polymeric fluids, which are viscoelastic. For compressible fluids, the normal stresses at solid surfaces are zero if the density is not changing with time, as is shown in Problem 3C.2.)

§3.2 THE EQUATION OF MOTION

To get the equation of motion we write a momentum balance over the volume element $\Delta x \Delta y \Delta z$ in Fig. 3.2-1 of the form

$$\begin{bmatrix} \text{rate of} \\ \text{increase} \\ \text{of momentum} \end{bmatrix} = \begin{bmatrix} \text{rate of} \\ \text{momentum} \\ \text{in} \end{bmatrix} - \begin{bmatrix} \text{rate of} \\ \text{momentum} \\ \text{out} \end{bmatrix} + \begin{bmatrix} \text{external} \\ \text{force on} \\ \text{the fluid} \end{bmatrix} \quad (3.2-1)$$

¹ L. D. Landau and E. M. Lifshitz, *Fluid Mechanics*, Pergamon Press, Oxford (1987), p. 21, point out that, for steady, isentropic flows, commonly encountered in aerodynamics, the incompressibility assumption is valid when the fluid velocity is small compared to the velocity of sound (i.e., low Mach number).

² Equation 3.1-5 is the basis for Chapter 2 in G. K. Batchelor, *An Introduction to Fluid Dynamics*, Cambridge University Press (1967), which is a lengthy discussion of the kinematical consequences of the equation of continuity.

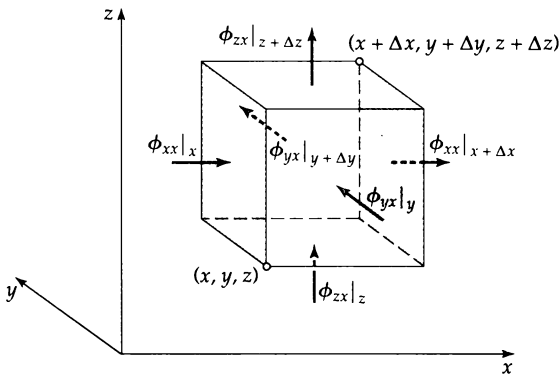


Fig. 3.2-1. Fixed volume element $\Delta x \Delta y \Delta z$, with six arrows indicating the flux of x -momentum through the surfaces by all mechanisms. The shaded faces are located at x and $x + \Delta x$.

Note that Eq. 3.2-1 is an extension of Eq. 2.1-1 to unsteady-state problems. Therefore we proceed in much the same way as in Chapter 2. However, in addition to including the unsteady-state term, we must allow the fluid to move through all six faces of the volume element. Remember that Eq. 3.2-1 is a vector equation with components in each of the three coordinate directions x , y , and z . We develop the x -component of each term in Eq. 3.2-1; the y - and z -components may be treated analogously.¹

First, we consider the rates of flow of the x -component of momentum into and out of the volume element shown in Fig. 3.2-1. Momentum enters and leaves $\Delta x \Delta y \Delta z$ by two mechanisms: convective transport (see §1.7), and molecular transport (see §1.2).

The rate at which the x -component of momentum enters across the shaded face at x by all mechanisms—both convective and molecular—is $(\phi_{xx})|_x \Delta y \Delta z$ and the rate at which it leaves the shaded face at $x + \Delta x$ is $(\phi_{xx})|_{x+\Delta x} \Delta y \Delta z$. The rates at which x -momentum enters and leaves through the faces at y and $y + \Delta y$ are $(\phi_{yx})|_y \Delta z \Delta x$ and $(\phi_{yx})|_{y+\Delta y} \Delta z \Delta x$, respectively. Similarly, the rates at which x -momentum enters and leaves through the faces at z and $z + \Delta z$ are $(\phi_{zx})|_z \Delta x \Delta y$ and $(\phi_{zx})|_{z+\Delta z} \Delta x \Delta y$. When these contributions are added we get for the net rate of addition of x -momentum

$$\Delta y \Delta z (\phi_{xx}|_x - \phi_{xx}|_{x+\Delta x}) + \Delta z \Delta x (\phi_{yx}|_y - \phi_{yx}|_{y+\Delta y}) + \Delta x \Delta y (\phi_{zx}|_z - \phi_{zx}|_{z+\Delta z}) \quad (3.2-2)$$

across all three pairs of faces.

Next there is the external force (typically the gravitational force) acting on the fluid in the volume element. The x -component of this force is

$$\rho g_x \Delta x \Delta y \Delta z \quad (3.2-3)$$

Equations 3.2-2 and 3.2-3 give the x -components of the three terms on the right side of Eq. 3.2-1. The sum of these terms must then be equated to the rate of increase of x -momentum within the volume element: $\Delta x \Delta y \Delta z \frac{\partial(\rho v_x)}{\partial t}$. When this is done, we have the x -component of the momentum balance. When this equation is divided by $\Delta x \Delta y \Delta z$ and the limit is taken as Δx , Δy , and Δz go to zero, the following equation results:

$$\frac{\partial}{\partial t} \rho v_x = - \left(\frac{\partial}{\partial x} \phi_{xx} + \frac{\partial}{\partial y} \phi_{yx} + \frac{\partial}{\partial z} \phi_{zx} \right) + \rho g_x \quad (3.2-4)$$

¹ In this book all the equations of change are derived by applying the conservation laws to a region $\Delta x \Delta y \Delta z$ fixed in space. The same equations can be obtained by using an arbitrary region fixed in space or one moving along with the fluid. These derivations are described in Problem 3D.1. Advanced students should become familiar with these derivations.

Here we have made use of the definitions of the partial derivatives. Similar equations can be developed for the y - and z -components of the momentum balance:

$$\frac{\partial}{\partial t} \rho v_y = -\left(\frac{\partial}{\partial x} \phi_{xy} + \frac{\partial}{\partial y} \phi_{yy} + \frac{\partial}{\partial z} \phi_{zy}\right) + \rho g_y \quad (3.2-5)$$

$$\frac{\partial}{\partial t} \rho v_z = -\left(\frac{\partial}{\partial x} \phi_{xz} + \frac{\partial}{\partial y} \phi_{yz} + \frac{\partial}{\partial z} \phi_{zz}\right) + \rho g_z \quad (3.2-6)$$

By using vector-tensor notation, these three equations can be written as follows:

$$\frac{\partial}{\partial t} \rho v_i = -[\nabla \cdot \boldsymbol{\phi}]_i + \rho g_i \quad i = x, y, z \quad (3.2-7)$$

That is, by letting i be successively x , y , and z , Eqs. 3.2-4, 5, and 6 can be reproduced. The quantities ρv_i are the Cartesian components of the vector $\rho \mathbf{v}$, which is the momentum per unit volume at a point in the fluid. Similarly, the quantities ρg_i are the components of the vector $\rho \mathbf{g}$, which is the external force per unit volume. The term $-[\nabla \cdot \boldsymbol{\phi}]_i$ is the i th component of the vector $-[\nabla \cdot \boldsymbol{\phi}]$.

When the i th component of Eq. 3.2-7 is multiplied by the unit vector in the i th direction and the three components are added together vectorially, we get

$$\frac{\partial}{\partial t} \rho \mathbf{v} = -[\nabla \cdot \boldsymbol{\phi}] + \rho \mathbf{g} \quad (3.2-8)$$

which is the differential statement of the law of conservation of momentum. It is the translation of Eq. 3.2-1 into mathematical symbols.

In Eq. 1.7-1 it was shown that the combined momentum flux tensor $\boldsymbol{\phi}$ is the sum of the convective momentum flux tensor $\rho \mathbf{v} \mathbf{v}$ and the molecular momentum flux tensor $\boldsymbol{\tau}$, and that the latter can be written as the sum of $p \boldsymbol{\delta}$ and $\boldsymbol{\tau}$. When we insert $\boldsymbol{\phi} = \rho \mathbf{v} \mathbf{v} + p \boldsymbol{\delta} + \boldsymbol{\tau}$ into Eq. 3.2-8, we get the following *equation of motion*:²

$\frac{\partial}{\partial t} \rho \mathbf{v}$	$=$	$-[\nabla \cdot \rho \mathbf{v} \mathbf{v}]$	$-\nabla p$	$-[\nabla \cdot \boldsymbol{\tau}]$	$+ \rho \mathbf{g}$	(3.2-9)
rate of increase of momentum per unit volume		rate of momentum addition by convection per unit volume	rate of momentum addition by molecular transport per unit volume		external force on fluid per unit volume	

In this equation ∇p is a vector called the “gradient of (the scalar) p ” sometimes written as “grad p .” The symbol $[\nabla \cdot \boldsymbol{\tau}]$ is a vector called the “divergence of (the tensor) $\boldsymbol{\tau}$ ” and $[\nabla \cdot \rho \mathbf{v} \mathbf{v}]$ is a vector called the “divergence of (the dyadic product) $\rho \mathbf{v} \mathbf{v}$.”

In the next two sections we give some formal results that are based on the equation of motion. The equations of change for mechanical energy and angular momentum are not used for problem solving in this chapter, but will be referred to in Chapter 7. Beginners are advised to skim these sections on first reading and to refer to them later as the need arises.

² This equation is attributed to A.-L. Cauchy, *Ex. de math.*, 2, 108–111 (1827). **(Baron) Augustin-Louis Cauchy** (1789–1857) (pronounced “Koh-shee” with the accent on the second syllable), originally trained as an engineer, made great contributions to theoretical physics and mathematics, including the calculus of complex variables.

§3.3 THE EQUATION OF MECHANICAL ENERGY

Mechanical energy is not conserved in a flow system, but that does not prevent us from developing an equation of change for this quantity. In fact, during the course of this book, we will obtain equations of change for a number of nonconserved quantities, such as internal energy, enthalpy, and entropy. The equation of change for mechanical energy, which involves only mechanical terms, may be derived from the equation of motion of §3.2. The resulting equation is referred to in many places in the text that follows.

We take the dot product of the velocity vector \mathbf{v} with the equation of motion in Eq. 3.2-9 and then do some rather lengthy rearranging, making use of the equation of continuity in Eq. 3.1-4. We also split up each of the terms containing p and τ into two parts. The final result is the *equation of change for kinetic energy*:

$$\begin{aligned} \frac{\partial}{\partial t} \left(\frac{1}{2} \rho v^2 \right) &= -(\nabla \cdot \frac{1}{2} \rho v^2 \mathbf{v}) - (\nabla \cdot p \mathbf{v}) - p(-\nabla \cdot \mathbf{v}) \\ \text{rate of} &\quad \text{rate of addition} & \text{rate of work} & \text{rate of reversible} \\ \text{increase of} &\quad \text{of kinetic energy} & \text{done by pressure} & \text{conversion of} \\ \text{kinetic energy} &\quad \text{by convection} & \text{of surroundings} & \text{kinetic energy into} \\ \text{per unit volume} &\quad \text{per unit volume} & \text{on the fluid} & \text{internal energy} \\ \\ -(\nabla \cdot (\tau \cdot \mathbf{v})) &= -(-\tau \cdot \nabla \mathbf{v}) + \rho(\mathbf{v} \cdot \mathbf{g}) & (3.3-1)^1 \\ \text{rate of work done} &\quad \text{rate of} & \text{rate of work} \\ \text{by viscous forces} &\quad \text{irreversible} & \text{by external force} \\ \text{on the fluid} &\quad \text{conversion} & \text{on the fluid} \\ &\quad \text{from kinetic to} & \\ &\quad \text{internal energy} & \end{aligned}$$

At this point it is not clear why we have attributed the indicated physical significance to the terms $p(\nabla \cdot \mathbf{v})$ and $(\tau \cdot \nabla \mathbf{v})$. Their meaning cannot be properly appreciated until one has studied the energy balance in Chapter 11. There it will be seen how these same two terms appear with opposite sign in the equation of change for internal energy.

We now introduce the *potential energy*² (per unit mass) $\hat{\Phi}$, defined by $\mathbf{g} = -\nabla \hat{\Phi}$. Then the last term in Eq. 3.3-1 may be rewritten as $-\rho(\mathbf{v} \cdot \nabla \hat{\Phi}) = -(\nabla \cdot \rho \mathbf{v} \hat{\Phi}) + \hat{\Phi}(\nabla \cdot \rho \mathbf{v})$. The equation of continuity in Eq. 3.1-4 may now be used to replace $+\hat{\Phi}(\nabla \cdot \rho \mathbf{v})$ by $-\hat{\Phi}(\partial \rho / \partial t)$. The latter may be written as $-\partial(\rho \hat{\Phi}) / \partial t$, if the potential energy is independent of the time. This is true for the gravitational field for systems that are located on the surface of the earth; then $\hat{\Phi} = gh$, where g is the (constant) gravitational acceleration and h is the elevation coordinate in the gravitational field.

With the introduction of the potential energy, Eq. 3.3-1 assumes the following form:

$$\begin{aligned} \frac{\partial}{\partial t} \left(\frac{1}{2} \rho v^2 + \rho \hat{\Phi} \right) &= -(\nabla \cdot (\frac{1}{2} \rho v^2 + \rho \hat{\Phi}) \mathbf{v}) \\ &\quad -(\nabla \cdot p \mathbf{v}) - p(-\nabla \cdot \mathbf{v}) - (\nabla \cdot [\tau \cdot \mathbf{v}]) - (-\tau \cdot \nabla \mathbf{v}) \end{aligned} \quad (3.3-2)$$

This is an *equation of change for kinetic-plus-potential energy*. Since Eqs. 3.3-1 and 3.3-2 contain only mechanical terms, they are both referred to as the *equation of change for mechanical energy*.

The term $p(\nabla \cdot \mathbf{v})$ may be either positive or negative depending on whether the fluid is undergoing *expansion* or *compression*. The resulting temperature changes can be rather large for gases in compressors, turbines, and shock tubes.

¹ The interpretation under the $(\tau \cdot \nabla \mathbf{v})$ term is correct only for Newtonian fluids; for viscoelastic fluids, such as polymers, this term may include reversible conversion to elastic energy.

² If $\mathbf{g} = -\delta_z g$ is a vector of magnitude g in the negative z direction, then the potential energy per unit mass is $\hat{\Phi} = gz$, where z is the elevation in the gravitational field.

The term $(-\tau : \nabla \mathbf{v})$ is always positive for *Newtonian* fluids,³ because it may be written as a sum of squared terms:

$$\begin{aligned} (-\tau : \nabla \mathbf{v}) &= \frac{1}{2}\mu \sum_i \sum_j \left[\left(\frac{\partial v_i}{\partial x_j} + \frac{\partial v_j}{\partial x_i} \right) - \frac{2}{3}(\nabla \cdot \mathbf{v})\delta_{ij} \right]^2 + \kappa(\nabla \cdot \mathbf{v})^2 \\ &= \mu\Phi_v + \kappa\Psi_v \end{aligned} \quad (3.3-3)$$

which serves to define the two quantities Φ_v and Ψ_v . When the index i takes on the values 1, 2, 3, the velocity components v_i become v_x , v_y , v_z and the Cartesian coordinates x_i become x , y , z . The symbol δ_{ij} is the Kronecker delta, which is 0 if $i \neq j$ and 1 if $i = j$.

The quantity $(-\tau : \nabla \mathbf{v})$ describes the degradation of mechanical energy into thermal energy that occurs in all flow systems (sometimes called the *viscous dissipation heating*).⁴ This heating can produce considerable temperature rises in systems with large viscosity and large velocity gradients, as in lubrication, rapid extrusion, and high-speed flight. (Another example of conversion of mechanical energy into heat is the rubbing of two sticks together to start a fire, which scouts are presumably able to do.)

When we speak of "isothermal systems," we mean systems in which there are no externally imposed temperature gradients and no appreciable temperature change resulting from expansion, contraction, or viscous dissipation.

The most important use of Eq. 3.3-2 is for the development of the macroscopic mechanical energy balance (or engineering Bernoulli equation) in Section 7.8.

§3.4 THE EQUATION OF ANGULAR MOMENTUM

Another equation can be obtained from the equation of motion by forming the cross product of the position vector \mathbf{r} (which has Cartesian components x , y , z) with Eq. 3.2-9. The equation of motion as derived in §3.2 does not contain the assumption that the stress (or momentum-flux) tensor τ is symmetric. (Of course, the expressions given in §2.3 for the Newtonian fluid are symmetric; that is, $\tau_{ij} = \tau_{ji}$.)

When the cross product is formed, we get—after some vector-tensor manipulations—the following *equation of change for angular momentum*:

$$\frac{\partial}{\partial t} \rho[\mathbf{r} \times \mathbf{v}] = -[\nabla \cdot \rho \mathbf{v}[\mathbf{r} \times \mathbf{v}]] - [\nabla \cdot [\mathbf{r} \times p\boldsymbol{\delta}^\dagger]] - [\nabla \cdot [\mathbf{r} \times \boldsymbol{\tau}^\dagger]] + [\mathbf{r} \times \rho \mathbf{g}] - [\boldsymbol{\epsilon} : \boldsymbol{\tau}] \quad (3.4-1)$$

Here $\boldsymbol{\epsilon}$ is a third-order tensor with components ϵ_{ijk} (the permutation symbol defined in §A.2). If the stress tensor $\boldsymbol{\tau}$ is symmetric, as for Newtonian fluids, the last term is zero. According to the kinetic theories of dilute gases, monatomic liquids, and polymers, the tensor $\boldsymbol{\tau}$ is symmetric, in the absence of electric and magnetic torques.¹ If, on the other hand, $\boldsymbol{\tau}$ is asymmetric, then the last term describes the rate of conversion of bulk angular momentum to internal angular momentum.

The assumption of a symmetric stress tensor, then, is equivalent to an assertion that there is no interconversion between bulk angular momentum and internal angular momentum and that the two forms of angular momentum are conserved separately. This

³ An amusing consequence of the viscous dissipation for air is the study by H. K. Moffatt [Nature, 404, 833–834 (2000)] of the way in which a spinning coin comes to rest on a table.

⁴ G. G. Stokes, *Trans. Camb. Phil. Soc.*, 9, 8–106 (1851), see pp. 57–59.

¹ J. S. Dahler and L. E. Scriven, *Nature*, 192, 36–37 (1961); S. de Groot and P. Mazur, *Nonequilibrium Thermodynamics*, North Holland, Amsterdam (1962), Chapter XII. A literature review can be found in G. D. C. Kuiken, *Ind. Eng. Chem. Res.*, 34, 3568–3572 (1995).

corresponds, in Eq. 0.3-8, to equating the cross-product terms and the internal angular momentum terms separately.

Eq. 3.4-1 will be referred to only in Chapter 7, where we indicate that the macroscopic angular momentum balance can be obtained from it.

§3.5 THE EQUATIONS OF CHANGE IN TERMS OF THE SUBSTANTIAL DERIVATIVE

Before proceeding we point out that several different time derivatives may be encountered in transport phenomena. We illustrate these by a homely example—namely, the observation of the concentration of fish in the Mississippi River. Because fish swim around, the fish concentration will in general be a function of position (x, y, z) and time (t).

The Partial Time Derivative $\partial/\partial t$

Suppose we stand on a bridge and observe the concentration of fish just below us as a function of time. We can then record the time rate of change of the fish concentration at a fixed location. The result is $(\partial c / \partial t)|_{x,y,z}$, the partial derivative of c with respect to t , at constant x, y , and z .

The Total Time Derivative d/dt

Now suppose that we jump into a motor boat and speed around on the river, sometimes going upstream, sometimes downstream, and sometimes across the current. All the time we are observing fish concentration. At any instant, the time rate of change of the observed fish concentration is

$$\frac{dc}{dt} = \left(\frac{\partial c}{\partial t} \right)_{x,y,z} + \frac{dx}{dt} \left(\frac{\partial c}{\partial x} \right)_{y,z,t} + \frac{dy}{dt} \left(\frac{\partial c}{\partial y} \right)_{z,x,t} + \frac{dz}{dt} \left(\frac{\partial c}{\partial z} \right)_{x,y,t} \quad (3.5-1)$$

in which $dx/dt, dy/dt$, and dz/dt are the components of the velocity of the boat.

The Substantial Time Derivative D/Dt

Next we climb into a canoe, and not feeling energetic, we just float along with the current, observing the fish concentration. In this situation the velocity of the observer is the same as the velocity \mathbf{v} of the stream, which has components v_x, v_y , and v_z . If at any instant we report the time rate of change of fish concentration, we are then giving

$$\frac{Dc}{Dt} = \frac{\partial c}{\partial t} + v_x \frac{\partial c}{\partial x} + v_y \frac{\partial c}{\partial y} + v_z \frac{\partial c}{\partial z} \quad \text{or} \quad \frac{Dc}{Dt} = \frac{\partial c}{\partial t} + (\mathbf{v} \cdot \nabla c) \quad (3.5-2)$$

The special operator $D/Dt = \partial/\partial t + \mathbf{v} \cdot \nabla$ is called the *substantial derivative* (meaning that the time rate of change is reported as one moves with the “substance”). The terms *material derivative*, *hydrodynamic derivative*, and *derivative following the motion* are also used.

Now we need to know how to convert equations expressed in terms of $\partial/\partial t$ into equations written with D/Dt . For any scalar function $f(x, y, z, t)$ we can do the following manipulations:

$$\begin{aligned} & \frac{\partial}{\partial t}(\rho f) + \left(\frac{\partial}{\partial x} \rho v_x f \right) + \left(\frac{\partial}{\partial y} \rho v_y f \right) + \left(\frac{\partial}{\partial z} \rho v_z f \right) \\ &= \rho \left(\frac{\partial f}{\partial t} + v_x \frac{\partial f}{\partial x} + v_y \frac{\partial f}{\partial y} + v_z \frac{\partial f}{\partial z} \right) + f \left(\frac{\partial \rho}{\partial t} + \frac{\partial}{\partial x} \rho v_x + \frac{\partial}{\partial y} \rho v_y + \frac{\partial}{\partial z} \rho v_z \right) \\ &= \rho \frac{Df}{Dt} \end{aligned} \quad (3.5-3)$$

Table 3.5-1 The Equations of Change for Isothermal Systems in the D/Dt -Form^a
Note: At the left are given the equation numbers for the $\partial/\partial t$ forms.

(3.1-4)	$\frac{D\rho}{Dt} = -\rho(\nabla \cdot \mathbf{v})$	(A)
(3.2-9)	$\rho \frac{D\mathbf{v}}{Dt} = -\nabla p - [\nabla \cdot \boldsymbol{\tau}] + \rho\mathbf{g}$	(B)
(3.3-1)	$\rho \frac{D}{Dt} (\frac{1}{2}\mathbf{v}^2) = -(\mathbf{v} \cdot \nabla p) - (\mathbf{v} \cdot [\nabla \cdot \boldsymbol{\tau}]) + \rho(\mathbf{v} \cdot \mathbf{g})$	(C)
(3.4-1)	$\rho \frac{D}{Dt} [\mathbf{r} \times \mathbf{v}] = -[\nabla \cdot [\mathbf{r} \times p\boldsymbol{\delta}^\dagger]] - [\nabla \cdot [\mathbf{r} \times \boldsymbol{\tau}^\dagger]] + [\mathbf{r} \times \rho\mathbf{g}]$	(D) ^a

^a Equations (A) through (C) are obtained from Eqs. 3.1-4, 3.2-9, and 3.3-1 with *no assumptions*. Equation (D) is written for symmetrical $\boldsymbol{\tau}$ only.

The quantity in the second parentheses in the second line is zero according to the equation of continuity. Consequently Eq. 3.5-3 can be written in vector form as

$$\frac{\partial}{\partial t} (\rho f) + (\nabla \cdot \rho \mathbf{v} f) = \rho \frac{Df}{Dt} \quad (3.5-4)$$

Similarly, for any vector function $\mathbf{f}(x, y, z, t)$,

$$\frac{\partial}{\partial t} (\rho \mathbf{f}) + [\nabla \cdot \rho \mathbf{v} \mathbf{f}] = \rho \frac{D\mathbf{f}}{Dt} \quad (3.5-5)$$

These equations can be used to rewrite the equations of change given in §§3.1 to 3.4 in terms of the substantial derivative as shown in Table 3.5-1.

Equation A in Table 3.5-1 tells how the density is decreasing or increasing as one moves along with the fluid, because of the compression [$(\nabla \cdot \mathbf{v}) < 0$] or expansion of the fluid [$(\nabla \cdot \mathbf{v}) > 0$]. Equation B can be interpreted as (mass) \times (acceleration) = the sum of the pressure forces, viscous forces, and the external force. In other words, Eq. 3.2-9 is equivalent to Newton's second law of motion applied to a small blob of fluid whose envelope moves locally with the fluid velocity \mathbf{v} (see Problem 3D.1).

We now discuss briefly the three most common simplifications of the equation of motion.¹

(i) For *constant* ρ and μ , insertion of the Newtonian expression for $\boldsymbol{\tau}$ from Eq. 1.2-7 into the equation of motion leads to the very famous *Navier-Stokes equation*, first developed from molecular arguments by Navier and from continuum arguments by Stokes:²

$$\rho \frac{D}{Dt} \mathbf{v} = -\nabla p + \mu \nabla^2 \mathbf{v} + \rho \mathbf{g} \quad \text{or} \quad \rho \frac{D}{Dt} \mathbf{v} = -\nabla \mathcal{P} + \mu \nabla^2 \mathbf{v} \quad (3.5-6, 7)$$

In the second form we have used the "modified pressure" $\mathcal{P} = p + \rho gh$ introduced in Chapter 2, where h is the elevation in the gravitational field and gh is the gravitational

¹ For discussions of the history of these and other famous fluid dynamics relations, see H. Rouse and S. Ince, *History of Hydraulics*, Iowa Institute of Hydraulics, Iowa City (1959).

² L. M. H. Navier, *Mémoires de l'Académie Royale des Sciences*, 6, 389–440 (1827); G. G. Stokes, *Proc. Cambridge Phil. Soc.*, 8, 287–319 (1845). The name Navier is pronounced "Nah-vyay."

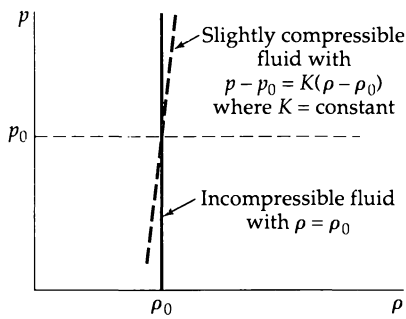


Fig. 3.5-1. The equation of state for a slightly compressible fluid and an incompressible fluid when T is constant.

potential energy per unit mass. Equation 3.5-6 is a standard starting point for describing isothermal flows of gases and liquids.

It must be kept in mind that, when constant ρ is assumed, the equation of state (at constant T) is a vertical line on a plot of p vs. ρ (see Fig. 3.5-1). Thus, the absolute pressure is no longer determinable from ρ and T , although pressure gradients and instantaneous differences remain determinate by Eq. 3.5-6 or Eq. 3.5-7. Absolute pressures are also obtainable if p is known at some point in the system.

(ii) When the *acceleration terms* in the Navier–Stokes equation are neglected—that is, when $\rho(D\mathbf{v}/Dt) = 0$ —we get

$$0 = -\nabla p + \mu\nabla^2\mathbf{v} + \rho\mathbf{g} \quad (3.5-8)$$

which is called the *Stokes flow equation*. It is sometimes called the *creeping flow equation*, because the term $\rho[\mathbf{v} \cdot \nabla \mathbf{v}]$, which is quadratic in the velocity, can be discarded when the flow is extremely slow. For some flows, such as the Hagen–Poiseuille tube flow, the term $\rho[\mathbf{v} \cdot \nabla \mathbf{v}]$ drops out, and a restriction to slow flow is not implied. The Stokes flow equation is important in lubrication theory, the study of particle motions in suspension, flow through porous media, and swimming of microbes. There is a vast literature on this subject.³

(iii) When *viscous forces are neglected*—that is, $[\nabla \cdot \tau] = 0$ —the equation of motion becomes

$$\rho \frac{D\mathbf{v}}{Dt} = -\nabla p + \rho\mathbf{g} \quad (3.5-9)$$

which is known as the *Euler equation* for “inviscid” fluids.⁴ Of course, there are no truly “inviscid” fluids, but there are many flows in which the viscous forces are relatively unimportant. Examples are the flow around airplane wings (except near the solid boundary), flow of rivers around the upstream surfaces of bridge abutments, some problems in compressible gas dynamics, and flow of ocean currents.⁵

³ J. Happel and H. Brenner, *Low Reynolds Number Hydrodynamics*, Martinus Nijhoff, The Hague (1983); S. Kim and S. J. Karrila, *Microhydrodynamics: Principles and Selected Applications*, Butterworth-Heinemann, Boston (1991).

⁴ L. Euler, *Mém. Acad. Sci. Berlin*, **11**, 217–273, 274–315, 316–361 (1755). The Swiss-born mathematician **Leonhard Euler** (1707–1783) (pronounced “Oiler”) taught in St. Petersburg, Basel, and Berlin and published extensively in many fields of mathematics and physics.

⁵ See, for example, D. J. Acheson, *Elementary Fluid Mechanics*, Clarendon Press, Oxford (1990), Chapters 3–5; and G. K. Batchelor, *An Introduction to Fluid Dynamics*, Cambridge University Press (1967), Chapter 6.

EXAMPLE 3.5-1

The Bernoulli Equation for the Steady Flow of Inviscid Fluids

The Bernoulli equation for steady flow of inviscid fluids is one of the most famous equations in classical fluid dynamics.⁶ Show how it is obtained from the Euler equation of motion.

SOLUTION

Omit the time-derivative term in Eq. 3.5-9, and then use the vector identity $[\mathbf{v} \cdot \nabla \mathbf{v}] = \frac{1}{2}\nabla(\mathbf{v} \cdot \mathbf{v}) - [\mathbf{v} \times [\nabla \times \mathbf{v}]]$ (Eq. A.4-23) to rewrite the equation as

$$\rho \nabla_{\frac{1}{2}} v^2 - \rho [\mathbf{v} \times [\nabla \times \mathbf{v}]] = -\nabla p - \rho g \nabla h \quad (3.5-10)$$

In writing the last term, we have expressed \mathbf{g} as $-\nabla \hat{\Phi} = -g \nabla h$, where h is the elevation in the gravitational field.

Next we divide Eq. 3.5-10 by ρ and then form the dot product with the unit vector $\mathbf{s} = \mathbf{v}/|\mathbf{v}|$ in the flow direction. When this is done the term involving the curl of the velocity field can be shown to vanish (a nice exercise in vector analysis), and $(\mathbf{s} \cdot \nabla)$ can be replaced by d/ds , where s is the distance along a streamline. Thus we get

$$\frac{d}{ds} \left(\frac{1}{2} v^2 \right) = -\frac{1}{\rho} \frac{d}{ds} p - g \frac{d}{ds} h \quad (3.5-11)$$

When this is integrated along a streamline from point 1 to point 2, we get

$$\frac{1}{2}(v_2^2 - v_1^2) + \int_{p_1}^{p_2} \frac{1}{\rho} dp + g(h_2 - h_1) = 0 \quad (3.5-12)$$

which is called the *Bernoulli equation*. It relates the velocity, pressure, and elevation of two points along a streamline in a fluid in steady-state flow. It is used in situations where it can be assumed that viscosity plays a rather minor role.

§3.6 USE OF THE EQUATIONS OF CHANGE TO SOLVE FLOW PROBLEMS

For most applications of the equation of motion, we have to insert the expression for τ from Eq. 1.2-7 into Eq. 3.2-9 (or, equivalently, the components of τ from Eq. 1.2-6 or Appendix B.1 into Eqs. 3.2-5, 3.2-6, and 3.2-7). Then to describe the flow of a Newtonian fluid at constant temperature, we need in general

The equation of continuity	Eq. 3.1-4
The equation of motion	Eq. 3.2-9
The components of τ	Eq. 1.2-6
The equation of state	$p = p(\rho)$
The equations for the viscosities	$\mu = \mu(\rho)$, $\kappa = \kappa(\rho)$

These equations, along with the necessary boundary and initial conditions, determine completely the pressure, density, and velocity distributions in the fluid. They are seldom used in their complete form to solve fluid dynamics problems. Usually restricted forms are used for convenience, as in this chapter.

If it is appropriate to assume constant density and viscosity, then we use

The equation of continuity	Eq. 3.1-4 and Table B.4
The Navier-Stokes equation	Eq. 3.5-6 and Tables B.5, 6, 7

along with initial and boundary conditions. From these one determines the pressure and velocity distributions.

⁶ Daniel Bernoulli (1700–1782) was one of the early researchers in fluid dynamics and also the kinetic theory of gases. His hydrodynamical ideas were summarized in D. Bernoulli, *Hydrodynamica sive de viribus et motibus fluidorum commentarii*, Argentorati (1738), however he did not actually give Eq. 3.5-12. The credit for the derivation of Eq. 3.5-12 goes to L. Euler, *Histoires de l'Académie de Berlin* (1755).

In Chapter 1 we gave the components of the stress tensor in Cartesian coordinates, and in this chapter we have derived the equations of continuity and motion in Cartesian coordinates. In Tables B.1, 4, 5, 6, and 7 we summarize these key equations in three much-used coordinate systems: Cartesian (x, y, z), cylindrical (r, θ, z), and spherical (r, θ, ϕ). Beginning students should not concern themselves with the derivation of these equations, but they should be very familiar with the tables in Appendix B and be able to use them for setting up fluid dynamics problems. Advanced students will want to go through the details of Appendix A and learn how to develop the expressions for the various ∇ -operations, as is done in §§A.6 and A.7.

In this section we illustrate how to set up and solve some problems involving the steady, isothermal, laminar flow of Newtonian fluids. The relatively simple analytical solutions given here are not to be regarded as ends in themselves, but rather as a preparation for moving on to the analytical or numerical solution of more complex problems, the use of various approximate methods, or the use of dimensional analysis.

The complete solution of viscous flow problems, including proofs of uniqueness and criteria for stability, is a formidable task. Indeed, the attention of some of the world's best applied mathematicians has been devoted to the challenge of solving the equations of continuity and motion. The beginner may well feel inadequate when faced with these equations for the first time. All we attempt to do in the illustrative examples in this section is to solve a few problems for stable flows that are known to exist. In each case we begin by making some *postulates* about the form for the pressure and velocity distributions: that is, we guess how p and v should depend on position in the problem being studied. Then we discard all the terms in the equations of continuity and motion that are unnecessary according to the postulates made. For example, if one postulates that v_x is a function of y alone, terms like $\partial v_x / \partial x$ and $\partial^2 v_x / \partial z^2$ can be discarded. When all the unnecessary terms have been eliminated, one is frequently left with a small number of relatively simple equations; and if the problem is sufficiently simple, an analytical solution can be obtained.

It must be emphasized that in listing the postulates, one makes use of *intuition*. The latter is based on our daily experience with flow phenomena. Our intuition often tells us that a flow will be symmetrical about an axis, or that some component of the velocity is zero. Having used our intuition to make such postulates, we must remember that the final solution is correspondingly restricted. However, by starting with the equations of change, when we have finished the "discarding process" we do at least have a complete listing of all the assumptions used in the solution. In some instances it is possible to go back and remove some of the assumptions and get a better solution.

In several examples to be discussed, we will find one solution to the fluid dynamical equations. However, because the full equations are nonlinear, there may be other solutions to the problem. Thus a complete solution to a fluid dynamics problem requires the specification of the limits on the stable flow regimes as well as any ranges of unstable behavior. That is, we have to develop a "map" showing the various flow regimes that are possible. Usually analytical solutions can be obtained for only the simplest flow regimes; the remainder of the information is generally obtained by experiment or by very detailed numerical solutions. In other words, although we know the differential equations that govern the fluid motion, much is yet unknown about how to solve them. This is a challenging area of applied mathematics, well above the level of an introductory textbook.

When difficult problems are encountered, a search should be made through some of the advanced treatises on fluid dynamics.¹

¹ R. Berker, *Handbuch der Physik*, Volume VIII-2, Springer, Berlin (1963), pp. 1–384; G. K. Batchelor, *An Introduction to Fluid Mechanics*, Cambridge University Press (1967); L. Landau and E. M. Lifshitz, *Fluid Mechanics*, Pergamon Press, Oxford, 2nd edition (1987); J. A. Schetz and A. E. Fuhs (eds.), *Handbook of Fluid Dynamics and Fluid Machinery*, Wiley-Interscience, New York (1996); R. W. Johnson (ed.), *The Handbook of Fluid Dynamics*, CRC Press, Boca Raton, Fla. (1998); C. Y. Wang, *Ann. Revs. Fluid Mech.*, **23**, 159–177 (1991).

We now turn to the illustrative examples. The first two are problems that were discussed in the preceding chapter; we rework these just to illustrate the use of the equations of change. Then we consider some other problems that would be difficult to set up by the shell balance method of Chapter 2.

EXAMPLE 3.6-1***Steady Flow in a Long Circular Tube***

Rework the tube-flow problem of Example 2.3-1 using the equations of continuity and motion. This illustrates the use of the tabulated equations for constant viscosity and density in cylindrical coordinates, given in Appendix B.

SOLUTION

We postulate that $\mathbf{v} = \delta_z v_z(r, z)$. This postulate implies that there is no radial flow ($v_r = 0$) and no tangential flow ($v_\theta = 0$), and that v_z does not depend on θ . Consequently, we can discard many terms from the tabulated equations of change, leaving

$$\text{equation of continuity} \quad \frac{\partial v_z}{\partial z} = 0 \quad (3.6-1)$$

$$r\text{-equation of motion} \quad 0 = -\frac{\partial \mathcal{P}}{\partial r} \quad (3.6-2)$$

$$\theta\text{-equation of motion} \quad 0 = -\frac{\partial \mathcal{P}}{\partial \theta} \quad (3.6-3)$$

$$z\text{-equation of motion} \quad 0 = -\frac{\partial \mathcal{P}}{\partial z} + \mu \frac{1}{r} \frac{\partial}{\partial r} \left(r \frac{\partial v_z}{\partial r} \right) \quad (3.6-4)$$

The first equation indicates that v_z depends only on r ; hence the partial derivatives in the second term on the right side of Eq. 3.6-4 can be replaced by ordinary derivatives. By using the modified pressure $\mathcal{P} = p + \rho gh$ (where h is the height above some arbitrary datum plane), we avoid the necessity of calculating the components of \mathbf{g} in cylindrical coordinates, and we obtain a solution valid for any orientation of the axis of the tube.

Equations 3.6-2 and 3.6-3 show that \mathcal{P} is a function of z alone, and the partial derivative in the first term of Eq. 3.6-4 may be replaced by an ordinary derivative. The only way that we can have a function of r plus a function of z equal to zero is for each term individually to be a constant—say, C_0 —so that Eq. 3.6-4 reduces to

$$\mu \frac{1}{r} \frac{d}{dr} \left(r \frac{dv_z}{dr} \right) = C_0 = \frac{d\mathcal{P}}{dz} \quad (3.6-5)$$

The \mathcal{P} equation can be integrated at once. The v_z -equation can be integrated by merely “peeling off” one operation after another on the left side (do not “work out” the compound derivative there). This gives

$$\mathcal{P} = C_0 z + C_1 \quad (3.6-6)$$

$$v_z = \frac{C_0}{4\mu} r^2 + C_2 \ln r + C_3 \quad (3.6-7)$$

The four constants of integration can be found from the boundary conditions:

$$\text{B.C. 1} \quad \text{at } z = 0, \quad \mathcal{P} = \mathcal{P}_0 \quad (3.6-8)$$

$$\text{B.C. 2} \quad \text{at } z = L, \quad \mathcal{P} = \mathcal{P}_L \quad (3.6-9)$$

$$\text{B.C. 3} \quad \text{at } r = R, \quad v_z = 0 \quad (3.6-10)$$

$$\text{B.C. 4} \quad \text{at } r = 0, \quad v_z = \text{finite} \quad (3.6-11)$$

The resulting solutions are:

$$\mathcal{P} = \mathcal{P}_0 - (\mathcal{P}_0 - \mathcal{P}_L)(z/L) \quad (3.6-12)$$

$$v_z = \frac{(\mathcal{P}_0 - \mathcal{P}_L)R^2}{4\mu L} \left[1 - \left(\frac{r}{R} \right)^2 \right] \quad (3.6-13)$$

Equation 3.6-13 is the same as Eq. 2.3-18. The pressure profile in Eq. 3.6-12 was not obtained in Example 2.3-1, but was tacitly postulated; we could have done that here, too, but we chose to work with a minimal number of postulates.

As pointed out in Example 2.3-1, Eq. 3.6-13 is valid only in the laminar-flow regime, and at locations not too near the tube entrance and exit. For Reynolds numbers above about 2100, a turbulent-flow regime exists downstream of the entrance region, and Eq. 3.6-13 is no longer valid.

EXAMPLE 3.6-2

Falling Film with Variable Viscosity

Set up the problem in Example 2.2-2 by using the equations of Appendix B. This illustrates the use of the equation of motion in terms of τ .

SOLUTION

As in Example 2.2-2 we postulate a steady-state flow with constant density, but with viscosity depending on x . We postulate, as before, that the x - and y -components of the velocity are zero and that $v_z = v_z(x)$. With these postulates, the equation of continuity is identically satisfied. According to Table B.1, the only nonzero components of τ are $\tau_{xz} = \tau_{zx} = -\mu(dv_z/dx)$. The components of the equation of motion in terms of τ are, from Table B.5,

$$0 = -\frac{\partial p}{\partial x} + \rho g \sin \beta \quad (3.6-14)$$

$$0 = -\frac{\partial p}{\partial y} \quad (3.6-15)$$

$$0 = -\frac{\partial p}{\partial z} - \frac{d}{dx} \tau_{xz} + \rho g \cos \beta \quad (3.6-16)$$

where β is the angle shown in Fig. 2.2-2.

Integration of Eq. 3.6-14 gives

$$p = \rho gx \sin \beta + f(y, z) \quad (3.6-17)$$

in which $f(y, z)$ is an arbitrary function. Equation 3.6-15 shows that f cannot be a function of y . We next recognize that the pressure in the gas phase is very nearly constant at the prevailing atmospheric pressure p_{atm} . Therefore, at the gas–liquid interface $x = 0$, the pressure is also constant at the value p_{atm} . Consequently, f can be set equal to p_{atm} and we obtain finally

$$p = \rho gx \sin \beta + p_{atm} \quad (3.6-18)$$

Equation 3.5-16 then becomes

$$\frac{d}{dx} \tau_{xz} = \rho g \cos \beta \quad (3.6-19)$$

which is the same as Eq. 2.2-10. The remainder of the solution is the same as in §2.2.

EXAMPLE 3.6-3

Operation of a Couette Viscometer

We mentioned earlier that the measurement of pressure difference vs. mass flow rate through a cylindrical tube is the basis for the determination of viscosity in commercial capillary viscometers. The viscosity may also be determined by measuring the torque required to turn a solid object in contact with a fluid. The forerunner of all rotational viscometers is the Couette instrument, which is sketched in Fig. 3.6-1.

The fluid is placed in the cup, and the cup is then made to rotate with a constant angular velocity Ω_o (the subscript “o” stands for *outer*). The rotating viscous liquid causes the suspended bob to turn until the torque produced by the momentum transfer in the fluid equals the product of the torsion constant k , and the angular displacement θ_b of the bob. The angular displacement can be measured by observing the deflection of a light beam reflected from a mirror mounted on the bob. The conditions of measurement are controlled so that there is a steady, tangential, laminar flow in the annular region between the two coaxial cylinders

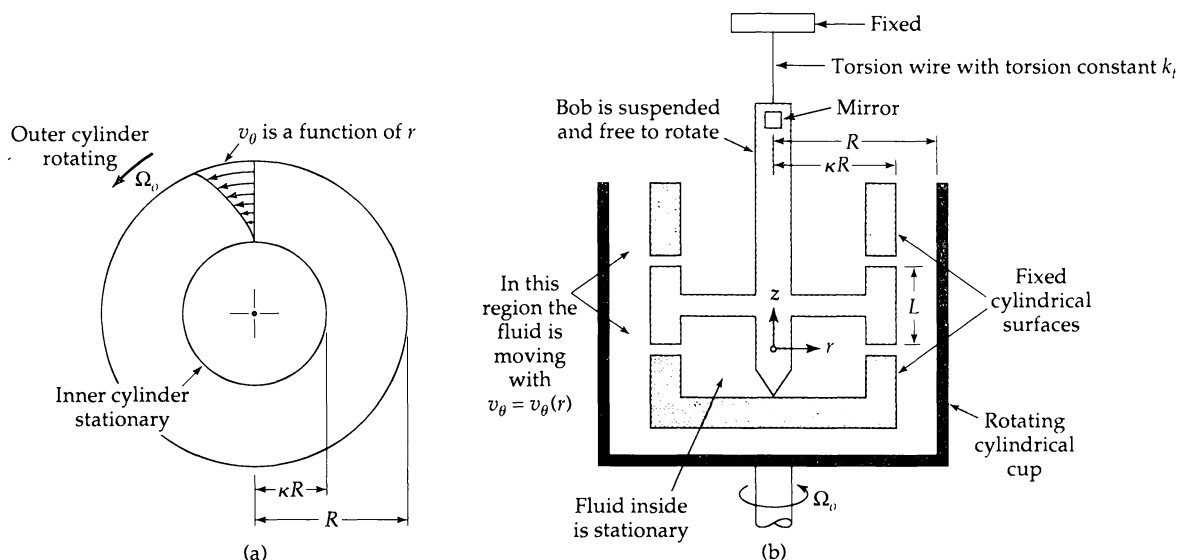


Fig. 3.6-1. (a) Tangential laminar flow of an incompressible fluid in the space between two cylinders; the outer one is moving with an angular velocity Ω_o . (b) A diagram of a Couette viscometer. One measures the angular velocity Ω_o of the cup and the deflection θ_b of the bob at steady-state operation. Equation 3.6-31 gives the viscosity μ in terms of Ω_o and the torque $T_z = k_t \theta_b$.

shown in the figure. Because of the arrangement used, end effects over the region including the bob height L are negligible.

To analyze this measurement, we apply the equations of continuity and motion for constant ρ and μ to the tangential flow in the annular region around the bob. Ultimately we want an expression for the viscosity in terms of (the z -component of) the torque T_z on the inner cylinder, the angular velocity Ω_o of the rotating cup, the bob height L , and the radii κR and R of the bob and cup, respectively.

SOLUTION

In the portion of the annulus under consideration the fluid moves in a circular pattern. Reasonable postulates for the velocity and pressure are: $v_\theta = v_\theta(r)$, $v_r = 0$, $v_z = 0$, and $p = p(r, z)$. We expect p to depend on z because of gravity and on r because of the centrifugal force.

For these postulates all the terms in the equation of continuity are zero, and the components of the equation of motion simplify to

$$\text{r-component} \quad -\rho \frac{v_\theta^2}{r} = -\frac{\partial p}{\partial r} \quad (3.6-20)$$

$$\theta\text{-component} \quad 0 = \frac{d}{dr} \left(\frac{1}{r} \frac{d}{dr} (rv_\theta) \right) \quad (3.6-21)$$

$$\text{z-component} \quad 0 = -\frac{\partial p}{\partial z} - \rho g \quad (3.6-22)$$

The second equation gives the velocity distribution. The third equation gives the effect of gravity on the pressure (the hydrostatic effect), and the first equation tells how the centrifugal force affects the pressure. For the problem at hand we need only the θ -component of the equation of motion.²

² See R. B. Bird, C. F. Curtiss, and W. E. Stewart, *Chem. Eng. Sci.*, 11, 114–117 (1959) for a method of getting $p(r, z)$ for this system. The time-dependent buildup to the steady-state profiles is given by R. B. Bird and C. F. Curtiss, *Chem. Eng. Sci.*, 11, 108–113 (1959).

A novice might have a compelling urge to perform the differentiations in Eq. 3.6-21 before solving the differential equation, but this should not be done. All one has to do is “peel off” one operation at a time—just the way you undress—as follows:

$$\frac{1}{r} \frac{d}{dr} (rv_\theta) = C_1 \quad (3.6-23)$$

$$\frac{d}{dr} (rv_\theta) = C_1 r \quad (3.6-24)$$

$$rv_\theta = \frac{1}{2} C_1 r^2 + C_2 \quad (3.6-25)$$

$$v_\theta = \frac{1}{2} C_1 r + \frac{C_2}{r} \quad (3.6-26)$$

The boundary conditions are that the fluid does not slip at the two cylindrical surfaces:

$$\text{B.C. 1} \quad \text{at } r = \kappa R, \quad v_\theta = 0 \quad (3.6-27)$$

$$\text{B.C. 2} \quad \text{at } r = R, \quad v_\theta = \Omega_o R \quad (3.6-28)$$

These boundary conditions can be used to get the constants of integration, which are then inserted in Eq. 3.6-26. This gives

$$v_\theta = \Omega_o R \frac{\left(\frac{r}{\kappa R} - \frac{\kappa R}{r} \right)}{\left(\frac{1}{\kappa} - \kappa \right)} \quad (3.6-29)$$

By writing the result in this form, with similar terms in the numerator and denominator, it is clear that both boundary conditions are satisfied and that the equation is dimensionally consistent.

From the velocity distribution we can find the momentum flux by using Table B.2:

$$\tau_{r\theta} = -\mu r \frac{d}{dr} \left(\frac{v_\theta}{r} \right) = -2\mu\Omega_o \left(\frac{R}{r} \right)^2 \left(\frac{\kappa^2}{1 - \kappa^2} \right) \quad (3.6-30)$$

The torque acting on the inner cylinder is then given by the product of the inward momentum flux ($-\tau_{r\theta}$), the surface of the cylinder, and the lever arm, as follows:

$$T_z = (-\tau_{r\theta})|_{r=\kappa R} \cdot 2\pi\kappa RL \cdot \kappa R = 4\pi\mu\Omega_o R^2 L \left(\frac{\kappa^2}{1 - \kappa^2} \right) \quad (3.6-31)$$

The torque is also given by $T_z = k_i\theta_b$. Therefore, measurement of the angular velocity of the cup and the angular deflection of the bob makes it possible to determine the viscosity. The same kind of analysis is available for other rotational viscometers.³

For any viscometer it is essential to know when turbulence will occur. The critical Reynolds number ($\Omega_o R^2 \rho / \mu$)_{crit}, above which the system becomes turbulent, is shown in Fig. 3.6-2 as a function of the radius ratio κ .

One might ask what happens if we hold the outer cylinder fixed and cause the inner cylinder to rotate with an angular velocity Ω_i (the subscript “*i*” stands for inner). Then the velocity distribution is

$$v_\theta = \Omega_i \kappa R \frac{\left(\frac{R}{r} - \frac{r}{R} \right)}{\left(\frac{1}{\kappa} - \kappa \right)} \quad (3.6-32)$$

This is obtained by making the same postulates (see before Eq. 3.6-20) and solving the same differential equation (Eq. 3.6-21), but with a different set of boundary conditions.

³ J. R. VanWazer, J. W. Lyons, K. Y. Kim, and R. E. Colwell, *Viscosity and Flow Measurement*, Wiley, New York (1963); K. Walters, *Rheometry*, Chapman and Hall, London (1975).

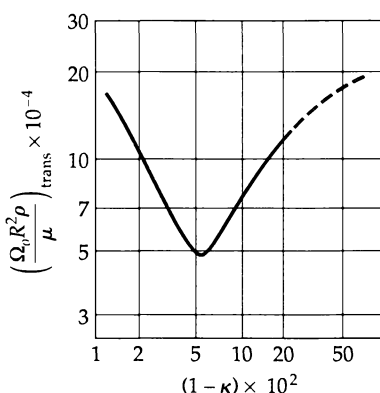


Fig. 3.6-2. Critical Reynolds number for the tangential flow in an annulus, with the outer cylinder rotating and the inner cylinder stationary [H. Schlichting, *Boundary Layer Theory*, McGraw-Hill, New York (1955), p. 357].

Equation 3.6-32 describes the flow accurately for small values of Ω_i . However, when Ω_i reaches a critical value ($\Omega_{i,crit} \approx 41.3(\mu/R^2(1-\kappa)^{3/2}\rho)$ for $\kappa \approx 1$) the fluid develops a secondary flow, which is superimposed on the primary (tangential) flow and which is periodic in the axial direction. A very neat system of toroidal vortices, called *Taylor vortices*, is formed, as depicted in Figs. 3.6-3 and 3.6-4(b). The loci of the centers of these vortices are circles, whose centers are located on the common axis of the cylinders. This is still laminar motion—but certainly inconsistent with the postulates made at the beginning of the problem. When the angular velocity Ω_i is increased further, the loci of the centers of the vortices become traveling waves; that is, the flow becomes, in addition, periodic in the tangential direction [see Fig. 3.6-4(c)]. Furthermore, the angular velocity of the traveling waves is approximately $\frac{1}{3}\Omega_i$. When the angular velocity Ω_i is further increased, the flow becomes turbulent. Figure 3.6-5 shows the various flow regimes, with the inner and outer cylinders both rotating, determined for a specific apparatus and a

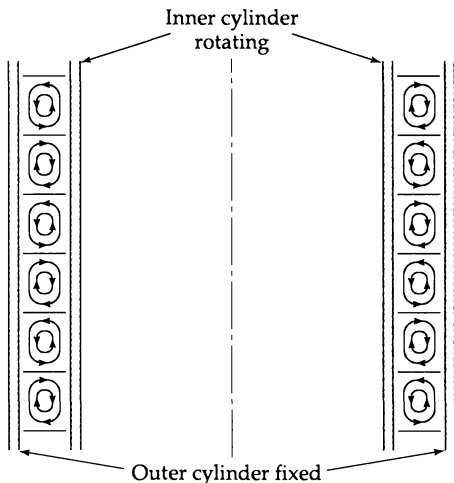


Fig. 3.6-3. Counter-rotating toroidal vortices, called *Taylor vortices*, observed in the annular space between two cylinders. The streamlines have the form of helices, with the axes wrapped around the common axis of the cylinders. This corresponds to Fig. 3.5-4(b).

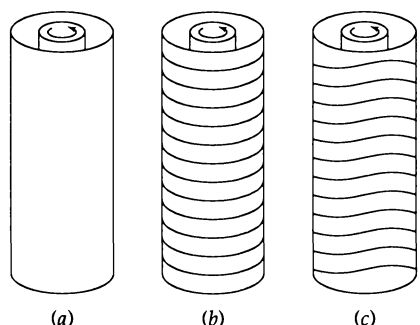


Fig. 3.6-4. Sketches showing the phenomena observed in the annular space between two cylinders: (a) purely tangential flow; (b) singly periodic flow (Taylor vortices); and (c) doubly periodic flow in which an undulatory motion is superposed on the Taylor vortices.

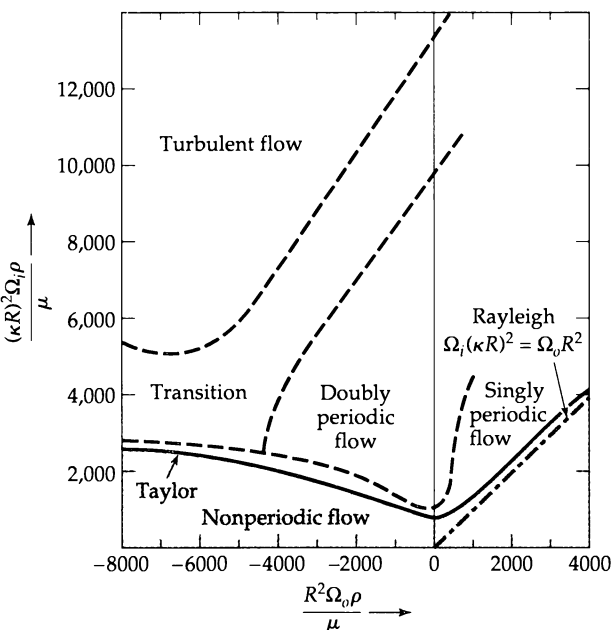


Fig. 3.6-5. Flow-regime diagram for the flow between two coaxial cylinders. The straight line labeled "Rayleigh" is Lord Rayleigh's analytic solution for an inviscid fluid. [See D. Coles, *J. Fluid. Mech.*, **21**, 385–425 (1965).]

specific fluid. This diagram demonstrates how complicated this apparently simple system is. Further details may be found elsewhere.^{4,5}

The preceding discussion should serve as a stern warning that intuitive postulates may be misleading. Most of us would not think about postulating the singly and doubly periodic solutions just described. Nonetheless, this information is contained in the Navier-Stokes equations. However, since problems involving instability and transitions between several flow regimes are extremely complex, we are forced to use a combination of theory and experiment to describe them. Theory alone cannot yet give us all the answers, and carefully controlled experiments will be needed for years to come.

EXAMPLE 3.6-4

Shape of the Surface of a Rotating Liquid

A liquid of constant density and viscosity is in a cylindrical container of radius R as shown in Fig. 3.6-6. The container is caused to rotate about its own axis at an angular velocity Ω . The cylinder axis is vertical, so that $g_r = 0$, $g_\theta = 0$, and $g_z = -g$, in which g is the magnitude of the gravitational acceleration. Find the shape of the free surface of the liquid when steady state has been established.

⁴ The initial work on this subject was done by John William Strutt (Lord Rayleigh) (1842–1919), who established the field of acoustics with his *Theory of Sound*, written on a houseboat on the Nile River. Some original references on Taylor instability are: J. W. Strutt (Lord Rayleigh), *Proc. Roy. Soc.*, **A93**, 148–154 (1916); G. I. Taylor, *Phil. Trans.*, **A223**, 289–343 (1923) and *Proc. Roy. Soc.* **A157**, 546–564 (1936); P. Schultz-Grunow and H. Hein, *Zeits. Flugwiss.*, **4**, 28–30 (1956); D. Coles, *J. Fluid. Mech.* **21**, 385–425 (1965). See also R. P. Feynman, R. B. Leighton, and M. Sands, *The Feynman Lectures in Physics*, Addison-Wesley, Reading, MA (1964), §41–6.

⁵ Other references on Taylor instability, as well as instability in other flow systems, are: L. D. Landau and E. M. Lifshitz, *Fluid Mechanics*, Pergamon, Oxford, 2nd edition (1987), pp. 99–106; S. Chandrasekhar, *Hydrodynamic and Hydromagnetic Stability*, Oxford University Press (1961), pp. 272–342; H. Schlichting and K. Gersten, *Boundary-Layer Theory*, 8th edition (2000), Chapter 15; P. G. Drazin and W. H. Reid, *Hydrodynamic Stability*, Cambridge University Press (1981); M. Van Dyke, *An Album of Fluid Motion*, Parabolic Press, Stanford (1982).

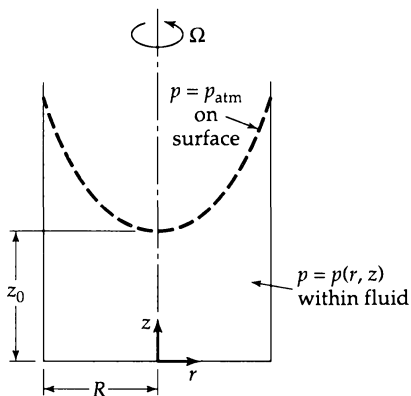


Fig. 3.6-6. Rotating liquid with a free surface, the shape of which is a paraboloid of revolution.

SOLUTION

Cylindrical coordinates are appropriate for this problem, and the equations of change are given in Tables B.2 and B.6. At steady state we postulate that v_r and v_z are both zero and that v_θ depends only on r . We also postulate that p depends on z because of the gravitational force and on r because of the centrifugal force but not on θ .

These postulates give $0 = 0$ for the equation of continuity, and the equation of motion gives:

$$r\text{-component} \quad -\rho \frac{v_\theta^2}{r} = -\frac{\partial p}{\partial r} \quad (3.6-33)$$

$$\theta\text{-component} \quad 0 = \mu \frac{d}{dr} \left(\frac{1}{r} \frac{d}{dr} (rv_\theta) \right) \quad (3.6-34)$$

$$z\text{-component} \quad 0 = -\frac{\partial p}{\partial z} - \rho g \quad (3.6-35)$$

The θ -component of the equation of motion can be integrated to give

$$v_\theta = \frac{1}{2} C_1 r + \frac{C_2}{r} \quad (3.6-36)$$

in which C_1 and C_2 are constants of integration. Because v_θ cannot be infinite at $r = 0$, the constant C_2 must be zero. At $r = R$ the velocity v_θ is $R\Omega$. Hence $C_1 = 2\Omega$ and

$$v_\theta = \Omega r \quad (3.6-37)$$

This states that each element of the rotating liquid moves as an element of a rigid body (we could have actually postulated that the liquid would rotate as a rigid body and written down Eq. 3.6-37 directly). When the result in Eq. 3.6-37 is substituted into Eq. 3.6-33, we then have these two equations for the pressure gradients:

$$\frac{\partial p}{\partial r} = \rho\Omega^2 r \quad \text{and} \quad \frac{\partial p}{\partial z} = -\rho g \quad (3.6-38, 39)$$

Each of these equations can be integrated, as follows:

$$p = \frac{1}{2}\rho\Omega^2 r^2 + f_1(\theta, z) \quad \text{and} \quad p = -\rho gz + f_2(r, \theta) \quad (3.6-40, 41)$$

where f_1 and f_2 are arbitrary functions of integration. Since we have postulated that p does not depend on θ , we can choose $f_1 = -\rho gz + C$ and $f_2 = \frac{1}{2}\rho\Omega^2 r^2 + C$, where C is a constant, and satisfy Eqs. 3.6-38 and 39. Thus the solution to those equations has the form

$$p = -\rho gz + \frac{1}{2}\rho\Omega^2 r^2 + C \quad (3.6-42)$$

The constant C may be determined by requiring that $p = p_{\text{atm}}$ at $r = 0$ and $z = z_0$, the latter being the elevation of the liquid surface at $r = 0$. When C is obtained in this way, we get

$$p - p_{\text{atm}} = -\rho g(z - z_0) + \frac{1}{2}\rho\Omega^2 r^2 \quad (3.6-43)$$

This equation gives the pressure at all points within the liquid. Right at the liquid-air interface, $p = p_{\text{atm}}$, and with this substitution Eq. 3.6-43 gives the shape of the liquid-air interface:

$$z - z_0 = \left(\frac{\Omega^2}{2g} \right) r^2 \quad (3.6-44)$$

This is the equation for a parabola. The reader can verify that the free surface of a liquid in a rotating annular container obeys a similar relation.

EXAMPLE 3.6-5

Flow near a Slowly Rotating Sphere

SOLUTION

A solid sphere of radius R is rotating slowly at a constant angular velocity Ω in a large body of quiescent fluid (see Fig. 3.6-7). Develop expressions for the pressure and velocity distributions in the fluid and for the torque T_z required to maintain the motion. It is assumed that the sphere rotates sufficiently slowly that it is appropriate to use the *creeping flow* version of the equation of motion in Eq. 3.5-8. This problem illustrates setting up and solving a problem in spherical coordinates.

The equations of continuity and motion in spherical coordinates are given in Tables B.4 and B.6, respectively. We postulate that, for steady creeping flow, the velocity distribution will have the general form $\mathbf{v} = \delta_\phi v_\phi(r, \theta)$, and that the modified pressure will be of the form $\mathcal{P} = \mathcal{P}(r, \theta)$. Since the solution is expected to be symmetric about the z -axis, there is no dependence on the angle ϕ .

With these postulates, the equation of continuity is exactly satisfied, and the components of the creeping flow equation of motion become

$$r\text{-component} \quad 0 = -\frac{\partial \mathcal{P}}{\partial r} \quad (3.6-45)$$

$$\theta\text{-component} \quad 0 = -\frac{1}{r} \frac{\partial \mathcal{P}}{\partial \theta} \quad (3.6-46)$$

$$\phi\text{-component} \quad 0 = \frac{1}{r^2} \frac{\partial}{\partial r} \left(r^2 \frac{\partial v_\phi}{\partial r} \right) + \frac{1}{r^2} \frac{\partial}{\partial \theta} \left(\frac{1}{\sin \theta} \frac{\partial}{\partial \theta} (v_\phi \sin \theta) \right) \quad (3.6-47)$$

The boundary conditions may be summarized as

$$\text{B.C. 1:} \quad \text{at } r = R, \quad v_r = 0, v_\theta = 0, v_\phi = R\Omega \sin \theta \quad (3.6-48)$$

$$\text{B.C. 2:} \quad \text{as } r \rightarrow \infty, \quad v_r \rightarrow 0, v_\theta \rightarrow 0, v_\phi \rightarrow 0 \quad (3.6-49)$$

$$\text{B.C. 3:} \quad \text{as } r \rightarrow \infty, \quad \mathcal{P} \rightarrow p_0 \quad (3.6-50)$$

where $\mathcal{P} = p + \rho g z$, and p_0 is the fluid pressure far from the sphere at $z = 0$.

Equation 3.6-47 is a partial differential equation for $v_\phi(r, \theta)$. To solve this, we try a solution of the form $v_\phi = f(r) \sin \theta$. This is just a guess, but it is consistent with the boundary condition in Eq. 3.6-48. When this trial form for the velocity distribution is inserted into Eq. 3.6-47 we get the following ordinary differential equation for $f(r)$:

$$\frac{d}{dr} \left(r^2 \frac{df}{dr} \right) - 2f = 0 \quad (3.6-51)$$

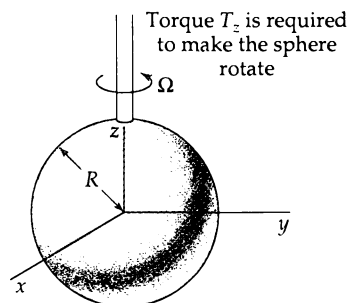


Fig. 3.6-7. A slowly rotating sphere in an infinite expanse of fluid. The primary flow is $v_\phi = \Omega R(R/r)^2 \sin \theta$.

This is an “equidimensional equation,” which may be solved by assuming a trial solution $f = r^n$ (see Eq. C.1-14). Substitution of this trial solution into Eq. 3.6-51 gives $n = 1, -2$. The solution of Eq. 3.6-51 is then

$$f = C_1 r + \frac{C_2}{r^2} \quad (3.6-52)$$

so that

$$v_\phi(r, \theta) = \left(C_1 r + \frac{C_2}{r^2} \right) \sin \theta \quad (3.6-53)$$

Application of the boundary conditions shows that $C_1 = 0$ and $C_2 = \Omega R^3$. Therefore the final expression for the velocity distribution is

$$v_\phi = \Omega R \left(\frac{R}{r} \right)^2 \sin \theta \quad (3.6-54)$$

Next we evaluate the torque needed to maintain the rotation of the sphere. This will be the integral, over the sphere surface, of the tangential force $(\tau_{r\phi}|_{r=R})R^2 \sin \theta d\theta d\phi$ exerted on the fluid by a solid surface element, multiplied by the lever arm $R \sin \theta$ for that element:

$$\begin{aligned} T_z &= \int_0^{2\pi} \int_0^\pi (\tau_{r\phi})|_{r=R} (R \sin \theta) R^2 \sin \theta d\theta d\phi \\ &= \int_0^{2\pi} \int_0^\pi (3\mu\Omega \sin \theta)(R \sin \theta) R^2 \sin \theta d\theta d\phi \\ &= 6\pi\mu\Omega R^3 \int_0^\pi \sin^3 \theta d\theta \\ &= 8\pi\mu\Omega R^3 \end{aligned} \quad (3.6-55)$$

In going from the first to the second line, we have used Table B.1, and in going from the second to the third line we have done the integration over the range of the ϕ variable. The integral in the third line is $\frac{4}{3}$.

As the angular velocity increases, deviations from the “primary flow” of Eq. 3.6-54 occur. Because of the centrifugal force effects, the fluid is pulled in toward the poles of the sphere and shoved outward from the equator as shown in Fig. 3.6-8. To describe this “secondary flow,” one has to include the $[\mathbf{v} \cdot \nabla \mathbf{v}]$ term in the equation of motion. This can be done by the use of a stream-function method.⁶

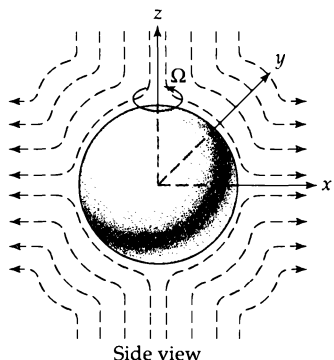


Fig. 3.6-8. Rough sketch showing the secondary flow which appears around a rotating sphere as the Reynolds number is increased.

⁶ See, for example, the development by O. Hassager in R. B. Bird, R. C. Armstrong, and O. Hassager, *Dynamics of Polymeric Liquids*, Vol. 1, Wiley-Interscience, New York, 2nd edition (1987), pp. 31–33. See also L. Landau and E. M. Lifshitz, *Fluid Mechanics*, Pergamon, Oxford, 2nd edition (1987), p. 65; and L. G. Leal, *Laminar Flow and Convective Transport Processes*, Butterworth-Heinemann, Boston (1992), pp. 180–181.

§3.7 DIMENSIONAL ANALYSIS OF THE EQUATIONS OF CHANGE

Suppose that we have taken experimental data on, or made photographs of, the flow through some system that cannot be analyzed by solving the equations of change analytically. An example of such a system is the flow of a fluid through an orifice meter in a pipe (this consists of a disk with a centered hole in it, placed in the tube, with a pressure-sensing device upstream and downstream of the disk). Suppose now that we want to scale up (or down) the experimental system, in order to build a new one in which exactly the same flow patterns occur [but appropriately scaled up (or down)]. First of all, we need to have *geometric similarity*: that is, the ratios of all dimensions of the pipe and orifice plate in the original system and in the scaled-up (or scaled-down) system must be the same. In addition, we must have *dynamic similarity*: that is, the dimensionless groups (such as the Reynolds number) in the differential equations and boundary conditions must be the same. The study of dynamic similarity is best understood by writing the equations of change, along with boundary and initial conditions, in dimensionless form.^{1,2}

For simplicity we restrict the discussion here to fluids of constant density and viscosity, for which the equations of change are Eqs. 3.1-5 and 3.5-7

$$(\nabla \cdot \mathbf{v}) = 0 \quad (3.7-1)$$

$$\rho \frac{D}{Dt} \mathbf{v} = -\nabla \mathcal{P} + \mu \nabla^2 \mathbf{v} \quad (3.7-2)$$

In most flow systems one can identify the following “scale factors”: a characteristic length l_0 , a characteristic velocity v_0 , and a characteristic modified pressure $\mathcal{P}_0 = p_0 + \rho gh_0$ (for example, these might be a tube diameter, the average flow velocity, and the modified pressure at the tube exit). Then we can define dimensionless variables and differential operators as follows:

$$\check{x} = \frac{x}{l_0} \quad \check{y} = \frac{y}{l_0} \quad \check{z} = \frac{z}{l_0} \quad \check{t} = \frac{v_0 t}{l_0} \quad (3.7-3)$$

$$\check{\mathbf{v}} = \frac{\mathbf{v}}{v_0} \quad \check{\mathcal{P}} = \frac{\mathcal{P} - \mathcal{P}_0}{\rho v_0^2} \quad \text{or} \quad \check{\mathcal{P}} = \frac{\mathcal{P} - \mathcal{P}_0}{\mu v_0 / l_0} \quad (3.7-4)$$

$$\check{\nabla} = l_0 \nabla = \delta_x (\partial / \partial \check{x}) + \delta_y (\partial / \partial \check{y}) + \delta_z (\partial / \partial \check{z}) \quad (3.7-5)$$

$$\check{\nabla}^2 = (\partial^2 / \partial \check{x}^2) + (\partial^2 / \partial \check{y}^2) + (\partial^2 / \partial \check{z}^2) \quad (3.7-6)$$

$$D/D\check{t} = (l_0/v_0)(D/Dt) \quad (3.7-7)$$

We have suggested two choices for the dimensionless pressure, the first one being convenient for high Reynolds numbers and the second for low Reynolds numbers. When the equations of change in Eqs. 3.7-1 and 3.7-2 are rewritten in terms of the dimensionless quantities, they become

$$(\check{\nabla} \cdot \check{\mathbf{v}}) = 0 \quad (3.7-8)$$

$$\frac{D}{D\check{t}} \check{\mathbf{v}} = -\check{\nabla} \check{\mathcal{P}} + \left[\frac{\mu}{l_0 v_0 \rho} \right] \check{\nabla}^2 \check{\mathbf{v}} \quad (3.7-9a)$$

or
$$\frac{D}{D\check{t}} \check{\mathbf{v}} = -\left[\frac{\mu}{l_0 v_0 \rho} \right] \check{\nabla} \check{\mathcal{P}} + \left[\frac{\mu}{l_0 v_0 \rho} \right] \check{\nabla}^2 \check{\mathbf{v}} \quad (3.7-9b)$$

¹ G. Birkhoff, *Hydrodynamics*, Dover, New York (1955), Chapter IV. Our dimensional analysis procedure corresponds to Birkhoff’s “complete inspectional analysis.”

² R. W. Powell, *An Elementary Text in Hydraulics and Fluid Mechanics*, Macmillan, New York (1951), Chapter VIII; and H. Rouse and S. Ince, *History of Hydraulics*, Dover, New York (1963) have interesting historical material regarding the dimensionless groups and the persons for whom they were named.

In these dimensionless equations, the four scale factors l_0 , v_0 , ρ , and μ appear in one dimensionless group. The reciprocal of this group is named after a famous fluid dynamicist³

$$\text{Re} = \left[\frac{l_0 v_0 \rho}{\mu} \right] = \text{Reynolds number} \quad (3.7-10)$$

The magnitude of this dimensionless group gives an indication of the relative importance of inertial and viscous forces in the fluid system.

From the two forms of the equation of motion given in Eq. 3.7-9, we can gain some perspective on the special forms of the Navier-Stokes equation given in §3.5. Equation 3.7-9a gives the Euler equation of Eq. 3.5-9 when $\text{Re} \rightarrow \infty$ and Eq. 3.7-9b gives the creeping flow equation of Eq. 3.5-8 when $\text{Re} \ll 1$. The regions of applicability of these and other asymptotic forms of the equation of motion are considered further in §§4.3 and 4.4.

Additional dimensionless groups may arise in the initial and boundary conditions; two that appear in problems with fluid-fluid interfaces are

$$\text{Fr} = \left[\frac{v_0^2}{l_0 g} \right] = \text{Froude number} \quad (3.7-11)^4$$

$$\text{We} = \left[\frac{\sigma}{l_0 v_0^2 \rho} \right] = \text{Weber number} \quad (3.7-12)^5$$

The first of these contains the gravitational acceleration g , and the second contains the interfacial tension σ , which may enter into the boundary conditions, as described in Problem 3C.5. Still other groups may appear, such as ratios of lengths in the flow system (for example, the ratio of tube diameter to the diameter of the hole in an orifice meter).

EXAMPLE 3.7-1

*Transverse Flow around a Circular Cylinder*⁶

The flow of an incompressible Newtonian fluid past a circular cylinder is to be studied experimentally. We want to know how the flow patterns and pressure distribution depend on the cylinder diameter, length, the approach velocity, and the fluid density and viscosity. Show how to organize the work so that the number of experiments needed will be minimized.

SOLUTION

For the analysis we consider an idealized flow system: a cylinder of diameter D and length L , submerged in an otherwise unbounded fluid of constant density and viscosity. Initially the fluid and the cylinder are both at rest. At time $t = 0$, the cylinder is abruptly made to move with velocity v_∞ in the negative x direction. The subsequent fluid motion is analyzed by using coordinates fixed in the cylinder axis as shown in Fig. 3.7-1.

The differential equations describing the flow are the equation of continuity (Eq. 3.7-1) and the equation of motion (Eq. 3.7-2). The initial condition for $t = 0$ is:

$$\text{I.C.} \quad \text{if } x^2 + y^2 > \frac{1}{4}D^2 \text{ or if } |z| > \frac{1}{2}L, \quad \mathbf{v} = \delta_x v_\infty \quad (3.7-13)$$

The boundary conditions for $t \geq 0$ and all z are:

$$\text{B.C. 1} \quad \text{as } x^2 + y^2 + z^2 \rightarrow \infty, \quad \mathbf{v} \rightarrow \delta_x v_\infty \quad (3.7-14)$$

$$\text{B.C. 2} \quad \text{if } x^2 + y^2 \leq \frac{1}{4}D^2 \text{ and } |z| \leq \frac{1}{2}L, \quad \mathbf{v} = 0 \quad (3.7-15)$$

$$\text{B.C. 3} \quad \text{as } x \rightarrow -\infty \text{ at } y = 0, \quad \mathcal{P} \rightarrow \mathcal{P}_\infty \quad (3.7-16)$$

³ See fn. 1 in §2.2.

⁴ William Froude (1810–1879) (rhymes with “food”) studied at Oxford and worked as a civil engineer concerned with railways and steamships. The Froude number is sometimes defined as the square root of the group given in Eq. 3.7-11.

⁵ Moritz Weber (1871–1951) (pronounced “Vayber”) was a professor of naval architecture in Berlin; another dimensionless group involving the surface tension in the *capillary number*, defined as $\text{Ca} = [\mu v_0 / \sigma]$.

⁶ This example is adapted from R. P. Feynman, R. B. Leighton, and M. Sands, *The Feynman Lectures on Physics*, Vol. II, Addison-Wesley, Reading, Mass. (1964), §41-4.

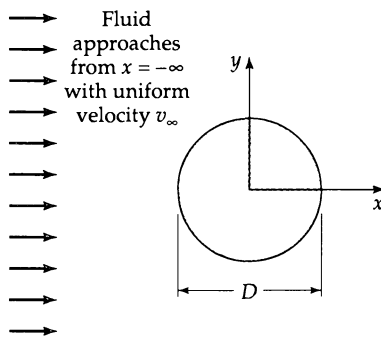


Fig. 3.7-1. Transverse flow around a cylinder.

Now we rewrite the problem in terms of variables made dimensionless with the characteristic length D , velocity v_∞ , and modified pressure \check{P}_∞ . The resulting dimensionless equations of change are

$$(\check{\nabla} \cdot \check{\mathbf{v}}) = 0, \quad \text{and} \quad \frac{\partial \check{\mathbf{v}}}{\partial \check{t}} + [\check{\mathbf{v}} \cdot \check{\nabla} \check{\mathbf{v}}] = -\check{\nabla} \check{P} + \frac{1}{Re} \check{\nabla}^2 \check{\mathbf{v}} \quad (3.7-17, 18)$$

in which $Re = Dv_\infty\rho/\mu$. The corresponding initial and boundary conditions are:

$$\text{I.C.} \quad \text{if } \check{x}^2 + \check{y}^2 > \frac{1}{4} \text{ or if } |\check{z}| > \frac{1}{2}(L/D), \quad \check{\mathbf{v}} = \check{\delta}_x \quad (3.7-19)$$

$$\text{B.C. 1} \quad \text{as } \check{x}^2 + \check{y}^2 + \check{z}^2 \rightarrow \infty, \quad \check{\mathbf{v}} \rightarrow \check{\delta}_x \quad (3.7-20)$$

$$\text{B.C. 2} \quad \text{if } \check{x}^2 + \check{y}^2 \leq \frac{1}{4} \text{ and } |\check{z}| \leq \frac{1}{2}(L/D), \quad \check{\mathbf{v}} = 0 \quad (3.7-21)$$

$$\text{B.C. 3} \quad \text{as } \check{x} \rightarrow -\infty \text{ at } y = 0, \quad \check{P} \rightarrow 0 \quad (3.7-22)$$

If we were bright enough to be able to solve the dimensionless equations of change along with the dimensionless boundary conditions, the solutions would have to be of the following form:

$$\check{\mathbf{v}} = \check{\mathbf{v}}(\check{x}, \check{y}, \check{z}, \check{t}, Re, L/D) \quad \text{and} \quad \check{P} = \check{P}(\check{x}, \check{y}, \check{z}, \check{t}, Re, L/D) \quad (3.7-23, 24)$$

That is, the dimensionless velocity and dimensionless modified pressure can depend only on the dimensionless parameters Re and L/D and the dimensionless independent variables \check{x} , \check{y} , \check{z} , and \check{t} .

This completes the dimensional analysis of the problem. We have not solved the flow problem, but have decided on a convenient set of dimensionless variables to restate the problem and suggest the form of the solution. The analysis shows that if we wish to catalog the flow patterns for flow past a cylinder, it will suffice to record them (e.g., photographically) for a series of Reynolds numbers $Re = Dv_\infty\rho/\mu$ and L/D values; thus, separate investigations into the roles of L , D , v_∞ , ρ , and μ are unnecessary. Such a simplification saves a lot of time and expense. Similar comments apply to the tabulation of numerical results, in the event that one decides to make a numerical assault on the problem.^{7,8}

⁷ Analytical solutions of this problem at very small Re and infinite L/D are reviewed in L. Rosenhead (ed.), *Laminar Boundary Layers*, Oxford University Press (1963), Chapter IV. An important feature of this two-dimensional problem is the absence of a “creeping flow” solution. Thus the $[\mathbf{v} \cdot \nabla \mathbf{v}]$ -term in the equation of motion has to be included, even in the limit as $Re \rightarrow 0$ (see Problem 3B.9). This is in sharp contrast to the situation for slow flow around a sphere (see §2.6 and §4.2) and around other finite, three-dimensional objects.

⁸ For computer studies of the flow around a long cylinder, see F. H. Harlow and J. E. From, *Scientific American*, 212, 104–110 (1965), and S. J. Sherwin and G. E. Karniadakis, *Comput. Math.*, 123, 189–229 (1995).

Experiments involve some necessary departures from the above analysis: the stream is finite in size, and fluctuations of velocity are inevitably present at the initial state and in the upstream fluid. These fluctuations die out rapidly near the cylinder at $\text{Re} < 1$. For Re approaching 40 the damping of disturbances gets slower, and beyond this approximate limit unsteady flow is always observed.

The observed flow patterns at large t vary strongly with the Reynolds number as shown in Fig. 3.7-2. At $\text{Re} \ll 1$ the flow is orderly, as shown in (a). At Re of about 10, a pair of vortices appears behind the cylinder, as may be seen in (b). This type of flow persists up to about $\text{Re} = 40$, when there appear two "separation points," at which the streamlines separate from the solid surface. Furthermore the flow becomes permanently unsteady; vortices begin to "peel off" from the cylinder and move downstream. With further increase in Re , the vortices separate regularly from alternate sides of the cylinder, as shown in (c); such a regular array of vortices is known as a "von Kármán vortex street." At still higher Re there is a disorderly fluctuating motion (turbulence) in the wake of the cylinder, as shown in (d). Finally, at Re near 10^6 , turbulence appears upstream of the separation point, and the wake abruptly narrows down as shown in (e). Clearly, the unsteady flows shown in the last three sketches would be very difficult to compute from the equations of change. It is much easier to observe them experimentally and correlate the results in terms of Eqs. 3.7-23 and 24.

Equations 3.7-23 and 24 can also be used for scale-up from a single experiment. Suppose that we wanted to predict the flow patterns around a cylinder of diameter $D_1 = 5$ ft, around which air is to flow with an approach velocity $(v_\infty)_1 = 30$ ft/s, by means of an ex-

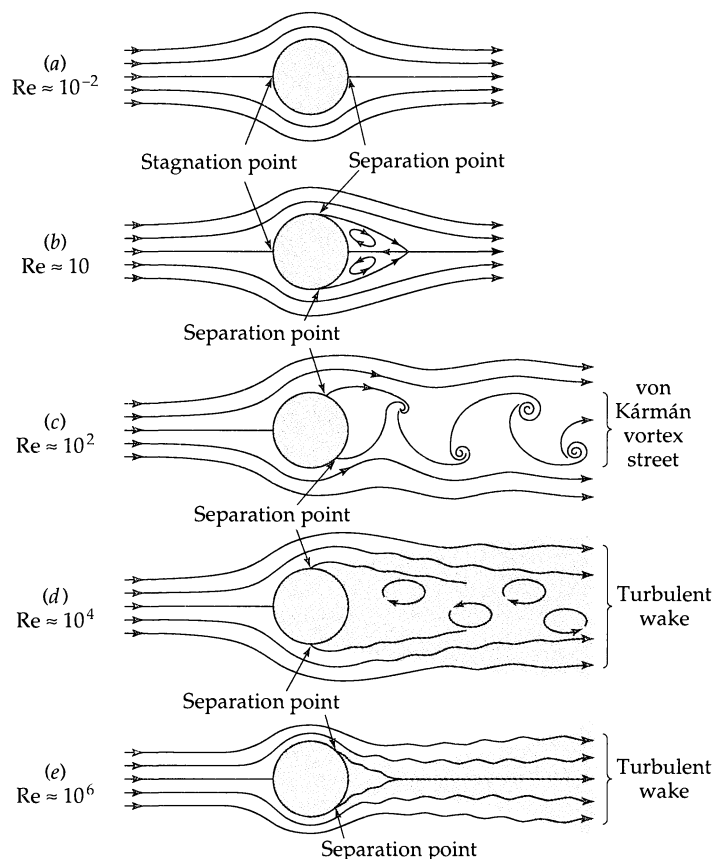


Fig. 3.7-2. The types of behavior for the flow around a cylinder, illustrating the various flow regimes that are observed as the Reynolds number increases. Regions of turbulent flow are shaded in gray.

periment on a scale model of diameter $D_{II} = 1$ ft. To have dynamic similarity, we must choose conditions such that $Re_{II} = Re_I$. Then if we use the same fluid in the small-scale experiment as in the large system, so that $\mu_{II}/\rho_{II} = \mu_I/\rho_I$, we find $(v_\infty)_{II} = 150$ ft/s as the required air velocity in the small-scale model. With the Reynolds numbers thus equalized, the flow patterns in the model and the full-scale system will look alike: that is, they are geometrically similar.

Furthermore, if Re is in the range of periodic vortex formation, the dimensionless time interval $t_v v_\infty / D$ between vortices will be the same in the two systems. Thus, the vortices will shed 25 times as fast in the model as in the full-scale system. The regularity of the vortex shedding at Reynolds numbers from about 10^2 to 10^4 is utilized commercially for precise flow metering in large pipelines.

EXAMPLE 3.7-2

Steady Flow in an Agitated Tank

SOLUTION

It is desired to predict the flow behavior in a large, unbaffled tank of oil, shown in Fig. 3.7-3, as a function of the impeller rotation speed. We propose to do this by means of model experiments in a smaller, geometrically similar system. Determine the conditions necessary for the model studies to provide a direct means of prediction.

We consider a tank of radius R , with a centered impeller of overall diameter D . At time $t = 0$, the system is stationary and contains liquid to a height H above the tank bottom. Immediately after time $t = 0$, the impeller begins rotating at a constant speed of N revolutions per minute. The drag of the atmosphere on the liquid surface is neglected. The impeller shape and initial position are described by the function $S_{imp}(r, \theta, z) = 0$.

The flow is governed by Eqs. 3.7-1 and 2, along with the initial condition

$$\text{at } t = 0, \text{ for } 0 \leq r < R \text{ and } 0 < z < H, \quad \mathbf{v} = 0 \quad (3.7-25)$$

and the following boundary conditions for the liquid region:

$$\text{tank bottom} \quad \text{at } z = 0 \text{ and } 0 \leq r < R, \quad \mathbf{v} = 0 \quad (3.7-26)$$

$$\text{tank wall} \quad \text{at } r = R, \quad \mathbf{v} = 0 \quad (3.7-27)$$

$$\text{impeller surface} \quad \text{at } S_{imp}(r, \theta - 2\pi Nt, z) = 0, \quad \mathbf{v} = 2\pi N r \hat{\mathbf{d}}_\theta \quad (3.7-28)$$

$$\text{gas-liquid interface} \quad \text{at } S_{int}(r, \theta, z, t) = 0, \quad (\mathbf{n} \cdot \mathbf{v}) = 0 \quad (3.7-29)$$

$$\text{and } \mathbf{n} p + [\mathbf{n} \cdot \boldsymbol{\tau}] = \mathbf{n} p_{atm} \quad (3.7-30)$$

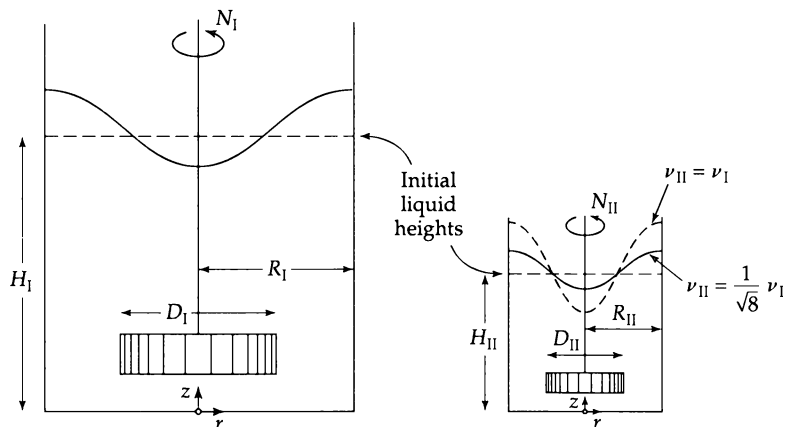


Fig. 3.7-3. Long-time average free-surface shapes, with $Re_I = Re_{II}$.

Equations 3.7-26 to 28 are the no-slip and impermeability conditions; the surface $S_{\text{imp}}(r, \theta - 2\pi Nt, z) = 0$ describes the location of the impeller after Nt rotations. Equation 3.7-29 is the condition of no mass flow through the gas–liquid interface, described by $S_{\text{int}}(r, \theta, z, t) = 0$, which has a local unit normal vector \mathbf{n} . Equation 3.7-30 is a force balance on an element of this interface (or a statement of the continuity of the normal component of the momentum flux tensor $\boldsymbol{\pi}$) in which the viscous contributions from the gas side are neglected. This interface is initially stationary in the plane $z = H$, and its motion thereafter is best obtained by measurement, though it is also predictable in principle by numerical solution of this equation system, which describes the initial conditions and subsequent acceleration $D\mathbf{v}/Dt$ of every fluid element.

Next we nondimensionalize the equations using the characteristic quantities $v_0 = ND$, $l_0 = D$, and $\mathcal{P}_0 = p_{\text{atm}}$ along with dimensionless polar coordinates $\check{r} = r/D$, θ , and $\check{z} = z/D$. Then the equations of continuity and motion appear as in Eqs. 3.7-8 and 9, with $\text{Re} = D^2N\rho/\mu$. The initial condition takes the form

$$\text{at } \check{t} = 0, \text{ for } \check{r} = \left[\frac{R}{D} \right] \text{ and } 0 < \check{z} < \left[\frac{H}{D} \right], \quad \check{\mathbf{v}} = 0 \quad (3.7-31)$$

and the boundary conditions become:

$$\text{tank bottom} \quad \text{at } \check{z} = 0 \text{ and } 0 < \check{r} < \left[\frac{R}{D} \right], \quad \check{\mathbf{v}} = 0 \quad (3.7-32)$$

$$\text{tank wall} \quad \text{at } \check{r} = \left[\frac{R}{D} \right], \quad \check{\mathbf{v}} = 0 \quad (3.7-33)$$

$$\text{impeller surface} \quad \text{at } \check{S}_{\text{imp}}(\check{r}, \theta - 2\pi\check{t}, \check{z}) = 0, \quad \check{\mathbf{v}} = 2\pi\check{r}\delta_\theta \quad (3.7-34)$$

$$\text{gas–liquid interface} \quad \text{at } \check{S}_{\text{int}}(\check{r}, \theta, \check{z}, \check{t}) = 0, \quad (\mathbf{n} \cdot \check{\mathbf{v}}) = 0 \quad (3.7-35)$$

$$\text{and } \mathbf{n}\check{\mathcal{P}} - \mathbf{n}\left[\frac{g}{DN^2} \right]\check{z} - \left[\frac{\mu}{D^2N\rho} \right][\mathbf{n} \cdot \check{\mathbf{y}}] = 0 \quad (3.7-36)$$

In going from Eq. 3.7-30 to 3.7-36 we have used Newton's law of viscosity in the form of Eq. 1.2-7 (but with the last term omitted, as is appropriate for incompressible liquids). We have also used the abbreviation $\check{\mathbf{y}} = \nabla\check{\mathbf{v}} + (\nabla\check{\mathbf{v}})^\dagger$ for the rate-of-deformation tensor, whose dimensionless Cartesian components are $\check{y}_i = \partial\check{v}_j/\partial\check{x}_i + (\partial\check{v}_i/\partial\check{x}_j)$.

The quantities in double brackets are known dimensionless quantities. The function $\check{S}_{\text{imp}}(\check{r}, \theta - 2\pi\check{t}, \check{z})$ is known for a given impeller design. The unknown function $\check{S}_{\text{int}}(\check{r}, \theta, \check{z}, \check{t})$ is measurable photographically, or in principle is computable from the problem statement.

By inspection of the dimensionless equations, we find that the velocity and pressure profiles must have the form

$$\check{\mathbf{v}} = \check{\mathbf{v}}\left(\check{r}, \theta, \check{z}, \check{t}; \frac{R}{D}, \frac{H}{D}, \text{Re}, \text{Fr}\right) \quad (3.7-37)$$

$$\check{\mathcal{P}} = \check{\mathcal{P}}\left(\check{r}, \theta, \check{z}, \check{t}; \frac{R}{D}, \frac{H}{D}, \text{Re}, \text{Fr}\right) \quad (3.7-38)$$

for a given impeller shape and location. The corresponding locus of the free surface is given by

$$\check{S}_{\text{int}} = \check{S}_{\text{int}}\left(\check{r}, \theta, \check{z}, \check{t}; \frac{R}{D}, \frac{H}{D}, \text{Re}, \text{Fr}\right) = 0 \quad (3.7-39)$$

in which $\text{Re} = D^2N\rho/\mu$ and $\text{Fr} = DN^2/g$. For time-smoothed observations at large \check{t} , the dependence on \check{t} will disappear, as will the dependence on θ for this axisymmetric tank geometry.

These results provide the necessary conditions for the proposed model experiment: the two systems must be (i) geometrically similar (same values of R/D and H/D , same impeller geometry and location), and (ii) operated at the same values of the Reynolds and Froude numbers. Condition (ii) requires that

$$\frac{D_l^2 N_l}{\nu_l} = \frac{D_{ll}^2 N_{ll}}{\nu_{ll}} \quad (3.7-40)$$

$$\frac{D_l N_l^2}{g_l} = \frac{D_{ll} N_{ll}^2}{g_{ll}} \quad (3.7-41)$$

in which the kinematic viscosity $\nu = \mu/\rho$ is used. Normally both tanks will operate in the same gravitational field $g_1 = g_{II}$, so that Eq. 3.7-41 requires

$$\frac{N_{II}}{N_I} = \left(\frac{D_I}{D_{II}} \right)^{1/2} \quad (3.7-42)$$

Substitution of this into Eq. 3.7-40 gives the requirement

$$\frac{\nu_{II}}{\nu_I} = \left(\frac{D_{II}}{D_I} \right)^{3/2} \quad (3.7-43)$$

This is an important result—namely, that the smaller tank (II) requires a fluid of smaller kinematic viscosity to maintain dynamic similarity. For example, if we use a scale model with $D_{II} = \frac{1}{2}D_I$, then we need to use a fluid with kinematic viscosity $\nu_{II} = \nu_I/\sqrt{8}$ in the scaled-down experiment. Evidently the requirements for dynamic similarity are more stringent here than in the previous example, because of the additional dimensionless group Fr .

In many practical cases, Eq. 3.7-43 calls for unattainably low values of ν_{II} . Exact scale-up from a single model experiment is then not possible. In some circumstances, however, the effect of one or more dimensionless groups may be known to be small, or may be predictable from experience with similar systems; in such situations, approximate scale-up from a single experiment is still feasible.⁹

This example shows the importance of including the boundary conditions in a dimensional analysis. Here the Froude number appeared only in the free-surface boundary condition Eq. 3.7-36. Failure to use this condition would result in the omission of the restriction in Eq. 3.7-42, and one might improperly choose $\nu_{II} = \nu_I$. If one did this, with $Re_{II} = Re_I$, the Froude number in the smaller tank would be too large, and the vortex would be too deep, as shown by the dotted line in Fig. 3.7-3.

EXAMPLE 3.7-3

Pressure Drop for Creeping Flow in a Packed Tube

Show that the mean axial gradient of the modified pressure $\check{\mathcal{P}}$ for creeping flow of a fluid of constant ρ and μ through a tube of radius R , uniformly packed for a length $L \gg D_p$ with solid particles of characteristic size $D_p \ll R$, is

$$\frac{\Delta\langle\check{\mathcal{P}}\rangle}{L} = \frac{\mu\langle v_z \rangle}{D_p^2} K(\text{geom}) \quad (3.7-44)$$

Here $\langle \dots \rangle$ denotes an average over a tube cross section within the packed length L , and the function $K(\text{geom})$ is a constant for a given bed geometry (i.e., a given shape and arrangement of the particles).

SOLUTION

We choose D_p as the characteristic length and $\langle v_z \rangle$ as the characteristic velocity. Then the interstitial fluid motion is determined by Eqs. 3.7-8 and 3.7-9b, with $\check{\mathbf{v}} = \mathbf{v}/\langle v_z \rangle$ and $\check{\mathcal{P}} = (\mathcal{P} - \mathcal{P}_0)D_p/\mu\langle v_z \rangle$, along with no-slip conditions on the solid surfaces and the modified pressure difference $\Delta\langle\check{\mathcal{P}}\rangle = \langle\check{\mathcal{P}}_0\rangle - \langle\check{\mathcal{P}}_L\rangle$. The solutions for $\check{\mathbf{v}}$ and $\check{\mathcal{P}}$ in creeping flow ($D_p\langle v_z \rangle\rho/\mu \rightarrow 0$) accordingly depend only on r , θ , and z for a given particle arrangement and shape. Then the mean axial gradient

$$\frac{D_p}{L} \int_0^{L/D_p} \left(-\frac{d\langle\check{\mathcal{P}}\rangle}{dz} \right) dz = \frac{D_p}{L} (\check{\mathcal{P}}_0 - \check{\mathcal{P}}_L) \quad (3.7-45)$$

depends only on the bed geometry as long as R and L are large relative to D_p . Inserting the foregoing expression for $\check{\mathcal{P}}$, we immediately obtain Eq. 3.7-44.

⁹ For an introduction to methods for scale-up with incomplete dynamic similarity, see R. W. Powell, *An Elementary Text in Hydraulics and Fluid Mechanics*, Macmillan, New York (1951).

QUESTIONS FOR DISCUSSION

1. What is the physical meaning of the term $\Delta x \Delta y (\rho v_z)|_z$ in Eq. 3.1-2? What is the physical meaning of $(\nabla \cdot \mathbf{v})$ of $(\nabla \cdot \rho \mathbf{v})$?
2. By making a mass balance over a volume element $(\Delta r)(r\Delta\theta)(\Delta z)$ derive the equation of continuity in cylindrical coordinates.
3. What is the physical meaning of the term $\Delta x \Delta y (\rho v_z v_z)|_z$ in Eq. 3.2-2? What is the physical meaning of $[\nabla \cdot \rho \mathbf{v} \mathbf{v}]$?
4. What happens when f is set equal to unity in Eq. 3.5-4?
5. Equation B in Table 3.5-1 is *not* restricted to fluids with constant density, even though ρ is to the left of the substantial derivative. Explain.
6. In the tangential annular flow problem in Example 3.5-3, would you expect the velocity profiles relative to the inner cylinder to be the same in the following two situations: (i) the inner cylinder is fixed and the outer cylinder rotates with an angular velocity Ω ; (ii) the outer cylinder is fixed and the inner cylinder rotates with an angular velocity $-\Omega$? Both flows are presumed to be laminar and stable.
7. Suppose that, in Example 3.6-4, there were two immiscible liquids in the rotating beaker. What would be the shape of the interface between the two liquid regions?
8. Would the system discussed in Example 3.6-5 be useful as a viscometer?
9. In Eq. 3.6-55, explain by means of a carefully drawn sketch the choice of limits in the integration and the meaning of each factor in the first integrand.
10. What factors would need to be taken into account in designing a mixing tank for use on the moon by using data from a similar tank on earth?

PROBLEMS

3A.1 Torque required to turn a friction bearing (Fig. 3A.1). Calculate the required torque in $\text{lb}_f \cdot \text{ft}$ and power consumption in horsepower to turn the shaft in the friction bearing shown in the figure. The length of the bearing surface on the shaft is 2 in., and the shaft is rotating at 200 rpm. The viscosity of the lubricant is 200 cp, and its density is $50 \text{ lb}_m/\text{ft}^3$. Neglect the effect of eccentricity.

Answers: $0.32 \text{ lb}_f \cdot \text{ft}$; $0.012 \text{ hp} = 0.009 \text{ kW}$

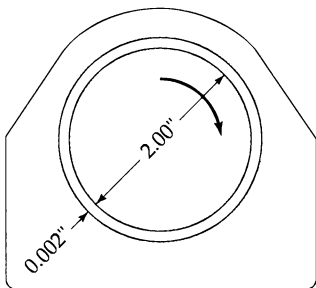


Fig. 3A.1. Friction bearing.

3A.2 Friction loss in bearings.¹ Each of two screws on a large motor-ship is driven by a 4000-hp engine. The shaft that connects the motor and the screw is 16 in. in diameter

and rests in a series of sleeve bearings that give a 0.005 in. clearance. The shaft rotates at 50 rpm, the lubricant has a viscosity of 5000 cp, and there are 20 bearings, each 1 ft in length. Estimate the fraction of engine power expended in rotating the shafts in their bearings. Neglect the effect of the eccentricity.

Answer: 0.115

3A.3 Effect of altitude on air pressure. When standing at the mouth of the Ontonagon River on the south shore of Lake Superior (602 ft above mean sea level), your portable barometer indicates a pressure of 750 mm Hg. Use the equation of motion to estimate the barometric pressure at the top of Government Peak (2023 ft above mean sea level) in the nearby Porcupine Mountains. Assume that the temperature at lake level is 70°F and that the temperature decreases with increasing altitude at a steady rate of 3°F per 1000 feet. The gravitational acceleration at the south shore of Lake Superior is about 32.19 ft/s², and its variation with altitude may be neglected in this problem.

Answer: $712 \text{ mm Hg} = 9.49 \times 10^4 \text{ N/m}^2$

3A.4 Viscosity determination with a rotating-cylinder viscometer. It is desired to measure the viscosities of sucrose solutions of about 60% concentration by weight at about 20°C with a rotating-cylinder viscometer such as that shown in Fig. 3.5-1. This instrument has an inner cylinder 4.000 cm in diameter surrounded by a rotating

¹ This problem was contributed by Prof. E. J. Crosby, University of Wisconsin.

concentric cylinder 4.500 cm in diameter. The length L is 4.00 cm. The viscosity of a 60% sucrose solution at 20°C is about 57 cp, and its density is about 1.29 g/cm³.

On the basis of past experience it seems possible that end effects will be important, and it is therefore decided to calibrate the viscometer by measurements on some known solutions of approximately the same viscosity as those of the unknown sucrose solutions.

Determine a reasonable value for the applied torque to be used in calibration if the torque measurements are reliable within 100 dyne/cm and the angular velocity can be measured within 0.5%. What will be the resultant angular velocity?

3A.5 Fabrication of a parabolic mirror. It is proposed to make a backing for a parabolic mirror, by rotating a pan of slow-hardening plastic resin at constant speed until it hardens. Calculate the rotational speed required to produce a mirror of focal length $f = 100$ cm. The focal length is one-half the radius of curvature at the axis, which in turn is given by

$$r_c = \left[1 + \left(\frac{dz}{dr} \right)^2 \right]^{3/2} \left(\frac{d^2 z}{dr^2} \right)^{-1} \quad (3A.5-1)$$

Answer: 21.1 rpm

3A.6 Scale-up of an agitated tank. Experiments with a small-scale agitated tank are to be used to design a geometrically similar installation with linear dimensions 10 times as large. The fluid in the large tank will be a heavy oil with $\mu = 13.5$ cp and $\rho = 0.9$ g/cm³. The large tank is to have an impeller speed of 120 rpm.

(a) Determine the impeller speed for the small-scale model, in accordance with the criteria for scale-up given in Example 3.7-2.

(b) Determine the operating temperature for the model if water is to be used as the stirred fluid.

Answers: (a) 380 rpm, (b) $T = 60^\circ$

3A.7 Air entrainment in a draining tank (Fig. 3A.7). A molasses storage tank 60 ft in diameter is to be built with a draw-off line 1 ft in diameter, 4 ft from the sidewall of the

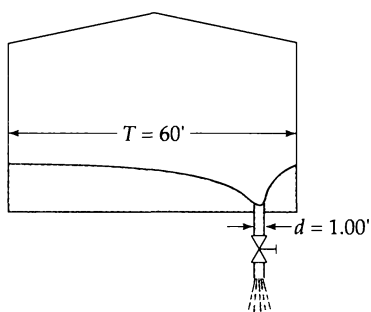


Fig. 3A.7. Draining of a molasses tank.

tank and extending vertically upward 1 ft from the tank bottom. It is known from experience that, as molasses is withdrawn from the tank, a vortex will form, and, as the liquid level drops, this vortex will ultimately reach the draw-off pipe, allowing air to be sucked into the molasses. This is to be avoided.

It is proposed to predict the minimum liquid level at which this entrainment can be avoided, at a draw-off rate of 800 gal/min, by a model study using a smaller tank. For convenience, water at 68°F is to be used for the fluid in the model study.

Determine the proper tank dimensions and operating conditions for the model if the density of the molasses is 1.286 g/cm³ and its viscosity is 56.7 cp. It may be assumed that, in either the full-size tank or the model, the vortex shape is dependent only on the amount of the liquid in the tank and the draw-off rate; that is, the vortex establishes itself very rapidly.

3B.1 Flow between coaxial cylinders and concentric spheres.

(a) The space between two coaxial cylinders is filled with an incompressible fluid at constant temperature. The radii of the inner and outer wetted surfaces are κR and R , respectively. The angular velocities of rotation of the inner and outer cylinders are Ω_i and Ω_o . Determine the velocity distribution in the fluid and the torques on the two cylinders needed to maintain the motion.

(b) Repeat part (a) for two concentric spheres.

Answers:

$$(a) v_\theta = \frac{\kappa R}{1 - \kappa^2} \left[(\Omega_o - \Omega_i \kappa^2) \left(\frac{r}{\kappa R} \right) + (\Omega_i - \Omega_o) \left(\frac{\kappa R}{r} \right) \right]$$

$$(b) v_\phi = \frac{\kappa R}{1 - \kappa^3} \left[(\Omega_o - \Omega_i \kappa^3) \left(\frac{r}{\kappa R} \right) + (\Omega_i - \Omega_o) \left(\frac{\kappa R}{r} \right)^2 \right] \sin \theta$$

3B.2 Laminar flow in a triangular duct (Fig. 3B.2).² One type of compact heat exchanger is shown in Fig. 3B.2(a). In order to analyze the performance of such an apparatus, it is necessary to understand the flow in a duct whose cross section is an equilateral triangle. This is done most easily by installing a coordinate system as shown in Fig. 3B.2(b).

(a) Verify that the velocity distribution for the laminar flow of a Newtonian fluid in a duct of this type is given by

$$v_z = \frac{(\mathcal{P}_0 - \mathcal{P}_L)}{4\mu LH} (y - H)(3x^2 - y^2) \quad (3B.2-1)$$

² An alternative formulation of the velocity profile is given by L. D. Landau and E. M. Lifshitz, *Fluid Mechanics*, Pergamon, Oxford, 2nd edition (1987), p. 54.

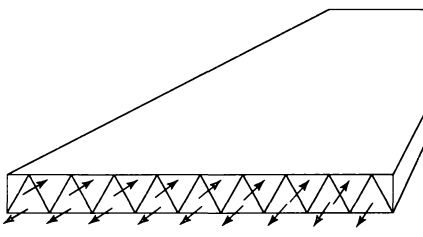


Fig. 3B.2. (a) Compact heat-exchanger element, showing channels of a triangular cross section; (b) coordinate system for an equilateral-triangular duct.

(b) From Eq. 3B.2-1 find the average velocity, maximum velocity, and mass flow rate.

$$\text{Answers: (b)} \langle v_z \rangle = \frac{(\mathcal{P}_0 - \mathcal{P}_L)H^2}{60\mu L} = \frac{9}{20} v_{z,\max}; \\ w = \frac{\sqrt{3}(\mathcal{P}_0 - \mathcal{P}_L)H^4\rho}{180\mu L}$$

3B.3 Laminar flow in a square duct.

(a) A straight duct extends in the z direction for a length L and has a square cross section, bordered by the lines $x = \pm B$ and $y = \pm B$. A colleague has told you that the velocity distribution is given by

$$v_z = \frac{(\mathcal{P}_0 - \mathcal{P}_L)B^2}{4\mu L} \left[1 - \left(\frac{x}{B} \right)^2 \right] \left[1 - \left(\frac{y}{B} \right)^2 \right] \quad (3B.3-1)$$

Since this colleague has occasionally given you wrong advice in the past, you feel obliged to check the result. Does it satisfy the relevant boundary conditions and the relevant differential equation?

(b) According to the review article by Berker,³ the mass rate of flow in a square duct is given by

$$w = \frac{0.563(\mathcal{P}_0 - \mathcal{P}_L)B^4\rho}{\mu L} \quad (3B.3-2)$$

Compare the coefficient in this expression with the coefficient that one obtains from Eq. 3B.3-1.

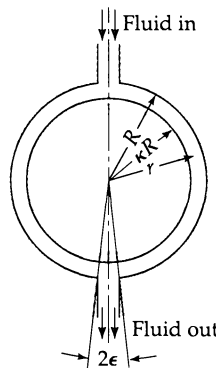


Fig. 3B.4. Creeping flow in the region between two stationary concentric spheres.

3B.4 Creeping flow between two concentric spheres (Fig. 3B.4). A very viscous Newtonian fluid flows in the space between two concentric spheres, as shown in the figure. It is desired to find the rate of flow in the system as a function of the imposed pressure difference. Neglect end effects and postulate that v_θ depends only on r and θ with the other velocity components zero.

(a) Using the equation of continuity, show that $v_\theta \sin \theta = u(r)$, where $u(r)$ is a function of r to be determined.

(b) Write the θ -component of the equation of motion for this system, assuming the flow to be slow enough that the $[\mathbf{v} \cdot \nabla \mathbf{v}]$ term is negligible. Show that this gives

$$0 = -\frac{1}{r} \frac{\partial \mathcal{P}}{\partial \theta} + \mu \left[\frac{1}{\sin \theta} \frac{1}{r^2} \frac{d}{dr} \left(r^2 \frac{du}{dr} \right) \right] \quad (3B.4-1)$$

(c) Separate this into two equations

$$\sin \theta \frac{d\mathcal{P}}{d\theta} = B; \quad \frac{\mu}{r} \frac{d}{dr} \left(r^2 \frac{du}{dr} \right) = B \quad (3B.4-2, 3)$$

where B is the separation constant, and solve the two equations to get

$$B = \frac{\mathcal{P}_2 - \mathcal{P}_1}{2 \ln \cot \frac{1}{2}\epsilon} \quad (3B.4-4)$$

$$u(r) = \frac{(\mathcal{P}_1 - \mathcal{P}_2)R}{4\mu \ln \cot (\epsilon/2)} \left[\left(1 - \frac{r}{R} \right) + \kappa \left(1 - \frac{R}{r} \right) \right] \quad (3B.4-5)$$

where \mathcal{P}_1 and \mathcal{P}_2 are the values of the modified pressure at $\theta = \epsilon$ and $\theta = \pi - \epsilon$, respectively.

(d) Use the results above to get the mass rate of flow

$$w = \frac{\pi(\mathcal{P}_1 - \mathcal{P}_2)R^3(1 - \kappa)^3\rho}{12\mu \ln \cot (\epsilon/2)} \quad (3B.4-6)$$

3B.5 Parallel-disk viscometer (Fig. 3B.5). A fluid, whose viscosity is to be measured, is placed in the gap of thickness B between the two disks of radius R . One measures the torque T_z required to turn the upper disk at an angular velocity Ω . Develop the formula for deducing the viscosity from these measurements. Assume creeping flow.

³ R. Berker, *Handbuch der Physik*, Vol. VIII/2, Springer, Berlin (1963); see pp. 67–77 for laminar flow in conduits of noncircular cross sections. See also W. E. Stewart, *AIChE Journal*, 8, 425–428 (1962).

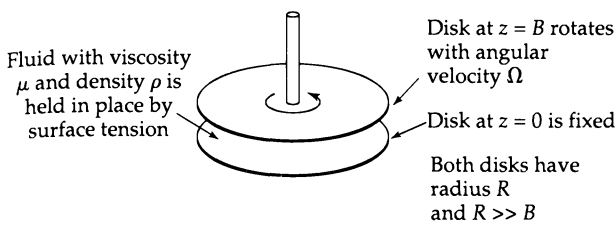


Fig. 3B.5. Parallel-disk viscometer.

- (a) Postulate that for small values of Ω the velocity profiles have the form $v_r = 0$, $v_z = 0$, and $v_\theta = rf(z)$; why does this form for the tangential velocity seem reasonable? Postulate further that $\mathcal{P} = \mathcal{P}(r, z)$. Write down the resulting simplified equations of continuity and motion.
- (b) From the θ -component of the equation of motion, obtain a differential equation for $f(z)$. Solve the equation for $f(z)$ and evaluate the constants of integration. This leads ultimately to the result $v_\theta = \Omega r(z/B)$. Could you have guessed this result?
- (c) Show that the desired working equation for deducing the viscosity is $\mu = 2BT_z/\pi\Omega R^4$.
- (d) Discuss the advantages and disadvantages of this instrument.

3B.6 Circulating axial flow in an annulus (Fig. 3B.6). A rod of radius κR moves upward with a constant velocity v_0 through a cylindrical container of inner radius R containing a Newtonian liquid. The liquid circulates in the cylinder, moving upward along the moving central rod and moving downward along the fixed container wall. Find the velocity distribution in the annular region, far from the end disturbances. Flows similar to this occur in the seals of some reciprocating machinery—for example, in the annular space between piston rings.

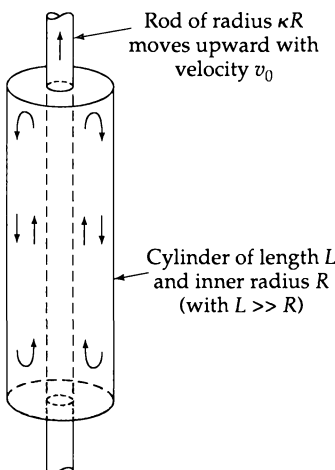


Fig. 3B.6. Circulating flow produced by an axially moving rod in a closed annular region.

(a) First consider the problem where the annular region is quite narrow—that is, where κ is just slightly less than unity. In that case the annulus may be approximated by a thin plane slit and the curvature can be neglected. Show that in this limit, the velocity distribution is given by

$$\frac{v_z}{v_0} = 3\left(\frac{\xi - \kappa}{1 - \kappa}\right)^2 - 4\left(\frac{\xi - \kappa}{1 - \kappa}\right) + 1 \quad (3B.6-1)$$

where $\xi = r/R$.

(b) Next work the problem without the thin-slit assumption. Show that the velocity distribution is given by

$$\frac{v_z}{v_0} = \frac{(1 - \xi^2)\left(1 - \frac{2\kappa^2}{1 - \kappa^2} \ln \frac{1}{\kappa}\right) - (1 - \kappa^2) \ln \frac{1}{\xi}}{(1 - \kappa^2) - (1 + \kappa^2) \ln \frac{1}{\kappa}} \quad (3B.6-2)$$

3B.7 Momentum fluxes for creeping flow into a slot (Fig. 3B.7). An incompressible Newtonian liquid is flowing very slowly into a thin slot of thickness $2B$ (in the y direction) and width W (in the z direction). The mass rate of flow in the slot is w . From the results of Problem 2B.3 it can be shown that the velocity distribution within the slot is

$$v_x = \frac{3w}{4BW\rho} \left[1 - \left(\frac{y}{B} \right)^2 \right] \quad v_y = 0 \quad v_z = 0 \quad (3B.7-1)$$

at locations not too near the inlet. In the region outside the slot the components of the velocity for *creeping flow* are

$$v_x = -\frac{2w}{\pi W\rho} \frac{x^3}{(x^2 + y^2)^2} \quad (3B.7-2)$$

$$v_y = -\frac{2w}{\pi W\rho} \frac{x^2 y}{(x^2 + y^2)^2} \quad (3B.7-3)$$

$$v_z = 0 \quad (3B.7-4)$$

Equations 3B.7-1 to 4 are only approximate in the region near the slot entry for both $x \geq 0$ and $x \leq 0$.

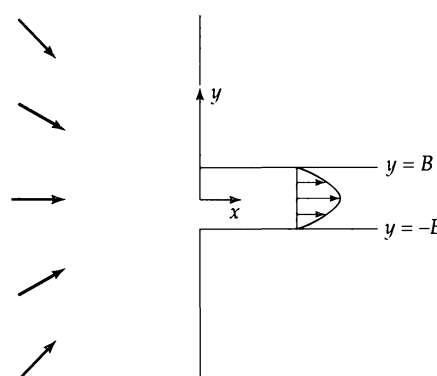


Fig. 3B.7. Flow of a liquid into a slot from a semi-infinite region $x < 0$.

- (a) Find the components of the convective momentum flux $\rho\mathbf{v}\mathbf{v}$ inside and outside the slot.
- (b) Evaluate the xx -component of $\rho\mathbf{v}\mathbf{v}$ at $x = -a, y = 0$.
- (c) Evaluate the xy -component of $\rho\mathbf{v}\mathbf{v}$ at $x = -a, y = +a$.
- (d) Does the total flow of kinetic energy through the plane $x = -a$ equal the total flow of kinetic energy through the slot?
- (e) Verify that the velocity distributions given in Eqs. 3B.7-1 to 4 satisfy the relation $(\nabla \cdot \mathbf{v}) = 0$.
- (f) Find the normal stress τ_{xx} at the plane $y = 0$ and also on the solid surface at $x = 0$.

(g) Find the shear stress τ_{yx} on the solid surface at $x = 0$. Is this result surprising? Does sketching the velocity profile v_y vs. x at some plane $y = a$ assist in understanding the result?

3B.8 Velocity distribution for creeping flow toward a slot (Fig. 3B.7).⁴ It is desired to get the velocity distribution given for the upstream region in the previous problem. We postulate that $v_\theta = 0, v_z = 0, v_r = v_r(r, \theta)$, and $\mathcal{P} = \mathcal{P}(r, \theta)$.

- (a) Show that the equation of continuity in cylindrical coordinates gives $v_r = f(\theta)/r$, where $f(\theta)$ is a function of θ for which $df/d\theta = 0$ at $\theta = 0$, and $f = 0$ at $\theta = \pi/2$.
- (b) Write the r - and θ -components of the creeping flow equation of motion, and insert the expression for $f(\theta)$ from (a).
- (c) Differentiate the r -component of the equation of motion with respect to θ and the θ -component with respect to r . Show that this leads to

$$\frac{d^3f}{d\theta^3} + 4 \frac{df}{d\theta} = 0 \quad (3B.8-1)$$

- (d) Solve this differential equation and obtain an expression for $f(\theta)$ containing three integration constants.
- (e) Evaluate the integration constants by using the two boundary conditions in (a) and the fact that the total mass-flow rate through any cylindrical surface must equal w . This gives

$$v_r = -\frac{2w}{\pi W\rho r} \cos^2 \theta \quad (3B.8-2)$$

- (f) Next from the equations of motion in (b) obtain $\mathcal{P}(r, \theta)$ as

$$\mathcal{P}(r, \theta) = \mathcal{P}_\infty - \frac{2\mu w}{\pi W\rho r^2} \cos 2\theta \quad (3B.8-3)$$

What is the physical meaning of \mathcal{P}_∞ ?

- (g) Show that the total normal stress exerted on the solid surface at $\theta = \pi/2$ is

$$(p + \tau_{\theta\theta})|_{\theta=\pi/2} = p_\infty + \frac{2\mu w}{\pi W\rho r^2} \quad (3B.8-4)$$

- (h) Next evaluate $\tau_{\theta r}$ on the same solid surface.

- (i) Show that the velocity profile obtained in Eq. 3B.8-2 is the equivalent to Eqs. 3B.7-2 and 3.

3B.9 Slow transverse flow around a cylinder (see Fig. 3.7-1). An incompressible Newtonian fluid approaches a stationary cylinder with a uniform, steady velocity v_∞ in the positive x direction. When the equations of change are solved for creeping flow, the following expressions⁵ are found for the pressure and velocity in the immediate vicinity of the cylinder (they are *not* valid at large distances):

$$p(r, \theta) = p_\infty - C\mu \frac{v_\infty \cos \theta}{r} - \rho gr \sin \theta \quad (3B.9-1)$$

$$v_r = Cv_\infty \left[\frac{1}{2} \ln \left(\frac{r}{R} \right) - \frac{1}{4} + \frac{1}{4} \left(\frac{R}{r} \right)^2 \right] \cos \theta \quad (3B.9-2)$$

$$v_\theta = -Cv_\infty \left[\frac{1}{2} \ln \left(\frac{r}{R} \right) + \frac{1}{4} - \frac{1}{4} \left(\frac{R}{r} \right)^2 \right] \sin \theta \quad (3B.9-3)$$

Here p_∞ is the pressure far from the cylinder at $y = 0$ and

$$C = \frac{2}{\ln (7.4/\text{Re})} \quad (3B.9-4)$$

with the Reynolds number defined as $\text{Re} = 2Rv_\infty\rho/\mu$.

- (a) Use these results to get the pressure p , the shear stress $\tau_{r\theta}$, and the normal stress τ_{rr} at the surface of the cylinder.
- (b) Show that the x -component of the force per unit area exerted by the liquid on the cylinder is

$$-\mathcal{P}|_{r=R} \cos \theta + \tau_{r\theta}|_{r=R} \sin \theta \quad (3B.9-5)$$

- (c) Obtain the force $F_x = 2C\pi L\mu v_\infty$ exerted in the x direction on a length L of the cylinder.

3B.10 Radial flow between parallel disks (Fig. 3B.10). A part of a lubrication system consists of two circular disks between which a lubricant flows radially. The flow takes place because of a modified pressure difference $\mathcal{P}_1 - \mathcal{P}_2$ between the inner and outer radii r_1 and r_2 , respectively.

- (a) Write the equations of continuity and motion for this flow system, assuming steady-state, laminar, incompressible Newtonian flow. Consider only the region $r_1 \leq r \leq r_2$ and a flow that is radially directed.

⁴ Adapted from R. B. Bird, R. C. Armstrong, and O. Hassager, *Dynamics of Polymeric Liquids*, Vol. 1, Wiley-Interscience, New York, 2nd edition (1987), pp. 42–43.

⁵ See G. K. Batchelor, *An Introduction to Fluid Dynamics*, Cambridge University Press (1967), pp. 244–246, 261.

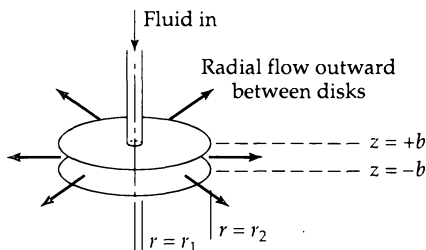


Fig. 3B.10. Outward radial flow in the space between two parallel, circular disks.

- (b) Show how the equation of continuity enables one to simplify the equation of motion to give

$$\rho \frac{\phi^2}{r^3} = -\frac{d\mathcal{P}}{dr} + \mu \frac{1}{r} \frac{d^2\phi}{dz^2} \quad (3B.10-1)$$

in which $\phi = rv_r$ is a function of z only. Why is ϕ independent of r ?

(c) It can be shown that no solution exists for Eq. 3B.10-1 unless the nonlinear term containing ϕ is omitted. Omission of this term corresponds to the “creeping flow assumption.” Show that for creeping flow, Eq. 3B.10-1 can be integrated with respect to r to give

$$0 = (\mathcal{P}_1 - \mathcal{P}_2) + \left(\mu \ln \frac{r_2}{r_1} \right) \frac{d^2\phi}{dz^2} \quad (3B.10-2)$$

- (d) Show that further integration with respect to z gives

$$v_r(r, z) = \frac{(\mathcal{P}_1 - \mathcal{P}_2)b^2}{2\mu r \ln(r_2/r_1)} \left[1 - \left(\frac{z}{b} \right)^2 \right] \quad (3B.10-3)$$

- (e) Show that the mass flow rate is

$$w = \frac{4\pi(\mathcal{P}_1 - \mathcal{P}_2)b^3\rho}{3\mu \ln(r_2/r_1)} \quad (3B.10-4)$$

- (f) Sketch the curves $\mathcal{P}(r)$ and $v_r(r, z)$.

3B.11 Radial flow between two coaxial cylinders. Consider an incompressible fluid, at constant temperature, flowing radially between two porous cylindrical shells with inner and outer radii κR and R .

(a) Show that the equation of continuity leads to $v_r = C/r$, where C is a constant.

(b) Simplify the components of the equation of motion to obtain the following expressions for the modified-pressure distribution:

$$\frac{d\mathcal{P}}{dr} = -\rho v_r \frac{dv_r}{dr} \quad \frac{d\mathcal{P}}{d\theta} = 0 \quad \frac{d\mathcal{P}}{dz} = 0 \quad (3B.11-1)$$

- (c) Integrate the expression for $d\mathcal{P}/dr$ above to get

$$\mathcal{P}(r) - \mathcal{P}(R) = \frac{1}{2}\rho[v_r(R)]^2 \left[1 - \left(\frac{R}{r} \right)^2 \right] \quad (3B.11-2)$$

- (d) Write out all the nonzero components of τ for this flow.
(e) Repeat the problem for concentric spheres.

3B.12 Pressure distribution in incompressible fluids. Penelope is staring at a beaker filled with a liquid, which for all practical purposes can be considered as incompressible; let its density be ρ_0 . She tells you she is trying to understand how the pressure in the liquid varies with depth. She has taken the origin of coordinates at the liquid-air interface, with the positive z -axis pointing away from the liquid. She says to you:

“If I simplify the equation of motion for an incompressible liquid at rest, I get $0 = -dp/dz - \rho_0 g$. I can solve this and get $p = p_{\text{atm}} - \rho_0 gz$. That seems reasonable—the pressure increases with increasing depth.

“But, on the other hand, the equation of state for any fluid is $p = p(\rho, T)$, and if the system is at constant temperature, this just simplifies to $p = p(\rho)$. And, since the fluid is incompressible, $p = p(\rho_0)$, and p must be a constant throughout the fluid! How can that be?”

Clearly Penelope needs help. Provide a useful explanation.

3B.13 Flow of a fluid through a sudden contraction.

(a) An incompressible liquid flows through a sudden contraction from a pipe of diameter D_1 into a pipe of smaller diameter D_2 . What does the Bernoulli equation predict for $\mathcal{P}_1 - \mathcal{P}_2$, the difference between the modified pressures upstream and downstream of the contraction? Does this result agree with experimental observations?

(b) Repeat the derivation for the isothermal horizontal flow of an ideal gas through a sudden contraction.

3B.14 Torricelli’s equation for efflux from a tank (Fig. 3B.14). A large uncovered tank is filled with a liquid to a height h . Near the bottom of the tank, there is a hole that allows the fluid to exit to the atmosphere. Apply Bernoulli’s equation to a streamline that extends from the surface of the liquid at the top to a point in the exit

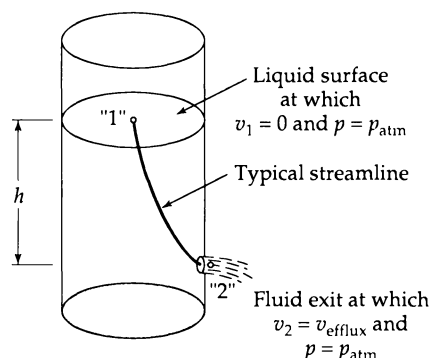


Fig. 3B.14. Fluid draining from a tank. Points “1” and “2” are on the same streamline.

stream just outside the vessel. Show that this leads to an efflux velocity $v_{\text{efflux}} = \sqrt{2gh}$. This is known as *Torricelli's equation*.

To get this result, one has to assume incompressibility (which is usually reasonable for most liquids), and that the height of the fluid surface is changing so slowly with time that the Bernoulli equation can be applied at any instant of time (the quasi-steady-state assumption).

3B.15 Shape of free surface in tangential annular flow.

(a) A liquid is in the annular space between two vertical cylinders of radii κR and R , and the liquid is open to the atmosphere at the top. Show that when the inner cylinder rotates with an angular velocity Ω_i , and the outer cylinder is fixed, the free liquid surface has the shape

$$z_R - z = \frac{1}{2g} \left(\frac{\kappa^2 R \Omega_i}{1 - \kappa^2} \right)^2 (\xi^{-2} + 4 \ln \xi - \xi^2) \quad (3B.15-1)$$

in which z_R is the height of the liquid at the outer-cylinder wall, and $\xi = r/R$.

(b) Repeat (a) but with the inner cylinder fixed and the outer cylinder rotating with an angular velocity Ω_o . Show that the shape of the liquid surface is

$$z_R - z = \frac{1}{2g} \left(\frac{\kappa^2 R \Omega_o}{1 - \kappa^2} \right)^2 [(\xi^{-2} - 1) + 4\kappa^{-2} \ln \xi - \kappa^{-4}(\xi^2 - 1)] \quad (3B.15-2)$$

(c) Draw a sketch comparing these two liquid-surface shapes.

3B.16 Flow in a slit with uniform cross flow (Fig. 3B.16). A fluid flows in the positive x -direction through a long flat duct of length L , width W , and thickness B , where $L \gg W \gg B$. The duct has porous walls at $y = 0$ and $y = B$, so that a constant cross flow can be maintained, with $v_y = v_0$, a constant, everywhere. Flows of this type are important in connection with separation processes using the sweep-diffusion effect. By carefully controlling the cross flow, one can concentrate the larger constituents (molecules, dust particles, etc.) near the upper wall.

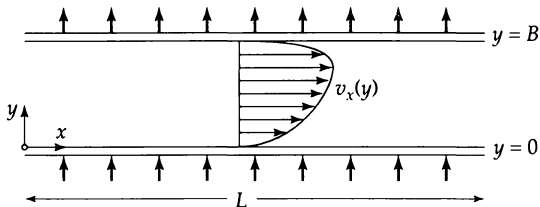


Fig. 3B.16. Flow in a slit of length L , width W , and thickness B . The walls at $y = 0$ and $y = B$ are porous, and there is a flow of the fluid in the y direction, with a uniform velocity $v_y = v_0$.

(a) Show that the velocity profile for the system is given by

$$v_x = \frac{(\mathcal{P}_0 - \mathcal{P}_L)B^2}{\mu L} \frac{1}{A} \left(\frac{y}{B} - \frac{e^{Ay/B} - 1}{e^A - 1} \right) \quad (3B.16-1)$$

in which $A = Bv_0\rho/\mu$.

(b) Show that the mass flow rate in the x direction is

$$w = \frac{(\mathcal{P}_0 - \mathcal{P}_L)B^3W\rho}{\mu L} \frac{1}{A} \left(\frac{1}{2} - \frac{1}{A} + \frac{1}{e^A - 1} \right) \quad (3B.16-2)$$

(c) Verify that the above results simplify to those of Problem 2B.3 in the limit that there is no cross flow at all (that is, $A \rightarrow 0$).

(d) A colleague has also solved this problem, but taking a coordinate system with $y = 0$ at the midplane of the slit, with the porous walls located at $y = \pm b$. His answer to part (a) above is

$$\langle v_x \rangle = \frac{e^{\alpha\eta} - \eta \sinh \alpha - \cosh \alpha}{(1/\alpha) \sinh \alpha - \cosh \alpha} \quad (3B.16-3)$$

in which $\alpha = bv_0\rho/\mu$ and $\eta = y/b$. Is this result equivalent to Eq. 3B.16-1?

3C.1 Parallel-disk compression viscometer⁶ (Fig. 3C.-1). A fluid fills completely the region between two circular disks of radius R . The bottom disk is fixed, and the upper disk is made to approach the lower one very slowly with a constant speed v_0 , starting from a height H_0 (and $H_0 \ll R$). The instantaneous height of the upper disk is $H(t)$. It is desired to find the force needed to maintain the speed v_0 .

This problem is inherently a rather complicated unsteady-state flow problem. However, a useful approximate solution can be obtained by making two simplifications in

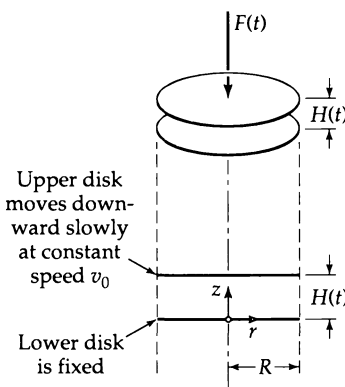


Fig. 3C.1. Squeezing flow in a parallel-disk compression viscometer.

⁶ J. R. Van Wazer, J. W. Lyons, K. Y. Kim, and R. E. Colwell, *Viscosity and Flow Measurement*, Wiley-Interscience, New York (1963), pp. 292–295.

the equations of change: (i) we assume that the speed v_0 is so slow that all terms containing time derivatives can be omitted; this is the so-called "quasi-steady-state" assumption; (ii) we use the fact that $H_0 \ll R$ to neglect quite a few terms in the equations of change by order-of-magnitude arguments. Note that the rate of decrease of the fluid volume between the disks is $\pi R^2 v_0$, and that this must equal the rate of outflow from between the disks, which is $2\pi R H \langle v_r \rangle|_{r=R}$. Hence

$$\langle v_r \rangle|_{r=R} = \frac{Rv_0}{2H(t)} \quad (3C.1-1)$$

We now argue that $v_r(r, z)$ will be of the order of magnitude of $\langle v_r \rangle|_{r=R}$ and that $v_z(r, z)$ is of the order of magnitude of v_0 , so that

$$v_r \approx (R/H)v_0; \quad v_z \approx -v_0 \quad (3C.1-2, 3)$$

and hence $|v_z| \ll v_r$. We may now estimate the order of magnitude of various derivatives as follows: as r goes from 0 to R , the radial velocity v_r goes from zero to approximately $(R/H)v_0$. By this kind of reasoning we get

$$\frac{\partial v_r}{\partial r} \approx \frac{(R/H)v_0 - 0}{R - 0} = \frac{v_0}{H} \quad (3C.1-4)$$

$$\frac{\partial v_z}{\partial z} \approx \frac{(-v_0) - 0}{H - 0} = -\frac{v_0}{H}, \text{ etc.} \quad (3C.1-5)$$

(a) By the above-outlined order-of-magnitude analysis, show that the continuity equation and the r -component of the equation of motion become (with g_z neglected)

$$\text{continuity: } \frac{1}{r} \frac{\partial}{\partial r} (rv_r) + \frac{\partial v_z}{\partial z} = 0 \quad (3C.1-6)$$

$$\text{motion } 0 = -\frac{dp}{dr} + \mu \frac{\partial^2 v_r}{\partial z^2} \quad (3C.1-7)$$

with the boundary conditions

$$\text{B.C. 1: at } z = 0, \quad v_r = 0, \quad v_z = 0 \quad (3C.1-8)$$

$$\text{B.C. 2: at } z = H(t), \quad v_r = 0, \quad v_z = -v_0 \quad (3C.1-9)$$

$$\text{B.C. 3: at } r = R, \quad p = p_{\text{atm}} \quad (3C.1-10)$$

(b) From Eqs. 3C.1-7 to 9 obtain

$$v_r = \frac{1}{2\mu} \left(\frac{dp}{dr} \right) z(z - H) \quad (3C.1-11)$$

(c) Integrate Eq. 3C.1-6 with respect to z and substitute the result from Eq. 3C.1-11 to get

$$v_0 = -\frac{H^3}{12\mu} \frac{1}{r} \frac{d}{dr} \left(r \frac{dp}{dr} \right) \quad (3C.1-12)$$

(d) Solve Eq. 3C.1-12 to get the pressure distribution

$$p = p_{\text{atm}} + \frac{3\mu v_0 R^2}{H^3} \left[1 - \left(\frac{r}{R} \right)^2 \right] \quad (3C.1-13)$$

(e) Integrate $[(p + \tau_{zz}) - p_{\text{atm}}]$ over the moving-disk surface to find the total force needed to maintain the disk motion:

$$F(t) = \frac{3\pi\mu v_0 R^4}{2[H(t)]^3} \quad (3C.1-14)$$

This result can be used to obtain the viscosity from the force and velocity measurements.

(f) Repeat the analysis for a viscometer that is operated in such a way that a centered, circular glob of liquid never completely fills the space between the two plates. Let the volume of the sample be V and obtain

$$F(t) = \frac{3\mu v_0 V^2}{2\pi[H(t)]^5} \quad (3C.1-15)$$

(g) Repeat the analysis for a viscometer that is operated with constant applied force, F_0 . The viscosity is then to be determined by measuring H as a function of time, and the upper-plate velocity is not a constant. Show that

$$\frac{1}{[H(t)]^2} = \frac{1}{H_0^2} + \frac{4F_0 t}{3\pi\mu R^4} \quad (3C.1-16)$$

3C.2 Normal stresses at solid surfaces for compressible fluids. Extend example 3.1-1 to compressible fluids. Show that

$$\tau_{zz}|_{z=0} = (\frac{4}{3}\mu + \kappa)(\partial \ln \rho / \partial t)|_{z=0} \quad (3C.2-1)$$

Discuss the physical significance of this result.

3C.3 Deformation of a fluid line (Fig. 3C.3). A fluid is contained in the annular space between two cylinders of radii κR and R . The inner cylinder is made to rotate with a constant angular velocity of Ω_i . Consider a line of fluid particles in the plane $z = 0$ extending from the inner cylinder to the outer cylinder and initially located at $\theta = 0$, normal to the two surfaces. How does this fluid line deform into a curve $\theta(r, t)$? What is the length, l , of the curve after N revolutions of the inner cylinder? Use Eq. 3.6-32.

$$\text{Answer: } \frac{l}{R} = \int_{\kappa}^1 \sqrt{1 + \frac{16\pi^2 N^2}{[(1/\kappa)^2 - 1]^2 \xi^4}} d\xi$$

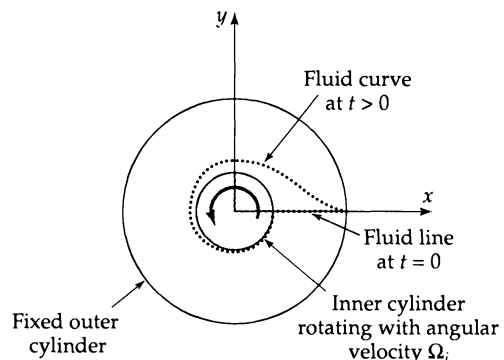


Fig. 3C.3. Deformation of a fluid line in Couette flow.

3C.4 Alternative methods of solving the Couette viscometer problem by use of angular momentum concepts (Fig. 3.6-1).

(a) By making a shell angular-momentum balance on a thin shell of thickness Δr , show that

$$\frac{d}{dr}(r^2\tau_{rr}) = 0 \quad (3C.4-1)$$

Next insert the appropriate expression for τ_{rr} in terms of the gradient of the tangential component of the velocity. Then solve the resulting differential equation with the boundary conditions to get Eq. 3.6-29.

(b) Show how to obtain Eq. 3C.4-1 from the *equation of change for angular momentum* given in Eq. 3.4-1.

3C.5 Two-phase interfacial boundary conditions. In §2.1, boundary conditions for solving viscous flow problems were given. At that point no mention was made of the role of interfacial tension. At the interface between two immiscible fluids, I and II, the following boundary condition should be used:⁷

$$\mathbf{n}^I(p^I - p^{II}) + [\mathbf{n}^I \cdot (\boldsymbol{\tau}^I - \boldsymbol{\tau}^{II})] = \mathbf{n}^I \left(\frac{1}{R_1} + \frac{1}{R_2} \right) \sigma \quad (3C.5-1)$$

This is essentially a momentum balance written for an interfacial element dS with no matter passing through it, and with no interfacial mass or viscosity. Here \mathbf{n}^I is the unit vector normal to dS and pointing into phase I. The quantities R_1 and R_2 are the principal radii of curvature at dS , and each of these is positive if its center lies in phase I. The sum $(1/R_1) + (1/R_2)$ can also be expressed as $(\nabla \cdot \mathbf{n}^I)$. The quantity σ is the interfacial tension, assumed constant.

(a) Show that, for a spherical droplet of I at rest in a second medium II, *Laplace's equation*

$$p^I - p^{II} = \left(\frac{1}{R_1} + \frac{1}{R_2} \right) \sigma \quad (3C.5-2)$$

relates the pressures inside and outside the droplet. Is the pressure in phase I greater than that in phase II, or the reverse? What is the relation between the pressures at a planar interface?

(b) Show that Eq. 3C.5-1 leads to the following dimensionless boundary condition

$$\begin{aligned} \mathbf{n}^I(\check{p}^I - \check{p}^{II}) + \mathbf{n}^I \left[\frac{\rho^{II} - \rho^I}{\rho^I} \right] \left[\frac{g l_0}{v_0^2} \right] \check{h} \\ \left[\frac{\mu^I}{l_0 v_0 \rho^I} \right] [\mathbf{n}^I \cdot \check{\gamma}^I] + \left[\frac{\mu^{II}}{l_0 v_0 \rho^{II}} \right] [\mathbf{n}^I \cdot \check{\gamma}^{II}] \\ = \mathbf{n}^I \left(\frac{1}{\check{R}_1} + \frac{1}{\check{R}_2} \right) \left[\frac{\sigma}{l_0 v_0^2 \rho^I} \right] \end{aligned} \quad (3C.5-3)$$

⁷ L. Landau and E. M. Lifshitz, *Fluid Mechanics*, Pergamon, Oxford, 2nd edition (1987), Eq. 61.13. More general formulas including the excess density and viscosity have been developed by L. E. Scriven, *Chem. Eng. Sci.*, **12**, 98–108 (1960).

in which $\check{h} = (h - h_0)/l_0$ is the dimensionless elevation of dS , $\check{\gamma}^I$ and $\check{\gamma}^{II}$ are dimensionless rate-of-deformation tensors, and $\check{R}_1 = R_1/l_0$ and $\check{R}_2 = R_2/l_0$ are dimensionless radii of curvature. Furthermore

$$\begin{aligned} \check{p}^I &= \frac{p^I - p_0 + \rho^I g(h - h_0)}{\rho^I v_0^2}; \\ \check{p}^{II} &= \frac{p^{II} - p_0 + \rho^{II} g(h - h_0)}{\rho^{II} v_0^2} \end{aligned} \quad (3C.5-4, 5)$$

In the above, the zero-subscripted quantities are the scale factors, valid in both phases. Identify the dimensionless groups that appear in Eq. 3C.5-3.

(c) Show how the result in (b) simplifies to Eq. 3.7-36 under the assumptions made in Example 3.7-2.

3D.1 Derivation of the equations of change by integral theorems (Fig. 3D.1).

(a) A fluid is flowing through some region of 3-dimensional space. Select an arbitrary “blob” of this fluid—that is, a region that is bounded by some surface $S(t)$ enclosing a volume $V(t)$, whose elements move with the local fluid velocity. Apply Newton's second law of motion to this system to get

$$\frac{d}{dt} \int_{V(t)} \rho v dV = - \int_{S(t)} [\mathbf{n} \cdot \boldsymbol{\pi}] dS + \int_{V(t)} \rho g dV \quad (3D.1-1)$$

in which the terms on the right account for the surface and volume forces acting on the system. Apply the Leibniz formula for differentiating an integral (see §A.5), recognizing that at all points on the surface of the blob, the surface velocity is identical to the fluid velocity. Next apply the Gauss theorem for a tensor (see §A.5) so that each term in the equation is a volume integral. Since the choice of the “blob” is arbitrary, all the integral signs may be removed, and the equation of motion in Eq. 3.2-9 is obtained.

(b) Derive the equation of motion by writing a momentum balance over an arbitrary region of volume V and surface S , fixed in space, through which a fluid is flowing. In doing this, just parallel the derivation given in §3.2 for a

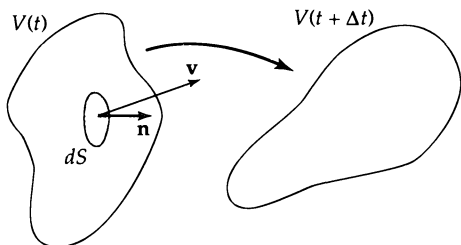


Fig. 3D.1. Moving “blob” of fluid to which Newton's second law of motion is applied. Every element of the fluid surface $dS(t)$ of the moving, deforming volume element $V(t)$ moves with the local, instantaneous fluid velocity $v(t)$.

rectangular fluid element. The Gauss theorem for a tensor is needed to complete the derivation.

This problem shows that applying Newton's second law of motion to an arbitrary moving "blob" of fluid is equivalent to setting up a momentum balance over an arbitrary fixed region of space through which the fluid is moving. Both (a) and (b) give the same result as that obtained in §3.2.

(c) Derive the equation of continuity using a volume element of arbitrary shape, both moving and fixed, by the methods outlined in (a) and (b).

3D.2 The equation of change for vorticity.

(a) By taking the curl of the Navier-Stokes equation of motion (in either the D/Dt form or the $\partial/\partial t$ form), obtain an equation for the *vorticity*, $\mathbf{w} = [\nabla \times \mathbf{v}]$ of the fluid; this equation may be written in two ways:

$$\frac{D}{Dt} \mathbf{w} = \nu \nabla^2 \mathbf{w} + [\mathbf{w} \cdot \nabla \mathbf{v}] \quad (3D.2-1)$$

$$\frac{D}{Dt} \mathbf{w} = \nu \nabla^2 \mathbf{w} + [\boldsymbol{\epsilon} : (\nabla \mathbf{v}) \cdot (\nabla \mathbf{v})] \quad (3D.2-2)$$

in which $\boldsymbol{\epsilon}$ is a third-order tensor whose components are the permutation symbol ϵ_{ijk} (see §A.2) and $\nu = \mu/\rho$ is the kinematic viscosity.

(b) How do the equations in (a) simplify for two-dimensional flows?

3D.3 Alternate form of the equation of motion.⁸ Show that, for an incompressible Newtonian fluid with constant viscosity, the equation of motion may be put into the form

$$4\nabla^2 p = \rho(\boldsymbol{\omega} : \boldsymbol{\omega}^\dagger - \dot{\boldsymbol{\gamma}} : \dot{\boldsymbol{\gamma}}) \quad (3D.3-2)$$

where

$$\dot{\boldsymbol{\gamma}} = \nabla \mathbf{v} + (\nabla \mathbf{v})^\dagger \text{ and } \boldsymbol{\omega} = \nabla \mathbf{v} - (\nabla \mathbf{v})^\dagger \quad (3D.3-2)$$

⁸ P. G. Saffman, *Vortex Dynamics*, Cambridge University Press, corrected edition (1995).

Velocity Distributions with More Than One Independent Variable

- §4.1 Time-dependent flow of Newtonian fluids
- §4.2^o Solving flow problems using a stream function
- §4.3^o Flow of inviscid fluids by use of the velocity potential
- §4.4^o Flow near solid surfaces by boundary-layer theory

In Chapter 2 we saw that viscous flow problems with straight streamlines can be solved by shell momentum balances. In Chapter 3 we introduced the equations of continuity and motion, which provide a better way to set up problems. The method was illustrated in §3.6, but there we restricted ourselves to flow problems in which only ordinary differential equations had to be solved.

In this chapter we discuss several classes of problems that involve the solutions of partial differential equations: unsteady-state flow (§4.1), viscous flow in more than one direction (§4.2), the flow of inviscid fluids (§4.3), and viscous flow in boundary layers (§4.4). Since all these topics are treated extensively in fluid dynamics treatises, we provide here only an introduction to them and illustrate some widely used methods for problem solving.

In addition to the analytical methods given in this chapter, there is also a rapidly expanding literature on numerical methods.¹ The field of computational fluid dynamics is already playing an important role in the field of transport phenomena. The numerical and analytical methods play roles complementary to one another, with the numerical methods being indispensable for complicated practical problems.

§4.1 TIME-DEPENDENT FLOW OF NEWTONIAN FLUIDS

In §3.6 only steady-state problems were solved. However, in many situations the velocity depends on both position and time, and the flow is described by partial differential equations. In this section we illustrate three techniques that are much used in fluid dynamics, heat conduction, and diffusion (as well as in many other branches of physics and engineering). In each of these techniques the problem of solving a partial differential equation is converted into a problem of solving one or more ordinary differential equations.

¹ R. W. Johnson (ed.), *The Handbook of Fluid Dynamics*, CRC Press, Boca Raton, Fla. (1998); C. Pozrikidis, *Introduction to Theoretical and Computational Fluid Dynamics*, Oxford University Press (1997).

The first example illustrates the *method of combination of variables* (or the *method of similarity solutions*). This method is useful only for semi-infinite regions, such that the initial condition and the boundary condition at infinity may be combined into a single new boundary condition.

The second example illustrates the *method of separation of variables*, in which the partial differential equation is split up into two or more ordinary differential equations. The solution is then an infinite sum of products of the solutions of the ordinary differential equations. These ordinary differential equations are usually discussed under the heading of "Sturm-Liouville" problems in intermediate-level mathematics textbooks.¹

The third example demonstrates the *method of sinusoidal response*, which is useful in describing the way a system responds to external periodic disturbances.

The illustrative examples are chosen for their physical simplicity, so that the major focus can be on the mathematical methods. Since all the problems discussed here are linear in the velocity, Laplace transforms can also be used, and readers familiar with this subject are invited to solve the three examples in this section by that technique.

EXAMPLE 4.1-1

Flow near a Wall

Suddenly Set in Motion

A semi-infinite body of liquid with constant density and viscosity is bounded below by a horizontal surface (the xz -plane). Initially the fluid and the solid are at rest. Then at time $t = 0$, the solid surface is set in motion in the positive x direction with velocity v_0 as shown in Fig. 4.4-1. Find the velocity v_x as a function of y and t . There is no pressure gradient or gravity force in the x direction, and the flow is presumed to be laminar.

SOLUTION

For this system $v_x = v_x(y, t)$, $v_y = 0$, and $v_z = 0$. Then from Table B.4 we find that the equation of continuity is satisfied directly, and from Table B.5 we get

$$\frac{\partial v_x}{\partial t} = \nu \frac{\partial^2 v_x}{\partial y^2} \quad (4.1-1)$$

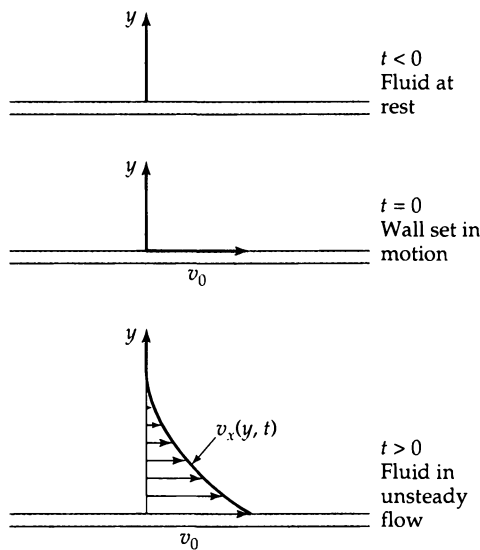


Fig. 4.1-1. Viscous flow of a fluid near a wall suddenly set in motion.

¹ See, for example, M. D. Greenberg, *Foundations of Applied Mathematics*, Prentice-Hall, Englewood Cliffs, N.J. (1978), §20.3.

in which $\nu = \mu/\rho$. The initial and boundary conditions are

$$\text{I.C.:} \quad \text{at } t \leq 0, \quad v_x = 0 \quad \text{for all } y \quad (4.1-2)$$

$$\text{B.C. 1:} \quad \text{at } y = 0, \quad v_x = v_0 \quad \text{for all } t > 0 \quad (4.1-3)$$

$$\text{B.C. 2:} \quad \text{at } y = \infty, \quad v_x = 0 \quad \text{for all } t > 0 \quad (4.1-4)$$

Next we introduce a dimensionless velocity $\phi = v_x/v_0$, so that Eq. 4.4-1 becomes

$$\frac{\partial \phi}{\partial t} = \nu \frac{\partial^2 \phi}{\partial y^2} \quad (4.1-5)$$

with $\phi(y, 0) = 0$, $\phi(0, t) = 1$, and $\phi(\infty, t) = 0$. Since the initial and boundary conditions contain only pure numbers, the solution to Eq. 4.1-5 has to be of the form $\phi = \phi(y, t; \nu)$. However, since ϕ is a dimensionless function, the quantities y , t , and ν must always appear in a dimensionless combination. The only dimensionless combinations of these three quantities are $y/\sqrt{\nu t}$ or powers or multiples thereof. We therefore conclude that

$$\phi = \phi(\eta), \quad \text{where } \eta = \frac{y}{\sqrt{4\nu t}} \quad (4.1-6)$$

This is the “method of combination of (independent) variables.” The “4” is included so that the final result in Eq. 4.1-14 will look neater; we know to do this only after solving the problem without it. The form of the solution in Eq. 4.1-6 is possible essentially because there is no characteristic length or time in the physical system.

We now convert the derivatives in Eq. 4.1-5 into derivatives with respect to the “combined variable” η as follows:

$$\frac{\partial \phi}{\partial t} = \frac{d\phi}{d\eta} \frac{\partial \eta}{\partial t} = -\frac{1}{2} \frac{\eta}{t} \frac{d\phi}{d\eta} \quad (4.1-7)$$

$$\frac{\partial \phi}{\partial y} = \frac{d\phi}{d\eta} \frac{\partial \eta}{\partial y} = \frac{d\phi}{d\eta} \frac{1}{\sqrt{4\nu t}} \quad \text{and} \quad \frac{\partial^2 \phi}{\partial y^2} = \frac{d^2\phi}{d\eta^2} \frac{1}{4\nu t} \quad (4.1-8)$$

Substitution of these expressions into Eq. 4.1-5 then gives

$$\frac{d^2\phi}{d\eta^2} + 2\eta \frac{d\phi}{d\eta} = 0 \quad (4.1-9)$$

This is an ordinary differential equation of the type given in Eq. C.1-8, and the accompanying boundary conditions are

$$\text{B.C. 1:} \quad \text{at } \eta = 0, \quad \phi = 1 \quad (4.1-10)$$

$$\text{B.C. 2:} \quad \text{at } \eta = \infty, \quad \phi = 0 \quad (4.1-11)$$

The first of these boundary conditions is the same as Eq. 4.1-3, and the second includes Eqs. 4.1-2 and 4. If now we let $d\phi/d\eta = \psi$, we get a first-order separable equation for ψ , and it may be solved to give

$$\psi = \frac{d\phi}{d\eta} = C_1 \exp(-\eta^2) \quad (4.1-12)$$

A second integration then gives

$$\phi = C_1 \int_0^\eta \exp(-\bar{\eta}^2) d\bar{\eta} + C_2 \quad (4.1-13)$$

The choice of 0 for the lower limit of the integral is arbitrary; another choice would lead to a different value of C_2 , which is still undetermined. Note that we have been careful to use an overbar for the variable of integration ($\bar{\eta}$) to distinguish it from the η in the upper limit.

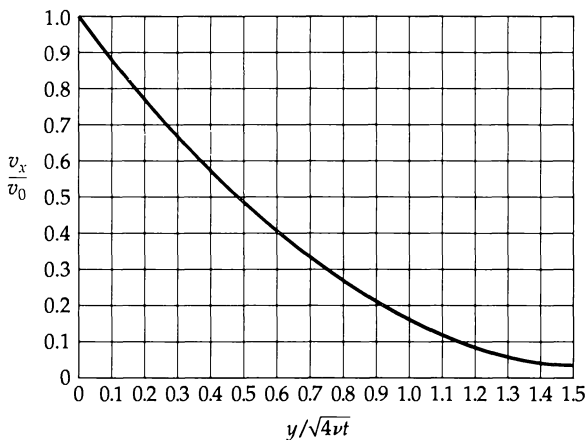


Fig. 4.1-2. Velocity distribution, in dimensionless form, for flow in the neighborhood of a wall suddenly set in motion.

Application of the two boundary conditions makes it possible to evaluate the two integration constants, and we get finally

$$\phi(\eta) = 1 - \frac{\int_0^\eta \exp(-\bar{\eta}^2) d\bar{\eta}}{\int_0^\eta \exp(-\bar{\eta}^2) d\bar{\eta}} = 1 - \frac{2}{\sqrt{\pi}} \int_0^\eta \exp(-\bar{\eta}^2) d\bar{\eta} = 1 - \text{erf } \eta \quad (4.1-14)$$

The ratio of integrals appearing here is called the *error function*, abbreviated $\text{erf } \eta$ (see §C.6). It is a well-known function, available in mathematics handbooks and computer software programs. When Eq. 4.1-14 is rewritten in the original variables, it becomes

$$\frac{v_x(y, t)}{v_0} = 1 - \text{erf} \frac{y}{\sqrt{4\nu t}} = \text{erfc} \frac{y}{\sqrt{4\nu t}} \quad (4.1-15)$$

in which $\text{erfc } \eta$ is called the *complementary error function*. A plot of Eq. 4.1-15 is given in Fig. 4.1-2. Note that, by plotting the result in terms of dimensionless quantities, only one curve is needed.

The complementary error function $\text{erfc } \eta$ is a monotone decreasing function that goes from 1 to 0 and drops to 0.01 when η is about 2.0. We can use this fact to define a “boundary-layer thickness” δ as that distance y for which v_x has dropped to a value of $0.01v_0$. This gives $\delta = 4\sqrt{\nu t}$ as a natural length scale for the diffusion of momentum. This distance is a measure of the extent to which momentum has “penetrated” into the body of the fluid. Note that this boundary-layer thickness is proportional to the square root of the elapsed time.

EXAMPLE 4.1-2

Unsteady Laminar Flow Between Two Parallel Plates

It is desired to re-solve the preceding illustrative example, but with a fixed wall at a distance b from the moving wall at $y = 0$. This flow system has a steady-state limit as $t \rightarrow \infty$, whereas the problem in Example 4.1-1 did not.

SOLUTION

As in Example 4.1-1, the equation for the x -component of the velocity is

$$\frac{\partial v_x}{\partial t} = \nu \frac{\partial^2 v_x}{\partial y^2} \quad (4.1-16)$$

The boundary conditions are now

$$\text{I.C.:} \quad \text{at } t \leq 0, \quad v_x = 0 \quad \text{for all } y \quad (4.1-17)$$

$$\text{B.C. 1:} \quad \text{at } y = 0, \quad v_x = v_0 \quad \text{for all } t > 0 \quad (4.1-18)$$

$$\text{B.C. 2:} \quad \text{at } y = b, \quad v_x = 0 \quad \text{for all } t > 0 \quad (4.1-19)$$

It is convenient to introduce the following dimensionless variables:

$$\phi = \frac{v_x}{v_0}; \quad \eta = \frac{y}{b}; \quad \tau = \frac{vt}{b^2} \quad (4.1-20)$$

The choices for dimensionless velocity and position ensure that these variables will go from 0 to 1. The choice of the dimensionless time is made so that there will be no parameters occurring in the transformed partial differential equation:

$$\frac{\partial \phi}{\partial \tau} = \frac{\partial^2 \phi}{\partial \eta^2} \quad (4.1-21)$$

The initial condition is $\phi = 0$ at $\tau = 0$, and the boundary conditions are $\phi = 1$ at $\eta = 0$ and $\phi = 0$ at $\eta = 1$.

We know that at infinite time the system attains a steady-state velocity profile $\phi_\infty(\eta)$ so that at $\tau = \infty$ Eq. 4.1-21 becomes

$$0 = \frac{d^2 \phi_\infty}{d \eta^2} \quad (4.1-22)$$

with $\phi_\infty = 1$ at $\eta = 0$, and $\phi_\infty = 0$ at $\eta = 1$. We then get

$$\phi_\infty = 1 - \eta \quad (4.1-23)$$

for the steady-state limiting profile.

We then can write

$$\phi(\eta, \tau) = \phi_\infty(\eta) - \phi_t(\eta, \tau) \quad (4.1-24)$$

where ϕ_t is the transient part of the solution, which fades out as time goes to infinity. Substitution of this expression into the original differential equation and boundary conditions then gives for ϕ_t

$$\frac{\partial \phi_t}{\partial \tau} = \frac{\partial^2 \phi_t}{\partial \eta^2} \quad (4.1-25)$$

with $\phi_t = \phi_\infty$ at $\tau = 0$, and $\phi_t = 0$ at $\eta = 0$ and 1 .

To solve Eq. 4.1-25 we use the "method of separation of (dependent) variables," in which we assume a solution of the form

$$\phi_t = f(\eta)g(\tau) \quad (4.1-26)$$

Substitution of this trial solution into Eq. 4.1-25 and then division by the product fg gives

$$\frac{1}{g} \frac{dg}{d\tau} = \frac{1}{f} \frac{d^2 f}{d\eta^2} \quad (4.1-27)$$

The left side is a function of τ alone, and the right side is a function of η alone. This means that both sides must equal a constant. We choose to designate the constant as $-c^2$ (we could equally well use c or $+c^2$, but experience tells us that these choices make the subsequent mathematics somewhat more complicated). Equation 4.1-27 can then be separated into two equations

$$\frac{dg}{d\tau} = -c^2 g \quad (4.1-28)$$

$$\frac{d^2 f}{d\eta^2} + c^2 f = 0 \quad (4.1-29)$$

These equations has the following solutions (see Eqs. C.1-1 and 3):

$$g = Ae^{-c^2 \tau} \quad (4.1-30)$$

$$f = B \sin c\eta + C \cos c\eta \quad (4.1-31)$$

in which A , B , and C are constants of integration.

We now apply the boundary and initial conditions in the following way:

B.C. 1: Because $\phi_t = 0$ at $\eta = 0$, the function f must be zero at $\eta = 0$. Hence C must be zero.

B.C. 2: Because $\phi_t = 0$ at $\eta = 1$, the function f must be zero at $\eta = 1$. This will be true if $B = 0$ or if $\sin c$ is zero. The first choice would lead to $f = 0$ for all η , and that would be physically unacceptable. Therefore we make the second choice, which leads to the requirement that $c = 0, \pm\pi, \pm 2\pi, \pm 3\pi, \dots$. We label these various admissible values of c (called "eigenvalues") as c_n and write

$$c_n = n\pi, \quad \text{with } n = 0, \pm 1, \pm 2, \pm 3, \dots \quad (4.1-32)$$

There are thus many admissible functions f_n (called "eigenfunctions") that satisfy Eq. 4.1-29 and the boundary conditions; namely,

$$f_n = B_n \sin n\pi\eta, \quad \text{with } n = 0, \pm 1, \pm 2, \pm 3, \dots \quad (4.1-33)$$

The corresponding functions satisfying Eq. 4.1-28 are called g_n and are given by

$$g_n = A_n \exp(-n^2\pi^2\tau), \quad \text{with } n = 0, \pm 1, \pm 2, \pm 3, \dots \quad (4.1-34)$$

I.C.: The combinations $f_n g_n$ satisfy the partial differential equation for ϕ_t in Eq. 4.1-25, and so will any superposition of such products. Therefore we write for the solution of Eq. 4.1-25

$$\phi_t = \sum_{n=-\infty}^{+\infty} D_n \exp(-n^2\pi^2\tau) \sin n\pi\eta \quad (4.1-35)$$

in which the expansion coefficients $D_n = A_n B_n$ have yet to be determined. In the sum, the term $n = 0$ does not contribute; also since $\sin(-n)\pi\eta = -\sin(+n)\pi\eta$, we may omit all the terms with negative values of n . Hence, Eq. 4.1-35 becomes

$$\phi_t = \sum_{n=1}^{\infty} D_n \exp(-n^2\pi^2\tau) \sin n\pi\eta \quad (4.1-36)$$

According to the initial condition, $\phi_t = 1 - \eta$ at $\tau = 0$, so that

$$1 - \eta = \sum_{n=1}^{\infty} D_n \sin n\pi\eta \quad (4.1-37)$$

We now have to determine all the D_n from this one equation! This is done by multiplying both sides of the equation by $\sin m\pi\eta$, where m is an integer, and then integrating over the physically pertinent range from $\eta = 0$ to $\eta = 1$, thus:

$$\int_0^1 (1 - \eta) \sin m\pi\eta d\eta = \sum_{n=1}^{\infty} D_n \int_0^1 \sin n\pi\eta \sin m\pi\eta d\eta \quad (4.1-38)$$

The left side gives $1/m\pi$; the integrals on the right side are zero when $n \neq m$ and $\frac{1}{2}$ when $n = m$. Hence the initial condition leads to

$$D_m = \frac{2}{m\pi} \quad (4.1-39)$$

The final expression for the dimensionless velocity profile is obtained from Eqs. 4.1-24, 36, and 39 as

$$\phi(\eta, \tau) = (1 - \eta) - \sum_{n=1}^{\infty} \left(\frac{2}{n\pi} \right) \exp(-n^2\pi^2\tau) \sin n\pi\eta \quad (4.1-40)$$

The solution thus consists of a steady-state-limit term minus a transient term, which fades out with increasing time.

Those readers who are encountering the method of separation of variables for the first time will have found the above sequence of steps rather long and complicated. However, no single step in the development is particularly difficult. The final solution in Eq. 4.1-40 looks rather involved because of the infinite sum. Actually, except for very small values of the time, only the first few terms in the series contribute appreciably.

Although we do not prove it here, the solution to this problem and that of the preceding problem are closely related.² In the limit of vanishingly small time, Eq. 4.1-40 becomes equivalent to Eq. 4.1-15. This is reasonable, since, at very small time, in this problem the fluid is in motion only very near the wall at $y = 0$, and the fluid cannot "feel" the presence of the wall at $y = b$. Since the solution and result in Example 4.1-1 are far simpler than those of this one, they are often used to represent the system if only small times are involved. This is, of course, an approximation, but a very useful one. It is often used in heat- and mass-transport problems as well.

EXAMPLE 4.1-3

Unsteady Laminar Flow near an Oscillating Plate

A semi-infinite body of liquid is bounded on one side by a plane surface (the xz -plane). Initially the fluid and solid are at rest. At time $t = 0$ the solid surface is made to oscillate sinusoidally in the x direction with amplitude X_0 and (circular) frequency ω . That is, the displacement X of the plane from its rest position is

$$X(t) = X_0 \sin \omega t \quad (4.1-41)$$

and the velocity of the fluid at $y = 0$ is then

$$v_x(0, t) = \frac{dX}{dt} = X_0 \omega \cos \omega t \quad (4.1-42)$$

We designate the amplitude of the velocity oscillation by $v_0 = X_0 \omega$ and rewrite Eq. 4.1-42 as

$$v_x(0, t) = v_0 \cos \omega t = v_0 \Re\{e^{i\omega t}\} \quad (4.1-43)$$

where $\Re\{z\}$ means "the real part of z ."

For oscillating systems we are generally not interested in the complete solution, but only the "periodic steady state" that exists after the initial "transients" have disappeared. In this state all the fluid particles in the system will be executing sinusoidal oscillations with frequency ω , but with phase and amplitude that are functions only of position. This "periodic steady state" solution may be obtained by an elementary technique that is widely used. Mathematically it is an asymptotic solution for $t \rightarrow \infty$.

SOLUTION

Once again the equation of motion is given by

$$\frac{\partial v_x}{\partial t} = \nu \frac{\partial^2 v_x}{\partial y^2} \quad (4.1-44)$$

and the initial and boundary conditions are given by

$$\text{I.C.:} \quad \text{at } t \leq 0, \quad v_x = 0 \quad \text{for all } y \quad (4.1-45)$$

$$\text{B.C. 1:} \quad \text{at } y = 0, \quad v_x = v_0 \Re\{e^{i\omega t}\} \quad \text{for all } t > 0 \quad (4.1-46)$$

$$\text{B.C. 2:} \quad \text{at } y = \infty, \quad v_x = 0 \quad \text{for all } t > 0 \quad (4.1-47)$$

The initial condition will not be needed, since we are concerned only with the fluid response after the plate has been oscillating for a long time.

We postulate an oscillatory solution of the form

$$v_x(y, t) = \Re\{v^\circ(y)e^{i\omega t}\} \quad (4.1-48)$$

² See H. S. Carslaw and J. C. Jaeger, *Conduction of Heat in Solids*, Oxford University Press, 2nd edition (1959), pp. 308–310, for a series solution that is particularly good for short times.

Here v^o is chosen to be a *complex* function of y , so that $v_x(y, t)$ will differ from $v_x(0, t)$ both in amplitude and phase. We substitute this trial solution into Eq. 4.1-44 and obtain

$$\Re\{v^o i \omega e^{i \omega t}\} = \nu \Re\left\{\frac{d^2 v^o}{dy^2} e^{i \omega t}\right\} \quad (4.1-49)$$

Next we make use of the fact that, if $\Re\{z_1 w\} = \Re\{z_2 w\}$, where z_1 and z_2 are two complex quantities and w is an arbitrary complex quantity, then $z_1 = z_2$. Then Eq. 4.1-49 becomes

$$\frac{d^2 v^o}{dy^2} - \left(\frac{i \omega}{\nu}\right) v^o = 0 \quad (4.1-50)$$

with the following boundary conditions:

$$\text{B.C. 1:} \quad \text{at } y = 0, \quad v^o = v_0 \quad (4.1-51)$$

$$\text{B.C. 2:} \quad \text{at } y = \infty, \quad v^o = 0 \quad (4.1-52)$$

Equation 4.1-50 is of the form of Eq. C.1-4 and has the solution

$$v^o = C_1 e^{\sqrt{i \omega / \nu} y} + C_2 e^{-\sqrt{i \omega / \nu} y} \quad (4.1-53)$$

Since $\sqrt{i} = \pm(1/\sqrt{2})(1+i)$, this equation can be rewritten as

$$v^o = C_1 e^{\sqrt{\omega/2\nu}(1+i)y} + C_2 e^{-\sqrt{\omega/2\nu}(1+i)y} \quad (4.1-54)$$

The second boundary condition requires that $C_1 = 0$, and the first boundary condition gives $C_2 = v_0$. Therefore the solution to Eq. 4.1-50 is

$$v^o = v_0 e^{-\sqrt{\omega/2\nu}(1+i)y} \quad (4.1-55)$$

From this result and Eq. 4.1-48, we get

$$\begin{aligned} v_x(y, t) &= \Re\{v_0 e^{-\sqrt{\omega/2\nu}(1+i)y} e^{i \omega t}\} \\ &= v_0 e^{-\sqrt{\omega/2\nu}y} \Re\{e^{-i(\sqrt{\omega/2\nu}y - \omega t)}\} \end{aligned} \quad (4.1-56)$$

or finally

$$v_x(y, t) = v_0 e^{-\sqrt{\omega/2\nu}y} \cos(\omega t - \sqrt{\omega/2\nu}y) \quad (4.1-57)$$

In this expression, the exponential describes the *attenuation* of the oscillatory motion—that is, the decrease in the amplitude of the fluid oscillations with increasing distance from the plate. In the argument of the cosine, the quantity $-\sqrt{\omega/2\nu}y$ is called the *phase shift*; that is, it describes how much the fluid oscillations at a distance y from the wall are “out-of-step” with the oscillations of the wall itself.

Keep in mind that Eq. 4.1-57 is not the complete solution to the problem as stated in Eqs. 4.1-44 to 47, but only the “periodic-steady-state” solution. The complete solution is given in Problem 4D.1.

§4.2 SOLVING FLOW PROBLEMS USING A STREAM FUNCTION

Up to this point the examples and problems have been chosen so that there was only one nonvanishing component of the fluid velocity. Solutions of the complete Navier-Stokes equation for flow in two or three dimensions are more difficult to obtain. The basic procedure is, of course, similar: one solves simultaneously the equations of continuity and motion, along with the appropriate initial and boundary conditions, to obtain the pressure and velocity profiles.

However, having both velocity and pressure as dependent variables in the equation of motion presents more difficulty in multidimensional flow problems than in the simpler ones discussed previously. It is therefore frequently convenient to eliminate the

pressure by taking the curl of the equation of motion, after making use of the vector identity $[\mathbf{v} \cdot \nabla \mathbf{v}] = \frac{1}{2}\nabla(\mathbf{v} \cdot \mathbf{v}) - [\mathbf{v} \times [\nabla \times \mathbf{v}]]$, which is given in Eq. A.4-23. For fluids of constant viscosity and density, this operation gives

$$\frac{\partial}{\partial t} [\nabla \times \mathbf{v}] - [\nabla \times [\mathbf{v} \times [\nabla \times \mathbf{v}]]] = \nu \nabla^2 [\nabla \times \mathbf{v}] \quad (4.2-1)$$

This is the *equation of change for the vorticity* $[\nabla \times \mathbf{v}]$; two other ways of writing it are given in Problem 3D.2.

For viscous flow problems one can then solve the vorticity equation (a third-order vector equation) together with the equation of continuity and the relevant initial and boundary conditions to get the velocity distribution. Once that is known, the pressure distribution can be obtained from the Navier–Stokes equation in Eq. 3.5-6. This method of solving flow problems is sometimes convenient even for the one-dimensional flows previously discussed (see, for example, Problem 4B.4).

For planar or axisymmetric flows the vorticity equation can be reformulated by introducing the *stream function* ψ . To do this, we express the two nonvanishing components of the velocity as derivatives of ψ in such a way that the equation of continuity is automatically satisfied (see Table 4.2-1). The component of the vorticity equation corresponding to the direction in which there is no flow then becomes a fourth-order scalar equation for ψ . The two nonvanishing velocity components can then be obtained after the equation for the scalar ψ has been found. The most important problems that can be treated in this way are given in Table 4.1-1.¹

The stream function itself is not without interest. Surfaces of constant ψ contain the *streamlines*,² which in steady-state flow are the paths of fluid elements. The volumetric rate of flow between the surfaces $\psi = \psi_1$ and $\psi = \psi_2$ is proportional to $\psi_2 - \psi_1$.

In this section we consider, as an example, the steady, creeping flow past a stationary sphere, which is described by the Stokes equation of Eq. 3.5-8, valid for $Re \ll 1$ (see the discussion right after Eq. 3.7-9). For creeping flow the second term on the left side of Eq. 4.2-1 is set equal to zero. The equation is then linear, and therefore there are many methods available for solving the problem.³ We use the stream function method based on Eq. 4.2-1.

EXAMPLE 4.2-1

Creeping Flow around a Sphere

Use Table 4.2-1 to set up the differential equation for the stream function for the flow of a Newtonian fluid around a stationary sphere of radius R at $Re \ll 1$. Obtain the velocity and pressure distributions when the fluid approaches the sphere in the positive z direction, as in Fig. 2.6-1.

¹ For a technique applicable to more general flows, see J. M. Robertson, *Hydrodynamics in Theory and Application*, Prentice-Hall, Englewood Cliffs, N.J. (1965), p. 77; for examples of three-dimensional flows using two stream functions, see Problem 4D.5 and also J. P. Sørensen and W. E. Stewart, *Chem. Eng. Sci.*, **29**, 819–825 (1974). A. Lahabbi and H.-C. Chang, *Chem. Eng. Sci.*, **40**, 434–447 (1985) dealt with high-Re flow through cubic arrays of spheres, including steady-state solutions and transition to turbulence. W. E. Stewart and M. A. McClelland, *AICHE Journal*, **29**, 947–956 (1983) gave matched asymptotic solutions for forced convection in three-dimensional flows with viscous heating.

² See, for example, G. K. Batchelor, *An Introduction to Fluid Dynamics*, Cambridge University Press (1967), §2.2. Chapter 2 of this book is an extensive discussion of the kinematics of fluid motion.

³ The solution given here follows that given by L. M. Milne-Thomson, *Theoretical Hydrodynamics*, Macmillan, New York, 3rd edition (1955), pp. 555–557. For other approaches, see H. Lamb, *Hydrodynamics*, Dover, New York (1945), §§337, 338. For a discussion of unsteady flow around a sphere, see R. Berker, in *Handbuch der Physik*, Volume VIII-2, Springer, Berlin (1963), §69; or H. Villat and J. Kravtchenko, *Leçons sur les Fluides Visqueux*, Gauthier-Villars, Paris (1943), Chapter VII. The problem of finding the forces and torques on objects of arbitrary shapes is discussed thoroughly by S. Kim and S. J. Karrila, *Microhydrodynamics: Principles and Selected Applications*, Butterworth-Heinemann, Boston (1991), Chapter II.

Table 4.2-1 Equations for the Stream Function^a

Type of motion	Coordinate system	Velocity components	Differential equations for ψ which are equivalent to the Navier–Stokes equation ^b	Expressions for operators
Two-dimensional (planar)	Rectangular with $v_z = 0$ and no z -dependence	$v_x = -\frac{\partial \psi}{\partial y}$ $v_y = +\frac{\partial \psi}{\partial x}$	$\frac{\partial}{\partial t}(\nabla^2 \psi) + \frac{\partial(\psi, \nabla^2 \psi)}{\partial(x, y)} = \nu \nabla^4 \psi$ (A)	$\nabla^2 \equiv \frac{\partial^2}{\partial x^2} + \frac{\partial^2}{\partial y^2}$ $\nabla^4 \psi \equiv \nabla^2(\nabla^2 \psi)$ $= \left(\frac{\partial^4}{\partial x^4} + 2 \frac{\partial^4}{\partial x^2 \partial y^2} + \frac{\partial^4}{\partial y^4} \right) \psi$
	Cylindrical with $v_z = 0$ with no z -dependence	$v_r = -\frac{1}{r} \frac{\partial \psi}{\partial \theta}$ $v_\theta = +\frac{\partial \psi}{\partial r}$	$\frac{\partial}{\partial t}(\nabla^2 \psi) + \frac{1}{r} \frac{\partial(\psi, \nabla^2 \psi)}{\partial(r, \theta)} = \nu \nabla^4 \psi$ (B)	$\nabla^2 \equiv \frac{\partial^2}{\partial r^2} + \frac{1}{r} \frac{\partial}{\partial r} + \frac{1}{r^2} \frac{\partial^2}{\partial \theta^2}$
Axisymmetrical	Cylindrical with $v_\theta = 0$ and no θ -dependence	$v_z = -\frac{1}{r} \frac{\partial \psi}{\partial r}$ $v_r = +\frac{1}{r} \frac{\partial \psi}{\partial z}$	$\frac{\partial}{\partial t}(E^2 \psi) - \frac{1}{r} \frac{\partial(\psi, E^2 \psi)}{\partial(r, z)} - \frac{2}{r^2} \frac{\partial \psi}{\partial z} E^2 \psi = \nu E^4 \psi$ (C)	$E^2 \equiv \frac{\partial^2}{\partial r^2} - \frac{1}{r} \frac{\partial}{\partial r} + \frac{\partial^2}{\partial z^2}$ $E^4 \psi \equiv E^2(E^2 \psi)$
	Spherical with $v_\phi = 0$ and no ϕ -dependence	$v_r = -\frac{1}{r^2 \sin \theta} \frac{\partial \psi}{\partial \theta}$ $v_\theta = +\frac{1}{r \sin \theta} \frac{\partial \psi}{\partial r}$	$\frac{\partial}{\partial t}(E^2 \psi) + \frac{1}{r^2 \sin \theta} \frac{\partial(\psi, E^2 \psi)}{\partial(r, \theta)}$ $- \frac{2E^2 \psi}{r^2 \sin^2 \theta} \left(\frac{\partial \psi}{\partial r} \cos \theta - \frac{1}{r} \frac{\partial \psi}{\partial \theta} \sin \theta \right) = \nu E^4 \psi$ (D)	$E^2 \equiv \frac{\partial^2}{\partial r^2} + \frac{\sin \theta}{r^2} \frac{\partial}{\partial \theta} \left(\frac{1}{\sin \theta} \frac{\partial}{\partial \theta} \right)$

^a Similar relations in general orthogonal coordinates may be found in S. Goldstein, *Modern Developments in Fluid Dynamics*, Dover, N.Y., (1965), pp. 114–115; in this reference, formulas are also given for axisymmetrical flows with a nonzero component of the velocity around the axis.

^b Here the Jacobians are designated by

$$\frac{\partial(f, g)}{\partial(x, y)} = \begin{vmatrix} \frac{\partial f}{\partial x} & \frac{\partial f}{\partial y} \\ \frac{\partial g}{\partial x} & \frac{\partial g}{\partial y} \end{vmatrix}$$

SOLUTION

For steady, creeping flow, the entire left side of Eq. D of Table 4.2-1 may be set equal to zero, and the ψ equation for axisymmetric flow becomes

$$E^4\psi = 0 \quad (4.2-2)$$

or, in spherical coordinates

$$\left[\frac{\partial^2}{\partial r^2} + \frac{\sin \theta}{r^2} \frac{\partial}{\partial \theta} \left(\frac{1}{\sin \theta} \frac{\partial \psi}{\partial \theta} \right) \right]^2 \psi = 0 \quad (4.2-3)$$

This is to be solved with the following boundary conditions:

$$\text{B.C. 1:} \quad \text{at } r = R, \quad v_r = -\frac{1}{r^2 \sin \theta} \frac{\partial \psi}{\partial \theta} = 0 \quad (4.2-4)$$

$$\text{B.C. 2:} \quad \text{at } r = R, \quad v_\theta = +\frac{1}{r \sin \theta} \frac{\partial \psi}{\partial r} = 0 \quad (4.2-5)$$

$$\text{B.C. 3:} \quad \text{as } r \rightarrow \infty, \quad \psi \rightarrow -\frac{1}{2}v_\infty r^2 \sin^2 \theta \quad (4.2-6)$$

The first two boundary conditions describe the no-slip condition at the sphere surface. The third implies that $v_z \rightarrow v_\infty$ far from the sphere (this can be seen by recognizing that $v_r = v_\infty \cos \theta$ and $v_\theta = -v_\infty \sin \theta$ far from the sphere).

We now postulate a solution of the form

$$\psi(r, \theta) = f(r) \sin^2 \theta \quad (4.2-7)$$

since it will at least satisfy the third boundary condition in Eq. 4.2-6. When it is substituted into Eq. 4.2-4, we get

$$\left(\frac{d^2}{dr^2} - \frac{2}{r^2} \right) \left(\frac{d^2}{dr^2} - \frac{2}{r^2} \right) f = 0 \quad (4.2-8)$$

The fact that the variable θ does not appear in this equation suggests that the postulate in Eq. 4.2-7 is satisfactory. Equation 4.2-8 is an "equidimensional" fourth-order equation (see Eq. C.1-14). When a trial solution of the form $f(r) = Cr^n$ is substituted into this equation, we find that n may have the values $-1, 1, 2$, and 4 . Therefore $f(r)$ has the form

$$f(r) = C_1 r^{-1} + C_2 r + C_3 r^2 + C_4 r^4 \quad (4.2-9)$$

To satisfy the third boundary condition, C_4 must be zero, and C_3 has to be $-\frac{1}{2}v_\infty$. Hence the stream function is

$$\psi(r, \theta) = (C_1 r^{-1} + C_2 r - \frac{1}{2}v_\infty r^2) \sin^2 \theta \quad (4.2-10)$$

The velocity components are then obtained by using Table 4.2-1 as follows:

$$v_r = -\frac{1}{r^2 \sin \theta} \frac{\partial \psi}{\partial \theta} = \left(v_\infty - 2 \frac{C_2}{r} - 2 \frac{C_1}{r^3} \right) \cos \theta \quad (4.2-11)$$

$$v_\theta = +\frac{1}{r \sin \theta} \frac{\partial \psi}{\partial r} = \left(-v_\infty + \frac{C_2}{r} - \frac{C_1}{r^3} \right) \sin \theta \quad (4.2-12)$$

The first two boundary conditions now give $C_1 = -\frac{1}{4}v_\infty R^2$ and $C_2 = \frac{3}{4}v_\infty R$, so that

$$v_r = v_\infty \left(1 - \frac{3}{2} \left(\frac{R}{r} \right) + \frac{1}{2} \left(\frac{R}{r} \right)^3 \right) \cos \theta \quad (4.2-13)$$

$$v_\theta = -v_\infty \left(1 - \frac{3}{4} \left(\frac{R}{r} \right) - \frac{1}{4} \left(\frac{R}{r} \right)^3 \right) \sin \theta \quad (4.2-14)$$

These are the velocity components given in Eqs. 2.6-1 and 2 without proof.

To get the pressure distribution, we substitute these velocity components into the r - and θ -components of the Navier–Stokes equation (given in Table B.7). After some tedious manipulations we get

$$\frac{\partial \mathcal{P}}{\partial r} = 3\left(\frac{\mu v_\infty}{R^2}\right)\left(\frac{R}{r}\right)^3 \cos \theta \quad (4.2-15)$$

$$\frac{\partial \mathcal{P}}{\partial \theta} = \frac{3}{2}\left(\frac{\mu v_\infty}{R}\right)\left(\frac{R}{r}\right)^2 \sin \theta \quad (4.2-16)$$

These equations may be integrated (cf. Eqs. 3.6-38 to 41), and, when use is made of the boundary condition that as $r \rightarrow \infty$ the modified pressure \mathcal{P} tends to p_0 (the pressure in the plane $z = 0$ far from the sphere), we get

$$p = p_0 - \rho g z - \frac{3}{2}\left(\frac{\mu v_\infty}{R}\right)\left(\frac{R}{r}\right)^2 \cos \theta \quad (4.2-17)$$

This is the same as the pressure distribution given in Eq. 2.6-4.

In §2.6 we showed how one can integrate the pressure and velocity distributions over the sphere surface to get the drag force. That method for getting the force of the fluid on the solid is general. Here we evaluate the “kinetic force” F_k by equating the rate of doing work on the sphere (force \times velocity) to the rate of viscous dissipation within the fluid, thus

$$F_k v_\infty = - \int_0^{2\pi} \int_0^\pi \int_R^\infty (\boldsymbol{\tau} : \nabla \mathbf{v}) r^2 dr \sin \theta d\theta d\phi \quad (4.2-18)$$

Insertion of the function $(-\boldsymbol{\tau} : \nabla \mathbf{v})$ in spherical coordinates from Table B.7 gives

$$\begin{aligned} F_k v_\infty &= \int_0^{2\pi} \int_0^\pi \int_R^\infty \left[2\left(\frac{\partial v_r}{\partial r}\right)^2 + 2\left(\frac{1}{r} \frac{\partial v_\theta}{\partial \theta} + \frac{v_r}{r}\right)^2 + 2\left(\frac{v_r}{r} + \frac{v_\theta \cot \theta}{r}\right)^2 \right. \\ &\quad \left. + \left(r \frac{\partial}{\partial r} \left(\frac{v_\theta}{r}\right) + \frac{1}{r} \frac{\partial v_r}{\partial \theta}\right)^2 \right] r^2 dr \sin \theta d\theta d\phi \end{aligned} \quad (4.2-19)$$

Then the velocity profiles from Eqs. 4.2-13 and 14 are substituted into Eq. 4.2-19. When the indicated differentiations and integrations (lengthy!) are performed, one finally gets

$$F_k = 6\pi\mu v_\infty R \quad (4.2-20)$$

which is *Stokes' law*.

As pointed out in §2.6, Stokes' law is restricted to $Re < 0.1$. The expression for the drag force can be improved by going back and including the $[\mathbf{v} \cdot \nabla \mathbf{v}]$ term. Then use of the *method of matched asymptotic expansions* leads to the following result⁴

$$F_k = 6\pi\mu v_\infty R [1 + \frac{3}{16} Re + \frac{9}{160} Re^2 (\ln \frac{1}{2} Re + \gamma + \frac{5}{3} \ln 2 - \frac{323}{360}) + \frac{27}{640} Re^3 \ln \frac{1}{2} Re + O(Re^3)] \quad (4.2-21)$$

where $\gamma = 0.5772$ is Euler's constant. This expression is good up to Re of about 1.

⁴ I. Proudman and J. R. A. Pearson, *J. Fluid Mech.* **2**, 237–262 (1957); W. Chester and D. R. Breach, *J. Fluid. Mech.* **37**, 751–760 (1969).

§4.3 FLOW OF INVISCID FLUIDS BY USE OF THE VELOCITY POTENTIAL¹

Of course, we know that inviscid fluids (i.e., fluids devoid of viscosity) do not actually exist. However, the Euler equation of motion of Eq. 3.5-9 has been found to be useful for describing the flows of low-viscosity fluids at $\text{Re} >> 1$ around streamlined objects and gives a reasonably good description of the velocity profile, except very near the object and beyond the line of separation.

Then the vorticity equation in Eq. 3D.2-1 may be simplified by omitting the term containing the kinematic viscosity. If, in addition, the flow is steady and two-dimensional, then the terms $\partial/\partial t$ and $[\mathbf{w} \cdot \nabla \mathbf{v}]$ vanish. This means that the vorticity $\mathbf{w} = [\nabla \times \mathbf{v}]$ is constant along a streamline. If the fluid approaching a submerged object has no vorticity far away from the object, then the flow will be such that $\mathbf{w} = [\nabla \times \mathbf{v}]$ will be zero throughout the entire flow field. That is, the flow will be *irrotational*.

To summarize, if we assume that $\rho = \text{constant}$ and $[\nabla \times \mathbf{v}] = 0$, then we can expect to get a reasonably good description of the flow of low-viscosity fluids around submerged objects in two-dimensional flows. This type of flow is referred to as *potential flow*.

Of course we know that this flow description will be inadequate in the neighborhood of solid surfaces. Near these surfaces we make use of a different set of assumptions, and these lead to *boundary-layer theory*, which is discussed in §4.4. By solving the potential flow equations for the “far field” and the boundary-layer equations for the “near field” and then matching the solutions asymptotically for large Re , it is possible to develop an understanding of the entire flow field around a streamlined object.²

To describe potential flow we start with the equation of continuity for an incompressible fluid and the Euler equation for an inviscid fluid (Eq. 3.5-9):

$$\text{(continuity)} \quad (\nabla \cdot \mathbf{v}) = 0 \quad (4.3-1)$$

$$\text{(motion)} \quad \rho \left(\frac{\partial \mathbf{v}}{\partial t} + \nabla_2^1 v^2 - [\mathbf{v} \times [\nabla \times \mathbf{v}]] \right) = -\nabla \mathcal{P} \quad (4.3-2)$$

In the equation of motion we have made use of the vector identity $[\mathbf{v} \cdot \nabla \mathbf{v}] = \nabla_2^1 v^2 - [\mathbf{v} \times [\nabla \times \mathbf{v}]]$ (see Eq. A.4-23).

For the two-dimensional, irrotational flow the statement that $[\nabla \times \mathbf{v}] = 0$ is

$$\text{(irrotational)} \quad \frac{\partial v_x}{\partial y} - \frac{\partial v_y}{\partial x} = 0 \quad (4.3-3)$$

and the equation of continuity is

$$\text{(continuity)} \quad \frac{\partial v_x}{\partial x} + \frac{\partial v_y}{\partial y} = 0 \quad (4.3-4)$$

The equation of motion for steady, irrotational flow can be integrated to give

$$\text{(motion)} \quad \frac{1}{2}\rho(v_x^2 + v_y^2) + \mathcal{P} = \text{constant} \quad (4.3-5)$$

That is, the sum of the pressure and the kinetic and potential energy per unit volume is constant throughout the entire flow field. This is the *Bernoulli equation* for incompressible, potential flow, and the constant is the same for all streamlines. (This has to be contrasted with Eq. 3.5-12, the Bernoulli equation for a compressible fluid in any kind of flow; there the sum of the three contributions is a different constant on each streamline.)

¹ R. H. Kirchhoff, Chapter 7 in *Handbook of Fluid Dynamics* (R. W. Johnson, ed.), CRC Press, Boca Raton, Fla. (1998).

² M. Van Dyke, *Perturbation Methods in Fluid Dynamics*, The Parabolic Press, Stanford, Cal. (1975).

We want to solve Eqs. 4.3-3 to 5 to obtain v_x , v_y , and \mathcal{P} as functions of x and y . We have already seen in the previous section that the equation of continuity in two-dimensional flows can be satisfied by writing the components of the velocity in terms of a *stream function* $\psi(x, y)$. However, any vector that has a zero curl can also be written as the gradient of a scalar function (that is, $[\nabla \times \mathbf{v}] = 0$ implies that $\mathbf{v} = -\nabla\phi$). It is very convenient, then, to introduce a *velocity potential* $\phi(x, y)$. Instead of working with the velocity components v_x and v_y , we choose to work with $\psi(x, y)$ and $\phi(x, y)$. We then have the following relations:

$$\text{(stream function)} \quad v_x = -\frac{\partial\psi}{\partial y} \quad v_y = \frac{\partial\psi}{\partial x} \quad (4.3-6, 7)$$

$$\text{(velocity potential)} \quad v_x = -\frac{\partial\phi}{\partial x} \quad v_y = -\frac{\partial\phi}{\partial y} \quad (4.3-8, 9)$$

Now Eqs. 4.3-3 and 4.3-4 will automatically be satisfied. By equating the expressions for the velocity components we get

$$\frac{\partial\phi}{\partial x} = \frac{\partial\psi}{\partial y} \quad \text{and} \quad \frac{\partial\phi}{\partial y} = -\frac{\partial\psi}{\partial x} \quad (4.3-10, 11)$$

These are the *Cauchy-Riemann equations*, which are the relations that must be satisfied by the real and imaginary parts of any analytic function³ $w(z) = \phi(x, y) + i\psi(x, y)$, where $z = x + iy$. The quantity $w(z)$ is called the *complex potential*. Differentiation of Eq. 4.3-10 with respect to x and Eq. 4.3-11 with respect to y and then adding gives $\nabla^2\phi = 0$. Differentiating with respect to the variables in reverse order and then subtracting gives $\nabla^2\psi = 0$. That is, both $\phi(x, y)$ and $\psi(x, y)$ satisfy the two-dimensional Laplace equation.⁴

As a consequence of the preceding development, it appears that *any* analytic function $w(z)$ yields a pair of functions $\phi(x, y)$ and $\psi(x, y)$ that are the velocity potential and stream function for *some* flow problem. Furthermore, the curves $\phi(x, y) = \text{constant}$ and $\psi(x, y) = \text{constant}$ are then the *equipotential lines* and *streamlines* for the problem. The velocity components are then obtained from Eqs. 4.3-6 and 7 or Eqs. 4.3-8 and 9 or from

$$\frac{dw}{dz} = -v_x + iv_y \quad (4.3-12)$$

in which dw/dz is called the *complex velocity*. Once the velocity components are known, the modified pressure can then be found from Eq. 4.3-5.

Alternatively, the equipotential lines and streamlines can be obtained from the *inverse function* $z(w) = x(\phi, \psi) + iy(\phi, \psi)$, in which $z(w)$ is *any* analytic function of w . Between the functions $x(\phi, \psi)$ and $y(\phi, \psi)$ we can eliminate ψ and get

$$F(x, y, \phi) = 0 \quad (4.3-13)$$

³ Some knowledge of the analytic functions of a complex variable is assumed here. Helpful introductions to the subject can be found in V. L. Streeter, E. B. Wylie, and K. W. Bedford, *Fluid Mechanics*, McGraw-Hill, New York, 9th ed. (1998), Chapter 8, and in M. D. Greenberg, *Foundations of Applied Mathematics*, Prentice-Hall, Englewood Cliffs, N.J. (1978), Chapters 11 and 12.

⁴ Even for three-dimensional flows the assumption of irrotational flow still permits the definition of a velocity potential. When $\mathbf{v} = -\nabla\phi$ is substituted into $(\nabla \cdot \mathbf{v}) = 0$, we get the three-dimensional Laplace equation $\nabla^2\phi = 0$. The solution of this equation is the subject of "potential theory," for which there is an enormous literature. See, for example, P. M. Morse and H. Feshbach, *Methods of Theoretical Physics*, McGraw-Hill, New York (1953), Chapter 11; and J. M. Robertson, *Hydrodynamics in Theory and Application*, Prentice-Hall, Englewood Cliffs, N.J. (1965), which emphasizes the engineering applications. There are many problems in flow through porous media, heat conduction, diffusion, and electrical conduction that are described by Laplace's equation.

Similar elimination of ϕ gives

$$G(x, y, \psi) = 0 \quad (4.3-14)$$

Setting $\phi = \text{constant}$ in Eq. 4.3-13 gives the equations for the equipotential lines for *some* flow problem, and setting $\psi = \text{constant}$ in Eq. 4.3-14 gives equations for the streamlines. The velocity components can be obtained from

$$-\frac{dz}{dw} = \frac{v_x + iv_y}{v_x^2 + v_y^2} \quad (4.3-15)$$

Thus from any analytic function $w(z)$, or its inverse $z(w)$, we can construct a flow net with streamlines $\psi = \text{constant}$ and equipotential lines $\phi = \text{constant}$. The task of finding $w(z)$ or $z(w)$ to satisfy a given flow problem is, however, considerably more difficult. Some special methods are available^{4,5} but it is frequently more expedient to consult a table of conformal mappings.⁶

In the next two illustrative examples we show how to use the complex potential $w(z)$ to describe the potential flow around a cylinder, and the inverse function $z(w)$ to solve the problem of the potential flow into a channel. In the third example we solve the flow in the neighborhood of a corner, which is treated further in §4.4 by the boundary-layer method. A few general comments should be kept in mind:

- (a) The streamlines are everywhere perpendicular to the equipotential lines. This property, evident from Eqs. 4.3-10, 11, is useful for the approximate construction of flow nets.
- (b) Streamlines and equipotential lines can be interchanged to get the solution of another flow problem. This follows from (a) and the fact that both ϕ and ψ are solutions to the two-dimensional Laplace equation.
- (c) Any streamline may be replaced by a solid surface. This follows from the boundary condition that the normal component of the velocity of the fluid is zero at a solid surface. The tangential component is not restricted, since in potential flow the fluid is presumed to be able to slide freely along the surface (the complete-slip assumption).

EXAMPLE 4.3-1

- (a) Show that the complex potential

Potential Flow around a Cylinder

$$w(z) = -v_\infty R \left(\frac{z}{R} + \frac{R}{z} \right) \quad (4.3-16)$$

describes the potential flow around a circular cylinder of radius R , when the approach velocity is v_∞ in the positive x direction.

- (b) Find the components of the velocity vector.
- (c) Find the pressure distribution on the cylinder surface, when the modified pressure far from the cylinder is \mathcal{P}_∞ .

SOLUTION

- (a) To find the stream function and velocity potential, we write the complex potential in the form $w(z) = \phi(x, y) + i\psi(x, y)$:

$$w(z) = -v_\infty x \left(1 + \frac{R^2}{x^2 + y^2} \right) - iv_\infty y \left(1 - \frac{R^2}{x^2 + y^2} \right) \quad (4.3-17)$$

⁵ J. Fuka, Chapter 21 in K. Rektorys, *Survey of Applicable Mathematics*, MIT Press, Cambridge, Mass. (1969).

⁶ H. Kober, *Dictionary of Conformal Representations*, Dover, New York, 2nd edition (1957).

Hence the stream function is

$$\psi(x, y) = -v_\infty y \left(1 - \frac{R^2}{x^2 + y^2} \right) \quad (4.3-18)$$

To make a plot of the streamlines it is convenient to rewrite Eq. 4.3-18 in dimensionless form

$$\Psi(X, Y) = -Y \left(1 - \frac{1}{X^2 + Y^2} \right) \quad (4.3-19)$$

in which $\Psi = \psi/v_\infty R$, $X = x/R$, and $Y = y/R$.

In Fig. 4.3-1 the streamlines are plotted as the curves $\Psi = \text{constant}$. The streamline $\Psi = 0$ gives a unit circle, which represents the surface of the cylinder. The streamline $\Psi = -\frac{3}{2}$ goes through the point $X = 0, Y = 2$, and so on.

(b) The velocity components are obtainable from the stream function by using Eqs. 4.3-6 and 7. They may also be obtained from the complex velocity according to Eq. 4.3-12, as follows:

$$\begin{aligned} \frac{dw}{dz} &= -v_\infty \left(1 - \frac{R^2}{z^2} \right) = -v_\infty \left(1 - \frac{R^2}{r^2} e^{-2i\theta} \right) \\ &= -v_\infty \left(1 - \frac{R^2}{r^2} (\cos 2\theta - i \sin 2\theta) \right) \end{aligned} \quad (4.3-20)$$

Therefore the velocity components as function of position are

$$v_x = v_\infty \left(1 - \frac{R^2}{r^2} \cos 2\theta \right) \quad (4.3-21)$$

$$v_y = -v_\infty \left(\frac{R^2}{r^2} \sin 2\theta \right) \quad (4.3-22)$$

(c) On the surface of the cylinder, $r = R$, and

$$\begin{aligned} v^2 &= v_x^2 + v_y^2 \\ &= v_\infty^2 [(1 - \cos 2\theta)^2 + (\sin 2\theta)^2] \\ &= 4v_\infty^2 \sin^2 \theta \end{aligned} \quad (4.3-23)$$

When θ is zero or π , the fluid velocity is zero; such points are known as *stagnation points*. From Eq. 4.3-5 we know that

$$\frac{1}{2}\rho v^2 + \mathcal{P} = \frac{1}{2}\rho v_\infty^2 + \mathcal{P}_\infty \quad (4.3-24)$$

Then from the last two equations we get the pressure distribution on the surface of the cylinder

$$(\mathcal{P} - \mathcal{P}_\infty) = \frac{1}{2}\rho v_\infty^2 (1 - 4 \sin^2 \theta) \quad (4.3-25)$$

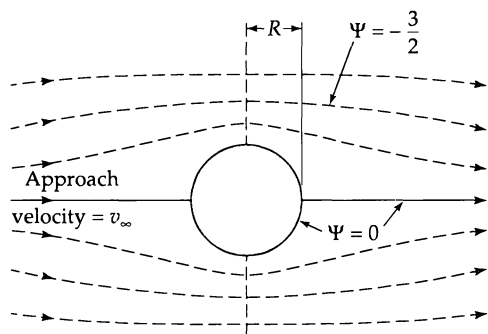


Fig. 4.3-1. The streamlines for the potential flow around a cylinder according to Eq. 4.3-19.

Note that the modified pressure distribution is symmetric about the x -axis; that is, for potential flow there is no form drag on the cylinder (*d'Alembert's paradox*).⁷ Of course, we know now that this is not really a paradox, but simply the result of the fact that the inviscid fluid does not permit applying the no-slip boundary condition at the interface.

EXAMPLE 4.3-2

Show that the inverse function

**Flow Into a
Rectangular Channel**

$$z(w) = \frac{w}{v_\infty} + \frac{b}{\pi} \exp(\pi w/bv_\infty) \quad (4.3-26)$$

represents the potential flow into a rectangular channel of half-width b . Here v_∞ is the magnitude of the velocity far downstream from the entrance to the channel.

SOLUTION

First we introduce dimensionless distance variables

$$X = \frac{\pi x}{b} \quad Y = \frac{\pi y}{b} \quad Z = X + iY = \frac{\pi z}{b} \quad (4.3-27)$$

and the dimensionless quantities

$$\Phi = \frac{\pi \phi}{bv_\infty} \quad \Psi = \frac{\pi \psi}{bv_\infty} \quad W = \Phi + i\Psi = \frac{\pi w}{bv_\infty} \quad (4.3-28)$$

The inverse function of Eq. 4.3-26 may now be expressed in terms of dimensionless quantities and split up into real and imaginary parts

$$Z = W + e^W = (\Phi + e^\Phi \cos \Psi) + i(\Psi + e^\Phi \sin \Psi) \quad (4.3-29)$$

Therefore

$$X = \Phi + e^\Phi \cos \Psi \quad Y = \Psi + e^\Phi \sin \Psi \quad (4.3-30, 31)$$

We can now set Ψ equal to a constant, and the streamline $Y = Y(X)$ is expressed parametrically in Φ . For example, the streamline $\Psi = 0$ is given by

$$X = \Phi + e^\Phi \quad Y = 0 \quad (4.3-32, 33)$$

As Φ goes from $-\infty$ to $+\infty$, X also goes from $-\infty$ to $+\infty$; hence the X -axis is a streamline. Next, the streamline $\Psi = \pi$ is given by

$$X = \Phi - e^\Phi \quad Y = \pi \quad (4.3-34, 35)$$

As Φ goes from $-\infty$ to $+\infty$, X goes from $-\infty$ to -1 and then back to $-\infty$; that is, the streamline doubles back on itself. We select this streamline to be one of the solid walls of the rectangular channel. Similarly, the streamline $\Psi = -\pi$ is the other wall. The streamlines $\Psi = C$, where $-\pi < C < \pi$, then give the flow pattern for the flow into the rectangular channel as shown in Fig. 4.3-2.

Next, from Eq. 4.3-29 the derivative $-dz/dw$ can be found:

$$-\frac{dz}{dw} = -\frac{1}{v_\infty} \frac{dZ}{dW} = -\frac{1}{v_\infty} (1 + e^W) = -\frac{1}{v_\infty} (1 + e^\Phi \cos \Psi + ie^\Phi \sin \Psi) \quad (4.3-36)$$

Comparison of this expression with Eq. 4.3-15 gives for the velocity components

$$\frac{v_x v_\infty}{v^2} = -(1 + e^\Phi \cos \Psi) \quad \frac{v_y v_\infty}{v^2} = -(e^\Phi \sin \Psi) \quad (4.3-37)$$

These equations have to be used in conjunction with Eqs. 4.3-30 and 31 to eliminate Φ and Ψ in order to get the velocity components as functions of position.

⁷ Hydrodynamic paradoxes are discussed in G. Birkhoff, *Hydrodynamics*, Dover, New York (1955).

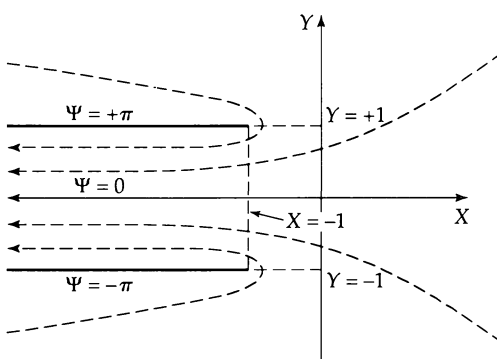


Fig. 4.3-2. The streamlines for the potential flow into a rectangular channel, as predicted from potential flow theory in Eqs. 4.3-30 and 31. A more realistic flow pattern is shown in Fig. 4.3-5.

EXAMPLE 4.3-3 Flow Near a Corner⁸

Figure 4.3-3 shows the potential flow in the neighborhood of two walls that meet at a corner at O . The flow in the neighborhood of this corner can be described by the complex potential

$$w(z) = -cz^\alpha \quad (4.3-38)$$

in which c is a constant. We can now consider two situations: (i) an “interior corner flow,” with $\alpha > 1$; and (ii) an “exterior corner flow,” with $\alpha < 1$.

- (a) Find the velocity components.
- (b) Obtain the tangential velocity at both parts of the wall.
- (c) Describe how to get the streamlines.
- (d) How can this result be applied to the flow around a wedge?

SOLUTION

- (a) The velocity components are obtained from the complex velocity

$$\frac{dw}{dz} = -caz^{\alpha-1} = -c\alpha r^{\alpha-1} e^{i(\alpha-1)\theta} \quad (4.3-39)$$

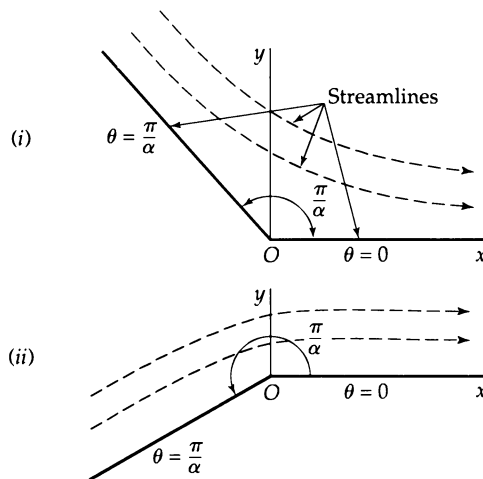


Fig. 4.3-3. Potential flow near a corner. On the left portion of the wall, $v_r = -cr^{\alpha-1}$, and on the right, $v_r = +cr^{\alpha-1}$. (i) Interior-corner flow, with $\alpha > 1$; and (ii) exterior-corner flow, with $\alpha < 1$.

⁸ R. L. Panton, *Compressible Flow*, Wiley, New York, 2nd edition (1996).

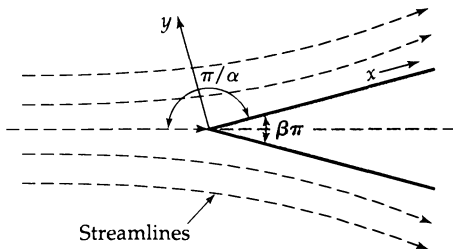


Fig. 4.3-4. Potential flow along a wedge. On the upper surface of the wedge, $v_x = cx^{\alpha-1} = cx^{\beta/(2-\beta)}$. The quantities α and β are related by $\beta = (2/\alpha)(\alpha - 1)$.

Hence from Eq. 4.3-12 we get

$$v_x = +c\alpha r^{\alpha-1} \cos(\alpha - 1)\theta \quad (4.3-40)$$

$$v_y = -c\alpha r^{\alpha-1} \sin(\alpha - 1)\theta \quad (4.3-41)$$

(b) The tangential velocity at the walls is

$$\text{at } \theta = 0: \quad v_x = v_r = c\alpha r^{\alpha-1} = c\alpha x^{\alpha-1} \quad (4.3-42)$$

$$\begin{aligned} \text{at } \theta = \pi/\alpha: \quad v_r &= v_x \cos \theta + v_y \sin \theta \\ &= +c\alpha r^{\alpha-1} \cos(\alpha - 1)\theta \cos \theta - c\alpha r^{\alpha-1} \sin(\alpha - 1)\theta \sin \theta \\ &= c\alpha r^{\alpha-1} \cos \alpha \theta \\ &= -c\alpha r^{\alpha-1} \end{aligned} \quad (4.3-43)$$

Hence, in Case (i), the incoming fluid at the wall decelerates as it approaches the junction, and the departing fluid accelerates as it moves away from the junction. In Case (ii) the velocity components become infinite at the corner as $\alpha - 1$ is then negative.

(c) The complex potential can be decomposed into its real and imaginary parts

$$w = \phi + i\psi = -cr^\alpha (\cos \alpha \theta + i \sin \alpha \theta) \quad (4.3-44)$$

Hence the stream function is

$$\psi = -cr^\alpha \sin \alpha \theta \quad (4.3-45)$$

To get the streamlines, one selects various values for the stream function—say, $\psi_1, \psi_2, \psi_3 \dots$ —and then for each value one plots r as a function of θ .

(d) Since for ideal flow any streamline may be replaced by a wall, and vice versa, the results found here for $\alpha > 0$ describe the inviscid flow over a wedge (see Fig. 4.3-4). We make use of this in Example 4.4-3.

A few words of warning are in order concerning the applicability of potential-flow theory to real systems:

- a. For the flow around a cylinder, the streamlines shown in Fig. 4.3-1 do not conform to any of the flow regimes sketched in Fig. 3.7-2.
- b. For the flow into a channel, the predicted flow pattern of Fig. 4.3-2 is unrealistic inside the channel and just upstream from the channel entrance. A much better approximation to the actual behavior is shown in Fig. 4.3-5.

Both of these failures of the elementary potential theory result from the phenomenon of *separation*: the departure of streamlines from a boundary surface.

Separation tends to occur at sharp corners of solid boundaries, as in channel flow, and on the downstream sides of bluff objects, as in the flow around a cylinder. Generally, separation is likely to occur in regions where the pressure increases in the direction

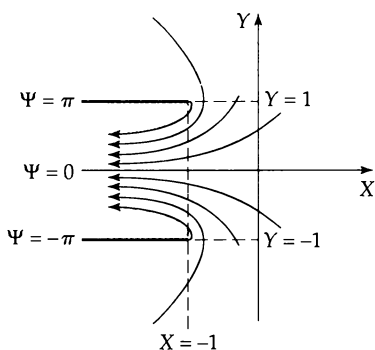


Fig. 4.3-5. Potential flow into a rectangular channel with separation, as calculated by H. von Helmholtz, *Phil. Mag.*, 36, 337–345 (1868). The streamlines for $\Psi = \pm\pi$ separate from the inner surface of the channel. The velocity along this separated streamline is constant. Between the separated streamline and the wall is an empty region.

of flow. Potential-flow analyses are not useful in the separated region. They can, however, be used upstream of this region if the location of the *separation streamline* is known. Methods of making such calculations have been highly developed. Sometimes the position of the separation streamline can be estimated successfully from potential-flow theory. This is true for flow into a channel, and, in fact, Fig. 4.3-5 was obtained in this way.⁹ For other systems, such as the flow around the cylinder, the separation point and separation streamline must be located by experiment. Even when the position of the separation streamline is not known, potential flow solutions may be valuable. For example, the flow field of Ex. 4.3-1 has been found useful for estimating aerosol impaction coefficients on cylinders.¹⁰ This success is a result of the fact that most of the particle impacts occur near the forward stagnation point, where the flow is not affected very much by the position of the separation streamline. Valuable semiquantitative conclusions concerning heat- and mass-transfer behavior can also be made on the basis of potential flow calculations ignoring the separation phenomenon.

The techniques described in this section all assume that the velocity vector can be written as the gradient of a scalar function that satisfies Laplace's equation. The equation of motion plays a much less prominent role than for the viscous flows discussed previously, and its primary use is for the determination of the pressure distribution once the velocity profiles are found.

§4.4 FLOW NEAR SOLID SURFACES BY BOUNDARY-LAYER THEORY

The potential flow examples discussed in the previous section showed how to predict the flow field by means of a stream function and a velocity potential. The solutions for the velocity distribution thus obtained do not satisfy the usual "no-slip" boundary condition at the wall. Consequently, the potential flow solutions are of no value in describing the transport phenomena in the immediate neighborhood of the wall. Specifically, the viscous drag force cannot be obtained, and it is also not possible to get reliable descriptions of interphase heat- and mass-transfer at solid surfaces.

To describe the behavior near the wall, we use *boundary-layer theory*. For the description of a viscous flow, we obtain an approximate solution for the velocity components in a very thin boundary layer near the wall, taking the viscosity into account. Then we "match" this solution to the potential flow solution that describes the flow outside the

⁹ H. von Helmholtz, *Phil Mag.* (4), 36, 337–345 (1868). Herman Ludwig Ferdinand von Helmholtz (1821–1894) studied medicine and became an army doctor; he then served as professor of medicine and later as professor of physics in Berlin.

¹⁰ W. E. Ranz, *Principles of Inertial Impaction*, Bulletin #66, Department of Engineering Research, Pennsylvania State University, University Park, Pa. (1956).

boundary layer. The success of the method depends on the thinness of the boundary layer, a condition that is met at high Reynolds number.

We consider the steady, two-dimensional flow of a fluid with constant ρ and μ around a submerged object, such as that shown in Fig. 4.4-1. We assert that the main changes in the velocity take place in a very thin region, the boundary layer, in which the curvature effects are not important. We can then set up a Cartesian coordinate system with x pointing downstream, and y perpendicular to the solid surface. The continuity equation and the Navier-Stokes equations then become:

$$\frac{\partial v_x}{\partial x} + \frac{\partial v_y}{\partial y} = 0 \quad (4.4-1)$$

$$\left(v_x \frac{\partial v_x}{\partial x} + v_y \frac{\partial v_x}{\partial y} \right) = -\frac{1}{\rho} \frac{\partial \mathcal{P}}{\partial x} + \nu \left(\frac{\partial^2 v_x}{\partial x^2} + \frac{\partial^2 v_x}{\partial y^2} \right) \quad (4.4-2)$$

$$\left(v_x \frac{\partial v_y}{\partial x} + v_y \frac{\partial v_y}{\partial y} \right) = -\frac{1}{\rho} \frac{\partial \mathcal{P}}{\partial y} + \nu \left(\frac{\partial^2 v_y}{\partial x^2} + \frac{\partial^2 v_y}{\partial y^2} \right) \quad (4.4-3)$$

Some of the terms in these equations can be discarded by order-of-magnitude arguments. We use three quantities as "yardsticks": the approach velocity v_∞ , some linear dimension l_0 of the submerged body, and an average thickness δ_0 of the boundary layer. The presumption that $\delta_0 \ll l_0$ allows us to make a number of rough calculations of orders of magnitude.

Since v_x varies from zero at the solid surface to v_∞ at the outer edge of the boundary layer, we can say that

$$\frac{\partial v_x}{\partial y} = O\left(\frac{v_\infty}{\delta_0}\right) \quad (4.4-4)$$

where O means "order of magnitude of." Similarly, the maximum variation in v_x over the length l_0 of the surface will be v_∞ , so that

$$\frac{\partial v_x}{\partial x} = O\left(\frac{v_\infty}{l_0}\right) \text{ and } \frac{\partial v_y}{\partial y} = O\left(\frac{v_\infty}{l_0}\right) \quad (4.4-5)$$

Here we have made use of the equation of continuity to get one more derivative (we are concerned here only with orders of magnitude and not the signs of the quantities). Integration of the second relation suggests that $v_y = O((\delta_0/l_0)v_\infty) \ll v_x$. The various terms in Eq. 4.4-2 may now be estimated as

$$v_x \frac{\partial v_x}{\partial x} = O\left(\frac{v_\infty^2}{l_0}\right); v_y \frac{\partial v_x}{\partial y} = O\left(\frac{v_\infty^2}{l_0}\right) \quad \frac{\partial^2 v_x}{\partial x^2} = O\left(\frac{v_\infty}{l_0^2}\right) \quad \frac{\partial^2 v_x}{\partial y^2} = O\left(\frac{v_\infty}{\delta_0^2}\right) \quad (4.4-6)$$

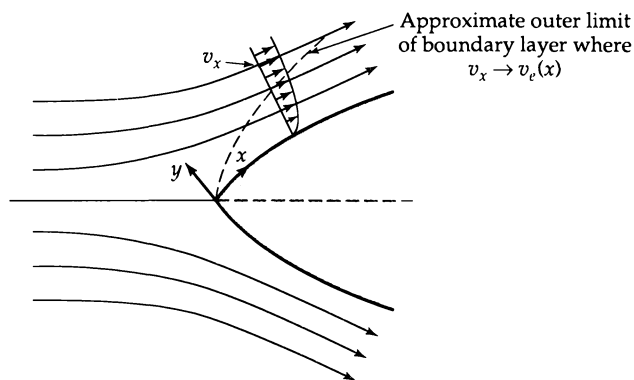


Fig. 4.4-1. Coordinate system for the two-dimensional flow around a submerged object. The boundary-layer thickness is greatly exaggerated for purposes of illustration. Because the boundary layer is in fact quite thin, it is permissible to use rectangular coordinates locally along the curved surface.

This suggests that $\partial^2 v_x / \partial x^2 \ll \partial^2 v_x / \partial y^2$, so that the former may be safely neglected. In the boundary layer it is expected that the terms on the left side of Eq. 4.4-2 should be of the same order of magnitude as those on the right side, and therefore

$$\frac{v_x^2}{l_0} = O\left(\nu \frac{v_\infty}{\delta_0^2}\right) \quad \text{or} \quad \frac{\delta_0}{l_0} = O\left(\sqrt{\frac{\nu}{v_\infty l_0}}\right) = O\left(\frac{1}{\sqrt{\text{Re}}}\right) \quad (4.4-7)$$

The second of these relations shows that the boundary-layer thickness is small compared to the dimensions of the submerged object in high-Reynolds-number flows.

Similarly it can be shown, with the help of Eq. 4.4-7, that three of the derivatives in Eq. 4.4-3 are of the same order of magnitude:

$$v_x \frac{\partial v_y}{\partial x}, v_y \frac{\partial v_y}{\partial y}, \nu \frac{\partial^2 v_y}{\partial y^2} = O\left(\frac{v_x^2 \delta_0}{l_0^2}\right) \gg \nu \frac{\partial^2 v_y}{\partial x^2} \quad (4.4-8)$$

Comparison of this result with Eq. 4.4-6 shows that $\partial \mathcal{P} / \partial y \ll \partial \mathcal{P} / \partial x$. This means that the y -component of the equation of motion is not needed and that the modified pressure can be treated as a function of x alone.

As a result of these order-of-magnitude arguments, we are left with the *Prandtl boundary layer equations*:¹

$$(continuity) \quad \frac{\partial v_x}{\partial x} + \frac{\partial v_y}{\partial y} = 0 \quad (4.4-9)$$

$$(motion) \quad v_x \frac{\partial v_x}{\partial x} + v_y \frac{\partial v_x}{\partial y} = -\frac{1}{\rho} \frac{d\mathcal{P}}{dx} + \nu \frac{\partial^2 v_x}{\partial y^2} \quad (4.4-10)$$

The modified pressure $\mathcal{P}(x)$ is presumed known from the solution of the corresponding potential-flow problem or from experimental measurements.

The usual boundary conditions for these equations are the no-slip condition ($v_x = 0$ at $y = 0$), the condition of no mass transfer from the wall ($v_y = 0$ at $y = 0$), and the statement that the velocity merges into the external (potential-flow) velocity at the outer edge of the boundary layer ($v_x(x, y) \rightarrow v_e(x)$). The function $v_e(x)$ is related to $\mathcal{P}(x)$ according to the potential-flow equation of motion in Eq. 4.3-5. Consequently the term $-(1/\rho)(d\mathcal{P}/dx)$ in Eq. 4.4-10 can be replaced by $v_e(dv_e/dx)$ for steady flow. Thus Eq. 4.4-10 may also be written as

$$v_x \frac{\partial v_x}{\partial x} + v_y \frac{\partial v_x}{\partial y} = v_e \frac{dv_e}{dx} + \nu \frac{\partial^2 v_x}{\partial y^2} \quad (4.4-11)$$

The equation of continuity may be solved for v_y by using the boundary condition that $v_y = 0$ at $y = 0$ (i.e., no mass transfer), and then this expression for v_y may be substituted into Eq. 4.4-11 to give

$$v_x \frac{\partial v_x}{\partial x} - \left(\int_0^y \frac{\partial v_x}{\partial x} dy \right) \frac{\partial v_x}{\partial y} = v_e \frac{dv_e}{dx} + \nu \frac{\partial^2 v_x}{\partial y^2} \quad (4.4-12)$$

This is a partial differential equation for the single dependent variable v_x .

¹ Ludwig Prandtl (1875–1953) (pronounced “Prahn-t'l”), who taught in Hannover and Göttingen and later served as the Director of the Kaiser Wilhelm Institute for Fluid Dynamics, was one of the people who shaped the future of his field at the beginning of the twentieth century; he made contributions to turbulent flow and heat transfer, but his development of the boundary-layer equations was his crowning achievement. L. Prandtl, *Verhandlungen des III Internationalen Mathematiker-Kongresses* (Heidelberg, 1904), Leipzig, pp. 484–491; L. Prandtl, *Gesammelte Abhandlungen*, 2, Springer-Verlag, Berlin (1961), pp. 575–584. For an introductory discussion of matched asymptotic expressions, see D. J. Acheson, *Elementary Fluid Mechanics*, Oxford University Press (1990), pp. 269–271. An exhaustive discussion of the subject may be found in M. Van Dyke, *Perturbation Methods in Fluid Dynamics*, The Parabolic Press, Stanford, Cal. (1975).

This equation may now be multiplied by ρ and integrated from $y = 0$ to $y = \infty$ to give the von Kármán momentum balance²

$$\mu \frac{\partial v_x}{\partial y} \Big|_{y=0} = \frac{d}{dx} \int_0^\infty \rho v_x (v_c - v_x) dy + \frac{dv_c}{dx} \int_0^\infty \rho (v_c - v_x) dy \quad (4.4-13)$$

Here use has been made of the condition that $v_x(x, y) \rightarrow v_c(x)$ as $y \rightarrow \infty$. The quantity on the left side of Eq. 4.4-13 is the shear stress exerted by the fluid on the wall: $-\tau_{yx}|_{y=0}$.

The original Prandtl boundary-layer equations, Eqs. 4.4-9 and 10, have thus been transformed into Eq. 4.4-11, Eq. 4.4-12, and Eq. 4.4-13, and any of these may be taken as the starting point for solving two-dimensional boundary-layer problems. Equation 4.4-13, with assumed expressions for the velocity profile, is the basis of many “approximate boundary-layer solutions” (see Example 4.4-1). On the other hand, the analytical or numerical solutions of Eqs. 4.4-11 or 12 are called “exact boundary-layer solutions” (see Example 4.4-2).

The discussion here is for steady, laminar, two-dimensional flows of fluids with constant density and viscosity. Corresponding equations are available for unsteady flow, turbulent flow, variable fluid properties, and three-dimensional boundary layers.³⁻⁶

Although many exact and approximate boundary-layer solutions have been obtained and applications of the theory to streamlined objects have been quite successful, considerable work remains to be done on flows with adverse pressure gradients (i.e., positive $\partial P/\partial x$) in Eq. 4.4-10, such as the flow on the downstream side of a blunt object. In such flows the streamlines usually separate from the surface before reaching the rear of the object (see Fig. 3.7-2). The boundary-layer approach described here is suitable for such flows only in the region upstream from the separation point.

EXAMPLE 4.4-1

Laminar Flow along a Flat Plate (Approximate Solution)

Use the von Kármán momentum balance to estimate the steady-state velocity profiles near a semi-infinite flat plate in a tangential stream with approach velocity v_∞ (see Fig. 4.4-2). For this system the potential-flow solution is $v_c = v_\infty$.

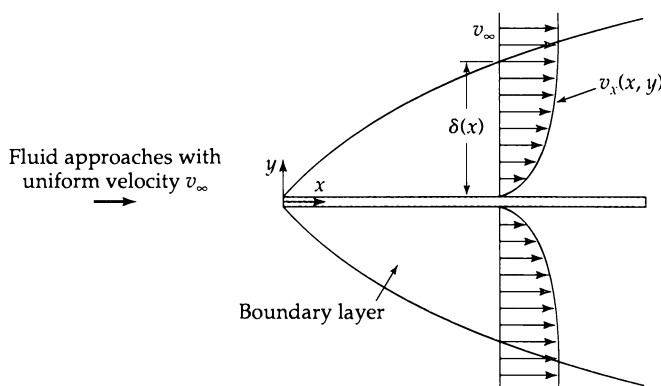


Fig. 4.4-2. Boundary-layer development near a flat plate of negligible thickness.

² Th. von Kármán, *Zeits. für angew. Math. u. Mech.*, 1, 233–252 (1921). Hungarian-born Theodor von Kármán taught in Göttingen, Aachen, and California Institute of Technology; he contributed much to the theory of turbulence and aerodynamics.

³ H. Schlichting and K. Gersten, *Boundary-Layer Theory*, Springer Verlag, Berlin, 8th edition (2000).

⁴ L. Rosenhead, *Laminar Boundary Layers*, Oxford University Press, London (1963).

⁵ K. Stewartson, *The Theory of Laminar Boundary Layers in Compressible Fluids*, Oxford University Press (1964).

⁶ W. H. Dorrance, *Viscous Hypersonic Flow*, McGraw-Hill, New York (1962).

SOLUTION

We know intuitively what the velocity profile $v_x(y)$ looks like. Hence we can guess a form for $v_x(y)$ and substitute it directly into the von Kármán momentum balance. One reasonable choice is to let $v_x(y)$ by a function of y/δ , where $\delta(x)$ is the “thickness” of the boundary layer. The function is so chosen that $v_x = 0$ at $y = 0$ and $v_x = v_\infty$ at $y = \delta$. This is tantamount to assuming geometrical similarity of the velocity profiles for various values of x . When this assumed profile is substituted into the von Kármán momentum balance, an ordinary differential equation for the boundary-layer thickness $\delta(x)$ is obtained. When this equation has been solved, the $\delta(x)$ so obtained can then be used to get the velocity profile and other quantities of interest.

For the present problem a plausible guess for the velocity distribution, with a reasonable shape, is

$$\frac{v_x}{v_\infty} = \frac{3}{2} \frac{y}{\delta} - \frac{1}{2} \left(\frac{y}{\delta} \right)^3 \quad \text{for } 0 \leq y \leq \delta(x) \quad (\text{boundary-layer region}) \quad (4.4-14)$$

$$\frac{v_x}{v_\infty} = 1 \quad \text{for } y \geq \delta(x) \quad (\text{potential flow region}) \quad (4.4-15)$$

This is “reasonable” because this velocity profile satisfies the no-slip condition at $y = 0$, and $\partial v_x / \partial y = 0$ at the outer edge of the boundary layer. Substitution of this profile into the von Kármán integral balance in Eq. 4.4-13 gives

$$\frac{3}{2} \frac{\mu v_\infty}{\delta} = \frac{d}{dx} \left(\frac{39}{280} \rho v_\infty^2 \delta \right) \quad (4.4-16)$$

This first-order, separable differential equation can now be integrated to give for the boundary-layer thickness

$$\delta(x) = \sqrt{\frac{280}{13} \frac{\nu x}{v_\infty}} = 4.64 \sqrt{\frac{\nu x}{v_\infty}} \quad (4.4-17)$$

Therefore, the boundary-layer thickness increases as the square root of the distance from the upstream end of the plate. The resulting approximate solution for the velocity distribution is then

$$\frac{v_x}{v_\infty} = \frac{3}{2} \left(y \sqrt{\frac{13}{280} \frac{\nu x}{v_\infty}} \right) - \frac{1}{2} \left(y \sqrt{\frac{13}{280} \frac{\nu x}{v_\infty}} \right)^3 \quad (4.4-18)$$

From this result we can estimate the drag force on a plate of finite size wetted on both sides. For a plate of width W and length L , integration of the momentum flux over the two solid surfaces gives:

$$F_x = 2 \int_0^W \int_0^L \left(+\mu \frac{\partial v_x}{\partial y} \right) \Big|_{y=0} dx dz = 1.293 \sqrt{\rho \mu L W^2 v_\infty^3} \quad (4.4-19)$$

The exact solution, given in the next example, gives the same result, but with a numerical coefficient of 1.328. Both solutions predict the drag force within the scatter of the experimental data. However, the exact solution gives somewhat better agreement with the measured velocity profiles.³ This additional accuracy is essential for stability calculations.

EXAMPLE 4.4-2

Obtain the exact solution for the problem given in the previous example.

Laminar Flow along a Flat Plate (Exact Solution)⁷**SOLUTION**

This problem may be solved by using the definition of the stream function in Table 4.2-1. Inserting the expressions for the velocity components in the first row of entries, we get

$$\frac{\partial \psi}{\partial y} \frac{\partial^2 \psi}{\partial x \partial y} - \frac{\partial \psi}{\partial x} \frac{\partial^2 \psi}{\partial y^2} = -\nu \frac{\partial^3 \psi}{\partial y^3} \quad (4.4-20)$$

⁷ This problem was treated originally by H. Blasius, *Zeits. Math. Phys.*, **56**, 1–37 (1908).

The boundary conditions for this equation for $\psi(x, y)$ are

$$\text{B.C. 1: at } y = 0, \quad \frac{\partial \psi}{\partial x} = v_y = 0 \quad \text{for } x \geq 0 \quad (4.4-21)$$

$$\text{B.C. 2: at } y = 0, \quad \frac{\partial \psi}{\partial y} = -v_x = 0 \quad \text{for } x \geq 0 \quad (4.4-22)$$

$$\text{B.C. 3: as } y \rightarrow \infty, \quad \frac{\partial \psi}{\partial y} = -v_x \rightarrow -v_\infty \quad \text{for } x \geq 0 \quad (4.4-23)$$

$$\text{B.C. 4: at } x = 0, \quad \frac{\partial \psi}{\partial y} = -v_x = -v_\infty \quad \text{for } y > 0 \quad (4.4-24)$$

Inasmuch as there is no characteristic length appearing in the above relations, the method of combination of independent variables seems appropriate. By dimensional arguments similar to those used in Example 4.1-1, we write

$$\frac{v_x}{v_\infty} = \Pi(\eta), \quad \text{where } \eta = y \sqrt{\frac{1}{2} \frac{v_x}{\nu x}} \quad (4.4-25)$$

The factor of 2 is included to avoid having any numerical factors occur in the differential equation in Eq. 4.4-27. The stream function that gives the velocity distribution in Eq. 4.4-25 is

$$\psi(x, y) = -\sqrt{2v_\infty \nu x} f(\eta), \quad \text{where } f(\eta) = \int_0^\eta \Pi'(\bar{\eta}) d\bar{\eta} \quad (4.4-26)$$

This expression for the stream function is consistent with Eq. 4.4-25 as may be seen by using the relation $v_x = -\partial \psi / \partial y$ (given in Table 4.2-1). Substitution of Eq. 4.4-26 into Eq. 4.4-20 gives

$$-ff'' = f''' \quad (4.4-27)$$

Substitution into the boundary conditions gives

$$\text{B.C. 1 and 2: at } \eta = 0, \quad f = 0 \quad \text{and} \quad f' = 0 \quad (4.4-28)$$

$$\text{B.C. 3 and 4: as } \eta \rightarrow \infty, \quad f' \rightarrow 1 \quad (4.4-29)$$

Thus the determination of the flow field is reduced to the solution of one third-order ordinary differential equation.

This equation, along with the boundary conditions given, can be solved by numerical integration, and accurate tables of the solution are available.^{3,4} The problem was originally solved by Blasius⁷ using analytic approximations that proved to be quite accurate. A plot of his solution is shown in Fig. 4.4-3 along with experimental data taken subsequently. The agreement between theory and experiment is remarkably good.

The drag force on a plate of width W and length L may be calculated from the dimensionless velocity gradient at the wall, $f''(0) = 0.4696 \dots$ as follows:

$$\begin{aligned} F_x &= 2 \int_0^W \int_0^L \left(+\mu \frac{\partial v_x}{\partial y} \right) \Big|_{y=0} dx dz \\ &= 2 \int_0^W \int_0^L \left(+\mu v_\infty \frac{df'}{d\eta} \frac{\partial \eta}{\partial y} \right) \Big|_{y=0} dx dz \\ &= 2 \int_0^W \int_0^L \mu v_\infty f''(0) \sqrt{\frac{1}{2} \frac{v_x}{\nu x}} dx dz \\ &= 1.328 \sqrt{\rho \mu L W^2 v_\infty^3} \end{aligned} \quad (4.4-30)$$

This result has also been confirmed experimentally.^{3,4}

Because of the approximations made in Eq. 4.4-10, the solution is most accurate at large local Reynolds numbers; that is, $\text{Re}_x = xv_\infty/\nu \gg 1$. The excluded region of lower Reynolds numbers is small enough to ignore in most drag calculations. More complete

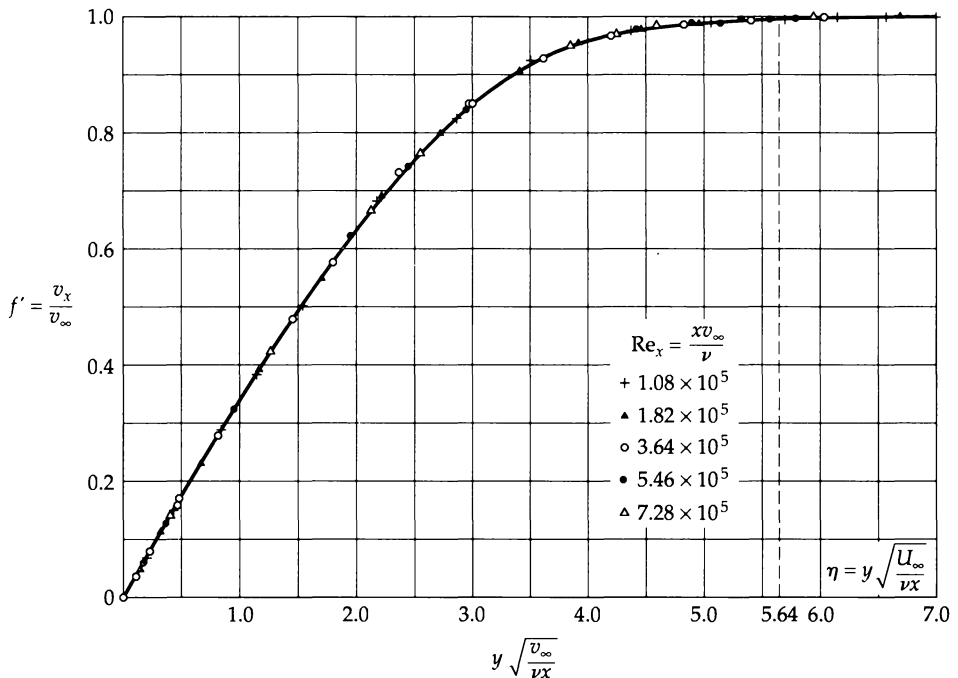


Fig. 4.4-3. Predicted and observed velocity profiles for tangential laminar flow along a flat plate. The solid line represents the solution of Eqs. 4.4-20 to 24, obtained by Blasius [see H. Schlichting, *Boundary-Layer Theory*, McGraw-Hill, New York, 7th edition (1979), p. 137].

analyses⁸ indicate that Eq. 4.4-30 is accurate to within 3% for $Lv_\infty/\nu \geq 10^4$ and within 0.3% for $Lv_\infty/\nu \geq 10^6$.

The growth of the boundary layer with increasing x eventually leads to an unstable situation, and turbulent flow sets in. The transition is found to begin somewhere in the range of local Reynolds number of $\text{Re}_x = xv_\infty/\nu \geq 3 \times 10^5$ to 3×10^6 , depending on the uniformity of the approaching stream.⁸ Upstream of the transition region the flow remains laminar, and downstream it is turbulent.

EXAMPLE 4.4-3

Flow near a Corner

We now want to treat the boundary-layer problem analogous to Example 4.3-3, namely the flow near a corner (see Fig. 4.3-4). If $\alpha > 1$, the problem may also be interpreted as the flow along a wedge of included angle $\beta\pi$, with $\alpha = 2/(2 - \beta)$. For this system the external flow v_e is known from Eqs. 4.3-42 and 43, where we found that

$$v_e(x) = cx^{\beta/(2-\beta)} \quad (4.4-31)$$

This was the expression that was found to be valid right at the wall (i.e., at $y = 0$). Here, it is assumed that the boundary layer is so thin that using the wall expression from ideal flow is adequate for the outer limit of the boundary-layer solution, at least for small values of x .

⁸ Y. H. Kuo, *J. Math. Phys.*, **32**, 83–101 (1953); I. Imai, *J. Aero. Sci.*, **24**, 155–156 (1957).

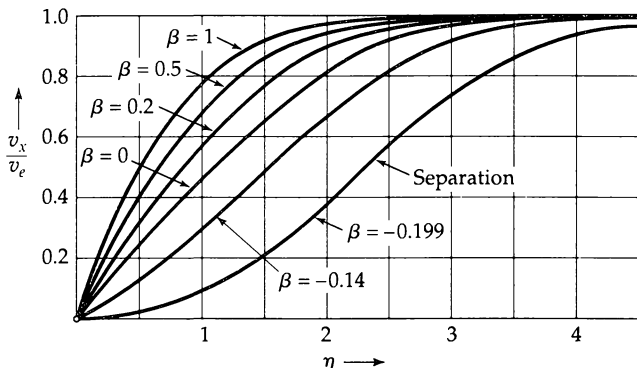


Fig. 4.4-4. Velocity profile for wedge flow with included angle $\beta\pi$. Negative values of β correspond to the flow around an “external corner” [see Fig. 4.3-4(ii)] with slip at the wall upstream of the corner.

SOLUTION

We now have to solve Eq. 4.4-11, using Eq. 4.4-31 for $v_e(x)$. When we introduce the stream function from the first row of Table 4.2-1, we obtain the following differential equation for ψ :

$$\frac{\partial \psi}{\partial y} \frac{\partial^2 \psi}{\partial x \partial y} - \frac{\partial \psi}{\partial x} \frac{\partial^2 \psi}{\partial y^2} = \left(\frac{c^2 \beta}{2 - \beta} \right) \frac{1}{x^{(2-3\beta)/(2-\beta)}} - \nu \frac{\partial^3 \psi}{\partial y^3} \quad (4.4-32)$$

which corresponds to Eq. 4.4-20 with the term $v_e(dv_e/dx)$ added. It was discovered⁹ that this equation can be reduced to a single ordinary differential equation by introducing a dimensionless stream function $f(\eta)$ by

$$\psi(x, y) = \sqrt{c\nu(2 - \beta)} x^{1/(2 - \beta)} f(\eta) \quad (4.4-33)$$

in which the independent variable is

$$\eta = \sqrt{\frac{c}{(2 - \beta)\nu}} \frac{y}{x^{(1-\beta)/(2-\beta)}} \quad (4.4-34)$$

Then Eq. 4.4-32 becomes the *Falkner-Skan equation*⁹

$$f''' - ff'' - \beta(1 - f'^2) = 0 \quad (4.4-35)$$

This equation has been solved numerically with the appropriate boundary conditions, and the results are shown in Fig. 4.4-4.

It can be seen that for positive values of β , which corresponds to the systems shown in Fig. 4.3-4(a) and Fig. 4.3-5, the fluid is accelerating and the velocity profiles are stable. For negative values of β , down to $\beta = -0.199$, the flows are decelerating but stable, and no separation occurs. However, if $\beta > -0.199$, the velocity gradient at the wall becomes zero, and separation of the flow occurs. Therefore, for the interior corner flows and for wedge flows, there is no separation, but for the exterior corner flows, separation may occur.

QUESTIONS FOR DISCUSSION

- For what types of problems is the method of combination of variables useful? The method of separation of variables?
- Can the flow near a cylindrical rod of infinite length suddenly set in motion in the axial direction be described by the method in Example 4.1-1?

⁹ V. M. Falkner and S. W. Skan, *Phil. Mag.*, **12**, 865–896 (1931); D. R. Hartree, *Proc. Camb. Phil. Soc.*, **33**, Part II, 223–239 (1937); H. Rouse (ed.), *Advanced Mechanics of Fluids*, Wiley, New York (1959), Chapter VII, Sec. D; H. Schlichting and K. Gersten, *Boundary-Layer Theory*, Springer-Verlag, Berlin (2000), pp. 169–173 (isothermal), 220–221 (nonisothermal); W. E. Stewart and R. Prober, *Int. J. Heat Mass Transfer*, **5**, 1149–1163 (1962); **6**, 221–229, 872 (1963), include wedge flow with heat and mass transfer.

3. What happens in Example 4.1-2 if one tries to solve Eq. 4.1-21 by the method of separation of variables without first recognizing that the solution can be written as the sum of a steady-state solution and a transient solution?
4. What happens if the separation constant after Eq. 4.1-27 is taken to be c or c^2 instead of $-c^2$?
5. Try solving the problem in Example 4.1-3 using trigonometric quantities in lieu of complex quantities.
6. How is the vorticity equation obtained and how may it be used?
7. How is the stream function defined, and why is it useful?
8. In what sense are the potential flow solutions and the boundary-layer flow solutions complementary?
9. List all approximate forms of the equations of change encountered thus far, and indicate their range of applicability.

PROBLEMS

4A.1 Time for attainment of steady flow in tube flow.

(a) A heavy oil, with a kinematic viscosity of $3.45 \times 10^{-4} \text{ m}^2/\text{s}$, is at rest in a long vertical tube with a radius of 0.7 cm. The fluid is suddenly allowed to flow from the bottom of the tube by virtue of gravity. After what time will the velocity at the tube center be within 10% of its final value?

(b) What is the result if water at 68°F is used?

Note: The result shown in Fig. 4D.2 should be used.

Answers: (a) $6.4 \times 10^{-2} \text{ s}$; (b) 22 s

4A.2 Velocity near a moving sphere.

A sphere of radius R is falling in creeping flow with a terminal velocity v_∞ through a quiescent fluid of viscosity μ . At what horizontal distance from the sphere does the velocity of the fluid fall to 1% of the terminal velocity of the sphere?

Answer: About 37 diameters

4A.3 Construction of streamlines for the potential flow around a cylinder.

Plot the streamlines for the flow around a cylinder using the information in Example 4.3-1 by the following procedure:

(a) Select a value of $\Psi = C$ (that is, select a streamline).

(b) Plot $Y = C + K$ (straight lines parallel to the X -axis) and $Y = K(X^2 + Y^2)$ (circles with radius $1/2K$, tangent to the X -axis at the origin).

(c) Plot the intersections of the lines and circles that have the same value of K .

(d) Join these points to get the streamline for $\Psi = C$.

Then select other values of C and repeat the process until the pattern of streamlines is clear.

4A.4 Comparison of exact and approximate profiles for flow along a flat plate.

Compare the values of v_x/v_∞ obtained from Eq. 4.4-18 with those from Fig. 4.4-3, at the following values of $y\sqrt{v_\infty/vx}$: (a) 1.5, (b) 3.0, (c) 4.0. Express the results as the ratio of the approximate to the exact values.

Answers: (a) 0.96; (b) 0.99; (c) 1.01

4A.5 Numerical demonstration of the von Kármán momentum balance.

(a) Evaluate the integrals in Eq. 4.4-13 numerically for the Blasius velocity profile given in Fig. 4.4-3.

(b) Use the results of (a) to determine the magnitude of the wall shear stress $\tau_{yx}|_{y=0}$.

(c) Calculate the total drag force, F_x , for a plate of width W and length L , wetted on both sides. Compare your result with that obtained in Eq. 4.4-30.

Answers: (a) $\int_0^\infty \rho v_x(v_e - v_x) dy = 0.664 \sqrt{\rho \mu v_\infty^3 x}$

$$\int_0^\infty \rho(v_e - v_x) dy = 1.73 \sqrt{\rho \mu v_\infty x}$$

4A.6 Use of boundary-layer equations. Air at 1 atm and 20°C flows tangentially on both sides of a thin, smooth flat plate of width $W = 10$ ft, and of length $L = 3$ ft in the direction of the flow. The velocity outside the boundary layer is constant at 20 ft/s.

- Compute the local Reynolds number $\text{Re}_x = xv_\infty/\nu$ at the trailing edge.
- Assuming laminar flow, compute the approximate boundary-layer thickness, in inches, at the trailing edge. Use the results of Example 4.4-1.
- Assuming laminar flow, compute the total drag of the plate in lb. Use the results of Examples 4.4-1 and 2.

4A.7 Entrance flow in conduits.

- Estimate the entrance length for laminar flow in a circular tube. Assume that the boundary-layer thickness δ is given adequately by Eq. 4.4-17, with v_∞ of the flat-plate problem corresponding to v_{\max} in the tube-flow problem. Assume further that the entrance length L_e can be taken to be the value of x at which $\delta = R$. Compare your result with the expression for L_e cited in §2.3—namely, $L_e = 0.035D \text{Re}$.
- Rewrite the transition Reynolds number $xv_\infty/\nu \approx 3.5 \times 10^5$ (for the flat plate) by inserting δ from Eq. 4.4-17 in place of x as the characteristic length. Compare the quantity $\delta v_\infty/\nu$ thus obtained with the corresponding minimum transition Reynolds number for the flow through long smooth tubes.
- Use the method of (a) to estimate the entrance length in the flat duct shown in Fig. 4C.1. Compare the result with that given in Problem 4C.1(d).

4B.1 Flow of a fluid with a suddenly applied constant wall stress. In the system studied in Example 4.1-1, let the fluid be at rest before $t = 0$. At time $t = 0$ a constant force is applied to the fluid at the wall in the positive x direction, so that the shear stress τ_{yx} takes on a new constant value τ_0 at $y = 0$ for $t > 0$.

- Differentiate Eq. 4.1-1 with respect to y and multiply by $-\mu$ to obtain a partial differential equation for $\tau_{yx}(y, t)$.
- Write the boundary and initial conditions for this equation.
- Solve using the method in Example 4.1-1 to obtain

$$\frac{\tau_{yx}}{\tau_0} = 1 - \operatorname{erf} \frac{y}{\sqrt{4\nu t}} \quad (4B.1-1)$$

- (d) Use the result in (c) to obtain the velocity profile. The following relation¹ will be helpful

$$\int_x^\infty (1 - \operatorname{erf} u) du = \frac{1}{\sqrt{\pi}} e^{-x^2} - x(1 - \operatorname{erf} x) \quad (4B.1-2)$$

4B.2 Flow near a wall suddenly set in motion (approximate solution) (Fig. 4B.2). Apply a procedure like that of Example 4.4-1 to get an approximate solution for Example 4.1.1.

- (a) Integrate Eq. 4.4-1 over y to get

$$\int_0^\infty \frac{\partial v_x}{\partial t} dy = \nu \left. \frac{\partial v_x}{\partial y} \right|_0^\infty \quad (4B.2-1)$$

Make use of the boundary conditions and the Leibniz rule for differentiating an integral (Eq. C.3-2) to rewrite Eq. 4B.2-1 in the form

$$\frac{d}{dt} \int_0^\infty \rho v_x dy = \tau_{yx}|_{y=0} \quad (4B.2-2)$$

Interpret this result physically.

¹ A useful summary of error functions and their properties can be found in H. S. Carslaw and J. C. Jaeger, *Conduction of Heat in Solids*, Oxford University Press, 2nd edition (1959), Appendix II.

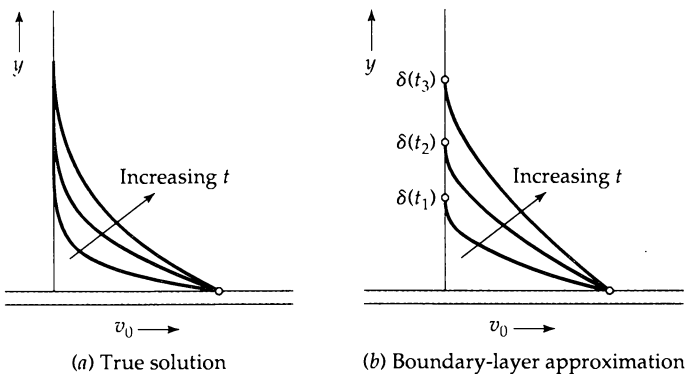


Fig. 4B.2. Comparison of true and approximate velocity profiles near a wall suddenly set in motion with velocity v_0 .

(b) We know roughly what the velocity profiles look like. We can make the following reasonable postulate for the profiles:

$$\frac{v_x}{v_\infty} = 1 - \frac{3}{2} \frac{y}{\delta(t)} + \frac{1}{2} \left(\frac{y}{\delta(t)} \right)^3 \quad \text{for } 0 \leq y \leq \delta(t) \quad (4B.2-3)$$

$$\frac{v_x}{v_\infty} = 1 \quad \text{for } y \geq \delta(t) \quad (4B.2-4)$$

Here $\delta(t)$ is a time-dependent boundary-layer thickness. Insert this approximate expression into Eq. 4B.2-2 to obtain

$$\delta \frac{d\delta}{dt} = 4\nu \quad (4B.2-5)$$

(c) Integrate Eq. 4B.2-5 with a suitable initial value of $\delta(t)$, and insert the result into Eq. 4B.2-3 to get the approximate velocity profiles.

(d) Compare the values of v_x/v_z obtained from (c) with those from Eq. 4.1-15 at $y/\sqrt{4vt} = 0.2, 0.5$, and 1.0 . Express the results as the ratio of the approximate value to the exact value.

Answer (d) 1.015, 1.026, 0.738

- 4B.3 Creeping flow around a spherical bubble.** When a liquid flows around a gas bubble, circulation takes place within the bubble. This circulation lowers the interfacial shear stress, and, to a first approximation, we may assume that it is entirely eliminated. Repeat the development of Ex. 4.2-1 for such a gas bubble, assuming it is spherical.

(a) Show that B.C. 2 of Ex. 4.2-1 is replaced by

$$\text{B.C. 2:} \quad \text{at } r = R, \quad \frac{d}{dr} \left(\frac{1}{r^2} \frac{df}{dr} \right) + 2 \frac{f}{r^4} = 0 \quad (4B.3-1)$$

and that the problem set-up is otherwise the same.

(b) Obtain the following velocity components:

$$v_r = v_x \left[1 - \left(\frac{R}{r} \right) \right] \cos \theta \quad (4B.3-2)$$

$$v_\theta = -v_\infty \left[1 - \frac{1}{2} \left(\frac{R}{r} \right) \right] \sin \theta \quad (4B.3-3)$$

(c) Next obtain the pressure distribution by using the equation of motion:

$$p = p_0 - \rho gh - \left(\frac{\mu v_x}{R}\right)\left(\frac{R}{r}\right)^2 \cos \theta \quad (4B.3-4)$$

- (d) Evaluate the total force of the fluid on the sphere to obtain

$$F_z = \frac{4}{3}\pi R^3 \rho g + 4\pi\mu R v_\infty \quad (4B.3-5)$$

This result may be obtained by the method of §2.6 or by integrating the z -component of $-(\mathbf{n} \cdot \boldsymbol{\pi})$ over the sphere surface (\mathbf{n} being the outwardly directed unit normal on the surface of the sphere).

4B.4 Use of the vorticity equation.

- (a) Work Problem 2B.3 using the y -component of the vorticity equation (Eq. 3D.2-1) and the following boundary conditions: at $x = \pm B$, $v_z = 0$ and at $x = 0$, $v_z = v_{z,\max}$. Show that this leads to

$$v_z = v_{z,\max}[1 - (x/B)^2] \quad (4B.4-1)$$

Then obtain the pressure distribution from the z -component of the equation of motion.

- (b) Work Problem 3B.6(b) using the vorticity equation, with the following boundary conditions: at $r = R$, $v_z = 0$ and at $r = \kappa R$, $v_z = v_0$. In addition an integral condition is needed to state that there is no net flow in the z direction. Find the pressure distribution in the system.

- (c) Work the following problems using the vorticity equation: 2B.6, 2B.7, 3B.1, 3B.10, 3B.16.

4B.5 Steady potential flow around a stationary sphere.²

In Example 4.2-1 we worked through the creeping flow around a sphere. We now wish to consider the flow of an incompressible, inviscid fluid in irrotational flow around a sphere. For such a problem, we know that the velocity potential must satisfy Laplace's equation (see text after Eq. 4.3-11).

- (a) State the boundary conditions for the problem.

- (b) Give reasons why the velocity potential ϕ can be postulated to be of the form $\phi(r, \theta) = f(r) \cos \theta$.

- (c) Substitute the trial expression for the velocity potential in (b) into Laplace's equation for the velocity potential.

- (d) Integrate the equation obtained in (c) and obtain the function $f(r)$ containing two constants of integration; determine these constants from the boundary conditions and find

$$\phi = -v_\infty R \left[\left(\frac{r}{R} \right) + \frac{1}{2} \left(\frac{R}{r} \right)^2 \right] \cos \theta \quad (4B.5-1)$$

- (e) Next show that

$$v_r = v_\infty \left[1 - \left(\frac{R}{r} \right)^3 \right] \cos \theta \quad (4B.5-2)$$

$$v_\theta = -v_\infty \left[1 + \frac{1}{2} \left(\frac{R}{r} \right)^3 \right] \sin \theta \quad (4B.5-3)$$

- (f) Find the pressure distribution, and then show that at the sphere surface

$$\mathcal{P} - \mathcal{P}_\infty = \frac{1}{2} \rho v_\infty^2 \left(1 - \frac{9}{4} \sin^2 \theta \right) \quad (4B.5-4)$$

4B.6 Potential flow near a stagnation point (Fig. 4B.6).

- (a) Show that the complex potential $w = -v_0 z^2$ describes the flow near a plane stagnation point.
 (b) Find the velocity components $v_x(x, y)$ and $v_y(x, y)$.
 (c) Explain the physical significance of v_0 .

² L. Landau and E. M. Lifshitz, *Fluid Mechanics*, Pergamon, Boston, 2nd edition (1987), pp. 21–26, contains a good collection of potential-flow problems.

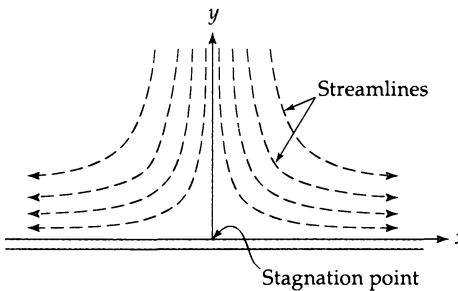


Fig. 4B.6. Two-dimensional potential flow near a stagnation point.

4B.7 Vortex flow.

(a) Show that the complex potential $w = (i\Gamma/2\pi) \ln z$ describes the flow in a vortex. Verify that the tangential velocity is given by $v_\theta = \Gamma/2\pi r$ and that $v_r = 0$. This type of flow is sometimes called a *free vortex*.

(b) Compare the functional dependence of v_θ on r in (a) with that which arose in Example 3.6-4. The latter kind of flow is sometimes called a *forced vortex*. Actual vortices, such as those that occur in a stirred tank, have a behavior intermediate between these two idealizations.

4B.8 The flow field about a line source. Consider the symmetric radial flow of an incompressible, inviscid fluid outward from an infinitely long uniform source, coincident with the z -axis of a cylindrical coordinate system. Fluid is being generated at a volumetric rate Γ per unit length of source.

(a) Show that the Laplace equation for the velocity potential for this system is

$$\frac{1}{r} \frac{d}{dr} \left(r \frac{d\phi}{dr} \right) = 0 \quad (4B.8-1)$$

(b) From this equation find the velocity potential, velocity, and pressure as functions of position:

$$\phi = -\frac{\Gamma}{2\pi} \ln r \quad v_r = \frac{\Gamma}{2\pi r} \quad P_\infty - P = \frac{\rho\Gamma^2}{8\pi^2 r^2} \quad (4B.8-2)$$

where P_∞ is the value of the modified pressure far away from the source.

(c) Discuss the applicability of the results in (b) to the flow field about a well drilled into a large body of porous rock.

(d) Sketch the flow net of streamlines and equipotential lines.

4B.9 Checking solutions to unsteady flow problems.

(a) Verify the solutions to the problems in Examples 4.1-1, 2, and 3 by showing that they satisfy the partial differential equations, initial conditions, and boundary conditions. To show that Eq. 4.1-15 satisfies the differential equation, one has to know how to differentiate an integral using the *Leibniz formula* given in §C.3.

(b) In Example 4.1-3 the initial condition is not satisfied by Eq. 4.1-57. Why?

4C.1 Laminar entrance flow in a slit³ (Fig. 4C.1). Estimate the velocity distribution in the entrance region of the slit shown in the figure. The fluid enters at $x = 0$ with $v_y = 0$ and $v_x = \langle v_x \rangle$, where $\langle v_x \rangle$ is the average velocity inside the slit. Assume that the velocity distribution in the entrance region $0 < x < L_e$ is

$$\frac{v_x}{v_e} = 2 \left(\frac{y}{\delta} \right) - \left(\frac{y}{\delta} \right)^2 \quad (\text{boundary layer region, } 0 < y < \delta) \quad (4C.1-1)$$

$$\frac{v_x}{v_e} = 1 \quad (\text{potential flow region, } \delta < y < B) \quad (4C.1-2)$$

in which δ and v_e are functions of x , yet to be determined.

³ A numerical solution to this problem using the Navier-Stokes equation has been given by Y. L. Wang and P. A. Longwell, *AIChE Journal*, 10, 323-329 (1964).

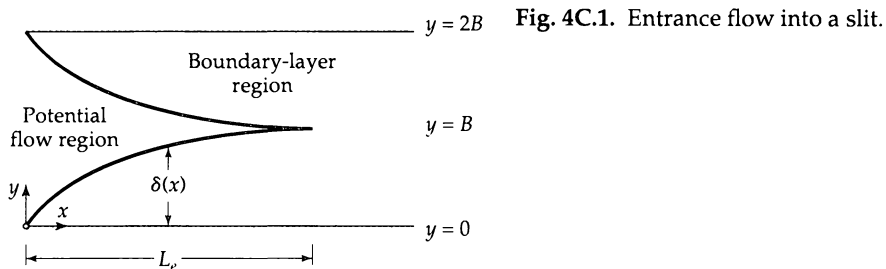


Fig. 4C.1. Entrance flow into a slit.

(a) Use the above two equations to get the mass flow rate w through an arbitrary cross section in the region $0 < x < L_e$. Then evaluate w from the inlet conditions and obtain

$$\frac{v_c(x)}{\langle v_x \rangle} = \frac{B}{B - \frac{1}{3}\delta(x)} \quad (4C.1-3)$$

(b) Next use Eqs. 4.4-13, 14, and 15 with ∞ replaced by B (why?) to obtain a differential equation for the quantity $\Delta = \delta/B$:

$$\frac{6\Delta + 7\Delta^2}{(3 - \Delta)^2} \frac{d\Delta}{dx} = 10 \left(\frac{\nu}{\langle v_x \rangle B^2} \right) \quad (4C.1-4)$$

(c) Integrate this equation with a suitable initial condition to obtain the following relation between the boundary-layer thickness and the distance down the duct:

$$\frac{\nu x}{\langle v_x \rangle B^2} = \frac{1}{10} \left[7\Delta + 48 \ln(1 - \frac{1}{3}\Delta) + \frac{27\Delta}{3 - \Delta} \right] \quad (4C.1-5)$$

(d) Compute the entrance length L_e from Eq. 4C.1-5, where L_e is that value of x for which $\delta(x) = B$.

(e) Using potential flow theory, evaluate $\mathcal{P} - \mathcal{P}_0$ in the entrance region, where \mathcal{P}_0 is the value of the modified pressure at $x = 0$.

Answers: (d) $L_e = 0.104 \langle v_x \rangle B^2 / \nu$; (e) $\mathcal{P} - \mathcal{P}_0 = \frac{1}{2} \rho \langle v_x \rangle^2 \left[1 - \left(\frac{3}{3 - \Delta} \right)^2 \right]$

4C.2 Torsional oscillatory viscometer (Fig. 4C.2). In the torsional oscillatory viscometer, the fluid is placed between a "cup" and "bob" as shown in the figure. The cup is made to undergo small sinusoidal oscillations in the tangential direction. This motion causes the bob, suspended by a torsion wire, to oscillate with the same frequency, but with a different amplitude

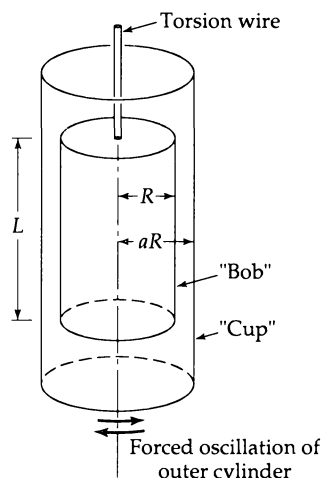


Fig. 4C.2. Sketch of a torsional oscillatory viscometer.

and phase. The amplitude ratio (ratio of amplitude of output function to input function) and phase shift both depend on the viscosity of the fluid and hence can be used for determining the viscosity. It is assumed throughout that the oscillations are of *small* amplitude. Then the problem is a linear one, and it can be solved either by Laplace transform or by the method outlined in this problem.

(a) First, apply Newton's second law of motion to the cylindrical bob for the special case that the annular space is completely evacuated. Show that the natural frequency of the system is $\omega_0 = \sqrt{k/I}$, in which I is the moment of inertia of the bob, and k is the spring constant for the torsion wire.

(b) Next, apply Newton's second law when there is a fluid of viscosity μ in the annular space. Let θ_R be the angular displacement of the bob at time t , and v_θ be the tangential velocity of the fluid as a function of r and t . Show that the equation of motion of the bob is

$$(Bob) \quad I \frac{d^2\theta_R}{dt^2} = -k\theta_R + (2\pi RL)(R) \left(\mu r \frac{\partial}{\partial r} \left(\frac{v_\theta}{r} \right) \right) \Big|_{r=R} \quad (4C.2-1)$$

If the system starts from rest, we have the initial conditions

$$\text{I.C.:} \quad \text{at } t = 0, \quad \theta_R = 0 \quad \text{and} \quad \frac{d\theta_R}{dt} = 0 \quad (4C.2-2)$$

(c) Next, write the equation of motion for the fluid along with the relevant initial and boundary conditions:

$$(Fluid) \quad \rho \frac{\partial v_\theta}{\partial t} = \mu \frac{\partial}{\partial r} \left(\frac{1}{r} \frac{\partial}{\partial r} (rv_\theta) \right) \quad (4C.2-3)$$

$$\text{I.C.:} \quad \text{at } t = 0, \quad v_\theta = 0 \quad (4C.2-4)$$

$$\text{B.C. 1:} \quad \text{at } r = R, \quad v_\theta = R \frac{d\theta_R}{dt} \quad (4C.2-5)$$

$$\text{B.C. 2:} \quad \text{at } r = aR, \quad v_\theta = aR \frac{d\theta_{aR}}{dt} \quad (4C.2-6)$$

The function $\theta_{aR}(t)$ is a specified sinusoidal function (the "input"). Draw a sketch showing θ_{aR} and θ_R as functions of time, and defining the *amplitude ratio* and the *phase shift*.

(d) Simplify the starting equations, Eqs. 4C.2-1 to 6, by making the assumption that a is only slightly greater than unity, so that the curvature may be neglected (the problem can be solved without making this assumption⁴). This suggests that a suitable dimensionless distance variable is $x = (r - R)/[(a - 1)R]$. Recast the entire problem in dimensionless quantities in such a way that $1/\omega_0 = \sqrt{I/k}$ is used as a characteristic time, and so that the viscosity appears in just one dimensionless group. The only choice turns out to be:

$$\text{time:} \quad \tau = \sqrt{\frac{k}{I}} t \quad (4C.2-7)$$

$$\text{velocity:} \quad \phi = \frac{2\pi R^3 L \rho (a - 1)}{k I} v_\theta \quad (4C.2-8)$$

$$\text{viscosity:} \quad M = \frac{\mu / \rho}{(a - 1)^2 R^2} \sqrt{\frac{I}{k}} \quad (4C.2-9)$$

$$\text{reciprocal of moment of inertia:} \quad A = \frac{2\pi R^4 L \rho (a - 1)}{I} \quad (4C.2-10)$$

⁴ H. Markovitz, *J. Appl. Phys.*, **23**, 1070–1077 (1952) has solved the problem without assuming a small spacing between the cup and bob. The cup-and-bob instrument has been used by L. J. Wittenberg, D. Ofe, and C. F. Curtiss, *J. Chem. Phys.*, **48**, 3253–3260 (1968), to measure the viscosity of liquid plutonium alloys.

Show that the problem can now be restated as follows:

$$(bob) \quad \frac{d^2\theta_R}{d\tau^2} = -\theta_R + M \left(\frac{\partial \phi}{\partial x} \right) \Big|_{x=0} \quad \text{at } t = 0, \theta_R = 0 \quad (4C.2-11)$$

$$(fluid) \quad \frac{\partial \phi}{\partial \tau} = M \frac{\partial^2 \phi}{\partial x^2} \quad \begin{cases} \text{at } \tau = 0, \phi = 0 \\ \text{at } x = 0, \phi = A(d\theta_R/dt) \\ \text{at } x = 1, \phi = A(d\theta_{aR}/dt) \end{cases} \quad (4C.2-12)$$

From these two equations we want to get θ_R and ϕ as functions of x and τ , with M and A as parameters.

(e) Obtain the “sinusoidal steady-state” solution by taking the input function θ_{aR} (the displacement of the cup) to be of the form

$$\theta_{aR}(\tau) = \theta_{aR}^0 \Re[e^{i\bar{\omega}\tau}] \quad (\theta_{aR}^0 \text{ is real}) \quad (4C.2-13)$$

in which $\bar{\omega} = \omega/\omega_0 = \omega\sqrt{I/k}$ is a dimensionless frequency. Then postulate that the bob and fluid motions will also be sinusoidal, but with different amplitudes and phases:

$$\theta_R(\tau) = \Re[\theta_R^0 e^{i\bar{\omega}\tau}] \quad (\theta_R^0 \text{ is complex}) \quad (4C.2-14)$$

$$\phi(x, \tau) = \Re[\phi^0(x)e^{i\bar{\omega}\tau}] \quad (\phi^0(x) \text{ is complex}) \quad (4C.2-15)$$

Verify that the amplitude ratio is given by $|\theta_R^0|/\theta_{aR}^0$, where $|\cdot|$ indicates the absolute magnitude of a complex quantity. Further show that the phase angle α is given by $\tan \alpha = \Im[\theta_R^0]/\Re[\theta_R^0]$, where \Re and \Im stand for the real and imaginary parts, respectively.

(f) Substitute the postulated solutions of (e) into the equations in (d) to obtain equations for the complex amplitudes θ_R^0 and ϕ^0 .

(g) Solve the equation for $\phi^0(x)$ and verify that

$$\frac{d\phi^0}{dx} \Big|_{x=0} = -\frac{A(i\bar{\omega})^{3/2}}{\sqrt{M}} \left(\frac{\theta_R^0 \cosh \sqrt{i\bar{\omega}/M} - \theta_{aR}^0}{\sinh \sqrt{i\bar{\omega}/M}} \right) \quad (4C.2-16)$$

(h) Next, solve the θ_R^0 equation to obtain

$$\frac{\theta_R^0}{\theta_{aR}^0} = \frac{AMi\bar{\omega}}{(1 - \bar{\omega}^2) \frac{\sinh \sqrt{i\bar{\omega}/M}}{\sqrt{i\bar{\omega}/M}} + AMi\bar{\omega} \cosh \sqrt{i\bar{\omega}/M}} \quad (4C.2-17)$$

from which the amplitude ratio $|\theta_R^0|/\theta_{aR}^0$ and phase shift α can be found.

(i) For high-viscosity fluids, we can seek a power series by expanding the hyperbolic functions in Eq. 4C.2-17 to get a power series in $1/M$. Show that this leads to

$$\frac{\theta_{aR}^0}{\theta_R^0} = 1 + \frac{i}{M} \left(\frac{\bar{\omega}^2 - 1}{A\bar{\omega}} + \frac{\bar{\omega}}{2} \right) - \frac{1}{M^2} \left(\frac{\bar{\omega}^2 - 1}{6A} + \frac{\bar{\omega}^2}{24} \right) + O\left(\frac{1}{M^3}\right) \quad (4C.2-18)$$

From this, find the amplitude ratio and the phase angle.

(j) Plot $|\theta_R^0|/\theta_{aR}^0$ versus $\bar{\omega}$ for $\mu/\rho = 10 \text{ cm}^2/\text{s}$, $L = 25 \text{ cm}$, $R = 5.5 \text{ cm}$, $I = 2500 \text{ gm/cm}^2$, $k = 4 \times 10^6 \text{ dyn cm}$. Where is the maximum in the curve?

4C.3 Darcy's equation for flow through porous media. For the flow of a fluid through a porous medium, the equations of continuity and motion may be replaced by

$$\text{smoothed continuity equation} \quad \varepsilon \frac{\partial p}{\partial t} = -(\nabla \cdot \rho \mathbf{v}_0) \quad (4C.3-1)$$

$$\text{Darcy's equation}^5 \quad \mathbf{v}_0 = -\frac{\kappa}{\mu} (\nabla p - \rho \mathbf{g}) \quad (4C.3-2)$$

⁵ Henry Philibert Gaspard Darcy (1803–1858) studied in Paris and became famous for designing the municipal water-supply system in Dijon, the city of his birth. H. Darcy, *Les Fontaines Publiques de la Ville de Dijon*, Victor Dalmont, Paris (1856). For further discussions of “Darcy’s law,” see J. Happel and H. Brenner, *Low Reynolds Number Hydrodynamics*, Martinus Nijhoff, Dordrecht (1983); and H. Brenner and D. A. Edwards, *Macrotransport Processes*, Butterworth-Heinemann, Boston (1993).

in which ϵ , the *porosity*, is the ratio of pore volume to total volume, and κ is the *permeability* of the porous medium. The velocity v_0 in these equations is the *superficial velocity*, which is defined as the volume rate of flow through a unit cross-sectional area of the solid plus fluid, averaged over a small region of space—small with respect to the macroscopic dimensions in the flow system, but large with respect to the pore size. The density and pressure are averaged over a region available to flow that is large with respect to the pore size. Equation 4C.3-2 was proposed empirically to describe the slow seepage of fluids through granular media.

When Eqs. 4C.3-1 and 2 are combined we get

$$\left(\frac{\epsilon\mu}{\kappa}\right)\frac{\partial p}{\partial t} = (\nabla \cdot \rho(\nabla p - \rho g)) \quad (4C.3-3)$$

for constant viscosity and permeability. This equation and the equation of state describe the motion of a fluid in a porous medium. For most purposes we may write the *equation of state* as

$$\rho = \rho_0 p^m e^{\beta p} \quad (4C.3-4)$$

in which ρ_0 is the fluid density at unit pressure, and the following parameters have been given:⁶

- | | | |
|----------------------------------|-------------|--------------------------|
| 1. Incompressible liquids | $m = 0$ | $\beta = 0$ |
| 2. Compressible liquids | $m = 0$ | $\beta \neq 0$ |
| 3. Isothermal expansion of gases | $\beta = 0$ | $m = 1$ |
| 4. Adiabatic expansion of gases | $\beta = 0$ | $m = C_V/C_p = 1/\gamma$ |

Show that Eqs. 4C.3-3 and 4 can be combined and simplified for these four categories to give (for gases it is customary to neglect the gravity terms since they are small compared with the pressure terms):

$$\text{Case 1. } \nabla^2 p = 0 \quad (4C.3-5)$$

$$\text{Case 2. } \left(\frac{\epsilon\mu\beta}{\kappa}\right)\frac{\partial p}{\partial t} = \nabla^2 p - (\nabla \cdot \rho^2 \beta g) \quad (4C.3-6)$$

$$\text{Case 3. } \left(\frac{2\epsilon\mu\rho_0}{\kappa}\right)\frac{\partial p}{\partial t} = \nabla^2 p^2 \quad (4C.3-7)$$

$$\text{Case 4. } \left(\frac{(m+1)\epsilon\mu\rho_0^{1/m}}{\kappa}\right)\frac{\partial p}{\partial t} = \nabla^2 p^{(1+m)/m} \quad (4C.3-8)$$

Note that Case 1 leads to *Laplace's equation*, Case 2 without the gravity term leads to the *heat-conduction or diffusion equation*, and Cases 3 and 4 lead to nonlinear equations.⁷

4C.4 Radial flow through a porous medium (Fig. 4C.4). A fluid flows through a porous cylindrical shell with inner and outer radii R_1 and R_2 , respectively. At these surfaces, the pressures are known to be p_1 and p_2 , respectively. The length of the cylindrical shell is h .

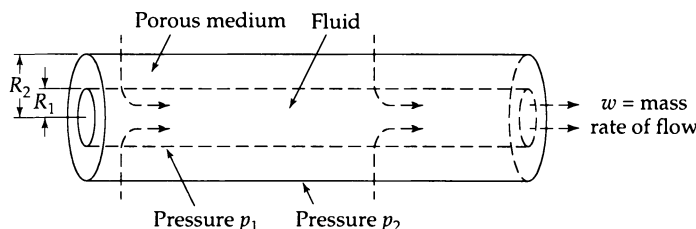


Fig. 4C.4. Radial flow through a porous medium.

⁶ M. Muskat, *Flow of Homogeneous Fluids Through Porous Media*, McGraw-Hill (1937).

⁷ For the boundary condition at a porous surface that bounds a moving fluid, see G. S. Beavers and D. D. Joseph, *J. Fluid Mech.*, **30**, 197–207 (1967) and G. S. Beavers, E. M. Sparrow, and B. A. Masha, *AIChE Journal*, **20**, 596–597 (1974).

(a) Find the pressure distribution, radial flow velocity, and mass rate of flow for an incompressible fluid.

(b) Rework (a) for a compressible liquid and for an ideal gas.

$$\text{Answers: (a)} \frac{\mathcal{P} - \mathcal{P}_1}{\mathcal{P}_2 - \mathcal{P}_1} = \frac{\ln(r/R_1)}{\ln(R_2/R_1)} \quad v_{0r} = -\frac{\kappa}{\mu r} \frac{\mathcal{P}_2 - \mathcal{P}_1}{\ln(\mathcal{P}_2/\mathcal{P}_1)} \quad w = \frac{2\pi\kappa h(p_2 - p_1)\rho}{\mu \ln(R_2/R_1)}$$

4D.1 Flow near an oscillating wall.⁸ Show, by using Laplace transforms, that the complete solution to the problem stated in Eqs. 4.1-44 to 47 is

$$\frac{v_x}{v_0} = e^{-\sqrt{\omega/2\nu}y} \cos(\omega t - \sqrt{\omega/2\nu}y) - \frac{1}{\pi} \int_0^\infty e^{-\bar{\omega}t} (\sin \sqrt{\omega/\nu}y) \frac{\bar{\omega}}{\omega^2 + \bar{\omega}^2} d\bar{\omega} \quad (4D.1-1)$$

4D.2 Start-up of laminar flow in a circular tube (Fig. 4D.2). A fluid of constant density and viscosity is contained in a very long pipe of length L and radius R . Initially the fluid is at rest. At time $t = 0$, a pressure gradient $(\mathcal{P}_0 - \mathcal{P}_L)/L$ is imposed on the system. Determine how the velocity profiles change with time.

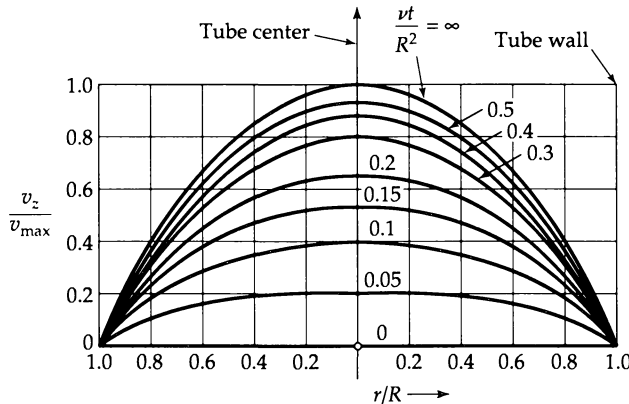


Fig. 4D.2. Velocity distribution for the unsteady flow resulting from a suddenly impressed pressure gradient in a circular tube [P. Szymanski, *J. Math. Pures Appl.*, Series 9, 11, 67–107 (1932)].

(a) Show that the relevant equation of motion can be put into dimensionless form as follows:

$$\frac{\partial \phi}{\partial \tau} = 4 + \frac{1}{\xi} \frac{\partial}{\partial \xi} \left(\xi \frac{\partial \phi}{\partial \xi} \right) \quad (4D.2-1)$$

in which $\xi = r/R$, $\tau = \mu t / \rho R^2$, and $\phi = [(\mathcal{P}_0 - \mathcal{P}_L)R^2 / 4\mu L]^{-1}v_z$.

(b) Show that the asymptotic solution for large time is $\phi_\infty = 1 - \xi^2$. Then define ϕ_t by $\phi(\xi, \tau) = \phi_\infty(\xi) - \phi_t(\xi, \tau)$, and solve the partial differential equation for ϕ_t by the method of separation of variables.

(c) Show that the final solution is

$$\phi(\xi, \tau) = (1 - \xi^2) - 8 \sum_{n=1}^{\infty} \frac{J_0(\alpha_n \xi)}{\alpha_n^3 J_1(\alpha_n)} \exp(-\alpha_n^2 \tau) \quad (4D.2-2)$$

in which $J_n(\xi)$ is the n th order Bessel function of ξ , and the α_n are the roots of the equation $J_0(\alpha_n) = 0$. The result is plotted in Fig. 4D.2.

⁸ H. S. Carslaw and J. C. Jaeger, *Conduction of Heat in Solids*, Oxford University Press, 2nd edition (1959), p. 319, Eq. (8), with $\varepsilon = \frac{1}{2}\pi$ and $\bar{\omega} = \kappa u^2$.

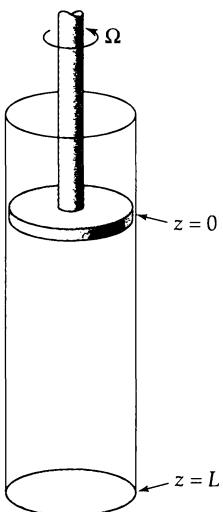


Fig. 4D.3. Rotating disk in a circular tube.

4D.3 Flows in the disk-and-tube system (Fig. 4D.3).⁹

- (a) A fluid in a circular tube is caused to move tangentially by a tightly fitting rotating disk at the liquid surface at $z = 0$; the bottom of the tube is located at $z = L$. Find the steady-state velocity distribution $v_\theta(r, z)$, when the angular velocity of the disk is Ω . Assume that creeping flow prevails throughout, so that there is no secondary flow. Find the limit of the solution as $L \rightarrow \infty$.
- (b) Repeat the problem for the unsteady flow. The fluid is at rest before $t = 0$, and the disk suddenly begins to rotate with an angular velocity Ω at $t = 0$. Find the velocity distribution $v_\theta(r, z, t)$ for a column of fluid of height L . Then find the solution for the limit as $L \rightarrow \infty$.
- (c) If the disk is oscillating sinusoidally in the tangential direction with amplitude Ω_0 , obtain the velocity distribution in the tube when the "oscillatory steady state" has been attained. Repeat the problem for a tube of infinite length.

4D.4 Unsteady annular flows.¹⁰

- (a) Obtain a solution to the Navier-Stokes equation for the start-up of *axial* annular flow by a sudden impressed pressure gradient. Check your result against the published solution.
- (b) Solve the Navier-Stokes equation for the unsteady *tangential* flow in an annulus. The fluid is at rest for $t < 0$. Starting at $t = 0$ the outer cylinder begins rotating with a constant angular velocity to cause laminar flow for $t > 0$. Compare your result with the published solution.¹¹

4D.5 Stream functions for steady three-dimensional flow.

- (a) Show that the velocity functions $\rho\mathbf{v} = [\nabla \times \mathbf{A}]$ and $\rho\mathbf{v} = [(\nabla\psi_1) \times (\nabla\psi_2)]$ both satisfy the equation of continuity identically for steady compressible flow. The functions ψ_1 , ψ_2 , and \mathbf{A} are arbitrary, except that their derivatives appearing in $(\nabla \cdot \rho\mathbf{v})$ must exist.
- (b) Show that, for the conditions of Table 4.2-1, the vector \mathbf{A} has the magnitude $-\rho\psi h_3$ and the direction of the coordinate normal to \mathbf{v} . Here h_3 is the scale factor for the third coordinate (see §A.7).
- (c) Show that the streamlines corresponding to Eq. 4.3-2 are given by the intersections of the surfaces $\psi_1 = \text{constant}$ and $\psi_2 = \text{constant}$. Sketch such a pair of surfaces for the flow in Fig. 4.3-1.
- (d) Use Stokes' theorem (Eq. A.5-4) to obtain an expression in terms of \mathbf{A} for the mass flow rate through a surface S bounded by a closed curve C . Show that the vanishing of \mathbf{v} on C does not imply the vanishing of \mathbf{A} on C .

⁹ W. Hort, *Z. tech. Phys.*, **10**, 213 (1920); C. T. Hill, J. D. Huppner, and R. B. Bird, *Chem. Engr. Sci.*, **21**, 815–817 (1966).

¹⁰ W. Müller, *Zeits. für angew. Math. u. Mech.*, **16**, 227–228 (1936).

¹¹ R. B. Bird and C. F. Curtiss, *Chem. Engr. Sci.*, **11**, 108–113 (1959).

Velocity Distributions in Turbulent Flow

- §5.1 Comparisons of laminar and turbulent flows
- §5.2 Time-smoothed equations of change for incompressible fluids
- §5.3 The time-smoothed velocity profile near a wall
- §5.4 Empirical expressions for the turbulent momentum flux
- §5.5 Turbulent flow in ducts
- §5.6° Turbulent flow in jets

In the previous chapters we discussed laminar flow problems only. We have seen that the differential equations describing laminar flow are well understood and that, for a number of simple systems, the velocity distribution and various derived quantities can be obtained in a straightforward fashion. The limiting factor in applying the equations of change is the mathematical complexity that one encounters in problems for which there are several velocity components that are functions of several variables. Even there, with the rapid development of computational fluid dynamics, such problems are gradually yielding to numerical solution.

In this chapter we turn our attention to turbulent flow. Whereas laminar flow is orderly, turbulent flow is chaotic. It is this chaotic nature of turbulent flow that poses all sorts of difficulties. In fact, one might question whether or not the equations of change given in Chapter 3 are even capable of describing the violently fluctuating motions in turbulent flow. Since the sizes of the turbulent eddies are several orders of magnitude larger than the mean free path of the molecules of the fluid, the equations of change *are* applicable. Numerical solutions of these equations are obtainable and can be used for studying the details of the turbulence structure. For many purposes, however, we are not interested in having such detailed information, in view of the computational effort required. Therefore, in this chapter we shall concern ourselves primarily with methods that enable us to describe the time-smoothed velocity and pressure profiles.

In §5.1 we start by comparing the experimental results for laminar and turbulent flows in several flow systems. In this way we can get some qualitative ideas about the main differences between laminar and turbulent motions. These experiments help to define some of the challenges that face the fluid dynamicist.

In §5.2 we define several *time-smoothed* quantities, and show how these definitions can be used to time-average the equations of change over a short time interval. These equations describe the behavior of the time-smoothed velocity and pressure. The time-smoothed equation of motion, however, contains the *turbulent momentum flux*. This flux

cannot be simply related to velocity gradients in the way that the momentum flux is given by Newton's law of viscosity in Chapter 1. At the present time the turbulent momentum flux is usually estimated experimentally or else modeled by some type of empiricism based on experimental measurements.

Fortunately, for turbulent flow near a solid surface, there are several rather general results that are very helpful in fluid dynamics and transport phenomena: the Taylor series development for the velocity near the wall; and the logarithmic and power law velocity profiles for regions further from the wall, the latter being obtained by dimensional reasoning. These expressions for the time-smoothed velocity distribution are given in §5.3.

In the following section, §5.4, we present a few of the empiricisms that have been proposed for the turbulent momentum flux. These empiricisms are of historical interest and have also been widely used in engineering calculations. When applied with proper judgment, these empirical expressions can be useful.

The remainder of the chapter is devoted to a discussion of two types of turbulent flows: flows in closed conduits (§5.5) and flows in jets (§5.6). These flows illustrate the two classes of flows that are usually discussed under the headings of *wall turbulence* and *free turbulence*.

In this brief introduction to turbulence we deal primarily with the description of the fully developed turbulent flow of an incompressible fluid. We do not consider the theoretical methods for predicting the inception of turbulence nor the experimental techniques devised for probing the structure of turbulent flow. We also give no discussion of the statistical theories of turbulence and the way in which the turbulent energy is distributed over the various modes of motion. For these and other interesting topics, the reader should consult some of the standard books on turbulence.¹⁻⁶ There is a growing literature on experimental and computational evidence for "coherent structures" (vortices) in turbulent flows.⁷

Turbulence is an important subject. In fact, most flows encountered in engineering are turbulent and not laminar! Although our understanding of turbulence is far from satisfactory, it is a subject that must be studied and appreciated. For the solution to industrial problems we cannot get neat analytical results, and, for the most part, such problems are attacked by using a combination of dimensional analysis and experimental data. This method is discussed in Chapter 6.

¹ S. Corrsin, "Turbulence: Experimental Methods," in *Handbuch der Physik*, Springer, Berlin (1963), Vol. VIII/2. **Stanley Corrsin** (1920–1986), a professor at The Johns Hopkins University, was an excellent experimentalist and teacher; he studied the interaction between chemical reactions and turbulence and the propagation of the double temperature correlations.

² A. A. Townsend, *The Structure of Turbulent Shear Flow*, Cambridge University Press, 2nd edition (1976); see also A. A. Townsend in *Handbook of Fluid Dynamics* (V. L. Streeter, ed.), McGraw-Hill (1961) for a readable survey.

³ J. O. Hinze, *Turbulence*, McGraw-Hill, New York, 2nd edition (1975).

⁴ H. Tennekes and J. L. Lumley, *A First Course in Turbulence*, MIT Press, Cambridge, Mass. (1972); Chapters 1 and 2 of this book provide an introduction to the physical interpretations of turbulent flow phenomena.

⁵ M. Lesieur, *La Turbulence*, Presses Universitaires de Grenoble (1994); this book contains beautiful color photographs of turbulent flow systems.

⁶ Several books that cover material beyond the scope of this text are: W. D. McComb, *The Physics of Fluid Turbulence*, Oxford University Press (1990); T. E. Faber, *Fluid Dynamics for Physicists*, Cambridge University Press (1995); U. Frisch, *Turbulence*, Cambridge University Press (1995).

⁷ P. Holmes, J. L. Lumley, and G. Berkooz, *Turbulence, Coherent Structures, Dynamical Systems, and Symmetry*, Cambridge University Press (1996); F. Waleffe, *Phys. Rev. Lett.*, **81**, 4140–4148 (1998).

§5.1 COMPARISONS OF LAMINAR AND TURBULENT FLOWS

Before discussing any theoretical ideas about turbulence, it is important to summarize the differences between laminar and turbulent flows in several simple systems. Specifically we consider the flow in conduits of circular and triangular cross section, flow along a flat plate, and flows in jets. The first three of these were considered for laminar flow in §2.3, Problem 3B.2, and §4.4.

Circular Tubes

For the steady, fully developed, laminar flow in a circular tube of radius R we know that the velocity distribution and the average velocity are given by

$$\frac{v_z}{v_{z,\max}} = 1 - \left(\frac{r}{R}\right)^2 \quad \text{and} \quad \frac{\langle v_z \rangle}{v_{z,\max}} = \frac{1}{2} \quad (\text{Re} < 2100) \quad (5.1-1, 2)$$

and that the pressure drop and mass flow rate w are linearly related:

$$\mathcal{P}_0 - \mathcal{P}_L = \left(\frac{8\mu L}{\pi\rho R^4}\right)w \quad (\text{Re} < 2100) \quad (5.1-3)$$

For turbulent flow, on the other hand, the velocity is fluctuating with time chaotically at each point in the tube. We can measure a “time-smoothed velocity” at each point with, say, a Pitot tube. This type of instrument is not sensitive to rapid velocity fluctuations, but senses the velocity averaged over several seconds. The time-smoothed velocity (which is defined in the next section) will have a z -component represented by \bar{v}_z , and its shape and average value will be given very roughly by¹

$$\frac{\bar{v}_z}{v_{z,\max}} \approx \left(1 - \frac{r}{R}\right)^{1/7} \quad \text{and} \quad \frac{\langle \bar{v}_z \rangle}{v_{z,\max}} \approx \frac{4}{5} \quad (10^4 < \text{Re} < 10^5) \quad (5.1-4, 5)$$

This $\frac{1}{7}$ -power expression for the velocity distribution is too crude to give a realistic velocity derivative at the wall. The laminar and turbulent velocity profiles are compared in Fig. 5.1-1.

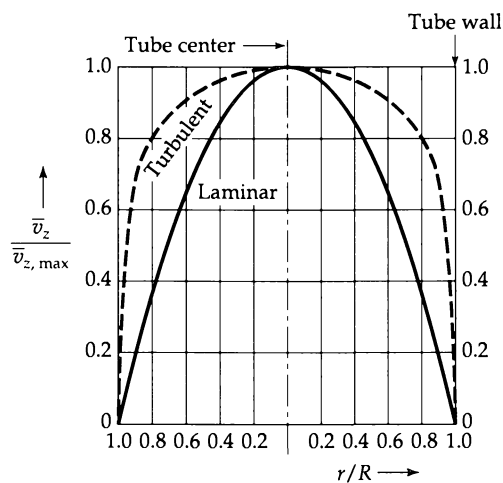


Fig. 5.1-1. Qualitative comparison of laminar and turbulent velocity profiles. For a more detailed description of the turbulent velocity distribution near the wall, see Fig. 5.5-3.

¹ H. Schlichting, *Boundary-Layer Theory*, McGraw-Hill, New York, 7th edition (1979), Chapter XX (tube flow), Chapters VII and XXI (flat plate flow), Chapters IX and XXIV (jet flows).

Over the same range of Reynolds numbers the mass rate of flow and the pressure drop are no longer proportional but are related approximately by

$$\mathcal{P}_0 - \mathcal{P}_L \approx 0.198 \left(\frac{2}{\pi} \right)^{7/4} \left(\frac{\mu^{1/4} L}{\rho R^{19/4}} \right) w^{7/4} \quad (10^4 < \text{Re} < 10^5) \quad (5.1-6)$$

The stronger dependence of pressure drop on mass flow rate for turbulent flow results from the fact that more energy has to be supplied to maintain the violent eddy motion in the fluid.

The laminar-turbulent transition in circular pipes normally occurs at a *critical Reynolds number* of roughly 2100, although this number may be higher if extreme care is taken to eliminate vibrations in the system.² The transition from laminar flow to turbulent flow can be demonstrated by the simple experiment originally performed by Reynolds. One sets up a long transparent tube equipped with a device for injecting a small amount of dye into the stream along the tube axis. When the flow is laminar, the dye moves downstream as a straight, coherent filament. For turbulent flow, on the other hand, the dye spreads quickly over the entire cross section, similarly to the motion of particles in Fig. 2.0-1, because of the eddying motion (turbulent diffusion).

Noncircular Tubes

For developed laminar flow in the triangular duct shown in Fig. 3B.2(b), the fluid particles move rectilinearly in the z direction, parallel to the walls of the duct. By contrast, in turbulent flow there is superposed on the time-smoothed flow in the z direction (the *primary flow*) a time-smoothed motion in the xy -plane (the *secondary flow*). The secondary flow is much weaker than the primary flow and manifests itself as a set of six vortices arranged in a symmetric pattern around the duct axis (see Fig. 5.1-2). Other noncircular tubes also exhibit secondary flows.

Flat Plate

In §4.4 we found that for the laminar flow around a flat plate, wetted on both sides, the solution of the boundary layer equations gave the drag force expression

$$F = 1.328 \sqrt{\rho \mu L W^2 v_\infty^3} \quad (\text{laminar}) \quad 0 < \text{Re}_L < 5 \times 10^5 \quad (5.1-7)$$

in which $\text{Re}_L = Lv_\infty/\mu$ is the Reynolds number for a plate of length L ; the plate width is W , and the approach velocity of the fluid is v_∞ .

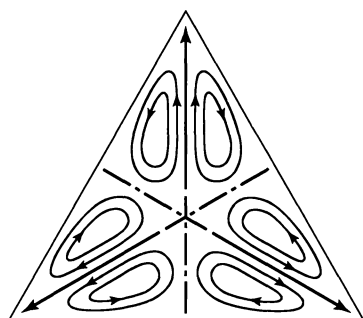


Fig. 5.1-2. Sketch showing the secondary flow patterns for turbulent flow in a tube of triangular cross section [H. Schlichting, *Boundary-Layer Theory*, McGraw-Hill, New York, 7th edition (1979), p. 613].

² O. Reynolds, *Phil. Trans. Roy. Soc.*, **174**, Part III, 935–982 (1883). See also A. A. Draad and F. M. T. Nieuwstadt, *J. Fluid Mech.*, **361**, 297–308 (1998).

Table 5.1-1 Dependence of Jet Parameters on Distance z from Wall

	Laminar flow			Turbulent flow		
	Width of jet	Centerline velocity	Mass flow rate	Width of jet	Centerline velocity	Mass flow rate
Circular jet	z	z^{-1}	z	z	z^{-1}	z
Plane jet	$z^{2/3}$	$z^{-1/3}$	$z^{1/3}$	z	$z^{-1/2}$	$z^{1/2}$

For turbulent flow, on the other hand, the dependence on the geometrical and physical properties is quite different:¹

$$F \approx 0.74 \sqrt[5]{\rho^4 \mu L^4 W^5 v_\infty^9} \quad (\text{turbulent}) \quad (5 \times 10^5 < \text{Re}_L < 10^7) \quad (5.1-8)$$

Thus the force is proportional to the $\frac{3}{2}$ -power of the approach velocity for laminar flow, but to the $\frac{9}{5}$ -power for turbulent flow. The stronger dependence on the approach velocity reflects the extra energy needed to maintain the irregular eddy motions in the fluid.

Circular and Plane Jets

Next we examine the behavior of jets that emerge from a flat wall, which is taken to be the xy -plane (see Fig. 5.6-1). The fluid comes out from a circular tube or a long narrow slot, and flows into a large body of the same fluid. Various observations on the jets can be made: the width of the jet, the centerline velocity of the jet, and the mass flow rate through a cross section parallel to the xy -plane. All these properties can be measured as functions of the distance z from the wall. In Table 5.1-1 we summarize the properties of the circular and two-dimensional jets for laminar and turbulent flow.¹ It is curious that, for the circular jet, the jet width, centerline velocity, and mass flow rate have exactly the same dependence on z in both laminar and turbulent flow. We shall return to this point later in §5.6.

The above examples should make it clear that the gross features of laminar and turbulent flow are generally quite different. One of the many challenges in turbulence theory is to try to explain these differences.

§5.2 TIME-SMOOTHED EQUATIONS OF CHANGE FOR INCOMPRESSIBLE FLUIDS

We begin by considering a turbulent flow in a tube with a constant imposed pressure gradient. If at one point in the fluid we observe one component of the velocity as a function of time, we find that it is fluctuating in a chaotic fashion as shown in Fig. 5.2-1(a). The fluctuations are irregular deviations from a mean value. The actual velocity can be regarded as the sum of the mean value (designated by an overbar) and the fluctuation (designated by a prime). For example, for the z -component of the velocity we write

$$v_z = \bar{v}_z + v'_z \quad (5.2-1)$$

which is sometimes called the *Reynolds decomposition*. The mean value is obtained from $v_z(t)$ by making a time average over a large number of fluctuations

$$\bar{v}_z = \frac{1}{t_0} \int_{t-\frac{1}{2}t_0}^{t+\frac{1}{2}t_0} v_z(s) ds \quad (5.2-2)$$

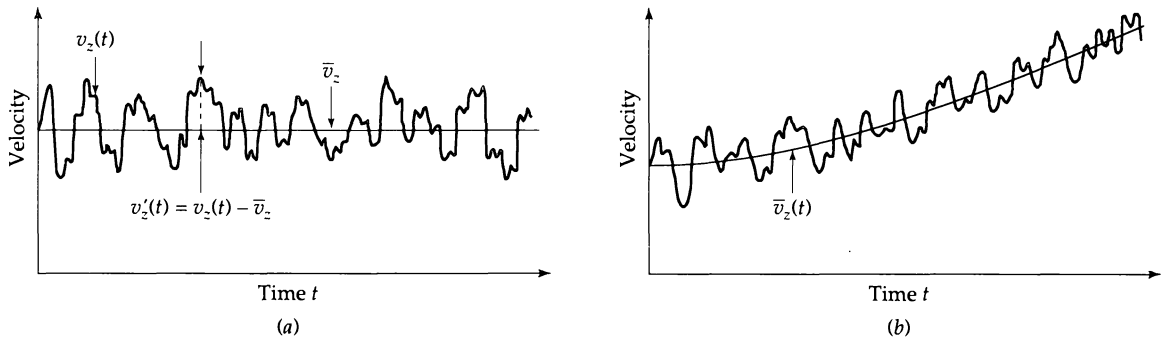


Fig. 5.2-1. Sketch showing the velocity component v_z as well as its time-smoothed value \bar{v}_z and its fluctuation v'_z in turbulent flow (a) for “steadily driven turbulent flow” in which \bar{v}_z does not depend on time, and (b) for a situation in which \bar{v}_z does depend on time.

the period t_0 being long enough to give a smooth averaged function. For the system at hand, the quantity \bar{v}_z , which we call the *time-smoothed velocity*, is independent of time, but of course depends on position. When the time-smoothed velocity does not depend on time, we speak of *steadily driven turbulent flow*. The same comments we have made for velocity can also be made for pressure.

Next we consider turbulent flow in a tube with a time-dependent pressure gradient. For such a flow one can define time-smoothed quantities as above, but one has to understand that the period t_0 must be small with respect to the changes in the pressure gradient, but still large with respect to the periods of fluctuations. For such a situation the time-smoothed velocity and the actual velocity are illustrated in Fig. 5.2-1(b).¹

According to the definition in Eq. 5.5-2, it is easy to verify that the following relations are true:

$$\overline{v'_z} = 0 \quad \overline{\bar{v}_z} = \bar{v}_z \quad \overline{\bar{v}_z v'_z} = 0 \quad \overline{\frac{\partial}{\partial x} v_z} = \frac{\partial}{\partial x} \bar{v}_z \quad \overline{\frac{\partial}{\partial t} v_z} = \frac{\partial}{\partial t} \bar{v}_z \quad (5.2-3)$$

The quantity $\overline{v'^2}$ will not, however, be zero, and in fact the ratio $\sqrt{\overline{v'^2}}/\langle \bar{v}_z \rangle$ can be taken to be a measure of the magnitude of the turbulent fluctuations. This quantity, known as the *intensity of turbulence*, may have values from 1 to 10% in the main part of a turbulent stream and values of 25% or higher in the neighborhood of a solid wall. Hence, it must be emphasized that we are not necessarily dealing with tiny disturbances; sometimes the fluctuations are actually quite violent and large.

Quantities such as $\overline{v'_x v'_y}$ are also nonzero. The reason for this is that the local motions in the x and y directions are *correlated*. In other words, the fluctuations in the x direction are not independent of the fluctuations in the y direction. We shall see presently that these time-smoothed values of the products of fluctuating properties have an important role in turbulent momentum transfer. Later we shall find similar correlations arising in turbulent heat and mass transport.

¹ One can also define the “overbar” quantities in terms of an “ensemble average.” For most purposes the results are equivalent or are assumed to be so. See, for example, A. A. Townsend, *The Structure of Turbulent Shear Flow*, Cambridge University Press, 2nd edition (1976). See also P. K. Kundu, *Fluid Mechanics*, Academic Press, New York (1990), p. 421, regarding the last of the formulas given in Eq. 5.2-3.

Having defined the time-smoothed quantities and discussed some of the properties of the fluctuating quantities, we can now move on to the time-smoothing of the equations of change. To keep the development as simple as possible, we consider here only the equations for a fluid of constant density and viscosity. We start by writing the equations of continuity and motion with \mathbf{v} replaced by its equivalent $\bar{\mathbf{v}} + \mathbf{v}'$ and p by its equivalent $\bar{p} + p'$. The equation of continuity is then $(\nabla \cdot \mathbf{v}) = 0$, and we write the x -component of the equation of motion, Eq. 3.5-6, in the $\partial/\partial t$ form by using Eq. 3.5-5:

$$\frac{\partial}{\partial x} (\bar{v}_x + v'_x) + \frac{\partial}{\partial y} (\bar{v}_y + v'_y) + \frac{\partial}{\partial z} (\bar{v}_z + v'_z) = 0 \quad (5.2-4)$$

$$\begin{aligned} \frac{\partial}{\partial t} \rho(\bar{v}_x + v'_x) &= -\frac{\partial}{\partial x} (\bar{p} + p') - \left(\frac{\partial}{\partial x} \rho(\bar{v}_x + v'_x)(\bar{v}_x + v'_x) + \frac{\partial}{\partial y} \rho(\bar{v}_y + v'_y)(\bar{v}_x + v'_x) \right. \\ &\quad \left. + \frac{\partial}{\partial z} \rho(\bar{v}_z + v'_z)(\bar{v}_x + v'_x) \right) + \mu \nabla^2 (\bar{v}_x + v'_x) + \rho g_x \end{aligned} \quad (5.2-5)$$

The y - and z -components of the equation of motion can be similarly written. We next time-smooth these equations, making use of the relations given in Eq. 5.2-3. This gives

$$\frac{\partial}{\partial x} \bar{v}_x + \frac{\partial}{\partial y} \bar{v}_y + \frac{\partial}{\partial z} \bar{v}_z = 0 \quad (5.2-6)$$

$$\begin{aligned} \frac{\partial}{\partial t} \rho \bar{v}_x &= -\frac{\partial}{\partial x} \bar{p} - \left(\frac{\partial}{\partial x} \rho \bar{v}_x \bar{v}_x + \frac{\partial}{\partial y} \rho \bar{v}_y \bar{v}_x + \frac{\partial}{\partial z} \rho \bar{v}_z \bar{v}_x \right) \\ &\quad - \left(\frac{\partial}{\partial x} \rho \bar{v}_x' \bar{v}_x' + \frac{\partial}{\partial y} \rho \bar{v}_y' \bar{v}_x' + \frac{\partial}{\partial z} \rho \bar{v}_z' \bar{v}_x' \right) + \mu \nabla^2 \bar{v}_x + \rho g_x \end{aligned} \quad (5.2-7)$$

with similar relations for the y - and z -components of the equation of motion. These are then the *time-smoothed equations of continuity and motion* for a fluid with constant density and viscosity. By comparing them with the corresponding equations in Eq. 3.1-5 and Eq. 3.5-6 (the latter rewritten in terms of $\partial/\partial t$), we conclude that

- a. The equation of continuity is the same as we had previously, except that \mathbf{v} is now replaced by $\bar{\mathbf{v}}$.
- b. The equation of motion now has $\bar{\mathbf{v}}$ and \bar{p} where we previously had \mathbf{v} and p . In addition there appear the dashed-underlined terms, which describe the momentum transport associated with the turbulent fluctuations.

We may rewrite Eq. 5.2-7 by introducing the *turbulent momentum flux tensor* $\bar{\tau}^{(t)}$ with components

$$\bar{\tau}_{xx}^{(t)} = \rho \bar{v}_x' \bar{v}_x' \quad \bar{\tau}_{xy}^{(t)} = \rho \bar{v}_y' \bar{v}_x' \quad \bar{\tau}_{xz}^{(t)} = \rho \bar{v}_z' \bar{v}_x' \text{ and so on} \quad (5.2-8)$$

These quantities are usually referred to as the *Reynolds stresses*. We may also introduce a symbol $\bar{\tau}^{(v)}$ for the time-smoothed viscous momentum flux. The components of this tensor have the same appearance as the expressions given in Appendices B.1 to B.3, except that the time-smoothed velocity components appear in them:

$$\bar{\tau}_{xx}^{(v)} = -2\mu \frac{\partial \bar{v}_x}{\partial x} \quad \bar{\tau}_{xy}^{(v)} = -\mu \left(\frac{\partial \bar{v}_y}{\partial x} + \frac{\partial \bar{v}_x}{\partial y} \right) \text{ and so on} \quad (5.2-9)$$

This enables us then to write the equations of change in vector-tensor form as

$$(\nabla \cdot \bar{\mathbf{v}}) = 0 \quad \text{and} \quad (\nabla \cdot \mathbf{v}') = 0 \quad (5.2-10, 11)$$

$$\frac{\partial}{\partial t} \rho \bar{\mathbf{v}} = -\nabla \bar{p} - [\nabla \cdot \rho \bar{\mathbf{v}} \bar{\mathbf{v}}] - [\nabla \cdot (\bar{\tau}^{(v)} + \bar{\tau}^{(t)})] + \rho \mathbf{g} \quad (5.2-12)$$

Equation 5.2-11 is an extra equation obtained by subtracting Eq. 5.2-10 from the original equation of continuity.

The principal result of this section is that the equation of motion in terms of the stress tensor, summarized in Appendix Table B.5, can be adapted for time-smoothed turbulent flow by changing all v_i to \bar{v}_i and p to \bar{p} as well as τ_{ij} to $\bar{\tau}_{ij} = \bar{\tau}_{ij}^{(v)} + \bar{\tau}_{ij}^{(t)}$ in any of the coordinate systems given.

We have now arrived at the main stumbling block in the theory of turbulence. The Reynolds stresses $\bar{\tau}_{ij}^{(t)}$ above are not related to the velocity gradients in a simple way as are the time-smoothed viscous stresses $\bar{\tau}_{ij}^{(v)}$ in Eq. 5.2-9. They are, instead, complicated functions of the position and the turbulence intensity. To solve flow problems we must have experimental information about the Reynolds stresses or else resort to some empirical expression. In §5.4 we discuss some of the empiricisms that are available.

Actually one can also obtain equations of change for the Reynolds stresses (see Problem 5D.1). However, these equations contain quantities like $v'_i v'_j v'_k$. Similarly, the equations of change for the $v'_i v'_j v'_k$ contain the next higher-order correlation $v'_i v'_j v'_k v'_l$, and so on. That is, there is a never-ending hierarchy of equations that must be solved. To solve flow problems one has to "truncate" this hierarchy by introducing empiricisms. If we use empiricisms for the Reynolds stresses, we then have a "first-order" theory. If we introduce empiricisms for the $v'_i v'_j v'_k$, we then have a "second-order theory," and so on. The problem of introducing empiricisms to get a closed set of equations that can be solved for the velocity and pressure distributions is referred to as the "closure problem." The discussion in §5.4 deals with closure at the first order. At the second order the " $k-\epsilon$ empiricism" has been extensively studied and widely used in computational fluid mechanics.²

§5.3 THE TIME-SMOOTHED VELOCITY PROFILE NEAR A WALL

Before we discuss the various empirical expressions used for the Reynolds stresses, we present here several developments that do not depend on any empiricisms. We are concerned here with the fully developed, time-smoothed velocity distribution in the neighborhood of a wall. We discuss several results: a Taylor expansion of the velocity near the wall, and the universal logarithmic and power law velocity distributions a little further out from the wall.

The flow near a flat surface is depicted in Fig. 5.3-1. It is convenient to distinguish four regions of flow:

- the *viscous sublayer* very near the wall, in which viscosity plays a key role
- the *buffer layer* in which the transition occurs between the viscous and inertial sublayers
- the *inertial sublayer* at the beginning of the main turbulent stream, in which viscosity plays at most a minor role
- the *main turbulent stream*, in which the time-smoothed velocity distribution is nearly flat and viscosity is unimportant

It must be emphasized that this classification into regions is somewhat arbitrary.

² J. L. Lumley, *Adv. Appl. Mech.*, **18**, 123–176 (1978); C. G. Speziale, *Ann. Revs. Fluid Mech.*, **23**, 107–157 (1991); H. Schlichting and K. Gersten, *Boundary-Layer Theory*, Springer, Berlin, 8th edition (2000), pp. 560–563.

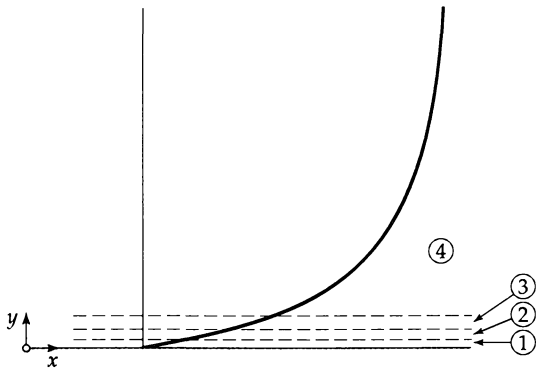


Fig. 5.3-1. Flow regions for describing turbulent flow near a wall: ① viscous sublayer, ② buffer layer, ③ inertial sublayer, ④ main turbulent stream.

The Logarithmic and Power Law Velocity Profiles in the Inertial Sublayer¹⁻⁴

Let the time-smoothed shear stress acting on the wall $y = 0$ be called τ_0 (this is the same as $-\bar{\tau}_{yx}|_{y=0}$). Then the shear stress in the inertial sublayer will not be very different from the value τ_0 . We now ask: On what quantities will the time-smoothed velocity gradient $d\bar{v}_x/dy$ depend? It should not depend on the viscosity, since, out beyond the buffer layer, momentum transport should depend primarily on the velocity fluctuations (loosely referred to as "eddy motion"). It may depend on the density ρ , the wall shear stress τ_0 , and the distance y from the wall. The only combination of these three quantities that has the dimensions of a velocity gradient is $\sqrt{\tau_0/\rho}/y$. Hence we write

$$\frac{d\bar{v}_x}{dy} = \frac{1}{\kappa} \sqrt{\frac{\tau_0}{\rho}} \frac{1}{y} \quad (5.3-1)$$

in which κ is an arbitrary dimensionless constant, which must be determined experimentally. The quantity $\sqrt{\tau_0/\rho}$ has the dimensions of velocity; it is called the *friction velocity* and given the symbol v_* . When Eq. 5.3-1 is integrated we get

$$\bar{v}_x = \frac{v_*}{\kappa} \ln y + \lambda' \quad (5.3-2)$$

λ' being an integration constant. To use dimensionless groupings, we rewrite Eq. 5.3-2 as

$$\frac{\bar{v}_x}{v_*} = \frac{1}{\kappa} \ln \left(\frac{y v_*}{\nu} \right) + \lambda \quad (5.3-3)$$

in which λ is a constant simply related to λ' ; the kinematic viscosity ν was included in order to construct the dimensionless argument of the logarithm. Experimentally it has been found that reasonable values of the constants² are $\kappa = 0.4$ and $\lambda = 5.5$, giving

$$\frac{\bar{v}_x}{v_*} = 2.5 \ln \left(\frac{y v_*}{\nu} \right) + 5.5 \quad \frac{y v_*}{\nu} > 30 \quad (5.3-4)$$

¹ L. Landau and E. M. Lifshitz, *Fluid Mechanics*, Pergamon, Oxford, 2nd edition (1987), pp. 172–178.

² H. Schlichting and K. Gersten, *Boundary-Layer Theory*, Springer-Verlag, Berlin, 8th edition (2000), §17.2.3.

³ T. von Kármán, *Nachr. Ges. Wiss. Göttingen, Math-Phys. Klasse* (1930), pp. 58–76; L. Prandtl, *Ergeb. Aerodyn. Versuch.*, Series 4, Göttingen (1932).

⁴ G. I. Barenblatt and A. J. Chorin, *Proc. Nat. Acad. Sci. USA*, **93**, 6749–6752 (1996) and *SIAM Rev.*, **40**, 265–291 (1981); G. I. Barenblatt, A. J. Chorin, and V. M. Prostokishin, *Proc. Nat. Acad. Sci. USA*, **94**, 773–776 (1997). See also G. I. Barenblatt, *Scaling, Self-Similarity, and Intermediate Asymptotics*, Cambridge University Press (1992), §10.2.

This is called the *von Kármán-Prandtl universal logarithmic velocity distribution*,³ it is intended to apply only in the inertial sublayer. Later we shall see (in Fig. 5.5-3) that this function describes moderately well the experimental data somewhat beyond the inertial sublayer.

If Eq. 5.3-1 were correct, then the constants κ and λ would indeed be “universal constants,” applicable at any Reynolds number. However, values of κ in the range 0.40 to 0.44 and values of λ in the range 5.0 to 6.3 can be found in the literature, depending on the range of Reynolds numbers. This suggests that the right side of Eq. 5.3-1 should be multiplied by some function of Reynolds number and that y could be raised to some power involving the Reynolds number. Theoretical arguments have been advanced⁴ that Eq. 5.3-1 should be replaced by

$$\frac{d\bar{v}_x}{dy} = \frac{v_*}{y} \left(B_0 + \frac{B_1}{\ln \text{Re}} \right) \left(\frac{y v_*}{\nu} \right)^{\beta_1 / \ln \text{Re}} \quad (5.3-5)$$

in which $B_0 = \frac{1}{2}\sqrt{3}$, $B_1 = \frac{15}{4}$, and $\beta_1 = \frac{3}{2}$. When Eq. 5.3-5 is integrated with respect to y , the *Barenblatt-Chorin universal velocity distribution* is obtained:

$$\frac{\bar{v}_x}{v_*} = \left(\frac{1}{\sqrt{3}} \ln \text{Re} + \frac{5}{2} \right) \left(\frac{y v_*}{\nu} \right)^{3/(2 \ln \text{Re})} \quad (5.3-6)$$

Equation 5.3-6 describes regions ③ and ④ of Fig. 5.3-1 better than does Eq. 5.3-4.⁴ Region ① is better described by Eq. 5.3-13.

Taylor-Series Development in the Viscous Sublayer

We start by writing a Taylor series for \bar{v}_x as a function of y , thus

$$\bar{v}_x(y) = \bar{v}_x(0) + \left. \frac{\partial \bar{v}_x}{\partial y} \right|_{y=0} y + \frac{1}{2!} \left. \frac{\partial^2 \bar{v}_x}{\partial y^2} \right|_{y=0} y^2 + \frac{1}{3!} \left. \frac{\partial^3 \bar{v}_x}{\partial y^3} \right|_{y=0} y^3 + \dots \quad (5.3-7)$$

To evaluate the terms in this series, we need the expression for the time-smoothed shear stress in the vicinity of a wall. For the special case of the steadily driven flow in a slit of thickness $2B$, the shear stress will be of the form $\bar{\tau}_{yx} = \bar{\tau}_{yx}^{(v)} + \bar{\tau}_{yx}^{(t)} = -\tau_0[1 - (y/B)]$. Then from Eqs. 5.2-8 and 9, we have

$$+ \mu \left. \frac{\partial \bar{v}_x}{\partial y} \right|_{y=0} - \rho \bar{v}_x' \bar{v}_y' = \tau_0 \left(1 - \frac{y}{B} \right) \quad (5.3-8)$$

Now we examine one by one the terms that appear in Eq. 5.3-7:⁵

- (i) The first term is zero by the no-slip condition.
- (ii) The coefficient of the second term can be obtained from Eq. 5.3-8, recognizing that both v_x' and v_y' are zero at the wall so that

$$\left. \frac{\partial \bar{v}_x}{\partial y} \right|_{y=0} = \frac{\tau_0}{\mu} \quad (5.3-9)$$

- (iii) The coefficient of the third term involves the second derivative, which may be obtained by differentiating Eq. 5.3-8 with respect to y and then setting $y = 0$, as follows,

$$\left. \frac{\partial^2 \bar{v}_x}{\partial y^2} \right|_{y=0} = \frac{\rho}{\mu} \left(v_x' \left. \frac{\partial v_y'}{\partial y} \right|_{y=0} + v_y' \left. \frac{\partial v_x'}{\partial y} \right|_{y=0} \right) - \frac{\tau_0}{\mu B} = -\frac{\tau_0}{\mu B} \quad (5.3-10)$$

since both v_x' and v_y' are zero at the wall.

⁵ A. A. Townsend, *The Structure of Turbulent Shear Flow*, Cambridge University Press, 2nd edition (1976), p. 163.

(iv) The coefficient of the fourth term involves the third derivative, which may be obtained from Eq. 5.3-8, and this is

$$\begin{aligned}\left.\frac{\partial^3 \bar{v}_x}{\partial y^3}\right|_{y=0} &= \frac{\rho}{\mu} \left(v'_x \frac{\partial^2 v'_y}{\partial y^2} + 2 \frac{\partial v'_y}{\partial y} \frac{\partial v'_x}{\partial y} + v'_y \frac{\partial^2 v'_x}{\partial y^2} \right) \Big|_{y=0} \\ &= -\frac{\rho}{\mu} \left(+2 \left(\frac{\partial v'_x}{\partial x} + \frac{\partial v'_z}{\partial z} \right) \frac{\partial v'_x}{\partial y} \right) \Big|_{y=0} = 0\end{aligned}\quad (5.3-11)$$

Here Eq. 5.2-11 has been used.

There appears to be no reason to set the next coefficient equal to zero, so we find that the Taylor series, in dimensionless quantities, has the form

$$\frac{\bar{v}_x}{v_*} = \frac{yv_*}{\nu} - \frac{1}{2} \left(\frac{\nu}{v_* B} \right) \left(\frac{yv_*}{\nu} \right)^2 + C \left(\frac{yv_*}{\nu} \right)^4 + \dots \quad (5.3-12)$$

The coefficient C has been obtained experimentally,⁶ and therefore we have the final result:

$$\frac{\bar{v}_x}{v_*} = \frac{yv_*}{\nu} \left[1 - \frac{1}{2} \left(\frac{\nu}{v_* B} \right) \left(\frac{yv_*}{\nu} \right) - \frac{1}{4} \left(\frac{yv_*}{14.5\nu} \right)^3 + \dots \right] \quad 0 < \frac{yv_*}{\nu} < 5 \quad (5.3-13)$$

The y^3 term in the brackets will turn out to be very important in connection with turbulent heat and mass transfer correlations in Chapters 13, 14, 21, and 22.

For the region $5 < yv_*/\nu < 30$ no simple analytical derivations are available, and empirical curve fits are sometimes used. One of these is shown in Fig. 5.5-3 for circular tubes.

§5.4 EMPIRICAL EXPRESSIONS FOR THE TURBULENT MOMENTUM FLUX

We now return to the problem of using the time-smoothed equations of change in Eqs. 5.2-11 and 12 to obtain the time-smoothed velocity and pressure distributions. As pointed out in the previous section, some information about the velocity distribution can be obtained without having a specific expression for the turbulent momentum flux $\bar{\tau}^{(t)}$. However, it has been popular among engineers to use various empiricisms for $\bar{\tau}^{(t)}$ that involve velocity gradients. We mention a few of these, and many more can be found in the turbulence literature.

The Eddy Viscosity of Boussinesq

By analogy with Newton's law of viscosity, Eq. 1.1-1, one may write for a turbulent shear flow¹

$$\bar{\tau}_{yx}^{(t)} = -\mu^{(t)} \frac{d\bar{v}_x}{dy} \quad (5.4-1)$$

⁶ C. S. Lin, R. W. Moulton, and G. L. Putnam, *Ind. Eng. Chem.*, **45**, 636–640 (1953); the numerical coefficient was determined from mass transfer experiments in circular tubes. The importance of the y^4 term in heat and mass transfer was recognized earlier by E. V. Murphree, *Ind. Eng. Chem.*, **24**, 726–736 (1932). Eger Vaughn Murphree (1898–1962) was captain of the University of Kentucky football team in 1920 and became President of the Standard Oil Development Company.

¹ J. Boussinesq, *Mém. prés. par div. savants à l'acad. sci. de Paris*, **23**, #1, 1–680 (1877), **24**, #2, 1–64 (1877). Joseph Valentin Boussinesq (1842–1929), university professor in Lille, wrote a two-volume treatise on heat, and is famous for the "Boussinesq approximation" and the idea of "eddy viscosity."

in which $\mu^{(t)}$ is the *turbulent viscosity* (often called the *eddy viscosity*, and given the symbol ε). As one can see from Table 5.1-1, for at least one of the flows given there, the circular jet, one might expect Eq. 5.4-1 to be useful. Usually, however, $\mu^{(t)}$ is a strong function of position and the intensity of turbulence. In fact, for some systems² $\mu^{(t)}$ may even be negative in some regions. It must be emphasized that the viscosity μ is a property of the *fluid*, whereas the eddy viscosity $\mu^{(t)}$ is primarily a property of the *flow*.

For two kinds of turbulent flows (i.e., flows along surfaces and flows in jets and wakes), special expressions for $\mu^{(t)}$ are available:

$$(i) \text{ Wall turbulence: } \mu^{(t)} = \mu \left(\frac{y v_*}{14.5 \nu} \right)^3 \quad 0 < \frac{y v_*}{\nu} < 5 \quad (5.4-2)$$

This expression, derivable from Eq. 5.3-13, is valid only very near the wall. It is of considerable importance in the theory of turbulent heat and mass transfer at fluid–solid interfaces.³

$$(ii) \text{ Free turbulence: } \mu^{(t)} = \rho \kappa_0 b (\bar{v}_{z,\max} - \bar{v}_{z,\min}) \quad (5.4-3)$$

in which κ_0 is a dimensionless coefficient to be determined experimentally, b is the width of the mixing zone at a downstream distance z , and the quantity in parentheses represents the maximum difference in the z -component of the time-smoothed velocities at that distance z . Prandtl⁴ found Eq. 5.4-3 to be a useful empiricism for jets and wakes.

The Mixing Length of Prandtl

By assuming that eddies move around in a fluid very much as molecules move around in a low-density gas (not a very good analogy) Prandtl⁵ developed an expression for momentum transfer in a turbulent fluid. The “mixing length” l plays roughly the same role as the mean free path in kinetic theory (see §1.4). This kind of reasoning led Prandtl to the following relation:

$$\bar{\tau}_{yx}^{(t)} = -\rho l^2 \left| \frac{d \bar{v}_x}{dy} \right| \frac{d \bar{v}_x}{dy} \quad (5.4-4)$$

If the mixing length were a universal constant, Eq. 5.4-4 would be very attractive, but in fact l has been found to be a function of position. Prandtl proposed the following expressions for l :

$$(i) \text{ Wall turbulence: } l = \kappa_1 y \quad (y = \text{distance from wall}) \quad (5.4-5)$$

$$(ii) \text{ Free turbulence: } l = \kappa_2 b \quad (b = \text{width of mixing zone}) \quad (5.4-6)$$

in which κ_1 and κ_2 are constants. A result similar to Eq. 5.4-4 was obtained by Taylor⁶ by his “vorticity transport theory” some years prior to Prandtl’s proposal.

² J. O. Hinze, *Appl. Sci. Res.*, **22**, 163–175 (1970); V. Krupa and S. Eskinazi, *J. Fluid. Mech.*, **20**, 555–579 (1964).

³ C. S. Lin, R. W. Moulton, and G. L. Putnam, *Ind. Eng. Chem.*, **45**, 636–640 (1953).

⁴ L. Prandtl, *Zeits. f. angew. Math. u. Mech.*, **22**, 241–243 (1942).

⁵ L. Prandtl, *Zeits. f. angew. Math. u. Mech.*, **5**, 136–139 (1925).

⁶ G. I. Taylor, *Phil. Trans. A215*, 1–26 (1915), and *Proc. Roy. Soc. (London)*, **A135**, 685–701 (1932).

The Modified van Driest Equation

There have been numerous attempts to devise empirical expressions that can describe the turbulent shear stress all the way from the wall to the main turbulent stream. Here we give a modification of the equation of van Driest.⁷ This is a formula for the mixing length of Eq. 5.4-4:

$$l = 0.4y \frac{1 - \exp(-yv_*/26\nu)}{\sqrt{1 - \exp(-0.26yv_*/\nu)}} \quad (5.4-7)$$

This relation has been found to be useful for predicting heat and mass transfer rates in flow in tubes.

In the next two sections and in several problems at the end of the chapter, we illustrate the use of the above empiricisms. Keep in mind that these expressions for the Reynolds stresses are little more than crutches that can be used for the representation of experimental data or for solving problems that fall into rather special classes.

EXAMPLE 5.4-1

Obtain an expression for $\bar{\tau}_{yx}^{(t)} = \rho \overline{v'_x v'_y}$ as a function of y in the neighborhood of the wall.

Development of the Reynolds Stress Expression in the Vicinity of the Wall

SOLUTION

(a) We start by making a Taylor series development of the three components of \mathbf{v}' :

$$\underline{v'_x(y)} = \underline{v'_x(0)} + \frac{\partial \underline{v'_x}}{\partial y} \Big|_{y=0} y + \frac{1}{2!} \frac{\partial^2 \underline{v'_x}}{\partial y^2} \Big|_{y=0} y^2 + \dots \quad (5.4-8)$$

$$\underline{v'_y(y)} = \underline{v'_y(0)} + \frac{\partial \underline{v'_y}}{\partial y} \Big|_{y=0} y + \frac{1}{2!} \frac{\partial^2 \underline{v'_y}}{\partial y^2} \Big|_{y=0} y^2 + \dots \quad (5.4-9)$$

$$\underline{v'_z(y)} = \underline{v'_z(0)} + \frac{\partial \underline{v'_z}}{\partial y} \Big|_{y=0} y + \frac{1}{2!} \frac{\partial^2 \underline{v'_z}}{\partial y^2} \Big|_{y=0} y^2 + \dots \quad (5.4-10)$$

The first term in Eqs. 5.4-8 and 10 must be zero because of the no-slip condition; the first term in Eq. 5.4-9 is zero in the absence of mass transfer. Next we can write Eq. 5.2-11 at $y = 0$,

$$\frac{\partial \underline{v'_x}}{\partial x} \Big|_{y=0} + \frac{\partial \underline{v'_y}}{\partial y} \Big|_{y=0} + \frac{\partial \underline{v'_z}}{\partial z} \Big|_{y=0} = 0 \quad (5.4-11)$$

The first and third terms in this equation are zero because of the no-slip condition. Therefore we have to conclude that the second term is zero as well. Hence all the dashed-underlined terms in Eqs. 5.4-8 to 10 are zero, and we may conclude that

$$\bar{\tau}_{yx}^{(t)} = \rho \overline{v'_x v'_y} = Ay^3 + By^4 + \dots \quad (5.4-12)$$

This suggests—but does not prove⁸—that the lead term in the Reynolds stress near a wall should be proportional to y^3 . Extensive studies of mass transfer rates in closed channels⁹ have, however, established that $A \neq 0$.

⁷ E. R. van Driest, *J. Aero. Sci.*, **23**, 1007–1011 and 1036 (1956). Van Driest's original equation did not have the square root divisor. This modification was made by O. T. Hanna, O. C. Sandall, and P. R. Mazet, *AIChE Journal*, **27**, 693–697 (1981) so that the turbulent viscosity would be proportional to y^3 as $y \rightarrow 0$, in accordance with Eq. 5.4-2.

⁸ H. Reichardt, *Zeits. f. angew. Math. u. Mech.*, **31**, 208–219 (1951). See also J. O. Hinze, *Turbulence*, McGraw-Hill, New York, 2nd edition (1975), pp. 620–621.

⁹ R. H. Notter and C. A. Sleicher, *Chem. Eng. Sci.*, **26**, 161–171 (1971); O. C. Sandall and O. T. Hanna, *AIChE Journal*, **25**, 190–192 (1979); D. W. Hubbard and E. N. Lightfoot, *Ind. Eng. Chem. Fundamentals*, **5**, 370–379 (1966).

(b) For the flow between parallel plates, we can use the expression found in Eq. 5.3-12 for the time-smoothed velocity profile to get the turbulent momentum flux:

$$\begin{aligned}\bar{\tau}_{yx}^{(t)} &= \rho \bar{v}_x' v_y' = -\tau_0 \left(1 - \frac{y}{B}\right) + \mu \frac{d\bar{v}_x}{dy} \\ &= -\tau_0 \left(1 - \frac{y}{B}\right) + \left(\tau_0 - \tau_0 \frac{y}{B} + Ay^3 + \dots\right)\end{aligned}\quad (5.4-13)$$

where $A = 4C(v_* / \nu)^4$. This is in accord with Eq. 5.4-12.

§5.5 TURBULENT FLOW IN DUCTS

We start this section with a short discussion of experimental measurements for turbulent flow in rectangular ducts, in order to give some impressions about the Reynolds stresses. In Figs. 5.5-1 and 2 are shown some experimental measurements of the time-smoothed quantities $v_z'^2$, $v_x'^2$, and $v_x'v_z'$ for the flow in the z direction in a rectangular duct.

In Fig. 5.5-1 note that quite close to the wall, $\sqrt{v_z'^2}$ is about 13% of the time-smoothed centerline velocity $\bar{v}_{z,\max}$, whereas $\sqrt{v_x'^2}$ is about 5%. This means that, near the wall, the velocity fluctuations in the flow direction are appreciably greater than those in the transverse direction. Near the center of the duct, the two fluctuation amplitudes are nearly equal and we say that the turbulence is nearly *isotropic* there.

In Fig. 5.5-2 the turbulent shear stress $\bar{\tau}_{xz}^{(t)} = \rho v_x' v_z'$ is compared with the total shear stress $\bar{\tau}_{xz} = \bar{\tau}_{xz}^{(t)} + \bar{\tau}_{xz}^{(v)}$ across the duct. It is evident that the turbulent contribution is the

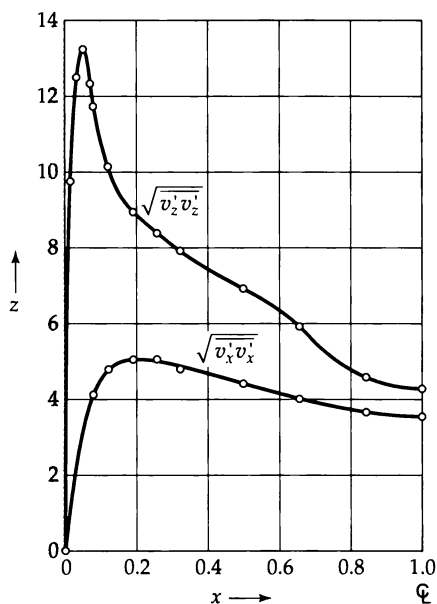


Fig. 5.5-1. Measurements of H. Reichardt [Naturwissenschaften, 404 (1938), Zeits. f. angew. Math. u. Mech., 13, 177–180 (1933), 18, 358–361 (1938)] for the turbulent flow of air in a rectangular duct with $\bar{v}_{z,\max} = 100 \text{ cm/s}$. Here the quantities $\sqrt{v_x' v_x'}$ and $\sqrt{v_z' v_z'}$ are shown.

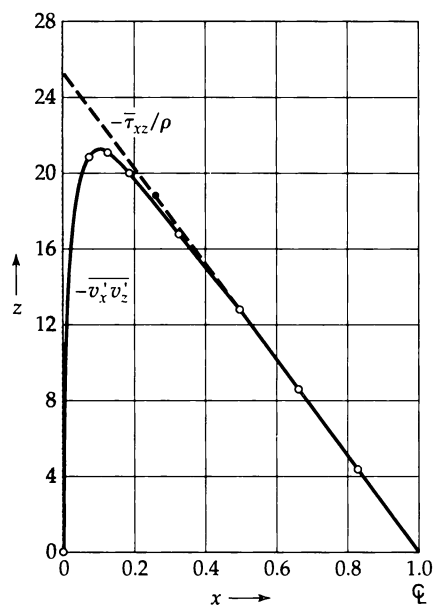


Fig. 5.5-2. Measurements of Reichardt (see Fig. 5.5-1) for the quantity $v_x' v_z'$ in a rectangular duct. Note that this quantity differs from $\bar{\tau}_{xz}/\rho$ only near the duct wall.

more important over most of the cross section and that the viscous contribution is important only in the vicinity of the wall. This is further illustrated in Example 5.5-3. Analogous behavior is observed in tubes of circular cross section.

EXAMPLE 5.5-1

Estimation of the Average Velocity in a Circular Tube

Apply the results of §5.3 to obtain the average velocity for turbulent flow in a circular tube.

SOLUTION

We can use the velocity distribution in the caption to Fig. 5.5-3. To get the average velocity in the tube, one should integrate over four regions: the viscous sublayer ($y^+ < 5$), the buffer zone $5 < y^+ < 30$, the inertial sublayer, and the main turbulent stream, which is roughly parabolic in shape. One can certainly do this, but it has been found that integrating the logarithmic profile of Eq. 5.3-4 (or the power law profile of Eq. 5.3-6) over the entire cross section gives results that are roughly of the right form. For the *logarithmic profile* one gets

$$\frac{\langle \bar{v}_z \rangle}{v_*} = 2.5 \ln \left(\frac{R v_*}{\nu} \right) + 1.75 \quad (5.5-1)$$

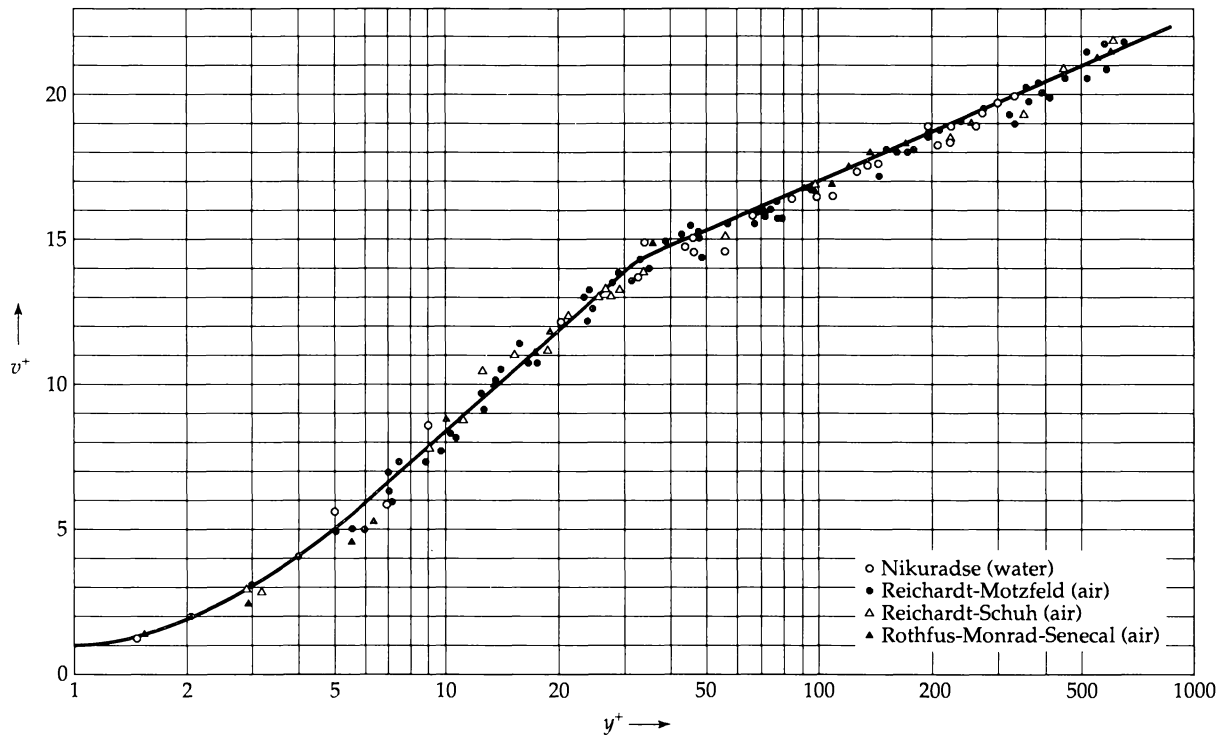


Fig. 5.5-3. Dimensionless velocity distribution for turbulent flow in circular tubes, presented as $v^+ = \bar{v}_z / v_*$ vs. $y^+ = y v_* \rho / \mu$, where $v_* = \sqrt{\tau_0 / \rho}$ and τ_0 is the wall shear stress. The solid curves are those suggested by Lin, Moulton, and Putnam [Ind. Eng. Chem., 45, 636–640 (1953)].

$$0 < y^+ < 5: \quad v^+ = y^+ [1 - \frac{1}{4}(y^+ / 14.5)^3]$$

$$5 < y^+ < 30: \quad v^+ = 5 \ln(y^+ + 0.205) - 3.27$$

$$30 < y^+: \quad v^+ = 2.5 \ln y^+ + 5.5$$

The experimental data are those of J. Nikuradse for water (○) [VDI Forschungsheft, H356 (1932)]; Reichardt and Motzfeld for air (●); Reichardt and Schuh (△) for air [H. Reichardt, NACA Tech. Mem. 1047 (1943)]; and R. R. Rothfus, C. C. Monrad, and V. E. Senecal for air (■) [Ind. Eng. Chem., 42, 2511–2520 (1950)].

If this is compared with experimental data on flow rate versus pressure drop, it is found that good agreement can be obtained by changing 2.5 to 2.45 and 1.75 to 2.0. This "fudging" of the constants would probably not be necessary if the integration over the cross section had been done by using the local expression for the velocity in the various layers. On the other hand, there is some virtue in having a simple logarithmic relation such as Eq. 5.5-1 to describe pressure drop vs. flow rate.

In a similar fashion the *power law profile* can be integrated over the entire cross section to give (see Ref. 4 of §5.3)

$$\frac{\langle \bar{v}_z \rangle}{v_*} = \frac{2}{(\alpha + 1)(\alpha + 2)} \left(\frac{1}{\sqrt{3}} \ln \text{Re} + \frac{5}{2} \right) \left(\frac{R v_*}{\nu} \right)^\alpha \quad (5.5-2)$$

in which $\alpha = 3/(2 \ln \text{Re})$. This relation is useful over the range $3.07 \times 10^3 < \text{Re} < 3.23 \times 10^6$.

EXAMPLE 5.5-2

Application of Prandtl's Mixing Length Formula to Turbulent Flow in a Circular Tube

Show how Eqs. 5.4-4 and 5 can be used to describe turbulent flow in a circular tube.

SOLUTION

Equation 5.2-12 gives for the steadily driven flow in a circular tube,

$$0 = \frac{\mathcal{P}_0 - \mathcal{P}_L}{L} - \frac{1}{r} \frac{d}{dr} (r \bar{\tau}_{rz}) \quad (5.5-3)$$

in which $\bar{\tau}_{rz} = \bar{\tau}_{rz}^{(v)} + \bar{\tau}_{rz}^{(t)}$. Over most of the tube the viscous contribution is quite small; here we neglect it entirely. Integration of Eq. 5.5-3 then gives

$$\bar{\tau}_{rz}^{(t)} = \frac{(\mathcal{P}_0 - \mathcal{P}_L)r}{2L} = \tau_0 \left(1 - \frac{y}{R} \right) \quad (5.5-4)$$

where τ_0 is the wall shear stress and $y = R - r$ is the distance from the tube wall.

According to the mixing length theory in Eq. 5.4-4, with the empirical expression in Eq. 5.4-5, we have for $d\bar{v}_z/dr$ negative

$$\bar{\tau}_{rz}^{(t)} = -\rho l^2 \left| \frac{d\bar{v}_z}{dr} \right| \frac{d\bar{v}_z}{dr} = +\rho (\kappa_1 y)^2 \left(\frac{d\bar{v}_z}{dy} \right)^2 \quad (5.5-5)$$

Substitution of this into Eq. 5.5-4 gives a differential equation for the time-smoothed velocity. If we follow Prandtl and extrapolate the inertial sublayer to the wall, then in Eq. 5.5-5 it is appropriate to replace $\bar{\tau}_{rz}^{(t)}$ by τ_0 . When this is done, Eq. 5.5-5 can be integrated to give

$$\bar{v}_z = \frac{v_*}{\kappa_1} \ln y + \text{constant} \quad (5.5-6)$$

Thus a logarithmic profile is obtained and hence the results from Example 5.5-1 can be used; that is, one can apply Eq. 5.5-6 as a very rough approximation over the entire cross section of the tube.

EXAMPLE 5.5-3

Relative Magnitude of Viscosity and Eddy Viscosity

Determine the ratio $\mu^{(t)}/\mu$ at $y = R/2$ for water flowing at a steady rate in a long, smooth, round tube under the following conditions:

$$R = \text{tube radius} = 3 \text{ in.} = 7.62 \text{ cm}$$

$$\tau_0 = \text{wall shear stress} = 2.36 \times 10^{-5} \text{ lb}_f/\text{in.}^2 = 0.163 \text{ Pa}$$

$$\rho = \text{density} = 62.4 \text{ lb}_m/\text{ft}^3 = 1000 \text{ kg/m}^3$$

$$\nu = \text{kinematic viscosity} = 1.1 \times 10^{-5} \text{ ft}^2/\text{s} = 1.02 \times 10^{-7} \text{ m}^2/\text{s}$$

SOLUTION

The expression for the time-smoothed momentum flux is

$$\bar{\tau}_{rz}^{(t)} = -\mu \frac{d\bar{v}_z}{dr} - \mu^{(t)} \frac{d\bar{v}_z}{dr} \quad (5.5-7)$$

This result may be solved for $\mu^{(t)}/\mu$ and the result can be expressed in terms of dimensionless variables:

$$\begin{aligned}\frac{\mu^{(t)}}{\mu} &= \frac{1}{\mu} \frac{\bar{\tau}_{rz}}{d\bar{v}_z/dy} - 1 \\ &= \frac{1}{\mu} \frac{\tau_0[1 - (y/R)]}{d\bar{v}_z/dy} - 1 \\ &= \frac{[1 - (y/R)]}{dv^+/dy^+} - 1\end{aligned}\quad (5.5-8)$$

where $y^+ = yv_*\rho/\mu$ and $v^+ = \bar{v}_z/v_*$. When $y = R/2$, the value of y^+ is

$$y^+ = \frac{yv_*\rho}{\mu} = \frac{(R/2)\sqrt{\tau_0/\rho\rho}}{\mu} = 485 \quad (5.5-9)$$

For this value of y^+ , the logarithmic distribution in the caption of Fig. 5.5-3 gives

$$\frac{dv^+}{dy^+} = \frac{2.5}{485} = 0.0052 \quad (5.5-10)$$

Substituting this into Eq. 5.5-8 gives

$$\frac{\mu^{(t)}}{\mu} = \frac{1/2}{0.0052} - 1 = 95 \quad (5.5-11)$$

This result emphasizes that, far from the tube wall, molecular momentum transport is negligible in comparison with eddy transport.

§5.6 TURBULENT FLOW IN JETS

In the previous section we discussed the flow in ducts, such as circular tubes; such flows are examples of *wall turbulence*. Another main class of turbulent flows is *free turbulence*, and the main examples of these flows are jets and wakes. The time-smoothed velocity in these types of flows can be described adequately by using Prandtl's expression for the eddy viscosity in Fig. 5.4-3, or by using Prandtl's mixing length theory with the empiricism given in Eq. 5.4-6. The former method is simpler, and hence we use it in the following illustrative example.

EXAMPLE 5.6-1

Time-Smoothed Velocity Distribution in a Circular Wall Jet¹⁻⁴

A jet of fluid emerges from a circular hole into a semi-infinite reservoir of the same fluid as depicted in Fig. 5.6-1. In the same figure we show roughly what we expect the profiles of the z-component of the velocity to look like. We would expect that for various values of z the profiles will be similar in shape, differing only by a scale factor for distance and velocity. We also can imagine that as the jet moves outward, it will create a net radial inflow so that some of the surrounding fluid will be dragged along. We want to find the time-smoothed velocity distribution in the jet and also the amount of fluid crossing each plane of constant z. Before working through the solution, it may be useful to review the information on jets in Table 5.1-1.

¹ H. Schlichting, *Boundary-Layer Theory*, McGraw-Hill, New York, 7th edition (1979), pp. 747–750.

² A. A. Townsend, *The Structure of Turbulent Shear Flow*, Cambridge University Press, 2nd edition (1976), Chapter 6.

³ J. O. Hinze, *Turbulence*, McGraw-Hill, New York, 2nd edition (1975), Chapter 6.

⁴ S. Goldstein, *Modern Developments in Fluid Dynamics*, Oxford University Press (1938), and Dover reprint (1965), pp. 592–597.

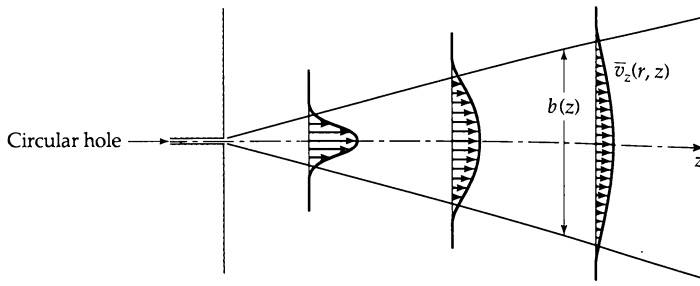


Fig. 5.6-1. Circular jet emerging from a plane wall.

SOLUTION

In order to use Eq. 5.4-3 it is necessary to know how b and $\bar{v}_{z,\max} - \bar{v}_{z,\min}$ vary with z for the circular jet. We know that the total rate of flow of z -momentum J will be the same for all values of z . We presume that the convective momentum flux is much greater than the viscous momentum flux. This permits us to postulate that the jet width b depends on J , on the density ρ and the kinematic viscosity ν of the fluid, and on the downstream distance z from the wall. The only combination of these variables that has the dimensions of length is $b \propto Jz/\rho\nu^2$, so that the jet width is proportional to z .

We next postulate that the velocity profiles are "similar," that is,

$$\frac{\bar{v}_z}{\bar{v}_{z,\max}} = f(\xi) \quad \text{where } \xi = \frac{r}{b(z)} \quad (5.6-1)$$

which seems like a plausible proposal; here $\bar{v}_{z,\max}$ is the velocity along the centerline. When this is substituted into the expression for the rate of momentum flow in the jet (neglecting the contribution from $\bar{\tau}_{xx}$)

$$J = \int_0^{2\pi} \int_0^\infty \rho \bar{v}_z^2 r dr d\theta \quad (5.6-2)$$

we find that

$$J = 2\pi \rho b^2 \bar{v}_{z,\max}^2 \int_0^\infty f^2 \xi d\xi = \text{constant} \times \rho b^2 \bar{v}_{z,\max}^2 \quad (5.6-3)$$

Since J does not depend on z and since b is proportional to z , then $\bar{v}_{z,\max}$ has to be inversely proportional to z .

The $\bar{v}_{z,\min}$ in Eq. 5.4-3 occurs at the outer edge of the jet and is zero. Therefore because $b \propto z$ and $\bar{v}_{z,\max} \propto z^{-1}$, we find from Eq. 5.4-3 that $\mu^{(t)}$ is a constant. Thus we can use the equations of motion for laminar flow and replace the viscosity μ by the eddy viscosity $\mu^{(t)}$, or ν by $\nu^{(t)}$.

In the jet the main motion is in the z direction; that is $|\bar{v}_r| \ll |\bar{v}_z|$. Hence we can use a boundary layer approximation (see §4.4) for the time-smoothed equations of change and write

$$\text{continuity: } \frac{1}{r} \frac{\partial}{\partial r} (r \bar{v}_r) + \frac{\partial \bar{v}_z}{\partial z} = 0 \quad (5.6-4)$$

$$\text{motion: } \bar{v}_r \frac{\partial \bar{v}_z}{\partial r} + \bar{v}_z \frac{\partial \bar{v}_z}{\partial z} = \nu^{(t)} \frac{1}{r} \frac{\partial}{\partial r} \left(r \frac{\partial \bar{v}_z}{\partial r} \right) \quad (5.6-5)$$

These equations are to be solved with the following boundary conditions:

$$\text{B.C. 1: } \bar{v}_r = 0 \quad \text{at } r = 0 \quad (5.6-6)$$

$$\text{B.C. 2: } \frac{\partial \bar{v}_z}{\partial r} = 0 \quad \text{at } r = 0 \quad (5.6-7)$$

$$\text{B.C. 3: } \bar{v}_z = 0 \quad \text{at } z = \infty \quad (5.6-8)$$

The last boundary condition is automatically satisfied, inasmuch as we have already found that $\bar{v}_{z,\max}$ is inversely proportional to z . We now seek a solution to Eq. 5.6-5 of the form of Eq. 5.6-1 with $b = z$.

To avoid working with two dependent variables, we introduce the stream function as discussed in §4.2. For axially symmetric flow, the stream function is defined as follows:

$$\bar{v}_z = -\frac{1}{r} \frac{\partial \psi}{\partial r} \quad \bar{v}_r = \frac{1}{r} \frac{\partial \psi}{\partial z} \quad (5.6-9, 10)$$

This definition ensures that the equation of continuity in Eq. 5.6-4 is satisfied. Since we know that \bar{v}_z is $z^{-1} \times$ some function of ξ , we deduce from Eq. 5.6-9 that ψ must be proportional to z . Furthermore ψ must have dimensions of (velocity) \times (length) 2 , hence the stream function must have the form

$$\psi(r, z) = \nu^{(t)} z F(\xi) \quad (5.6-11)$$

in which F is a dimensionless function of $\xi = r/z$. From Eqs. 5.6-9 and 10 we then get

$$\bar{v}_z = -\frac{\nu^{(t)}}{z} \frac{F'}{\xi} \quad \bar{v}_r = \frac{\nu^{(t)}}{z} \left(\frac{F}{\xi} - F' \right) \quad (5.6-12, 13)$$

The first two boundary conditions may now be rewritten as

$$\text{B.C. 1:} \quad \text{at } \xi = 0, \quad \frac{F}{\xi} - F' = 0 \quad (5.6-14)$$

$$\text{B.C. 2:} \quad \text{at } \xi = 0, \quad \frac{F''}{\xi} - \frac{F'}{\xi^2} = 0 \quad (5.6-15)$$

If we expand F in a Taylor series about $\xi = 0$,

$$F(\xi) = a + b\xi + c\xi^2 + d\xi^3 + e\xi^4 + \dots \quad (5.6-16)$$

then the first boundary condition gives $a = 0$, and the second gives $b = d = 0$. We will use this result presently.

Substitution of the velocity expressions of Eqs. 5.6-12 and 13 into the equation of motion in Eq. 5.6-5 then gives a third-order differential equation for F ,

$$\frac{d}{d\xi} \left(\frac{FF'}{\xi} \right) = \frac{d}{d\xi} \left(F'' - \frac{F'}{\xi} \right) \quad (5.6-17)$$

This may be integrated to give

$$\frac{FF'}{\xi} = F'' - \frac{F'}{\xi} + C_1 \quad (5.6-18)$$

in which the constant of integration must be zero; this can be seen by using the Taylor series in Eq. 5.6-16 along with the fact that a , b , and d are all zero.

Equation 5.6-18 was first solved by Schlichting.⁵ First one changes the independent variable by setting $\xi = \ln \beta$. The resulting second-order differential equation contains only the dependent variable and its first two derivatives. Equations of this type can be solved by elementary methods. The first integration gives

$$\xi F' = 2F + \frac{1}{2}F^2 + C_2 \quad (5.6-19)$$

Once again, knowing the behavior of F near $\xi = 0$, we conclude that the second constant of integration is zero. Equation 5.6-19 is then a first-order separable equation, and it may be solved to give

$$F(\xi) = -\frac{(C_3 \xi)^2}{1 + \frac{1}{4}(C_3 \xi)^2} \quad (5.6-20)$$

⁵ H. Schlichting, *Zeits. f. angew. Math. u. Mech.*, **13**, 260–263 (1933).

in which C_3 is the third constant of integration. Substitution of this into Eqs. 5.6-12 and 13 then gives

$$\bar{v}_z = \frac{\nu^{(t)}}{z} \frac{2C_3^2}{[1 + \frac{1}{4}(C_3 r/z)^2]^2} \quad (5.6-21)$$

$$\bar{v}_r = \frac{C_3 \nu^{(t)}}{z} \frac{(C_3 r/z) - \frac{1}{4}(C_3 r/z)^3}{[1 + \frac{1}{4}(C_3 r/z)^2]^2} \quad (5.6-22)$$

When the above expression for \bar{v}_z is substituted into Eq. 5.6-2 for J , we get an expression for the third integration constant in terms of J :

$$C_3 = \sqrt{\frac{3}{16\pi}} \sqrt{J} \frac{1}{\rho \nu^{(t)}} \quad (5.6-23)$$

The last three equations then give the time-smoothed velocity profiles in terms of J , ρ , and $\nu^{(t)}$.

A measurable quantity in jet flow is the radial position corresponding to an axial velocity one-half the centerline value; we call this half-width $b_{1/2}$. From Eq. 5.6-21 we then obtain

$$\frac{\bar{v}_z(b_{1/2}, z)}{\bar{v}_{z,\max}(z)} = \frac{1}{2} = \frac{1}{[1 + \frac{1}{4}(C_3 b_{1/2}/z)^2]^2} \quad (5.6-24)$$

Experiments indicate⁶ that $b_{1/2} = 0.0848z$. When this is inserted into Eq. 5.6-24, it is found that $C_3 = 15.1$. Using this value, we can get the turbulent viscosity $\nu^{(t)}$ as a function of J and ρ from Eq. 5.6-23.

Figure 5.6-2 gives a comparison of the above axial velocity profile with experimental data. The calculated curve obtained from the Prandtl mixing length theory is also shown.⁷ Both methods appear to give reasonably good curve fits of the experimental profiles. The

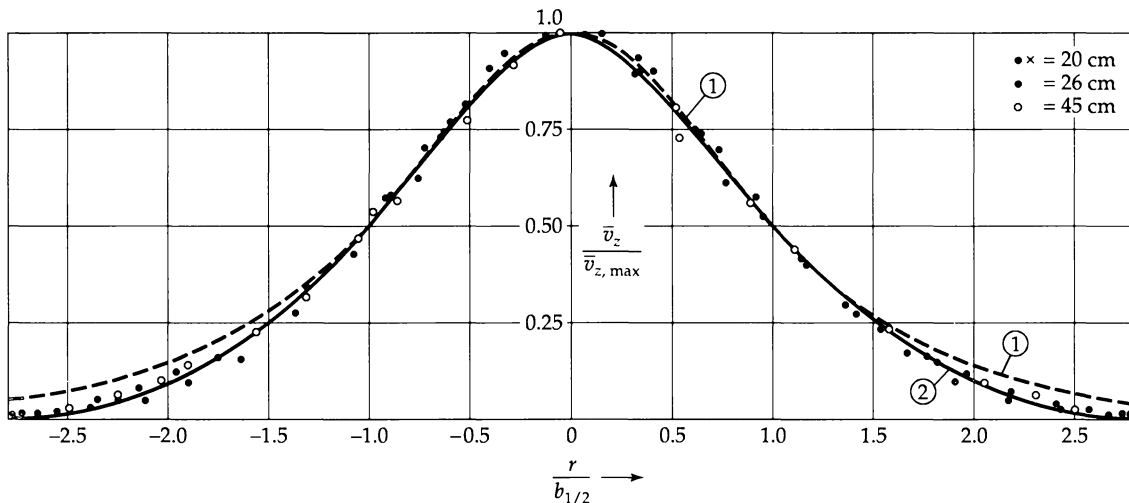


Fig. 5.6-2. Velocity distribution in a circular jet in turbulent flow [H. Schlichting, *Boundary-Layer Theory*, McGraw-Hill, New York, 7th edition (1979), Fig. 24.9]. The eddy viscosity calculation (curve 1) and the Prandtl mixing length calculation (curve 2) are compared with the measurements of H. Reichardt [VDI *Forschungsheft*, 414 (1942), 2nd edition (1951)]. Further measurements by others are cited by S. Corrsin ["Turbulence: Experimental Methods," in *Handbuch der Physik*, Vol. VIII/2, Springer, Berlin (1963)].

⁶ H. Reichardt, *VDI Forschungsheft*, 414 (1942).

⁷ W. Tollmien, *Zeits. f. angew. Math. u. Mech.*, 6, 468–478 (1926).

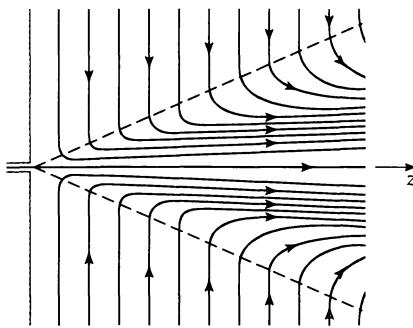


Fig. 5.6-3. Streamline pattern in a circular jet in turbulent flow [H. Schlichting, *Boundary-Layer Theory*, McGraw-Hill, New York, 7th edition (1979), Fig. 24.10].

eddy viscosity method seems to be somewhat better in the neighborhood of the maximum, whereas the mixing length results are better in the outer part of the jet.

Once the velocity profiles are known, the streamlines can be obtained. From the streamlines, shown in Fig. 5.6-3, it can be seen how the jet draws in fluid from the surrounding mass of fluid. Hence the mass of fluid carried by the jet increases with the distance from the source. This mass rate of flow is

$$w = \int_0^{2\pi} \int_0^{\infty} \rho \bar{v}_z r dr d\theta = 8\pi\rho\nu^{(t)} z \quad (5.6-25)$$

This result corresponds to an entry in Table 5.1-1.

The two-dimensional jet issuing from a thin slot may be analyzed similarly. In that problem, however, the turbulent viscosity is a function of position.

QUESTIONS FOR DISCUSSION

1. Compare and contrast the procedures for solving laminar flow problems and turbulent flow problems.
2. Why must Eq. 5.1-4 *not* be used for evaluating the velocity gradient at the solid boundary?
3. What does the logarithmic profile of Eq. 5.3-4 give for the fluid velocity at the wall? Why does this not create a problem in Example 5.5-1 when the logarithmic profile is integrated over the cross section of the tube?
4. Discuss the physical interpretation of each term in Eq. 5.2-12.
5. Why is the absolute value sign used in Eq. 5.4-4? How is it eliminated in Eq. 5.5-5?
6. In Example 5.6-1, how do we know that the momentum flow through any plane of constant z is a constant? Can you imagine a modification of the jet problem in which that would not be the case?
7. Go through some of the volumes of *Ann. Revs. Fluid Mech.* and summarize the topics in turbulent flow that are found there.
8. In Eq. 5.3-1 why do we investigate the functional dependence of the velocity gradient rather than the velocity itself?
9. Why is turbulence such a difficult topic?

PROBLEMS

- 5A.1 Pressure drop needed for laminar-turbulent transition.** A fluid with viscosity 18.3 cp and density 1.32 g/cm^3 is flowing in a long horizontal tube of radius 1.05 in. (2.67 cm). For what pressure gradient will the flow become turbulent?

Answer: 42 psi/mi ($1.8 \times 10^5 \text{ Pa/km}$)

5A.2 Velocity distribution in turbulent pipe flow. Water is flowing through a long, straight, level run of smooth 6.00 in. i.d. pipe, at a temperature of 68°F. The pressure gradient along the length of the pipe is 1.0 psi/mi.

- (a) Determine the wall shear stress τ_0 in psi ($\text{lb}_f/\text{in.}^2$) and Pa.
- (b) Assume the flow to be turbulent and determine the radial distances from the pipe wall at which $\bar{v}_z/\bar{v}_{z,\max} = 0.0, 0.1, 0.2, 0.4, 0.7, 0.85, 1.0$.
- (c) Plot the complete velocity profile, $\bar{v}_z/\bar{v}_{z,\max}$ vs. $y = R - r$.
- (d) Is the assumption of turbulent flow justified?
- (e) What is the mass flow rate?

5B.1 Average flow velocity in turbulent tube flow.

- (a) For the turbulent flow in smooth circular tubes, the function¹

$$\frac{\bar{v}_z}{\bar{v}_{z,\max}} = \left(1 - \frac{r}{R}\right)^{1/n} \quad (5B.1-1)$$

is sometimes useful for curve-fitting purposes: near $\text{Re} = 4 \times 10^3$, $n = 6$; near $\text{Re} = 1.1 \times 10^5$, $n = 7$; and near $\text{Re} = 3.2 \times 10^6$, $n = 10$. Show that the ratio of average to maximum velocity is

$$\frac{\langle \bar{v}_z \rangle}{\bar{v}_{z,\max}} = \frac{2n^2}{(n+1)(2n+1)} \quad (5B.1-2)$$

and verify the result in Eq. 5.1-5.

- (b) Sketch the logarithmic profile in Eq. 5.3-4 as a function of r when applied to a circular tube of radius R . Then show how this function may be integrated over the tube cross section to get Eq. 5.5-1. List all the assumptions that have been made to get this result.

5B.2 Mass flow rate in a turbulent circular jet.

- (a) Verify that the velocity distributions in Eqs. 5.6-21 and 22 do indeed satisfy the differential equations and boundary conditions.
- (b) Verify that Eq. 5.6-25 follows from Eq. 5.6-21.

5B.3 The eddy viscosity expression in the viscous sublayer. Verify that Eq. 5.4-2 for the eddy viscosity comes directly from the Taylor series expression in Eq. 5.3-13.

5C.1 Two-dimensional turbulent jet. A fluid jet issues forth from a slot perpendicular to the xy -plane and emerges in the z direction into a semi-infinite medium of the same fluid. The width of the slot in the y direction is W . Follow the pattern of Example 5.6-1 to find the time-smoothed velocity profiles in the system.

- (a) Assume the similar profiles

$$\bar{v}_z/\bar{v}_{z,\max} = f(\xi) \quad \text{with } \xi = x/z \quad (5C.1-1)$$

Show that the momentum conservation statement leads to the fact that the centerline velocity must be proportional to $z^{-1/2}$.

- (b) Introduce a stream function ψ such that $\bar{v}_z = -\partial\psi/\partial x$ and $\bar{v}_x = +\partial\psi/\partial z$. Show that the result in (a) along with dimensional considerations leads to the following form for ψ :

$$\psi = z^{1/2} \sqrt{J/\rho W F(\xi)} \quad (5C.1-2)$$

Here $F(\xi)$ is a dimensionless stream function, which will be determined from the equation of motion for the fluid.

¹ H. Schlichting, *Boundary-Layer Theory*, McGraw-Hill, New York, 7th edition (1979), pp. 596–600.

- (c) Show that Eq. 5.4-2 and dimensional considerations lead to the following form for the turbulent kinematic viscosity:

$$\nu^{(t)} = \mu^{(t)} / \rho = \lambda \sqrt{J/\rho} W z^{1/2} \quad (5C.1-3)$$

Here λ is a dimensionless constant that has to be determined from experiments.

- (d) Rewrite the equation of motion for the jet using the expression for the turbulent kinematic viscosity from (c) and the stream function from (b). Show that this leads to the following differential equation:

$$\frac{1}{2} F'^2 + \frac{1}{2} FF'' - \lambda F''' = 0 \quad (5C.1-4)$$

For the sake of convenience, introduce a new variable

$$\eta = \xi / 4\lambda = x / 4\lambda z \quad (5C.1-5)$$

and rewrite Eq. 5C.1-4.

- (e) Next verify that the boundary conditions for Eq. 5C.1-4 are $F(0) = 0$, $F'(0) = 0$, and $F'(\infty) = 0$.
(f) Show that Eq. 5C.1-4 can be integrated to give

$$2FF' - F'' = \text{constant} \quad (5C.1-6)$$

and that the boundary conditions require that the constant be zero.

- (g) Show that further integration leads to

$$F^2 - F' = C^2 \quad (5C.1-7)$$

where C is a constant of integration.

- (h) Show that another integration leads to

$$F = -C \tanh C\eta \quad (5C.1-8)$$

and that the axial velocity can be found from this to be

$$\bar{v}_z = \frac{\sqrt{J/\rho} WC^2}{4\lambda \sqrt{z}} \operatorname{sech}^2 C\eta \quad (5C.1-9)$$

- (i) Next show that putting the axial velocity into the expression for the total momentum of the jet leads to the value $C = \sqrt[3]{3\lambda}$ for the integration constant. Rewrite Eq. 5C.1-9 in terms of λ rather than C . The value of $\lambda = 0.0102$ gives good agreement with the experimental data.² The agreement is believed to be slightly better than that for the Prandtl mixing length empiricism.

- (j) Show that the mass flow rate across any line $z = \text{constant}$ is given by

$$w = 2\sqrt[3]{3\lambda} \sqrt{\frac{J\rho z}{W}} \quad (5C.1-10)$$

- 5C.2 Axial turbulent flow in an annulus.** An annulus is bounded by cylindrical walls at $r = aR$ and $r = R$ (where $a < 1$). Obtain expressions for the turbulent velocity profiles and the mass flow rate. Apply the logarithmic profile of Eq. 5.3-3 for the flow in the neighborhood of each wall. Assume that the location of the maximum in the velocity occurs on the same cylindrical surface $r = bR$ found for laminar annular flow:

$$b = \sqrt{\frac{1 - a^2}{2 \ln(1/a)}} \quad (5C.2-1)$$

² H. Schlichting, *Boundary-Layer Theory*, McGraw-Hill, New York, 4th edition (1960), p. 607 and Fig. 23.7.

Measured velocity profiles suggest that this assumption for b is reasonable, at least for high Reynolds numbers.³ Assume further that κ in Eq. 5.3-3 is the same for the inner and outer walls.

- (a) Show that direct application of Eq. 5.3-3 leads immediately to the following velocity profiles⁴ in the region $r < b$ (designated by $<$) and $r > b$ (designated by $>$):

$$\frac{\bar{v}_z^<}{v_*^<} = \frac{1}{\kappa} \ln \left(\frac{(r - aR)v_*^<}{\nu} \right) + \lambda^< \quad \text{where } v_*^< = v_{**} \sqrt{\frac{b^2 - a^2}{a}} \quad (5C.2-2)$$

$$\frac{\bar{v}_z^>}{v_*^>} = \frac{1}{\kappa} \ln \left(\frac{(r - aR)v_*^>}{\nu} \right) + \lambda^> \quad \text{where } v_*^> = v_{**} \sqrt{1 - b^2} \quad (5C.2-3)$$

in which $v_{**} = \sqrt{(\mathcal{P}_0 - \mathcal{P}_L)R/2L\rho}$.

- (b) Obtain a relation between the constants $\lambda^<$ and $\lambda^>$ by requiring that the velocity be continuous at $r = bR$.

- (c) Use the results of (b) to show that the mass flow rate through the annulus is

$$w = \pi R^2 \rho v_{**} \left\{ (1 - a^2) \sqrt{1 - b^2} \left[\frac{1}{\kappa} \ln \frac{R(1 - b)\sqrt{1 - b^2} v_{**}}{\nu} + \lambda^> \right] - B \right\} \quad (5C.2-4)$$

in which B is

$$B = \frac{(b^2 - a^2)^{3/2}}{\kappa \sqrt{a}} \left(\frac{a}{a + b} + \frac{1}{2} \right) + \frac{(1 - b^2)^{3/2}}{\kappa} \left(\frac{1}{1 + b} + \frac{1}{2} \right) \quad (5C.2-5)$$

5C.3 Instability in a simple mechanical system (Fig. 5C.3).

- (a) A disk is rotating with a constant angular velocity Ω . Above the center of the disk a sphere of mass m is suspended by a massless rod of length L . Because of the rotation of the disk, the sphere experiences a centrifugal force and the rod makes an angle θ with the vertical. By making a force balance on the sphere, show that

$$\cos \theta = \frac{g}{\Omega^2 L} \quad (5C.3-1)$$

What happens when Ω goes to zero?

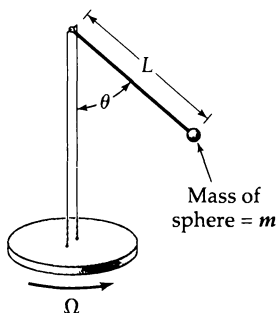


Fig. 5C.3. A simple mechanical system for illustrating concepts in stability.

³ J. G. Knudsen and D. L. Katz, *Fluid Dynamics and Heat Transfer*, McGraw-Hill, New York (1958); R. Rothfus (1948), J. E. Walker (1957), and G. A. Whan (1956), Doctoral theses, Carnegie Institute of Technology (now Carnegie-Mellon University), Pittsburgh, Pa.

⁴ W. Tiedt, *Berechnung des laminaren u. turbulenten Reibungswiderstandes konzentrischer u. exzentrischer Ringspalten*, Technischer Bericht Nr. 4, Inst. f. Hydraulik u. Hydraulologie, Technische Hochschule, Darmstadt (1968); D. M. Meter and R. B. Bird, *AIChE Journal*, 7, 41–45 (1961) did the same analysis using the Prandtl mixing length theory.

(b) Show that, if Ω is below some threshold value Ω_{thr} , the angle θ is zero. Above the threshold value, show that there are two admissible values for θ . Explain by means of a carefully drawn sketch of θ vs. Ω . Above Ω_{thr} label the two curves *stable* and *unstable*.

(c) In (a) and (b) we considered only the steady-state operation of the system. Next show that the equation of motion for the sphere of mass m is

$$mL \frac{d^2\theta}{dt^2} = m\Omega^2 L \sin \theta \cos \theta - mg \sin \theta \quad (5C.3-2)$$

Show that for steady-state operation this leads to Eq. 5C.3-1. We now want to use this equation to make a small-amplitude stability analysis. Let $\theta = \theta_0 + \theta_1$, where θ_0 is a steady-state solution (independent of time) and θ_1 is a very small perturbation (dependent on time).

(d) Consider first the lower branch in (b), which is $\theta_0 = 0$. Then $\sin \theta = \sin \theta_1 \approx \theta_1$ and $\cos \theta = \cos \theta_1 \approx 1$, so that Eq. 5B.2-2 becomes

$$\frac{d^2\theta_1}{dt^2} = \left(\Omega^2 - \frac{g}{L} \right) \theta_1 \quad (5C.3-3)$$

We now try a small-amplitude oscillation of the form $\theta_1 = A \Re\{e^{-i\omega t}\}$ and find that

$$\omega_{\pm} = \pm i \sqrt{\Omega^2 - \frac{g}{L}} \quad (5C.3-4)$$

Now consider two cases: (i) If $\Omega^2 < g/L$, both ω_+ and ω_- are real, and hence θ_1 oscillates; this indicates that for $\Omega^2 < g/L$ the system is stable. (ii) If $\Omega^2 > g/L$, the root ω_+ is positive imaginary and $e^{-i\omega t}$ will increase indefinitely with time; this indicates that for $\Omega^2 > g/L$ the system is unstable with respect to infinitesimal perturbations.

(e) Next consider the upper branch in (b). Do an analysis similar to that in (d). Set up the equation for θ_1 and drop terms in the square of θ_1 (that is, linearize the equation). Once again try a solution of the form $\theta_1 = A \Re\{e^{-i\omega t}\}$. Show that for the upper branch the system is stable with respect to infinitesimal perturbations.

(f) Relate the above analysis, which is for a system with one degree of freedom, to the problem of laminar-turbulent transition for the flow of a Newtonian fluid in the flow between two counter-rotating cylinders. Read the discussion by Landau and Lifshitz⁵ on this point.

5D.1 Derivation of the equation of change for the Reynolds stresses. At the end of §5.2 it was pointed out that there is an equation of change for the Reynolds stresses. This can be derived by (a) multiplying the i th component of the vector form of Eq. 5.2-5 by v'_i and time smoothing, (b) multiplying the j th component of the vector form of Eq. 5.2-5 by v'_j and time smoothing, and (c) adding the results of (a) and (b). Show that one finally gets

$$\begin{aligned} \rho \frac{D}{Dt} \overline{\mathbf{v}' \mathbf{v}'} = & -\rho \overline{\mathbf{v}' \mathbf{v}' \cdot \nabla \bar{\mathbf{v}}} - \rho \overline{\mathbf{v}' \mathbf{v}' \cdot \nabla \bar{\mathbf{v}}}^t - \rho \overline{\nabla \cdot \mathbf{v}' \mathbf{v}' \mathbf{v}'} \\ & - \overline{\mathbf{v}' \nabla p'} - \overline{\mathbf{v}' \nabla p'}^t + \mu \left\{ \overline{\mathbf{v}' \nabla^2 \mathbf{v}'} + \overline{\mathbf{v}' \nabla^2 \mathbf{v}'}^t \right\} \end{aligned} \quad (5D.1-1)$$

Equations 5.2-10 and 11 will be needed in this development.

5D.2 Kinetic energy of turbulence. By taking the trace of Eq. 5D.1-1 obtain the following:

$$\frac{D}{Dt} \left(\frac{1}{2} \rho \overline{\mathbf{v}'^2} \right) = -\rho \overline{(\mathbf{v}' \mathbf{v}' \cdot \nabla \bar{\mathbf{v}})} - (\nabla \cdot \frac{1}{2} \rho \overline{\mathbf{v}'^2 \mathbf{v}'}) - (\nabla \cdot \overline{p' \mathbf{v}'}) + \mu \overline{(\mathbf{v}' \cdot \nabla^2 \mathbf{v}')} \quad (5D.2-1)$$

Interpret the equation.⁶

⁵ L. Landau and E. M. Lifshitz, *Fluid Mechanics*, Pergamon, Oxford, 2nd edition (1987), §§26–27.

⁶ H. Tennekes and J. L. Lumley, *A First Course in Turbulence*, MIT Press, Cambridge, Mass. (1972), §3.2.

Interphase Transport in Isothermal Systems

- §6.1 Definition of friction factors
- §6.2 Friction factors for flow in tubes
- §6.3 Friction factors for flow around spheres
- §6.4^o Friction factors for packed columns

In Chapters 2–4 we showed how laminar flow problems may be formulated and solved. In Chapter 5 we presented some methods for solving turbulent flow problems by dimensional arguments or by semiempirical relations between the momentum flux and the gradient of the time-smoothed velocity. In this chapter we show how flow problems can be solved by a combination of dimensional analysis and experimental data. The technique presented here has been widely used in chemical, mechanical, aeronautical, and civil engineering, and it is useful for solving many practical problems. It is a topic worth learning well.

Many engineering flow problems fall into one of two broad categories: flow in channels and flow around submerged objects. Examples of channel flow are the pumping of oil through pipes, the flow of water in open channels, and extrusion of plastics through dies. Examples of flow around submerged objects are the motion of air around an airplane wing, motion of fluid around particles undergoing sedimentation, and flow across tube banks in heat exchangers.

In channel flow the main object is usually to get a relationship between the volume rate of flow and the pressure drop and/or elevation change. In problems involving flow around submerged objects the desired information is generally the relation between the velocity of the approaching fluid and the drag force on the object. We have seen in the preceding chapters that, if one knows the velocity and pressure distributions in the system, then the desired relationships for these two cases may be obtained. The derivation of the Hagen–Poiseuille equation in §2.3 and the derivation of the Stokes equation in §2.6 and §4.2 illustrate the two categories we are discussing here.

For many systems the velocity and pressure profiles cannot be easily calculated, particularly if the flow is turbulent or the geometry is complicated. One such system is the flow through a packed column; another is the flow in a tube in the shape of a helical coil. For such systems we can take carefully chosen experimental data and then construct “correlations” of dimensionless variables that can be used to estimate the flow behavior in geometrically similar systems. This method is based on §3.7.

We start in §6.1 by defining the “friction factor,” and then we show in §§6.2 and 6.3 how to construct friction factor charts for flow in circular tubes and flow around spheres. These are both systems we have already studied and, in fact, several results from earlier chapters are included in these charts. Finally in §6.4 we examine the flow in packed columns, to illustrate the treatment of a geometrically complicated system. The more complex problem of fluidized beds is not included in this chapter.¹

§6.1 DEFINITION OF FRICTION FACTORS

We consider the steadily driven flow of a fluid of constant density in one of two systems: (a) the fluid flows in a straight conduit of uniform cross section; (b) the fluid flows around a submerged object that has an axis of symmetry (or two planes of symmetry) parallel to the direction of the approaching fluid. There will be a force F_{f-s} exerted by the fluid on the solid surfaces. It is convenient to split this force into two parts: F_s , the force that would be exerted by the fluid even if it were stationary; and F_k , the additional force associated with the motion of the fluid (see §2.6 for the discussion of F_s and F_k for flow around spheres). In systems of type (a), F_k points in the same direction as the average velocity $\langle v \rangle$ in the conduit, and in systems of type (b), F_k points in the same direction as the approach velocity v_∞ .

For both types of systems we state that the magnitude of the force F_k is proportional to a characteristic area A and a characteristic kinetic energy K per unit volume; thus

$$F_k = AKf \quad (6.1-1)^1$$

in which the proportionality constant f is called the *friction factor*. Note that Eq. 6.1-1 is *not* a law of fluid dynamics, but only a definition for f . This is a useful definition, because the dimensionless quantity f can be given as a relatively simple function of the Reynolds number and the system shape.

Clearly, for any given flow system, f is not defined until A and K are specified. Let us now see what the customary definitions are:

(a) For *flow in conduits*, A is usually taken to be the wetted surface, and K is taken to be $\frac{1}{2}\rho\langle v \rangle^2$. Specifically, for circular tubes of radius R and length L we define f by

$$F_k = (2\pi RL)\left(\frac{1}{2}\rho\langle v \rangle^2\right)f \quad (6.1-2)$$

Generally, the quantity measured is not F_k , but rather the pressure difference $p_0 - p_L$ and the elevation difference $h_0 - h_L$. A force balance on the fluid between 0 and L in the direction of flow gives for fully developed flow

$$\begin{aligned} F_k &= [(p_0 - p_L) + \rho g(h_0 - h_L)]\pi R^2 \\ &= (\mathcal{P}_0 - \mathcal{P}_L)\pi R^2 \end{aligned} \quad (6.1-3)$$

Elimination of F_k between the last two equations then gives

$$f = \frac{1}{4} \left(\frac{D}{L} \right) \left(\frac{\mathcal{P}_0 - \mathcal{P}_L}{\frac{1}{2}\rho\langle v \rangle^2} \right) \quad (6.1-4)$$

¹ R. Jackson, *The Dynamics of Fluidized Beds*, Cambridge University Press (2000).

¹ For systems lacking symmetry, the fluid exerts both a force and a torque on the solid. For discussions of such systems see J. Happel and H. Brenner, *Low Reynolds Number Hydrodynamics*, Martinus Nijhoff, The Hague (1983), Chapter 5; H. Brenner, in *Adv. Chem. Engr.*, **6**, 287–438 (1966); S. Kim and S. J. Karrila, *Microhydrodynamics: Principles and Selected Applications*, Butterworth-Heinemann, Boston (1991), Chapter 5.

in which $D = 2R$ is the tube diameter. Equation 6.1-4 shows how to calculate f from experimental data. The quantity f is sometimes called the *Fanning friction factor*.²

(b) For flow around submerged objects, the characteristic area A is usually taken to be the area obtained by projecting the solid onto a plane perpendicular to the velocity of the approaching fluid; the quantity K is taken to be $\frac{1}{2}\rho v_\infty^2$, where v_∞ is the approach velocity of the fluid at a large distance from the object. For example, for flow around a sphere of radius R , we define f by the equation

$$F_k = (\pi R^2)(\frac{1}{2}\rho v_\infty^2)f \quad (6.1-5)$$

If it is not possible to measure F_k , then we can measure the terminal velocity of the sphere when it falls through the fluid (in that case, v_∞ has to be interpreted as the terminal velocity of the sphere). For the steady-state fall of a sphere in a fluid, the force F_k is just counterbalanced by the gravitational force on the sphere less the buoyant force (cf. Eq. 2.6-14):

$$F_k = \frac{4}{3}\pi R^3 \rho_{\text{sph}} g - \frac{4}{3}\pi R^3 \rho g \quad (6.1-6)$$

Elimination of F_k between Eqs. 6.1-5 and 6.1-6 then gives

$$f = \frac{4}{3} \frac{gD}{v_\infty^2} \left(\frac{\rho_{\text{sph}} - \rho}{\rho} \right) \quad (6.1-7)$$

This expression can be used to obtain f from terminal velocity data. The friction factor used in Eqs. 6.1-5 and 7 is sometimes called the *drag coefficient* and given the symbol c_D .

We have seen that the “drag coefficient” for submerged objects and the “friction factor” for channel flow are defined in the same general way. For this reason we prefer to use the same symbol and name for both of them.

§6.2 FRICTION FACTORS FOR FLOW IN TUBES

We now combine the definition of f in Eq. 6.1-2 with the dimensional analysis of §3.7 to show what f must depend on in this kind of system. We consider a “test section” of inner radius R and length L , shown in Fig. 6.2-1, carrying a fluid of constant density and viscosity at a steady mass flow rate. The pressures P_0 and P_L at the ends of the test section are known.

² This friction factor definition is due to J. T. Fanning, *A Practical Treatise on Hydraulic and Water Supply Engineering*, Van Nostrand, New York, 1st edition (1877), 16th edition (1906); the name “Fanning” is used to avoid confusion with the “Moody friction factor,” which is larger by a factor of 4 than the f used here [L. F. Moody, *Trans. ASME*, **66**, 671–684 (1944)].

If we use the “friction velocity” $v_* = \sqrt{\tau_0/\rho} = \sqrt{(P_0 - P_L)R/2L\rho}$, introduced in §5.3, then Eq. 6.1-4 assumes the form

$$f = 2(v_*/\langle v \rangle)^2 \quad (6.1-4a)$$

John Thomas Fanning (1837–1911) studied architectural and civil engineering, served as an officer in the Civil War, and after the war became prominent in hydraulic engineering. The 14th edition of his book *A Practical Treatise on Hydraulic and Water-Supply Engineering* appeared in 1899.

³ For the translational motion of a sphere in three dimensions, one can write approximately

$$F_k = (\pi R^2)(\frac{1}{2}\rho v_\infty^2)f\mathbf{n} \quad (6.1-5a)$$

where \mathbf{n} is a unit vector in the direction of \mathbf{v}_∞ . See Problem 6C.1.

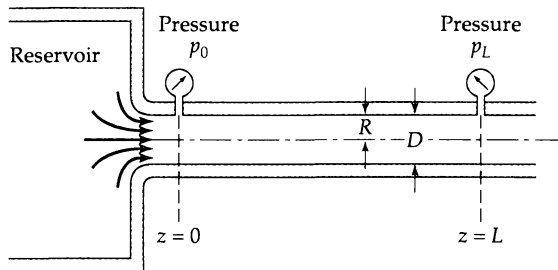


Fig. 6.2-1. Section of a circular pipe from $z = 0$ to $z = L$ for the discussion of dimensional analysis.

The system is either in steady laminar flow or steadily driven turbulent flow (i.e., turbulent flow with a steady total throughput). In either case the force in the z direction of the fluid on the inner wall of the test section is

$$F_k(t) = \int_0^L \int_0^{2\pi} \left(-\mu \frac{\partial v_z}{\partial r} \right) \Big|_{r=R} R d\theta dz \quad (6.2-1)$$

In turbulent flow the force may be a function of time, not only because of the turbulent fluctuations, but also because of occasional ripping off of the boundary layer from the wall, which results in some distances with long time scales. In laminar flow it is understood that the force will be independent of time.

Equating Eqs. 6.2-1 and 6.1-2, we get the following expression for the friction factor:

$$f(t) = \frac{\int_0^L \int_0^{2\pi} \left(-\mu \frac{\partial v_z}{\partial r} \right) \Big|_{r=R} R d\theta dz}{(2\pi RL)(\frac{1}{2}\rho(v_z)^2)} \quad (6.2-2)$$

Next we introduce the dimensionless quantities from §3.7: $\check{r} = r/D$, $\check{z} = z/D$, $\check{v}_z = v_z/\langle v_z \rangle$, $\check{t} = \langle v_z \rangle t/D$, $\check{\mathcal{P}} = (\mathcal{P} - \mathcal{P}_0)/\rho(v_z)^2$, and $\text{Re} = D\langle v_z \rangle \rho / \mu$. Then Eq. 6.2-2 may be rewritten as

$$f(\check{t}) = \frac{1}{\pi} \frac{D}{L} \frac{1}{\text{Re}} \int_0^{L/D} \int_0^{2\pi} \left(-\frac{\partial \check{v}_z}{\partial \check{r}} \right) \Big|_{\check{r}=1/2} d\theta d\check{z} \quad (6.2-3)$$

This relation is valid for laminar or turbulent flow in circular tubes. We see that for flow systems in which the drag depends on viscous forces alone (i.e., no "form drag") the product of $f\text{Re}$ is essentially a dimensionless velocity gradient averaged over the surface.

Recall now that, in principle, $\partial \check{v}_z / \partial \check{r}$ can be evaluated from Eqs. 3.7-8 and 9 along with the boundary conditions¹

$$\text{B.C. 1:} \quad \text{at } \check{r} = \frac{1}{2}, \quad \check{v} = 0 \quad \text{for } z > 0 \quad (6.2-4)$$

$$\text{B.C. 2:} \quad \text{at } \check{z} = 0, \quad \check{v} = \check{\mathbf{d}}_z \quad (6.2-5)$$

$$\text{B.C. 3:} \quad \text{at } \check{r} = 0 \text{ and } \check{z} = 0, \quad \check{\mathcal{P}} = 0 \quad (6.2-6)$$

¹ Here we follow the customary practice of neglecting the $(\partial^2 / \partial \check{z}^2)\mathbf{v}$ terms of Eq. 3.7-9, on the basis of order-of-magnitude arguments such as those given in §4.4. With those terms suppressed, we do not need an outlet boundary condition on \mathbf{v} .

and appropriate initial conditions. The uniform inlet velocity profile in Eq. 6.2-5 is accurate except very near the wall, for a well-designed nozzle and upstream system. If Eqs. 3.7-8 and 9 could be solved with these boundary and initial conditions to get \check{v} and \check{P} , the solutions would necessarily be of the form

$$\check{v} = \check{v}(\check{r}, \theta, \check{z}, \check{t}; \text{Re}) \quad (6.2-7)$$

$$\check{P} = \check{P}(\check{r}, \theta, \check{z}, \check{t}; \text{Re}) \quad (6.2-8)$$

That is, the functional dependence of \check{v} and \check{P} must, in general, include all the dimensionless variables and the one dimensionless group appearing in the differential equations. No additional dimensionless groups enter via the preceding boundary conditions. As a consequence, $\partial\check{v}_z/\partial\check{r}$ must likewise depend on $\check{r}, \theta, \check{z}, \check{t}$, and Re . When $\partial\check{v}_z/\partial\check{r}$ is evaluated at $\check{r} = \frac{1}{2}$ and then integrated over \check{z} and θ in Eq. 6.2-3, the result depends only on \check{t} , Re , and L/D (the latter appearing in the upper limit in the integration over \check{z}). Therefore we are led to the conclusion that $f(\check{t}) = f(\text{Re}, L/D, \check{t})$, which, when time averaged, becomes

$$f = f(\text{Re}, L/D) \quad (6.2-9)$$

when the time average is performed over an interval long enough to include any long-time turbulent disturbances. The measured friction factor then depends only on the Reynolds number and the length-to-diameter ratio.

The dependence of f on L/D arises from the development of the time-average velocity distribution from its flat entry shape toward more rounded profiles at downstream z values. This development occurs within an entrance region, of length $L_e \cong 0.03D \text{ Re}$ for laminar flow or $L_e \approx 60D$ for turbulent flow, beyond which the shape of the velocity distribution is "fully developed." In the transportation of fluids, the entrance length is usually a small fraction of the total; then Eq. 6.2-9 reduces to the long-tube form

$$f = f(\text{Re}) \quad (6.2-10)$$

and f can be evaluated experimentally from Eq. 6.1-4, which was written for fully developed flow at the inlet and outlet.

Equations 6.2-9 and 10 are useful results, since they provide a guide for the systematic presentation of data on flow rate versus pressure difference for laminar and turbulent flow in circular tubes. For *long* tubes we need only a single curve of f plotted versus the single combination $D\langle\bar{v}_z\rangle\rho/\mu$. Think how much simpler this is than plotting pressure drop versus the flow rate for separate values of D , L , ρ , and μ , which is what the uninitiated might do.

There is much experimental information for pressure drop versus flow rate in tubes, and hence f can be calculated from the experimental data by Eq. 6.1-4. Then f can be plotted versus Re for smooth tubes to obtain the *solid* curves shown in Fig. 6.2-2. These solid curves describe the laminar and turbulent behavior for fluids flowing in *long, smooth, circular* tubes.

Note that the *laminar* curve on the friction factor chart is merely a plot of the *Hagen-Poiseuille* equation in Eq. 2.3-21. This can be seen by substituting the expression for $(P_0 - P_L)$ from Eq. 2.3-21 into Eq. 6.1-4 and using the relation $w = \rho\langle v_z \rangle \pi R^2$; this gives

$$f = \frac{16}{\text{Re}} \begin{cases} \text{Re} < 2100 & \text{stable} \\ \text{Re} > 2100 & \text{usually unstable} \end{cases} \quad (6.2-11)$$

in which $\text{Re} = D\langle\bar{v}_z\rangle\rho/\mu$; this is exactly the laminar line in Fig. 6.2-2.

Analogous *turbulent* curves have been constructed by using *experimental data*. Some analytical curve-fit expressions are also available. For example, Eq. 5.1-6 can be put into the form

$$f = \frac{0.0791}{\text{Re}^{1/4}} \quad 2.1 \times 10^3 < \text{Re} < 10^5 \quad (6.2-12)$$

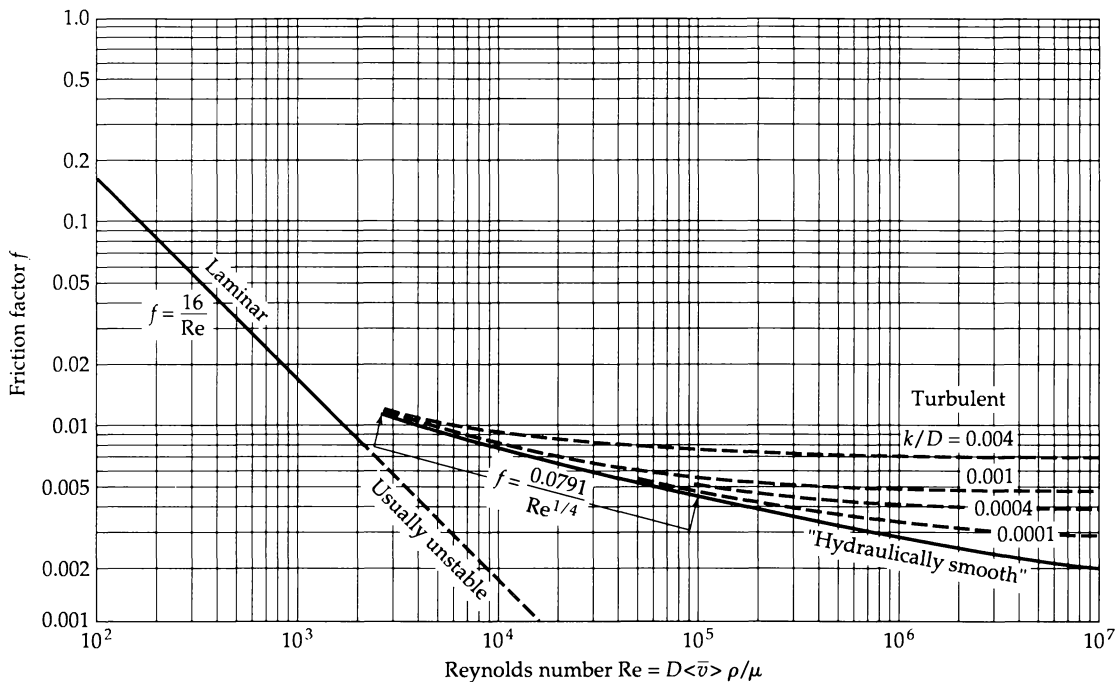


Fig. 6.2-2. Friction factor for tube flow (see definition of f in Eqs. 6.1-2 and 6.1-3. [Curves of L. F. Moody, *Trans. ASME*, **66**, 671–684 (1944) as presented in W. L. McCabe and J. C. Smith, *Unit Operations of Chemical Engineering*, McGraw-Hill, New York (1954).]

which is known as the *Blasius formula*.² Equation 5.5-1 (with 2.5 replaced by 2.45 and 1.75 by 2.00) is equivalent to

$$\frac{1}{\sqrt{f}} = 4.0 \log_{10} \text{Re} \sqrt{f} - 0.4 \quad 2.3 \times 10^3 < \text{Re} < 4 \times 10^6 \quad (6.2-13)$$

which is known as the *Prandtl formula*.³ Finally, corresponding to Eq. 5.5-2, we have

$$f = \frac{2}{\Psi^{2/(\alpha+1)}} \quad \text{where} \quad \Psi = \frac{\epsilon^{3/2}(\sqrt{3} + 5\alpha)}{2^\alpha \alpha(\alpha + 1)(\alpha + 2)} \quad (6.2-14)$$

and $\alpha = 3/(2 \ln \text{Re})$. This has been found to represent the experimental data well for $3.07 \times 10^3 < \text{Re} < 3.23 \times 10^6$. Equation 6.2-14 is called the *Barenblatt formula*.⁴

A further relation, which includes the dashed curves for rough pipes in Fig. 6.2-2, is the empirical *Haaland equation*⁵

$$\frac{1}{\sqrt{f}} = -3.6 \log_{10} \left[\frac{6.9}{\text{Re}} + \left(\frac{k/D}{3.7} \right)^{10/9} \right] \quad \begin{cases} 4 \times 10^4 < \text{Re} < 10^8 \\ 0 < k/D < 0.05 \end{cases} \quad (6.2-15)$$

² H. Blasius, *Forschungsarbeiten des Ver. Deutsch. Ing.*, no. 131 (1913).

³ L. Prandtl, *Essentials of Fluid Dynamics*, Hafner, New York (1952), p. 165.

⁴ G. I. Barenblatt, *Scaling, Self-Similarity, and Intermediate Asymptotics*, Cambridge University Press (1996), §10.2.

⁵ S. E. Haaland, *Trans. ASME, JFE*, **105**, 89–90 (1983). For other empiricisms see D. J. Zigrang and N. D. Sylvester, *AIChE Journal*, **28**, 514–515 (1982).

This equation is stated⁵ to be accurate within 1.5%. As can be seen in Fig. 6.2-2, the frictional resistance to flow increases with the height, k , of the protuberances. Of course, k has to enter into the correlation in a dimensionless fashion and hence appears via the ratio k/D .

For turbulent flow in noncircular tubes it is common to use the following empiricism: First we define a "mean hydraulic radius" R_h as follows:

$$R_h = S/Z \quad (6.2-16)$$

in which S is the cross section of the conduit and Z is the wetted perimeter. Then we can use Eq. 6.1-4 and Fig. 6.2-2, with the diameter D of the circular pipe replaced by $4R_h$. That is, we calculate pressure differences by replacing Eq. 6.1-4 by

$$f = \left(\frac{R_h}{L} \right) \left(\frac{\mathcal{P}_0 - \mathcal{P}_L}{\frac{1}{2} \rho (v_z)^2} \right) \quad (6.2-17)$$

and getting f from Fig. 6.2-2 with a Reynolds number defined as

$$Re_h = \frac{4R_h \langle v_z \rangle \rho}{\mu} \quad (6.2-18)$$

This estimation method of Eqs. 6.2-16 to 18 should *not* be used for *laminar* flow.

EXAMPLE 6.2-1

Pressure Drop Required for a Given Flow Rate

What pressure gradient is required to cause diethylaniline, $C_6H_5N(C_2H_5)_2$, to flow in a horizontal, smooth, circular tube of inside diameter $D = 3$ cm at a mass rate of 1028 g/s at $20^\circ C$? At this temperature the density of diethylaniline is $\rho = 0.935 \text{ g/cm}^3$ and its viscosity is $\mu = 1.95 \text{ cp}$.

SOLUTION

The Reynolds number for the flow is

$$\begin{aligned} Re &= \frac{D \langle v_z \rangle \rho}{\mu} = \frac{Dw}{(\pi D^2/4)\mu} = \frac{4w}{\pi D \mu} \\ &= \frac{4(1028 \text{ g/s})}{\pi(3 \text{ cm})(1.95 \times 10^{-2} \text{ g/cm} \cdot \text{s})} = 2.24 \times 10^4 \end{aligned} \quad (6.2-19)$$

From Fig. 6.2-2, we find that for this Reynolds number the friction factor f has a value of 0.0063 for smooth tubes. Hence the pressure gradient required to maintain the flow is (according to Eq. 6.1-4)

$$\begin{aligned} \frac{p_0 - p_L}{L} &= \left(\frac{4}{D} \right) \left(\frac{1}{2} \rho \langle v_z \rangle^2 \right) f = \frac{2}{D} \rho \left(\frac{4w}{\pi D^2 \mu} \right)^2 f \\ &= \frac{32w^2 f}{\pi^2 D^5 \mu} = \frac{(32)(1028)^2(0.0063)}{\pi^2 (3.0)^5 (0.935)} \\ &= 95 (\text{dyne/cm}^2)/\text{cm} = 0.071 (\text{mm Hg})/\text{cm} \end{aligned} \quad (6.2-20)$$

EXAMPLE 6.2-2

Flow Rate for a Given Pressure Drop

Determine the flow rate, in pounds per hour, of water at $68^\circ F$ through a 1000-ft length of horizontal 8-in. schedule 40 steel pipe (internal diameter 7.981 in.) under a pressure difference of 3.00 psi. For such a pipe use Fig. 6.2-2 and assume that $k/D = 2.3 \times 10^{-4}$.

SOLUTION

We want to use Eq. 6.1-4 and Fig. 6.2-2 to solve for $\langle v_z \rangle$ when $p_0 - p_L$ is known. However, the quantity $\langle v_z \rangle$ appears explicitly on the left side of the equation and implicitly on the right side in f , which depends on $Re = D \langle v_z \rangle \rho / \mu$. Clearly a trial-and-error solution can be found.

However, if one has to make more than a few calculations of $\langle v_z \rangle$, it is advantageous to develop a systematic approach; we suggest two methods here. Because experimental data are often presented in graphical form, it is important for engineering students to use their originality in devising special methods such as those described here.

Method A. Figure 6.2-2 may be used to construct a plot⁶ of Re versus the group $Re\sqrt{f}$, which does not contain $\langle v_z \rangle$:

$$Re\sqrt{f} = \frac{D\langle v_z \rangle \rho}{\mu} \sqrt{\frac{(p_0 - p_L)D}{2L\rho\langle v_z \rangle^2}} = \frac{D\rho}{\mu} \sqrt{\frac{(p_0 - p_L)D}{2L\rho}} \quad (6.2-21)$$

The quantity $Re\sqrt{f}$ can be computed for this problem, and a value of the Reynolds number can be read from the Re versus $Re\sqrt{f}$ plot. From Re the average velocity and flow rate can then be calculated.

Method B. Figure 6.2-2 may also be used directly without any replotted, by devising a scheme that is equivalent to the graphical solution of two simultaneous equations. The two equations are

$$f = f(Re, k/D) \quad \text{curve given in Fig. 6.2-2} \quad (6.2-22)$$

$$f = \frac{(Re\sqrt{f})^2}{Re^2} \quad \text{straight line of slope } -2 \text{ on log-log plot} \quad (6.2-23)$$

The procedure is then to compute $Re\sqrt{f}$ according to Eq. 6.2-21 and then to plot Eq. 6.2-23 on the log-log plot of f versus Re in Fig. 6.2-2. The intersection point gives the Reynolds number of the flow, from which $\langle v_z \rangle$ can then be computed.

For the problem at hand, we have

$$\begin{aligned} p_0 - p_L &= (3.00 \text{ lb}_f/\text{in.}^2)(32.17 \text{ lb}_m/\text{ft lb}_f \text{ s}^2)(144 \text{ in.}^2/\text{ft}^2) \\ &= 1.39 \times 10^4 \text{ lb}_m/\text{ft} \cdot \text{s}^2 \end{aligned}$$

$$D = (7.981 \text{ in.})(\frac{1}{12} \text{ ft/in.}) = 0.665 \text{ ft}$$

$$L = 1000 \text{ ft}$$

$$\rho = 62.3 \text{ lb}_m/\text{ft}^3$$

$$\begin{aligned} \mu &= (1.03 \text{ cp})(6.72 \times 10^{-4}(\text{lb}_m/\text{ft} \cdot \text{s})/\text{cp}) \\ &= 6.93 \times 10^{-4} \text{ lb}_m/\text{ft} \cdot \text{s} \end{aligned}$$

Then according to Eq. 6.2-21,

$$\begin{aligned} Re\sqrt{f} &= \frac{D\rho}{\mu} \sqrt{\frac{(p_0 - p_L)D}{2L\rho}} = \frac{(0.665)(62.3)}{(6.93 \times 10^{-4})} \sqrt{\frac{(1.39 \times 10^4)(0.665)}{2(1000)(62.3)}} \\ &= 1.63 \times 10^4 \quad (\text{dimensionless}) \end{aligned} \quad (6.2-24)$$

The line of Eq. 6.2-23 for this value of $Re\sqrt{f}$ passes through $f = 1.0$ at $Re = 1.63 \times 10^4$ and through $f = 0.01$ at $Re = 1.63 \times 10^5$. Extension of the straight line through these points to the curve of Fig. 6.2-2 for $k/D = 0.00023$ gives the solution to the two simultaneous equations:

$$Re = \frac{D\langle v_z \rangle \rho}{\mu} = \frac{4w}{\pi D \mu} = 2.4 \times 10^5 \quad (6.2-25)$$

Solving for w then gives

$$\begin{aligned} w &= (\pi/4)D\mu Re \\ &= (0.7854)(0.665)(6.93 \times 10^{-4})(3600)(2.4 \times 10^5) \\ &= 3.12 \times 10^5 \text{ lb}_m/\text{hr} = 39 \text{ kg/s} \end{aligned} \quad (6.2-26)$$

⁶ A related plot was proposed by T. von Kármán, *Nachr. Ges. Wiss. Göttingen, Fachgruppen*, I, 5, 58–76 (1930).

§6.3 FRICTION FACTORS FOR FLOW AROUND SPHERES

In this section we use the definition of the friction factor in Eq. 6.1-5 along with the dimensional analysis of §3.7 to determine the behavior of f for a stationary sphere in an infinite stream of fluid approaching with a uniform, steady velocity v_∞ . We have already studied the flow around a sphere in §2.6 and §4.2 for $\text{Re} < 0.1$ (the “creeping flow” region). At Reynolds numbers above about 1 there is a significant unsteady eddy motion in the wake of the sphere. Therefore, it will be necessary to do a time average over a time interval long with respect to this eddy motion.

Recall from §2.6 that the total force acting in the z direction on the sphere can be written as the sum of a contribution from the normal stresses (F_n) and one from the tangential stresses (F_t). One part of the normal-stress contribution is the force that would be present even if the fluid were stationary, F_s . Thus the “kinetic force,” associated with the fluid motion, is

$$F_k = (F_n - F_s) + F_t = F_{\text{form}} + F_{\text{friction}} \quad (6.3-1)$$

The forces associated with the form drag and the friction drag are then obtained from

$$F_{\text{form}}(t) = \int_0^{2\pi} \int_0^\pi (-\bar{\mathcal{P}}|_{r=R} \cos \theta) R^2 \sin \theta d\theta d\phi \quad (6.3-2)$$

$$F_{\text{friction}}(t) = \int_0^{2\pi} \int_0^\pi \left(-\mu \left[r \frac{\partial}{\partial r} \left(\frac{v_\theta}{r} \right) + \frac{1}{r} \frac{\partial v_r}{\partial \theta} \right] \Big|_{r=R} \sin \theta \right) R^2 \sin \theta d\theta d\phi \quad (6.3-3)$$

Since v_r is zero everywhere on the sphere surface, the term containing $\partial v_r / \partial \theta$ is zero.

If now we split f into two parts as follows

$$f = f_{\text{form}} + f_{\text{friction}} \quad (6.3-4)$$

then, from the definition in Eq. 6.1-5, we get

$$f_{\text{form}}(\check{t}) = \frac{2}{\pi} \int_0^{2\pi} \int_0^\pi (-\bar{\mathcal{P}}|_{\check{r}=1} \cos \theta) \sin \theta d\theta d\phi \quad (6.3-5)$$

$$f_{\text{friction}}(\check{t}) = -\frac{4}{\pi} \frac{1}{\text{Re}} \int_0^{2\pi} \int_0^\pi \left[\check{r} \frac{\partial}{\partial \check{r}} \left(\frac{\check{v}_\theta}{\check{r}} \right) \right] \Big|_{\check{r}=1} \sin^2 \theta d\theta d\phi \quad (6.3-6)$$

The friction factor is expressed here in terms of dimensionless variables

$$\check{\mathcal{P}} = \frac{\bar{\mathcal{P}}}{\rho v_\infty^2} \quad \check{v}_\theta = \frac{v_\theta}{v_\infty} \quad \check{r} = \frac{r}{R} \quad \check{t} = \frac{v_\infty t}{R} \quad (6.3-7)$$

and a Reynolds number defined as

$$\text{Re} = \frac{D v_\infty \rho}{\mu} = \frac{2 R v_\infty \rho}{\mu} \quad (6.3-8)$$

To evaluate $f(\check{t})$ one would have to know $\check{\mathcal{P}}$ and \check{v}_θ as functions of \check{r} , θ , ϕ , and \check{t} .

We know that for incompressible flow these distributions can *in principle* be obtained from the solution of Eqs. 3.7-8 and 9 along with the boundary conditions

$$\text{B.C. 1:} \quad \text{at } \check{r} = 1, \quad \check{v}_r = 0 \quad \text{and} \quad \check{v}_\theta = 0 \quad (6.3-9)$$

$$\text{B.C. 2:} \quad \text{at } \check{r} = \infty, \quad \check{v}_z = 1 \quad (6.3-10)$$

$$\text{B.C. 3:} \quad \text{at } \check{r} = \infty, \quad \check{\mathcal{P}} = 0 \quad (6.3-11)$$

and some appropriate initial condition on \check{v} . Because no additional dimensionless groups enter via the boundary and initial conditions, we know that the dimensionless pressure and velocity profiles will have the following form:

$$\check{\mathcal{P}} = \check{\mathcal{P}}(\check{r}, \theta, \phi, \check{t}; \text{Re}) \quad \check{v} = \check{v}(\check{r}, \theta, \phi, \check{t}; \text{Re}) \quad (6.3-12)$$

When these expressions are substituted into Eqs. 6.3-5 and 6, it is then evident that the friction factor in Eq. 6.3-4 must have the form $f(t) = f(\text{Re}, t)$, which, when time averaged over the turbulent fluctuations, simplifies to

$$f = f(\text{Re}) \quad (6.3-13)$$

by using arguments similar to those in §6.2. Hence from the definition of the friction factor and the dimensionless form of the equations of change and the boundary conditions, we find that f must be a function of Re alone.

Many experimental measurements of the drag force on spheres are available, and when these are plotted in dimensionless form, Fig. 6.3-1 results. For this system there is no sharp transition from an unstable laminar flow curve to a stable turbulent flow curve as for long tubes at a Reynolds number of about 2100 (see Fig. 6.2-2). Instead, as the approach velocity increases, f varies smoothly and moderately up to Reynolds numbers of the order of 10^5 . The kink in the curve at about $\text{Re} = 2 \times 10^5$ is associated with the shift of the boundary layer separation zone from in front of the equator to in back of the equator of the sphere.¹

We have juxtaposed the discussions of tube flow and flow around a sphere to emphasize the fact that various flow systems behave quite differently. Several points of difference between the two systems are:

Flow in Tubes	Flow Around Spheres
• Rather well defined laminar-turbulent transition at about $\text{Re} = 2100$	• No well defined laminar-turbulent transition
• The only contribution to f is the friction drag	• Contributions to f from both friction and form drag
• No boundary layer separation	• There is a kink in the f vs. Re curve associated with a shift in the separation zone

The general shape of the curves in Figs. 6.1-2 and 6.3-1 should be carefully remembered.

For the *creeping flow region*, we already know that the drag force is given by *Stokes' law*, which is a consequence of solving the continuity equation and the Navier-Stokes equation of motion without the $\rho Dv/Dt$ term. Stokes' law can be rearranged into the form of Eq. 6.1-5 to get

$$F_k = (\pi R^2)(\frac{1}{2}\rho v_\infty^2) \left(\frac{24}{Dv_\infty \rho / \mu} \right) \quad (6.3-14)$$

Hence for *creeping flow* around a sphere

$$f = \frac{24}{\text{Re}} \quad \text{for } \text{Re} < 0.1 \quad (6.3-15)$$

and this is the straight-line asymptote as $\text{Re} \rightarrow 0$ of the friction factor curve in Fig. 6.3-1.

For higher values of the Reynolds number, Eq. 4.2-21 can describe f accurately up to about $\text{Re} = 1$. However, the empirical expression²

$$f = \left(\sqrt{\frac{24}{\text{Re}}} + 0.5407 \right)^2 \quad \text{for } \text{Re} < 6000 \quad (6.3-16)$$

¹ R. K. Adair, *The Physics of Baseball*, Harper and Row, New York (1990).

² F. F. Abraham, *Physics of Fluids*, **13**, 2194 (1970); M. Van Dyke, *Physics of Fluids*, **14**, 1038–1039 (1971).

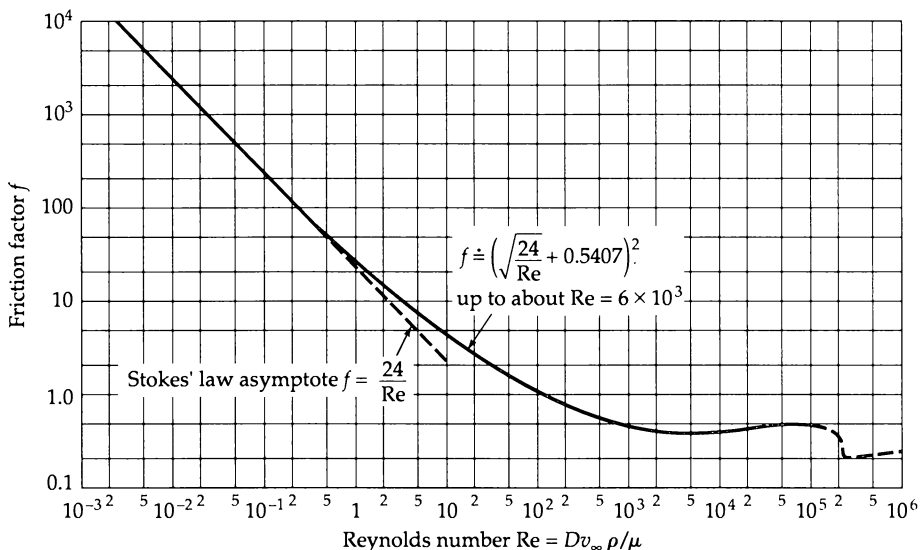


Fig. 6.3-1. Friction factor (or drag coefficient) for spheres moving relative to a fluid with a velocity v_∞ . The definition of f is given in Eq. 6.1-5. [Curve taken from C. E. Lapple, "Dust and Mist Collection," in *Chemical Engineers' Handbook*, (J. H. Perry, ed.), McGraw-Hill, New York, 3rd edition (1950), p. 1018.]

is both simple and useful. It is important to remember that

$$f \approx 0.44 \quad \text{for } 5 \times 10^2 < \text{Re} < 1 \times 10^5 \quad (6.3-17)$$

which covers a remarkable range of Reynolds numbers. Eq. 6.3-17 is sometimes called *Newton's resistance law*; it is handy for a seat-of-the-pants calculation. According to this, the drag force is proportional to the square of the approach velocity of the fluid.

Many extensions of Fig. 6.3-1 have been made, but a systematic study is beyond the scope of this text. Among the effects that have been investigated are wall effects³ (see Prob. 6C.2), fall of droplets with internal circulation,⁴ hindered settling (i.e., fall of clusters of particles⁵ that interfere with one another), unsteady flow,⁶ and the fall of non-spherical particles.⁷

EXAMPLE 6.3-1

Determination of the Diameter of a Falling Sphere

Glass spheres of density $\rho_{\text{sph}} = 2.62 \text{ g/cm}^3$ are to be allowed to fall through liquid CCl_4 at 20°C in an experiment for studying human reaction times in making time observations with stopwatches and more elaborate devices. At this temperature the relevant properties of CCl_4 are $\rho = 1.59 \text{ g/cm}^3$ and $\mu = 9.58 \text{ millipoises}$. What diameter should the spheres be to have a terminal velocity of about 65 cm/s ?

³ J. R. Strom and R. C. Kintner, *AIChE Journal*, **4**, 153–156 (1958).

⁴ L. Landau and E. M. Lifshitz, *Fluid Mechanics*, Pergamon, Oxford, 2nd edition (1987), pp. 65–66; S. Hu and R. C. Kintner, *AIChE Journal*, **1**, 42–48 (1955).

⁵ C. E. Lapple, *Fluid and Particle Mechanics*, University of Delaware Press, Newark, Del. (1951), Chapter 13; R. F. Probstein, *Physicochemical Hydrodynamics*, Wiley, New York, 2nd edition (1994), §5.4.

⁶ R. R. Hughes and E. R. Gilliland, *Chem. Eng. Prog.*, **48**, 497–504 (1952); L. Landau and E. M. Lifshitz, *Fluid Mechanics*, Pergamon, Oxford, 2nd edition (1987), pp. 90–91.

⁷ E. S. Pettyjohn and E. B. Christiansen, *Chem. Eng. Prog.*, **44**, 147 (1948); H. A. Becker, *Can. J. Chem. Eng.*, **37**, 885–891 (1959); S. Kim and S. J. Karrila, *Microhydrodynamics: Principles and Selected Applications*, Butterworth-Heinemann, Boston (1991), Chapter 5.

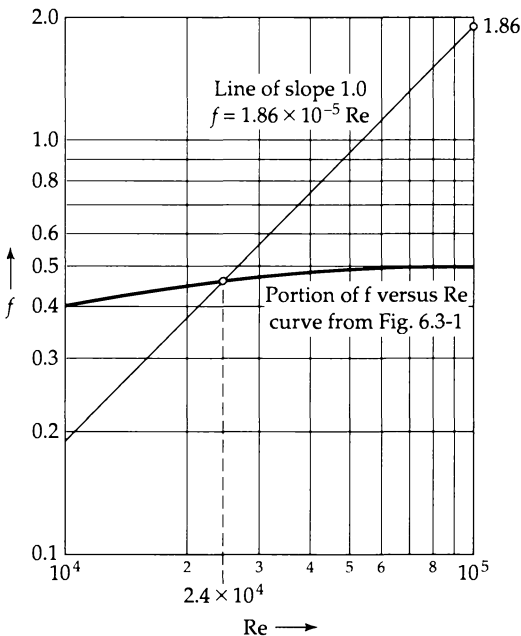


Fig. 6.3-2. Graphical procedure used in Example 6.3-1.

SOLUTION

To find the sphere diameter, we have to solve Eq. 6.1-7 for D . However, in this equation one has to know D in order to get f ; and f is given by the solid curve in Fig. 6.3-1. A trial-and-error procedure can be used, taking $f = 0.44$ as a first guess.

Alternatively, we can solve Eq. 6.1-7 for f and then note that f/Re is a quantity independent of D :

$$\frac{f}{Re} = \frac{4}{3} \frac{g\mu}{\rho v_\infty^3} \left(\frac{\rho_{\text{sph}} - \rho}{\rho} \right) \quad (6.3-18)$$

The quantity on the right side can be calculated with the information above, and we call it C . Hence we have two simultaneous equations to solve:

$$f = C Re \quad \text{from Eq. 6.3-18} \quad (6.3-19)$$

$$f = f(Re) \quad \text{from Fig. 6.3-1} \quad (6.3-20)$$

Equation 6.3-19 is a straight line with slope of unity on the log-log plot of f versus Re .

For the problem at hand we have

$$C = \frac{4}{3} \frac{(980)(9.58 \times 10^{-3})}{(1.59)(65)^3} \left(\frac{2.62 - 1.59}{1.59} \right) = 1.86 \times 10^{-5} \quad (6.3-21)$$

Hence at $Re = 10^5$, according to Eq. 6.3-19, $f = 1.86$. The line of slope 1 passing through $f = 1.86$ at $Re = 10^5$ is shown in Fig. 6.3-2. This line intersects the curve of Eq. 6.3-20 (i.e., the curve of Fig. 6.3-1) at $Re = Dv_\infty\rho/\mu = 2.4 \times 10^4$. The sphere diameter is then found to be

$$D = \frac{Re \mu}{\rho v_\infty} = \frac{(2.4 \times 10^4)(9.58 \times 10^{-3})}{(1.59)(65)} = 2.2 \text{ cm} \quad (6.3-22)$$

§6.4 FRICTION FACTORS FOR PACKED COLUMNS

In the preceding two sections we have discussed the friction factor correlations for two simple flow systems of rather wide interest. Friction factor charts are available for a number of other systems, such as transverse flow past a cylinder, flow across tube

banks, flow near baffles, and near flow around rotating disks. These and many more are summarized in various reference works.¹ One complex system of considerable interest in chemical engineering is the packed column, widely used for catalytic reactors and for separation processes.

There have been two main approaches for developing friction factor expressions for packed columns. In one method the packed column is visualized as a bundle of tangled tubes of weird cross section; the theory is then developed by applying the previous results for single straight tubes to the collection of crooked tubes. In the second method the packed column is regarded as a collection of submerged objects, and the pressure drop is obtained by summing up the resistances of the submerged particles.² The tube bundle theories have been somewhat more successful, and we discuss them here. Figure 6.4-1(a) depicts a packed column, and Fig. 6.4-1(b) illustrates the tube bundle model.

A variety of materials may be used for the packing in columns: spheres, cylinders, Berl saddles, and so on. It is assumed throughout the following discussion that the packing is statistically uniform, so that there is no "channeling" (in actual practice, channeling frequently occurs, and then the development given here does not apply). It is further assumed that the diameter of the packing particles is small in comparison to the diameter of the column in which the packing is contained, and that the column diameter is uniform.

We define the friction factor for the packed column analogously to Eq. 6.1-4:

$$f = \frac{1}{4} \left(\frac{D_p}{L} \right) \left(\frac{\mathcal{P}_0 - \mathcal{P}_L}{\frac{1}{2} \rho v_0^2} \right) \quad (6.4-1)$$

in which L is the length of the packed column, D_p is the effective particle diameter (defined presently), and v_0 is the *superficial velocity*; this is the volume flow rate divided by the empty column cross section, $v_0 = w/\rho S$.

The pressure drop through a representative tube in the tube bundle model is given by Eq. 6.2-17

$$\mathcal{P}_0 - \mathcal{P}_L = \frac{1}{2} \rho (v)^2 \left(\frac{L}{R_h} \right) f_{\text{tube}} \quad (6.4-2)$$

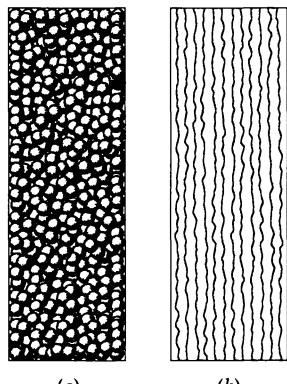


Fig. 6.4-1. (a) A cylindrical tube packed with spheres;
(b) a "tube bundle" model for the packed column in (a).

¹ P. C. Carman, *Flow of Gases through Porous Media*, Butterworths, London (1956); J. G. Richardson, Section 16 in *Handbook of Fluid Dynamics* (V. L. Streeter, ed.), McGraw-Hill, New York (1961); M. Kaviany, Chapter 21 in *The Handbook of Fluid Dynamics* (R. W. Johnson, ed.), CRC Press, Boca Raton, Fla. (1998).

² W. E. Ranz, *Chem. Eng. Prog.*, **48**, 274–253 (1952); H. C. Brinkman, *Appl. Sci. Research.*, **A1**, 27–34, 81–86, 333–346 (1949). **Henri Coenraad Brinkman** (1908–1961) did research on viscous dissipation heating, flow in porous media, and plasma physics; he taught at the University of Bandung, Indonesia, from 1949 to 1954, where he wrote *The Application of Spinor Invariants to Atomic Physics*.

in which the friction factor for a single tube, f_{tube} , is a function of the Reynolds number $\text{Re}_h = 4R_h \langle v \rangle \rho / \mu$. When this pressure difference is substituted into Eq. 6.4-1, we get

$$f = \frac{1}{4} \frac{D_p \langle v \rangle^2}{R_h v_0^2} f_{\text{tube}} = \frac{1}{4\epsilon^2} \frac{D_p}{R_h} f_{\text{tube}} \quad (6.4-3)$$

In the second expression, we have introduced the *void fraction*, ϵ , the fraction of space in the column not occupied by the packing. Then $v_0 = \langle v \rangle \epsilon$, which results from the definition of the superficial velocity. We now need an expression for R_h .

The hydraulic radius can be expressed in terms of the void fraction ϵ and the wetted surface a per unit volume of bed as follows:

$$\begin{aligned} R_h &= \left(\frac{\text{cross section available for flow}}{\text{wetted perimeter}} \right) \\ &= \left(\frac{\text{volume available for flow}}{\text{total wetted surface}} \right) \\ &= \frac{\left(\frac{\text{volume of voids}}{\text{volume of bed}} \right)}{\left(\frac{\text{wetted surface}}{\text{volume of bed}} \right)} = \frac{\epsilon}{a} \end{aligned} \quad (6.4-4)$$

The quantity a is related to the “specific surface” a_v (total particle surface per volume of particles) by

$$a_v = \frac{a}{1 - \epsilon} \quad (6.4-5)$$

The quantity a_v is in turn used to define the mean particle diameter D_p as follows:

$$D_p = \frac{6}{a_v} \quad (6.4-6)$$

This definition is chosen because, for spheres of uniform diameter, D_p is exactly the diameter of a sphere. From the last three expressions we find that the hydraulic radius is $R_h = D_p \epsilon / 6(1 - \epsilon)$. When this is substituted into Eq. 6.4-3, we get

$$f = \frac{3}{2} \left(\frac{1 - \epsilon}{\epsilon^3} \right) f_{\text{tube}} \quad (6.4-7)$$

We now adapt this result to laminar and turbulent flows by inserting appropriate expressions for f_{tube} .

(a) For *laminar flow* in tubes, $f_{\text{tube}} = 16/\text{Re}_h$. This is exact for circular tubes only. To account for the fact that the fluid is flowing through tubes that are noncircular and that its path is quite tortuous, it has been found that replacing 16 by 100/3 allows the tube bundle model to describe the packed-column data. When this modified expression for the tube friction factor is used, Eq. 6.4-7 becomes

$$f = \frac{(1 - \epsilon)^2}{\epsilon^3} \frac{75}{(D_p G_0 / \mu)} \quad (6.4-8)$$

in which $G_0 = \rho v_0$ is the mass flux through the system. When this expression for f is substituted into Eq. 6.4-1 we get

$$\frac{\mathcal{P}_0 - \mathcal{P}_L}{L} = 150 \left(\frac{\mu v_0}{D_p^2} \right) \frac{(1 - \epsilon)^2}{\epsilon^3} \quad (6.4-9)$$

which is the *Blake-Kozeny equation*.³ Equations 6.4-8 and 9 are generally good for $(D_p G_0 / \mu(1 - \varepsilon)) < 10$ and for void fractions less than $\varepsilon = 0.5$.

(b) For *highly turbulent flow* a treatment similar to the above can be given. We begin again with the expression for the friction factor definition for flow in a circular tube. This time, however, we note that, for highly turbulent flow in tubes with any appreciable roughness, the friction factor is a function of the roughness only, and is independent of the Reynolds number. If we assume that the tubes in all packed columns have similar roughness characteristics, then the value of f_{tube} may be taken to be the same constant for all systems. Taking $f_{\text{tube}} = 7/12$ proves to be an acceptable choice. When this is inserted into Eq. 6.4-7, we get

$$f = \frac{7}{8} \left(\frac{1 - \varepsilon}{\varepsilon^3} \right) \quad (6.4-10)$$

When this is substituted into Eq. 6.4-1, we get

$$\frac{\mathcal{P}_0 - \mathcal{P}_L}{L} = \frac{7}{4} \left(\frac{\rho v_0^2}{D_p} \right) \frac{1 - \varepsilon}{\varepsilon^3} \quad (6.4-11)$$

which is the *Burke-Plummer*⁴ equation, valid for $(D_p G_0 / \mu(1 - \varepsilon)) > 1000$. Note that the dependence on the void fraction is different from that for laminar flow.

(c) For the *transition region*, we may superpose the pressure drop expressions for (a) and (b) above to get

$$\frac{\mathcal{P}_0 - \mathcal{P}_L}{L} = 150 \left(\frac{\mu v_0}{D_p^2} \right) \frac{(1 - \varepsilon)^2}{\varepsilon^3} + \frac{7}{4} \left(\frac{\rho v_0^2}{D_p} \right) \frac{1 - \varepsilon}{\varepsilon^3} \quad (6.4-12)$$

For very small v_0 , this simplifies to the Blake-Kozeny equation, and for very large v_0 , to the Burke-Plummer equation. Such empirical superpositions of asymptotes often lead to satisfactory results. Equation 6.4-12 may be rearranged to form dimensionless groups:

$$\left(\frac{(\mathcal{P}_0 - \mathcal{P}_L)\rho}{G_0^2} \right) \left(\frac{D_p}{L} \right) \left(\frac{\varepsilon^3}{1 - \varepsilon} \right) = 150 \left(\frac{1 - \varepsilon}{D_p G_0 / \mu} \right) + \frac{7}{4} \quad (6.4-13)$$

This is the *Ergun equation*,⁵ which is shown in Fig. 6.4-2 along with the Blake-Kozeny and Burke-Plummer equations and experimental data. It has been applied with success to gas flow through packed columns by using the density $\bar{\rho}$ of the gas at the arithmetic average of the end pressures. Note that G_0 is constant through the column, whereas v_0 changes through the column for a compressible fluid. For large pressure drops, however, it seems more appropriate to apply Eq. 6.4-12 locally by expressing the pressure gradient in differential form.

The Ergun equation is but one of many⁶ that have been proposed for describing packed columns. For example, the *Tallmadge equation*⁷

$$\left(\frac{(\mathcal{P}_0 - \mathcal{P}_L)\rho}{G_0^2} \right) \left(\frac{D_p}{L} \right) \left(\frac{\varepsilon^3}{1 - \varepsilon} \right) = 150 \left(\frac{1 - \varepsilon}{D_p G_0 / \mu} \right) + 4.2 \left(\frac{1 - \varepsilon}{D_p G_0 / \mu} \right)^{1/6} \quad (6.4-14)$$

is reported to give good agreement with experimental data over the range $0.1 < (D_p G_0 / \mu(1 - \varepsilon)) < 10^5$.

³ F. C. Blake, *Trans. Amer. Inst. Chem. Engrs.*, **14**, 415–421 (1922); J. Kozeny, *Sitzungsber. Akad. Wiss. Wien, Abt. IIa*, **136**, 271–306 (1927).

⁴ S. P. Burke and W. B. Plummer, *Ind. Eng. Chem.*, **20**, 1196–1200 (1928).

⁵ S. Ergun, *Chem. Engr. Prog.*, **48**, 89–94 (1952).

⁶ I. F. Macdonald, M. S. El-Sayed, K. Mow, and F. A. Dullien, *Ind. Eng. Chem. Fundam.*, **18**, 199–208 (1979).

⁷ J. A. Tallmadge, *AIChE Journal*, **16**, 1092–1093 (1970).

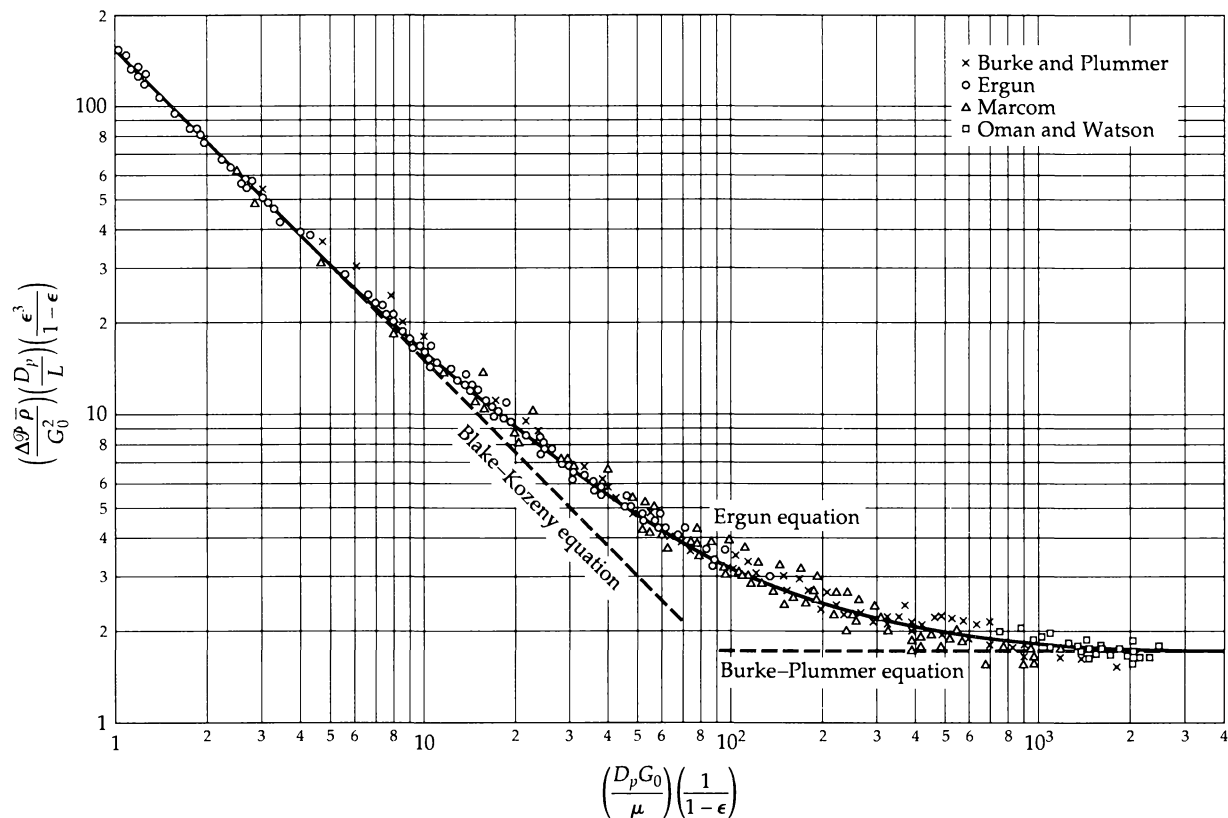


Fig. 6.4-2. The Ergun equation for flow in packed beds, and the two related asymptotes, the Blake–Kozeny equation and the Burke–Plummer equation [S. Ergun, *Chem. Eng. Prog.*, **48**, 89–94 (1952)].

The above discussion of packed beds illustrates how one can often combine solutions of elementary problems to create useful models for complex systems. The constants appearing in the models are then determined from experimental data. As better data become available the modeling can be improved.

QUESTIONS FOR DISCUSSION

- How are graphs of friction factors versus Reynolds numbers generated from experimental data, and why are they useful?
- Compare and contrast the friction factor curves for flow in tubes and flow around spheres. Why do they have different shapes?
- In Fig. 6.2-2, why does the f versus Re curve for turbulent flow lie above the curve for laminar flow rather than below?
- Discuss the caveat after Eq. 6.2-18. Will the use of the mean hydraulic radius for laminar flow predict a pressure drop that is too high or too low for a given flow rate?
- Can friction factor correlations be used for unsteady flows?
- What is the connection, if any, between the Blake–Kozeny equation (Eq. 6.4-9) and Darcy’s law (Eq. 4C.3-2)?

7. Discuss the flow of water through a 1/2-in. rubber garden hose that is attached to a house faucet with a pressure of 70 psig available.
8. Why was Eq. 6.4-12 rewritten in the form of Eq. 6.4-13?
9. A baseball announcer says: "Because of the high humidity today, the baseball cannot go as far through the heavy humid air as it would on a dry day." Comment critically on this statement.

PROBLEMS

6A.1 Pressure drop required for a pipe with fittings.

What pressure drop is needed for pumping water at 20°C through a pipe of 25 cm diameter and 1234 m length at a rate of 1.97 m/s? The pipe is at the same elevation throughout and contains four standard radius 90° elbows and two 45° elbows. The resistance of a standard radius 90° elbow is roughly equivalent to that offered by a pipe whose length is 82 diameters; a 45° elbow, 15 diameters. (An alternative method for calculating losses in fittings is given in §7.5.)

Answer: 4630 psi = 21.5 MPa

6A.2 Pressure difference required for flow in pipe with elevation change (Fig. 6A.2).

Water at 68°F is to be pumped through 95 ft of standard 3-in. pipe (internal diameter 3.068 in.) into an overhead reservoir.

(a) What pressure is required at the outlet of the pump to

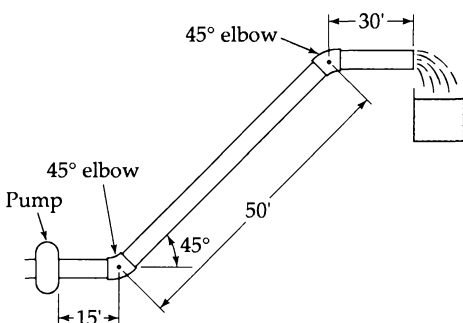


Fig. 6A.2. Pipe flow system.

supply water to the overhead reservoir at a rate of 18 gal/min? At 68°F the viscosity of water is 1.002 cp and the density is 0.9982 g/ml.

(b) What percentage of the pressure drop is needed for overcoming the pipe friction?

Answer: (a) 15.2 psig

6A.3 Flow rate for a given pressure drop.

How many gal/hr of water at 68°F can be delivered through a 1320-ft length of smooth 6.00-in. i.d. pipe under a pressure difference of 0.25 psi? Assume that the pipe is "hydraulically smooth."

(a) Solve by Method A of Example 6.2-2.

(b) Solve by Method B of Example 6.2-2.

Answer: 4070 gal/hr

6A.4 Motion of a sphere in a liquid.

A hollow sphere, 5.00 mm in diameter, with a mass of 0.0500 g, is released in a column of liquid and attains a terminal velocity of 0.500 cm/s. The liquid density is 0.900 g/cm³. The local gravitational acceleration is 980.7 cm/sec². The sphere is far enough from the containing walls so that their effect can be neglected.

(a) Compute the drag force on the sphere in dynes.

(b) Compute the friction factor.

(c) Determine the viscosity of the liquid in centipoises.

Answers: (a) 8.7 dynes; (b) $f = 396$; (c) 370 cp

6A.5 Sphere diameter for a given terminal velocity.

(a) Explain how to find the sphere diameter D corresponding to given values of v_∞ , ρ , ρ_s , μ , and g by making a direct construction on Fig. 6.3-1.

(b) Rework Problem 2A.4 by using Fig. 6.3-1.

(c) Rework (b) when the gas velocity is 10 ft/s.

6A.6 Estimation of void fraction of a packed column.

A tube of 146 sq. in. cross section and 73 in. height is packed with spherical particles of diameter 2 mm. When a pressure difference of 158 psi is maintained across the column, a 60% aqueous sucrose solution at 20°C flows through the bed at a rate of 244 lb/min. At this temperature, the viscosity of the solution is 56.5 cp and its density is 1.2865 g/cm³. What is the void fraction of the bed? Discuss the usefulness of this method of obtaining the void fraction.

Answer: 0.30

6A.7 Estimation of pressure drops in annular flow.

For flow in an annulus formed by cylindrical surfaces of diameters D and κD (with $\kappa < 1$) the friction factors for laminar and turbulent flow are

$$\text{Laminar} \quad f = \frac{16}{Re_\kappa} \quad (6A.7-1)$$

$$\text{Turbulent} \quad \sqrt{\frac{1}{f}} = G \log_{10}(Re_\kappa \sqrt{f}) - H \quad (6A.7-2)$$

in which the Reynolds number is defined by

$$Re_\kappa = K \frac{D(1 - \kappa)(\langle \bar{v}_z \rangle \rho)}{\mu} \quad (6A.7-3)$$

The values of G , H , and K are given as:¹

κ	G	H	K
0.00	4.000	0.400	1.000
0.05	3.747	0.293	0.7419
0.10	3.736	0.239	0.7161
0.15	3.738	0.208	0.7021
0.20	3.746	0.186	0.6930
0.30	3.771	0.154	0.6820
0.40	3.801	0.131	0.6759
0.50	3.833	0.111	0.6719
0.60	3.866	0.093	0.6695
0.70	3.900	0.076	0.6681
0.80	3.933	0.060	0.6672
0.90	3.967	0.046	0.6668
1.00	4.000	0.031	0.6667

Equation 6A.7-2 is based on Problem 5C.2 and reproduces the experimental data within about 3% up to Reynolds numbers of 20,000.

(a) Verify that Eqs. 6A.7-1 and 2 are equivalent to the results given in §2.4.

(b) An annular duct is formed from cylindrical surfaces of diameters 6 in. and 15 in. It is desired to pump water at 60°F at a rate of 1500 cu ft per second. How much pressure drop is required per unit length of conduit, if the annulus is horizontal? Use Eq. 6A.7-2.

(c) Repeat (b) using the “mean hydraulic radius” empiricism.

6A.8 Force on a water tower in a gale. A water tower has a spherical storage tank 40 ft in diameter. In a 100-mph gale what is the force of the wind on the spherical tank at 0°C? Take the density of air to be 1.29 g/liter or 0.08 lb/ft³ and the viscosity to be 0.017 cp.

Answer: 17,000 lb_f

6A.9 Flow of gas through a packed column. A horizontal tube with diameter 4 in. and length 5.5 ft is packed with glass spheres of diameter 1/16 in., and the void fraction is 0.41. Carbon dioxide is to be pumped through the tube at 300K, at which temperature its viscosity is known to be 1.495×10^{-4} g/cm · s. What will be the mass flow rate through the column when the inlet and outlet pressures are 25 atm and 3 atm, respectively?

Answer: 480 g/s

¹ D. M. Meter and R. B. Bird, *AIChE Journal*, 7, 41–45 (1961).

6A.10 Determination of pipe diameter. What size of circular pipe is needed to produce a flow rate of 250 firkins per fortnight when there is a pressure drop of 3×10^5 scruples per square barleycorn? The pipe is horizontal. (The authors are indebted to Professor R. S. Kirk of the University of Massachusetts, who introduced them to these units.)

6B.1 Effect of error in friction factor calculations. In a calculation using the Blasius formula for turbulent flow in pipes, the Reynolds number used was too low by 4%. Calculate the resulting error in the friction factor.

Answer: Too high by 1%

6B.2 Friction factor for flow along a flat plate.²

(a) An expression for the drag force on a flat plate, wetted on both sides, is given in Eq. 4.4-30. This equation was derived by using laminar boundary layer theory and is known to be in good agreement with experimental data. Define a friction factor and Reynolds number, and obtain the f versus Re relation.

(b) For turbulent flow, an approximate boundary layer treatment based on the 1/7 power velocity distribution gives

$$F_k = 0.072 \rho v_\infty^2 WL (L v_\infty \rho / \mu)^{-1/5} \quad (6B.2-1)$$

When 0.072 is replaced by 0.074, this relation describes the drag force within experimental error for $5 \times 10^5 < Lv_\infty \rho / \mu < 2 \times 10^7$. Express the corresponding friction factor as a function of the Reynolds number.

6B.3 Friction factor for laminar flow in a slit. Use the results of Problem 2B.3 to show that for the laminar flow in a thin slit of thickness $2B$ the friction factor is $f = 12/Re$, if the Reynolds number is defined as $Re = 2B\langle v_z \rangle \rho / \mu$. Compare this result for f with what one would get from the mean hydraulic radius empiricism.

6B.4 Friction factor for a rotating disk.³ A thin circular disk of radius R is immersed in a large body of fluid with density ρ and viscosity μ . If a torque T_z is required to make the disk rotate at an angular velocity Ω , then a friction factor f may be defined analogously to Eq. 6.1-1 as follows,

$$T_z / R = AKf \quad (6B.4-1)$$

where reasonable definitions for K and A are $K = \frac{1}{2}\rho(\Omega R)^2$ and $A = 2(\pi R^2)$. An appropriate choice for the Reynolds number for the system is $Re = R^2 \Omega \rho / \mu$.

For laminar flow, an exact boundary layer development gives

$$T_z = 0.616 \pi \rho R^4 \sqrt{\mu \Omega^3 / \rho} \quad (6B.4-2)$$

² H. Schlichting, *Boundary-Layer Theory*, McGraw-Hill, New York, 7th edition (1979), Chapter XXI.

³ T. von Kármán, *Zeits. für angew. Math. u. Mech.*, 1, 233–252 (1921).

For turbulent flow, an approximate boundary layer treatment based on the 1/7 power velocity distribution leads to

$$\mathcal{T} = 0.073 \rho \Omega^2 R^5 \sqrt[5]{\mu / R^2 \Omega \rho} \quad (6B.4-3)$$

Express these results as relations between f and Re .

6B.5 Turbulent flow in horizontal pipes. A fluid is flowing with a mass flow rate w in a smooth horizontal pipe of length L and diameter D as the result of a pressure difference $p_0 - p_L$. The flow is known to be turbulent.

The pipe is to be replaced by one of diameter $D/2$ but with the same length. The same fluid is to be pumped at the same mass flow rate w . What pressure difference will be needed?

- (a) Use Eq. 6.2-12 as a suitable equation for the friction factor.
- (b) How can this problem be solved using Fig. 6.2-2 if Eq. 6.2-12 is not appropriate?

Answer: (a) A pressure difference 27 times greater will be needed.

6B.6 Inadequacy of mean hydraulic radius for laminar flow.

(a) For laminar flow in an annulus with radii κR and R , use Eqs. 6.2-17 and 18 to get an expression for the average velocity in terms of the pressure difference analogous to the exact expression given in Eq. 2.4-16.

- (b) What is the percentage of error in the result in (a) for $\kappa = \frac{1}{2}$?

Answer: 47%

6B.7 Falling sphere in Newton's drag-law region. A sphere initially at rest at $z = 0$ falls under the influence of gravity. Conditions are such that, after a negligible interval, the sphere falls with a resisting force proportional to the square of the velocity.

- (a) Find the distance z that the sphere falls as a function of t .
- (b) What is the terminal velocity of the sphere? Assume that the density of the fluid is much less than the density of the sphere.

Answer: (a) The distance is $z = (1/c^2 g) \ln \cosh cgt$, where $c^2 = \frac{3}{8}(0.44)(\rho/\rho_{\text{sph}})(1/gR)$; (b) $1/c$

6B.8 Design of an experiment to verify the f vs. Re chart for spheres. It is desired to design an experiment to test the friction factor chart in Fig. 6.3-1 for flow around a sphere. Specifically, we want to test the plotted value $f = 1$ at $\text{Re} = 100$. This is to be done by dropping bronze spheres ($\rho_{\text{sph}} = 8 \text{ g/cm}^3$) in water ($\rho = 1 \text{ g/cm}^3$, $\mu = 10^{-2} \text{ g/cm} \cdot \text{s}$). What sphere diameter must be used?

- (a) Derive a formula that gives the required diameter as a function of f , Re , g , μ , ρ , and ρ_{sph} for terminal velocity conditions.

- (b) Insert numerical values and find the value of the sphere diameter.

Answers: (a) $D = \sqrt[3]{\frac{3f \text{Re}^2 \mu^2}{4(\rho_{\text{sph}} - \rho)pg}}$; (b) $D = 0.048 \text{ cm}$

6B.9 Friction factor for flow past an infinite cylinder.⁴ The flow past a long cylinder is very different from the flow past a sphere, and the method introduced in §4.2 cannot be used to describe this system. It is found that, when the fluid approaches with a velocity v_∞ , the kinetic force acting on a length L of the cylinder is

$$F_k = \frac{4\pi\mu v_\infty L}{\ln(7.4/\text{Re})} \quad (6B.9-1)$$

The Reynolds number is defined here as $\text{Re} = Dv_\infty\rho/\mu$. Equation 6B.9-1 is valid only up to about $\text{Re} = 1$. In this range of Re , what is the formula for the friction factor as a function of the Reynolds number?

6C.1 Two-dimensional particle trajectories. A sphere of radius R is fired horizontally (in the x direction) at high velocity in still air above level ground. As it leaves the propelling device, an identical sphere is dropped from the same height above the ground (in the y direction).

(a) Develop differential equations from which the particle trajectories can be computed, and that will permit comparison of the behavior of the two spheres. Include the effects of fluid friction, and make the assumption that steady-state friction factors may be used (this is a "quasi-steady-state assumption").

- (b) Which sphere will reach the ground first?
- (c) Would the answer to (b) have been the same if the sphere Reynolds numbers had been in the Stokes' law region?

Answers: (a) $\frac{dv_x}{dt} = -\frac{3}{8} \frac{v_x}{R} \sqrt{v_x^2 + v_y^2} f \frac{\rho_{\text{air}}}{\rho_{\text{sph}}}$,
 $\frac{dv_y}{dt} = -\frac{3}{8} \frac{v_y}{R} \sqrt{v_x^2 + v_y^2} f \frac{\rho_{\text{air}}}{\rho_{\text{sph}}} + \left(1 - \frac{\rho_{\text{air}}}{\rho_{\text{sph}}}\right)g$,

in which $f = f(\text{Re})$ as given by Fig. 5.3-1, with

$$\text{Re} = \frac{2R\sqrt{v_x^2 + v_y^2}\rho_{\text{air}}}{\mu_{\text{air}}}$$

6C.2 Wall effects for a sphere falling in a cylinder.⁵⁻⁷

(a) Experiments on friction factors of spheres are generally performed in cylindrical tubes. Show by dimensional analysis that, for such an arrangement, the friction factor for the sphere will have the following dependence:

$$f = f(\text{Re}, R/R_{\text{cyl}}) \quad (6C.2-1)$$

Here $\text{Re} = 2Rv_\infty\rho/\mu$, in which R is the sphere radius, v_∞ is the terminal velocity of the sphere, and R_{cyl} is the inside

⁴ G. K. Batchelor, *An Introduction to Fluid Dynamics*, Cambridge University Press (1967), pp. 244–246, 257–261. For flow past finite cylinders, see J. Happel and H. Brenner, *Low Reynolds Number Hydrodynamics*, Martinus Nijhoff, The Hague (1983), pp. 227–230.

radius of the cylinder. For the *creeping flow* region, it has been found empirically that the dependence of f on R/R_{cyl} may be described by the *Ladenburg–Faxén correction*,⁵ so that

$$f = \frac{24}{\text{Re}} \left(1 + 2.1 \frac{R}{R_{\text{cyl}}} \right) \quad (6C.2-2)$$

Wall effects for falling droplets have also been studied.⁶

(b) Design an experiment to check the graph for spheres in Fig. 6.3-1. Select sphere sizes, cylinder dimensions, and appropriate materials for the experiment.

6C.3 Power input to an agitated tank (Fig. 6C.3). Show by dimensional analysis that the power, P , imparted by a rotating impeller to an incompressible fluid in an agitated tank may be correlated, for any specific tank and impeller shape, by the expression

$$\frac{P}{\rho N^3 D^5} = \Phi \left(\frac{D^2 N \rho}{\mu}, \frac{DN^2}{g}, Nt \right) \quad (6C.3-1)$$

Here N is the rate of rotation of the impeller, D is the impeller diameter, t is the time since the start of the operation, and Φ is a function whose form has to be determined experimentally.

For the commonly used geometry shown in the figure, the power is given by the sum of two integrals representing the contributions of friction drag of the cylindrical tank

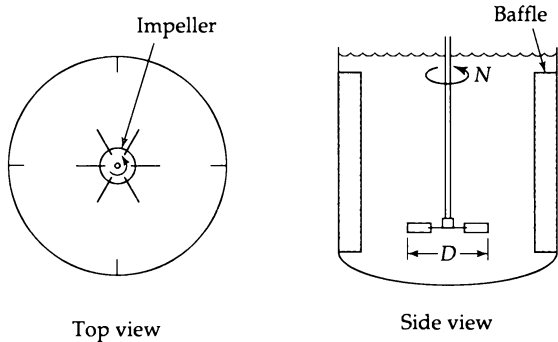


Fig. 6C.3. Agitated tank with a six-bladed impeller and four vertical baffles.

⁵ R. Ladenburg, *Ann. Physik* (4), **23**, 447 (1907); H. Faxén, dissertation, Uppsala (1921). For extensive discussions of wall effects for falling spheres, see J. Happel and H. Brenner, *Low Reynolds Number Hydrodynamics*, Martinus Nijhoff, The Hague (1983).

⁶ J. R. Strom and R. C. Kintner, *AICHE Journal*, **4**, 153–156 (1958).

body and bottom and the form drag of the radial baffles, respectively:

$$P = NT_z = N \left(\int_S R (\partial v_\theta / \partial n)_{\text{surf}} dS + \int_A R p_{\text{surf}} dA \right) \quad (6C.3-2)$$

Here T_z is the torque required to turn the impeller, S is the total surface area of the tank, A is the surface area of the baffles, (considered positive on the "upstream" side and negative on the "downstream side"), R is the radial distance to any surface element dS or dA from the impeller axis of rotation, and n is the distance measured normally into the fluid from any element of tank surface dS .

The desired solution may now be obtained by dimensional analysis of the equations of motion and continuity by rewriting the integrals above in dimensionless form. Here it is convenient to use D , DN , and $\rho N^2 D^2$ for the characteristic length, velocity, and pressure, respectively.

6D.1 Friction factor for a bubble in a clean liquid.^{7,8}

When a gas bubble moves through a liquid, the bulk of the liquid behaves as if it were in potential flow; that is, the flow field in the liquid phase is very nearly given by Eqs. 4B.5-2 and 3.

The drag force is closely related to the energy dissipation in the liquid phase (see Eq. 4.2-18)

$$F_k v_\infty = E_v \quad (6D.1-1)$$

Show that for irrotational flow the general expression for the energy dissipation can be transformed into the following surface integral:

$$E_v = \mu f (\mathbf{n} \cdot \nabla v^2) dS \quad (6D.1-2)$$

Next show that insertion of the potential flow velocity profiles into Eq. 6D.1-2, and use of Eq. 6D.1-1 leads to

$$f = \frac{48}{\text{Re}} \quad (6D.1-3)$$

A somewhat improved calculation that takes into account the dissipation in the boundary layer and in the turbulent wake leads to the following result:⁹

$$f = \frac{48}{\text{Re}} \left(1 - \frac{2.2}{\sqrt{\text{Re}}} \right) \quad (6D.1-4)$$

This result seems to hold rather well up to a Reynolds number of about 200.

⁷ L. Landau and E. M. Lifshitz, *Fluid Mechanics*, Pergamon, Oxford (1987), pp. 182–183.

⁸ G. K. Batchelor, *An Introduction to Fluid Dynamics*, Cambridge University Press, (1967), pp. 367–370.

⁹ D. W. Moore, *J. Fluid Mech.*, **16**, 161–176 (1963).

Macroscopic Balances for Isothermal Flow Systems

- §7.1 The macroscopic mass balance
- §7.2 The macroscopic momentum balance
- §7.3 The macroscopic angular momentum balance
- §7.4 The macroscopic mechanical energy balance
- §7.5 Estimation of the viscous loss
- §7.6 Use of the macroscopic balances for steady-state problems
- §7.7^O Use of the macroscopic balances for unsteady-state problems
- §7.8^{*} Derivation of the macroscopic mechanical energy balance

In the first four sections of Chapter 3 the *equations of change* for isothermal systems were presented. These equations were obtained by writing conservation laws over a “microscopic system”—namely, a small element of volume through which the fluid is flowing. In this way partial differential equations were obtained for the changes in mass, momentum, angular momentum, and mechanical energy in the system. The microscopic system has no solid bounding surfaces, and the interactions of the fluid with solid surfaces in specific flow systems are accounted for by boundary conditions on the differential equations.

In this chapter we write similar conservation laws for “macroscopic systems”—that is, large pieces of equipment or parts thereof. A sample macroscopic system is shown in Fig. 7.0-1. The balance statements for such a system are called the *macroscopic balances*; for

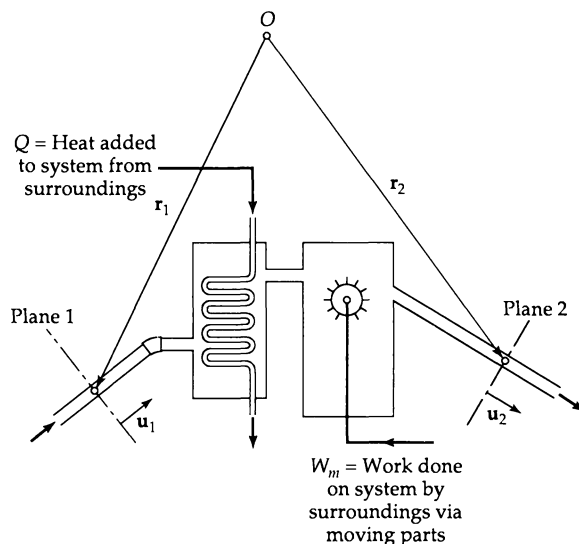


Fig. 7.0-1. Macroscopic flow system with fluid entering at plane 1 and leaving at plane 2. It may be necessary to add heat at a rate Q to maintain the system temperature constant. The rate of doing work on the system by the surroundings by means of moving surfaces is W_m . The symbols \mathbf{u}_1 and \mathbf{u}_2 denote unit vectors in the direction of flow at planes 1 and 2. The quantities \mathbf{r}_1 and \mathbf{r}_2 are position vectors giving the location of the centers of the inlet and outlet planes with respect to some designated origin of coordinates.

unsteady-state systems, these are ordinary differential equations, and for steady-state systems, they are algebraic equations. The macroscopic balances contain terms that account for the interactions of the fluid with the solid surfaces. The fluid can exert forces and torques on the surfaces of the system, and the surroundings can do work W_m on the fluid by means of moving surfaces.

The macroscopic balances can be obtained from the equations of change by integrating the latter over the entire volume of the flow system:^{1,2}

$$\int_{V(t)} (\text{eq. of continuity}) dV = \text{macroscopic mass balance}$$

$$\int_{V(t)} (\text{eq. of motion}) dV = \text{macroscopic momentum balance}$$

$$\int_{V(t)} (\text{eq. of angular momentum}) dV = \text{macroscopic angular momentum balance}$$

$$\int_{V(t)} (\text{eq. of mechanical energy}) dV = \text{macroscopic mechanical energy balance}$$

The first three of these macroscopic balances can be obtained either by writing the conservation laws directly for the macroscopic system or by doing the indicated integrations. However, to get the macroscopic mechanical energy balance, the corresponding equation of change must be integrated over the macroscopic system.

In §§7.1 to 7.3 we set up the macroscopic mass, momentum, and angular momentum balances by writing the conservation laws. In §7.4 we present the macroscopic mechanical energy balance, postponing the detailed derivation until §7.8. In the macroscopic mechanical energy balance, there is a term called the “friction loss,” and we devote §7.5 to estimation methods for this quantity. Then in §7.6 and §7.7 we show how the set of macroscopic balances can be used to solve flow problems.

The macroscopic balances have been widely used in many branches of engineering. They provide global descriptions of large systems without much regard for the details of the fluid dynamics inside the systems. Often they are useful for making an initial appraisal of an engineering problem and for making order-of-magnitude estimates of various quantities. Sometimes they are used to derive approximate relations, which can then be modified with the help of experimental data to compensate for terms that have been omitted or about which there is insufficient information.

In using the macroscopic balances one often has to decide which terms can be omitted, or one has to estimate some of the terms. This requires (i) intuition, based on experience with similar systems, (ii) some experimental data on the system, (iii) flow visualization studies, or (iv) order-of-magnitude estimates. This will be clear when we come to specific examples.

The macroscopic balances make use of nearly all the topics covered thus far; therefore Chapter 7 provides a good opportunity for reviewing the preceding chapters.

§7.1 THE MACROSCOPIC MASS BALANCE

In the system shown in Fig. 7.0-1 the fluid enters the system at plane 1 with cross section S_1 and leaves at plane 2 with cross section S_2 . The average velocity is $\langle v_1 \rangle$ at the entry plane and $\langle v_2 \rangle$ at the exit plane. In this and the following sections, we introduce two assumptions that are not very restrictive: (i) at the planes 1 and 2 the time-smoothed veloc-

¹ R. B. Bird, *Chem. Eng. Sci.*, **6**, 123–131 (1957); *Chem. Eng. Educ.*, **27**(2), 102–109 (Spring 1993).

² J. C. Slattery and R. A. Gaggioli, *Chem. Eng. Sci.*, **17**, 893–895 (1962).

ity is perpendicular to the relevant cross section, and (ii) at planes 1 and 2 the density and other physical properties are uniform over the cross section.

The law of conservation of mass for this system is then

$$\frac{d}{dt} m_{\text{tot}} = \rho_1 \langle v_1 \rangle S_1 - \rho_2 \langle v_2 \rangle S_2 \quad (7.1-1)$$

rate of rate of rate of
increase mass in mass out
of mass at plane 1 at plane 2

Here $m_{\text{tot}} = \int \rho dV$ is the total mass of fluid contained in the system between planes 1 and 2. We now introduce the symbol $w = \rho \langle v \rangle S$ for the mass rate of flow, and the notation $\Delta w = w_2 - w_1$ (exit value minus entrance value). Then the *unsteady-state macroscopic mass balance* becomes

$$\frac{d}{dt} m_{\text{tot}} = -\Delta w \quad (7.1-2)$$

If the total mass of fluid does not change with time, then we get the *steady-state macroscopic mass balance*

$$\Delta w = 0 \quad (7.1-3)$$

which is just the statement that the rate of mass entering equals the rate of mass leaving.

For the macroscopic mass balance we use the term "steady state" to mean that the time derivative on the left side of Eq. 7.1-2 is zero. Within the system, because of the possibility for moving parts, flow instabilities, and turbulence, there may well be regions of unsteady flow.

EXAMPLE 7.1-1

Draining of a Spherical Tank

A spherical tank of radius R and its drainpipe of length L and diameter D are completely filled with a heavy oil. At time $t = 0$ the valve at the bottom of the drainpipe is opened. How long will it take to drain the tank? There is an air vent at the very top of the spherical tank. Ignore the amount of oil that clings to the inner surface of the tank, and assume that the flow in the drainpipe is laminar.

SOLUTION

We label three planes as in Fig. 7.1-1, and we let the instantaneous liquid level above plane 2 be $h(t)$. Then, at any time t the total mass of liquid in the sphere is

$$m_{\text{tot}} = \pi R h^2 \left(1 - \frac{1}{3} \frac{h}{R}\right) \rho \quad (7.1-4)$$

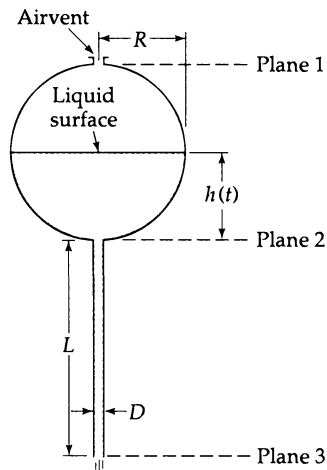


Fig. 7.1-1. Spherical tank with drainpipe.

which can be obtained by using integral calculus. Since no fluid crosses plane 1 we know that $w_1 = 0$. The outlet mass flow rate w_2 , as determined from the Hagen–Poiseuille formula, is

$$w_2 = \frac{\pi(\mathcal{P}_2 - \mathcal{P}_3)D^4\rho}{128\mu L} = \frac{\pi(\rho gh + \rho gL)D^4\rho}{128\mu L} \quad (7.1-5)$$

The Hagen–Poiseuille formula was derived for steady-state flow, but we use it here since the volume of liquid in the tank is changing slowly with time; this is an example of a “quasi-steady-state” approximation. When these expressions for m_{tot} and w_2 are substituted into Eq. 7.1-2, we get, after some rearrangement,

$$-\frac{(2R - h)h}{h + L} \frac{dh}{dt} = \frac{\rho g D^4}{128\mu L} \quad (7.1-6)$$

We now abbreviate the constant on the right side of the equation as A . The equation is easier to integrate if we make the change of variable $H = h + L$ so that

$$\frac{[H - (2R + L)](H - L)}{H} \frac{dH}{dt} = A \quad (7.1-7)$$

We now integrate this equation between $t = 0$ (when $h = 2R$ or $H = 2R + L$), and $t = t_{\text{efflux}}$ (when $h = 0$ or $H = L$). This gives for the efflux time

$$t_{\text{efflux}} = \frac{L^2}{A} \left[2 \frac{R}{L} \left(1 + \frac{R}{L} \right) - \left(1 + 2 \frac{R}{L} \right) \ln \left(1 + 2 \frac{R}{L} \right) \right] \quad (7.1-8)$$

in which A is given by the right side of Eq. 7.1-6. Note that we have obtained this result without any detailed analysis of the fluid motion within the sphere.

§7.2 THE MACROSCOPIC MOMENTUM BALANCE

We now apply the law of conservation of momentum to the system in Fig. 7.0-1, using the same two assumptions mentioned in the previous section, plus two additional assumptions: (iii) the forces associated with the stress tensor τ are neglected at planes 1 and 2, since they are generally small compared to the pressure forces at the entry and exit planes, and (iv) the pressure does not vary over the cross section at the entry and exit planes.

Since momentum is a vector quantity, each term in the balance must be a vector. We use unit vectors \mathbf{u}_1 and \mathbf{u}_2 to represent the direction of flow at planes 1 and 2. The law of conservation of momentum then reads

$$\frac{d}{dt} \mathbf{P}_{\text{tot}} = \rho_1 \langle v_1^2 \rangle S_1 \mathbf{u}_1 - \rho_2 \langle v_2^2 \rangle S_2 \mathbf{u}_2 + p_1 S_1 \mathbf{u}_1 - p_2 S_2 \mathbf{u}_2 + \mathbf{F}_{s \rightarrow f} + m_{\text{tot}} \mathbf{g} \quad (7.2-1)$$

rate of increase of momentum in plane 1	rate of momentum out of plane 2	rate of momentum force on fluid at plane 1	pressure force on fluid at plane 1	pressure force on fluid at plane 2	force of solid surface on fluid	force of gravity on fluid
---	---------------------------------	--	------------------------------------	------------------------------------	---------------------------------	---------------------------

Here $\mathbf{P}_{\text{tot}} = \int \rho \mathbf{v} dV$ is the total momentum in the system. The equation states that the total momentum within the system changes because of the convection of momentum into and out of the system, and because of the various forces acting on the system: the pressure forces at the ends of the system, the force of the solid surfaces acting on the fluid in the system, and the force of gravity acting on the fluid within the walls of the system. The subscript “ $s \rightarrow f$ ” serves as a reminder of the direction of the force.

By introducing the symbols for the mass rate of flow and the Δ symbol we finally get for the *unsteady-state macroscopic momentum balance*

$$\frac{d}{dt} \mathbf{P}_{\text{tot}} = -\Delta \left(\frac{\langle v^2 \rangle}{\langle v \rangle} w + pS \right) \mathbf{u} + \mathbf{F}_{s \rightarrow f} + m_{\text{tot}} \mathbf{g} \quad (7.2-2)$$

If the total amount of momentum in the system does not change with time, then we get the *steady-state macroscopic momentum balance*

$$\mathbf{F}_{f \rightarrow s} = -\Delta \left(\frac{\langle v^2 \rangle}{\langle v \rangle} w + pS \right) \mathbf{u} + m_{\text{tot}} \mathbf{g} \quad (7.2-3)$$

Once again we emphasize that this is a vector equation. It is useful for computing the force of the fluid on the solid surfaces, $\mathbf{F}_{f \rightarrow s}$, such as the force on a pipe bend or a turbine blade. Actually we have already used a simplified version of the above equation in Eq. 6.1-3.

Notes regarding turbulent flow: (i) For turbulent flow it is customary to replace $\langle v \rangle$ by $\langle \bar{v} \rangle$ and $\langle v^2 \rangle$ by $\langle \bar{v}^2 \rangle$; in the latter we are neglecting the term $\langle \bar{v}'^2 \rangle$, which is generally small with respect to $\langle \bar{v}^2 \rangle$. (ii) Then we further replace $\langle \bar{v}^2 \rangle / \langle \bar{v} \rangle$ by $\langle \bar{v} \rangle$. The error in doing this is quite small; for the empirical $\frac{1}{7}$ power law velocity profile given in Eq. 5.1-4, $\langle \bar{v}^2 \rangle / \langle \bar{v} \rangle = \frac{50}{49} \langle \bar{v} \rangle$, so that the error is about 2%. (iii) When we make this assumption we will normally drop the angular brackets and overbars to simplify the notation. That is, we will let $\langle \bar{v}_1 \rangle \equiv v_1$ and $\langle \bar{v}_1^2 \rangle \equiv \bar{v}_1^2$, with similar simplifications for quantities at plane 2.

EXAMPLE 7.2-1

Force Exerted by a Jet (Part a)

A turbulent jet of water emerges from a tube of radius $R_1 = 2.5$ cm with a speed $v_1 = 6$ m/s, as shown in Fig. 7.2-1. The jet impinges on a disk-and-rod assembly of mass $m = 5.5$ kg, which is free to move vertically. The friction between the rod and the sleeve will be neglected. Find the height h at which the disk will "float" as a result of the jet.¹ Assume that the water is incompressible.

SOLUTION

To solve this problem one has to imagine how the jet behaves. In Fig. 7.2-1(a) we make the assumption that the jet has a constant radius, R_1 , between the tube exit and the disk, whereas in Fig. 7.2-1(b) we assume that the jet spreads slightly. In this example, we make the first assumption, and in Example 7.4-1 we account for the jet spreading.

We apply the z-component of the steady-state momentum balance between planes 1 and 2. The pressure terms can be omitted, since the pressure is atmospheric at both planes. The z component of the fluid velocity at plane 2 is zero. The momentum balance then becomes

$$mg = v_1(\rho v_1 \pi R_1^2) - (\pi R_1^2 h) \rho g \quad (7.2-4)$$

When this is solved for h , we get (in SI units)

$$h = \frac{v_1^2}{g} - \frac{m}{\rho \pi R_1^2} = \frac{(6)^2}{(9.807)} - \frac{5.5}{\pi(0.025)^2} = 0.87 \text{ m} \quad (7.2-5)$$

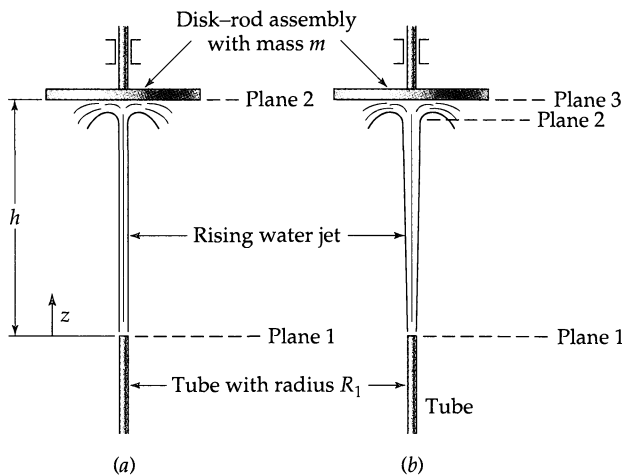


Fig. 7.2-1. Sketches corresponding to the two solutions to the jet-and-disk problem. In (a) the water jet is assumed to have a uniform radius R_1 . In (b) allowance is made for the spreading of the liquid jet.

¹ K. Federhofer, *Aufgaben aus der Hydromechanik*, Springer-Verlag, Vienna (1954), pp. 36 and 172.

§7.3 THE MACROSCOPIC ANGULAR MOMENTUM BALANCE

The development of the macroscopic angular momentum balance parallels that for the (linear) momentum balance in the previous section. All we have to do is to replace "momentum" by "angular momentum" and "force" by "torque."

To describe the angular momentum and torque we have to select an origin of coordinates with respect to which these quantities are evaluated. The origin is designated by "O" in Fig. 7.0-1, and the locations of the midpoints of planes 1 and 2 with respect to this origin are given by the position vectors \mathbf{r}_1 and \mathbf{r}_2 .

Once again we make assumptions (i)–(iv) introduced in §§7.1 and 7.2. With these assumptions the rate of entry of angular momentum at plane 1, which is $\int [\mathbf{r} \times \rho \mathbf{v}] (\mathbf{v} \cdot \mathbf{u}) dS$ evaluated at that plane, becomes $\rho_1 \langle v_1^2 \rangle S_1 [\mathbf{r}_1 \times \mathbf{u}_1]$, with a similar expression for the rate at which angular momentum leaves the system at 2.

The *unsteady-state macroscopic angular momentum balance* may now be written as

$$\frac{d}{dt} \mathbf{L}_{\text{tot}} = \rho_1 \langle v_1^2 \rangle S_1 [\mathbf{r}_1 \times \mathbf{u}_1] - \rho_2 \langle v_2^2 \rangle S_2 [\mathbf{r}_2 \times \mathbf{u}_2]$$

rate of increase of angular momentum	rate of angular momentum in at plane 1	rate of angular momentum out at plane 2
--------------------------------------	--	---

$$+ p_1 S_1 [\mathbf{r}_1 \times \mathbf{u}_1] - p_2 S_2 [\mathbf{r}_2 \times \mathbf{u}_2] + \mathbf{T}_{s \rightarrow f} + \mathbf{T}_{\text{ext}} \quad (7.3-1)$$

torque due to pressure on fluid at plane 1	torque due to pressure on fluid at plane 2	torque of solid surface on fluid
--	--	----------------------------------

Here $\mathbf{L}_{\text{tot}} = \int \rho [\mathbf{r} \times \mathbf{v}] dV$ is the total angular momentum within the system, and $\mathbf{T}_{\text{ext}} = \int [\mathbf{r} \times \rho \mathbf{g}] dV$ is the torque on the fluid in the system resulting from the gravitational force. This equation can also be written as

$$\boxed{\frac{d}{dt} \mathbf{L}_{\text{tot}} = -\Delta \left(\frac{\langle v^2 \rangle}{\langle v \rangle} w + pS \right) [\mathbf{r} \times \mathbf{u}] + \mathbf{T}_{s \rightarrow f} + \mathbf{T}_{\text{ext}}} \quad (7.3-2)$$

Finally, the *steady-state macroscopic angular momentum balance* is

$$\mathbf{T}_{f \rightarrow s} = -\Delta \left(\frac{\langle v^2 \rangle}{\langle v \rangle} w + pS \right) [\mathbf{r} \times \mathbf{u}] + \mathbf{T}_{\text{ext}} \quad (7.3-3)$$

This gives the torque exerted by the fluid on the solid surfaces.

EXAMPLE 7.3-1

Torque on a Mixing Vessel

A mixing vessel, shown in Fig. 7.3-1, is being operated at steady state. The fluid enters tangentially at plane 1 in turbulent flow with a velocity v_1 and leaves through the vertical pipe with a velocity v_2 . Since the tank is baffled there is no swirling motion of the fluid in the vertical exit pipe. Find the torque exerted on the mixing vessel.

SOLUTION

The origin of the coordinate system is taken to be on the tank axis in a plane passing through the axis of the entrance pipe and parallel to the tank top. Then the vector $[\mathbf{r}_1 \times \mathbf{u}_1]$ is a vector pointing in the z direction with magnitude R . Furthermore $[\mathbf{r}_2 \times \mathbf{u}_2] = 0$, since the two vectors are collinear. For this problem Eq. 7.3-3 gives

$$\mathbf{T}_{f \rightarrow s} = (\rho v_1^2 S_1 + p_1 S_1) R \delta_z \quad (7.3-4)$$

Thus the torque is just "force \times lever arm," as would be expected. If the torque is sufficiently large, the equipment must be suitably braced to withstand the torque produced by the fluid motion and the inlet pressure.

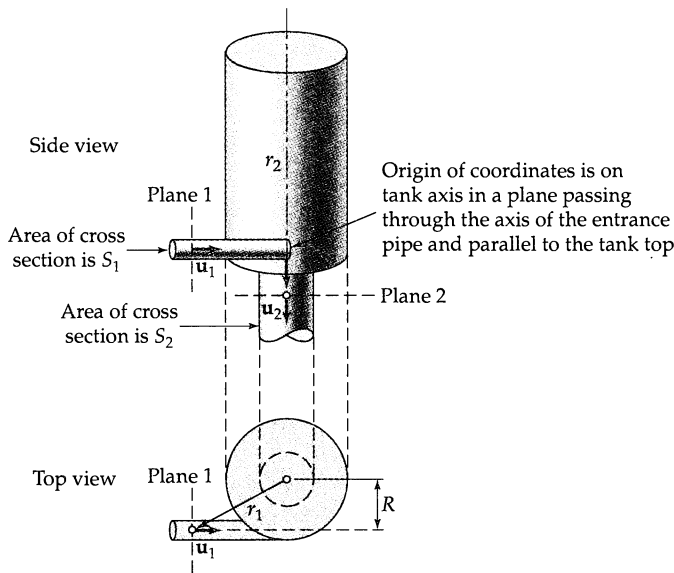


Fig. 7.3-1. Torque on a tank, showing side view and top view.

§7.4 THE MACROSCOPIC MECHANICAL ENERGY BALANCE

Equations 7.1-2, 7.2-2, and 7.3-2 have been set up by applying the laws of conservation of mass, (linear) momentum, and angular momentum over the macroscopic system in Fig. 7.0-1. The three macroscopic balances thus obtained correspond to the equations of change in Eqs. 3.1-4, 3.2-9, and 3.4-1, and, in fact, they are very similar in structure. These three macroscopic balances can also be obtained by integrating the three equations of change over the volume of the flow system.

Next we want to set up the macroscopic mechanical energy balance, which corresponds to the equation of mechanical energy in Eq. 3.3-2. There is no way to do this directly as we have done in the preceding three sections, since there is no conservation law for mechanical energy. In this instance we *must* integrate the equation of change of mechanical energy over the volume of the flow system. The result, which has made use of the same assumptions (i–iv) used above, is the *unsteady-state macroscopic mechanical energy balance* (sometimes called the *engineering Bernoulli equation*). The equation is derived in §7.8; here we state the result and discuss its meaning:

$$\frac{d}{dt} (K_{\text{tot}} + \Phi_{\text{tot}}) = \left(\frac{1}{2} \rho_1 \langle v_1^3 \rangle + \rho_1 \hat{\Phi}_1(v_1) \right) S_1 - \left(\frac{1}{2} \rho_2 \langle v_2^3 \rangle + \rho_2 \hat{\Phi}_2(v_2) \right) S_2 + (p_1 \langle v_1 \rangle S_1 - p_2 \langle v_2 \rangle S_2) + W_m + \int_{V(t)} p (\nabla \cdot \mathbf{v}) dV + \int_{V(t)} (\boldsymbol{\tau} : \nabla \mathbf{v}) dV \quad (7.4-1)$$

rate of increase rate at which kinetic rate at which kinetic
 of kinetic and and potential energy and potential energy
 potential energy enter system at plane 1 leave system at plane 2
 in system

net rate at which the rate of rate at which rate at which
 surroundings do doing mechanical mechanical
 work on the fluid work on energy increases energy
 at planes 1 and 2 by fluid by or decreases decreases
 the pressure moving because of expansion because of
 surfaces or compression of fluid viscous
 or dissipation¹

¹ This interpretation of the term is valid only for Newtonian fluids; polymeric liquids have elasticity and the interpretation given above no longer holds.

Here $K_{\text{tot}} = \int_2^1 \rho v^2 dV$ and $\Phi_{\text{tot}} = \int \rho \hat{\Phi} dV$ are the total kinetic and potential energies within the system. According to Eq. 7.4-1, the total mechanical energy (i.e., kinetic plus potential) changes because of a difference in the rates of addition and removal of mechanical energy, because of work done on the fluid by the surroundings, and because of compressibility effects and viscous dissipation. Note that, at the system entrance (plane 1), the force $p_1 S_1$ multiplied by the velocity $\langle v_1 \rangle$ gives the rate at which the surroundings do work on the fluid. Furthermore, W_m is the work done by the surroundings on the fluid by means of moving surfaces.

The macroscopic mechanical energy balance may now be written more compactly as

$$\boxed{\frac{d}{dt} (K_{\text{tot}} + \Phi_{\text{tot}}) = -\Delta \left(\frac{1}{2} \frac{\langle v^3 \rangle}{\langle v \rangle} + \hat{\Phi} + \frac{p}{\rho} \right) w + W_m - E_c - E_v} \quad (7.4-2)$$

in which the terms E_c and E_v are defined as follows:

$$E_c = - \int_{V(t)} p (\nabla \cdot \mathbf{v}) dV \quad \text{and} \quad E_v = - \int_{V(t)} (\boldsymbol{\tau} : \nabla \mathbf{v}) dV \quad (7.4-3, 4)$$

The *compression term* E_c is positive in compression and negative in expansion; it is zero when the fluid is assumed to be incompressible. The term E_v is the *viscous dissipation* (or *friction loss*) term, which is always positive for Newtonian liquids, as can be seen from Eq. 3.3-3. (For polymeric fluids, which are viscoelastic, E_v is not necessarily positive; these fluids are discussed in the next chapter.)

If the total kinetic plus potential energy in the system is not changing with time, we get

$$\boxed{\Delta \left(\frac{1}{2} \frac{\langle v^3 \rangle}{\langle v \rangle} + gh + \frac{p}{\rho} \right) w = W_m - E_c - E_v} \quad (7.4-5)$$

which is the *steady-state macroscopic mechanical energy balance*. Here h is the height above some arbitrarily chosen datum plane.

Next, if we assume that it is possible to draw a representative streamline through the system, we may combine the $\Delta(p/\rho)$ and E_c terms to get the following *approximate* relation (see §7.8)

$$\Delta \left(\frac{p}{\rho} \right) w + E_c \approx w \int_1^2 \frac{1}{\rho} dp \quad (7.4-6)$$

Then, after dividing Eq. 7.4-5 by $w_1 = w_2 = w$, we get

$$\boxed{\Delta \left(\frac{1}{2} \frac{\langle v^3 \rangle}{\langle v \rangle} \right) + g \Delta h + \int_1^2 \frac{1}{\rho} dp = \hat{W}_m - \hat{E}_v} \quad (7.4-7)$$

Here $\hat{W}_m = W_m/w$ and $\hat{E}_v = E_v/w$. Equation 7.4-7 is the version of the steady-state mechanical energy balance that is most often used. For isothermal systems, the integral term can be calculated as long as an expression for density as a function of pressure is available.

Equation 7.4-7 should now be compared with Eq. 3.5-12, which is the “classical” Bernoulli equation for an inviscid fluid. If, to the right side of Eq. 3.5-12, we just add the work \hat{W}_m done by the surroundings and subtract the viscous dissipation term \hat{E}_v , and reinterpret the velocities as appropriate averages over the cross sections, then we get Eq. 7.4-7. This provides a “plausibility argument” for Eq. 7.4-7 and still preserves the fundamental idea that the macroscopic mechanical energy balance is derived from the equation of motion (that is, from the law of conservation of momentum). The full derivation of the macroscopic mechanical energy balance is given in §7.8 for those who are interested.

Notes for turbulent flow: (i) For turbulent flows we replace $\langle v^3 \rangle$ by $\langle \bar{v}^3 \rangle$, and ignore the contribution from the turbulent fluctuations. (ii) It is common practice to replace the

quotient $\langle \bar{v}^3 \rangle / \langle \bar{v} \rangle$ by $\langle \bar{v} \rangle^2$. For the empirical $\frac{1}{7}$ power law velocity profile given in Eq. 5.1-4, it can be shown that $\langle \bar{v}^3 \rangle / \langle \bar{v} \rangle = \frac{43200}{40817} \langle \bar{v} \rangle^2$, so that the error amounts to about 6%. (iii) We further omit the brackets and overbars to simplify the notation in turbulent flow.

EXAMPLE 7.4-1

Force Exerted by a Jet (Part b)

Continue the problem in Example 7.2-1 by accounting for the spreading of the jet as it moves upward.

SOLUTION

We now permit the jet diameter to increase with increasing z as shown in Fig. 7.2-1(b). It is convenient to work with three planes and to make balances between pairs of planes. The separation between planes 2 and 3 is taken to be quite small.

A mass balance between planes 1 and 2 gives

$$w_1 = w_2 \quad (7.4-8)$$

Next we apply the mechanical energy balance of Eq. 7.4-5 or 7.4-7 between the same two planes. The pressures at planes 1 and 2 are both atmospheric, and there is no work done by moving parts W_m . We assume that the viscous dissipation term E_v can be neglected. If z is measured upward from the tube exit, then $g\Delta h = g(h_2 - h_1) \approx g(h - 0)$, since planes 2 and 3 are so close together. Thus the mechanical energy balance gives

$$\frac{1}{2}(v_2^2 - v_1^2) + gh = 0 \quad (7.4-9)$$

We now apply the z-momentum balance between planes 2 and 3. Since the region is very small, we neglect the last term in Eq. 7.2-3. Both planes are at atmospheric pressure, so the pressure terms do not contribute. The fluid velocity is zero at plane 3, so there are only two terms left in the momentum balance

$$mg = v_2 w_2 \quad (7.4-10)$$

From the above three equations we get

$$\begin{aligned} h &= \frac{v_1^2}{2g} \left(1 - \frac{v_2^2}{v_1^2} \right) && \text{from Eq. 7.4-9} \\ &= \frac{v_1^2}{2g} \left(1 - \frac{(mg/w_2)^2}{v_1^2} \right) && \text{from Eq. 7.4-10} \\ &= \frac{v_1^2}{2g} \left(1 - \left(\frac{mg}{v_1 w_1} \right)^2 \right) && \text{from Eq. 7.4-8} \end{aligned} \quad (7.4-11)$$

in which mg and $v_1 w_1 = \pi R_1^2 \rho v_1^2$ are known. When the numerical values are substituted into Eq. 7.4-10, we get $h = 0.77$ m. This is probably a better result than the value of 0.87 m obtained in Example 7.2-1, since it accounts for the spreading of the jet. We have not, however, considered the clinging of the water to the disk, which gives the disk-rod assembly a somewhat greater effective mass. In addition, the frictional resistance of the rod in the sleeve has been neglected. It is necessary to run an experiment to assess the validity of Eq. 7.4-10.

§7.5 ESTIMATION OF THE VISCOSITY LOSS

This section is devoted to methods for estimating the viscous loss (or friction loss), E_v , which appears in the macroscopic mechanical energy balance. The general expression for E_v is given in Eq. 7.4-4. For incompressible Newtonian fluids, Eq. 3.3-3 may be used to rewrite E_v as

$$E_v = \int \mu \Phi_v dV \quad (7.5-1)$$

which shows that it is the integral of the local rate of viscous dissipation over the volume of the entire flow system.

We now want to examine E_v from the point of view of dimensional analysis. The quantity Φ_v is a sum of squares of velocity gradients; hence it has dimensions of $(v_0/l_0)^2$, where v_0 and l_0 are a characteristic velocity and length, respectively. We can therefore write

$$E_v = (\rho v_0^3 l_0^2) (\mu / l_0 v_0 \rho) \int \check{\Phi}_v d\check{V} \quad (7.5-2)$$

where $\check{\Phi}_v = (l_0/v_0)^2 \Phi_v$ and $d\check{V} = l_0^{-3} dV$ are dimensionless quantities. If we make use of the dimensional arguments of §§3.7 and 6.2, we see that the integral in Eq. 7.5-2 depends only on the various dimensionless groups in the equations of change and on various geometrical factors that enter into the boundary conditions. Hence, if the only significant dimensionless group is a Reynolds number, $Re = l_0 v_0 \rho / \mu$, then Eq. 7.5-2 must have the general form

$$E_v = (\rho v_0^3 l_0^2) \times \left(\begin{array}{l} \text{a dimensionless function of } Re \\ \text{and various geometrical ratios} \end{array} \right) \quad (7.5-3)$$

In *steady-state flow* we prefer to work with the quantity $\hat{E}_v = E_v/w$, in which $w = \rho \langle v \rangle S$ is the mass rate of flow passing through *any* cross section of the flow system. If we select the reference velocity v_0 to be $\langle v \rangle$ and the reference length l_0 to be \sqrt{S} , then

$$\hat{E}_v = \frac{1}{2} \langle v \rangle^2 e_v \quad (7.5-4)$$

in which e_v , the *friction loss factor*, is a function of a Reynolds number and relevant dimensionless geometrical ratios. The factor $\frac{1}{2}$ has been introduced in keeping with the form of several related equations. We now want to summarize what is known about the friction loss factor for the various parts of a piping system.

For a straight conduit the friction loss factor is closely related to the friction factor. We consider only the steady flow of a fluid of constant density in a straight conduit of arbitrary, but constant, cross section S and length L . If the fluid is flowing in the z direction under the influence of a pressure gradient and gravity, then Eqs. 7.2-2 and 7.4-7 become

$$(z\text{-momentum}) \quad F_{f \rightarrow s} = (p_1 - p_2)S + (\rho S L) g_z \quad (7.5-5)$$

$$(\text{mechanical energy}) \quad \hat{E}_v = \frac{1}{\rho} (p_1 - p_2) + L g_z \quad (7.5-6)$$

Multiplication of the second of these by ρS and subtracting gives

$$\hat{E}_v = \frac{F_{f \rightarrow s}}{\rho S} \quad (7.5-7)$$

If, in addition, the flow is *turbulent* then the expression for $F_{f \rightarrow s}$ in terms of the mean hydraulic radius R_h may be used (see Eqs. 6.2-16 to 18) so that

$$\hat{E}_v = \frac{1}{2} \langle v \rangle^2 \frac{L}{R_h} f \quad (7.5-8)$$

in which f is the friction factor discussed in Chapter 6. Since this equation is of the form of Eq. 7.5-4, we get a simple relation between the friction loss factor and the friction factor

$$e_v = \frac{L}{R_h} f \quad (7.5-9)$$

for turbulent flow in sections of straight pipe with uniform cross section. For a similar treatment for conduits of variable cross section, see Problem 7B.2.

Table 7.5-1 Brief Summary of Friction Loss Factors for Use with Eq. 7.5-10
(Approximate Values for Turbulent Flow)^a

Disturbances	e_v
Sudden changes in cross-sectional area ^b	
Rounded entrance to pipe	0.05
Sudden contraction	$0.45(1 - \beta)$
Sudden expansion ^c	$\left(\frac{1}{\beta} - 1\right)^2$
Orifice (sharp-edged)	$2.71(1 - \beta)(1 - \beta^2) \frac{1}{\beta^2}$
Fittings and valves	
90° elbows (rounded)	0.4–0.9
90° elbows (square)	1.3–1.9
45° elbows	0.3–0.4
Globe valve (open)	6–10
Gate valve (open)	0.2

^a Taken from H. Kramers, *Physische Transportverschijnselen*, Technische Hogeschool Delft, Holland (1958), pp. 53–54.

^b Here $\beta = (\text{smaller cross-sectional area}) / (\text{larger cross-sectional area})$.

^c See derivation from the macroscopic balances in Example 7.6-1. If $\beta = 0$, then $\hat{E}_v = \frac{1}{2}\langle v \rangle^2$, where $\langle v \rangle$ is the velocity *upstream* from the enlargement.

Most flow systems contain various “obstacles,” such as fittings, sudden changes in diameter, valves, or flow measuring devices. These also contribute to the friction loss \hat{E}_v . Such additional resistances may be written in the form of Eq. 7.5-4, with e_v determined by one of two methods: (a) simultaneous solution of the macroscopic balances, or (b) experimental measurement. Some rough values of e_v are tabulated in Table 7.5-1 for the convention that $\langle v \rangle$ is the average velocity *downstream* from the disturbance. These e_v values are for *turbulent flow* for which the Reynolds number dependence is not too important.

Now we are in a position to rewrite Eq. 7.4-7 in the *approximate* form frequently used for *turbulent flow* calculations in a system composed of various kinds of piping and additional resistances:

$$\frac{1}{2}(v_2^2 - v_1^2) + g(z_2 - z_1) + \int_{p_1}^{p_2} \frac{1}{\rho} dp = \hat{W}_m - \sum_i \left(\frac{1}{2} v^2 \frac{L}{R_h} f \right)_i - \sum_i \left(\frac{1}{2} v^2 e_v \right)_i \quad (7.5-10)$$

sum over all sections of straight conduits sum over all fittings, valves, meters, etc.

Here R_h is the mean hydraulic radius defined in Eq. 6.2-16, f is the friction factor defined in Eq. 6.1-4, and e_v is the friction loss factor given in Table 7.5-1. Note that the v_1 and v_2 in the first term refer to the velocities at planes 1 and 2; the v in the first sum is the average velocity in the i th pipe segment; and the v in the second sum is the average velocity *downstream* from the i th fitting, valve, or other obstacle.

EXAMPLE 7.5-1

Power Requirement for Pipeline Flow

What is the required power output from the pump at steady state in the system shown in Fig. 7.5-1? The water ($\rho = 62.4 \text{ lb}_m/\text{ft}^3$; $\mu = 1.0 \text{ cp}$) is to be delivered to the upper tank at a rate of 12 ft³/min. All of the piping is 4-in. internal diameter smooth circular pipe.

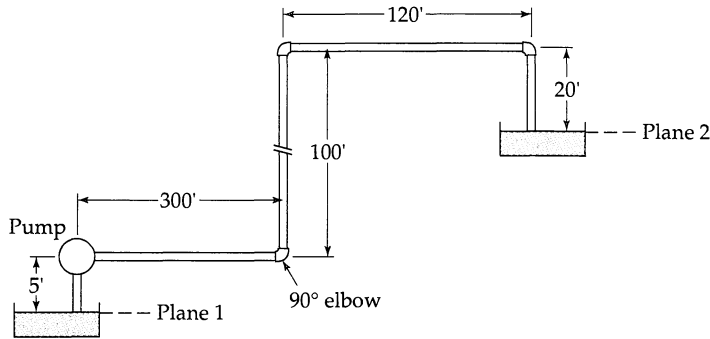


Fig. 7.5-1. Pipeline flow with friction losses because of fittings. Planes 1 and 2 are just under the surface of the liquid.

SOLUTION

The average velocity in the pipe is

$$\langle v \rangle = \frac{w/\rho}{\pi R^2} = \frac{(12/60)}{\pi(1/6)^2} = 2.30 \text{ ft/s} \quad (7.5-11)$$

and the Reynolds number is

$$Re = \frac{D\langle v \rangle \rho}{\mu} = \frac{(1/3)(2.30)(62.4)}{(1.0)(6.72 \times 10^{-4})} = 7.11 \times 10^4 \quad (7.5-12)$$

Hence the flow is *turbulent*.

The contribution to \hat{E}_v from the various lengths of pipe will be

$$\begin{aligned} \sum_i \left(\frac{1}{2} v^2 \frac{L}{R_h} f \right)_i &= \frac{2v^2 f}{D} \sum_i L_i \\ &= \frac{2(2.30)^2(0.0049)}{(1/3)} (5 + 300 + 100 + 120 + 20) \\ &= (0.156)(545) = 85 \text{ ft}^2/\text{s}^2 \end{aligned} \quad (7.5-13)$$

The contribution to \hat{E}_v from the sudden contraction, the three 90° elbows, and the sudden expansion (see Table 7.5-1) will be

$$\sum_i \left(\frac{1}{2} v^2 e_v \right)_i = \frac{1}{2}(2.30)^2(0.45 + 3 \cdot \frac{1}{2}) + 1 = 8 \text{ ft}^2/\text{s}^2 \quad (7.5-14)$$

Then from Eq. 7.5-10 we get

$$0 + (32.2)(105 - 20) + 0 = \hat{W}_m - 85 - 8 \quad (7.5-15)$$

Solving for \hat{W}_m we get

$$\hat{W}_m = 2740 + 85 - 8 \approx 2830 \text{ ft}^2/\text{s}^2 \quad (7.5-16)$$

This is the work (per unit mass of fluid) done *on* the fluid *in* the pump. Hence the pump does $2830 \text{ ft}^2/\text{s}^2$ or $2830/32.2 = 88 \text{ ft lb}_f/\text{lb}_m$ of work on the fluid passing through the system. The mass rate of flow is

$$w = (12/60)(62.4) = 12.5 \text{ lb}_m/\text{s} \quad (7.5-17)$$

Consequently

$$\hat{W}_m = w \hat{W}_m = (12.5)(88) = 1100 \text{ ft lb}_f/\text{s} = 2 \text{ hp} = 1.5 \text{ kW} \quad (7.5-18)$$

which is the power delivered by the pump.

Table 7.6-1 Steady-State Macroscopic Balances for Turbulent Flow in Isothermal Systems

Mass:	$\sum w_1 - \sum w_2 = 0$	(A)
Momentum:	$\Sigma(v_1 w_1 + p_1 S_1) \mathbf{u}_1 - \Sigma(v_2 w_2 + p_2 S_2) \mathbf{u}_2 + m_{\text{tot}} \mathbf{g} = \mathbf{F}_{f \rightarrow s}$	(B)
Angular momentum:	$\Sigma(v_1 w_1 + p_1 S_1)[\mathbf{r}_1 \times \mathbf{u}_1] - \Sigma(v_2 w_2 + p_2 S_2)[\mathbf{r}_2 \times \mathbf{u}_2] + \mathbf{T}_{\text{ext}} = \mathbf{T}_{f \rightarrow s}$	(C)
Mechanical energy:	$\Sigma\left(\frac{1}{2}v_1^2 + gh_1 + \frac{p_1}{\rho_1}\right)w_1 - \Sigma\left(\frac{1}{2}v_2^2 + gh_2 + \frac{p_2}{\rho_2}\right)w_2 = -W_m + E_c + E_v$	(D)

Notes:

- (a) All formulas here assume flat velocity profiles.
- (b) $\sum w_i = w_{1a} + w_{1b} + w_{1c} + \dots$, where $w_{1a} = \rho_{1a} v_{1a} S_{1a}$, etc.
- (c) h_1 and h_2 are elevations above an arbitrary datum plane.
- (d) All equations are written for compressible flow; for incompressible flow, $E_c = 0$.

§7.6 USE OF THE MACROSCOPIC BALANCES FOR STEADY-STATE PROBLEMS

In §3.6 we saw how to set up the differential equations to calculate the velocity and pressure profiles for isothermal flow systems by simplifying the equations of change. In this section we show how to use the set of steady-state macroscopic balances to obtain the algebraic equations for describing large systems.

For each problem we start with the four macroscopic balances. By keeping track of the discarded or approximated terms, we automatically have a complete listing of the assumptions inherent in the final result. All of the examples given here are for isothermal, incompressible flow. The incompressibility assumption means that the velocity of the fluid must be less than the velocity of sound in the fluid and the pressure changes must be small enough that the resulting density changes can be neglected.

The steady-state macroscopic balances may be easily generalized for systems with multiple inlet streams (called 1a, 1b, 1c, ...) and multiple outlet streams (called 2a, 2b, 2c, ...). These balances are summarized in Table 7.6-1 for turbulent flow (where the velocity profiles are regarded as flat).

EXAMPLE 7.6-1

Pressure Rise and Friction Loss in a Sudden Enlargement

An incompressible fluid flows from a small circular tube into a large tube in turbulent flow, as shown in Fig. 7.6-1. The cross-sectional areas of the tubes are S_1 and S_2 . Obtain an expression for the pressure change between planes 1 and 2 and for the friction loss associated with the sudden enlargement in cross section. Let $\beta = S_1/S_2$, which is less than unity.

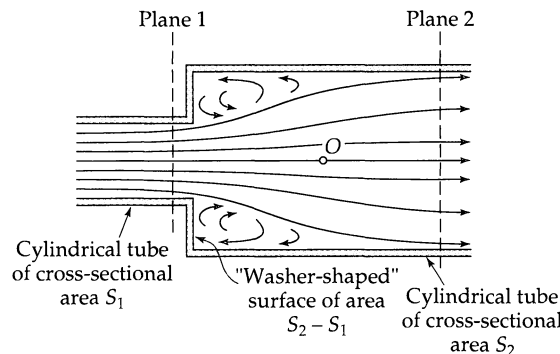


Fig. 7.6-1. Flow through a sudden enlargement.

SOLUTION

(a) **Mass balance.** For steady flow the mass balance gives

$$w_1 = w_2 \quad \text{or} \quad \rho_1 v_1 S_1 = \rho_2 v_2 S_2 \quad (7.6-1)$$

For a fluid of constant density, this gives

$$\frac{v_1}{v_2} = \frac{1}{\beta} \quad (7.6-2)$$

(b) **Momentum balance.** The downstream component of the momentum balance is

$$\mathbf{F}_{f \rightarrow s} = (v_1 w_1 - v_2 w_2) + (p_1 S_1 - p_2 S_2) \quad (7.6-3)$$

The force $\mathbf{F}_{f \rightarrow s}$ is composed of two parts: the viscous force on the cylindrical surfaces parallel to the direction of flow, and the pressure force on the washer-shaped surface just to the right of plane 1 and perpendicular to the flow axis. The former contribution we neglect (by intuition) and the latter we take to be $p_1(S_2 - S_1)$ by assuming that the pressure on the washer-shaped surface is the same as that at plane 1. We then get, by using Eq. 7.6-1,

$$-p_1(S_2 - S_1) = \rho v_2 S_2 (v_1 - v_2) + (p_1 S_1 - p_2 S_2) \quad (7.6-4)$$

Solving for the pressure difference gives

$$p_2 - p_1 = \rho v_2 (v_1 - v_2) \quad (7.6-5)$$

or, in terms of the downstream velocity,

$$p_2 - p_1 = \rho v_2^2 \left(\frac{1}{\beta} - 1 \right) \quad (7.6-6)$$

Note that the momentum balance predicts (correctly) a *rise* in pressure.

(c) **Angular momentum balance.** This balance is not needed. If we take the origin of coordinates on the axis of the system at the center of gravity of the fluid located between planes 1 and 2, then $[\mathbf{r}_1 \times \mathbf{u}_1]$ and $[\mathbf{r}_2 \times \mathbf{u}_2]$ are both zero, and there are no torques on the fluid system.

(d) **Mechanical energy balance.** There is no compressive loss, no work done via moving parts, and no elevation change, so that

$$\hat{E}_v = \frac{1}{2}(v_1^2 - v_2^2) + \frac{1}{\rho}(p_1 - p_2) \quad (7.6-7)$$

Insertion of Eq. 7.6-6 for the pressure rise then gives, after some rearrangement,

$$\hat{E}_v = \frac{1}{2} v_2^2 \left(\frac{1}{\beta} - 1 \right)^2 \quad (7.6-8)$$

which is an entry in Table 7.5-1.

This example has shown how to use the macroscopic balances to estimate the friction loss factor for a simple resistance in a flow system. Because of the assumptions mentioned after Eq. 7.6-3, the results in Eqs. 7.6-6 and 8 are approximate. If great accuracy is needed, a correction factor based on experimental data should be introduced.

EXAMPLE 7.6-2*Performance of a Liquid-Liquid Ejector*

A diagram of a liquid-liquid ejector is shown in Fig. 7.6-2. It is desired to analyze the mixing of the two streams, both of the same fluid, by means of the macroscopic balances. At plane 1 the two fluid streams merge. Stream 1a has a velocity v_0 and a cross-sectional area $\frac{1}{3}S_1$, and stream 1b has a velocity $\frac{1}{2}v_0$ and a cross-sectional area $\frac{2}{3}S_1$. Plane 2 is chosen far enough downstream that the two streams have mixed and the velocity is almost uniform at v_2 . The flow is

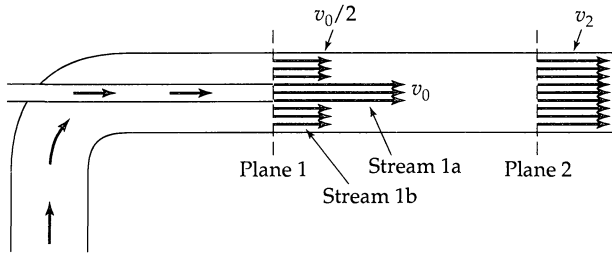


Fig. 7.6-2. Flow in a liquid-liquid ejector pump.

turbulent and the velocity profiles at planes 1 and 2 are assumed to be flat. In the following analysis $\mathbf{F}_{f-\infty}$ is neglected, since it is felt to be less important than the other terms in the momentum balance.

SOLUTION

(a) **Mass balance.** At steady state, Eq. (A) of Table 7.6-1 gives

$$w_{1a} + w_{1b} = w_2 \quad (7.6-9)$$

or

$$\rho v_0 (\frac{1}{3} S_1) + \rho (\frac{1}{2} v_0) (\frac{2}{3} S_1) = \rho v_2 S_2 \quad (7.6-10)$$

Hence, since $S_1 = S_2$, this equation gives

$$v_2 = \frac{2}{3} v_0 \quad (7.6-11)$$

for the velocity of the exit stream. We also note, for later use, that $w_{1a} = w_{1b} = \frac{1}{2} w_2$.

(b) **Momentum balance.** From Eq. (B) of Table 7.6-1 the component of the momentum balance in the flow direction is

$$(v_{1a} w_{1a} + v_{1b} w_{1b} + p_1 S_1) - (v_2 w_2 + p_2 S_2) = 0 \quad (7.6-12)$$

or using the relation at the end of (a)

$$\begin{aligned} (p_2 - p_1) S_2 &= (\frac{1}{2}(v_{1a} + v_{1b}) - v_2) w_2 \\ &= (\frac{1}{2}(v_0 + \frac{1}{2}v_0) - \frac{2}{3}v_0)(\rho(\frac{2}{3}v_0)S_2) \end{aligned} \quad (7.6-13)$$

from which

$$p_2 - p_1 = \frac{1}{18}\rho v_0^2 \quad (7.6-14)$$

This is the expression for the pressure rise resulting from the mixing of the two streams.

(c) **Angular momentum balance.** This balance is not needed.

(d) **Mechanical energy balance.** Equation (D) of Table 7.6-1 gives

$$(\frac{1}{2}v_{1a}^2 w_{1a} + \frac{1}{2}v_{1b}^2 w_{1b}) - \left(\frac{1}{2}v_2^2 + \frac{p_2 - p_1}{\rho} \right) w_2 = E_v \quad (7.6-15)$$

or, using the relation at the end of (a), we get

$$(\frac{1}{2}v_{1a}^2 (\frac{1}{2}w_2) + \frac{1}{2}(\frac{1}{2}v_0)^2 (\frac{1}{2}w_2)) - (\frac{1}{2}(\frac{2}{3}v_0)^2 + \frac{1}{18}v_0^2) w_2 = E_v \quad (7.6-16)$$

Hence

$$\hat{E}_v = \frac{E_v}{w_2} = \frac{5}{144} v_0^2 \quad (7.6-17)$$

is the energy dissipation per unit mass. The preceding analysis gives fairly good results for liquid-liquid ejector pumps. In gas-gas ejectors, however, the density varies significantly and it is necessary to include the macroscopic total energy balance as well as an equation of state in the analysis. This is discussed in Example 15.3-2.

EXAMPLE 7.6-3**Thrust on a Pipe Bend**

Water at 95°C is flowing at a rate of 2.0 ft³/s through a 60° bend, in which there is a contraction from 4 to 3 in. internal diameter (see Fig. 7.6-3). Compute the force exerted on the bend if the pressure at the downstream end is 1.1 atm. The density and viscosity of water at the conditions of the system are 0.962 g/cm³ and 0.299 cp, respectively.

SOLUTION

The Reynolds number for the flow in the 3-in. pipe is

$$\begin{aligned} \text{Re} &= \frac{D\langle v \rangle \rho}{\mu} = \frac{4w}{\pi D \mu} \\ &= \frac{4(2.0 \times (12 \times 2.54)^3)(0.962)}{\pi(3 \times 2.54)(0.00299)} = 3 \times 10^6 \end{aligned} \quad (7.6-18)$$

At this Reynolds number the flow is highly turbulent, and the assumption of flat velocity profiles is reasonable.

(a) **Mass balance.** For steady-state flow, $w_1 = w_2$. If the density is constant throughout,

$$\frac{v_1}{v_2} = \frac{S_2}{S_1} \equiv \beta \quad (7.6-19)$$

in which β is the ratio of the smaller to the larger cross section.

(b) **Mechanical energy balance.** For steady, incompressible flow, Eq. (d) of Table 7.6-1 becomes, for this problem,

$$\frac{1}{2}(v_2^2 - v_1^2) + g(h_2 - h_1) + \frac{1}{\rho}(p_2 - p_1) + \hat{E}_v = 0 \quad (7.6-20)$$

According to Table 7.5-1 and Eq. 7.5-4, we can take the friction loss as approximately $\frac{2}{5}(\frac{1}{2}v_2^2) = \frac{1}{5}v_2^2$. Inserting this into Eq. 7.6-20 and using the mass balance we get

$$p_1 - p_2 = \rho v_2^2 (\frac{1}{2} - \frac{1}{2}\beta^2 + \frac{1}{5}) + \rho g(h_2 - h_1) \quad (7.6-21)$$

This is the pressure drop through the bend in terms of the known velocity v_2 and the known geometrical factor β .

(c) **Momentum balance.** We now have to consider both the x - and y -components of the momentum balance. The inlet and outlet unit vectors will have x - and y -components given by $u_{1x} = 1$, $u_{1y} = 0$, $u_{2x} = \cos \theta$, and $u_{2y} = \sin \theta$.

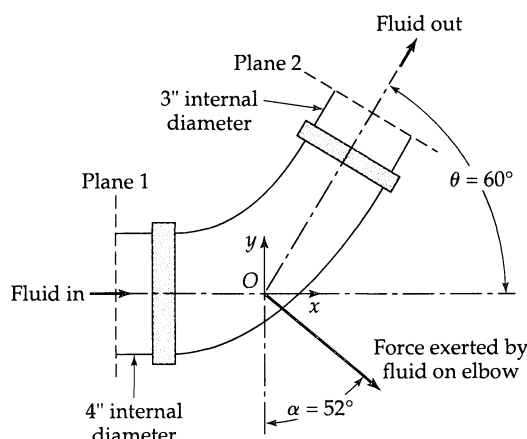


Fig. 7.6-3. Reaction force at a reducing bend in a pipe.

The x -component of the momentum balance then gives

$$F_x = (v_1 w_1 + p_1 S_1) - (v_2 w_2 + p_2 S_2) \cos \theta \quad (7.6-22)$$

where F_x is the x -component of $\mathbf{F}_{f \rightarrow s}$. Introducing the specific expressions for w_1 and w_2 , we get

$$\begin{aligned} F_x &= v_1(\rho v_1 S_1) - v_2(\rho v_2 S_2) \cos \theta + p_1 S_1 - p_2 S_2 \cos \theta \\ &= \rho v_2^2 S_2 (\beta - \cos \theta) + (p_1 - p_2) S_1 + p_2 (S_1 - S_2 \cos \theta) \end{aligned} \quad (7.6-23)$$

Substituting into this the expression for $p_1 - p_2$ from Eq. 7.6-21 gives

$$\begin{aligned} F_x &= \rho v_2^2 S_2 (\beta - \cos \theta) + \rho v_2^2 S_2 \beta^{-1} \left(\frac{7}{10} - \frac{1}{2} \beta^2 \right) \\ &\quad + \rho g (h_2 - h_1) S_2 \beta^{-1} + p_2 S_2 (\beta^{-1} - \cos \theta) \\ &= w^2 (\rho S_2)^{-1} \left(\frac{7}{10} \beta^{-1} - \cos \theta + \frac{1}{2} \beta \right) \\ &\quad + \rho g (h_2 - h_1) S_2 \beta^{-1} + p_2 S_2 (\beta^{-1} - \cos \theta) \end{aligned} \quad (7.6-24)$$

The y -component of the momentum balance is

$$F_y = -(v_2 w_2 + p_2 S_2) \sin \theta - m_{\text{tot}} g \quad (7.6-25)$$

or

$$F_y = -w^2 (\rho S_2)^{-1} \sin \theta - p_2 S_2 \sin \theta - \pi R^2 L \rho g \quad (7.6-26)$$

in which R and L are the radius and length of a roughly equivalent cylinder.

We now have the components of the reaction force in terms of known quantities. The numerical values needed are

$$\begin{aligned} \rho &= 60 \text{ lb}_m/\text{ft}^3 & S_2 &= \frac{1}{64} \pi = 0.049 \text{ ft}^2 \\ w &= (2.0)(60) = 120 \text{ lb}_m/\text{s} & \beta &= S_2/S_1 = 3^2/4^2 = 0.562 \\ \cos \theta &= \frac{1}{2} & R & \approx \frac{1}{8} \text{ ft} \\ \sin \theta &= \frac{1}{2}\sqrt{3} & L & \approx \frac{5}{6} \text{ ft} \\ p_2 &= 16.2 \text{ lb}_f/\text{in.}^2 & h_2 - h_1 & \approx \frac{1}{2} \text{ ft} \end{aligned}$$

With these values we then get

$$\begin{aligned} F_x &= \frac{(120)^2}{2(0.049)(32.2)} \left(\frac{7}{10} \frac{1}{0.562} - \frac{1}{2} + \frac{0.562}{2} \right) + (60)(\frac{1}{2})(0.049) \left(\frac{1}{0.562} \right) \\ &\quad + (16.2)(0.049)(144) \left(\frac{1}{0.562} - \frac{1}{2} \right) \text{lb}_f \\ &= (152)(1.24 - 0.50 + 0.28) + 2.6 + (144)(1.78 - 0.50) \\ &= 155 + 2.6 + 146 = 304 \text{ lb}_f = 1352 \text{ N} \end{aligned} \quad (7.6-27)$$

$$\begin{aligned} F_y &= -\frac{(120)^2}{2(0.049)(32.2)} \left(\frac{1}{2}\sqrt{3} \right) - (16.2)(0.049)(144) \left(\frac{1}{2}\sqrt{3} \right) - \pi \left(\frac{1}{8} \right)^2 \left(\frac{5}{6} \right) (60) \text{ lb}_f \\ &= -132 - 99 - 2.5 = 234 \text{ lb}_f = 1041 \text{ N} \end{aligned} \quad (7.6-28)$$

Hence the magnitude of the force is

$$|\mathbf{F}| = \sqrt{F_x^2 + F_y^2} = \sqrt{304^2 + 234^2} = 384 \text{ lb}_f = 1708 \text{ N} \quad (7.6-29)$$

The angle that this force makes with the vertical is

$$\alpha = \arctan(F_x/F_y) = \arctan 1.30 = 52^\circ \quad (7.6-30)$$

In looking back over the calculation, we see that all the effects we have included are important, with the possible exception of the gravity terms of 2.6 lb_f in F_x and 2.5 lb_f in F_y .

EXAMPLE 7.6-4**The Impinging Jet**

A rectangular incompressible fluid jet of thickness b_1 emerges from a slot of width c , hits a flat plate and splits into two streams of thicknesses b_{2a} and b_{2b} as shown in Fig. 7.6-4. The emerging turbulent jet stream has a velocity v_1 and a mass flow rate w_1 . Find the velocities and mass rates of flow in the two streams on the plate.¹

SOLUTION

We neglect viscous dissipation and gravity, and assume that the velocity profiles of all three streams are flat and that their pressures are essentially equal. The macroscopic balances then give

Mass balance

$$w_1 = w_{2a} + w_{2b} \quad (7.6-31)$$

Momentum balance (in the direction parallel to the plate)

$$v_1 w_1 \cos \theta = v_{2a} w_{2a} - v_{2b} w_{2b} \quad (7.6-32)$$

Mechanical energy balance

$$\frac{1}{2} v_1^2 w_1 = \frac{1}{2} v_{2a}^2 w_{2a} + \frac{1}{2} v_{2b}^2 w_{2b} \quad (7.6-33)$$

Angular momentum balance (put the origin of coordinates on the centerline of the jet and at an altitude of $\frac{1}{2}b_1$; this is done so that there will be no angular momentum of the incoming jet)

$$0 = (v_{2a} w_{2a}) \cdot \frac{1}{2}(b_1 - b_{2a}) - (v_{2b} w_{2b}) \cdot \frac{1}{2}(b_1 - b_{2b}) \quad (7.6-34)$$

This last equation can be rewritten to eliminate the b 's in favor of the w 's. Since $w_1 = \rho v_1 b_1 c$ and $w_{2a} = \rho v_{2a} b_{2a} c$, we can replace $b_1 - b_{2a}$ by $(w_1 / \rho v_1 c) - (w_{2a} / \rho v_{2a} c)$ and replace $b_1 - b_{2b}$ correspondingly. Then the angular momentum balance becomes

$$(v_{2a} w_{2a}) \left(\frac{w_1}{v_1} - \frac{w_{2a}}{v_{2a}} \right) = (v_{2b} w_{2b}) \left(\frac{w_1}{v_1} - \frac{w_{2b}}{v_{2b}} \right) \quad (7.6-35)$$

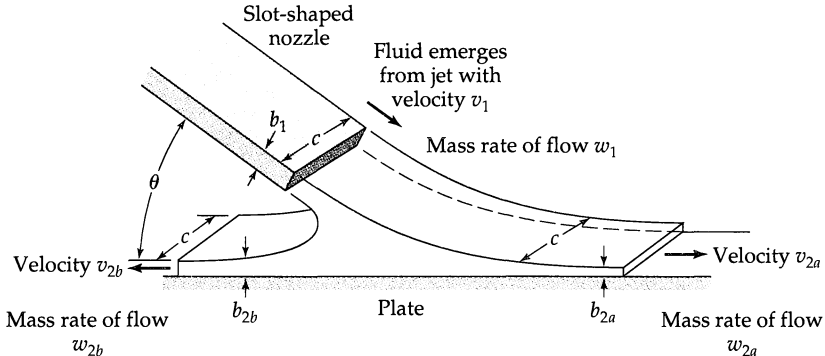


Fig. 7.6-4. Jet impinging on a wall and splitting into two streams. The point O , which is the origin of coordinates for the angular momentum balance, is taken to be the intersection of the centerline of the incoming jet and a plane that is at an elevation $\frac{1}{2}b_1$.

¹ For alternative solutions to this problem, see G. K. Batchelor, *An Introduction to Fluid Dynamics*, Cambridge University Press (1967), pp. 392–394, and S. Whitaker, *Introduction to Fluid Dynamics*, Prentice-Hall, Englewood Cliffs, N.J. (1968), p. 260. An application of the compressible impinging jet problem has been given by J. V. Foa, U.S. Patent 3,361,336 (Jan. 2, 1968). There, use is made of the fact that if the slot-shaped nozzle moves to the left in Fig. 7.6-4 (i.e., left with respect to the plate), then, for a compressible fluid, the right stream will be cooler than the jet and the left stream will be warmer.

or

$$w_{2a}^2 - w_{2b}^2 = \frac{w_1}{v_1} (v_{2a}w_{2a} - v_{2b}w_{2b}) \quad (7.6-36)$$

Now Eqs. 7.6-31, 32, 33, and 36 are four equations with four unknowns. When these are solved we find that

$$v_{2a} = v_1 \quad w_{2a} = \frac{1}{2}w_1(1 + \cos \theta) \quad (7.6-37, 38)$$

$$v_{2b} = v_1 \quad w_{2b} = \frac{1}{2}w_1(1 - \cos \theta) \quad (7.6-39, 40)$$

Hence the velocities of all three streams are equal. The same result is obtained by applying the classical Bernoulli equation for the flow of an inviscid fluid (see Example 3.5-1).

EXAMPLE 7.6-5

Isothermal Flow of a Liquid Through an Orifice

A common method for determining the mass rate of flow through a pipe is to measure the pressure drop across some "obstacle" in the pipe. An example of this is the orifice, which is a thin plate with a hole in the middle. There are pressure taps at planes 1 and 2, upstream and downstream of the orifice plate. Fig. 7.6-5(a) shows the orifice meter, the pressure taps, and the general behavior of the velocity profiles as observed experimentally. The velocity profile at plane 1

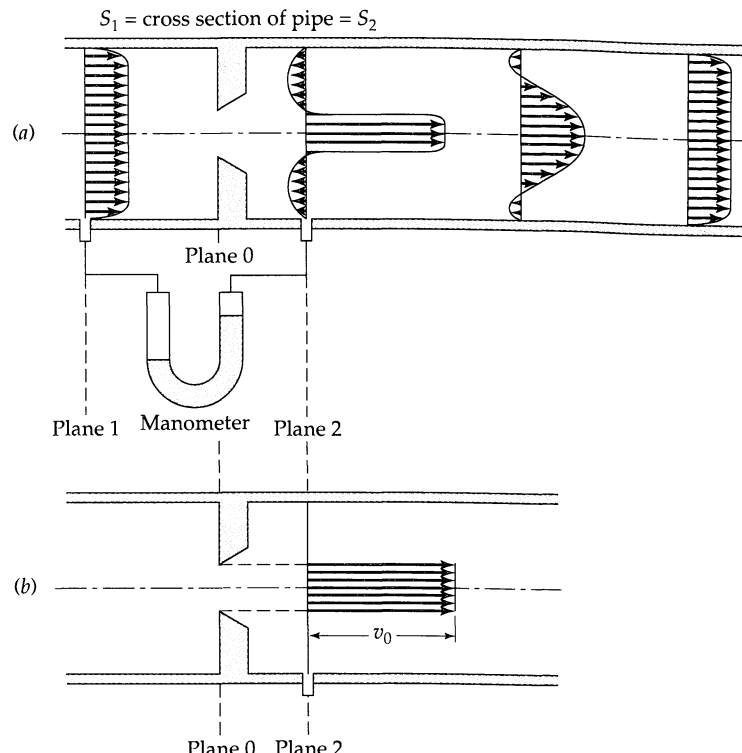


Fig. 7.6-5. (a) A sharp-edged orifice, showing the approximate velocity profiles at several planes near the orifice plate. The fluid jet emerging from the hole is somewhat smaller than the hole itself. In highly turbulent flow this jet necks down to a minimum cross section at the *vena contracta*. The extent of this necking down can be given by the *contraction coefficient*, $C_c = (S_{\text{vena contracta}}/S_0)$. According to inviscid flow theory, $C_c = \pi/(\pi + 2) = 0.611$ if $S_0/S_1 = 0$ [H. Lamb, *Hydrodynamics*, Dover, New York (1945), p. 99]. Note that there is some back flow near the wall. (b) Approximate velocity profile at plane 2 used to estimate $\langle v_2^3 \rangle / \langle v_2 \rangle$.

will be assumed to be flat. In Fig. 7.6-5(b) we show an approximate velocity profile at plane 2, which we use in the application of the macroscopic balances. The standard orifice meter equation is obtained by applying the macroscopic mass and mechanical energy balances.

SOLUTION

(a) **Mass balance.** For a fluid of constant density with a system for which $S_1 = S_2 = S$, the mass balance in Eq. 7.1-1 gives

$$\langle v_1 \rangle = \langle v_2 \rangle \quad (7.6-41)$$

With the assumed velocity profiles this becomes

$$v_1 = \frac{S_0}{S} v_0 \quad (7.6-42)$$

and the volume rate of flow is $w = \rho v_1 S$.

(b) **Mechanical energy balance.** For a constant-density fluid in a flow system with no elevation change and no moving parts, Eq. 7.4-5 gives

$$\frac{1}{2} \frac{\langle v_2^2 \rangle}{\langle v_2 \rangle} - \frac{1}{2} \frac{\langle v_1^2 \rangle}{\langle v_1 \rangle} + \frac{p_2 - p_1}{\rho} + \hat{E}_v = 0 \quad (7.6-43)$$

The viscous loss \hat{E}_v is neglected, even though it is certainly not equal to zero. With the assumed velocity profiles, Eq. 7.6-43 then becomes

$$\frac{1}{2}(v_0^2 - v_1^2) + \frac{p_2 - p_1}{\rho} = 0 \quad (7.6-44)$$

When Eqs. 7.6-42 and 44 are combined to eliminate v_0 , we can solve for v_1 to get

$$v_1 = \sqrt{\frac{2(p_1 - p_2)}{\rho} \frac{1}{(S/S_0)^2 - 1}} \quad (7.6-45)$$

We can now multiply by ρS to get the volume rate of flow. Then to account for the errors introduced by neglecting \hat{E}_v and by the assumptions regarding the velocity profiles we include a *discharge coefficient*, C_d , and obtain

$$w = C_d S_0 \sqrt{\frac{2\rho(p_1 - p_2)}{1 - (S_0/S)^2}} \quad (7.6-46)$$

Experimental discharge coefficients have been correlated as a function of S_0/S and the Reynolds number.² For Reynolds numbers greater than 10^4 , C_d approaches about 0.61 for all practical values of S_0/S .

This example has illustrated the use of the macroscopic balances to get the general form of the result, which is then modified by introducing a multiplicative function of dimensionless groups to correct for errors introduced by unwarranted assumptions. This combination of macroscopic balances and dimensional considerations is often used and can be quite useful.

§7.7 USE OF THE MACROSCOPIC BALANCES FOR UNSTEADY-STATE PROBLEMS

In the preceding section we have illustrated the use of the macroscopic balances for solving steady-state problems. In this section we turn our attention to unsteady-state problems. We give two examples to illustrate the use of the time-dependent macroscopic balance equations.

² G. L. Tuve and R. E. Sprenkle, *Instruments*, 6, 202–205, 225, 232–234 (1935); see also R. H. Perry and C. H. Chilton, *Chemical Engineers' Handbook*, McGraw-Hill, New York, 5th edition (1973), Fig. 5-18; *Fluid Meters: Their Theory and Applications*, 6th edition, American Society of Mechanical Engineers, New York (1971), pp. 58–65; Measurement of Fluid Flow Using Small Bore Precision Orifice Meters, American Society of Mechanical Engineers, MFC-14-M, New York (1995).

EXAMPLE 7.7-1

Acceleration Effects in Unsteady Flow from a Cylindrical Tank

SOLUTION

An open cylinder of height H and radius R is initially entirely filled with a liquid. At time $t = 0$ the liquid is allowed to drain out through a small hole of radius R_0 at the bottom of the tank (see Fig. 7.7-1).

(a) Find the efflux time by using the unsteady-state mass balance and by assuming Torricelli's equation (see Problem 3B.14) to describe the relation between efflux velocity and the instantaneous height of the liquid.

(b) Find the efflux time using the unsteady-state mass and mechanical energy balances.

(a) We apply Eq. 7.1-2 to the system in Fig. 7.7-1, taking plane 1 to be at the top of the tank (so that $w_1 = 0$). If the instantaneous liquid height is $h(t)$, then

$$\frac{d}{dt} (\pi R^2 h \rho) = -\rho v_2 (\pi R_0^2) \quad (7.7-1)$$

Here we have assumed that the velocity profile at plane 2 is flat. According to Torricelli's equation $v_2 = \sqrt{2gh}$, so that Eq. 7.7-1 becomes

$$\frac{dh}{dt} = -\left(\frac{R_0}{R}\right)^2 \sqrt{2gh} \quad (7.7-2)$$

When this is integrated from $t = 0$ to $t = t_{\text{efflux}}$ we get

$$t_{\text{efflux}} = \sqrt{\frac{2NH}{g}} \quad (7.7-3)$$

in which $N = (R/R_0)^4 \gg 1$. This is effectively a quasi-steady-state solution, since we have used the unsteady-state mass balance along with Torricelli's equation, which was derived for a steady-state flow.

(b) We now use Eq. 7.7-1 and the mechanical energy balance in Eq. 7.4-2. In the latter, the terms W_m and E_v are identically zero, and we assume that E_v is negligibly small, since the velocity gradients in the system will be small. We take the datum plane for the potential energy to be at the bottom of the tank, so that $\Phi_2 = gz_2 = 0$; at plane 1 no liquid is entering, and therefore the potential energy term is not needed there. Since the top of the tank is open to the atmosphere and the tank is discharging into the atmosphere, the pressure contributions cancel one another.

To get the total kinetic energy in the system at any time t , we have to know the velocity of every fluid element in the tank. At every point in the tank, we assume that the fluid is moving downward at the same velocity, namely $v_2(R_0/R)^2$ so that the kinetic energy per unit volume is everywhere $\frac{1}{2}\rho v_2^2(R_0/R)^4$.

To get the total potential energy in the system at any time t , we have to integrate the potential energy per unit volume $\rho g z$ over the volume of fluid from 0 to h . This gives $\pi R^2 \rho g (\frac{1}{2}h^2)$.

Therefore the mechanical energy balance in Eq. 7.4-2 becomes

$$\frac{d}{dt} [(\pi R^2 h)(\frac{1}{2}\rho v_2^2)(R_0/R)^4 + \pi R^2 \rho g (\frac{1}{2}h^2)] = -\frac{1}{2}v_2^2 (\rho v_2 \pi R_0^2) \quad (7.7-4)$$

From the unsteady-state mass balance, $v_2 = -(R/R_0)^2(dh/dt)$. When this is inserted into Eq. 7.7-4 we get (after dividing by dh/dt)

$$2h \frac{d^2h}{dt^2} - (N - 1)\left(\frac{dh}{dt}\right)^2 + 2gh = 0 \quad (7.7-5)$$

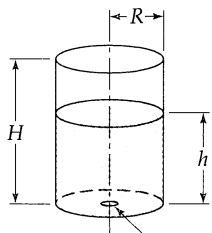


Fig. 7.7-1. Flow out of a cylindrical tank.

This is to be solved with the two initial conditions:

$$\text{I.C. 1:} \quad \text{at } t = 0, \quad h = H \quad (7.7-6)$$

$$\text{I.C. 2:} \quad \text{at } t = 0, \quad \frac{dh}{dt} = \sqrt{2gH}(R_0/R)^2 \quad (7.7-7)$$

The second of these is Torricelli's equation at the initial instant of time.

The second-order differential equation for h can be converted to a first-order equation for the function $u(h)$ by making the change of variable $(dh/dt)^2 = u$. This gives

$$h \frac{du}{dh} - (N-1)u + 2gh = 0 \quad (7.7-8)$$

The solution to this first-order equation can be verified to be¹

$$u = Ch^{N-1} + 2gh/(N-2) \quad (7.7-9)$$

The second initial condition then gives $C = -4g/[N(N-2)H^{N-2}]$ for the integration constant; since $N \gg 1$, we need not concern ourselves with the special case that $N = 2$. We can next take the square root of Eq. 7.7-9 and introduce a dimensionless liquid height $\eta = h/H$; this gives

$$\frac{d\eta}{dt} = \pm \sqrt{\frac{2g}{(N-2)H}} \sqrt{\eta - \frac{2}{N} \eta^{N-1}} \quad (7.7-10)$$

in which the minus sign must be chosen on physical grounds. This separable, first-order equation can be integrated from $t = 0$ to $t = t_{\text{efflux}}$ to give

$$t_{\text{efflux}} = \sqrt{\frac{(N-2)H}{2g}} \int_0^1 \frac{d\eta}{\sqrt{\eta - (2/N)\eta^{N-1}}} \equiv \sqrt{\frac{2NH}{g}} \phi(N) \quad (7.7-11)$$

The function $\phi(N)$ gives the deviation from the quasi-steady-state solution obtained in Eq. 7.7-3. This function can be evaluated as follows:

$$\begin{aligned} \phi(N) &= \frac{1}{2} \sqrt{\frac{N-2}{N}} \int_0^1 \frac{d\eta}{\sqrt{\eta - (2/N)\eta^{N-1}}} \\ &= \frac{1}{2} \sqrt{\frac{N-2}{N}} \int_0^1 \frac{1}{\sqrt{\eta}} \left(1 - \frac{2}{N} \eta^{N-2}\right)^{-1/2} d\eta \\ &= \frac{1}{2} \sqrt{\frac{N-2}{N}} \int_0^1 \frac{1}{\sqrt{\eta}} \left(1 + \frac{1}{2} \left(\frac{2}{N} \eta^{N-2}\right) + \frac{3}{8} \left(\frac{2}{N} \eta^{N-2}\right)^2 + \dots\right) d\eta \end{aligned} \quad (7.7-12)$$

The integrations can now be performed. When the result is expanded in inverse powers of N , one finds that

$$\phi(N) = 1 - \frac{1}{N} + O\left(\frac{1}{N^3}\right) \quad (7.7-13)$$

Since $N = (R/R_0)^4$ is a very large number, it is evident that the factor $\phi(N)$ differs only very slightly from unity.

It is instructive now to return to Eq. 7.7-4 and omit the term describing the change in total kinetic energy with time. If this is done, one obtains exactly the expression for efflux time in Eq. 7.7-3 (or Eq. 7.7-11, with $\phi(N) = 1$). We can therefore conclude that in this type of problem, the change in kinetic energy with time can safely be neglected.

¹ See E. Kamke, *Differentialgleichungen: Lösungsmethoden und Lösungen*, Chelsea Publishing Company, New York (1948), p. 311, #1.94; G. M. Murphy, *Ordinary Differential Equations and Their Solutions*, Van Nostrand, Princeton, N.J. (1960), p. 236, #157.

EXAMPLE 7.7-2*Manometer Oscillations²***SOLUTION**

The liquid in a U-tube manometer, initially at rest, is set in motion by suddenly imposing a pressure difference $p_a - p_b$. Determine the differential equation for the motion of the manometer fluid, assuming incompressible flow and constant temperature. Obtain an expression for the tube radius for which critical damping occurs. Neglect the motion of the gas above the manometer liquid. The notation is summarized in Fig. 7.7-2.

We designate the manometric liquid as the system to which we apply the macroscopic balances. In that case, there are no planes 1 and 2 through which liquid enters or exits. The free liquid surfaces are capable of performing work on the surroundings, W_m , and hence play the role of the moving mechanical parts in §7.4. We apply the mechanical energy balance of Eq. 7.4-2, with E_c set equal to zero (since the manometer liquid is regarded as incompressible). Because of the choice of the system, both w_1 and w_2 are zero, so that the only terms on the right side are $-W_m$ and $-E_v$.

To evaluate dK_{tot}/dt and E_v it is necessary to make some kind of assumption about the velocity profile. Here we take the velocity profile to be parabolic:

$$v(r, t) = 2\langle v \rangle \left[1 - \left(\frac{r}{R} \right)^2 \right] \quad (7.7-14)$$

in which $\langle v \rangle = dh/dt$ is a function of time, defined to be positive when the flow is from left to right.

The kinetic energy term may then be evaluated as follows:

$$\begin{aligned} \frac{dK_{\text{tot}}}{dt} &= \frac{d}{dt} \int_0^L \int_0^{2\pi} \int_0^R \left(\frac{1}{2} \rho v^2 \right) r dr d\theta dl \\ &= 2\pi L \left(\frac{1}{2} \rho \right) \frac{d}{dt} \int_0^R v^2 r dr \\ &= 2\pi L R^2 \left(\frac{1}{2} \rho \right) \frac{d}{dt} \int_0^1 (2\langle v \rangle (1 - \xi^2))^2 \xi d\xi \\ &= \frac{4}{3} \rho L S \langle v \rangle \frac{d}{dt} \langle v \rangle \end{aligned} \quad (7.7-15)$$

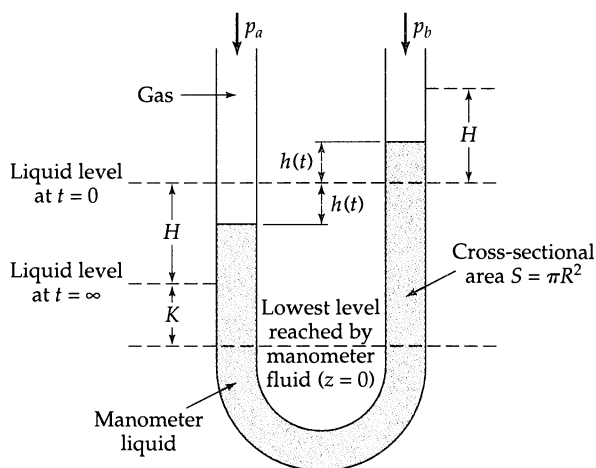


Fig. 7.7-2. Damped oscillations of a manometer fluid.

² For a summary of experimental and theoretical work on manometer oscillations, see J. C. Biery, *AIChE Journal*, 9, 606–614 (1963); 10, 551–557 (1964); 15, 631–634 (1969). Biery's experimental data show that the assumption made in Eq. 7.7-14 is not very good.

Here l is a coordinate running along the axis of the manometer tube, and L is the distance along this axis from one manometer interface to the other—that is, the total length of the manometer fluid. The dimensionless coordinate ξ is r/R , and S is the cross-sectional area of the tube.

The change of potential energy with time is given by

$$\begin{aligned}\frac{d\Phi_{\text{tot}}}{dt} &= \frac{d}{dt} \int_0^L \int_0^{2\pi} \int_0^R (\rho g z) r dr d\theta dl \\ &= \frac{d}{dt} \left[\left(\begin{array}{l} \text{integral over portion} \\ \text{below } z = 0, \text{ which} \\ \text{is constant} \end{array} \right) + \rho g S \int_0^{K+H-h} z dz + \rho g S \int_0^{K+H+h} z dz \right] \\ &= 2\rho g Sh \frac{dh}{dt}\end{aligned}\quad (7.7-16)$$

The viscous loss term can also be evaluated as follows:

$$\begin{aligned}E_v &= - \int_0^L \int_0^{2\pi} \int_0^R (\tau : \nabla v) r dr d\theta dl \\ &= 2\pi L \mu \int_0^R \left(\frac{dv}{dr} \right)^2 r dr \\ &= 8\pi L \mu \langle v \rangle^2 \int_0^1 (-2\xi)^2 \xi d\xi \\ &= 8LS\mu \langle v \rangle^2 / R^2\end{aligned}\quad (7.7-17)$$

Furthermore, the net work done by the surroundings on the system is

$$W_m = (p_a - p_b)S\langle v \rangle \quad (7.7-18)$$

Substitution of the above terms into the mechanical energy balance and letting $\langle v \rangle = dh/dt$ then gives the differential equation for $h(t)$ as

$$\frac{d^2h}{dt^2} + \left(\frac{6\mu}{\rho R^2} \right) \frac{dh}{dt} + \left(\frac{3g}{2L} \right) h = \frac{3}{4} \left(\frac{p_a - p_b}{\rho L} \right) \quad (7.7-19)$$

which is to be solved with the initial conditions that $h = 0$ and $dh/dt = 0$ at $t = 0$. This second-order, linear, nonhomogeneous equation can be rendered homogeneous by introducing a new variable k defined by

$$k = 2h - \frac{p_a - p_b}{\rho L} \quad (7.7-20)$$

Then the equation for the motion of the manometer liquid is

$$\frac{d^2k}{dt^2} + \left(\frac{6\mu}{\rho R^2} \right) \frac{dk}{dt} + \left(\frac{3g}{2L} \right) k = 0 \quad (7.7-21)$$

This equation also arises in describing the motion of a mass connected to a spring and dashpot as well as the current in an RLC circuit (see Eq. C.1-7).

We now try a solution of the form $k = e^{mt}$. Substituting this trial function into Eq. 7.7-21 shows that there are two admissible values for m :

$$m_{\pm} = \frac{1}{2}[-(6\mu/\rho R^2) \pm \sqrt{(6\mu/\rho R^2)^2 - (6g/L)}] \quad (7.7-22)$$

and the solution is

$$k = C_+ e^{m_+ t} + C_- e^{m_- t} \quad \text{when } m_+ \neq m_- \quad (7.7-23)$$

$$k = C_1 e^{mt} + C_2 t e^{mt} \quad \text{when } m_+ = m_- = m \quad (7.7-24)$$

with the constants being determined by the initial conditions.

The type of motion that the manometer liquid exhibits depends on the value of the discriminant in Eq. 7.7-22:

- (a) If $(6\mu/\rho R^2)^2 > (6g/L)$, the system is *overdamped*, and the liquid moves slowly to its final position.
- (b) If $(6\mu/\rho R^2)^2 < (6g/L)$, the system is *underdamped*, and the liquid oscillates about its final position, the oscillations becoming smaller and smaller.
- (c) If $(6\mu/\rho R^2)^2 = (6g/L)$, the system is *critically damped*, and the liquid moves to its final position in the most rapid monotone fashion.

The tube radius for critical damping is then

$$R_{cr} = \left(\frac{6\mu^2 L}{\rho^2 g} \right)^{1/4} \quad (7.7-25)$$

If the tube radius R is greater than R_{cr} , an oscillatory motion occurs.

§7.8 DERIVATION OF THE MACROSCOPIC MECHANICAL ENERGY BALANCE¹

In Eq. 7.4-2 the macroscopic mechanical energy balance was presented without proof. In this section we show how the equation is obtained by integrating the equation of change for mechanical energy (Eq. 3.3-2) over the entire volume of the flow system of Fig. 7.0-1. We begin by doing the formal integration:

$$\begin{aligned} \int_{V(t)} \frac{\partial}{\partial t} \left(\frac{1}{2} \rho v^2 + \rho \hat{\Phi} \right) dV = & - \int_{V(t)} (\nabla \cdot (\frac{1}{2} \rho v^2 + \rho \hat{\Phi}) \mathbf{v}) dV - \int_{V(t)} (\nabla \cdot p \mathbf{v}) dV - \int_{V(t)} (\nabla \cdot [\boldsymbol{\tau} \cdot \mathbf{v}]) dV \\ & + \int_{V(t)} p (\nabla \cdot \mathbf{v}) dV + \int_{V(t)} (\boldsymbol{\tau} : \nabla \mathbf{v}) dV \end{aligned} \quad (7.8-1)$$

Next we apply the 3-dimensional Leibniz formula (Eq. A.5-5) to the left side and the Gauss divergence theorem (Eq. A.5-2) to terms 1, 2, and 3 on the right side.

$$\begin{aligned} \frac{d}{dt} \int_{V(t)} \left(\frac{1}{2} \rho v^2 + \rho \hat{\Phi} \right) dV = & - \int_{S(t)} (\mathbf{n} \cdot (\frac{1}{2} \rho v^2 + \rho \hat{\Phi}) (\mathbf{v} - \mathbf{v}_s)) dS - \int_{S(t)} (\mathbf{n} \cdot p \mathbf{v}) dS \\ & - \int_{S(t)} (\mathbf{n} \cdot [\boldsymbol{\tau} \cdot \mathbf{v}]) dS + \int_{V(t)} p (\nabla \cdot \mathbf{v}) dV + \int_{V(t)} (\boldsymbol{\tau} : \nabla \mathbf{v}) dV \end{aligned} \quad (7.8-2)$$

The term containing \mathbf{v}_s , the velocity of the surface of the system, arises from the application of the Leibniz formula. The surface $S(t)$ consists of four parts:

- the fixed surface S_f (on which both \mathbf{v} and \mathbf{v}_s are zero)
- the moving surfaces S_m (on which $\mathbf{v} = \mathbf{v}_s$ with both nonzero)
- the cross section of the entry port S_1 (where $\mathbf{v}_s = 0$)
- the cross section of the exit port S_2 (where $\mathbf{v}_s = 0$)

Presently each of the surface integrals will be split into four parts corresponding to these four surfaces.

We now interpret the terms in Eq. 7.8-2 and, in the process, introduce several assumptions; these assumptions have already been mentioned in §§7.1 to 7.4, but now the reasons for them will be made clear.

¹ R. B. Bird, *Korean J. Chem. Eng.*, **15**, 105–123 (1998), §3.

The term on the left side can be interpreted as the time rate of change of the total kinetic and potential energy ($K_{\text{tot}} + \Phi_{\text{tot}}$) within the “control volume,” whose shape and volume are changing with time.

We next examine one by one the five terms on the right side:

Term 1 (including the minus sign) contributes only at the entry and exit ports and gives the rates of influx and efflux of kinetic and potential energy:

$$\text{Term 1} = (\frac{1}{2}\rho_1\langle v_1^3 \rangle S_1 + \rho_1\hat{\Phi}_1\langle v_1 \rangle S_1) - (\frac{1}{2}\rho_2\langle v_2^3 \rangle S_2 + \rho_2\hat{\Phi}_2\langle v_2 \rangle S_2) \quad (7.8-3)$$

The angular brackets indicate an average over the cross section. To get this result we have to assume that the fluid density and potential energy per unit mass are constant over the cross section, and that the fluid is flowing parallel to the tube walls at the entry and exit ports. The first term in Eq. 7.8-3 is positive, since at plane 1, $(-\mathbf{n} \cdot \mathbf{v}) = (\mathbf{u}_1 \cdot (\mathbf{u}_1 v_1)) = v_1$, and the second term is negative, since at plane 2, $(-\mathbf{n} \cdot \mathbf{v}) = (-\mathbf{u}_2 \cdot (\mathbf{u}_2 v_2)) = -v_2$.

Term 2 (including the minus sign) gives no contribution on S_f since \mathbf{v} is zero there. On each surface element dS of S_m there is a force $-\mathbf{n}pdS$ acting on a surface moving with a velocity \mathbf{v} , and the dot product of these quantities gives the rate at which the surroundings do work on the fluid through the moving surface element dS . We use the symbol $W_m^{(p)}$ to indicate the sum of all these surface terms. Furthermore, the integrals over the stationary surfaces S_1 and S_2 give the work required to push the fluid into the system at plane 1 minus the work required to push the fluid out of the system at plane 2. Therefore term 2 finally gives

$$\text{Term 2} = p_1\langle v_1 \rangle S_1 - p_2\langle v_2 \rangle S_2 + W_m^{(p)} \quad (7.8-4)$$

Here we have assumed that the pressure does not vary over the cross section at the entry and exit ports.

Term 3 (including the minus sign) gives no contribution on S_f since \mathbf{v} is zero there. The integral over S_m can be interpreted as the rate at which the surroundings do work on the fluid by means of the viscous forces, and this integral is designated as $W_m^{(\tau)}$. At the entry and exit ports it is conventional to neglect the work terms associated with the viscous forces, since they are generally quite small compared with the pressure contributions. Therefore we get

$$\text{Term 3} = W_m^{(\tau)} \quad (7.8-5)$$

We now introduce the symbol $W_m = W_m^{(p)} + W_m^{(\tau)}$ to represent the total rate at which the surroundings do work on the fluid within the system through the agency of the moving surfaces.

Terms 4 and 5 cannot be further simplified, and hence we define

$$\text{Term 4} = + \int_{V(t)} p(\nabla \cdot \mathbf{v}) dV = -E_c \quad (7.8-6)$$

$$\text{Term 5} = + \int_{V(t)} (\mathbf{r} : \nabla \mathbf{v}) dV = -E_v \quad (7.8-7)$$

For Newtonian fluids the viscous loss E_v is the rate at which mechanical energy is *irreversibly* degraded into thermal energy because of the viscosity of the fluid and is always a positive quantity (see Eq. 3.3-3). We have already discussed methods for estimating E_v in §7.5. (For viscoelastic fluids, which we discuss in Chapter 8, E_v has to be interpreted differently and may even be negative.) The compression term E_c is the rate at which mechanical energy is *reversibly* changed into thermal energy because of the compressibility of the fluid; it may be either positive or negative. If the fluid is being regarded as incompressible, then E_c is zero.

When all the contributions are inserted into Eq. 7.8-2 we finally obtain the macroscopic mechanical energy balance:

$$\begin{aligned} \frac{d}{dt} (K_{\text{tot}} + \Phi_{\text{tot}}) &= (\frac{1}{2}\rho_1(v_1^3)S_1 + \rho_1\hat{\Phi}_1(v_1)S_1 + p_1(v_1)S_1) - (\frac{1}{2}\rho_2(v_2^3)S_2 \\ &\quad + \rho_2\hat{\Phi}_2(v_2)S_2 + p_2(v_2)S_2) + W_m - E_c - E_v \end{aligned} \quad (7.8-8)$$

If, now, we introduce the symbols $w_1 = \rho_1(v_1)S_1$ and $w_2 = \rho_2(v_2)S_2$ for the mass rates of flow in and out, then Eq. 7.8-8 can be rewritten in the form of Eq. 7.4-2. Several assumptions have been made in this development, but normally they are not serious. If the situation warrants, one can go back and include the neglected effects.

It should be noted that the above derivation of the mechanical energy balance does not require that the system be isothermal. Therefore the results in Eqs. 7.4-2 and 7.8-8 are valid for nonisothermal systems.

To get the mechanical energy balance in the form of Eq. 7.4-7 we have to develop an *approximate* expression for E_c . We imagine that there is a representative streamline running through the system, and we introduce a coordinate s along the streamline. We assume that pressure, density, and velocity do not vary over the cross section. We further imagine that at each position along the streamline, there is a cross section $S(s)$ perpendicular to the s -coordinate, so that we can write $dV = S(s)ds$. If there are moving parts in the system and if the system geometry is complex, it may not be possible to do this.

We start by using the fact that $(\nabla \cdot \rho v) = 0$ at steady state so that

$$E_c = - \int_V p(\nabla \cdot v) dV = + \int_V \frac{p}{\rho} (v \cdot \nabla \rho) dV \quad (7.8-9)$$

Then we use the assumption that the pressure and density are constant over the cross section to write approximately

$$E_c \approx \int_1^2 \frac{p}{\rho} \left(v \frac{dp}{ds} \right) S(s) ds \quad (7.8-10)$$

Even though ρ , v , and S are functions of the streamline coordinate s , their product, $w = \rho v S$, is a constant for steady-state operation and hence may be taken outside the integral. This gives

$$E_c \approx w \int_1^2 \frac{p}{\rho^2} \frac{dp}{ds} ds = -w \int_1^2 p \frac{d}{ds} \left(\frac{1}{\rho} \right) ds \quad (7.8-11)$$

Then an integration by parts can be performed:

$$E_c \approx -w \left[\frac{p}{\rho} \Big|_1^2 - \int_1^2 \frac{1}{\rho} \frac{dp}{ds} ds \right] = -w \Delta \left(\frac{p}{\rho} \right) + w \int_1^2 \frac{1}{\rho} dp \quad (7.8-12)$$

When this result is put into Eq. 7.4-5, the approximate relation in Eq. 7.4-7 is obtained. Because of the questionable nature of the assumptions made (the existence of a representative streamline and the constancy of p and ρ over a cross section), it seems preferable to use Eq. 7.4-5 rather than Eq. 7.4-7. Also, Eq. 7.4-5 is easily generalized to systems with multiple inlet and outlet ports, whereas Eq. 7.4-7 is not; the generalization is given in Eq. (D) of Table 7.6-1.

QUESTIONS FOR DISCUSSION

1. Discuss the origin, meaning, and use of the macroscopic balances, and explain what assumptions have been made in deriving them.
2. How does one decide which macroscopic balances to use for a given problem? What auxiliary information might one need in order to solve problems with the macroscopic balances?
3. Are friction factors and friction loss factors related? If so, how?

4. Discuss the viscous loss E_v and the compression term E_c , with regard to physical interpretation, sign, and methods of estimation.
5. How is the macroscopic mechanical energy balance related to the Bernoulli equation for inviscid fluids? How is it derived?
6. What happens in Example 7.3-1 if one makes a different choice for the origin of the coordinate system?
7. In Example 7.5-1 what would be the error in the final result if the estimation of the viscous loss E_v were off by a factor of 2? Under what circumstances would such an error be more serious?
8. In Example 7.5-1 what would happen if 5 ft were replaced by 50 ft?
9. In Example 7.6-3, how would the results be affected if the outlet pressure were 11 atm instead of 1.1 atm?
10. List all the assumptions that are inherent in the equations given in Table 7.6-1.

PROBLEMS

- 7A.1 Pressure rise in a sudden enlargement** (Fig. 7.6-1). An aqueous salt solution is flowing through a sudden enlargement at a rate of 450 U.S. gal/min = $0.0384 \text{ m}^3/\text{s}$. The inside diameter of the smaller pipe is 5 in. and that of the large pipe is 9 in. What is the pressure rise in pounds per square inch if the density of the solution is $63 \text{ lb}_m/\text{ft}^3$? Is the flow in the smaller pipe laminar or turbulent?

Answer: $0.056 \text{ psi} = 386 \text{ N/m}^2$

- 7A.2 Pumping a hydrochloric acid solution** (Fig. 7A.2). A dilute HCl solution of constant density and viscosity ($\rho = 62.4 \text{ lb}_m/\text{ft}^3$, $\mu = 1 \text{ cp}$) is to be pumped from tank 1 to tank 2 with no overall change in elevation. The pressures in the gas spaces of the two tanks are $p_1 = 1 \text{ atm}$ and $p_2 = 4 \text{ atm}$. The pipe radius is 2 in. and the Reynolds number is 7.11×10^4 . The average velocity in the pipe is to be 2.30 ft/s. What power must be delivered by the pump?

Answer: $2.3 \text{ hp} = 1.7 \text{ kW}$

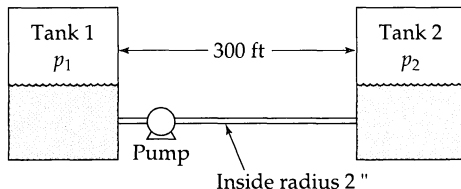


Fig. 7A.2. Pumping of a hydrochloric acid solution.

- 7A.3 Compressible gas flow in a cylindrical pipe.** Gaseous nitrogen is in isothermal turbulent flow at 25°C through a straight length of horizontal pipe with 3-in. inside diameter at a rate of $0.28 \text{ lb}_m/\text{s}$. The absolute pressures at the inlet and outlet are 2 atm and 1 atm, respectively. Evaluate the viscous loss \bar{E}_v , assuming ideal gas behavior.

Answer: $26.3 \text{ Btu/lb}_m = 6.12 \times 10^3 \text{ J/kg}$

- 7A.4 Incompressible flow in an annulus.** Water at 60°F is being delivered from a pump through a coaxial annular conduit 20.3 ft long at a rate of 241 U.S. gal/min. The inner and outer radii of the annular space are 3 in. and 7 in. The inlet is 5 ft lower than the outlet. Determine the power output required from the pump. Use the mean hydraulic radius empiricism to solve the problem. Assume that the pressures at the pump inlet and the annular outlet are the same.

Answer: $0.31 \text{ hp} = 0.23 \text{ kW}$

- 7A.5 Force on a U-bend (Fig. 7A.5).** Water at 68°F ($\rho = 62.4 \text{ lb}_m/\text{ft}^3$, $\mu = 1 \text{ cp}$) is flowing in turbulent flow in a U-shaped pipe bend at $3 \text{ ft}^3/\text{s}$. What is the horizontal force exerted by the water on the U-bend?

Answer: 903 lb,

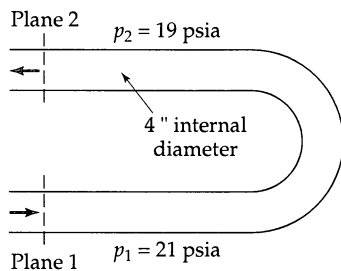


Fig. 7A.5. Flow in a U-bend; both arms of the bend are at the same elevation.

- 7A.6 Flow-rate calculation (Fig. 7A.6).** For the system shown in the figure, calculate the volume flow rate of water at 68°F .

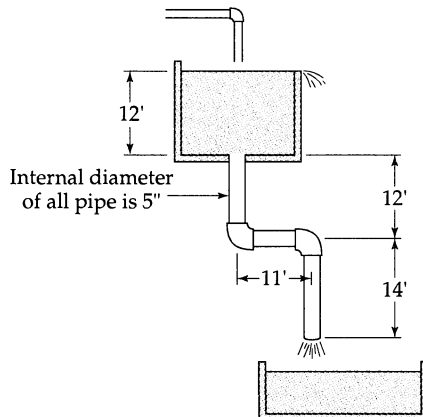


Fig. 7A.6. Flow from a constant-head tank.

- 7A.7 Evaluation of various velocity averages from Pitot tube data.** Following are some experimental data¹ for a Pitot tube traverse for the flow of water in a pipe of internal radius 3.06 in.:

Position	Distance from tube center (in.)	Local velocity (ft/s)	Position	Distance from tube center (in.)	Local velocity (ft/s)
1	2.80	7.85	6	0.72	11.70
2	2.17	10.39	7	1.43	11.47
3	1.43	11.31	8	2.17	11.10
4	0.72	11.66	9	2.80	9.26
5	0.00	11.79			

Plot these data and find out whether the flow is laminar or turbulent. Then use Simpson's rule for numerical integration to compute $\langle v \rangle / v_{\max}$, $\langle v^2 \rangle / v_{\max}^2$, and $\langle v^3 \rangle / v_{\max}^3$. Are these results consistent with the values of $50/49$ (given just before Example 7.2-1) and $43200/40817$ (given just before Example 7.4-1)?

¹ B. Bird, C. E. thesis, University of Wisconsin (1915).

7B.1 Velocity averages from the $\frac{1}{7}$ power law. Evaluate the velocity ratios in Problem 7A.7 according to the velocity distribution in Eq. 5.1-4.

7B.2 Relation between force and viscous loss for flow in conduits of variable cross section. Equation 7.5-6 gives the relation $F_{f \rightarrow s} = \rho S \hat{E}_v$ between the drag force and viscous loss for straight conduits of arbitrary, but constant, cross section. Here we consider a straight channel whose cross section varies gradually with the downstream distance. We restrict ourselves to axisymmetrical channels, so that the force $F_{f \rightarrow s}$ is axially directed.

If the cross section and pressure at the entrance are S_1 and p_1 , and those at the exit are S_2 and p_2 , then prove that the relation analogous to Eq. 7.5-7 is

$$F_{f \rightarrow s} = \rho S_m \hat{E}_v + p_m (S_1 - S_2) \quad (7B.2-1)$$

where

$$\frac{1}{S_m} = \frac{1}{2} \left(\frac{1}{S_1} + \frac{1}{S_2} \right) \quad (7B.2-2)$$

$$p_m = \frac{p_1 S_1 + p_2 S_2}{S_1 + S_2} \quad (7B.2-3)$$

Interpret the results.

7B.3 Flow through a sudden enlargement (Fig. 7.6-1). A fluid is flowing through a sudden enlargement, in which the initial and final diameters are D_1 and D_2 respectively. At what ratio D_2/D_1 will the pressure rise $p_2 - p_1$ be a maximum for a given value of v_1 ?

Answer: $D_2/D_1 = \sqrt{2}$

7B.4 Flow between two tanks (Fig. 7B.4). *Case I:* A fluid flows between two tanks A and B because $p_A > p_B$. The tanks are at the same elevation and there is no pump in the line. The connecting line has a cross-sectional area S_I and the mass rate of flow is w for a pressure drop of $(p_A - p_B)_I$.

Case II: It is desired to replace the connecting line by two lines, each with cross section S_{II} = $\frac{1}{2}S_I$. What pressure difference $(p_A - p_B)_{II}$ is needed to give the same total mass flow rate as in Case I? Assume turbulent flow and use the Blasius formula (Eq. 6.2-12) for the friction factor. Neglect entrance and exit losses.

Answer: $(p_A - p_B)_{II}/(p_A - p_B)_I = 2^{5/8}$

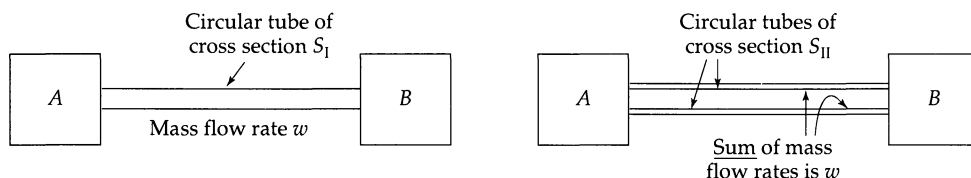


Fig. 7B.4. Flow between two tanks.

7B.5 Revised design of an air duct (Fig. 7B.5). A straight, horizontal air duct was to be installed in a factory. The duct was supposed to be 4 ft \times 4 ft in cross section. Because of an obstruction, the duct may be only 2 ft high, but it may have any width. How wide should the duct be to have the same terminal pressures and same volume rate of flow? Assume that the flow is turbulent and that the Blasius formula (Eq. 6.2-12) is satisfactory for this calculation. Air can be regarded as incompressible in this situation.

- (a) Write the simplified versions of the mechanical energy balance for ducts I and II.
- (b) Equate the pressure drops for the two ducts and obtain an equation relating the widths and heights of the two ducts.

(c) Solve the equation in (b) numerically to find the width that should be used for duct II.

Answer: (c) 9.2 ft

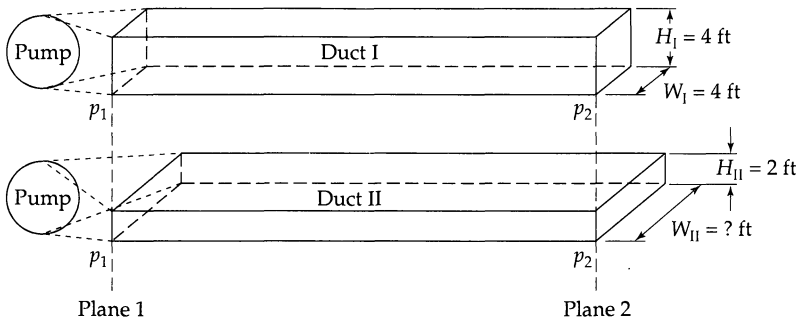


Fig. 7B.5. Installation of an air duct.

- 7B.6** **Multiple discharge into a common conduit**² (Fig. 7B.6). Extend Example 7.6-1 to an incompressible fluid discharging from several tubes into a larger tube with a net increase in cross section. Such systems are important in heat exchangers of certain types, for which the expansion and contraction losses account for an appreciable fraction of the overall pressure drop. The flows in the small tubes and the large tube may be laminar or turbulent. Analyze this system by means of the macroscopic mass, momentum, and mechanical energy balances.

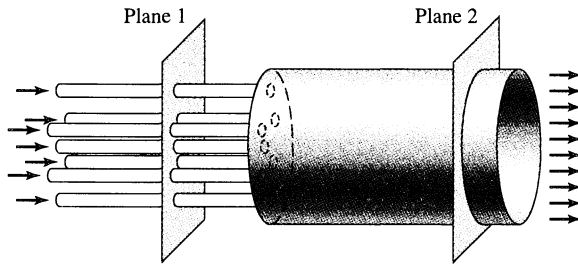


Fig. 7B.6. Multiple discharge into a common conduit. The total cross sectional area at plane 1 available for flow is S_1 and that at plane 2 is S_2 .

- 7B.7** **Inventory variations in a gas reservoir.** A natural gas reservoir is to be supplied from a pipeline at a steady rate of w_1 lb_m/hr. During a 24-hour period, the fuel demand from the reservoir, w_2 , varies approximately as follows,

$$w_2 = A + B \cos \omega t \quad (7B.7-1)$$

where ωt is a dimensionless time measured from the time of peak demand (approximately 6 A.M.).

- (a) Determine the maximum, minimum, and average values of w_2 for a 24-hour period in terms of A and B .
- (b) Determine the required value of w_1 in terms of A and B .
- (c) Let $m_{\text{tot}} = m_{\text{tot}}^0$ at $t = 0$, and integrate the unsteady mass balance with this initial condition to obtain m_{tot} as a function of time.
- (d) If $A = 5000$ lb_m/hr, $B = 2000$ lb_m/hr, and $\rho = 0.044$ lb_m/ft³ in the reservoir, determine the absolute minimum reservoir capacity in cubic feet to meet the demand without interruption. At what time of day must the reservoir be full to permit such operation?
- (e) Determine the minimum reservoir capacity in cubic feet required to permit maintaining at least a three-day reserve at all times.

Answer: 3.47×10^5 ft³; 8.53×10^6 ft³

² W. M. Kays, *Trans. ASME*, **72**, 1067–1074 (1950).

7B.8 Change in liquid height with time (Fig. 7.1-1).

- (a) Derive Eq. 7.1-4 by using integral calculus.
 (b) In Example 7.1-1, obtain the expression for the liquid height h as a function of time t .
 (c) Make a graph of Eq. 7.1-8 using dimensionless quantities. Is this useful?

7B.9 Draining of a cylindrical tank with exit pipe (Fig. 7B.9).

- (a) Rework Example 7.1-1, but with a cylindrical tank instead of a spherical tank. Use the quasi-steady-state approach; that is, use the unsteady-state mass balance along with the Hagen-Poiseuille equation for the laminar flow in the pipe.
 (b) Rework the problem for turbulent flow in the pipe.

Answer: (a) $t_{\text{efflux}} = \frac{128\mu LR^2}{\rho g D^4} \ln \left(1 + \frac{H}{L} \right)$

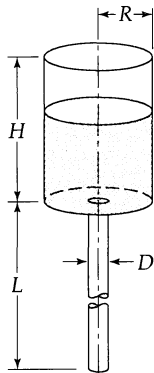


Fig. 7B.9. A cylindrical tank with a long pipe attached. The fluid surface and pipe exit are open to the atmosphere.

7B.10 Efflux time for draining a conical tank (Fig. 7B.10). A conical tank, with dimensions given in the figure, is initially filled with a liquid. The liquid is allowed to drain out by gravity. Determine the efflux time. In parts (a)–(c) take the liquid in the cone to be the “system.”

- (a) First use an unsteady macroscopic mass balance to show that the exit velocity is

$$v_2 = -\frac{z^2}{z_2^2} \frac{dz}{dt} \quad (7B.10-1)$$

- (b) Write the unsteady-state mechanical energy balance for the system. Discard the viscous loss term and the term containing the time derivative of the kinetic energy, and give reasons for doing so. Show that this leads to

$$v_2 = \sqrt{2g(z - z_2)} \quad (7B.10-2)$$

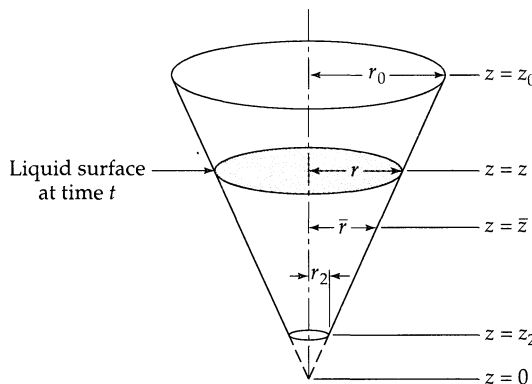


Fig. 7B.10. A conical container from which a fluid is allowed to drain. The quantity r is the radius of the liquid surface at height z , and \bar{r} is the radius of the cone at some arbitrary height \bar{z} .

- (c) Combine the results of (a) and (b). Solve the resulting differential equation with an appropriate initial condition to get the liquid level z as a function of t . From this get the efflux time

$$t_{\text{efflux}} = \frac{1}{5} \left(\frac{z_0}{z_2} \right)^2 \sqrt{\frac{2z_0}{g}} \quad (7B.10-3)$$

List all the assumptions that have been made and discuss how serious they are. How could these assumptions be avoided?

- (d) Rework part (b) by choosing plane 1 to be stationary and slightly below the liquid surface at time t . It is understood that the liquid surface does not go below plane 1 during the differential time interval dt over which the unsteady mechanical energy balance is made. With this choice of plane 1 the derivative $d\Phi_{\text{tot}}/dt$ is zero and there is no work term W_m . Furthermore the conditions at plane 1 are very nearly those at the liquid surface. Then with the pseudo-steady-state approximation that the derivative dK_{tot}/dt is approximately zero and the neglect of the viscous loss term, the mechanical energy balance, with $w_1 = w_2$, takes the form

$$0 = \frac{1}{2}(v_1^2 - v_2^2) + g(h_1 - h_2) \quad (7B.10-4)$$

- 7B.11 Disintegration of wood chips** (Fig. 7B.11). In the manufacture of paper pulp the cellulose fibers of wood chips are freed from the lignin binder by heating in alkaline solutions under pressure in large cylindrical tanks called digesters. At the end of the "cooking" period, a small port in one end of the digester is opened, and the slurry of softened wood chips is allowed to blow against an impact plate to complete the breakup of the chips and the separation of the fibers. Estimate the velocity of the discharging stream and the additional force on the impact plate shortly after the discharge begins. Frictional effects inside the digester, and the small kinetic energy of the fluid inside the tank, may be neglected. (Note: See Problem 7B.10 for two different methods for selecting the entrance and exit planes.)

Answer: 2810 lb_m/s (or 1275 kg/s); 10,900 lb_f (or 48,500 N)

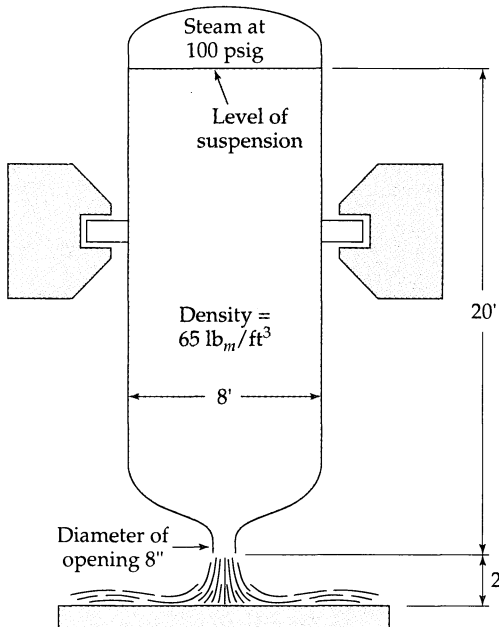


Fig. 7B.11. Pulp digester.

- 7B.12 Criterion for Vapor-Free Flow in a Pipeline.** To ensure that a pipeline is completely liquid-filled, it is necessary that $p > p_{\text{vap}}$ at every point. Apply this criterion to the system in Fig. 7.5-1, by using mechanical energy balances over appropriate portions of the system.

7C.1 End corrections in tube viscometers (Fig. 7C.1).³ In analyzing tube-flow viscometric data to determine viscosity, one compares pressure drop versus flow rate data with the theoretical expression (the Hagen–Poiseuille equation of Eq. 2.3-21). The latter assumes that the flow is fully developed in the region between the two planes at which the pressure is measured. In an apparatus such as that shown in the figure, the pressure is known at the tube exit (2) and also above the fluid in the reservoir (1). However, in the entrance region of the tube, the velocity profiles are not yet fully developed. Hence the theoretical expression relating the pressure drop to the flow rate is not valid.

There is, however, a method in which the Hagen–Poiseuille equation can be used, by making flow measurements in two tubes of different lengths, L_A and L_B ; the shorter of the two tubes must be long enough so that the velocity profiles are fully developed at the exit. Then the end section of the long tube, of length $L_B - L_A$, will be a region of fully developed flow. If we knew the value of $\mathcal{P}_0 - \mathcal{P}_4$ for this region, then we could apply the Hagen–Poiseuille equation.

Show that proper combination of the mechanical energy balances, written for the systems 1–2, 3–4, and 0–4 gives the following expression for $\mathcal{P}_0 - \mathcal{P}_4$ when each viscometer has the *same flow rate*.

$$\frac{\mathcal{P}_0 - \mathcal{P}_4}{L_B - L_A} = \frac{p_B - p_A}{L_B - L_A} + \rho g \left(1 + \frac{L_B - L_A}{L_B - L_A} \right) \quad (7C.1-1)$$

where $\mathcal{P}_0 = p_0 + \rho g z_0$. Explain carefully how you would use Eq. 7C.1-1 to analyze experimental measurements. Is Eq. 7C.1-1 valid for ducts with noncircular, uniform cross section?

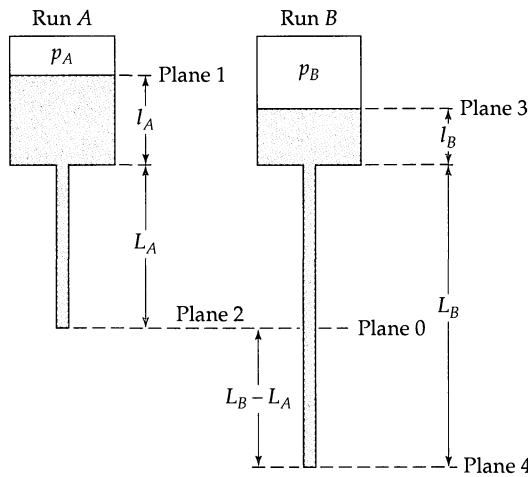


Fig. 7C.1. Two tube viscometers with the same flow rate and the same exit pressure. The pressures p_A and p_B are maintained by an inert gas.

7D.1 Derivation of the macroscopic balances from the equations of change. Derive the macroscopic mass and momentum balances by integrating the equations of continuity and motion over the flow system of Fig. 7.0-1. Follow the procedure given in §7.8 for the macroscopic mechanical energy balance, using the Gauss divergence theorem and the Leibniz formula.

³ A. G. Fredrickson, PhD Thesis, University of Wisconsin (1959); *Principles and Applications of Rheology*, Prentice-Hall, Englewood Cliffs, N.J. (1964), §9.2.

Chapter 8

Polymeric Liquids

- §8.1 Examples of the behavior of polymeric liquids
- §8.2 Rheometry and material functions
- §8.3 Non-Newtonian viscosity and the generalized Newtonian models
- §8.4^O Elasticity and the linear viscoelastic models
- §8.5[•] The corotational derivatives and the nonlinear viscoelastic models
- §8.6[•] Molecular theories for polymeric liquids

In the first seven chapters we have considered only *Newtonian fluids*. The relations between stresses and velocity gradients are described by Eq. 1.1-2 for simple shear flow and by Eq. 1.2-6 (or Eq. 1.2-7) for arbitrary time-dependent flows. For the Newtonian fluid, two material parameters are needed—the two coefficients of viscosity μ and κ —which depend on temperature, pressure, and composition, but not on the velocity gradients. All gases and all liquids composed of “small” molecules (up to molecular weights of about 5000) are accurately described by the Newtonian fluid model.

There are many fluids that are not described by Eq. 1.2-6, and these are called *non-Newtonian fluids*. These structurally complex fluids include polymer solutions, polymer melts, soap solutions, suspensions, emulsions, pastes, and some biological fluids. In this chapter we focus on polymeric liquids.

Because they contain high-molecular-weight molecules with many internal degrees of freedom, polymer solutions and molten polymers have behavior qualitatively different from that of Newtonian fluids. Their viscosities depend strongly on the velocity gradients, and in addition they may display pronounced “elastic effects.” Also in the steady simple shear flow between two parallel plates, there are nonzero and unequal normal stresses (τ_{xx} , τ_{yy} , and τ_{zz}) that do not arise in Newtonian fluids. In §8.1 we describe some experiments that emphasize the differences between Newtonian and polymeric fluids.

In dealing with Newtonian fluids the science of the measurement of viscosity is called *viscometry*, and in earlier chapters we have seen examples of simple flow systems that can be used as *viscometers* (the circular tube, the cone–plate system, and coaxial cylinders). To characterize non-Newtonian fluids we have to measure not only the viscosity, but the normal stresses and the viscoelastic responses as well. The science of measurement of these properties is called *rheometry*, and the instruments are called *rheometers*. We treat this subject briefly in §8.2. The science of *rheology* includes all aspects of the study of deformation and flow of non-Hookean solids and non-Newtonian liquids.

After the first two sections, which deal with experimental facts, we turn to the presentation of various non-Newtonian “models” (that is, empirical expressions for the stress tensor) that are commonly used for describing polymeric liquids. In §8.3 we start with the *generalized Newtonian models*, which are relatively simple, but which can describe only the non-Newtonian viscosity (and not the viscoelastic effects). Then in §8.4 we give examples of *linear viscoelastic models*, which can describe the viscoelastic responses, but

only in flows with exceedingly small displacement gradients. Next in §8.5 we give several *nonlinear viscoelastic models*, and these are intended to be applicable in all flow situations. As we go from elementary to more complicated models, we enlarge the set of observed phenomena that we can describe (but also the mathematical difficulties). Finally in §8.6 there is a brief discussion about the kinetic theory approach to polymer fluid dynamics.

Polymeric liquids are encountered in the fabrication of plastic objects, and as additives to lubricants, foodstuffs, and inks. They represent a vast and important class of liquids, and many scientists and engineers must deal with them. Polymer fluid dynamics, heat transfer, and diffusion form a rapidly growing part of the subject of transport phenomena, and there are many textbooks,¹ treatises,² and journals devoted to the subject. The subject has also been approached from the kinetic theory standpoint, and molecular theories of the subject have contributed much to our understanding of the mechanical, thermal, and diffusional behavior of these fluids.³ Finally, for those interested in the history of the subject, the reader is referred to the book by Tanner and Walters.⁴

§8.1 EXAMPLES OF THE BEHAVIOR OF POLYMERIC LIQUIDS

In this section we discuss several experiments that contrast the flow behavior of Newtonian and polymeric fluids.¹

Steady-State Laminar Flow in Circular Tubes

Even for the steady-state, axial, laminar flow in circular tubes, there is an important difference between the behavior of Newtonian liquids and that of polymeric liquids. For Newtonian liquids the velocity distribution, average velocity, and pressure drop are given by Eqs. 2.3-18, 2.3-20, and 2.3-21, respectively.

For polymeric liquids, experimental data suggest that the following equations are reasonable:

$$\frac{v_z}{v_{z,\max}} \approx 1 - \left(\frac{r}{R}\right)^{(1/n)+1} \quad \text{and} \quad \frac{\langle v_z \rangle}{v_{z,\max}} \approx \frac{(1/n) + 1}{(1/n) + 3} \quad (8.1-1, 2)$$

where n is a positive parameter characterizing the fluid, usually with a value less than unity. That is, the velocity profile is more blunt than it is for the Newtonian fluid, for which $n = 1$. It is further found experimentally that

$$\mathcal{P}_0 - \mathcal{P}_L \sim w^n \quad (8.1-3)$$

The pressure drop thus increases much less rapidly with the mass flow rate than for Newtonian fluids, for which the relation is linear.

¹ A. S. Lodge, *Elastic Liquids*, Academic Press, New York (1964); R. B. Bird, R. C. Armstrong, and O. Hassager, *Dynamics of Polymeric Liquids*, Vol. 1., *Fluid Mechanics*, Wiley-Interscience, New York, 2nd edition (1987); R. I. Tanner, *Engineering Rheology*, Clarendon Press, Oxford (1985).

² H. A. Barnes, J. F. Hutton, and K. Walters, *An Introduction to Rheology*, Elsevier, Amsterdam (1989); H. Giesekus, *Phänomenologische Rheologie: Eine Einführung*, Springer Verlag, Berlin (1994). Books emphasizing the engineering aspects of the subject include Z. Tadmor and C. G. Gogos, *Principles of Polymer Processing*, Wiley, New York (1979), D. G. Baird and D. I. Collias, *Polymer Processing: Principles and Design*, Butterworth-Heinemann, Boston (1995), J. Dealy and K. Wissbrun, *Melt Rheology and its Role in Plastics Processing*, Van Nostrand Reinhold, New York (1990).

³ R. B. Bird, C. F. Curtiss, R. C. Armstrong, and O. Hassager, *Dynamics of Polymeric Liquids*, Vol. 2, *Kinetic Theory*, Wiley-Interscience, New York, 2nd edition (1987); C. F. Curtiss and R. B. Bird, *Adv. Polymer Sci.*, **125**, 1-101 (1996) and *J. Chem. Phys.*, **111**, 10362-10370 (1999).

⁴ R. I. Tanner and K. Walters, *Rheology: An Historical Perspective*, Elsevier, Amsterdam (1998).

¹ More details about these and other experiments can be found in R. B. Bird, R. C. Armstrong, and O. Hassager, *Dynamics of Polymeric Liquids*, Vol. 1, *Fluid Dynamics*, Wiley-Interscience, New York, 2nd edition (1987), Chapter 2. See also A. S. Lodge, *Elastic Liquids*, Academic Press, New York (1964), Chapter 10.

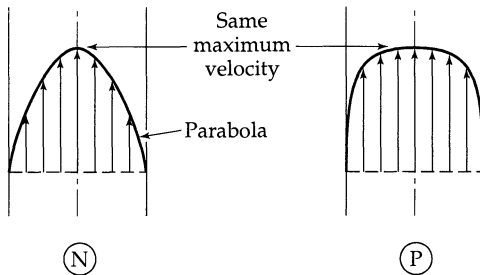


Fig. 8.1-1. Laminar flow in a circular tube. The symbols \textcircled{N} (Newtonian liquid) and \textcircled{P} (Polymeric liquid) are used in this and the next six figures.

In Fig. 8.1-1 we show typical velocity profiles for laminar flow of Newtonian and polymeric fluids for the same maximum velocity. This simple experiment suggests that the polymeric fluids have a viscosity that depends on the velocity gradient. This point will be elaborated on in §8.3.

For laminar flow in tubes of noncircular cross section, polymeric liquids exhibit secondary flows superposed on the axial motion. Recall that for turbulent Newtonian flows secondary flows are also observed—in Fig. 5.1-2 it is shown that the fluid moves toward the corners of the conduit and then back in toward the center. For laminar flow of polymeric fluids, the secondary flows go in the opposite direction—from the corners of the conduit and then back toward the walls.² In turbulent flows the secondary flows result from inertial effects, whereas in the flow of polymers the secondary flows are associated with the “normal stresses.”

Recoil after Cessation of Steady-State Flow in a Circular Tube

We start with a fluid at rest in a circular tube and, with a syringe, we “draw” a dye line radially in the fluid as shown in Fig. 8.1-2. Then we pump the fluid and watch the dye deform.³

For a Newtonian fluid the dye line deforms into a continuously stretching parabola. If the pump is turned off, the dye parabola stops moving. After some time diffusion occurs and the parabola begins to get fuzzy, of course.

For a *Polymeric liquid* the dye line deforms into a curve that is more blunt than a parabola (see Eq. 8.1-1). If the pump is stopped and the fluid is not axially constrained, the fluid will begin to “recoil” and will retreat from this maximum stretched shape; that

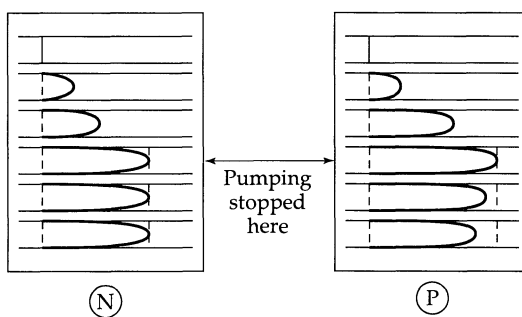


Fig. 8.1-2. Constrained recoil after cessation of flow in a circular tube, observed in polymeric liquids, but not in Newtonian liquids.

² B. Gervang and P. S. Larsen, *J. Non-Newtonian Fluid Mech.*, **39**, 217–237 (1991).

³ For the details of this experiment see N. N. Kapoor, M.S. thesis, University of Minnesota, Minneapolis (1964), as well as A. G. Fredrickson, *Principles and Applications of Rheology*, Prentice-Hall, Englewood Cliffs, N.J. (1964), p. 120.

is, the fluid snaps back somewhat like a rubber band. However, whereas a rubber band returns to its original shape, the fluid retreats only part way toward its original configuration.

If we permit ourselves an anthropomorphism, we can say that a rubber band has "perfect memory," since it returns to its initial unstressed state. The polymeric fluid, on the other hand, has a "fading memory," since it gradually "forgets" its original state. That is, as it recoils, its memory becomes weaker and weaker.

Fluid recoil is a manifestation of *elasticity*, and any complete description of polymeric fluids must be able to incorporate the idea of elasticity into the expression for the stress tensor. The theory must also include the notion of fading memory.

"Normal Stress" Effects

Other striking differences in the behavior of Newtonian and polymeric liquids appear in the "normal stress" effects. The reason for this nomenclature will be given in the next section.

A rotating rod in a beaker of a Newtonian fluid causes the fluid to undergo a tangential motion. At steady state, the fluid surface is lower near the rotating rod. Intuitively we know that this comes about because the centrifugal force causes the fluid to move radially toward the beaker wall. For a *polymeric liquid*, on the other hand, the fluid moves toward the rotating rod, and, at steady state, the fluid surface is as shown in Fig. 8.1-3. This phenomenon is called the *Weissenberg rod-climbing effect*.⁴ Evidently some kinds of forces are induced that cause the polymeric liquid to behave in a way that is qualitatively different from that of a Newtonian liquid.

In a closely related experiment, we can put a rotating disk on the surface of a fluid in a cylindrical container as shown in Fig. 8.1-4. If the fluid is Newtonian, the rotating disk causes the fluid to move in a tangential direction (the "primary flow"), but, in addition, the fluid moves slowly outward toward the cylinder wall because of the centrifugal force, then moves downward, and then back up along the cylinder axis. This superposed radial and axial flow is weaker than the primary flow and is termed a "secondary flow." For a *polymeric liquid*, the fluid also develops a primary tangential flow with a weak ra-

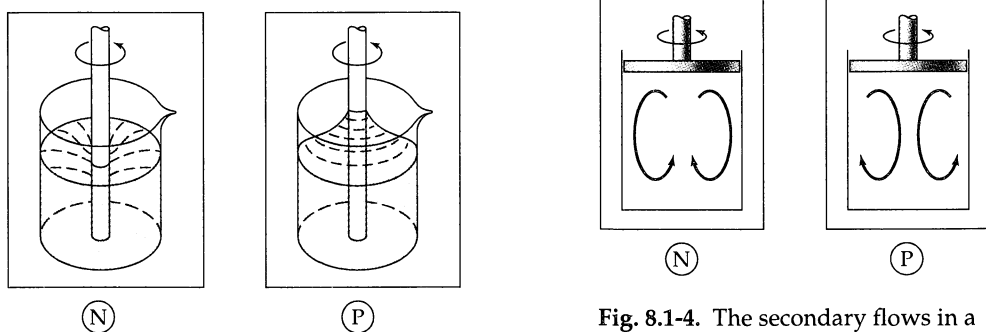


Fig. 8.1-3. The free surface of a liquid near a rotating rod. The polymeric liquid shows the Weissenberg rod-climbing effect.

Fig. 8.1-4. The secondary flows in a cylindrical container with a rotating disk at the liquid surface have the opposite directions for Newtonian and polymeric fluids.

⁴ This phenomenon was first described by F. H. Garner and A. H. Nissan, *Nature*, **158**, 634–635 (1946) and by R. J. Russel, Ph.D. thesis, Imperial College, University of London (1946), p. 58. The experiment was analyzed by K. Weissenberg, *Nature*, **159**, 310–311 (1947).

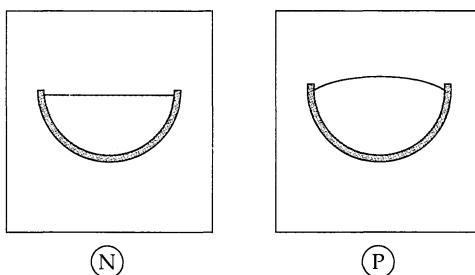


Fig. 8.1-5. Flow down a tilted semicylindrical trough. The convexity of the polymeric liquid surface is somewhat exaggerated here.

dial and axial secondary flow, but the latter goes in a direction opposite to that seen in the Newtonian fluid.⁵

In another experiment we can let a liquid flow down a tilted, semi-cylindrical trough as shown in Fig. 8.1-5. If the fluid is Newtonian, the liquid surface is flat, except for the meniscus effects at the outer edges. For most *Polymeric liquids*, however, the liquid surface is found to be slightly convex. The effect is small but reproducible.⁶

Some Other Experiments

The operation of a simple siphon is familiar to everyone. We know from experience that, if the fluid is Newtonian, the removal of the siphon tube from the liquid means that the siphoning action ceases. However, as may be seen in Fig. 8.1-6, for polymeric liquids the siphoning can continue even when the siphon is lifted several centimeters above the liquid surface. This is called the *tubeless siphon* effect. One can also just lift some of the fluid up over the edge of the beaker and then the fluid will flow upward along the inside of the beaker and then down the outside until the beaker is nearly empty.⁷

In another experiment a long cylindrical rod, with its axis in the z direction, is made to oscillate back and forth in the x direction with the axis parallel to the z axis (see Fig.

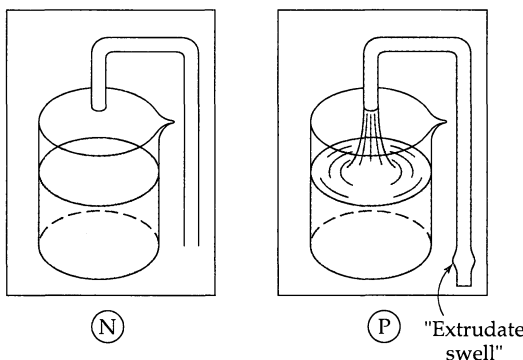


Fig. 8.1-6. Siphoning continues to occur when the tube is raised above the surface of a polymeric liquid, but not so for a Newtonian liquid. Note the swelling of the polymeric liquid as it leaves the siphon tube.

⁵ C. T. Hill, J. D. Huppler, and R. B. Bird, *Chem. Eng. Sci.* **21**, 815–817 (1966); C. T. Hill, *Trans. Soc. Rheol.*, **16**, 213–245 (1972). Theoretical analyses have been given by J. M. Kramer and M. W. Johnson, Jr., *Trans. Soc. Rheol.* **16**, 197–212 (1972), and by J. P. Nirschl and W. E. Stewart, *J. Non-Newtonian Fluid Mech.*, **16**, 233–250 (1984).

⁶ This experiment was first done by R. I. Tanner, *Trans. Soc. Rheol.*, **14**, 483–507 (1970), prompted by a suggestion by A. S. Wineman and A. C. Pipkin, *Acta Mech.* **2**, 104–115 (1966). See also R. I. Tanner, *Engineering Rheology*, Oxford University Press (1985), 102–105.

⁷ D. F. James, *Nature*, **212**, 754–756 (1966).

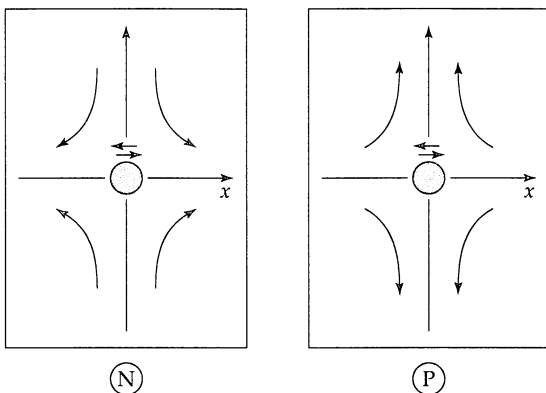


Fig. 8.1-7. The “acoustical streaming” near a laterally oscillating rod, showing that the induced secondary flow goes in the opposite directions for Newtonian and polymeric fluids.

8.1-7). In a Newtonian fluid, a secondary flow is induced whereby the fluid moves toward the cylinder from above and below (i.e., from the $+y$ and $-y$ directions, and moves away to the left and right (i.e., toward the $-x$ and $+x$ direction). For the *Polymeric liquid*, however, the induced secondary motion is in the opposite direction: the fluid moves inward from the left and right along the x axis and outward in the up and down directions along the y axis.⁸

The preceding examples are only a few of many interesting experiments that have been performed.⁹ The polymeric behavior can be illustrated easily and inexpensively with a 0.5% aqueous solution of polyethylene oxide.

There are also some fascinating effects that occur when even tiny quantities of polymers are present. The most striking of these is the phenomenon of *drag reduction*.¹⁰ With only parts per million of some polymers (“drag-reducing agents”), the friction loss in turbulent pipe flow may be lowered dramatically—by 30–50%. Such polymeric drag-reducing agents are used by fire departments to increase the flow of water, and by oil companies to lower the costs for pumping crude oil over long distances.

For discussions of other phenomena that arise in polymeric fluids, the reader should consult the summary articles in *Annual Review of Fluid Mechanics*.¹¹

§8.2 RHEOMETRY AND MATERIAL FUNCTIONS

The experiments described in §8.1 make it abundantly clear that polymeric liquids do not obey Newton’s law of viscosity. In this section we discuss several simple, controllable flows in which the stress components can be measured. From these experiments one can measure a number of *material functions* that describe the mechanical response of complex fluids. Whereas incompressible Newtonian fluids are described by only one material constant (the viscosity), one can measure many different material functions for non-Newtonian liquids. Here we show how a few of the more commonly used material

⁸ C. F. Chang and W. R. Schowalter, *J. Non-Newtonian Fluid Mech.*, **6**, 47–67 (1979).

⁹ The book by D. V. Boger and K. Walters, *Rheological Phenomena in Focus*, Elsevier, Amsterdam (1993), contains many photographs of fluid behavior in a variety of non-Newtonian flow systems.

¹⁰ This is sometimes called the *Toms phenomenon*, since it was perhaps first reported in B. A. Toms, *Proc. Int. Congress on Rheology*, North-Holland, Amsterdam (1949). The phenomenon has also been studied in connection with the drag-reducing nature of fish slime [T. L. Daniel, *Biol. Bull.*, **160**, 376–382 (1981)], which is thought to explain, at least in part, “Gray’s paradox”—the fact that fish seem to be able to swim faster than energy considerations permit.

¹¹ For example, M. M. Denn, *Ann. Rev. Fluid Mech.*, **22**, 13–34 (1990); E. S. G. Shaqfeh, *Ann. Rev. Fluid Mech.*, **28**, 129–185 (1996); G. G. Fuller, *Ann. Rev. Fluid Mech.*, **22**, 387–417 (1992).

functions are defined and measured. Information about the actual measurement equipment and other material functions can be found elsewhere.^{1,2} It is assumed throughout this chapter that the polymeric liquids can be regarded as incompressible.

Steady Simple Shear Flow

We consider now the steady shear flow between a pair of parallel plates, where the velocity profile is given by $v_x = \dot{\gamma}y$, the other velocity components being zero (see Fig. 8.2-1). The quantity $\dot{\gamma}$, here taken to be positive, is called the "shear rate." For a Newtonian fluid the shear stress τ_{yx} is given by Eq. 1.1-2, and the normal stresses (τ_{xx} , τ_{yy} , and τ_{zz}) are all zero.

For incompressible non-Newtonian fluids, the normal stresses are nonzero and unequal. For these fluids it is conventional to define three material functions as follows:

$$\tau_{yx} = -\eta \frac{dv_x}{dy} \quad (8.2-1)$$

$$\tau_{xx} - \tau_{yy} = -\Psi_1 \left(\frac{dv_x}{dy} \right)^2 \quad (8.2-2)$$

$$\tau_{yy} - \tau_{zz} = -\Psi_2 \left(\frac{dv_x}{dy} \right)^2 \quad (8.2-3)$$

in which η is the non-Newtonian viscosity, Ψ_1 is the first normal stress coefficient, and Ψ_2 is the second normal stress coefficient. These three quantities— η , Ψ_1 , Ψ_2 —are all functions of the shear rate $\dot{\gamma}$. For many polymeric liquids η may decrease by a factor of as much as 10^4 as the shear rate increases. Similarly, the normal stress coefficients may decrease by a factor of as much as 10^7 over the usual range of shear rates. For polymeric fluids made up of flexible macromolecules, the functions $\eta(\dot{\gamma})$ and $\Psi_1(\dot{\gamma})$ have been found experimentally to be positive, whereas $\Psi_2(\dot{\gamma})$ is almost always negative. It can be shown that for positive $\Psi_1(\dot{\gamma})$ the fluid behaves as though it were under tension in the flow (or x) direction, and that the negative $\Psi_2(\dot{\gamma})$ means that the fluid is under tension in the transverse (or z) direction. For the Newtonian fluid $\eta = \mu$, $\Psi_1 = 0$, and $\Psi_2 = 0$.

The strongly shear-rate-dependent non-Newtonian viscosity is connected with the behavior given in Eqs. 8.1-1 to 3, as is shown in the next section. The positive Ψ_1 is primarily responsible for the Weissenberg rod-climbing effect. Because of the tangential flow, there is a tension in the tangential direction, and this tension pulls the fluid toward the rotating rod, overcoming the centrifugal force. The secondary flows in the disk-and-cylinder experiment (Fig. 8.1-4) can also be explained qualitatively in terms of the positive Ψ_1 . Also, the negative Ψ_2 can be shown to explain the convex surface shape in the tilted-trough experiment (Fig. 8.1-5).

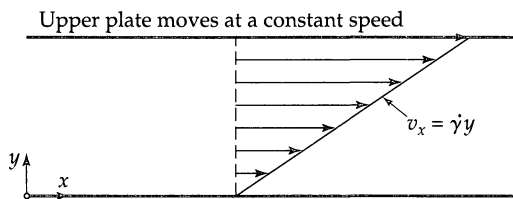


Fig. 8.2-1. Steady simple shear flow between parallel plates, with shear rate $\dot{\gamma}$. For Newtonian fluids in this flow, $\tau_{xx} = \tau_{yy} = \tau_{zz} = 0$, but for polymeric fluids the normal stresses are in general nonzero and unequal.

¹ J. R. Van Wazer, J. W. Lyons, K. Y. Kim, and R. E. Colwell, *Viscosity and Flow Measurement*, Interscience (Wiley), New York (1963).

² K. Walters, *Rheometry*, Wiley, New York (1975).

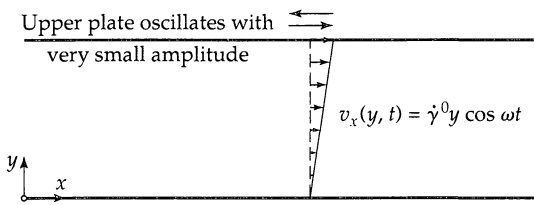


Fig. 8.2-2. Small-amplitude oscillatory motion. For small plate spacing and highly viscous fluids, the velocity profile may be assumed to be linear.

Many ingenious devices have been developed to measure the three material functions for steady shearing flow, and the theories needed for the use of the instruments are explained in detail elsewhere.² See Problem 8C.1 for the use of the cone-and-plate instrument for measuring the material functions.

Small-Amplitude Oscillatory Motion

A standard method for measuring the elastic response of a fluid is the small-amplitude oscillatory shear experiment, depicted in Fig. 8.2-2. Here the top plate moves back and forth in sinusoidal fashion, and with a tiny amplitude. If the plate spacing is extremely small and the fluid has a very high viscosity, then the velocity profile will be nearly linear, so that $v_x(y, t) = \dot{\gamma}^0 y \cos \omega t$, in which $\dot{\gamma}^0$, a real quantity, gives the amplitude of the shear rate excursion.

The shear stress required to maintain the oscillatory motion will also be periodic in time and, in general, of the form

$$\tau_{yx} = -\eta' \dot{\gamma}^0 \cos \omega t - \eta'' \dot{\gamma}^0 \sin \omega t \quad (8.2-4)$$

in which η' and η'' are the components of the *complex viscosity*, $\eta^* = \eta' - i\eta''$, which is a function of the frequency. The first (in-phase) term is the "viscous response," and the second (out-of-phase) term is the "elastic response." Polymer chemists use the curves of $\eta'(\omega)$ and $\eta''(\omega)$ (or the storage and loss moduli, $G' = \eta''\omega$ and $G'' = \eta'\omega$) for "characterizing" polymers, since much is known about the connection between the shapes of these curves and the chemical structure.³ For the Newtonian fluid, $\eta' = \mu$ and $\eta'' = 0$.

Steady-State Elongational Flow

A third experiment that can be performed involves the stretching of the fluid, in which the velocity distribution is given by $v_z = \dot{\varepsilon}z$, $v_x = -\frac{1}{2}\dot{\varepsilon}x$, and $v_y = -\frac{1}{2}\dot{\varepsilon}y$ (see Fig. 8.2-3), where the positive quantity $\dot{\varepsilon}$ is called the "elongation rate." Then the relation

$$\tau_{zz} - \tau_{xx} = -\bar{\eta} \frac{dv_z}{dz} \quad (8.2-5)$$

defines the *elongational viscosity* $\bar{\eta}$, which depends on $\dot{\varepsilon}$. When $\dot{\varepsilon}$ is negative, the flow is referred to as *biaxial stretching*. For the Newtonian fluid it can be shown that $\bar{\eta} = 3\mu$, and this is sometimes called the "Trouton viscosity."

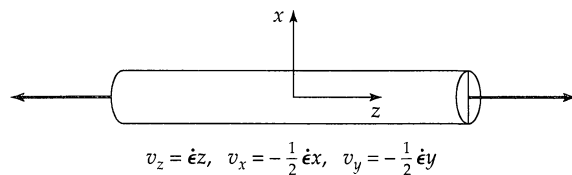


Fig. 8.2-3. Steady elongational flow with elongation rate $\dot{\varepsilon} = dv_z/dz$.

³ J. D. Ferry, *Viscoelastic Properties of Polymers*, Wiley, New York, 3rd edition (1980).

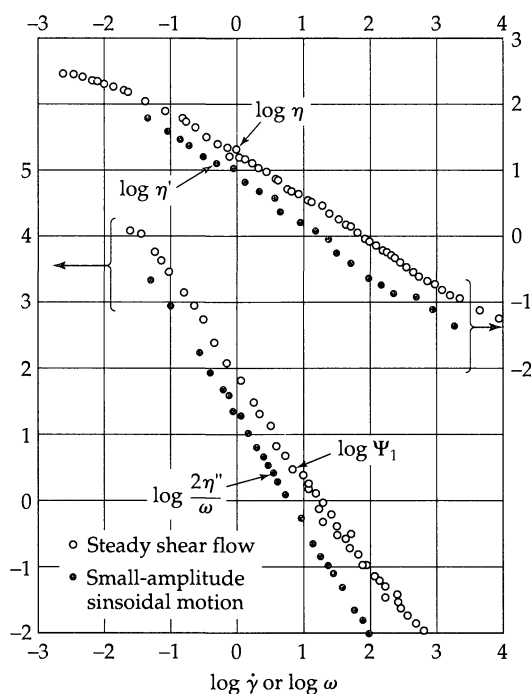


Fig. 8.2-4. The material functions $\eta(\dot{\gamma})$, $\Psi_1(\dot{\gamma})$, $\eta'(\omega)$, and $\eta''(\omega)$ for a 1.5% polyacrylamide solution in a 50/50 mixture of water and glycerin. The quantities η , η' , and η'' are given in $\text{Pa} \cdot \text{s}$, and Ψ_1 in $\text{Pa} \cdot \text{s}^2$. Both $\dot{\gamma}$ and ω are given in s^{-1} . The data are from J. D. Huppner, E. Ashare, and L. Holmes, *Trans. Soc. Rheol.*, **11**, 159–179 (1967), as replotted by J. M. Wiest. The oscillatory normal stresses have also been studied experimentally and theoretically (see M. C. Williams and R. B. Bird, *Ind. Eng. Chem. Fundam.*, **3**, 42–48 (1964); M. C. Williams, *J. Chem. Phys.*, **42**, 2988–2989 (1965); E. B. Christiansen and W. R. Leppard, *Trans. Soc. Rheol.*, **18**, 65–86 (1974), in which the ordinate of Fig. 15 should be multiplied by 39.27.

The elongational viscosity $\bar{\eta}$ cannot be measured for all fluids, since a steady-state elongational flow cannot always be attained.⁴

The three experiments described above are only a few of the rheometric tests that can be performed. Other tests include stress relaxation after cessation of flow, stress growth at the inception of flow, recoil, and creep—each of which can be performed in shear, elongation, and other types of flow. Each experiment results in the definition of one or more material functions. These can be used for fluid characterization and also for determining the empirical constants in the models described in §§8.3 to 8.5.

Some sample material functions are displayed in Figs. 8.2-4 to 8.2-6. Since there is a wide range of complex fluids, as regards chemical structure and constitution,

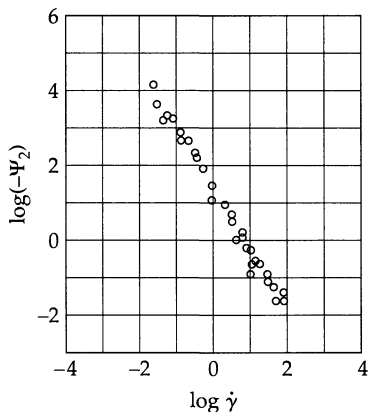


Fig. 8.2-5. Dependence of the second normal stress coefficient on shear rate for a 2.5% solution of polyacrylamide in a 50/50 mixture of water and glycerin. The quantity Ψ_2 is given in $\text{Pa} \cdot \text{s}^2$, and ω is in s^{-1} . The data of E. B. Christiansen and W. R. Leppard, *Trans. Soc. Rheol.*, **18**, 65–86 (1974), have been replotted by J. M. Wiest.

⁴ C. J. S. Petrie, *Elongational Flows*, Pitman, London (1979); J. Meissner, *Chem. Engr. Commun.*, **33**, 159–180 (1985).

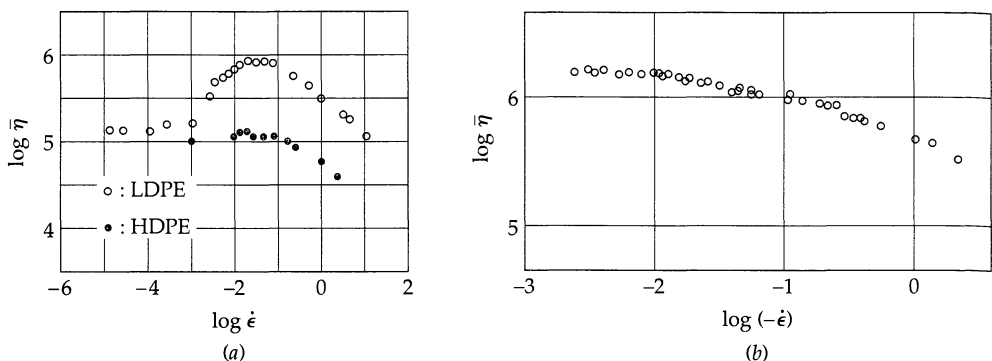


Fig. 8.2-6. (a) Elongational viscosity for uniaxial stretching of low- and high-density polyethylene. [From H. Münstedt and H. M. Laun, *Rheol. Acta*, **20**, 211–221 (1981).] (b) Elongational viscosity for biaxial stretching of low-density polyethylene, deduced from flow-birefringence data. [From J. A. van Aken and H. Janeschitz-Kriegl, *Rheol. Acta*, **20**, 419–432 (1981).] In both graphs the quantity $\bar{\eta}$ is given in $\text{Pa} \cdot \text{s}$ and $\dot{\epsilon}$ is in s^{-1} .

there are many types of mechanical responses in these various experiments. More complete discussions of the data obtained in rheometric experiments are given elsewhere.⁵

§8.3 NON-NEWTONIAN VISCOSITY AND THE GENERALIZED NEWTONIAN MODELS

This is the first of three sections devoted to empirical stress tensor expressions for non-Newtonian fluids. One might say, very roughly, that these three sections satisfy three different groups of people:

- §8.3 The generalized Newtonian models are primarily used to describe steady-state shear flows and have been widely used by *engineers* for designing flow systems.
- §8.4 The linear viscoelastic models are primarily used to describe unsteady-state flows in systems with very small displacement gradients and have been used mainly by *chemists* interested in understanding polymer structure.
- §8.5 The nonlinear viscoelastic models represent an attempt to describe all types of flow (including the two listed above) and have been developed largely by *physicists* and *applied mathematicians* interested in finding an all-inclusive theory.

Actually the three classes of models are interrelated, and each is important for understanding the subject of non-Newtonian flow. In the following discussion of non-Newtonian models, we assume throughout that the fluids are incompressible.

The *generalized Newtonian models*¹ discussed here are the simplest of the three types of models to be discussed. However, they can describe only the non-Newtonian viscosity, and none of the normal stress effects, time-dependent effects, or elastic effects. Nonethe-

⁵ R. B. Bird, R. C. Armstrong, and O. Hassager, *Dynamics of Polymeric Liquids*, Vol. 1, *Fluid Mechanics*, Wiley-Interscience, 2nd edition (1987).

¹ K. Hohenemser and W. Prager, *Zeits. f. Math. u. Mech.*, **12**, 216–226 (1932); J. G. Oldroyd, *Proc. Camb. Phil. Soc.*, **45**, 595–611 (1949), and **47**, 410–418 (1950). James Gardner Oldroyd (1921–1982), a professor at the University of Liverpool, made many contributions to the theory of non-Newtonian fluids, in particular his ideas on the construction of constitutive equations and the principles of continuum mechanics.

less, in many processes in the polymer industry, such as pipe flow with heat transfer, distributor design, extrusion, and injection molding, the non-Newtonian viscosity and its enormous variation with shear rate are central to describing the flows of interest.

For incompressible Newtonian fluids the expression for the stress tensor is given by Eq. 1.2-7 with the last term omitted:

$$\tau = -\mu(\nabla v + (\nabla v)^\dagger) \equiv -\mu\dot{\gamma} \quad (8.3-1)$$

in which we have introduced the symbol $\dot{\gamma} = \nabla v + (\nabla v)^\dagger$, the *rate-of-strain tensor* (or *rate-of-deformation tensor*). The generalized Newtonian fluid model is obtained by simply replacing the constant viscosity μ by the non-Newtonian viscosity η , a function of the shear rate, which in general can be written as the “magnitude of the rate-of-strain tensor” $\dot{\gamma} = \sqrt{\frac{1}{2}(\dot{\gamma}; \dot{\gamma})}$; it is understood that when the square root is taken, the sign must be so chosen that $\dot{\gamma}$ is a positive quantity. Then the generalized Newtonian fluid model is

$$\tau = -\eta(\nabla v + (\nabla v)^\dagger) \equiv -\eta\dot{\gamma} \quad \text{with } \eta = \eta(\dot{\gamma}) \quad (8.3-2)$$

The components of the rate-of-strain tensor $\dot{\gamma}$ can be obtained in Cartesian, cylindrical, and spherical coordinates from the right sides of the equations in Table B.1 by omitting the $(\nabla \cdot v)$ terms as well as the factor $(-\mu)$ in the remaining terms.

We now have to give an empiricism for the non-Newtonian viscosity function $\eta(\dot{\gamma})$. Dozens of such expressions have been proposed, but we mention only two here:

(a) The simplest empiricism for $\eta(\dot{\gamma})$ is the two-parameter *power law* expression:²

$$\eta = m\dot{\gamma}^{n-1} \quad (8.3-3)$$

in which m and n are constants characterizing the fluid. This simple relation describes the non-Newtonian viscosity curve over the linear portion of the log-log plot of the viscosity versus shear rate for many materials (see, for example, the viscosity data in Fig. 8.2-4). The parameter m has units of $\text{Pa} \cdot \text{s}^n$, and $n - 1$ is the slope of the $\log \eta$ vs. $\log \dot{\gamma}$ plot. Some sample values of power law parameters are given in Table 8.3-1.

Although the power law model was proposed as an empirical expression, it will be seen in Eq. 8.6-11 that a simple molecular theory leads to a power law expression for high shear rates, with $n = \frac{1}{3}$.

Table 8.3-1 Power Law Parameters for Aqueous Solutions^a

Solution	Temperature (K)	$m(\text{Pa} \cdot \text{s}^n)$	$n(—)$
2.0% hydroxyethylcellulose	293	93.5	0.189
	313	59.7	0.223
	333	38.5	0.254
0.5% hydroxyethylcellulose	293	0.84	0.509
	313	0.30	0.595
	333	0.136	0.645
1.0% polyethylene oxide	293	0.994	0.532
	313	0.706	0.544
	333	0.486	0.599

^a R. M. Turian, Ph.D. Thesis, University of Wisconsin, Madison (1964), pp. 142–148.

² W. Ostwald, *Kolloid-Zeitschrift*, **36**, 99–117 (1925); A. de Waele, *Oil Color Chem. Assoc. J.*, **6**, 33–88 (1923).

Table 8.3-2 Parameters in the Carreau Model for Some Solutions of Linear Polystyrene in 1-Chloronaphthalene^a

Properties of solution		Parameters in Eq. 8.3-4 (η_∞ is taken to be zero)		
M_w (g/mol)	c (g/ml)	η_0 (Pa · s)	λ (s)	n (---)
3.9×10^5	0.45	8080	1.109	0.304
3.9×10^5	0.30	135	3.61×10^{-2}	0.305
1.1×10^5	0.52	1180	9.24×10^{-2}	0.441
1.1×10^5	0.45	166	1.73×10^{-2}	0.538
3.7×10^4	0.62	3930	1×10^{-1}	0.217

^a Values of the parameters are taken from K. Yasuda, R. C. Armstrong, and R. E. Cohen, *Rheol. Acta*, **20**, 163–178 (1981).

(b) A better curve fit for most data can be obtained by using the four-parameter *Carreau equation*,³ which is

$$\frac{\eta - \eta_\infty}{\eta_0 - \eta_\infty} = [1 + (\lambda \dot{\gamma})^2]^{(n-1)/2} \quad (8.3-4)$$

in which η_0 is the zero shear rate viscosity, η_∞ is the infinite shear rate viscosity, λ is a parameter with units of time, and n is a dimensionless parameter. Some sample parameters for the Carreau model are given in Table 8.3-2.

We now give some examples of how to use the power law model. These are extensions of problems discussed in Chapters 2 and 3 for Newtonian fluids.⁴

EXAMPLE 8.3-1

Laminar Flow of an Incompressible Power Law Fluid in a Circular Tube^{4,5}

Derive the expression for the mass flow rate of a polymer liquid, described by the power law model. The fluid is flowing in a long circular tube of radius R and length L , as a result of a pressure difference, gravity, or both.

SOLUTION

Equation 2.3-13 gives the shear stress distribution for any fluid in developing steady flow in a circular tube. Into this expression we have to insert the shear stress for the power law fluid (instead of using Eq. 2.3-14). This expression may be obtained from Eqs. 8.3-2 and 3 above.

$$\tau_{rz} = -m\dot{\gamma}^{n-1} \frac{dv_z}{dr} \quad (8.3-5)$$

Since v_z is postulated to be a function of r alone, from Eq. B.1-13 we find that $\dot{\gamma} = \sqrt{\frac{1}{2}(\dot{\gamma}:\dot{\gamma})} = \sqrt{(dv_z/dr)^2}$. We have to choose the sign for the square root so that $\dot{\gamma}$ will be positive. Since dv_z/dr is negative in tube flow, we have to choose the minus sign, so that

$$\tau_{rz} = -m \left(-\frac{dv_z}{dr} \right)^{n-1} \frac{dv_z}{dr} = m \left(-\frac{dv_z}{dr} \right)^n \quad (8.3-6)$$

³ P. J. Carreau, Ph.D. thesis, University of Wisconsin, Madison (1968). See also K. Yasuda, R. C. Armstrong, and R. E. Cohen, *Rheol. Acta*, **20**, 163–178 (1981).

⁴ For additional examples, including nonisothermal flows, see R. B. Bird, R. C. Armstrong, and O. Hassager, *Dynamics of Polymeric Liquids*, Vol. 1. *Fluid Mechanics*, Wiley-Interscience, New York, 2nd edition (1998), Chapter 4.

⁵ M. Reiner, *Deformation, Strain and Flow*, Interscience, New York, 2nd edition (1960), pp. 243–245.

Combining Eq. 8.3-6 and 2.3-13 then gives the following differential equation for the velocity:

$$m \left(-\frac{dv_z}{dr} \right)^n = \left(\frac{\mathcal{P}_0 - \mathcal{P}_L}{2L} \right) r \quad (8.3-7)$$

After taking the n th root the equation may be integrated, and when the no-slip boundary condition at $r = R$ is used, we get

$$v_z = \left(\frac{(\mathcal{P}_0 - \mathcal{P}_L)R}{2mL} \right)^{1/n} \frac{R}{(1/n) + 1} \left[1 - \left(\frac{r}{R} \right)^{(1/n)+1} \right] \quad (8.3-8)$$

for the velocity distribution (see Eq. 8.1-1). When this is integrated over the cross section of the circular tube we get

$$w = \frac{\pi R^3 \rho}{(1/n) + 3} \left(\frac{(\mathcal{P}_0 - \mathcal{P}_L)R}{2mL} \right)^{1/n} \quad (8.3-9)$$

which simplifies to the Hagen–Poiseuille law for Newtonian fluids (Eq. 2.3-21) when $n = 1$ and $m = \mu$. Equation 8.3-9 can be used along with data on pressure drop versus flow rate to determine the power law parameters m and n .

EXAMPLE 8.3-2

Flow of a Power Law Fluid in a Narrow Slit⁴

The flow of a Newtonian fluid in a narrow slit is solved in Problem 2B.3. Find the velocity distribution and the mass flow rate for a power law fluid flowing in the slit.

SOLUTION

The expression for the shear stress τ_{xz} as a function of position x in Eq. 2B.3-1 can be taken over here, since it does not depend on the type of fluid. The power law formula for τ_{xz} from Eq. 8.3-3 is

$$\tau_{xz} = m \left(-\frac{dv_z}{dx} \right)^n \quad \text{for } 0 \leq x \leq B \quad (8.3-10)$$

$$\tau_{xz} = -m \left(\frac{dv_z}{dx} \right)^n \quad \text{for } -B \leq x \leq 0 \quad (8.3-11)$$

To get the velocity distribution for $0 \leq x \leq B$, we substitute τ_{xz} from Eq. 8.3-10 into Eq. 2B.3-1 to get:

$$m \left(-\frac{dv_z}{dx} \right)^n = \frac{(\mathcal{P}_0 - \mathcal{P}_L)x}{L} \quad 0 \leq x \leq B \quad (8.3-12)$$

Integrating and using the no-slip boundary condition at $x = B$ gives

$$v_z = \left(\frac{(\mathcal{P}_0 - \mathcal{P}_L)B}{mL} \right)^{1/n} \frac{B}{(1/n) + 1} \left[1 - \left(\frac{x}{B} \right)^{(1/n)+1} \right] \quad 0 \leq x \leq B \quad (8.3-13)$$

Since we expect the velocity profile to be symmetric about the midplane $x = 0$, we can get the mass rate of flow as follows:

$$\begin{aligned} w &= \int_0^W \int_{-B}^B \rho v_z dx dy = 2 \int_0^W \int_0^B \rho v_z dx dy \\ &= 2 \left(\frac{(\mathcal{P}_0 - \mathcal{P}_L)B}{mL} \right)^{1/n} \frac{WB^2 \rho}{(1/n) + 1} \int_0^1 \left[1 - \left(\frac{x}{B} \right)^{(1/n)+1} \right] d\left(\frac{x}{B} \right) \\ &= \frac{2WB^2 \rho}{(1/n) + 2} \left(\frac{(\mathcal{P}_0 - \mathcal{P}_L)B}{mL} \right)^{1/n} \end{aligned} \quad (8.3-14)$$

When $n = 1$ and $m = \mu$, the Newtonian result in Problem 2B.3 is recovered. Experimental data on pressure drop and mass flow rate through a narrow slit can be used with Eq. 8.3-14 to determine the power law parameters.

EXAMPLE 8.3-3

Rework Example 3.6-3 for a power law fluid.

Tangential Annular Flow of a Power Law Fluid^{4,5}

SOLUTION

Equations 3.6-20 and 3.6-22 remain unchanged for a non-Newtonian fluid, but in lieu of Eq. 3.6-21 we write the θ -component of the equation of motion in terms of the shear stress by using Table B.5:

$$0 = -\frac{1}{r^2} \frac{d}{dr} (r^2 \tau_{r\theta}) \quad (8.3-15)$$

For the postulated velocity profile, we get for the power law model (with the help of Table B.1)

$$\begin{aligned} \tau_{r\theta} &= -\eta r \frac{d}{dr} \left(\frac{v_\theta}{r} \right) \\ &= -m \left(r \frac{d}{dr} \left(\frac{v_\theta}{r} \right) \right)^{n-1} r \frac{d}{dr} \left(\frac{v_\theta}{r} \right) \\ &= -m \left(r \frac{d}{dr} \left(\frac{v_\theta}{r} \right) \right)^n \end{aligned} \quad (8.3-16)$$

Combining Eqs. 8.3-15 and 16 we get

$$\frac{d}{dr} \left(r^2 m \left(r \frac{d}{dr} \left(\frac{v_\theta}{r} \right) \right)^n \right) = 0 \quad (8.3-17)$$

Integration gives

$$r^2 \left(r \frac{d}{dr} \left(\frac{v_\theta}{r} \right) \right)^n = C_1 \quad (8.3-18)$$

Dividing by r^2 and taking the n th root gives a first-order differential equation for the angular velocity

$$\frac{d}{dr} \left(\frac{v_\theta}{r} \right) = \frac{1}{r} \left(\frac{C_1}{r^2} \right)^{1/n} \quad (8.3-19)$$

This may be integrated with the boundary conditions in Eqs. 3.6-27 and 28 to give

$$\frac{v_\theta}{\Omega_o r} = \frac{1 - (\kappa R/r)^{2/n}}{1 - \kappa^{2/n}} \quad (8.3-20)$$

The (z-component of the) torque needed on the outer cylinder to maintain the motion is then

$$\begin{aligned} T_z &= (-\tau_{r\theta})|_{r=R} \cdot 2\pi RL \cdot R \\ &= m \left(r \frac{d}{dr} \left(\frac{v_\theta}{r} \right) \right)^n \Big|_{r=R} \cdot 2\pi RL \cdot R \end{aligned} \quad (8.3-21)$$

Combining Eqs. 8.3-20 and 21 then gives

$$T_z = 2\pi m \Omega_o (\kappa R)^2 L \left(\frac{(2/n)}{1 - \kappa^{2/n}} \right)^n \quad (8.3-22)$$

The Newtonian result can be recovered by setting $n = 1$ and $m = \mu$. Equation 8.3-22 can be used along with torque versus angular velocity data to determine the power law parameters m and n .

§8.4 ELASTICITY AND THE LINEAR VISCOELASTIC MODELS

Just after Eq. 1.2-3, in the discussion about generalizing Newton's "law of viscosity," we specifically excluded time derivatives and time integrals in the construction of a linear expression for the stress tensor in terms of the velocity gradients. In this section, we

allow for the inclusion of time derivatives or time integrals, but still require a linear relation between τ and $\dot{\gamma}$. This leads to *linear viscoelastic* models.

We start by writing Newton's expression for the stress tensor for an incompressible viscous liquid along with Hooke's analogous expression for the stress tensor for an incompressible elastic solid:¹

$$\text{Newton: } \tau = -\mu(\nabla v + (\nabla v)^\dagger) \equiv -\mu\dot{\gamma} \quad (8.4-1)$$

$$\text{Hooke: } \tau = -G(\nabla u + (\nabla u)^\dagger) \equiv -G\gamma \quad (8.4-2)$$

In the second of these expressions G is the elastic modulus, and u is the "displacement vector," which gives the distance and direction that a point in the solid has moved from its initial position as a result of the applied stresses. The quantity γ is called the "infinitesimal strain tensor." The rate-of-strain tensor and the infinitesimal strain tensor are related by $\dot{\gamma} = \partial\gamma/\partial t$. The Hookean solid has a perfect memory; when imposed stresses are removed, the solid returns to its initial configuration. Hooke's law is valid only for very small displacement gradients, ∇u . Now we want to combine the ideas embodied in Eqs. 8.4-1 and 2 to describe viscoelastic fluids.

The Maxwell Model

The simplest equation for describing a fluid that is both viscous and elastic is the following *Maxwell model*:²

$$\tau + \lambda_1 \frac{\partial}{\partial t} \tau = -\eta_0 \dot{\gamma} \quad (8.4-3)$$

Here λ_1 is a time constant (the *relaxation time*) and η_0 is the *zero shear rate viscosity*. When the stress tensor changes imperceptibly with time, then Eq. 8.4-3 has the form of Eq. 8.4-1 for a Newtonian liquid. When there are very rapid changes in the stress tensor with time, then the first term on the left side of Eq. 8.4-3 can be omitted, and when the equation is integrated with respect to time, we get an equation of the form of Eq. 8.4-2 for the Hookean solid. In that sense, Eq. 8.4-3 incorporates both viscosity and elasticity.

A simple experiment that illustrates the behavior of a viscoelastic liquid involves "silly putty." This material flows easily when squeezed slowly between the palms of the hands, and this indicates that it is a viscous fluid. However, when it is rolled into a ball, the ball will bounce when dropped onto a hard surface. During the impact the stresses change rapidly, and the material behaves as an elastic solid.

The Jeffreys Model

The Maxwell model of Eq. 8.4-3 is a linear relation between the stresses and the velocity gradients, involving a time derivative of the stresses. One could also include a time derivative of the velocity gradients and still have a linear relation:

$$\tau + \lambda_1 \frac{\partial}{\partial t} \tau = -\eta_0 \left(\dot{\gamma} + \lambda_2 \frac{\partial}{\partial t} \dot{\gamma} \right) \quad (8.4-4)$$

¹ R. Hooke, *Lectures de Potentia Restitutiva* (1678).

² This relation was proposed by J. C. Maxwell, *Phil. Trans. Roy. Soc.*, A157, 49–88 (1867), to investigate the possibility that gases might be viscoelastic.

This *Jeffreys model*³ contains three constants: the zero shear rate viscosity and two time constants (the constant λ_2 is called the *retardation time*).

One could clearly add terms containing second, third, and higher derivatives of the stress and rate-of-strain tensors with appropriate multiplicative constants, to get a still more general linear relation among the stress and rate-of-strain tensors. This gives greater flexibility in fitting experimental data.

The Generalized Maxwell Model

Another way of generalizing Maxwell's original idea is to "superpose" equations of the form of Eq. 8.4-3 and write the *generalized Maxwell model* as

$$\tau(t) = \sum_{k=1}^{\infty} \tau_k(t) \quad \text{where } \tau_k + \lambda_k \frac{\partial}{\partial t} \tau_k = -\eta_k \dot{\gamma} \quad (8.4-5, 6)$$

in which there are many relaxation times λ_k (with $\lambda_1 \geq \lambda_2 \geq \lambda_3 \dots$) and many constants η_k with dimensions of viscosity. Much is known about the constants in this model from polymer molecular theories and the extensive experiments that have been done on polymeric liquids.⁴

The total number of parameters can be reduced to three by using the following empirical expressions:⁵

$$\eta_k = \eta_0 \frac{\lambda_k}{\sum \lambda_j} \quad \text{and} \quad \lambda_k = \frac{\lambda}{k^\alpha} \quad (8.4-7, 8)$$

in which η_0 is the zero shear rate viscosity, λ is a time constant, and α is a dimensionless constant (usually between 1.5 and 4).

Since Eq. 8.4-6 is a linear differential equation, it can be integrated analytically, with the condition that the fluid is at rest at $t = -\infty$. Then when the various τ_k are summed according to Eq. 8.4-5, we get the integral form of the generalized Maxwell model:

$$\tau(t) = - \int_{-\infty}^t \left\{ \sum_{k=1}^{\infty} \frac{\eta_k}{\lambda_k} \exp[-(t-t')/\lambda_k] \right\} \dot{\gamma}(t') dt' = - \int_{-\infty}^t G(t-t') \dot{\gamma}(t') dt' \quad (8.4-9)$$

In this form, the "fading memory" idea is clearly present: the stress at time t depends on the velocity gradients at all past times t' , but, because of the exponentials in the integrand, greatest weight is given to times t' that are near t ; that is, the fluid "memory" is better for recent times than for more remote times in the past. The quantity within braces {} is called the *relaxation modulus* of the fluid and is denoted by $G(t-t')$. The integral ex-

³ This model was suggested by H. Jeffreys, *The Earth*, Cambridge University Press, 1st edition (1924), and 2nd edition (1929), p. 265, to describe the propagation of waves in the earth's mantle. The parameters in this model have been related to the structure of suspensions and emulsions by H. Fröhlich and R. Sack, *Proc. Roy. Soc.*, **A185**, 415–430 (1946) and by J. G. Oldroyd, *Proc. Roy. Soc.*, **A218**, 122–132 (1953), respectively. Another interpretation of Eq. 8.4-4 is to regard it as the sum of a Newtonian solvent contribution (s) and a polymer contribution (p), the latter being described by a Maxwell model:

$$\tau_s = -\eta_s \dot{\gamma}; \quad \tau_p + \lambda_1 \frac{\partial}{\partial t} \tau_p = -\eta_p \dot{\gamma} \quad (8.4-4a, b)$$

so that $\tau = \tau_s + \tau_p$. Then if Eqs. 8.4-4a, 8.4-4b, and λ_1 times the time derivative of Eq. 8.4-4a are added, we get the Jeffreys model of Eq. 8.4-4, with $\eta_0 = \eta_s + \eta_p$ and $\lambda_2 = (\eta_s/(\eta_s + \eta_p))\lambda_1$.

⁴ J. D. Ferry, *Viscoelastic Properties of Polymers*, Wiley, New York, 3rd edition (1980). See also N. W. Tschoegl, *The Phenomenological Theory of Linear Viscoelastic Behavior*, Springer-Verlag, Berlin (1989); and R. B. Bird, R. C. Armstrong, and O. Hassager, *Dynamics of Polymeric Liquids*, Vol. 1, *Fluid Mechanics*, Wiley-Interscience, New York, 2nd edition (1987), Chapter 5.

⁵ T. W. Spriggs, *Chem. Eng. Sci.*, **20**, 931–940 (1965).

pression in Eq. 8.4-9 is sometimes more convenient for solving linear viscoelastic problems than are the differential equations in Eqs. 8.4-5 and 6.

The Maxwell, Jeffreys, and generalized Maxwell models are all examples of linear viscoelastic models, and their use is restricted to motions with very small displacement gradients. Polymeric liquids have many internal degrees of freedom and therefore many relaxation times are needed to describe their linear response. For this reason, the generalized Maxwell model has been widely used for interpreting experimental data on linear viscoelasticity. By fitting Eq. 8.4-9 to experimental data one can determine the relaxation function $G(t - t')$. One can then relate the shapes of the relaxation functions to the molecular structure of the polymer. In this way a sort of "mechanical spectroscopy" is developed, which can be used to investigate structure via linear viscoelastic measurements (such as the complex viscosity).

Models describing flows with very small displacement gradients might seem to have only limited interest to engineers. However, an important reason for studying them is that some background in linear viscoelasticity helps us in the study of nonlinear viscoelasticity, where flows with large displacement gradients are discussed.

EXAMPLE 8.4-1

Small-Amplitude Oscillatory Motion

Obtain an expression for the components of the complex viscosity by using the generalized Maxwell model. The system is described in Fig. 8.2-2.

SOLUTION

We use the yx -component of Eq. 8.4-9, and for this problem the yx -component of the rate-of-strain tensor is

$$\dot{\gamma}_{yx}(t) = \frac{\partial v_x}{\partial y} = \dot{\gamma}^0 \cos \omega t \quad (8.4-10)$$

where ω is the angular frequency. When this is substituted into Eq. 8.4-9, with the relaxation modulus (in braces) expressed as $G(t - t')$, we get

$$\begin{aligned} \tau_{yx} &= - \int_{-\infty}^t G(t - t') \dot{\gamma}^0 \cos \omega t' dt' \\ &= - \dot{\gamma}^0 \int_0^\infty G(s) \cos \omega(t - s) ds \\ &= - \dot{\gamma}^0 \left[\int_0^\infty G(s) \cos \omega s ds \right] \cos \omega t - \dot{\gamma}^0 \left[\int_0^\infty G(s) \sin \omega s ds \right] \sin \omega t \end{aligned} \quad (8.4-11)$$

in which $s = t - t'$. When this equation is compared with Eq. 8.2-4, we obtain

$$\eta'(\omega) = \int_0^\infty G(s) \cos \omega s ds \quad (8.4-12)$$

$$\eta''(\omega) = \int_0^\infty G(s) \sin \omega s ds \quad (8.4-13)$$

for the components of the complex viscosity $\eta^* = \eta' - i\eta''$. When the generalized Maxwell expression for the relaxation modulus is introduced and the integrals are evaluated, we find that

$$\eta'(\omega) = \sum_{k=1}^{\infty} \frac{\eta_k}{1 + (\lambda_k \omega)^2} \quad (8.4-14)$$

$$\eta''(\omega) = \sum_{k=1}^{\infty} \frac{\eta_k \lambda_k}{1 + (\lambda_k \omega)^2} \quad (8.4-15)$$

If the empiricisms in Eqs. 8.4-7 and 8 are used, it can be shown that both η' and η'' decrease as $1/\omega^{1-(1/\alpha)}$ at very high frequencies (see Fig. 8.2-4).

EXAMPLE 8.4-2

Unsteady Viscoelastic Flow Near an Oscillating Plate

Extend Example 4.1-3 to viscoelastic fluids, using the Maxwell model, and obtain the attenuation and phase shift in the "periodic steady state."

SOLUTION

For the postulated shearing flow, the equation of motion, written in terms of the stress tensor component gives

$$\rho \frac{\partial v_x}{\partial t} = -\frac{\partial}{\partial y} \tau_{yx} \quad (8.4-16)$$

The Maxwell model in integral form is like Eq. 8.4-9, but with a single exponential:

$$\tau_{yx}(y, t) = -\int_{-\infty}^t \left\{ \frac{\eta_0}{\lambda_1} \exp[-(t - t')/\lambda_1] \right\} \frac{\partial v_x(y, t')}{\partial y} dt' \quad (8.4-17)$$

Combining these two equations, we get

$$\rho \frac{\partial v_x}{\partial t} = \int_{-\infty}^t \left\{ \frac{\eta_0}{\lambda_1} \exp[-(t - t')/\lambda_1] \right\} \frac{\partial^2 v_x(y, t')}{\partial y^2} dt' \quad (8.4-18)$$

As in Example 4.1-3 we postulate a solution of the form

$$v_x(y, t) = \Re\{v^0(y)e^{i\omega t}\} \quad (8.4-19)$$

where $v^0(y)$ is complex. Substituting this into Eq. 8.4-19, we get

$$\begin{aligned} \rho \Re[i\omega v^0 e^{i\omega t}] &= \int_{-\infty}^t \left\{ \frac{\eta_0}{\lambda_1} \exp[-(t - t')/\lambda_1] \right\} \Re \left\{ \frac{d^2 v^0}{dy^2} e^{i\omega t'} \right\} dt' \\ &= \Re \left\{ \frac{d^2 v^0}{dy^2} e^{i\omega t} \int_0^\infty \frac{\eta_0}{\lambda_1} e^{-s/\lambda_1} e^{-i\omega s} ds \right\} \\ &= \Re \left\{ \frac{d^2 v^0}{dy^2} e^{i\omega t} \left[\frac{\eta_0}{1 + i\lambda_1 \omega} \right] \right\} \end{aligned} \quad (8.4-20)$$

Removing the real operator then gives an equation for $v^0(y)$

$$\frac{d^2 v^0}{dy^2} - \left[\frac{i\omega(1 + i\lambda_1 \omega)}{\eta_0} \right] v^0 = 0 \quad (8.4-21)$$

Then if the complex quantity in the brackets [] is set equal to $(\alpha + i\beta)^2$, the solution to the differential equation is

$$v^0 = v_0 e^{-(\alpha + i\beta)y} \quad (8.4-22)$$

Multiplying this by $e^{i\omega t}$ and taking the real part gives

$$v_x(y, t) = v_0 e^{-\alpha y} \cos(\omega t - \beta y) \quad (8.4-23)$$

This result has the same form as that in Eq. 4.1-57, but the quantities α and β depend on frequency:

$$\alpha(\omega) = \sqrt{\frac{\rho\omega}{2\eta_0}} [\sqrt{1 + (\lambda_1\omega)^2} - \lambda_1\omega]^{+1/2} \quad (8.4-24)$$

$$\beta(\omega) = \sqrt{\frac{\rho\omega}{2\eta_0}} [\sqrt{1 + (\lambda_1\omega)^2} - \lambda_1\omega]^{-1/2} \quad (8.4-25)$$

That is, with increasing frequency, α decreases and β increases, because of the fluid elasticity. This result shows how elasticity affects the transmission of shear waves near an oscillating surface.

Note that there is an important difference between the problems in the last two examples. In Example 8.4-1 the velocity profile is prescribed, and we have derived an expression for the shear stress required to maintain the motion; the equation of motion was not used. In Example 8.4-2 no assumption was made about the velocity distribution, and we derived the velocity distribution by using the equation of motion.

§8.5 THE COROTATIONAL DERIVATIVES AND THE NONLINEAR VISCOELASTIC MODELS

In the previous section it was shown that the inclusion of time derivatives (or time integrals) in the stress tensor expression allows for the description of elastic effects. The linear viscoelastic models can describe the complex viscosity and the transmission of small-amplitude shearing waves. It can also be shown that the linear models can describe elastic recoil, although the results are restricted to flows with negligible displacement gradients (and hence of little practical interest).

In this section we introduce the hypothesis^{1,2} that the relation between the stress tensor and the kinematic tensors at a fluid particle should be independent of the instantaneous orientation of that particle in space. This seems like a reasonable hypothesis; if you measure the stress-strain relation in a rubber band, it should not matter whether you are stretching the rubber band in the north-south direction or the east-west direction, or even rotating as you take data (provided, of course, that you do not rotate so rapidly that centrifugal forces interfere with the measurements).

One way to implement the above hypothesis is to introduce at each fluid particle a corotating coordinate frame. This orthogonal frame rotates with the local instantaneous angular velocity as it moves along with the fluid particle through space (see Fig. 8.5-1). In the corotating coordinate system we can now write down some kind of relation

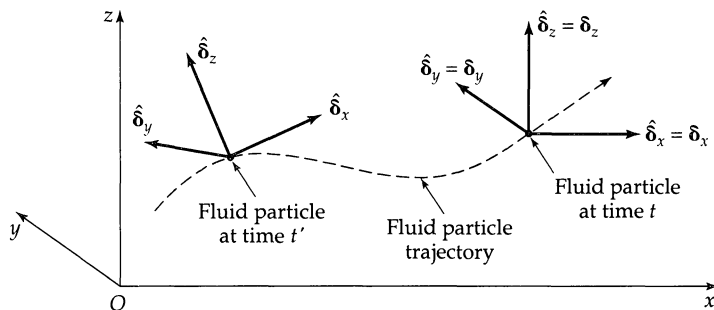


Fig. 8.5-1. Fixed coordinate frame with origin at O , and the corotating frame with unit vectors $\hat{\delta}_1, \hat{\delta}_2, \hat{\delta}_3$ that move with a fluid particle and rotate with the local, instantaneous angular velocity $\frac{1}{2}[\nabla \times \mathbf{v}]$ of the fluid.

¹ G. Jaumann, *Grundlagen der Bewegungslehre*, Leipzig (1905); *Sitzungsberichte Akad. Wiss. Wien, IIa*, **120**, 385–530 (1911); S. Zaremba, *Bull. Int. Acad. Sci., Cracovie*, 594–614, 614–621 (1903). **Gustaf Andreas Johannes Jaumann** (1863–1924) (pronounced “Yow-mahn”) who taught at the German university in Brünn (now Brno), for whom the “Jaumann derivative” is named, was an important contributor to the field of continuum mechanics at the beginning of the twentieth century; he was the first to give the equation of change for entropy, including the “entropy flux” and the “rate of entropy production” (see §24.1).

² J. G. Oldroyd, *Proc. Roy. Soc., A* **245**, 278–297 (1958). For an extension of the corotational idea, see L. E. Wedgewood, *Rheol. Acta*, **38**, 91–99 (1999).

between the stress tensor and the rate-of-strain tensor; for example, we can write the Jeffreys model and then add some additional nonlinear terms for good measure:

$$\hat{\tau} + \lambda_1 \frac{\partial}{\partial t} \hat{\tau} + \frac{1}{2} \mu_0 (\text{tr } \hat{\tau}) \hat{\gamma} - \frac{1}{2} \mu_1 [\hat{\gamma} \cdot \hat{\tau} + \hat{\tau} \cdot \hat{\gamma}] = -\eta_0 \left(\hat{\gamma} + \lambda_2 \frac{\partial}{\partial t} \hat{\gamma} - \mu_2 [\hat{\gamma} \cdot \hat{\gamma}] \right) \quad (8.5-1)$$

in which the circumflexes ($\hat{\cdot}$) on the tensors indicate that their components are those with respect to the corotating coordinate frame. In Eq. 8.5-1 the constants λ_1 , λ_2 , μ_0 , μ_1 , and μ_2 all have dimensions of time.

Since the equations of continuity and motion are written for the usual xyz -coordinate frame, fixed in space, it seems reasonable to transform Eq. 8.5-1 from the $\hat{x}\hat{y}\hat{z}$ frame into the xyz frame. This is a purely mathematical problem, which was worked out long ago,¹ and the solution is well known. It can be shown that the partial time derivatives $\partial/\partial t$, $\partial^2/\partial t^2$, \dots are changed into *corotational* (or *Jaumann*¹⁻⁴) *time derivatives* $\mathcal{D}/\mathcal{D}t$, $\mathcal{D}^2/\mathcal{D}t^2$, \dots . The corotational time derivative of a second-order tensor is defined as

$$\frac{\mathcal{D}}{\mathcal{D}t} \boldsymbol{\alpha} = \frac{D}{Dt} \boldsymbol{\alpha} + \frac{1}{2} [\boldsymbol{\omega} \cdot \boldsymbol{\alpha} - \boldsymbol{\alpha} \cdot \boldsymbol{\omega}] \quad (8.5-2)$$

in which $\boldsymbol{\omega} = \nabla \mathbf{v} - (\nabla \mathbf{v})^\dagger$ is the *vorticity tensor*, and D/Dt is the substantial time derivative defined in §3.5. The tensor dot products appearing in Eq. 8.5-1, with components in the $\hat{x}\hat{y}\hat{z}$ frame, transform into the corresponding dot products, with the components given in the xyz frame.

When transformed into the xyz frame, Eq. 8.5-1 becomes

$$\boldsymbol{\tau} + \lambda_1 \frac{\mathcal{D}}{\mathcal{D}t} \boldsymbol{\tau} + \frac{1}{2} \mu_0 (\text{tr } \boldsymbol{\tau}) \dot{\gamma} - \frac{1}{2} \mu_1 [\boldsymbol{\tau} \cdot \dot{\gamma} + \dot{\gamma} \cdot \boldsymbol{\tau}] = -\eta_0 \left(\dot{\gamma} + \lambda_2 \frac{\mathcal{D}}{\mathcal{D}t} \dot{\gamma} - \mu_2 [\dot{\gamma} \cdot \dot{\gamma}] \right) \quad (8.5-3)$$

which is the *Oldroyd 6-constant model*. This model, then, has no dependence on the local instantaneous orientation of the fluid particles in space. It should be emphasized that Eq. 8.5-3 is an empirical model; the use of the corotating frame guarantees only that the instantaneous local rotation of the fluid has been “subtracted off.”

With proper choice of these parameters most of the observed phenomena in polymer fluid dynamics can be described *qualitatively*. As a result this model has been widely used in exploratory fluid dynamics calculations. A 3-constant simplification of Eq. 8.5-3 with $\mu_1 = \lambda_1$, $\mu_2 = \lambda_2$, and $\mu_0 = 0$ is called the *Oldroyd-B model*. In Example 8.5-1 we show what Eq. 8.5-3 gives for the material functions defined in §8.2.

Another nonlinear viscoelastic model is the 3-constant *Giesekus model*,⁵ which contains a term that is quadratic in the stress components:

$$\boldsymbol{\tau} + \lambda \left(\frac{\mathcal{D}}{\mathcal{D}t} \boldsymbol{\tau} - \frac{1}{2} [\boldsymbol{\tau} \cdot \dot{\gamma} + \dot{\gamma} \cdot \boldsymbol{\tau}] \right) - \alpha \frac{\lambda}{\eta_0} \{\boldsymbol{\tau} \cdot \boldsymbol{\tau}\} = -\eta_0 \dot{\gamma} \quad (8.5-4)$$

Here λ is a time constant, η_0 is the zero shear rate viscosity, and α is a dimensionless parameter. This model gives reasonable shapes for most material functions, and the analytical expressions for them are summarized in Table 8.5-1. Because of the $\{\boldsymbol{\tau} \cdot \boldsymbol{\tau}\}$ term, they

³ J. D. Goddard and C. Miller, *Rheol. Acta*, **5**, 177–184 (1966).

⁴ R. B. Bird, R. C. Armstrong, and O. Hassager, *Dynamics of Polymeric Liquids*, Vol. 1, *Fluid Mechanics*, Wiley, New York, 1st edition (1977), Chapters 7 and 8; the corotational models are not discussed in the second edition of this book, where emphasis is placed on the use of “convected coordinates” and the “codeforming” frame. For differential models, either the corotating or codeforming frame can be used, but the former is simpler conceptually and mathematically.

⁵ H. Giesekus, *J. Non-Newtonian Fluid Mech.*, **11**, 69–109 (1982); **12**, 367–374; *Rheol. Acta*, **21**, 366–375 (1982). See also R. B. Bird and J. M. Wiest, *J. Rheol.*, **29**, 519–532 (1985), and R. B. Bird, R. C. Armstrong, and O. Hassager, *Dynamics of Polymeric Liquids*, Vol. 1, *Fluid Dynamics*, Wiley-Interscience, New York, 2nd edition (1987), §7.3(c).

Table 8.5-1 Material Functions for the Giesekus Model

Steady shear flow:

$$\frac{\eta}{\eta_0} = \frac{(1-f)^2}{1 + (1-2\alpha)f} \quad (\text{A})$$

$$\frac{\Psi_1}{2\eta_0\lambda} = \frac{f(1-\alpha f)}{\alpha(1-f)} \frac{1}{(\lambda\dot{\gamma})^2} \quad (\text{B})$$

$$\frac{\Psi_2}{\eta_0\lambda} = -f \frac{1}{(\lambda\dot{\gamma})^2} \quad (\text{C})$$

where

$$f = \frac{1-\chi}{1 + (1-2\alpha)\chi} \quad \text{and} \quad \chi^2 = \frac{[1 + 16\alpha(1-\alpha)(\lambda\dot{\gamma})^2]^{1/2} - 1}{8\alpha(1-\alpha)(\lambda\dot{\gamma})^2} \quad (\text{D}, \text{E})$$

Small-amplitude oscillatory shear flow:

$$\frac{\eta'}{\eta_0} = \frac{1}{1 + (\lambda\omega)^2} \quad \text{and} \quad \frac{\eta''}{\eta_0} = \frac{\lambda\omega}{1 + (\lambda\omega)^2} \quad (\text{F}, \text{G})$$

Steady elongational flow:

$$\frac{\bar{\eta}}{3\eta_0} = \frac{1}{6\alpha} \left[3 + \frac{1}{\lambda\dot{\epsilon}} (\sqrt{1 - 4(1-2\alpha)\lambda\dot{\epsilon}} + 4(\lambda\dot{\epsilon})^2) - \sqrt{1 + 2(1-2\alpha)\lambda\dot{\epsilon} + (\lambda\dot{\epsilon})^2} \right] \quad (\text{H})$$

are not particularly simple. Superpositions of Giesekus models can be made to describe the shapes of the measured material functions almost quantitatively.⁶ The model has been used widely for fluid dynamics calculations.

EXAMPLE 8.5-1

Material Functions for the Oldroyd 6-Constant Model^{2,4}

Obtain the material functions for steady shear flow, small amplitude oscillatory motion, and steady uniaxial elongational flow. Make use of the fact that in shear flows, the stress tensor components τ_{xz} and τ_{yz} are zero, and that in elongational flow, the off-diagonal elements of the stress tensor are zero (these results are obtained by symmetry arguments⁷).

SOLUTION

(a) First we simplify Eq. 8.5-3 for *unsteady shear flow*, with the velocity distribution $v_x(y, t) = \dot{\gamma}(t)y$. By writing out the components of the equation we get

$$\left(1 + \lambda_1 \frac{\partial}{\partial t}\right) \tau_{xx} - (\lambda_1 + \mu_1) \tau_{yx} \dot{\gamma} = +\eta_0(\lambda_2 + \mu_2) \dot{\gamma}^2 \quad (8.5-5)$$

$$\left(1 + \lambda_1 \frac{\partial}{\partial t}\right) \tau_{yy} + (\lambda_1 - \mu_1) \tau_{yx} \dot{\gamma} = -\eta_0(\lambda_2 - \mu_2) \dot{\gamma}^2 \quad (8.5-6)$$

$$\left(1 + \lambda_1 \frac{\partial}{\partial t}\right) \tau_{zz} = 0 \quad (8.5-7)$$

$$\left(1 + \lambda_1 \frac{\partial}{\partial t}\right) \tau_{yx} + \frac{1}{2}(\lambda_1 - \mu_1 + \mu_0) \tau_{xx} \dot{\gamma} - \frac{1}{2}(\lambda_1 + \mu_1 - \mu_0) \tau_{yy} \dot{\gamma} + \frac{1}{2}\mu_0 \tau_{zz} \dot{\gamma} = -\eta_0 \left(1 + \lambda_2 \frac{\partial}{\partial t}\right) \dot{\gamma} \quad (8.5-8)$$

⁶ W. R. Burghardt, J.-M. Li, B. Khomami, and B. Yang, *J. Rheol.*, **147**, 149–165 (1999).

⁷ See, for example, R. B. Bird, R. C. Armstrong, and O. Hassager, *Dynamics of Polymeric Liquids*, Vol. 1, *Fluid Dynamics*, Wiley-Interscience, New York, 2nd edition (1987), §3.2.

(b) For steady-state shear flow, Eqs. 8.5-7 gives $\tau_{zz} = 0$, and the other three equations give a set of simultaneous algebraic equations that can be solved to get the remaining stress tensor components. Then with the definitions of the material functions in §8.2, we can obtain

$$\frac{\eta}{\eta_0} = \frac{1 + [\lambda_1\lambda_2 + (\mu_0 - \mu_1)\mu_2]\dot{\gamma}^2}{1 + [\lambda_1^2 + (\mu_0 - \mu_1)\mu_1]\dot{\gamma}^2} = \frac{1 + \sigma_2\dot{\gamma}^2}{1 + \sigma_1\dot{\gamma}^2} \quad (8.5-9)$$

$$\frac{\Psi_1}{2\eta_0\lambda_1} = \frac{1 + \sigma_2\dot{\gamma}^2}{1 + \sigma_1\dot{\gamma}^2} - \frac{\lambda_2}{\lambda_1} \quad (8.5-10)$$

$$\frac{\Psi_2}{\eta_0\lambda_1} = -\left(1 - \frac{\mu_1}{\lambda_1}\right) \frac{1 + \sigma_2\dot{\gamma}^2}{1 + \sigma_1\dot{\gamma}^2} + \left(1 - \frac{\mu_2}{\lambda_2}\right) \frac{\lambda_2}{\lambda_1} \quad (8.5-11)$$

The model thus gives a shear-rate-dependent viscosity as well as shear-rate-dependent normal-stress coefficients. (For the Oldroyd-B model the viscosity and normal-stress coefficients are independent of the shear rate.) For most polymers the non-Newtonian viscosity decreases with the shear rate, and for such fluids we conclude that $0 < \sigma_2 < \sigma_1$. Moreover, since measured values of $|\tau_{yx}|$ always increase monotonically with shear rate, we also require that $\sigma_2 > \frac{1}{9}\sigma_1$. Although the model gives shear-rate-dependent viscosity and normal stresses, the shapes of the curves are not in satisfactory agreement with experimental data over a wide range of shear rates.

If $\mu_1 < \lambda_1$ and $\mu_2 < \lambda_2$, the second normal-stress coefficient has the opposite sign of the first normal-stress coefficient, in agreement with the data for most polymeric liquids. Since the second normal-stress coefficient is much smaller than the first for many fluids and in some flows plays a negligible role, setting $\mu_1 = \lambda_1$ and $\mu_2 = \lambda_2$ may be reasonable, thereby reducing the number of parameters from 6 to 4.

This discussion shows how to evaluate a proposed empirical model by comparing the model predictions with experimental data obtained in rheometric experiments. We have also seen that the experimental data may necessitate restrictions on the parameters. Clearly this is a tremendous task, but it is not unlike the problem that the thermodynamicist faces in developing empirical equations of state for mixtures, for example. The rheologist, however, is dealing with tensor equations, whereas the thermodynamicist is concerned only with scalar equations.

(c) For small-amplitude oscillatory motion the nonlinear terms in Eqs. 8.5-5 to 8 may be omitted, and the material functions are the same as those obtained from the Jeffreys model of linear viscoelasticity:

$$\frac{\eta'}{\eta_0} = \frac{1 + \lambda_1\lambda_2\omega^2}{1 + \lambda_1^2\omega^2} \quad \text{and} \quad \frac{\eta''}{\eta_0} = \frac{(\lambda_1 - \lambda_2)\omega}{1 + \lambda_1^2\omega^2} \quad (8.5-12, 13)$$

For η' to be a monotone decreasing function of the frequency and for η'' to be positive (as seen in all experiments), we have to require that $\lambda_2 < \lambda_1$. Here again, the model gives qualitatively correct results, but the shapes of the curves are not correct.

(d) For the steady elongational flow defined in §8.2, the Oldroyd 6-constant model gives

$$\frac{\bar{\eta}}{3\eta_0} = \frac{1 - \mu_2\dot{\epsilon} + \mu_2(3\mu_0 - 2\mu_1)\dot{\epsilon}^2}{1 - \mu_1\dot{\epsilon} + \mu_1(3\mu_0 - 2\mu_1)\dot{\epsilon}^2} \quad (8.5-14)$$

Since, for most polymers, the slope of the elongational viscosity versus elongation rate curve is positive at $\dot{\epsilon} = 0$, we must require that $\mu_1 > \mu_2$. Equation 8.5-14 predicts that the elongational viscosity may become infinite at some finite value of the elongation rate; this may possibly present a problem in fiber-stretching calculations.

Note that the time constants λ_1 and λ_2 do not appear in the expression for elongational viscosity, whereas the constants μ_0 , μ_1 , and μ_2 do not enter into the components of the complex viscosity in Eqs. 8.5-14 and 15. This emphasizes the fact that a wide range of rheometric experiments is necessary for determining the parameters in an empirical expression for the stress tensor. To put it in another way, various experiments emphasize different parts of the model.

§8.6 MOLECULAR THEORIES FOR POLYMERIC LIQUIDS^{1,2,3}

It should be evident from the previous section that proposing and testing empirical expressions for the stress tensor in nonlinear viscoelasticity is a formidable task. Recall that, in turbulence, seeking empirical expressions for the Reynolds stress tensor is equally daunting. However, in nonlinear viscoelasticity we have the advantage that we can narrow the search for stress tensor expressions considerably by using molecular theory. Although the kinetic theory of polymers is considerably more complicated than the kinetic theory of gases, it nonetheless guides us in suggesting possible forms for the stress tensor. However, the constants appearing in the molecular expressions must still be determined from rheometric measurements.

The kinetic theories for polymers can be divided roughly into two classes: *network theories* and *single-molecule theories*:

a. The network theories³ were originally developed for describing the mechanical properties of rubber. One imagines that the polymer molecules in the rubber are joined chemically during vulcanization. The theories have been extended to describe molten polymers and concentrated solutions by postulating an ever-changing network in which the junction points are temporary, formed by adjacent strands that move together for a while and then gradually pull apart (see Fig. 8.6-1). It is necessary in the theory to make some empirical statements about the rates of formation and rupturing of the junctions.

b. The single-molecule theories¹ were originally designed for describing the polymer molecules in a very dilute solution, where polymer–polymer interactions are infrequent. The molecule is usually represented by means of some kind of “bead spring” model, a series of small spheres connected by linear or nonlinear springs in such a way as to represent the molecular architecture; the bead spring model is then allowed to move about in the solvent, with the beads experiencing a Stokes’ law drag force by the solvent as well as being buffeted about by Brownian motion (see Fig. 8.6-2a). Then from the kinetic theory one obtains the “distribution function” for the orientations of the molecules (modeled as bead spring structures); once this function is known, various macroscopic properties can be calculated. The same kind of theory may be applied to concentrated solutions and molten polymers by examining the motion of a single bead spring model in the “mean force field” exerted by the surrounding molecules. That is,

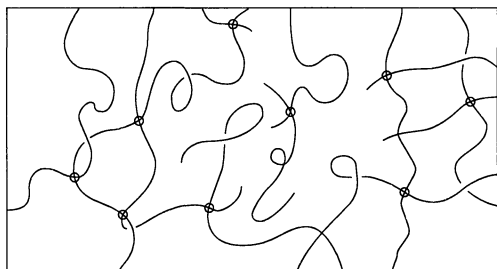


Fig. 8.6-1. Portion of a polymer network formed by “temporary junctions,” indicated here by circles.

¹ R. B. Bird, C. F. Curtiss, R. C. Armstrong, and O. Hassager, *Dynamics of Polymeric Liquids*, Vol. 2, *Kinetic Theory*, Wiley-Interscience, New York, 2nd edition (1987).

² M. Doi and S. F. Edwards, *The Theory of Polymer Dynamics*, Clarendon Press, Oxford (1986); J. D. Schieber, “Polymer Dynamics,” in *Encyclopedia of Applied Physics*, Vol. 14, VCH Publishers, Inc. (1996), pp. 415–443. R. B. Bird and H. C. Öttinger, *Ann. Rev. Phys. Chem.*, **43**, 371–406 (1992).

³ A. S. Lodge, *Elastic Liquids*, Academic Press, New York (1964); *Body Tensor Fields in Continuum Mechanics*, Academic Press, New York (1974); *Understanding Elastomer Molecular Network Theory*, Bannatek Press, Madison, Wis. (1999).

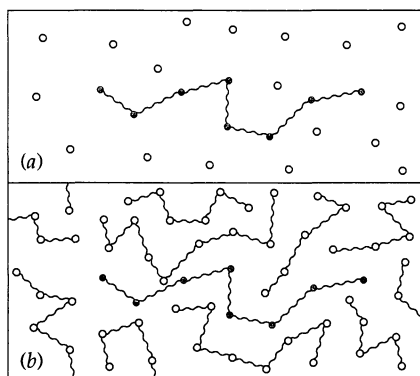


Fig. 8.6-2. Single-molecule bead spring models for (a) a dilute polymer solution, and (b) an undiluted polymer (a polymer “melt” with no solvent). In the dilute solution, the polymer molecule can move about in all directions through the solvent. In the undiluted polymer, a typical polymer molecule (black beads) is constrained by the surrounding molecules and tends to execute snakelike motion (“reptation”) by sliding back and forth along its backbone direction.

because of the proximity of the surrounding molecules, it is easier for the “beads” of the model to move in the direction of the polymer chain backbone than perpendicular to it. In other words, the polymer finds itself executing a sort of snakelike motion, called “reptation” (see Fig. 8.6-2b).

As an illustration of the kinetic theory approach we discuss the results for a simple system: a dilute solution of a polymer, modeled as an elastic dumbbell consisting of two beads connected by a spring. We take the spring to be nonlinear and finitely extensible, with the force in the connecting spring being given by⁴

$$\mathbf{F}^{(c)} = \frac{HQ}{1 - (Q/Q_0)^2} \quad (8.6-1)$$

in which H is a spring constant, \mathbf{Q} is the end-to-end vector of the dumbbell representing the stretching and orientation of the dumbbell, and Q_0 is the maximum elongation of the spring. The friction coefficient for the motion of the beads through the solvent is given by Stokes' law as $\zeta = 6\pi\eta_s a$, where a is the bead radius and η_s is the solvent viscosity. Although this model is greatly oversimplified, it does embody the key physical ideas of molecular orientation, molecular stretching, and finite extensibility.

When the details of the kinetic theory are worked out, one gets the following expression for the stress tensor, written as the sum of a Newtonian solvent and a polymer contribution (see fn. 3 in §8.4):⁵

$$\boldsymbol{\tau} = \boldsymbol{\tau}_s + \boldsymbol{\tau}_p \quad (8.6-2)$$

Here

$$\boldsymbol{\tau}_s = -\eta_s \dot{\boldsymbol{\gamma}} \quad (8.6-3)$$

$$Z\boldsymbol{\tau}_p + \lambda_H \left(\frac{\mathcal{D}}{\mathcal{D}t} \boldsymbol{\tau}_p - \frac{1}{2} [\boldsymbol{\tau}_p \cdot \dot{\boldsymbol{\gamma}} + \dot{\boldsymbol{\gamma}} \cdot \boldsymbol{\tau}_p] \right) - \lambda_H (\boldsymbol{\tau}_p - n\kappa T \mathbf{d}) \frac{D \ln Z}{Dt} = -n\kappa T \lambda_H \dot{\boldsymbol{\gamma}} \quad (8.6-4)$$

where n is the number density of polymer molecules (i.e., dumbbells), $\lambda_H = \zeta/4H$ is a time constant (typically between 0.01 and 10 seconds), $Z = 1 + (3/b)[1 - (\text{tr } \boldsymbol{\tau}_p)/3n\kappa T]$, and $b = HQ_0^2/\kappa T$ is the finite extensibility parameter, usually between 10 and 100. The

⁴ H. R. Warner, Jr., *Ind. Eng. Chem. Fundamentals*, **11**, 379–387 (1972); R. L. Christiansen and R. B. Bird, *J. Non-Newtonian Fluid Mech.*, **3**, 161–177 (1977/1978).

⁵ R. I. Tanner, *Trans. Soc. Rheol.*, **19**, 37–65 (1975); R. B. Bird, P. J. Dotson, and N. L. Johnson, *J. Non-Newtonian Fluid Mech.*, **7**, 213–235 (1980)—in the last publication, Eqs. 58–85 are in error.

molecular theory has thus resulted in a model with four adjustable constants: η_s , λ_H , n , and b , which can be determined from rheometric experiments. Thus the molecular theory suggests the form of the stress tensor expression, and the rheometric data are used to determine the values of the parameters. The model described by Eqs. 8.6-2, 3, and 4 is called the FENE-P model (finitely extensible nonlinear elastic model, in the Peterlin approximation) in which $(Q/Q_0)^2$ in Eq. 8.6-1 is replaced by $\langle Q^2 \rangle / Q_0^2$.

This model is more difficult to work with than the Oldroyd 6-constant model, because it is nonlinear in the stresses. However, it gives better shapes for some of the material functions. Also, since we are dealing here with a molecular model, we can get information about the molecular stretching and orientation after a flow problem has been solved. For example, it can be shown that the average molecular stretching is given by $\langle Q^2 \rangle / Q_0^2 = 1 - Z^{-1}$ where the angular brackets indicate a statistical average.

The following examples illustrate how one obtains the material functions for the model and compares the results with experimental data. If the model is acceptable, then it must be combined with the equations of continuity and motion to solve interesting flow problems. This requires large-scale computing.

EXAMPLE 8.6-1

Material Functions for the FENE-P Model

Obtain the material functions for the steady-state shear flow and the steady-state elongational flow of a polymer described by the FENE-P model.

SOLUTION

(a) For steady-state shear flow the model gives the following equations for the nonvanishing components of the polymer contribution to the stress tensor:

$$Z\tau_{p,xx} = 2\tau_{p,yx}\lambda_H\dot{\gamma} \quad (8.6-5)$$

$$Z\tau_{p,yx} = -n\kappa T\lambda_H\dot{\gamma} \quad (8.6-6)$$

Here the quantity Z is given by

$$Z = 1 + (3/b)[1 - (\tau_{p,xx}/3n\kappa T)] \quad (8.6-7)$$

These equations can be combined to give a cubic equation for the dimensionless shear stress contribution $T_{yx} = \tau_{p,yx}/3n\kappa T$

$$T_{yx}^3 + 3pT_{yx} + 2q = 0 \quad (8.6-8)$$

in which $p = (b/54) + (1/18)$ and $q = (b/108)\lambda_H\dot{\gamma}$. This cubic equation may be solved to give⁶

$$T_{yx} = -2p^{1/2} \sinh(\frac{1}{3} \operatorname{arcsinh} qp^{-3/2}) \quad (8.6-9)$$

The non-Newtonian viscosity based on this function is shown in Fig. 8.6-3 along with some experimental data for some polymethyl-methacrylate solutions. From Eq. 8.6-9 we find for the limiting values of the viscosity

$$\text{For } \dot{\gamma} = 0: \quad \eta - \eta_s = n\kappa T\lambda_H \left(\frac{b}{b+3} \right) \quad (8.6-10)$$

$$\text{For } \dot{\gamma} \rightarrow \infty: \quad \eta - \eta_s \sim n\kappa T\lambda_H \left(\frac{b}{2} \frac{1}{\lambda_H^2 \dot{\gamma}^2} \right)^{1/3} \quad (8.6-11)$$

Hence, at high shear rates one obtains a power law behavior (Eq. 8.3-3) with $n = \frac{1}{3}$. This can be taken as a molecular justification for use of the power law model.

⁶ K. Rektorys, *Survey of Applicable Mathematics*, MIT Press, Cambridge, MA (1969), pp. 78–79.

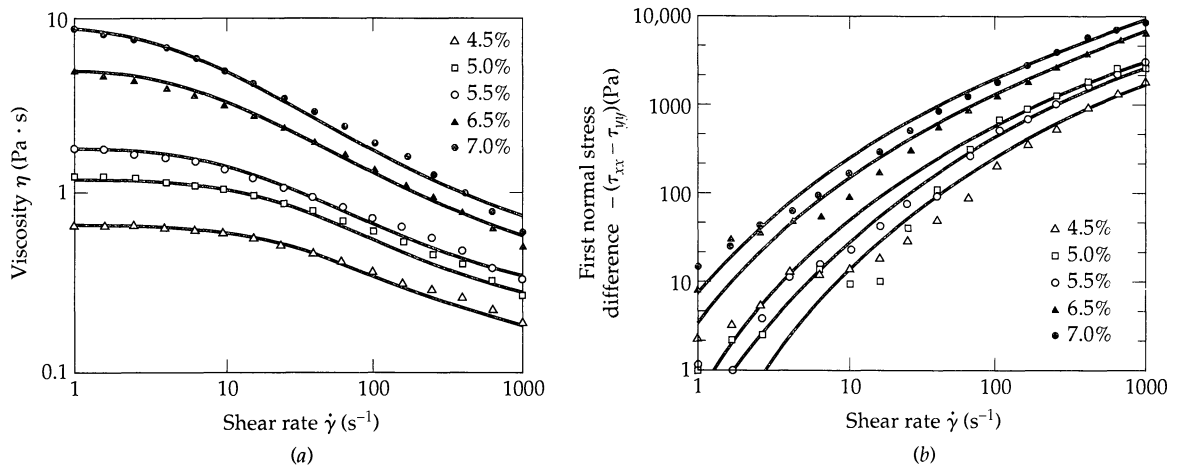


Fig. 8.6-3. Viscosity and first-normal-stress difference data for polymethylmethacrylate solutions from D. D. Joseph, G. S. Beavers, A. Cers, C. Dewald, A. Hoger, and P. T. Than, *J. Rheol.*, 28, 325–345 (1984), along with the FENE-P curves for the following constants, determined by L. E. Wedgewood:

Polymer concentration [%]	η_0 [Pa · s]	λ_H [s]	a [Pa]	b [- - -]
4.5	0.13	0.157	3.58	47.9
5.0	0.19	0.192	5.94	38.3
5.5	0.25	0.302	5.98	30.6
6.5	0.38	0.447	11.8	25.0
7.0	0.45	0.553	19.1	16.0

The quantity $a = n\kappa T$ was taken to be a parameter determined from the rheometric data.

From Eq. 8.6-5 one finds that Ψ_1 is given by $\Psi_1 = 2(\eta - \eta_s)^2/n\kappa T$; a comparison of this result with experimental data is shown in Fig. 8.6-3. The second normal stress coefficient Ψ_2 for this model is zero. As pointed out above, once we have solved the flow problem, we can also get the molecular stretching from the quantity Z . In Fig. 8.6-4 we show how the molecules are stretched, on the average, as a function of the shear rate.

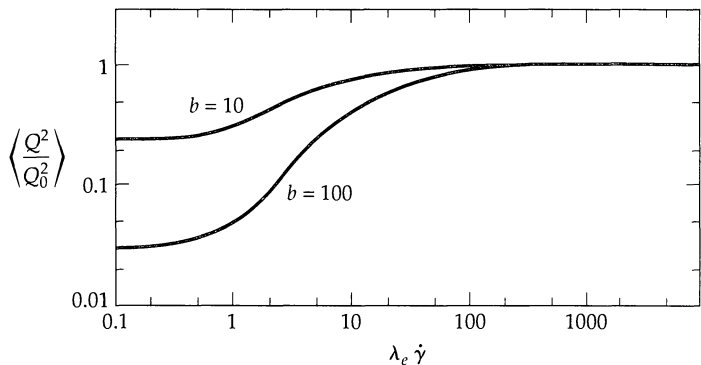


Fig. 8.6-4. Molecular stretching as a function of shear rate $\dot{\gamma}$ in steady shear flow, according to the FENE-P dumbbell model. The experimentally accessible time constant $\lambda_e = [\eta_0]\eta_s M/RT$, where $[\eta_0]$ is the zero shear rate intrinsic viscosity, is related to λ_H by $\lambda_e = \lambda_H b/(b + 3)$. [From R. B. Bird, P. J. Dotson, and N. L. Johnson, *J. Non-Newtonian Fluid Mech.*, 7, 213–235 (1980).]

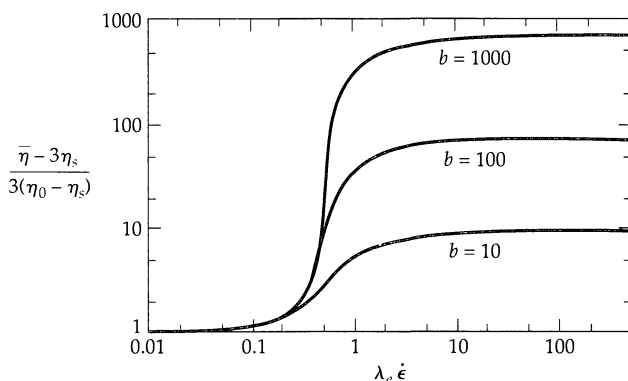


Fig. 8.6-5. Steady elongational viscosity $\bar{\eta}$ as a function of the elongation rate $\dot{\epsilon}$ according to the FENE-P dumbbell model. The time constant is given by $\lambda_e = \lambda_H b / (b + 3)$. [From R. B. Bird, P. J. Dotson, and N. L. Johnson, *J. Non-Newtonian Fluid Mech.*, **7**, 213–235 (1980).]

(b) For steady-state elongational flow we get

$$Z\tau_{p,xx} + \tau_{p,xx}\lambda_H\dot{\epsilon} = +n\kappa T\lambda_H\dot{\epsilon} \quad (8.6-12)$$

$$Z\tau_{p,yy} + \tau_{p,yy}\lambda_H\dot{\epsilon} = +n\kappa T\lambda_H\dot{\epsilon} \quad (8.6-13)$$

$$Z\tau_{p,zz} - 2\tau_{p,zz}\lambda_H\dot{\epsilon} = -2n\kappa T\lambda_H\dot{\epsilon} \quad (8.6-14)$$

$$Z = 1 + \frac{3}{b} \left(1 - \frac{\tau_{p,xx} + \tau_{p,yy} + \tau_{p,zz}}{3n\kappa T} \right) \quad (8.6-15)$$

This set of equations leads to a cubic equation for $\tau_{p,xx} - \tau_{p,zz}$, from which the elongational viscosity can be obtained (see Fig. 8.6-5). Limited experimental data on polymer solutions indicate that the shapes of the curves are probably approximately correct.

The limiting expressions for the elongational viscosity are

$$\text{For } \dot{\epsilon} = 0: \quad \bar{\eta} - 3\eta_s = 3n\kappa T\lambda_H \left(\frac{b}{b+3} \right) \quad (8.6-16)$$

$$\text{For } \dot{\epsilon} \rightarrow \infty: \quad \bar{\eta} - 3\eta_s = 2n\kappa T\lambda_H b \quad (8.6-17)$$

Having found the stresses in the system, we can then get the average stretching of the molecules as a function of the elongation rate; this is shown in Fig. 8.6-6.

It is worth noting that for a typical value of b —say, 50—the elongational viscosity can increase by a factor of about 30 as the elongation rate increases, thereby having a profound effect on flows in which there is a strong elongational component.⁷

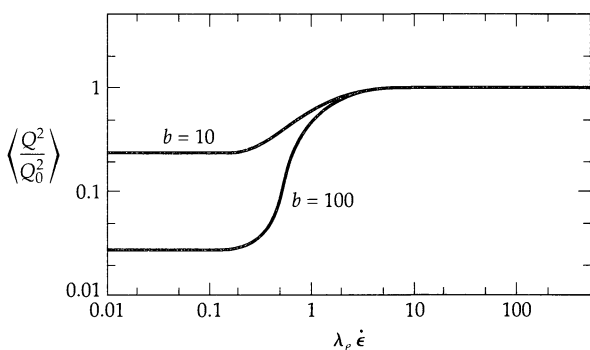


Fig. 8.6-6. Molecular stretching as a function of the elongation rate $\dot{\epsilon}$ in steady elongational flow, as predicted by the FENE-P dumbbell model. The time constant is given by $\lambda_e = \lambda_H b / (b + 3)$. [From R. B. Bird, P. J. Dotson, and N. L. Johnson, *J. Non-Newtonian Fluid Mech.*, **7**, 213–235 (1980).]

⁷ The FENE-P and Giesekus models have been used successfully to describe the details of turbulent drag reduction, which is closely related to elongational viscosity, by R. Sureshkumar, A. N. Beris and R. A. Handler, *Phys. Fluids*, **9**, 743–755 (1997), and C. D. Dimitropoulos, R. Sureshkumar, and A. N. Beris, *J. Non-Newtonian Fluid Mechanics*, **79**, 433–468 (1998).

QUESTIONS FOR DISCUSSION

1. Compare the behavior of Newtonian liquids and polymeric liquids in the various experiments discussed in §§8.1 and 8.2.
2. Why do we deal only with differences in normal stresses for incompressible liquids (see Eqs. 8.2-2 and 3)?
3. In Fig. 8.2-2 the postulated velocity profile is linear in y . What would you expect the velocity distribution to look like if the gap between the plates were not small and the fluid had a very low viscosity?
4. How is the parameter n in Eq. 8.3-3 related to the parameter n in Eq. 8.3-4? How is it related to the slope of the non-Newtonian velocity curve from the dumbbell kinetic theory model in §8.6?
5. What limitations have to be placed on use of the generalized Newtonian models and the linear viscoelastic models?
6. Compare and contrast Examples 8.4-1 and 2 regarding the geometry of the flow system and the assumptions regarding the velocity profiles.
7. To what extent does the Oldroyd model in Eq. 8.5-3 include a generalized Newtonian model and a linear viscoelastic model? Can the Oldroyd model describe effects that are not described by these other models?
8. Why is it necessary to put restrictions on the parameters in the Oldroyd model? What is the relation between these restrictions and the subject of rheometry?
9. What advantages do molecular expressions for the stress tensor have over the empirical expressions?
10. For what kinds of industrial problems would you use the various kinds of models described in this chapter?
11. Why may the power law model be unsatisfactory for describing the axial flow in an annulus?

PROBLEMS

- 8A.1 Flow of a polyisoprene solution in a pipe.** A 13.5% (by weight) solution of polyisoprene in isopentane has the following power law parameters at 323 K: $n = 0.2$ and $m = 5 \times 10^3 \text{ Pa} \cdot \text{s}^n$. It is being pumped (in laminar flow) through a horizontal pipe that has a length of 10.2 m and an internal diameter of 1.3 cm. It is desired to use another pipe with a length of 30.6 m with the same mass flow rate and the same pressure drop. What should the pipe radius be?
- 8A.2 Pumping of a polyethylene oxide solution.** A 1% aqueous solution of polyethylene oxide at 333 K has power law parameters $n = 0.6$ and $m = 0.50 \text{ Pa} \cdot \text{s}^n$. The solution is being pumped between two tanks, with the first tank at pressure p_1 and the second at pressure p_2 . The pipe carrying the solution has a length of 14.7 m and an internal diameter of 0.27 m. It has been decided to replace the single pipe by a pair of pipes of the same length, but with smaller diameter. What diameter should these pipes have so that the mass flow rate will be the same as in the single pipe?
- 8B.1 Flow of a polymeric film.** Work the problem in §2.2 for the power law fluid. Show that the result simplifies properly to the Newtonian result.
- 8B.2 Power law flow in a narrow slit.** In Example 8.3-2 show how to derive the velocity distribution for the region $-B \leq x \leq 0$. Is it possible to combine this result with that in Eq. 8.3-13 into one equation?
- 8B.3 Non-Newtonian flow in an annulus.** Rework Problem 2B.7 for the annular flow of a power law fluid with the flow being driven by the axial motion of the inner cylinder.
- (a) Show that the velocity distribution for the fluid is

$$\frac{v_z}{v_0} = \frac{(r/R)^{1-(1/n)} - 1}{\kappa^{1-(1/n)} - 1} \quad (8B.3-1)$$

(b) Verify that the result in (a) simplifies to the Newtonian result when n goes to unity.

(c) Show that the mass flow rate in the annular region is given by

$$w = \frac{2\pi R^2 v_0 \rho}{\kappa^{1-(1/n)} - 1} \left(\frac{1 - \kappa^{3-(1/n)}}{3 - (1/n)} - \frac{1 - \kappa^2}{2} \right) \quad (\text{for } n \neq \frac{1}{3}) \quad (8B.3-2)$$

(d) What is the mass flow rate for fluids with $n = \frac{1}{3}$?

(e) Simplify Eq. 8B.3-2 for the Newtonian fluid.

8B.4 Flow of a polymeric liquid in a tapered tube. Work Problem 2B.10 for a power law fluid, using the lubrication approximation.

8B.5 Slit flow of a Bingham fluid.¹ For thick suspensions and pastes it is found that no flow occurs until a certain critical stress, the *yield stress*, is reached, and then the fluid flows in such a way that part of the stream is in "plug flow." The simplest model of a fluid with a yield value is the *Bingham model*:

$$\begin{cases} \eta = \infty & \text{when } \tau \leq \tau_0 \\ \eta = \mu_0 + \frac{\tau_0}{\dot{\gamma}} & \text{when } t \geq \tau_0 \end{cases} \quad (8B.5-1)$$

in which τ_0 is the yield stress, the stress below which no flow occurs, and μ_0 is a parameter with units of viscosity. The quantity $\tau = \sqrt{\frac{1}{2}(\boldsymbol{\tau} : \boldsymbol{\tau})}$ is the magnitude of the stress tensor.

Find the mass flow rate in a slit for the Bingham fluid (see Problem 2B.3 and Example 8.3-2). The expression for the shear stress τ_{xz} as a function of position x in Eq. 2B.3-1 can be taken over here, since it does not depend on the type of fluid. We see that $|\tau_{xz}|$ is just equal to the yield stress τ_0 at $x = \pm x_0$, where x_0 is defined by

$$\tau_0 = \frac{\mathcal{P}_0 - \mathcal{P}_L}{L} x_0 \quad (8B.5-2)$$

(a) Show that the upper equation of Eq. 8B.5-1 requires that $dv_z/dx = 0$ for $|x| \leq x_0$, since $\tau_{xz} = -\eta dv_z/dx$ and τ_{xz} is finite; this is then the "plug-flow" region. Then show that, since for x positive, $\dot{\gamma} = -dv_z/dx$, and for x negative, $\dot{\gamma} = +dv_z/dx$, the lower equation of Eq. 8.3-5 requires that

$$\tau_{xz} = \begin{cases} -\mu_0(dv_z/dx) + \tau_0 & \text{for } +x_0 \leq x \leq +B \\ -\mu_0(dv_z/dx) - \tau_0 & \text{for } -B \leq x \leq -x_0 \end{cases} \quad (8B.5-3)$$

(b) To get the velocity distribution for $+x_0 \leq x \leq +B$, substitute the upper relation from Eq. 8B.5-3 into Eq. 2B.3-1 and get the differential equation for v_z . Show that this may be integrated with the boundary condition that the velocity is zero at $x = B$ to give

$$v_z = \frac{(\mathcal{P}_0 - \mathcal{P}_L)B^2}{2\mu_0 L} \left[1 - \left(\frac{x}{B} \right)^2 \right] - \frac{\tau_0 B}{\mu_0} \left(1 - \frac{x}{B} \right) \quad \text{for } +x_0 \leq x \leq +B \quad (8B.5-4)$$

What is the velocity in the range $|x| \leq x_0$? Draw a sketch of $v_z(x)$.

(c) The mass flow rate can then be obtained from

$$w = W\rho \int_{-B}^{+B} v_z dx = 2W\rho \int_0^B v_z dx = 2W\rho \int_{x_0}^B x \left(-\frac{dv_z}{dx} \right) dx \quad (8B.5-5)$$

¹ E. C. Bingham, *Fluidity and Plasticity*, McGraw-Hill, New York (1922), pp. 215–218. See R. B. Bird, G. C. Dai, and B. J. Yarusso, *Reviews in Chemical Engineering*, 1, 1–70 (1982) for a review of models with a yield stress.

The integration by parts allows the integration to be done more easily. Show that the final result is

$$w = \frac{2}{3} \frac{(\mathcal{P}_0 - \mathcal{P}_L)WB^3\rho}{\mu_0 L} \left[1 - \frac{3}{2} \left(\frac{\tau_0 L}{(\mathcal{P}_0 - \mathcal{P}_L)B} \right) + \frac{1}{2} \left(\frac{\tau_0 L}{(\mathcal{P}_0 - \mathcal{P}_L)B} \right)^3 \right] \quad (8B.5-6)$$

Verify that, when the yield stress goes to zero, this result simplifies to the Newtonian fluid result in Problem 2B.3.

- 8B.6 Derivation of the Buckingham–Reiner equation.²** Rework Example 8.3-1 for the Bingham model. First find the velocity distribution. Then show that the mass rate of flow is given by

$$w = \frac{\pi(\mathcal{P}_0 - \mathcal{P}_L)R^4\rho}{8\mu_0 L} \left[1 - \frac{4}{3} \left(\frac{\tau_0}{\tau_R} \right) + \frac{1}{3} \left(\frac{\tau_0}{\tau_R} \right)^4 \right] \quad (8B.6-1)$$

in which $\tau_R = (\mathcal{P}_0 - \mathcal{P}_L)R/2L$ is the shear stress at the tube wall. This expression is valid only when $\tau_R \geq \tau_0$.

- 8B.7 The complex-viscosity components for the Jeffreys fluid.**

(a) Work Example 8.4-1 for the Jeffreys model of Eq. 8.4-4, and show that the results are Eqs. 8.5-12 and 13. How are these results related to Eqs. (G) and (H) of Table 8.5-1?

(b) Obtain the complex-viscosity components for the Jeffreys model by using the superposition suggested in fn. 3 of §8.4.

- 8B.8 Stress relaxation after cessation of shear flow.** A viscoelastic fluid is in steady-state flow between a pair of parallel plates, with $v_x = \dot{\gamma}y$. If the flow is suddenly stopped (i.e., $\dot{\gamma}$ becomes zero), the stresses do not go to zero as would be the case for a Newtonian fluid. Explore this *stress relaxation* phenomenon using a 3-constant Oldroyd model (Eq. 8.5-3 with $\lambda_2 = \mu_2 = \mu_1 = \mu_0 = 0$).

(a) Show that in steady-state flow

$$\tau_{yx} = -\eta_0 \dot{\gamma} \frac{1}{1 + (\lambda_1 \dot{\gamma})^2} \quad (8B.8-1)$$

To what extent does this expression agree with the experimental data in Fig. 8.2-4?

(b) By using Example 8.5-1 (part a) show that, if the flow is stopped at $t = 0$, the shear stress for $t \geq 0$ will be

$$\tau_{yx} = -\eta_0 \dot{\gamma} \frac{1}{1 + (\lambda_1 \dot{\gamma})^2} e^{-t/\lambda_1} \quad (8B.8-2)$$

This shows why λ_1 is called the “relaxation time.” This relaxation of stresses after the fluid motion has stopped is characteristic of viscoelastic materials.

(c) What is the normal stress τ_{xx} during steady shear flow and after cessation of the flow?

- 8B.9 Draining of a tank with an exit pipe** (Fig. 7B.9). Rework Problem 7B.9(a) for the power law fluid.

- 8B.10 The Giesekus model.**

(a) Use the results in Table 8.5-1 to get the limiting values for the non-Newtonian viscosity and the normal stress differences as the shear rate goes to zero.

(b) Find the limiting expressions for the non-Newtonian viscosity and the two normal-stress coefficients in the limit as the shear rate becomes infinitely large.

(c) What is the steady-state elongational viscosity in the limit that the elongation rate tends to zero? Show that the elongational viscosity has a finite limit as the elongation rate goes to infinity.

² E. Buckingham, *Proc. ASTM*, **21**, 1154–1161 (1921); M. Reiner, *Deformation and Flow*, Lewis, London (1949).

8C.1 The cone-and-plate viscometer (Fig. 2B.11).³ Review the Newtonian analysis of the cone-and-plate instrument in Problem 2B.11 and then do the following:

(a) Show that the shear rate $\dot{\gamma}$ is uniform throughout the gap and equal to $\dot{\gamma} = -\dot{\gamma}_{\theta\phi} = \Omega/\psi_0$. Because of the uniformity of $\dot{\gamma}$, the components of the stress tensor are also constant throughout the gap.

(b) Show that the non-Newtonian viscosity is then obtained from measurements of the torque T_z and rotation speed Ω by using

$$\eta(\dot{\gamma}) = \frac{3T_z\psi_0}{2\pi R^3\Omega} \quad (8C.1-1)$$

(c) Show that for the cone-and-plate system the radial component of the equation of motion is

$$0 = -\frac{\partial p}{\partial r} - \frac{1}{r^2} \frac{\partial}{\partial r} (r^2 \tau_{rr}) + \frac{\tau_{00} - \tau_{\phi\phi}}{r} \quad (8C.1-2)$$

if the centrifugal force term $-\rho\dot{\phi}^2/r$ can be neglected. Rearrange this to get

$$0 = -\partial\pi_{rr}/\partial \ln r + (\tau_{\phi\phi} - \tau_{00}) + 2(\tau_{00} - \tau_{rr}) \quad (8C.1-3)$$

Then introduce the normal stress coefficients, and use the result of (a) to replace $\partial\pi_{rr}/\partial \ln r$ by $\partial\pi_{\theta\theta}/\partial \ln r$, to get

$$\partial\pi_{\theta\theta}/\partial \ln r = -(\Psi_1 + 2\Psi_2)\dot{\gamma}^2 \quad (8C.1-4)$$

Integrate this from r to R and use the boundary condition $\pi_{rr}(R) = p_a$ to get

$$\begin{aligned} \pi_{\theta\theta}(r) &= \pi_{\theta\theta}(R) - (\Psi_1 + 2\Psi_2)\dot{\gamma}^2 \ln(r/R) \\ &= p_a - \Psi_2\dot{\gamma}^2 - (\Psi_1 + 2\Psi_2)\dot{\gamma}^2 \ln(r/R) \end{aligned} \quad (8C.1-5)$$

in which p_a is the atmospheric pressure acting on the fluid at the rim of the cone-and-plate instrument.

(d) Show that the total thrust in the z direction exerted by the fluid on the cone is

$$F_z = \int_0^{2\pi} \int_0^R [\pi_{\theta\theta}(r) - p_a] r dr d\theta = \frac{1}{2}\pi R^2 \Psi_1 \dot{\gamma}^2 \quad (8C.1-6)$$

From this one can obtain the first normal-stress coefficient by measuring the force that the fluid exerts.

(e) Suggest a method for measuring the second normal-stress coefficient using results in part (c) if small pressure transducers are flush-mounted in the plate at several different radial locations.

8C.2 Squeezing flow between parallel disks (Fig. 3C.1).⁴ Rework Problem 3C.1(g) for the power law fluid. This device can be useful for determining the power law parameters for materials that are highly viscous. Show that the power law analog of Eq. 3C.1-16 is

$$\frac{1}{H_0^{(n+1)/n}} = \frac{1}{H_0^{(n+1)/n}} + \frac{2(n+1)}{2n+1} \left(\frac{n+3}{\pi m R^{n+3}} \right)^{1/n} F_0^{1/n} t \quad (8C.2-1)$$

³ R. B. Bird, R. C. Armstrong, and O. Hassager, *Dynamics of Polymeric Liquids*, Vol. 1, *Fluid Mechanics*, Wiley-Interscience, New York, 2nd Edition (1987), pp. 521–524.

⁴ P. J. Leider, *Ind. Eng. Chem. Fundam.*, **13**, 342–346 (1974); R. J. Grimm, *AIChE Journal*, **24**, 427–439 (1978).

8C.3 Verification of Giesekus viscosity function.⁵

(a) To check the shear-flow entries in Table 8.5-1, introduce dimensionless stress tensor components $T_{ij} = (\lambda / \eta_0) \tau_{ij}$ and a dimensionless shear rate $\dot{\Gamma} = \lambda \dot{\gamma}$, and then show that for steady-state shear flow Eq. 8.5-4 becomes

$$T_{xx} - 2\dot{\Gamma}T_{yx} - \alpha(T_{xx}^2 + T_{yx}^2) = 0 \quad (8C.3-1)$$

$$T_{yy} - \alpha(T_{yx}^2 + T_{yy}^2) = 0 \quad (8C.3-2)$$

$$T_{yx} - \dot{\Gamma}T_{yy} - \alpha T_{yx}(T_{xx} + T_{yy}) = -\dot{\Gamma} \quad (8C.3-3)$$

There is also a fourth equation, which leads to $T_{zz} = 0$.

(b) Rewrite these equations in terms of the dimensionless normal-stress differences $N_1 = T_{xx} - T_{yy}$ and $N_2 = T_{yy} - T_{zz}$, and T_{yx} .

(c) It is difficult to solve the equations in (b) to get the dimensionless shear stress and normal-stress differences in terms of the dimensionless shear rate. Instead, solve for N_1 , T_{yx} , and $\dot{\Gamma}$ as functions of N_2 :

$$T_{yx}^2 = \frac{N_2(1 - \alpha N_2)}{\alpha} \quad (8C.3-4)$$

$$N_1 = -\frac{2N_2(1 - \alpha N_2)}{\alpha(1 - N_2)} \quad (8C.3-5)$$

$$\dot{\Gamma}^2 = \frac{N_2(1 - \alpha N_2)[1 + (1 - 2\alpha)N_2]^2}{\alpha(1 - N_2)^4} \quad (8C.3-6)$$

(d) Solve the last equation for N_2 as a function of $\dot{\Gamma}$ to get

$$N_2 = f(\chi) = (1 - \chi) / [1 + (1 - 2\alpha)\chi] \quad (8C.3-7)$$

where

$$\chi^2 = \frac{\sqrt{1 + 16\alpha(1 - \alpha)\dot{\Gamma}^2} - 1}{8\alpha(1 - \alpha)\dot{\Gamma}^2} = 1 - 4\alpha(1 - \alpha)\dot{\Gamma}^2 + \dots \quad (8C.3-8)$$

Then get the expression for the non-Newtonian viscosity and plot the curve of $\eta(\dot{\gamma})$.

8C.4 Tube Flow for the Oldroyd 6-Constant Model. Find the mass flow rate for the steady flow in a long circular tube⁶ using Eq. 8.5-3.

8C.5 Chain Models with Rigid-Rod Connectors. Read and discuss the following publications: M. Gottlieb, *Computers in Chemistry*, **1**, 155–160 (1977); O. Hassager, *J. Chem. Phys.*, **60**, 2111–2124 (1974); X. J. Fan and T. W. Liu, *J. Non-Newtonian Fluid Mech.*, **19**, 303–321 (1986); T. W. Liu, *J. Chem. Phys.*, **90**, 5826–5842 (1989); H. H. Saab, R. B. Bird, and C. F. Curtiss, *J. Chem. Phys.*, **77**, 4758–4766 (1982); J. D. Schieber, *J. Chem. Phys.*, **87**, 4917–4927, 4928–4936 (1987). Why are rodlike connectors more difficult to handle than springs? What kinds of problems can be solved by computer simulations?

⁵ H. Giesekus, *J. Non-Newtonian Fluid Mech.*, **11**, 69–109 (1982).

⁶ M. C. Williams and R. B. Bird, *AIChE Journal*, **8**, 378–382 (1962).

Part Two

Energy Transport

Thermal Conductivity and the Mechanisms of Energy Transport

- §9.1 Fourier's law of heat conduction (molecular energy transport)
- §9.2 Temperature and pressure dependence of heat conductivity
- §9.3^o Theory of thermal conductivity of gases at low density
- §9.4^o Theory of thermal conductivity of liquids
- §9.5^o Thermal conductivity of solids
- §9.6^o Effective thermal conductivity of composite solids
- §9.7 Convective transport of energy
- §9.8 Work associated with molecular motions

It is common knowledge that some materials such as metals conduct heat readily, whereas others such as wood act as thermal insulators. The physical property that describes the rate at which heat is conducted is the thermal conductivity k .

Heat conduction in fluids can be thought of as *molecular energy transport*, inasmuch as the basic mechanism is the motion of the constituent molecules. Energy can also be transported by the bulk motion of a fluid, and this is referred to as *convective energy transport*; this form of transport depends on the density ρ of the fluid. Another mechanism is that of *diffusive energy transport*, which occurs in mixtures that are interdiffusing. In addition, energy can be transmitted by means of *radiative energy transport*, which is quite distinct in that this form of transport does not require a material medium as do conduction and convection. This chapter introduces the first two mechanisms, conduction and convection. Radiation is treated separately in Chapter 16, and the subject of diffusive heat transport arises in §19.3 and again in §24.2.

We begin in §9.1 with the definition of the thermal conductivity k by Fourier's law for the heat flux vector \mathbf{q} . In §9.2 we summarize the temperature and pressure dependence of k for fluids by means of the principle of corresponding states. Then in the next four sections we present information about thermal conductivities of gases, liquids, solids, and solid composites, giving theoretical results when available.

Since in Chapters 10 and 11 we will be setting up problems by using the law of conservation of energy, we need to know not only how *heat* moves into and out of a system but also how *work* is done on or by a system by means of molecular mechanisms. The nature of the molecular work terms is discussed in §9.8. Finally, by combining the conductive heat flux, the convective energy flux, and the work flux we can create a *combined energy flux vector* \mathbf{e} , which is useful in setting up energy balances.

§9.1 FOURIER'S LAW OF HEAT CONDUCTION (MOLECULAR ENERGY TRANSPORT)

Consider a slab of solid material of area A located between two large parallel plates a distance Y apart. We imagine that initially (for time $t < 0$) the solid material is at a temperature T_0 throughout. At $t = 0$ the lower plate is suddenly brought to a slightly higher temperature T_1 and maintained at that temperature. As time proceeds, the temperature profile in the slab changes, and ultimately a linear steady-state temperature distribution is attained (as shown in Fig. 9.1-1). When this steady-state condition has been reached, a constant rate of heat flow Q through the slab is required to maintain the temperature difference $\Delta T = T_1 - T_0$. It is found then that for sufficiently small values of ΔT the following relation holds:

$$\frac{Q}{A} = k \frac{\Delta T}{Y} \quad (9.1-1)$$

That is, the rate of heat flow per unit area is proportional to the temperature decrease over the distance Y . The constant of proportionality k is the *thermal conductivity* of the slab. Equation 9.1-1 is also valid if a liquid or gas is placed between the two plates, provided that suitable precautions are taken to eliminate convection and radiation.

In subsequent chapters it is better to work with the above equation in differential form. That is, we use the limiting form of Eq. 9.1-1 as the slab thickness approaches zero. The local rate of heat flow per unit area (heat flux) in the positive y direction is designated by q_y . In this notation Eq. 9.1-1 becomes

$$q_y = -k \frac{dT}{dy} \quad (9.1-2)$$

This equation, which serves to define k , is the one-dimensional form of *Fourier's law of heat conduction*.^{1,2} It states that the heat flux by conduction is proportional to the temper-

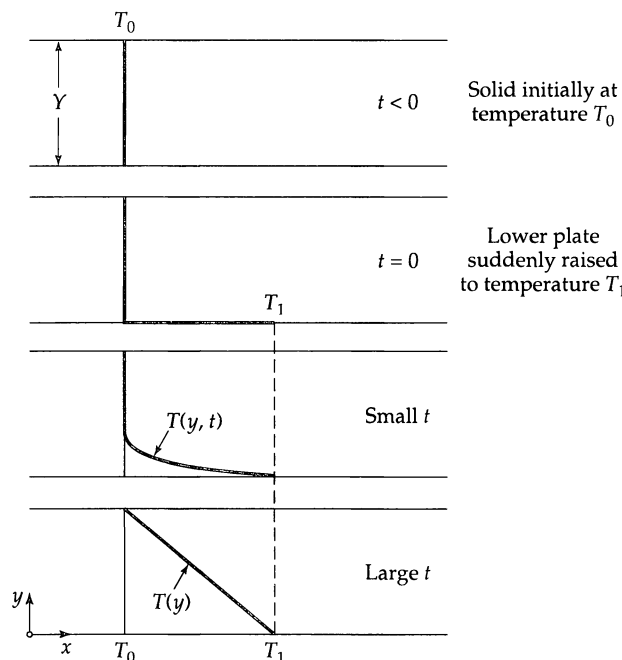


Fig. 9.1-1. Development of the steady-state temperature profile for a solid slab between two parallel plates. See Fig. 1.1-1 for the analogous situation for momentum transport.

ture gradient, or, to put it pictorially, "heat slides downhill on the temperature versus distance graph." Actually Eq. 9.1-2 is not really a "law" of nature, but rather a suggestion, which has proven to be a very useful empiricism. However, it does have a theoretical basis, as discussed in Appendix D.

If the temperature varies in all three directions, then we can write an equation like Eq. 9.1-2 for each of the coordinate directions:

$$q_x = -k \frac{\partial T}{\partial x} \quad q_y = -k \frac{\partial T}{\partial y} \quad q_z = -k \frac{\partial T}{\partial z} \quad (9.1-3, 4, 5)$$

If each of these equations is multiplied by the appropriate unit vector and the equations are then added, we get

$$\mathbf{q} = -k \nabla T \quad (9.1-6)$$

which is the three-dimensional form of Fourier's law. This equation describes the molecular transport of heat in isotropic media. By "isotropic" we mean that the material has no preferred direction, so that heat is conducted with the same thermal conductivity k in all directions.

Some solids, such as single noncubic crystals, fibrous materials, and laminates, are anisotropic.³ For such substances one has to replace Eq. 9.1-6 by

$$\mathbf{q} = -[\boldsymbol{\kappa} \cdot \nabla T] \quad (9.1-7)$$

in which $\boldsymbol{\kappa}$ is a symmetric second-order tensor called the *thermal conductivity tensor*. Thus, the heat flux vector does not point in the same direction as the temperature gradient. For polymeric liquids in the shearing flow $v_x(y, t)$, the thermal conductivity may increase above the equilibrium value by 20% in the x direction and decrease by 10% in the z direction. Anisotropic heat conduction in packed beds is discussed briefly in §9.6.

¹ J. B. Fourier, *Théorie analytique de la chaleur*, *Œuvres de Fourier*, Gauthier-Villars et Fils, Paris (1822). (Baron) Jean-Baptiste-Joseph Fourier (pronounced "Foo-ree-ay") (1768–1830) was not only a brilliant mathematician and the originator of the Fourier series and the Fourier transform, but also famous as an Egyptologist and a political figure (he was prefect of the province of Isère).

² Some authors prefer to write Eq. 9.1-2 in the form

$$q_y = -J_e k \frac{dT}{dy} \quad (9.1-2a)$$

in which J_e is the "mechanical equivalent of heat," which displays explicitly the conversion of thermal units into mechanical units. For example, in the c.g.s. system one would use the following units: $q_y [=]$ erg/cm²·s, $k [=]$ cal/cm·s·C, $T [=]$ C, $y [=]$ cm, and $J_e [=]$ erg/cal. We will not use Eq. 9.1-2a in this book.

³ Although polymeric liquids at rest are isotropic, kinetic theory suggests that when they are flowing the heat conduction is anisotropic [see B. H. A. A. van den Brule, *Rheol. Acta*, **28**, 257–266 (1989); and C. F. Curtiss and R. B. Bird, *Advances in Polymer Science*, **25**, 1–101 (1996)]. Experimental measurements for shear and elongational flows have been reported by D. C. Venerus, J. D. Schieber, H. Iddir, J. D. Guzman, and A. W. Broerman, *Phys. Rev. Letters*, **82**, 366–369 (1999); A. W. Broerman, D. C. Venerus, and J. D. Schieber, *J. Chem. Phys.*, **111**, 6965–6969 (1999); H. Iddir, D. C. Venerus, and J. D. Schieber, *AIChE Journal*, **46**, 610–615 (2000). For oriented polymer solids, enhanced thermal conductivity in the direction of orientation has been measured by B. Poulaert, J.-C. Chielens, C. Vandenhende, J.-P. Issi, and R. Legras, *Polymer Comm.*, **31**, 148–151 (1989). In connection with the bead spring models of polymer thermal conductivity, it has been shown by R. B. Bird, C. F. Curtiss, and K. J. Beers [*Rheol. Acta*, **36**, 269–276 (1997)] that the predicted thermal conductivity is exceedingly sensitive to the form of the potential energy used for describing the springs.

Another possible generalization of Eq. 9.1-6 is to include a term containing the time derivative of \mathbf{q} multiplied by a time constant, by analogy with the Maxwell model of linear viscoelasticity in Eq. 8.4-3. There seems to be little experimental evidence that such a generalization is warranted.⁴

The reader will have noticed that Eq. 9.1-2 for heat conduction and Eq. 1.1-2 for viscous flow are quite similar. In both equations the flux is proportional to the negative of the gradient of a macroscopic variable, and the coefficient of proportionality is a physical property characteristic of the material and dependent on the temperature and pressure. For the situations in which there is three-dimensional transport, we find that Eq. 9.1-6 for heat conduction and Eq. 1.2-7 for viscous flow differ in appearance. This difference arises because energy is a scalar, whereas momentum is a vector, and the heat flux \mathbf{q} is a vector with three components, whereas the momentum flux $\boldsymbol{\tau}$ is a second-order tensor with nine components. We can anticipate that the transport of energy and momentum will in general not be mathematically analogous except in certain geometrically simple situations.

In addition to the thermal conductivity k , defined by Eq. 9.1-2, a quantity known as the *thermal diffusivity* α is widely used. It is defined as

$$\alpha = \frac{k}{\rho \hat{C}_p} \quad (9.1-8)$$

Here \hat{C}_p is the heat capacity at constant pressure; the circumflex (\wedge) over the symbol indicates a quantity "per unit mass." Occasionally we will need to use the symbol \tilde{C}_p in which the tilde (\sim) over the symbol stands for a quantity "per mole."

The thermal diffusivity α has the same dimensions as the kinematic viscosity ν —namely, (length)²/time. When the assumption of constant physical properties is made, the quantities ν and α occur in similar ways in the equations of change for momentum and energy transport. Their ratio ν/α indicates the relative ease of momentum and energy transport in flow systems. This dimensionless ratio

$$\text{Pr} = \frac{\nu}{\alpha} = \frac{\hat{C}_p \mu}{k} \quad (9.1-9)$$

is called the *Prandtl number*.⁵ Another dimensionless group that we will encounter in subsequent chapters is the *Péclet number*,⁶ $\text{Pé} = \text{RePr}$.

The units that are commonly used for thermal conductivity and related quantities are given in Table 9.1-1. Other units, as well as the interrelations among the various systems, may be found in Appendix F.

Thermal conductivity can vary all the way from about 0.01 W/m · K for gases to about 1000 W/m · K for pure metals. Some experimental values of the thermal con-

⁴ The linear theory of thermoviscoelasticity does predict relaxation effects in heat conduction, as discussed by R. M. Christensen, *Theory of Viscoelasticity*, Academic Press, 2nd edition (1982). The effect has also been found from a kinetic theory treatment of the energy equation by R. B. Bird and C. F. Curtiss, *J. Non-Newtonian Fluid Mechanics*, **79**, 255–259 (1998).

⁵ This dimensionless group, named for Ludwig Prandtl, involves only the physical properties of the fluid.

⁶ Jean-Claude-Eugène Péclet (pronounced "Pay-clay" with the second syllable accented) (1793–1857) authored several books including one on heat conduction.

Table 9.1-1 Summary of Units for Quantities in Eqs. 9.1-2 and 9

	SI	c.g.s.	British
q_y	W/m^2	$\text{cal}/\text{cm}^2 \cdot \text{s}$	$\text{Btu}/\text{hr} \cdot \text{ft}^2$
T	K	C	F
y	m	cm	ft
k	$\text{W}/\text{m} \cdot \text{K}$	$\text{cal}/\text{cm} \cdot \text{s} \cdot \text{C}$	$\text{Btu}/\text{hr} \cdot \text{ft} \cdot \text{F}$
\hat{C}_p	$\text{J}/\text{K} \cdot \text{kg}$	$\text{cal}/\text{C} \cdot \text{g}$	$\text{Btu}/\text{F} \cdot \text{lb}_m$
α	m^2/s	cm^2/s	ft^2/s
μ	$\text{Pa} \cdot \text{s}$	$\text{g}/\text{cm} \cdot \text{s}$	$\text{lb}_m/\text{ft} \cdot \text{hr}$
Pr	—	—	—

Note: The watt (W) is the same as J/s, the joule (J) is the same as N · m, the newton (N) is kg · m/s², and the Pascal (Pa) is N/m². For more information on interconversion of units, see Appendix F.

ductivity of gases, liquids, liquid metals, and solids are given in Tables 9.1-2, 9.1-3, 9.1-4, and 9.1-5. In making calculations, experimental values should be used when possible. In the absence of experimental data, one can make estimates by using the methods outlined in the next several sections or by consulting various engineering handbooks.⁷

Table 9.1-2 Thermal Conductivities, Heat Capacities, and Prandtl Numbers of Some Common Gases at 1 atm Pressure^a

Gas	Temperature T (K)	Thermal conductivity k ($\text{W}/\text{m} \cdot \text{K}$)	Heat capacity \hat{C}_p ($\text{J}/\text{kg} \cdot \text{K}$)	Prandtl number Pr (—)
H_2	100	0.06799	11,192	0.682
	200	0.1282	13,667	0.724
	300	0.1779	14,316	0.720
O_2	100	0.00904	910	0.764
	200	0.01833	911	0.734
	300	0.02657	920	0.716
NO	200	0.01778	1015	0.781
	300	0.02590	997	0.742
CO_2	200	0.00950	734	0.783
	300	0.01665	846	0.758
CH_4	100	0.01063	2073	0.741
	200	0.02184	2087	0.721
	300	0.03427	2227	0.701

^a Taken from J. O. Hirschfelder, C. F. Curtiss, and R. B. Bird, *Molecular Theory of Gases and Liquids*, Wiley, New York, 2nd corrected printing (1964), Table 8.4-10. The k values are measured, the \hat{C}_p values are calculated from spectroscopic data, and μ is calculated from Eq. 1.4-18. The values of \hat{C}_p for H_2 represent a 3:1 ortho-para mixture.

⁷ For example, W. M. Rohsenow, J. P. Hartnett, and Y. I. Cho, eds., *Handbook of Heat Transfer*, McGraw-Hill, New York (1998); Landolt-Börnstein, *Zahlenwerte und Funktionen*, Vol. II, 5, Springer (1968–1969).

Table 9.1-3 Thermal Conductivities, Heat Capacities, and Prandtl Numbers for Some Nonmetallic Liquids at Their Saturation Pressures^a

Liquid	Temperature <i>T</i> (K)	Thermal conductivity <i>k</i> (W/m · K)	Viscosity $\mu \times 10^4$ (Pa · s)	Heat capacity $\hat{C}_p \times 10^{-3}$ (J/kg · K)	Prandtl number Pr (—)
1-Pentene	200	0.1461	6.193	1.948	8.26
	250	0.1307	3.074	2.070	4.87
	300	0.1153	1.907	2.251	3.72
CCl_4	250	0.1092	20.32	0.8617	16.0
	300	0.09929	8.828	0.8967	7.97
	350	0.08935	4.813	0.9518	5.13
$(\text{C}_2\text{H}_5)_2\text{O}$	250	0.1478	3.819	2.197	5.68
	300	0.1274	2.213	2.379	4.13
	350	0.1071	1.387	2.721	3.53
$\text{C}_2\text{H}_5\text{OH}$	250	0.1808	30.51	2.120	35.8
	300	0.1676	10.40	2.454	15.2
	350	0.1544	4.486	2.984	8.67
Glycerol	300	0.2920	7949	2.418	6580
	350	0.2977	365.7	2.679	329
	400	0.3034	64.13	2.940	62.2
H_2O	300	0.6089	8.768	4.183	6.02
	350	0.6622	3.712	4.193	2.35
	400	0.6848	2.165	4.262	1.35

^a The entries in this table were prepared from functions provided by T. E. Daubert, R. P. Danner, H. M. Sibul, C. C. Stebbins, J. L. Oscarson, R. L. Rowley, W. V. Wilding, M. E. Adams, T. L. Marshall, and N. A. Zundel, *DIPPR® Data Compilation of Pure Compound Properties*, Design Institute for Physical Property Data®, AIChE, New York, NY (2000).

EXAMPLE 9.1-1*Measurement of Thermal Conductivity*

A plastic panel of area $A = 1 \text{ ft}^2$ and thickness $Y = 0.252 \text{ in.}$ was found to conduct heat at a rate of 3.0 W at steady state with temperatures $T_0 = 24.00^\circ\text{C}$ and $T_1 = 26.00^\circ\text{C}$ imposed on the two main surfaces. What is the thermal conductivity of the plastic in $\text{cal}/\text{cm} \cdot \text{s} \cdot \text{K}$ at 25°C ?

SOLUTION

First convert units with the aid of Appendix F:

$$A = 144 \text{ in.}^2 \times (2.54)^2 = 929 \text{ cm}^2$$

$$Y = 0.252 \text{ in.} \times 2.54 = 0.640 \text{ cm}$$

$$Q = 3.0 \text{ W} \times 0.23901 = 0.717 \text{ cal/s}$$

$$\Delta T = 26.00 - 24.00 = 2.00 \text{ K}$$

Substitution into Eq. 9.1-1 then gives

$$k = \frac{QY}{A\Delta T} = \frac{0.717 \times 0.640}{929 \times 2} = 2.47 \times 10^{-4} \text{ cal/cm} \cdot \text{s} \cdot \text{K} \quad (9.1-20)$$

For ΔT as small as 2 degrees C, it is reasonable to assume that the value of k applies at the average temperature, which in this case is 25°C . See Problem 10B.12 and 10C.1 for methods of accounting for the variation of k with temperature.

Table 9.1-4 Thermal Conductivities, Heat Capacities, and Prandtl Numbers of Some Liquid Metals at Atmospheric Pressure^a

Metal	Temperature \bar{T} (K)	Thermal conductivity k (W/m · K)	Heat capacity \bar{C}_p (J/kg · K)	Prandtl number ^c Pr (—)
Hg	273.2	8.20	140.2	0.0288
	373.2	10.50	137.2	0.0162
	473.2	12.34	156.9	0.0116
Pb	644.2	15.9	15.9	0.024
	755.2	15.5	15.5	0.017
	977.2	15.1	14.6 ^b	0.013 ^b
Bi	589.2	16.3	14.4	0.0142
	811.2	15.5	15.4	0.0110
	1033.2	15.5	16.4	0.0083
Na	366.2	86.2	13.8	0.011
	644.2	72.8	13.0	0.0051
	977.2	59.8	12.6	0.0037
K	422.2	45.2	795	0.0066
	700.2	39.3	753	0.0034
	977.2	33.1	753	0.0029
Na-K alloy ^c	366.2	25.5	1130	0.026
	644.2	27.6	1054	0.0091
	977.2	28.9	1042	0.0058

^a Data taken from *Liquid Metals Handbook*, 2nd edition, U.S. Government Printing Office, Washington, D.C. (1952), and from E. R. G. Eckert and R. M. Drake, Jr., *Heat and Mass Transfer*, McGraw-Hill, New York, 2nd edition (1959), Appendix A.

^b Based on an extrapolated heat capacity.

^c 56% Na by weight, 44% K by weight.

Table 9.1-5 Experimental Values of Thermal Conductivities of Some Solids^a

Substance	Temperature \bar{T} (K)	Thermal conductivity k (W/m · K)
Aluminum	373.2	205.9
	573.2	268
	873.2	423
Cadmium	273.2	93.0
	373.2	90.4
	291.2	384.1
Copper	373.2	379.9
	291.2	46.9
	373.2	44.8
Steel	273.2	63.93
	373.2	59.8
	—	63
Tin	273.2	92
Brick (common red)	—	1.7
Concrete (stone)	—	0.71
Graphite	—	5.0
Sand (dry)	—	0.389
Wood (fir)	—	0.126
parallel to axis	—	0.038

^a Data taken from the *Reactor Handbook*, Vol. 2, Atomic Energy Commission AECD-3646, U.S. Government Printing Office, Washington, D.C. (May 1955), pp. 1766 *et seq.*

§9.2 TEMPERATURE AND PRESSURE DEPENDENCE OF THERMAL CONDUCTIVITY

When thermal conductivity data for a particular compound cannot be found, one can make an estimate by using the corresponding-states chart in Fig. 9.2-1, which is based on thermal conductivity data for several monatomic substances. This chart, which is similar to that for viscosity shown in Fig. 1.3-1, is a plot of the reduced thermal conductivity $k_r = k/k_c$, which is the thermal conductivity at pressure p and temperature T divided by the thermal conductivity at the critical point. This quantity is plotted as a function of the reduced temperature $T_r = T/T_c$ and the reduced pressure $p_r = p/p_c$. Figure 9.2-1 is based on a limited amount of experimental data for monatomic substances, but may be used

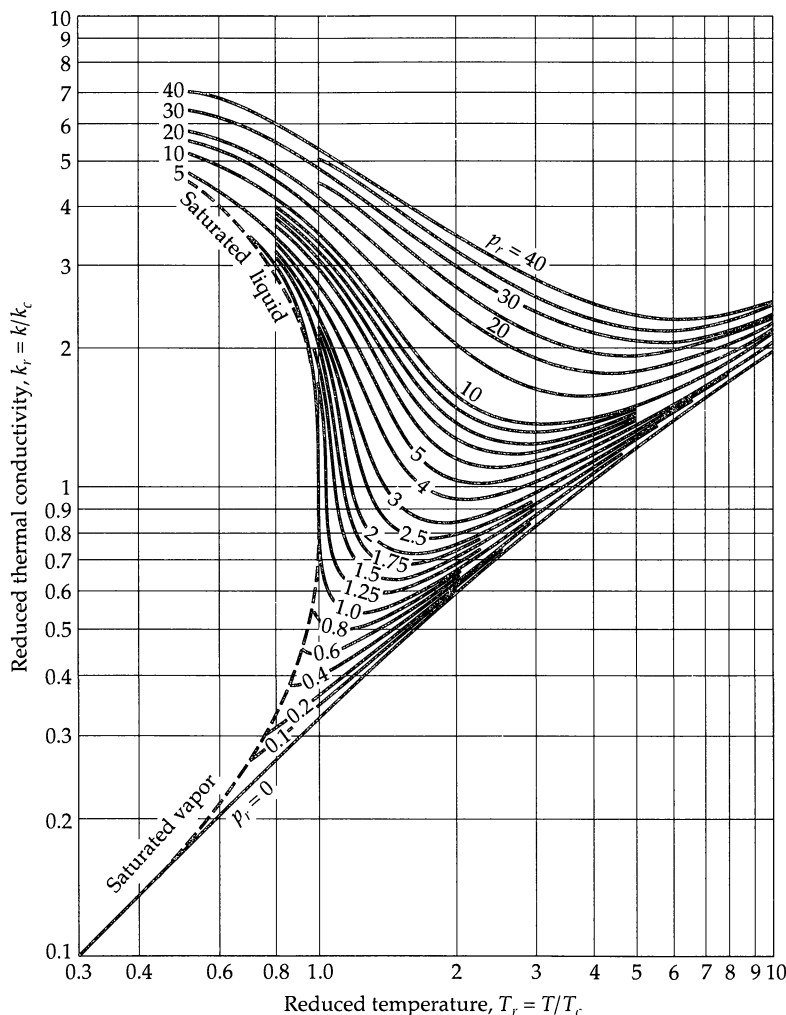


Fig. 9.2-1. Reduced thermal conductivity for monatomic substances as a function of the reduced temperature and pressure [E. J. Owens and G. Thodos, *AIChE Journal*, 3, 454–461 (1957)]. A large-scale version of this chart may be found in O. A. Hougen, K. M. Watson, and R. A. Ragatz, *Chemical Process Principles Charts*, 2nd edition, Wiley, New York (1960).

for rough estimates for polyatomic materials. It should *not* be used in the neighborhood of the critical point.¹

It can be seen that the thermal conductivity of a gas approaches a limiting function of T at low pressures; for most gases this limit is reached at about 1 atm pressure. The thermal conductivities of *gases* at low density *increase* with increasing temperature, whereas the thermal conductivities of most *liquids* *decrease* with increasing temperature. The correlation is less reliable in the liquid region; polar or associated liquids, such as water, may exhibit a maximum in the curve of k versus T . The main virtue of the corresponding-states chart is that one gets a global view of the behavior of the thermal conductivity of gases and liquids.

The quantity k_c may be estimated in one of two ways: (i) given k at a known temperature and pressure, preferably close to the conditions at which k is to be estimated, one can read k_r from the chart and compute $k_c = k/k_r$; or (ii) one can estimate a value of k in the low-density region by the methods given in §9.3 and the proceed as in (i). Values of k_c obtained by method (i) are given in Appendix E.

For mixtures, one might estimate the thermal conductivity by methods analogous to those described in §1.3. Very little is known about the accuracy of pseudocritical procedures as applied to thermal conductivity, largely because there are so few data on mixtures at elevated pressures.

EXAMPLE 9.2-1

Effect of Pressure on Thermal Conductivity

Estimate the thermal conductivity of ethane at 153°F and 191.9 atm from the experimental value² $k = 0.0159 \text{ Btu/hr} \cdot \text{ft} \cdot \text{F}$ at 1 atm and 153°F.

SOLUTION

Since a measured value of k is known, we use method (i). First we calculate p_r and T_r at the condition of the measured value:

$$T_r = \frac{153 + 460}{(1.8)(305.4)} = 1.115 \quad p_r = \frac{1}{48.2} = 0.021 \quad (9.2-1)$$

From Fig. 9.2-1 we read $k_r = 0.36$. Hence k_c is

$$k_c = \frac{k}{k_r} = \frac{0.0159}{0.36} = 0.0442 \text{ Btu/hr} \cdot \text{ft} \cdot \text{F} \quad (9.2-2)$$

At 153°F ($T_r = 1.115$) and 191.9 atm ($p_r = 3.98$), we read from the chart $k_r = 2.07$. The predicted thermal conductivity is then

$$k = k_r k_c = (2.07)(0.0422) = 0.0914 \text{ Btu/hr} \cdot \text{ft} \cdot \text{F} \quad (9.2-3)$$

An observed value of 0.0453 Btu/hr · ft · F has been reported.² The poor agreement shows that one should not rely heavily on this correlation for polyatomic substances nor for conditions near the critical point.

¹ In the vicinity of the critical point, where the thermal conductivity diverges, it is customary to write $k = k^b + \Delta k$, where k^b is the "background" contribution and Δk is the "critical enhancement" contribution. The k_c being used in the corresponding states correlation is the background contribution. For the behavior of transport properties near the critical point, see J. V. Sengers and J. Luettmer Strathmann, in *Transport Properties of Fluids* (J. H. Dymond, J. Millat, and C. A. Nieto de Castro, eds.), Cambridge University Press (1995); E. P. Sakonidou, H. R. van den Berg, C. A. ten Seldam, and J. V. Sengers, *J. Chem. Phys.*, **105**, 10535–10555 (1996) and **109**, 717–736 (1998).

² J. M. Lenoir, W. A. Junk, and E. W. Comings, *Chem. Eng. Progr.*, **49**, 539–542 (1949).

§9.3 THEORY OF THERMAL CONDUCTIVITY OF GASES AT LOW DENSITY

The thermal conductivities of dilute *monatomic* gases are well understood and can be described by the kinetic theory of gases at low density. Although detailed theories for *polyatomic* gases have been developed,¹ it is customary to use some simple approximate theories. Here, as in §1.5, we give a simplified mean free path derivation for monatomic gases, and then summarize the result of the Chapman–Enskog kinetic theory of gases.

We use the model of rigid, nonattracting spheres of mass m and diameter d . The gas as a whole is at rest ($\mathbf{v} = 0$), but the molecular motions must be accounted for.

As in §1.5, we use the following results for a rigid-sphere gas:

$$\bar{u} = \sqrt{\frac{8kT}{\pi m}} = \text{mean molecular speed} \quad (9.3-1)$$

$$Z = \frac{1}{4}n\bar{u} = \text{wall collision frequency per unit area} \quad (9.3-2)$$

$$\lambda = \frac{1}{\sqrt{2}\pi d^2 n} = \text{mean free path} \quad (9.3-3)$$

The molecules reaching any plane in the gas have had, on an average, their last collision at a distance a from the plane, where

$$a = \frac{2}{3}\lambda \quad (9.3-4)$$

In these equations k is the Boltzmann constant, n is the number of molecules per unit volume, and m is the mass of a molecule.

The only form of energy that can be exchanged in a collision between two smooth rigid spheres is translational energy. The mean translational energy per molecule under equilibrium conditions is

$$\frac{1}{2}m\bar{u}^2 = \frac{3}{2}kT \quad (9.3-5)$$

as shown in Prob. 1C.1. For such a gas, the molar heat capacity at constant volume is

$$\tilde{C}_V = \left(\frac{\partial \tilde{U}}{\partial T} \right)_V = \tilde{N} \frac{d}{dT} (\frac{1}{2}m\bar{u}^2) = \frac{3}{2}R \quad (9.3-6)$$

in which R is the gas constant. Equation 9.3-6 is satisfactory for monatomic gases up to temperatures of several thousand degrees.

To determine the thermal conductivity, we examine the behavior of the gas under a temperature gradient dT/dy (see Fig. 9.3-1). We assume that Eqs. 9.3-1 to 6 remain valid in this nonequilibrium situation, except that $\frac{1}{2}m\bar{u}^2$ in Eq. 9.3-5 is taken as the average kinetic energy for molecules that had their last collision in a region of temperature T . The heat flux q_y across any plane of constant y is found by summing the kinetic energies of the molecules that cross the plane per unit time in the positive y direction and subtracting the kinetic energies of the equal number that cross in the negative y direction:

$$\begin{aligned} q_y &= Z(\frac{1}{2}m\bar{u}^2)|_{y-a} - \frac{1}{2}m\bar{u}^2|_{y+a}) \\ &= \frac{3}{2}kZ(T|_{y-a} - T|_{y+a}) \end{aligned} \quad (9.3-7)$$

¹ C. S. Wang Chang, G. E. Uhlenbeck, and J. de Boer, *Studies in Statistical Mechanics*, Wiley-Interscience, New York, Vol. II (1964), pp. 241–265; E. A. Mason and L. Monchick, *J. Chem. Phys.*, **35**, 1676–1697 (1961) and **36**, 1622–1639, 2746–2757 (1962); L. Monchick, A. N. G. Pereira, and E. A. Mason, *J. Chem. Phys.*, **42**, 3241–3256 (1965). For an introduction to the kinetic theory of the transport properties, see R. S. Berry, S. A. Rice, and J. Ross, *Physical Chemistry*, 2nd edition (2000), Chapter 28.

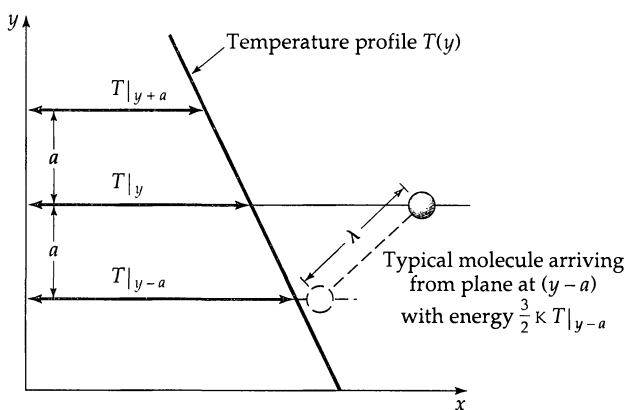


Fig. 9.3-1. Molecular transport of (kinetic) energy from plane at $(y - a)$ to plane at y .

Equation 9.3-7 is based on the assumption that all molecules have velocities representative of the region of their last collision and that the temperature profile $T(y)$ is linear for a distance of several mean free paths. In view of the latter assumption we may write

$$T|_{y-a} = T|_y - \frac{2}{3}\lambda \frac{dT}{dy} \quad (9.3-8)$$

$$T|_{y+a} = T|_y + \frac{2}{3}\lambda \frac{dT}{dy} \quad (9.3-9)$$

By combining the last three equations we get

$$q_y = -\frac{1}{2}nK\bar{u} \lambda \frac{dT}{dy} \quad (9.3-10)$$

This corresponds to Fourier's law of heat conduction (Eq. 9.1-2) with the thermal conductivity given by

$$k = \frac{1}{2}nK\bar{u}\lambda = \frac{1}{3}\rho\hat{C}_V\bar{u}\lambda \quad (\text{monatomic gas}) \quad (9.3-11)$$

in which $\rho = nm$ is the gas density, and $\hat{C}_V = \frac{3}{2}K/m$ (from Eq. 9.3-6).

Substitution of the expressions for \bar{u} and λ from Eqs. 9.3-1 and 3 then gives

$$k = \frac{\sqrt{mKT/\pi}}{\pi d^2} \frac{K}{m} = \frac{2}{3\pi} \frac{\sqrt{\pi mKT}}{\pi d^2} \hat{C}_V \quad (\text{monatomic gas}) \quad (9.3-12)$$

which is the thermal conductivity of a dilute gas composed of rigid spheres of diameter d . This equation predicts that k is independent of pressure. Figure 9.2-1 indicates that this prediction is in good agreement with experimental data up to about 10 atm for most gases. The predicted temperature dependence is too weak, as was the case for viscosity.

For a more accurate treatment of the monatomic gas, we turn again to the rigorous Chapman-Enskog treatment discussed in §1.5. The Chapman-Enskog formula² for the thermal conductivity of a monatomic gas at low density and temperature T is

$$k = \frac{25}{32} \frac{\sqrt{\pi mKT}}{\pi \sigma^2 \Omega_k} \hat{C}_V \quad \text{or} \quad k = 1.9891 \times 10^{-4} \frac{\sqrt{T/M}}{\sigma^2 \Omega_k} \quad (\text{monatomic gas}) \quad (9.3-13)$$

In the second form of this equation, $k [=] \text{cal/cm} \cdot \text{s} \cdot \text{K}$, $T [=] \text{K}$, $\sigma [=] \text{\AA}$, and the "collision integral" for thermal conductivity, Ω_k , is identical to that for viscosity, Ω_μ , in §1.4.

² J. O. Hirschfelder, C. F. Curtiss, and R. B. Bird, *Molecular Theory of Gases and Liquids*, Wiley, New York, 2nd corrected printing (1964), p. 534.

Values of $\Omega_k = \Omega_\mu$ are given for the Lennard-Jones intermolecular potential in Table E.2 as a function of the dimensionless temperature kT/ε . Equation 9.3-13, together with Table E.2, has been found to be remarkably accurate for predicting thermal conductivities of *monatomic* gases when the parameters σ and ε deduced from viscosity measurements are used (that is, the values given in Table E.1).

Equation 9.3-13 is very similar to the corresponding viscosity formula, Eq. 1.4-14. From these two equations we can then get

$$k = \frac{15}{4} \frac{R}{M} \mu = \frac{5}{2} \hat{C}_V \mu \quad (\text{monatomic gas}) \quad (9.3-14)$$

The simplified rigid-sphere theory (see Eqs. 1.4-8 and 9.3-11) gives $k = \hat{C}_V \mu$ and is thus in error by a factor 2.5. This is not surprising in view of the many approximations that were made in the simple treatment.

So far we have discussed only *monatomic* gases. We know from the discussion in §0.3 that, in binary collisions between diatomic molecules, there may be interchanges between kinetic and internal (i.e., vibrational and rotational) energy. Such interchanges are not taken into account in the Chapman-Enskog theory for monatomic gases. It can therefore be anticipated that the Chapman-Enskog theory will not be adequate for describing the thermal conductivity of polyatomic molecules.

A simple semiempirical method of accounting for the energy exchange in polyatomic gases was developed by Eucken.³ His equation for thermal conductivity of a polyatomic gas at low density is

$$k = \left(\hat{C}_p + \frac{5}{4} \frac{R}{M} \right) \mu \quad (\text{polyatomic gas}) \quad (9.3-15)$$

This *Eucken formula* includes the monatomic formula (Eq. 9.3-14) as a special case, because $\hat{C}_p = \frac{5}{2}(R/M)$ for monatomic gases. Hirschfelder⁴ obtained a formula similar to that of Eucken by using multicomponent-mixture theory (see Example 19.4-4). Other theories, correlations, and empirical formulas are also available.^{5,6}

Equation 9.3-15 provides a simple method for estimating the Prandtl number, defined in Eq. 9.1-8:

$$\Pr = \frac{\hat{C}_p \mu}{k} = \frac{\tilde{C}_p}{\tilde{C}_p + \frac{5}{4}R} \quad (\text{polyatomic gas}) \quad (9.3-16)$$

This equation is fairly satisfactory for nonpolar polyatomic gases at low density, as can be seen in Table 9.3-1; it is less accurate for polar molecules.

The thermal conductivities for gas mixtures at low density may be estimated by a method⁷ analogous to that previously given for viscosity (see Eqs. 1.4-15 and 16):

$$k_{\text{mix}} = \sum_{\alpha=1}^N \frac{x_\alpha k_\alpha}{\sum_\beta x_\beta \Phi_{\alpha\beta}} \quad (9.3-17)$$

The x_α are the mole fractions, and the k_α are the thermal conductivities of the pure chemical species. The coefficients $\Phi_{\alpha\beta}$ are identical to those appearing in the viscosity equation

³ A. Eucken, *Physik. Z.*, **14**, 324–333 (1913); “Eucken” is pronounced “Oy-ken.”

⁴ J. O. Hirschfelder, *J. Chem. Phys.*, **26**, 274–281, 282–285 (1957).

⁵ J. H. Ferziger and H. G. Kaper, *Mathematical Theory of Transport Processes in Gases*, North-Holland, Amsterdam (1972).

⁶ R. C. Reid, J. M. Prausnitz, and B. E. Poling, *The Properties of Gases and Liquids*, McGraw-Hill, New York, 4th edition (1987).

⁷ E. A. Mason and S. C. Saxena, *Physics of Fluids*, **1**, 361–369 (1958). Their method is an approximation to a more accurate method given by J. O. Hirschfelder, *J. Chem. Phys.*, **26**, 274–281, 282–285 (1957). With Professor Mason’s approval we have omitted here an empirical factor 1.065 in his Φ_{ij} expression for $i \neq j$ to establish self-consistency for mixtures of identical species.

Table 9.3-1 Predicted and Observed Values of the Prandtl Number for Gases at Atmospheric Pressure^a

Gas	T(K)	$\hat{C}_p \mu / k$ from Eq. 9.3-16	$\hat{C}_p \mu / k$ from observed values of \hat{C}_p , μ , and k
Ne ^b	273.2	0.667	0.66
Ar ^b	273.2	0.667	0.67
H ₂	90.6	0.68	0.68
	273.2	0.73	0.70
	673.2	0.74	0.65
N ₂	273.2	0.74	0.73
O ₂	273.2	0.74	0.74
Air	273.2	0.74	0.73
CO	273.2	0.74	0.76
NO	273.2	0.74	0.77
Cl ₂	273.2	0.76	0.76
H ₂ O	373.2	0.77	0.94
	673.2	0.78	0.90
CO ₂	273.2	0.78	0.78
SO ₂	273.2	0.79	0.86
NH ₃	273.2	0.77	0.85
C ₂ H ₄	273.2	0.80	0.80
C ₂ H ₆	273.2	0.83	0.77
CHCl ₃	273.2	0.86	0.78
CCl ₄	273.2	0.89	0.81

^a Calculated from values given by M. Jakob, *Heat Transfer*, Wiley, New York (1949), pp. 75–76.^b J. O. Hirschfelder, C. F. Curtiss, and R. B. Bird, *Molecular Theory of Gases and Liquids*, Wiley, New York, corrected printing (1964), p. 16.

(see Eq. 1.4-16). All values of k_α in Eq. 9.3-17 and μ_α in Eq. 1.4-16 are low-density values at the given temperature. If viscosity data are not available, they may be estimated from k and \hat{C}_p via Eq. 9.3-15. Comparisons with experimental data⁷ indicate an average deviation of about 4% for mixtures containing nonpolar polyatomic gases, including O₂, N₂, CO, C₂H₂, and CH₄.

EXAMPLE 9.3-1

Compute the thermal conductivity of Ne at 1 atm and 373.2K.

SOLUTION**Computation of the Thermal Conductivity of a Monatomic Gas at Low Density**

From Table E.1 the Lennard-Jones constants for neon are $\sigma = 2.789 \text{ \AA}$ and $\varepsilon/k = 35.7 \text{ K}$, and its molecular weight M is 20.183. Then, at 373.2K, we have $\kappa T/\varepsilon = 373.2/35.7 = 10.45$. From Table E.2 we find that $\Omega_k = \Omega_\mu = 0.821$. Substitution into Eq. 9.3-13 gives

$$\begin{aligned} k &= (1.9891 \times 10^{-4}) \frac{\sqrt{T/M}}{\sigma^2 \Omega_k} \\ &= (1.9891 \times 10^{-4}) \frac{\sqrt{(373.2)/(20.183)}}{(2.789)^2(0.821)} \\ &= 1.338 \times 10^{-4} \text{ cal/cm} \cdot \text{s} \cdot \text{K} \end{aligned} \quad (9.3-18)$$

A measured value of $1.35 \times 10^{-4} \text{ cal/cm} \cdot \text{s} \cdot \text{K}$ has been reported⁸ at 1 atm and 373.2K.⁸ W. G. Kannuluik and E. H. Carman, *Proc. Phys. Soc. (London)*, **65B**, 701–704 (1952).

EXAMPLE 9.3-2

Estimate the thermal conductivity of molecular oxygen at 300K and low pressure.

Estimation of the Thermal Conductivity of a Polyatomic Gas at Low Density

SOLUTION

The molecular weight of O₂ is 32.0000; its molar heat capacity \tilde{C}_p at 300°K and low pressure is 7.019 cal/g-mole · K. From Table E.1 we find the Lennard-Jones parameters for molecular oxygen to be $\sigma = 3.433 \text{ \AA}$ and $\varepsilon/k = 113\text{K}$. At 300K, then, $kT/\varepsilon = 300/113 = 2.655$. From Table E.2, we find $\Omega_\mu = 1.074$. The viscosity, from Eq. 1.4-18, is

$$\begin{aligned}\mu &= (2.6693 \times 10^{-5}) \frac{\sqrt{MT}}{\sigma^2 \Omega_\mu} \\ &= (2.6693 \times 10^{-5}) \frac{\sqrt{(32.00)(300)}}{(3.433)^2(1074)} \\ &= 2.065 \times 10^{-5} \text{ g/cm} \cdot \text{s}\end{aligned}\quad (9.3-19)$$

Then, from Eq. 9.3-15, the Eucken approximation to the thermal conductivity is

$$\begin{aligned}k &= (\tilde{C}_p + \frac{5}{4}R)(\mu/M) \\ &= (7.019 + 2.484)((2.065 \times 10^{-4})/(32.000)) \\ &= 6.14 \times 10^{-5} \text{ cal/cm} \cdot \text{s} \cdot \text{K}\end{aligned}\quad (9.3-20)$$

This compares favorably with the experimental value of $6.35 \times 10^{-5} \text{ cal/cm} \cdot \text{s} \cdot \text{K}$ in Table 9.1-1.

EXAMPLE 9.3-3

Prediction of the Thermal Conductivity of a Gas Mixture at Low Density

Predict the thermal conductivity of the following gas mixture at 1 atm and 293K from the given data on the pure components at the same pressure and temperature:

Species	α	Mole fraction x_α	Molecular weight M_α	$\mu_\alpha \times 10^7$ (g/cm · s)	$k_\alpha \times 10^7$ (cal/cm · s · K)
CO ₂	1	0.133	44.010	1462	383
O ₂	2	0.039	32.000	2031	612
N ₂	3	0.828	28.016	1754	627

SOLUTION

Use Eqs. 9.3-17 and 18. We note that the $\Phi_{\alpha\beta}$ for this gas mixture at these conditions have already been computed in the viscosity calculation in Example 1.5-2. In that example we evaluated the following summations, which also appear in Eq. 9.3-17:

$$\begin{array}{ccccc} \alpha \rightarrow & 1 & 2 & 3 \\ \sum_{\beta=1}^3 x_\beta \Phi_{\alpha\beta} & 0.763 & 1.057 & 1.049 \end{array}$$

Substitution in Eq. 9.3-17 gives

$$\begin{aligned}k_{\text{mix}} &= \sum_{\alpha=1}^N \frac{x_\alpha k_\alpha}{\sum_{\beta} x_\beta \Phi_{\alpha\beta}} \\ &= \frac{(0.133)(383)(10^{-7})}{0.763} + \frac{(0.039)(612)(10^{-7})}{1.057} + \frac{(0.828)(627)(10^{-7})}{1.049} \\ &= 584 \times (10^{-7}) \text{ cal/cm} \cdot \text{s} \cdot \text{K}\end{aligned}\quad (9.3-22)$$

No data are available for comparison at these conditions.

§9.4 THEORY OF THERMAL CONDUCTIVITY OF LIQUIDS

A very detailed kinetic theory for the thermal conductivity of monatomic liquids was developed a half-century ago,¹ but it has not yet been possible to implement it for practical calculations. As a result we have to use rough theories or empirical estimation methods.²

We choose to discuss here Bridgman's simple theory³ of energy transport in pure liquids. He assumed that the molecules are arranged in a cubic lattice, with a center-to-center spacing given by $(\tilde{V}/\tilde{N})^{1/3}$, in which \tilde{V}/\tilde{N} is the volume per molecule. He further assumed energy to be transferred from one lattice plane to the next at the sonic velocity v_s for the given fluid. The development is based on a reinterpretation of Eq. 9.3-11 of the rigid-sphere gas theory:

$$k = \frac{1}{3} \rho \hat{C}_V \bar{u} \lambda = \rho \hat{C}_V |\bar{u}_y| a \quad (9.4-1)$$

The heat capacity at constant volume of a monatomic liquid is about the same as for a solid at high temperature, which is given by the Dulong and Petit formula⁴ $\hat{C}_V = 3(\kappa/m)$. The mean molecular speed in the y direction, $|\bar{u}_y|$, is replaced by the sonic velocity v_s . The distance a that the energy travels between two successive collisions is taken to be the lattice spacing $(\tilde{V}/\tilde{N})^{1/3}$. Making these substitutions in Eq. 9.4-1 gives

$$k = 3(\tilde{N}/\tilde{V})^{2/3} \kappa v_s \quad (9.4-2)$$

which is *Bridgman's equation*. Experimental data show good agreement with Eq. 9.4-2, even for polyatomic liquids, but the numerical coefficient is somewhat too high. Better agreement is obtained if the coefficient is changed to 2.80:

$$k = 2.80(\tilde{N}/\tilde{V})^{2/3} \kappa v_s \quad (9.4-3)^5$$

This equation is limited to densities well above the critical density, because of the tacit assumption that each molecule oscillates in a "cage" formed by its nearest neighbors. The success of this equation for polyatomic fluids seems to imply that the energy transfer in collisions of polyatomic molecules is incomplete, since the heat capacity used here, $\hat{C}_V = 3(\kappa/m)$, is less than the heat capacities of polyatomic liquids.

The velocity of low-frequency sound is given (see Problem 11C.1) by

$$v_s = \sqrt{\frac{C_p}{C_V} \left(\frac{\partial p}{\partial \rho} \right)_T} \quad (9.4-4)$$

The quantity $(\partial p / \partial \rho)_T$ may be obtained from isothermal compressibility measurements or from an equation of state, and (C_p / C_V) is very nearly unity for liquids, except near the critical point.

¹ J. H. Irving and J. G. Kirkwood, *J. Chem. Phys.*, **18**, 817–829 (1950). This theory has been extended to polymeric liquids by C. F. Curtiss and R. B. Bird, *J. Chem. Phys.*, **107**, 5254–5267 (1997).

² R. C. Reid, J. M. Prausnitz, and B. E. Poling, *The Properties of Gases and Liquids*, McGraw-Hill, New York (1987); L. Riedel, *Chemie-Ing.-Techn.*, **27**, 209–213 (1955).

³ P. W. Bridgman, *Proc. Am. Acad. Arts and Sci.*, **59**, 141–169 (1923). Bridgman's equation is often misquoted, because he gave it in terms of a little-known gas constant equal to $\frac{3}{2}\kappa$.

⁴ This empirical equation has been justified, and extended, by A. Einstein [*Ann. Phys.* [4], **22**, 180–190 (1907)] and P. Debye [*Ann. Phys.*, [4] **39**, 789–839 (1912)].

⁵ Equation 9.4-3 is in approximate agreement with a formula derived by R. E. Powell, W. E. Roseveare, and H. Eyring, *Ind. Eng. Chem.*, **33**, 430–435 (1941).

EXAMPLE 9.4-1

Prediction of the Thermal Conductivity of a Liquid

The density of liquid CCl_4 at 20°C and 1 atm is 1.595 g/cm^3 , and its isothermal compressibility $(1/\rho)(\partial\rho/\partial p)_T$ is $90.7 \times 10^{-6} \text{ atm}^{-1}$. What is its thermal conductivity?

SOLUTION

First compute

$$\begin{aligned}\left(\frac{\partial p}{\partial \rho}\right)_T &= \frac{1}{\rho(1/\rho)(\partial\rho/\partial p)_T} = \frac{1}{(1.595)(90.7 \times 10^{-6})} = 6.91 \times 10^3 \text{ atm} \cdot \text{cm}^3/\text{g} \\ &= 7.00 \times 10^9 \text{ cm}^2/\text{s}^2 \text{ (using Appendix F)}\end{aligned}\quad (9.4-5)$$

Assuming that $C_p/C_V = 1.0$, we get from Eq. 9.4-4

$$v_s = \sqrt{(1.0)(7.00 \times 10^9)} = 8.37 \times 10^4 \text{ cm/s} \quad (9.4-6)$$

The molar volume is $\tilde{V} = M/\rho = 153.84/1.595 = 96.5 \text{ cm}^3/\text{g-mole}$. Substitution of these values in Eq. 9.4-3 gives

$$\begin{aligned}k &= 2.80(\tilde{N}/\tilde{V})^{2/3} Kv_s \\ &= 2.80\left(\frac{6.023 \times 10^{23}}{0.965 \times 10^2}\right)^{2/3} (1.3805 \times 10^{-16})(8.37 \times 10^4) \\ &= 1.10 \times 10^4 \text{ (cm}^{-2}\text{)(erg/K)(cm/s)} \\ &= 0.110 \text{ W/m} \cdot \text{K}\end{aligned}\quad (9.4-7)$$

The experimental value given in Table 9.1-2 is $0.103 \text{ W/m} \cdot \text{K}$.

§9.5 THERMAL CONDUCTIVITY OF SOLIDS

Thermal conductivities of solids have to be measured experimentally, since they depend on many factors that are difficult to measure or predict.¹ In crystalline materials, the phase and crystallite size are important; in amorphous solids the degree of molecular orientation has a considerable effect. In porous solids, the thermal conductivity is strongly dependent on the void fraction, the pore size, and the fluid contained in the pores. A detailed discussion of thermal conductivity of solids has been given by Jakob.²

In general, metals are better heat conductors than nonmetals, and crystalline materials conduct heat more readily than amorphous materials. Dry porous solids are very poor heat conductors and are therefore excellent for thermal insulation. The conductivities of most pure metals decrease with increasing temperature, whereas the conductivities of nonmetals increase; alloys show intermediate behavior. Perhaps the most useful of the rules of thumb is that thermal and electrical conductivity go hand in hand.

For pure metals, as opposed to alloys, the thermal conductivity k and the electrical conductivity k_e are related approximately³ as follows:

$$\frac{k}{k_e T} = L = \text{constant} \quad (9.5-1)$$

This is the *Wiedemann–Franz–Lorenz equation*; this equation can also be explained theoretically (see Problem 9A.6). The “Lorenz number” L is about 22 to $29 \times 10^{-9} \text{ volt}^2/\text{K}^2$ for

¹ A. Goldsmith, T. E. Waterman, and H. J. Hirschhorn, eds., *Handbook of Thermophysical Properties of Solids*, Macmillan, New York (1961).

² M. Jakob, *Heat Transfer*, Vol. 1, Wiley, New York (1949), Chapter 6. See also W. H. Rohsenow, J. P. Hartnett, and Y. I. Cho, eds., *Handbook of Heat Transfer*, McGraw-Hill, New York (1998).

³ G. Wiedemann and R. Franz, *Ann. Phys. u. Chemie*, **89**, 497–531 (1853); L. Lorenz, *Poggendorff's Annalen*, **147**, 429–452 (1872).

pure metals at 0°C and changes but little with temperatures above 0°C, increases of 10–20% per 1000°C being typical. At very low temperatures (−269.4°C for mercury) metals become superconductors of electricity but not of heat, and L thus varies strongly with temperature near the superconducting region. Equation 9.5-1 is of limited use for alloys, since L varies strongly with composition and, in some cases, with temperature.

The success of Eq. 9.5-1 for pure metals is due to the fact that free electrons are the major heat carriers in pure metals. The equation is not suitable for nonmetals, in which the concentration of free electrons is so low that energy transport by molecular motion predominates.

§9.6 EFFECTIVE THERMAL CONDUCTIVITY OF COMPOSITE SOLIDS

Up to this point we have discussed homogeneous materials. Now we turn our attention briefly to the thermal conductivity of two-phase solids—one solid phase dispersed in a second solid phase, or solids containing pores, such as granular materials, sintered metals, and plastic foams. A complete description of the heat transport through such materials is clearly extremely complicated. However, for steady conduction these materials can be regarded as homogeneous materials with an *effective thermal conductivity* k_{eff} , and the temperature and heat flux components are reinterpreted as the analogous quantities averaged over a volume that is large with respect to the scale of the heterogeneity but small with respect to the overall dimensions of the heat conduction system.

The first major contribution to the estimation of the conductivity of heterogeneous solids was by Maxwell.¹ He considered a material made of spheres of thermal conductivity k_1 embedded in a continuous solid phase with thermal conductivity k_0 . The volume fraction ϕ of embedded spheres is taken to be sufficiently small that the spheres do not “interact” thermally; that is, one needs to consider only the thermal conduction in a large medium containing only one embedded sphere. Then by means of a surprisingly simple derivation, Maxwell showed that for *small volume fraction* ϕ

$$\frac{k_{\text{eff}}}{k_0} = 1 + \frac{3\phi}{\left(\frac{k_1 + 2k_0}{k_1 - k_0}\right) - \phi} \quad (9.6-1)$$

(see Problems 11B.8 and 11C.5).

For *large volume fraction* ϕ , Rayleigh² showed that, if the spheres are located at the intersections of a cubic lattice, the thermal conductivity of the composite is given by

$$\frac{k_{\text{eff}}}{k_0} = 1 + \frac{3\phi}{\left(\frac{k_1 + 2k_0}{k_1 - k_0}\right) - \phi + 1.569\left(\frac{k_1 - k_0}{3k_1 - 4k_0}\right)\phi^{10/3} + \dots} \quad (9.6-2)$$

Comparison of this result with Eq. 9.6-1 shows that the interaction between the spheres is small, even at $\phi = \frac{1}{6}\pi$, the maximum possible value of ϕ for the cubic lattice arrangement. Therefore the simpler result of Maxwell is often used, and the effects of nonuniform sphere distribution are usually neglected.

¹ Maxwell's derivation was for electrical conductivity, but the same arguments apply for thermal conductivity. See J. C. Maxwell, *A Treatise on Electricity and Magnetism*, Oxford University Press, 3rd edition (1891, reprinted 1998), Vol. 1, §314; H. S. Carslaw and J. C. Jaeger, *Conduction of Heat in Solids*, Clarendon Press, Oxford, 2nd edition (1959), p. 428.

² J. W. Strutt (Lord Rayleigh), *Phil. Mag.* (5), **34**, 431–502 (1892).

For *nonspherical inclusions*, however, Eq. 9.6-1 does require modification. Thus for square arrays of long cylinders parallel to the z axis, Rayleigh² showed that the zz component of the thermal conductivity tensor κ is

$$\frac{\kappa_{\text{eff}, zz}}{k_0} = 1 + \left(\frac{k_1 - k_0}{k_0} \right) \phi \quad (9.6-3)$$

and the other two components are

$$\frac{\kappa_{\text{eff}, zz}}{k_0} = \frac{\kappa_{\text{eff}, yy}}{k_0} = 1 + \frac{2\phi}{\left(\frac{k_1 + k_0}{k_1 - k_0} \right) - \phi + \left(\frac{k_1 - k_0}{k_1 + k_0} \right) (0.30584\phi^4 + 0.013363\phi^8 + \dots)} \quad (9.6-4)$$

That is, the composite solid containing aligned embedded cylinders is anisotropic. The effective thermal conductivity tensor has been computed up to $O(\phi^2)$ for a medium containing spheroidal inclusions.³

For *complex nonspherical inclusions*, often encountered in practice, no exact treatment is possible, but some approximate relations are available.^{4,5,6} For simple unconsolidated granular beds the following expression has proven successful:

$$\frac{k_{\text{eff}}}{k_0} = \frac{(1 - \phi) + \alpha\phi(k_1/k_0)}{(1 - \phi) + \alpha\phi} \quad (9.6-5)$$

in which

$$\alpha = \frac{1}{3} \sum_{k=1}^3 \left[1 + \left(\frac{k_1}{k_0} - 1 \right) g_k \right]^{-1} \quad (9.6-6)$$

The g_k are “shape factors” for the granules of the medium,⁷ and they must satisfy $g_1 + g_2 + g_3 = 1$. For spheres $g_1 = g_2 = g_3 = \frac{1}{3}$, and Eq. 9.6-5 reduces to Eq. 9.6-1. For unconsolidated soils,⁵ $g_1 = g_2 = \frac{1}{8}$ and $g_3 = \frac{3}{4}$. The structure of consolidated porous beds—for example, sandstones—is considerably more complex. Some success is claimed for predicting the effective conductivity of such substances,^{4,6,8} but the generality of the methods is not yet known.

For *solids containing gas pockets*,⁹ thermal radiation (see Chapter 16) may be important. The special case of parallel planar fissures perpendicular to the direction of heat conduction is particularly important for high-temperature insulation. For such systems it may be shown that

$$\frac{k_{\text{eff}}}{k_0} = \frac{1}{1 - \phi + \left(\frac{k_1}{k_0\phi} + \frac{4\sigma T^3 L}{k_0} \right)^{-1}} \quad (9.6-7)$$

where σ is the Stefan–Boltzmann constant, k_1 is the thermal conductivity of the gas, and L is the total thickness of the material in the direction of the heat conduction. A modification of this equation for fissures of other shapes and orientations is available.⁷

³ S.-Y. Lu and S. Kim, *AIChE Journal*, **36**, 927–938 (1990).

⁴ V. I. Odelevskii, *J. Tech. Phys. (USSR)*, **24**, 667 and 697 (1954); F. Euler, *J. Appl. Phys.*, **28**, 1342–1346 (1957).

⁵ D. A. de Vries, *Mededelingen van de Landbouwhogeschool te Wageningen*, (1952); see also Ref. 6 and D. A. de Vries, Chapter 7 in *Physics of Plant Environment*, W. R. van Wijk, ed., Wiley, New York (1963).

⁶ W. Woodside and J. H. Messmer, *J. Appl. Phys.*, **32**, 1688–1699, 1699–1706 (1961).

⁷ A. L. Loeb, *J. Amer. Ceramic Soc.*, **37**, 96–99 (1954).

⁸ Sh. N. Plyat, *Soviet Physics JETP*, **2**, 2588–2589 (1957).

⁹ M. Jakob, *Heat Transfer*, Wiley, New York (1959), Vol. 1, §6.5.

For *gas-filled granular beds*^{6,9} a different type of complication arises. Since the thermal conductivities of gases are much lower than those of solids, most of the gas-phase heat conduction is concentrated near the points of contact of adjacent solid particles. As a result, the distances over which the heat is conducted through the gas may approach the mean free path of the gas molecules. When this is true, the conditions for the developments of §9.3 are violated, and the thermal conductivity of the gas decreases. Very effective insulators can thus be prepared from partially evacuated beds of fine powders.

Cylindrical ducts filled with granular materials through which a fluid is flowing (in the z direction) are of considerable importance in separation processes and chemical reactors. In such systems the effective thermal conductivities in the radial and axial directions are quite different and are designated¹⁰ by $\kappa_{\text{eff},rr}$ and $\kappa_{\text{eff},zz}$. Conduction, convection, and radiation all contribute to the flow of heat through the porous medium.¹¹ For highly turbulent flow, the energy is transported primarily by the tortuous flow of the fluid in the interstices of the granular material; this gives rise to a highly anisotropic thermal conductivity. For a bed of uniform spheres, the radial and axial components are approximately

$$\kappa_{\text{eff},rr} = \frac{1}{10} \rho \hat{C}_p v_0 D_p; \quad \kappa_{\text{eff},zz} = \frac{1}{2} \rho \hat{C}_p v_0 D_p \quad (9.6-8, 9)$$

in which v_0 is the "superficial velocity" defined in §4.3 and §6.4, and D_p is the diameter of the spherical particles. These simplified relations hold for $\text{Re} = D_p v_0 \rho / \mu$ greater than 200. The behavior at lower Reynolds numbers is discussed in several references.¹² Also, the behavior of the effective thermal conductivity tensor as a function of the Péclet number has been studied in considerable detail.¹³

§9.7 CONVECTIVE TRANSPORT OF ENERGY

In §9.1 we gave Fourier's law of heat conduction, which accounts for the energy transported through a medium by virtue of the molecular motions.

Energy may also be transported by the bulk motion of the fluid. In Fig. 9.7-1 we show three mutually perpendicular elements of area dS at the point P , where the fluid

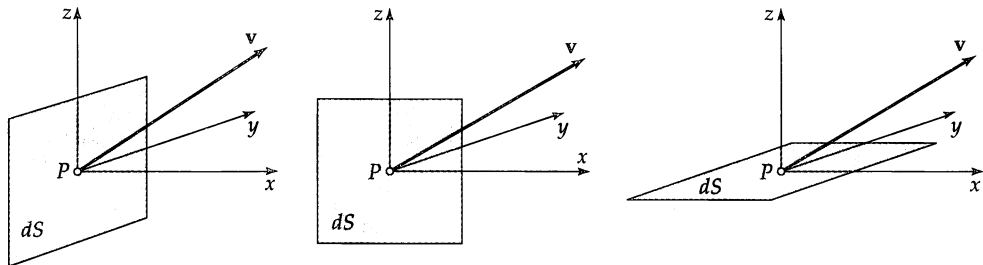


Fig. 9.7-1. Three mutually perpendicular surface elements of area dS across which energy is being transported by convection by the fluid moving with the velocity v . The volume rate of flow across the face perpendicular to the x -axis is $v_x dS$, and the rate of flow of energy across dS is then $(\frac{1}{2}\rho v^2 + \rho \hat{U})v_x dS$. Similar expressions can be written for the surface elements perpendicular to the y - and z -axes.

¹⁰ See Eq. 9.1-7 for the modification of Fourier's law for anisotropic materials. The subscripts rr and zz emphasize that these quantities are components of a second-order symmetrical tensor.

¹¹ W. B. Argo and J. M. Smith, *Chem. Engr. Progress*, **49**, 443–451 (1953).

¹² J. Beek, *Adv. Chem. Engr.*, **3**, 203–271 (1962); H. Kramers and K. R. Westerterp, *Elements of Chemical Reactor Design and Operation*, Academic Press, New York (1963), §III.9; O. Levenspiel and K. B. Bischoff, *Adv. Chem. Engr.*, **4**, 95–198 (1963).

¹³ D. L. Koch and J. F. Brady, *J. Fluid Mech.*, **154**, 399–427 (1985).

velocity is \mathbf{v} . The volume rate of flow across the surface element dS perpendicular to the x -axis is $v_x dS$. The rate at which energy is being swept across the same surface element is then

$$(\frac{1}{2}\rho v^2 + \rho \hat{U})v_x dS \quad (9.7-1)$$

in which $\frac{1}{2}\rho v^2 = \frac{1}{2}\rho(v_x^2 + v_y^2 + v_z^2)$ is the kinetic energy per unit volume, and $\rho \hat{U}$ is the internal energy per unit volume.

The definition of the internal energy in a nonequilibrium situation requires some care. From the *continuum* point of view, the internal energy at position \mathbf{r} and time t is assumed to be the same function of the local, instantaneous density and temperature that one would have at equilibrium. From the *molecular* point of view, the internal energy consists of the sum of the kinetic energies of all the constituent atoms (relative to the flow velocity \mathbf{v}), the intramolecular potential energies, and the intermolecular energies, within a small region about the point \mathbf{r} at time t .

Recall that, in the discussion of molecular collisions in §0.3, we found it convenient to regard the energy of a colliding pair of molecules to be the sum of the kinetic energies referred to the center of mass of the molecule plus the intramolecular potential energy of the molecule. Here also we split the energy of the fluid (regarded as a continuum) into kinetic energy associated with the bulk fluid motion and the internal energy associated with the kinetic energy of the molecules with respect to the flow velocity and the intra- and intermolecular potential energies.

We can write expressions similar to Eq. 9.7-1 for the rate at which energy is being swept through the surface elements perpendicular to the y - and z -axes. If we now multiply each of the three expressions by the corresponding unit vector and add, we then get, after division by dS ,

$$(\frac{1}{2}\rho v^2 + \rho \hat{U})\delta_x v_x + (\frac{1}{2}\rho v^2 + \rho \hat{U})\delta_y v_y + (\frac{1}{2}\rho v^2 + \rho \hat{U})\delta_z v_z = (\frac{1}{2}\rho v^2 + \rho \hat{U})\mathbf{v} \quad (9.7-2)$$

and this quantity is called the *convective energy flux vector*. To get the convective energy flux across a unit surface whose normal unit vector is \mathbf{n} , we form the dot product $(\mathbf{n} \cdot (\frac{1}{2}\rho v^2 + \rho \hat{U})\mathbf{v})$. It is understood that this is the flux from the negative side of the surface to the positive side. Compare this with the convective momentum flux in Fig. 1.7-2.

§9.8 WORK ASSOCIATED WITH MOLECULAR MOTIONS

Presently we will be concerned with applying the law of conservation of energy to "shells" (as in the shell balances in Chapter 10) or to small elements of volume fixed in space (to develop the equation of change for energy in §11.1). The law of conservation of energy for an open flow system is an extension of the first law of classical thermodynamics (for a closed system at rest). In the latter we state that the change in internal energy is equal to the amount of heat added to the system plus the amount of work done on the system. For flow systems we shall need to account for the heat added to the system (by molecular motions and by bulk fluid motion) and also for the work done on the system by the molecular motions. Therefore it is appropriate that we develop here the expression for the rate of work done by the molecular motions.

First we recall that, when a force \mathbf{F} acts on a body and causes it to move through a distance $d\mathbf{r}$, the work done is $dW = (\mathbf{F} \cdot d\mathbf{r})$. Then the rate of doing work is $dW/dt = (\mathbf{F} \cdot d\mathbf{r}/dt) = (\mathbf{F} \cdot \mathbf{v})$ —that is, the dot product of the force times the velocity. We now apply this formula to the three perpendicular planes at a point P in space shown in Fig. 9.8-1.

First we consider the surface element perpendicular to the x -axis. The fluid on the minus side of the surface exerts a force $\pi_x dS$ on the fluid that is on the plus side (see

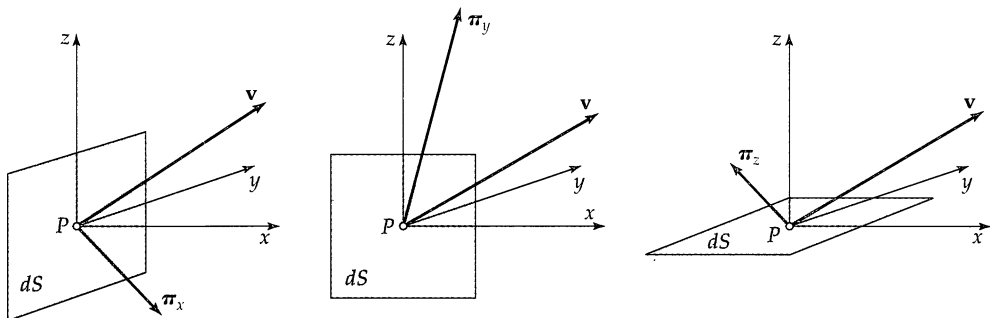


Fig. 9.8-1. Three mutually perpendicular surface elements of area dS at point P along with the stress vectors $\boldsymbol{\pi}_x$, $\boldsymbol{\pi}_y$, $\boldsymbol{\pi}_z$ acting on these surfaces. In the first figure, the rate at which work is done by the fluid on the minus side of dS on the fluid on the plus side of dS is then $(\boldsymbol{\pi}_x \cdot \mathbf{v})dS = [\boldsymbol{\pi} \cdot \mathbf{v}]_x dS$. Similar expressions hold for the surface elements perpendicular to the other two coordinate axes.

Table 1.2-1). Since the fluid is moving with a velocity \mathbf{v} , the rate at which work is done by the minus fluid on the plus fluid is $(\boldsymbol{\pi}_x \cdot \mathbf{v})dS$. Similar expressions may be written for the work done across the other two surface elements. When written out in component form, these rate of work expressions, per unit area, become

$$(\boldsymbol{\pi}_x \cdot \mathbf{v}) = \pi_{xx}v_x + \pi_{xy}v_y + \pi_{xz}v_z \equiv [\boldsymbol{\pi} \cdot \mathbf{v}]_x \quad (9.8-1)$$

$$(\boldsymbol{\pi}_y \cdot \mathbf{v}) = \pi_{yx}v_x + \pi_{yy}v_y + \pi_{yz}v_z \equiv [\boldsymbol{\pi} \cdot \mathbf{v}]_y \quad (9.8-2)$$

$$(\boldsymbol{\pi}_z \cdot \mathbf{v}) = \pi_{zx}v_x + \pi_{zy}v_y + \pi_{zz}v_z \equiv [\boldsymbol{\pi} \cdot \mathbf{v}]_z \quad (9.8-3)$$

When these scalar components are multiplied by the unit vectors and added, we get the "rate of doing work vector per unit area," and we can call this, for short, the *work flux*:

$$[\boldsymbol{\pi} \cdot \mathbf{v}] = \hat{\delta}_x(\boldsymbol{\pi}_x \cdot \mathbf{v}) + \hat{\delta}_y(\boldsymbol{\pi}_y \cdot \mathbf{v}) + \hat{\delta}_z(\boldsymbol{\pi}_z \cdot \mathbf{v}) \quad (9.8-4)$$

Furthermore, the rate of doing work across a unit area of surface with orientation given by the unit vector \mathbf{n} is $(\mathbf{n} \cdot [\boldsymbol{\pi} \cdot \mathbf{v}])$.

Equations 9.8-1 to 9.8-4 are easily written for cylindrical coordinates by replacing x, y, z by r, θ, z and, for spherical coordinates by replacing x, y, z by r, θ, ϕ .

We now define, for later use, the *combined energy flux vector* \mathbf{e} as follows:

$$\mathbf{e} = (\frac{1}{2}\rho v^2 + \rho \hat{U})\mathbf{v} + [\boldsymbol{\pi} \cdot \mathbf{v}] + \mathbf{q} \quad (9.8-5)$$

The \mathbf{e} vector is the sum of (a) the convective energy flux, (b) the rate of doing work (per unit area) by molecular mechanisms, and (c) the rate of transporting heat (per unit area) by molecular mechanisms. All the terms in Eq. 9.8-5 have the same sign convention, so that e_x is the energy transport in the positive x direction per unit area per unit time.

The total molecular stress tensor $\boldsymbol{\pi}$ can now be split into two parts: $\boldsymbol{\pi} = \rho \hat{\delta} + \boldsymbol{\tau}$ so that $[\boldsymbol{\pi} \cdot \mathbf{v}] = p\mathbf{v} + [\boldsymbol{\tau} \cdot \mathbf{v}]$. The term $p\mathbf{v}$ can then be combined with the internal energy term $\rho \hat{U}\mathbf{v}$ to give an enthalpy term $\rho \hat{U}\mathbf{v} + p\mathbf{v} = \rho(\hat{U} + (p/\rho))\mathbf{v} = \rho(\hat{U} + p\hat{V})\mathbf{v} = \rho \hat{H}\mathbf{v}$, so that

$$\mathbf{e} = (\frac{1}{2}\rho v^2 + \rho \hat{H})\mathbf{v} + [\boldsymbol{\tau} \cdot \mathbf{v}] + \mathbf{q} \quad (9.8-6)$$

We shall usually use the \mathbf{e} vector in this form. For a surface element dS of orientation \mathbf{n} , the quantity $(\mathbf{n} \cdot \mathbf{e})$ gives the convective energy flux, the heat flux, and the work flux across the surface element dS from the negative side to the positive side of dS .

Table 9.8-1 Summary of Notation for Energy Fluxes

Symbol	Meaning	Reference
$(\frac{1}{2}\rho v^2 + \rho \hat{U})\mathbf{v}$	convective energy flux vector	Eq. 9.7-2
\mathbf{q}	molecular heat flux vector	Eq. 9.1-6
$[\boldsymbol{\pi} \cdot \mathbf{v}]$	molecular work flux vector	Eq. 9.8-4
$\mathbf{e} = \mathbf{q} + [\boldsymbol{\pi} \cdot \mathbf{v}] + (\frac{1}{2}\rho v^2 + \rho \hat{U})\mathbf{v}$ $= \mathbf{q} + [\boldsymbol{\tau} \cdot \mathbf{v}] + (\frac{1}{2}\rho v^2 + \rho \hat{H})\mathbf{v}$	combined energy flux vector	Eq. 9.8-5, 6

In Table 9.8-1 we summarize the notation for the various energy flux vectors introduced in this section. All of them have the same sign convention.

To evaluate the enthalpy in Eq. 9.8-6, we make use of the standard equilibrium thermodynamics formula

$$d\hat{H} = \left(\frac{\partial \hat{H}}{\partial T}\right)_p dT + \left(\frac{\partial \hat{H}}{\partial p}\right)_T dp = \hat{C}_p dT + \left[\hat{V} - T\left(\frac{\partial \hat{V}}{\partial T}\right)_p\right]dp \quad (9.8-7)$$

When this is integrated from some reference state p°, T° to the state p, T , we then get¹

$$\hat{H} - \hat{H}^\circ = \int_{T^\circ}^T \hat{C}_p dT + \int_{p^\circ}^p \left[\hat{V} - T\left(\frac{\partial \hat{V}}{\partial T}\right)_p \right] dp \quad (9.8-8)$$

in which \hat{H}° is the enthalpy per unit mass at the reference state. The integral over p is zero for an ideal gas and $(1/\rho)(p - p^\circ)$ for fluids of constant density. The integral over T becomes $\hat{C}_p(T - T^\circ)$ if the heat capacity can be regarded as constant over the relevant temperature range. It is assumed that Eq. 9.8-7 is valid in nonequilibrium systems, where p and T are the *local* values of the pressure and temperature.

QUESTIONS FOR DISCUSSION

- Define and give the dimensions of thermal conductivity k , thermal diffusivity α , heat capacity \hat{C}_p , heat flux \mathbf{q} , and combined energy flux \mathbf{e} . For the dimensions use m = mass, l = length, T = temperature, and t = time.
- Compare the orders of magnitude of the thermal conductivities of gases, liquids, and solids.
- In what way are Newton's law of viscosity and Fourier's law of heat conduction similar? Dissimilar?
- Are gas viscosities and thermal conductivities related? If so, how?
- Compare the temperature dependence of the thermal conductivities of gases, liquids, and solids.
- Compare the orders of magnitudes of Prandtl numbers for gases and liquids.
- Are the thermal conductivities of gaseous Ne²⁰ and Ne²² the same?
- Is the relation $\hat{C}_p - \hat{C}_V = R$ true only for ideal gases, or is it also true for liquids? If it is not true for liquids, what formula should be used?
- What is the kinetic energy flux in the axial direction for the laminar Poiseuille flow of a Newtonian liquid in a circular tube?
- What is $[\boldsymbol{\pi} \cdot \mathbf{v}] = p\mathbf{v} + [\boldsymbol{\tau} \cdot \mathbf{v}]$ for Poiseuille flow?

¹ See, for example, R. J. Silbey and R. A. Alberty, *Physical Chemistry*, Wiley, 3rd edition (2001), §2.11.

PROBLEMS

9A.1 Prediction of thermal conductivities of gases at low density.

(a) Compute the thermal conductivity of argon at 100°C and atmospheric pressure, using the Chapman–Enskog theory and the Lennard-Jones constants derived from viscosity data. Compare your result with the observed value¹ of 506×10^{-7} cal/cm · s · K.

(b) Compute the thermal conductivities of NO and CH₄ at 300K and atmospheric pressure from the following data for these conditions:

	$\mu \times 10^7$ (g/cm · s)	\hat{C}_p (cal/g-mole · K)
NO	1929	7.15
CH ₄	1116	8.55

Compare your results with the experimental values given in Table 9.1-1.

9A.2 Computation of the Prandtl numbers for gases at low density.

(a) By using the Eucken formula and experimental heat capacity data, estimate the Prandtl number at 1 atm and 300K for each of the gases listed in the table.

(b) For the same gases, compute the Prandtl number directly by substituting the following values of the physical properties into the defining formula $\text{Pr} = \hat{C}_p \mu / k$, and compare the values with the results obtained in (a). All properties are given at low pressure and 300K.

Gas ^a	$\hat{C}_p \times 10^{-3}$ J/kg · K	$\mu \times 10^5$ Pa · s	k W/m · K
He	5.193	1.995	0.1546
Ar	0.5204	2.278	0.01784
H ₂	14.28	0.8944	0.1789
Air	1.001	1.854	0.02614
CO ₂	0.8484	1.506	0.01661
H ₂ O	1.864	1.041	0.02250

^a The entries in this table were prepared from functions provided by T. E. Daubert, R. P. Danner, H. M. Sibul, C. C. Stebbins, J. L. Oscarson, R. L. Rowley, W. V. Wilding, M. E. Adams, T. L. Marshall, and N. A. Zundel, *DIPPR ® Data Compilation of Pure Compound Properties*, Design Institute for Physical Property Data®, AIChE, New York (2000).

¹ W. G. Kannuluik and E. H. Carman, *Proc. Phys. Soc. (London)*, **65B**, 701–704 (1952).

9A.3 Estimation of the thermal conductivity of a dense gas.

Predict the thermal conductivity of methane at 110.4 atm and 127°F by the following methods:

(a) Use Fig. 9.2-1. Obtain the necessary critical properties from Appendix E.

(b) Use the Eucken formula to get the thermal conductivity at 127°F and low pressure. Then apply a pressure correction by using Fig. 9.2-1. The experimental value² is 0.0282 Btu/hr · ft · F.

Answer: (a) 0.0294 Btu/hr · ft · F.

9A.4 Prediction of the thermal conductivity of a gas mixture.

Calculate the thermal conductivity of a mixture containing 20 mole % CO₂ and 80 mole % H₂ at 1 atm and 300K. Use the data of Problem 9A.2 for your calculations.

Answer: 2850×10^7 cal/cm · s · K

9A.5 Estimation of the thermal conductivity of a pure liquid.

Predict the thermal conductivity of liquid H₂O at 40°C and 40 megabars pressure (1 megabar = 10^6 dyn/cm²). The isothermal compressibility, $(1/\rho)(\partial\rho/\partial p)_T$, is 38×10^{-6} megabar⁻¹ and the density is 0.9938 g/cm³. Assume that $\hat{C}_p = \hat{C}_V$.

Answer: 0.375 Btu/hr · ft · F

9A.6 Calculation of the Lorenz number.

(a) Application of kinetic theory to the “electron gas” in a metal³ gives for the Lorenz number

$$L = \frac{\pi^2}{3} \left(\frac{k}{e} \right)^2 \quad (9A.6-1)$$

in which k is the Boltzmann constant and e is the charge on the electron. Compute L in the units given under Eq. 9.5-1.

(b) The electrical resistivity, $1/k_e$, of copper at 20°C is 1.72×10^{-6} ohm · cm. Estimate its thermal conductivity in W/m · K using Eq. 9A.6-1, and compare your result with the experimental value given in Table 9.1-4.

Answers: (a) 2.44×10^{-8} volt²/K²; (b) 416 W/m · K

9A.7 Corroboration of the Wiedemann–Franz–Lorenz law.

Given the following experimental data at 20°C for pure metals, compute the corresponding values of the Lorenz number, L , defined in Eq. 9.5-1.

² J. M. Lenoir, W. A. Junk, and E. W. Comings, *Chem. Engr. Prog.*, **49**, 539–542 (1953).

³ J. E. Mayer and M. G. Mayer, *Statistical Mechanics*, Wiley, New York (1946), p. 412; P. Drude, *Ann. Phys.*, **1**, 566–613 (1900).

Metal	$k_e \times 10^6$ (ohm · cm)	k (cal/cm · s · K)
Na	4.6	0.317
Ni	6.9	0.140
Cu	1.69	0.92
Al	2.62	0.50

9A.8. Thermal conductivity and Prandtl number of a polyatomic gas.

(a) Estimate the thermal conductivity of CH₄ at 1500K and 1.37 atm. The molar heat capacity at constant pressure⁴ at 1500K is 20.71 cal/g-mole · K.

(b) What is the Prandtl number at the same pressure and temperature?

Answers: (a) 5.03×10^{-4} cal/cm · s · K; (b) 0.89

9A.9. Thermal conductivity of gaseous chlorine. Use Eq. 9.3-15 to calculate the thermal conductivity of gaseous chlorine. To do this you will need to use Eq. 1.4-14 to estimate the viscosity, and will also need the following values of the heat capacity:

T (K)	200	300	400	500	600
\tilde{C}_p (cal/g-mole · K)	(8.06)	8.12	8.44	8.62	6.74

Check to see how well the calculated values agree with the following experimental thermal conductivity data⁵

T (K)	p (mm Hg)	$k \times 10^5$ cal/cm · s · K
198	50	1.31 ± 0.03
275	220	1.90 ± 0.02
276	120	1.93 ± 0.01
	220	1.92 ± 0.01
363	100	2.62 ± 0.02
	200	2.61 ± 0.02
395	210	3.04 ± 0.02
453	150	3.53 ± 0.03
	250	3.42 ± 0.02
495	250	3.72 ± 0.07
553	100	4.14 ± 0.04
583	170	4.43 ± 0.04
	210	4.45 ± 0.08
676	150	5.07 ± 0.10
	250	4.90 ± 0.03

9A.10. Thermal conductivity of chlorine-air mixtures. Using Eq. 9.3-17, predict thermal conductivities of chlorine-air mixtures at 297K and 1 atm for the following mole fractions of chlorine: 0.25, 0.50, 0.75. Air may be considered a single substance, and the following data may be assumed:

Substance ^a	μ (Pa · s)	k (W/m · K)	\hat{C}_p (J/kg · K)
Air	1.854×10^{-5}	2.614×10^{-2}	1.001×10^3
Chlorine	1.351×10^{-5}	8.960×10^{-3}	4.798×10^2

^a The entries in this table were prepared from functions provided by T. E. Daubert, R. P. Danner, H. M. Sibul, C. C. Stebbins, J. L. Oscarson, R. L. Rowley, W. V. Wilding, M. E. Adams, T. L. Marshall, and N. A. Zundel, *DIPPR ® Data Compilation of Pure Compound Properties*, Design Institute for Physical Property Data®, AIChE, New York (2000).

9A.11. Thermal conductivity of quartz sand. A typical sample of quartz sand has the following properties at 20°C:

Component	Volume fraction	k cal/cm · s · K
$i = 1$: Silica	0.510	20.4×10^{-3}
$i = 2$: Feldspar	0.063	7.0×10^{-3}
Continuous phase ($i = 0$) is one of the following:		
(i) Water	0.427	1.42×10^{-3}
(ii) Air	0.427	0.0615×10^{-3}

Estimate the effective thermal conductivity of the sand (i) when it is water saturated, and (ii) when it is completely dry.

(a) Use the following generalization of Eqs. 9.6-5 and 6:

$$\frac{k_{\text{eff}}}{k_0} = \frac{\sum_{i=0}^N \alpha_i \phi_i (k_i/k_0)}{\sum_{i=0}^N \alpha_i \phi_i} \quad (9A.11-1)$$

$$\alpha_i = \frac{1}{3} \sum_{i=1}^3 \left[1 + \left(\frac{k_i}{k_0} - 1 \right) g_i \right]^{-1} \quad (9A.11-2)$$

Here N is the number of solid phases. Compare the prediction for spheres ($g_1 = g_2 = g_3 = \frac{1}{3}$) with the recommendation of de Vries ($g_1 = g_2 = \frac{1}{8}; g_3 = \frac{3}{4}$).

(b) Use Eq. 9.6-1 with $k_1 = 18.9 \times 10^{-3}$ cal/cm · s · K, which is the volume-average thermal conductivity of the two solids. Observed values, accurate within about 3%, are 6.2 and 0.58×10^{-3} cal/cm · s · K for wet and dry sand, respectively.⁶ The particles were believed to be best approxi-

⁴ O. A. Hougen, K. M. Watson, and R. A. Ragatz, *Chemical Process Principles*, Vol. 1, Wiley, New York (1954), p. 253.

⁵ Interpolated from data of E. U. Frank, *Z. Elektrochem.*, 55, 636 (1951), as reported in *Nouveau Traité de Chimie Minerale*, P. Pascal, ed., Masson et C^e, Paris (1960), pp. 158–159.

⁶ The behavior of partially wetted soil has been treated by D. A. de Vries, Chapter 7 in *Physics and Plant Environment*, W. R. van Wijk, ed., Wiley, New York (1963).

mated as oblate spheroids, with an axis ratio of 4, for which $g_1 = g_2 = 0.144$; $g_3 = 0.712$.

Answer: (a) From Eq. 9.6-4, 4.93×10^{-3} cal/cm · s · K (spherical), and 6.22×10^{-3} cal/cm · s · K. From Eq. 9.6-1, 5.0×10^{-3} cal/cm · s · K

9A.12. Calculation of molecular diameters from transport properties.

(a) Determine the molecular diameter d for argon from Eq. 1.4-9 and the experimental viscosity given in Problem 9A.2.

(b) Repeat part (a), but using Eq. 9.3-12 and the measured thermal conductivity in Problem 9A.2. Compare this result with the value obtained in (a).

(c) Calculate and compare the values of the Lennard-Jones collision diameter σ from the same experimental data used in (a) and (b), using $\varepsilon/k = 124\text{K}$.

(d) What can be concluded from the above calculations?

Answer: (a) 2.95 Å; (b) 1.88 Å; (c) 3.415 Å from Eq. 1.4-14, 3.425 Å from Eq. 9.3-13

9C.1. Enskog theory for dense gases. Enskog⁷ developed a kinetic theory for the transport properties of dense gases. He showed that for molecules that are idealized as rigid spheres of diameter σ_0

$$\frac{\mu}{\mu^\circ} \frac{\tilde{V}}{b_0} = \frac{1}{y} + 0.8 + 0.761y \quad (9C.1-1)$$

$$\frac{k}{k^\circ} \frac{\tilde{V}}{b_0} = \frac{1}{y} + 1.2 + 0.755y \quad (9C.1-2)$$

Here μ° and k° are the low-pressure properties (computed, for example, from Eqs. 1.4-14 and 9.3-13), \tilde{V} is the molar volume, and $b_0 = \frac{2}{3}\pi N\sigma_0^3$, where N is Avogadro's number. The quantity y is related to the equation of state of a gas of rigid spheres:

$$y = \frac{p\tilde{V}}{RT} - 1 = \left(\frac{b_0}{\tilde{V}}\right) + 0.6250\left(\frac{b_0}{\tilde{V}}\right)^2 + 0.2869\left(\frac{b_0}{\tilde{V}}\right)^3 + \dots \quad (9C.1-3)$$

⁷ D. Enskog, *Kungliga Svenska Vetenskapsakademiens Handlingar*, 62, No. 4 (1922), in German. See also J. O. Hirschfelder, C. F. Curtiss, and R. B. Bird, *Molecular Theory of Gases and Liquids*, 2nd printing with corrections (1964), pp. 647–652.

These three equations give the density corrections to the viscosity and thermal conductivity of a hypothetical gas made up of rigid spheres.

Enskog further suggested that for real gases, (i) y can be given empirically by

$$y = \frac{\tilde{V}}{RT} \left[T \left(\frac{\partial p}{\partial T} \right)_{\tilde{V}} - 1 \right] \quad (9C.1-4)$$

where experimental $p\tilde{V}-T$ data are used, and (ii) b_0 can be determined by fitting the minimum in the curve of $(\mu/\mu^\circ)\tilde{V}$ versus y .

(a) A useful way to summarize the equation of state is to use the corresponding-states presentation⁸ of $Z = Z(p_r, T_r)$, where $Z = p\tilde{V}/RT$, $p_r = p/p_c$, and $T_r = T/T_c$. Show that the quantity y defined by Eq. 9C.1-4 can be computed as a function of the reduced pressure and temperature from

$$y = Z \frac{1 + (\partial \ln Z / \partial \ln T_r)_p}{1 - (\partial \ln Z / \partial \ln p_r)_{T_r}} \quad (9C.1-5)$$

(b) Show how Eqs. 9C.1-1, 2, and 5, together with the Hougen-Watson Z -chart and the Uyehara-Watson μ/μ_c chart in Fig. 1.3-1, can be used to develop a chart of k/k_c as a function of p_r and T_r . What would be the limitations of the resulting chart? Such a procedure (but using specific $p\tilde{V}-T$ data instead of the Hougen-Watson Z -chart) was used by Comings and Nathan.⁹

(c) How might one use the Redlich and Kwong¹⁰ equation of state

$$\left(p + \frac{a}{\sqrt{T\tilde{V}(\tilde{V} + b)}} \right) (\tilde{V} - b) = RT \quad (9C.1-6)$$

for the same purpose? The quantities a and b are constants characteristic of each gas.

⁸ O. A. Hougen and K. M. Watson, *Chemical Process Principles*, Vol. II, Wiley, New York (1947), p. 489.

⁹ E. W. Comings and M. F. Nathan, *Ind. Eng. Chem.*, **39**, 964–970 (1947).

¹⁰ O. Redlich and J. N. S. Kwong, *Chem. Rev.*, **44**, 233–244 (1949).

Shell Energy Balances and Temperature Distributions in Solids and Laminar Flow

- §10.1 Shell energy balances; boundary conditions
- §10.2 Heat conduction with an electrical heat source
- §10.3 Heat conduction with a nuclear heat source
- §10.4 Heat conduction with a viscous heat source
- §10.5 Heat conduction with a chemical heat source
- §10.6 Heat conduction through composite walls
- §10.7 Heat conduction in a cooling fin
- §10.8 Forced convection
- §10.9 Free convection

In Chapter 2 we saw how certain simple viscous flow problems are solved by a two-step procedure: (i) a momentum balance is made over a thin slab or shell perpendicular to the direction of momentum transport, which leads to a first-order differential equation that gives the momentum flux distribution; (ii) then into the expression for the momentum flux we insert Newton's law of viscosity, which leads to a first-order differential equation for the fluid velocity as a function of position. The integration constants that appear are evaluated by using the boundary conditions, which specify the velocity or momentum flux at the bounding surfaces.

In this chapter we show how a number of heat conduction problems are solved by an analogous procedure: (i) an energy balance is made over a thin slab or shell perpendicular to the direction of the heat flow, and this balance leads to a first-order differential equation from which the heat flux distribution is obtained; (ii) then into this expression for the heat flux, we substitute Fourier's law of heat conduction, which gives a first-order differential equation for the temperature as a function of position. The integration constants are then determined by use of boundary conditions for the temperature or heat flux at the bounding surfaces.

It should be clear from the similar wording of the preceding two paragraphs that the mathematical methods used in this chapter are the same as those introduced in Chapter 2—only the notation and terminology are different. However, we will encounter here a number of physical phenomena that have no counterpart in Chapter 2.

After a brief introduction to the shell energy balance in §10.1, we give an analysis of the heat conduction in a series of uncomplicated systems. Although these examples are

somewhat idealized, the results find application in numerous standard engineering calculations. The problems were chosen to introduce the beginner to a number of important physical concepts associated with the heat transfer field. In addition, they serve to show how to use a variety of boundary conditions and to illustrate problem solving in Cartesian, cylindrical, and spherical coordinates. In §§10.2–10.5 we consider four kinds of heat sources: electrical, nuclear, viscous, and chemical. In §§10.6 and 10.7 we cover two topics with widespread applications—namely, heat flow through composite walls and heat loss from fins. Finally, in §§10.8 and 10.9, we analyze two limiting cases of heat transfer in moving fluids: forced convection and free convection. The study of these topics paves the way for the general equations in Chapter 11.

§10.1 SHELL ENERGY BALANCES; BOUNDARY CONDITIONS

The problems discussed in this chapter are set up by means of shell energy balances. We select a slab (or shell), the surfaces of which are normal to the direction of heat conduction, and then we write for this system a statement of the law of conservation of energy. For *steady-state* (i.e., time-independent) systems, we write:

$$\left\{ \begin{array}{l} \text{rate of} \\ \text{energy in} \\ \text{by convective} \\ \text{transport} \end{array} \right\} - \left\{ \begin{array}{l} \text{rate of} \\ \text{energy out} \\ \text{by convective} \\ \text{transport} \end{array} \right\} + \left\{ \begin{array}{l} \text{rate of} \\ \text{energy in} \\ \text{by molecular} \\ \text{transport} \end{array} \right\} - \left\{ \begin{array}{l} \text{rate of} \\ \text{energy out} \\ \text{by molecular} \\ \text{transport} \end{array} \right\} + \\ \left\{ \begin{array}{l} \text{rate of} \\ \text{work done} \\ \text{on system} \\ \text{by molecular} \\ \text{transport} \end{array} \right\} - \left\{ \begin{array}{l} \text{rate of} \\ \text{work done} \\ \text{by system} \\ \text{by molecular} \\ \text{transport} \end{array} \right\} + \left\{ \begin{array}{l} \text{rate of} \\ \text{work done} \\ \text{on system} \\ \text{by external} \\ \text{forces} \end{array} \right\} + \left\{ \begin{array}{l} \text{rate of} \\ \text{energy} \\ \text{production} \end{array} \right\} = 0 \quad (10.1-1)$$

The *convective transport* of energy was discussed in §9.7, and the *molecular transport* (heat conduction) in §9.1. The *molecular work terms* were explained in §9.8. These three terms can be added to give the “combined energy flux” \mathbf{e} , as shown in Eq. 9.8-6. In setting up problems here (and in the next chapter) we will use the \mathbf{e} vector along with the expression for the enthalpy in Eq. 9.8-8. Note that in nonflow systems (for which \mathbf{v} is zero) the \mathbf{e} vector simplifies to the \mathbf{q} vector, which is given by Fourier’s law.

The *energy production* term in Eq. 10.1-1 includes (i) the degradation of electrical energy into heat, (ii) the heat produced by slowing down of neutrons and nuclear fragments liberated in the fission process, (iii) the heat produced by viscous dissipation, and (iv) the heat produced in chemical reactions. The chemical reaction heat source will be discussed further in Chapter 19. Equation 10.1-1 is a statement of the first law of thermodynamics, written for an “open” system at steady-state conditions. In Chapter 11 this same statement—extended to unsteady-state systems—will be written as an equation of change.

After Eq. 10.1-1 has been written for a thin slab or shell of material, the thickness of the slab or shell is allowed to approach zero. This procedure leads ultimately to an expression for the temperature distribution containing constants of integration, which we evaluate by use of boundary conditions. The commonest types of boundary conditions are:

- The temperature may be specified at a surface.
- The heat flux normal to a surface may be given (this is equivalent to specifying the normal component of the temperature gradient).
- At interfaces the continuity of temperature and of the heat flux normal to the interface are required.

- d. At a solid-fluid interface, the normal heat flux component may be related to the difference between the solid surface temperature T_0 and the “bulk” fluid temperature T_b :

$$q = h(T_0 - T_b) \quad (10.1-2)$$

This relation is referred to as *Newton's law of cooling*. It is not really a “law” but rather the defining equation for h , which is called the *heat transfer coefficient*. Chapter 14 deals with methods for estimating heat-transfer coefficients.

All four types of boundary conditions are encountered in this chapter. Still other kinds of boundary conditions are possible, and they will be introduced as needed.

§10.2 HEAT CONDUCTION WITH AN ELECTRICAL HEAT SOURCE

The first system we consider is an electric wire of circular cross section with radius R and electrical conductivity k_e ohm $^{-1}$ cm $^{-1}$. Through this wire there is an electric current with current density I amp/cm 2 . The transmission of an electric current is an irreversible process, and some electrical energy is converted into heat (thermal energy). The rate of heat production per unit volume is given by the expression

$$S_e = \frac{I^2}{k_e} \quad (10.2-1)$$

The quantity S_e is the heat source resulting from electrical dissipation. We assume here that the temperature rise in the wire is not so large that the temperature dependence of either the thermal or electrical conductivity need be considered. The surface of the wire is maintained at temperature T_0 . We now show how to find the radial temperature distribution within the wire.

For the energy balance we take the system to be a cylindrical shell of thickness Δr and length L (see Fig. 10.2-1). Since $\mathbf{v} = 0$ in this system, the only contributions to the energy balance are

Rate of heat in across cylindrical surface at r $(2\pi rL)q_r|_r) = (2\pi rLq_r)|_r \quad (10.2-2)$

Rate of heat out across cylindrical surface at $r + \Delta r$ $(2\pi(r + \Delta r)L)(q_r|_{r+\Delta r}) = (2\pi rLq_r)|_{r+\Delta r} \quad (10.2-3)$

Rate of thermal energy production by electrical dissipation $(2\pi r\Delta rL)S_e \quad (10.2-4)$

The notation q_r means “heat flux in the r direction,” and $(\dots)|_{r+\Delta r}$ means “evaluated at $r + \Delta r$.” Note that we take “in” and “out” to be in the positive r direction.

We now substitute these quantities into the energy balance of Eq. 9.1-1. Division by $2\pi L\Delta r$ and taking the limit as Δr goes to zero gives

$$\lim_{\Delta r \rightarrow 0} \frac{(rq_r)|_{r+\Delta r} - (rq_r)|_r}{\Delta r} = S_e r \quad (10.2-5)$$

The expression on the left side is the first derivative of rq_r with respect to r , so that Eq. 10.2-5 becomes

$$\frac{d}{dr}(rq_r) = S_e r \quad (10.2-6)$$

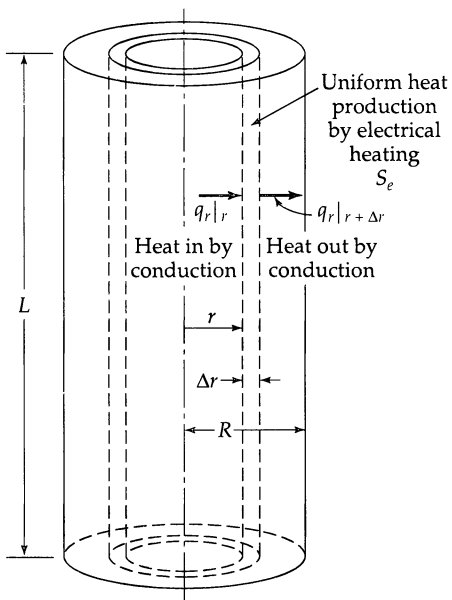


Fig. 10.2-1. An electrically heated wire, showing the cylindrical shell over which the energy balance is made.

This is a first-order differential equation for the energy flux, and it may be integrated to give

$$q_r = \frac{S_e r}{2} + \frac{C_1}{r} \quad (10.2-7)$$

The integration constant C_1 must be zero because of the boundary condition that

$$\text{B.C. 1:} \quad \text{at } r = 0, \quad q_r \text{ is not infinite} \quad (10.2-8)$$

Hence the final expression for the heat flux distribution is

$$q_r = \frac{S_e r}{2}$$

(10.2-9)

This states that the heat flux increases linearly with r .

We now substitute Fourier's law in the form $q_r = -k(dT/dr)$ (see Eq. B.2-4) into Eq. 10.2-9 to obtain

$$-k \frac{dT}{dr} = \frac{S_e r}{2} \quad (10.2-10)$$

When k is assumed to be constant, this first-order differential equation can be integrated to give

$$T = -\frac{S_e r^2}{4k} + C_2$$

(10.2-11)

The integration constant is determined from

$$\text{B.C. 2:} \quad \text{at } r = R, \quad T = T_0 \quad (10.2-12)$$

Hence $C_2 = (S_e R^2 / 4k) + T_0$ and Eq. 10.2-11 becomes

$$T - T_0 = \frac{S_e R^2}{4k} \left[1 - \left(\frac{r}{R} \right)^2 \right]$$

(10.2-13)

Equation 10.2-13 gives the temperature rise as a parabolic function of the distance r from the wire axis.

Once the temperature and heat flux distributions are known, various information about the system may be obtained:

(i) *Maximum temperature rise* (at $r = 0$)

$$T_{\max} - T_0 = \frac{S_e R^2}{4k} \quad (10.2-14)$$

(ii) *Average temperature rise*

$$\langle T \rangle - T_0 = \frac{\int_0^{2\pi} \int_0^R (T(r) - T_0) r dr d\theta}{\int_0^{2\pi} \int_0^R r dr d\theta} = \frac{S_e R^2}{8k} \quad (10.2-15)$$

Thus the temperature rise, averaged over the cross section, is half the maximum temperature rise.

(iii) *Heat outflow at the surface* (for a length L of wire)

$$Q|_{r=R} = 2\pi RL \cdot q_r|_{r=R} = 2\pi RL \cdot \frac{S_e R}{2} = \pi R^2 L \cdot S_e \quad (10.2-16)$$

This result is not surprising, since, at steady state, all the heat produced by electrical dissipation in the volume $\pi R^2 L$ must leave through the surface $r = R$.

The reader, while going through this development, may well have had the feeling of *déjà vu*. There is, after all, a pronounced similarity between the heated wire problem and the viscous flow in a circular tube. Only the notation is different:

	Tube flow	Heated wire
First integration gives	$\tau_{rz}(r)$	$q_r(r)$
Second integration gives	$v_z(r)$	$T(r) - T_0$
Boundary condition at $r = 0$	$\tau_{rz} = \text{finite}$	$q_r = \text{finite}$
Boundary condition at $r = R$	$v_z = 0$	$T - T_0 = 0$
Transport property	μ	k
Source term	$(\mathcal{P}_0 - \mathcal{P}_L)/L$	S_e
Assumptions	$\mu = \text{constant}$	$k, k_e = \text{constant}$

That is, when the quantities are properly chosen, the differential equations and the boundary conditions for the two problems are identical, and the physical processes are said to be "analogous." Not all problems in momentum transfer have analogs in energy and mass transport. However, when such analogies can be found, they may be useful in taking over known results from one field and applying them in another. For example, the reader should have no trouble in finding a heat conduction analog for the viscous flow in a liquid film on an inclined plane.

There are many examples of heat conduction problems in the electrical industry.¹ The minimizing of temperature rises inside electrical machinery prolongs insulation life. One example is the use of internally liquid-cooled stator conductors in very large (500,000 kw) AC generators.

¹ M. Jakob, *Heat Transfer*, Vol. 1, Wiley, New York (1949), Chapter 10, pp. 167–199.

To illustrate further problems in electrical heating, we give two examples concerning the temperature rise in wires: the first indicates the order of magnitude of the heating effect, and the second shows how to handle different boundary conditions. In addition, in Problem 10C.2 we show how to take into account the temperature dependence of the thermal and electrical conductivities.

EXAMPLE 10.2-1

Voltage Required for a Given Temperature Rise in a Wire Heated by an Electric Current

A copper wire has a radius of 2 mm and a length of 5 m. For what voltage drop would the temperature rise at the wire axis be 10°C, if the surface temperature of the wire is 20°C?

SOLUTION

Combining Eq. 10.2-14 and 10.2-1 gives

$$T_{\max} - T_0 = \frac{I^2 R^2}{4k_e k} \quad (10.2-17)$$

The current density is related to the voltage drop E over a length L by

$$I = k_e \frac{E}{L} \quad (10.2-18)$$

Hence

$$T_{\max} - T_0 = \frac{E^2 R^2}{4L^2} \left(\frac{k_e}{k} \right) \quad (10.2-19)$$

from which

$$E = 2 \frac{L}{R} \sqrt{\frac{k}{k_e T_0}} \sqrt{T_0(T_{\max} - T_0)} \quad (10.2-20)$$

For copper, the Lorenz number of §9.5 is $k/k_e T_0 = 2.23 \times 10^{-8}$ volt²/K². Therefore, the voltage drop needed to cause a 10°C temperature rise is

$$\begin{aligned} E &= 2 \left(\frac{5000 \text{ mm}}{2 \text{ mm}} \right) \sqrt{2.23 \times 10^{-8} \frac{\text{volt}}{\text{K}}} \sqrt{(293)(10)} \text{ K} \\ &= (5000)(1.49 \times 10^{-4})(54.1) = 40 \text{ volts} \end{aligned} \quad (10.2-21)$$

EXAMPLE 10.2.2

Heated Wire with Specified Heat Transfer Coefficient and Ambient Air Temperature

Repeat the analysis in §10.2, assuming that T_0 is not known, but that instead the heat flux at the wall is given by Newton's "law of cooling" (Eq. 10.1-2). Assume that the heat transfer coefficient h and the ambient air temperature T_{air} are known.

SOLUTION I

The solution proceeds as before through Eq. 10.2-11, but the second integration constant is determined from Eq. 10.1-2:

$$\text{B.C. } 2': \quad \text{at } r = R, \quad -k \frac{dT}{dr} = h(T - T_{\text{air}}) \quad (10.2-22)$$

Substituting Eq. 10.2-11 into Eq. 10.2-22 gives $C_2 = (S_e R / 2h) + (S_e R^2 / 4k) + T_{\text{air}}$, and the temperature profile is then

$$T - T_{\text{air}} = \frac{S_e R^2}{4k} \left[1 - \left(\frac{r}{R} \right)^2 \right] + \frac{S_e R}{2h} \quad (10.2-23)$$

From this the surface temperature of the wire is found to be $T_{\text{air}} + S_e R / 2h$.

SOLUTION II

Another method makes use of the result obtained previously in Eq. 10.2-13. Although T_0 is not known in the present problem, we can nonetheless use the result. From Eqs. 10.1-2 and 10.2-16 we can get the temperature difference

$$T_0 - T_{\text{air}} = \frac{\pi R^2 L S_c}{h(2\pi RL)} = \frac{S_c R}{2h} \quad (10.2-24)$$

Subtraction of Eq. 10.2-24 from Eq. 10.2-13 enables us to eliminate the unknown T_0 and gives Eq. 10.2-23.

§10.3 HEAT CONDUCTION WITH A NUCLEAR HEAT SOURCE

We consider a spherical nuclear fuel element as shown in Fig. 10.3-1. It consists of a sphere of fissionable material with radius $R^{(F)}$, surrounded by a spherical shell of aluminum "cladding" with outer radius $R^{(C)}$. Inside the fuel element, fission fragments are produced that have very high kinetic energies. Collisions between these fragments and the atoms of the fissionable material provide the major source of thermal energy in the reactor. Such a volume source of thermal energy resulting from nuclear fission we call S_n (cal/cm³ · s). This source will not be uniform throughout the sphere of fissionable material; it will be the smallest at the center of the sphere. For the purpose of this problem, we assume that the source can be approximated by a simple parabolic function

$$S_n = S_{n0} \left[1 + b \left(\frac{r}{R^{(F)}} \right)^2 \right] \quad (10.3-1)$$

Here S_{n0} is the volume rate of heat production at the center of the sphere, and b is a dimensionless positive constant.

We select as the system a spherical shell of thickness Δr within the sphere of fissionable material. Since the system is not in motion, the energy balance will consist only of heat conduction terms and a source term. The various contributions to the energy balance are:

Rate of heat in by conduction at r	$q_r^{(F)} _r \cdot 4\pi r^2 = (4\pi r^2 q_r^{(F)}) _r$	(10.3-2)
--	---	----------

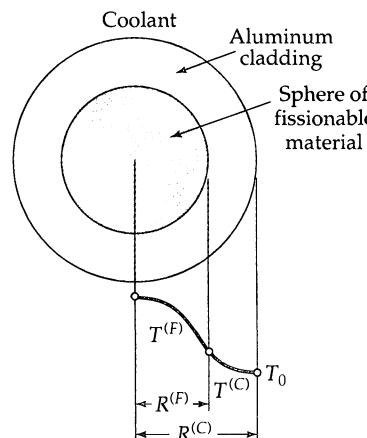


Fig. 10.3-1. A spherical nuclear fuel assembly, showing the temperature distribution within the system.

Rate of heat out
by conduction
at $r + \Delta r$

$$q_r^{(F)}|_{r+\Delta r} \cdot 4\pi(r + \Delta r)^2 = (4\pi r^2 q_r^{(F)})|_{r+\Delta r} \quad (10.3-3)$$

Rate of thermal
energy produced
by nuclear fission

$$S_n \cdot 4\pi r^2 \Delta r \quad (10.3-4)$$

Substitution of these terms into the energy balance of Eq. 10.1-1 gives, after dividing by $4\pi \Delta r$ and taking the limit as $\Delta r \rightarrow 0$

$$\lim_{\Delta r \rightarrow 0} \frac{(r^2 q_r^{(F)})|_{r+\Delta r} - (r^2 q_r^{(F)})|_r}{\Delta r} = S_n r^2 \quad (10.3-5)$$

Taking the limit and introducing the expression in Eq. 10.3-1 leads to

$$\frac{d}{dr} (r^2 q_r^{(F)}) = S_{n0} \left[1 + b \left(\frac{r}{R^{(F)}} \right)^2 \right] r^2 \quad (10.3-6)$$

The differential equation for the heat flux $q_r^{(C)}$ in the cladding is of the same form as Eq. 10.3-6, except that there is no significant source term:

$$\frac{d}{dr} (r^2 q_r^{(C)}) = 0 \quad (10.3-7)$$

Integration of these two equations gives

$$q_r^{(F)} = S_{n0} \left(\frac{r}{3} + \frac{b}{R^{(F)2}} \frac{r^3}{5} \right) + \frac{C_1^{(F)}}{r^2} \quad (10.3-8)$$

$$q_r^{(C)} = + \frac{C_1^{(C)}}{r^2} \quad (10.3-9)$$

in which $C_1^{(F)}$ and $C_1^{(C)}$ are integration constants. These are evaluated by means of the boundary conditions:

$$\text{B.C. 1: } \text{at } r = 0, \quad q_r^{(F)} \text{ is not infinite} \quad (10.3-10)$$

$$\text{B.C. 2: } \text{at } r = R^{(F)}, \quad q_r^{(F)} = q_r^{(C)} \quad (10.3-11)$$

Evaluation of the constants then leads to

$$q_r^{(F)} = S_{n0} \left(\frac{r}{3} + \frac{b}{R^{(F)2}} \frac{r^3}{5} \right) \quad (10.3-12)$$

$$q_r^{(C)} = S_{n0} \left(\frac{1}{3} + \frac{b}{5} \right) \frac{R^{(F)3}}{r^2} \quad (10.3-13)$$

These are the heat flux distributions in the fissionable sphere and in the spherical-shell cladding.

Into these distributions we now substitute Fourier's law of heat conduction (Eq. B.2-7):

$$-k^{(F)} \frac{dT^{(F)}}{dr} = S_{n0} \left(\frac{r}{3} + \frac{b}{R^{(F)2}} \frac{r^3}{5} \right) \quad (10.3-14)$$

$$-k^{(C)} \frac{dT^{(C)}}{dr} = S_{n0} \left(\frac{1}{3} + \frac{b}{5} \right) \frac{R^{(F)3}}{r^2} \quad (10.3-15)$$

These equations may be integrated for constant $k^{(F)}$ and $k^{(C)}$ to give

$$T^{(F)} = -\frac{S_{n0}}{k^{(F)}} \left(\frac{r^2}{6} + \frac{b}{R^{(F)2}} \frac{r^4}{20} \right) + C_2^{(F)} \quad (10.3-16)$$

$$T^{(C)} = +\frac{S_{n0}}{k^{(C)}} \left(\frac{1}{3} + \frac{b}{5} \right) \frac{R^{(F)3}}{r} + C_2^{(C)} \quad (10.3-17)$$

The integration constants can be determined from the boundary conditions

$$\text{B.C. 3:} \quad \text{at } r = R^{(F)}, \quad T^{(F)} = T^{(C)} \quad (10.3-18)$$

$$\text{B.C. 4:} \quad \text{at } r = R^{(C)}, \quad T^{(C)} = T_0 \quad (10.3-19)$$

where T_0 is the known temperature at the outside of the cladding. The final expressions for the temperature profiles are

$$\boxed{T^{(F)} = \frac{S_{n0}R^{(F)2}}{6k^{(F)}} \left\{ \left[1 - \left(\frac{r}{R^{(F)}} \right)^2 \right] + \frac{3}{10} b \left[1 - \left(\frac{r}{R^{(F)}} \right)^4 \right] \right\} + \frac{S_{n0}R^{(F)2}}{3k^{(C)}} \left(1 + \frac{3}{5} b \right) \left(1 - \frac{R^{(F)}}{R^{(C)}} \right)} \quad (10.3-20)$$

$$\boxed{T^{(C)} = \frac{S_{n0}R^{(F)2}}{3k^{(C)}} \left(1 + \frac{3}{5} b \right) \left(\frac{R^{(F)}}{r} - \frac{R^{(F)}}{R^{(C)}} \right)} \quad (10.3-21)$$

To find the maximum temperature in the sphere of fissionable material, all we have to do is set r equal to zero in Eq. 10.3-20. This is a quantity one might well want to know when making estimates of thermal deterioration.

This problem has illustrated two points: (i) how to handle a position-dependent source term, and (ii) the application of the continuity of temperature and normal heat flux at the boundary between two solid materials.

§10.4 HEAT CONDUCTION WITH A VISCOUS HEAT SOURCE

Next we consider the flow of an incompressible Newtonian fluid between two coaxial cylinders as shown in Fig. 10.4-1. The surfaces of the inner and outer cylinders are maintained at $T = T_0$ and $T = T_b$, respectively. We can expect that T will be a function of r alone.

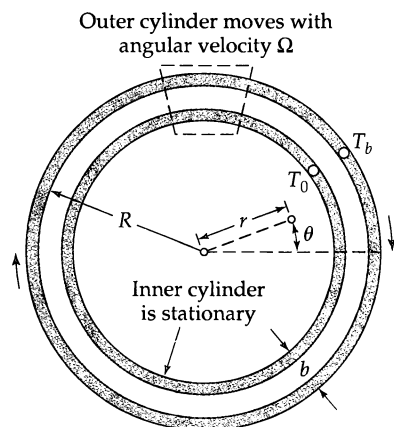


Fig. 10.4-1. Flow between cylinders with viscous heat generation. That part of the system enclosed within the dotted lines is shown in modified form in Fig. 10.4-2.

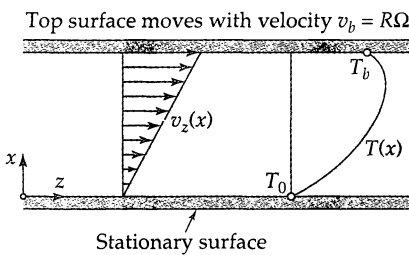


Fig. 10.4-2. Modification of a portion of the flow system in Fig. 10.4-1, in which the curvature of the bounding surfaces is neglected.

As the outer cylinder rotates, each cylindrical shell of fluid “rubs” against an adjacent shell of fluid. This friction between adjacent layers of the fluid produces heat; that is, the mechanical energy is degraded into thermal energy. The volume heat source resulting from this “viscous dissipation,” which can be designated by S_v , appears automatically in the shell balance when we use the combined energy flux vector e defined at the end of Chapter 9, as we shall see presently.

If the slit width b is small with respect to the radius R of the outer cylinder, then the problem can be solved approximately by using the somewhat simplified system depicted in Fig. 10.4-2. That is, we ignore curvature effects and solve the problem in Cartesian coordinates. The velocity distribution is then $v_z = v_b(x/b)$, where $v_b = \Omega R$.

We now make an energy balance over a shell of thickness Δx , width W , and length L . Since the fluid is in motion, we use the combined energy flux vector e as written in Eq. 9.8-6. The balance then reads

$$WL e_x|_x - WL e_x|_{x+\Delta x} = 0 \quad (10.4-1)$$

Dividing by $WL \Delta x$ and letting the shell thickness Δx go to zero then gives

$$\frac{de_x}{dx} = 0 \quad (10.4-2)$$

This equation may be integrated to give

$$e_x = C_1 \quad (10.4-3)$$

Since we do not know any boundary conditions for e_x , we cannot evaluate the integration constant at this point.

We now insert the expression for e_x from Eq. 9.8-6. Since the velocity component in the x direction is zero, the term $(\frac{1}{2}\rho v^2 + \rho \hat{U})\mathbf{v}$ can be discarded. The x -component of \mathbf{q} is $-k(dT/dx)$ according to Fourier’s law. The x -component of $[\boldsymbol{\tau} \cdot \mathbf{v}]$ is, as shown in Eq. 9.8-1, $\tau_{xx}v_x + \tau_{xy}v_y + \tau_{xz}v_z$. Since the only nonzero component of the velocity is v_z and since $\tau_{xz} = -\mu(dv_z/dx)$ according to Newton’s law of viscosity, the x -component of $[\boldsymbol{\tau} \cdot \mathbf{v}]$ is $-\mu v_z(dv_z/dx)$. We conclude, then, that Eq. 10.4-3 becomes

$$-k \frac{dT}{dx} - \mu v_z \frac{dv_z}{dx} = C_1 \quad (10.4-4)$$

When the linear velocity profile $v_z = v_b(x/b)$ is inserted, we get

$$-k \frac{dT}{dx} - \mu x \left(\frac{v_b}{b} \right)^2 = C_1 \quad (10.4-5)$$

in which $\mu(v_b/b)^2$ can be identified as the rate of viscous heat production per unit volume S_v .

When Eq. 10.4-5 is integrated we get

$$T = -\left(\frac{\mu}{k}\right)\left(\frac{v_b}{b}\right)^2 \frac{x^2}{2} - \frac{C_1}{k}x + C_2 \quad (10.4-6)$$

The two integration constants are determined from the boundary conditions

$$\text{B.C. 1:} \quad \text{at } x = 0, \quad T = T_0 \quad (10.4-7)$$

$$\text{B.C. 2:} \quad \text{at } x = b, \quad T = T_b \quad (10.4-8)$$

This yields finally, for $T_b \neq T_0$

$$\boxed{\left(\frac{T - T_0}{T_b - T_0} \right) = \frac{1}{2} \text{Br} \frac{x}{b} \left(1 - \frac{x}{b} \right) + \frac{x}{b}} \quad (10.4-9)$$

Here $\text{Br} = \mu v_b^2 / k(T_b - T_0)$ is the dimensionless *Brinkman number*,¹ which is a measure of the importance of the viscous dissipation term. If $T_b = T_0$, then Eq. 10.4-9 can be written as

$$\frac{T - T_0}{T_0} = \frac{1}{2} \frac{\mu v_b^2}{k T_0} \frac{x}{b} \left(1 - \frac{x}{b} \right) + \frac{x}{b} \quad (10.4-10)$$

and the maximum temperature is at $x/b = \frac{1}{2}$.

If the temperature rise is appreciable, the temperature dependence of the viscosity has to be taken into account. This is discussed in Problem 10C.1.

The viscous heating term $S_v = \mu(v_b/b)^2$ may be understood by the following arguments. For the system in Fig. 10.4-2, the rate at which work is done is the force acting on the upper plate times the velocity with which it moves, or $(-\tau_{xz}WL)(v_b)$. The rate of energy addition per unit volume is then obtained by dividing this quantity by WLb , which gives $(-\tau_{xz}v_b/b) = \mu(v_b/b)^2$. This energy all appears as heat and is hence S_v .

In most flow problems viscous heating is not important. However if there are large velocity gradients, then it cannot be neglected. Examples of situations where viscous heating must be accounted for include: (i) flow of a lubricant between rapidly moving parts, (ii) flow of molten polymers through dies in high-speed extrusion, (iii) flow of highly viscous fluids in high-speed viscometers, and (iv) flow of air in the boundary layer near an earth satellite or rocket during reentry into the earth's atmosphere. The first two of these are further complicated because many lubricants and molten plastics are non-Newtonian fluids. Viscous heating for non-Newtonian fluids is illustrated in Problem 10B.5.

§10.5 HEAT CONDUCTION WITH A CHEMICAL HEAT SOURCE

A chemical reaction is being carried out in a tubular, fixed-bed flow reactor with inner radius R as shown in Fig. 10.5-1. The reactor extends from $z = -\infty$ to $z = +\infty$ and is divided into three zones:

Zone I: Entrance zone packed with noncatalytic spheres

Zone II: Reaction zone packed with catalyst spheres, extending from $z = 0$ to $z = L$

Zone III: Exit zone packed with noncatalytic spheres

It is assumed that the fluid proceeds through the reactor tube in "plug flow"—that is, with axial velocity uniform at a superficial value $v_0 = w/\pi R^2 \rho$ (see text below Eq. 6.4-1 for the definition of "superficial velocity"). The density, mass flow rate, and superficial

¹ H. C. Brinkman, *Appl. Sci. Research*, **A2**, 120–124 (1951), solved the viscous dissipation heating problem for the Poiseuille flow in a circular tube. Other dimensionless groups that may be used for characterizing viscous heating have been summarized by R. B. Bird, R. C. Armstrong, and O. Hassager, *Dynamics of Polymeric Liquids*, Vol. 1, 2nd edition, Wiley, New York (1987), pp. 207–208.

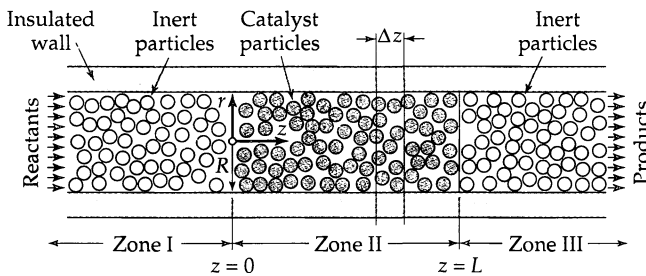


Fig. 10.5-1. Fixed-bed axial-flow reactor. Reactants enter at $z = -\infty$ and leave at $z = +\infty$. The reaction zone extends from $z = 0$ to $z = L$.

velocity are all treated as independent of r and z . In addition, the reactor wall is assumed to be well insulated, so that the temperature can be considered essentially independent of r . It is desired to find the steady-state axial temperature distribution $T(z)$ when the fluid enters at $z = -\infty$ with a uniform temperature T_1 .

When a chemical reaction occurs, thermal energy is produced or consumed when the reactant molecules rearrange to form the products. The volume rate of thermal energy production by chemical reaction, S_c , is in general a complicated function of pressure, temperature, composition, and catalyst activity. For simplicity, we represent S_c here as a function of temperature only: $S_c = S_{c1}F(\Theta)$, where $\Theta = (T - T_0)/(T_1 - T_0)$. Here T is the local temperature in the catalyst bed (assumed equal for catalyst and fluid), and S_{c1} and T_0 are empirical constants for the given reactor inlet conditions.

For the shell balance we select a disk of radius R and thickness Δz in the catalyst zone (see Fig. 10.5-1), and we choose Δz to be much larger than the catalyst particle dimensions. In setting up the energy balance, we use the combined energy flux vector e inasmuch as we are dealing with a flow system. Then, at steady state, the energy balance is

$$\pi R^2 e_z|_z - \pi R^2 e_z|_{z+\Delta z} + (\pi R^2 \Delta z) S_c = 0 \quad (10.5-1)$$

Next we divide by $\pi R^2 \Delta z$ and take the limit as Δz goes to zero. Strictly speaking, this operation is not "legal," since we are not dealing with a continuum but rather with a granular structure. Nevertheless, we perform this limiting process with the understanding that the resulting equation describes, not point values, but rather average values of e_z and S_c for reactor cross sections of constant z . This gives

$$\frac{de_z}{dz} = S_c \quad (10.5-2)$$

Now we substitute the z -component of Eq. 9.8-6 into this equation to get

$$\frac{d}{dz} \left(\frac{1}{2} \rho v^2 + \rho \hat{H} \right) v_z + \tau_{zz} v_z + q_z = S_c \quad (10.5-3)$$

We now use Fourier's law for q_z , Eq. 1.2-6 for τ_{zz} , and the enthalpy expression in Eq. 9.8-8 (with the assumption that the heat capacity is constant) to get

$$\frac{d}{dz} \left(\frac{1}{2} \rho v_z^2 + \rho \hat{C}_p (T - T^\circ) v_z + (p - p^\circ) v_z - \mu v_z \frac{dv_z}{dz} - \kappa_{\text{eff},zz} \frac{dT}{dz} \right) = S_c \quad (10.5-4)$$

in which the effective thermal conductivity in the z direction $\kappa_{\text{eff},zz}$ has been used (see Eq. 9.6-9). The first and fourth terms on the left side may be discarded, since the velocity is not changing with z . The third term may be discarded if the pressure does not change

significantly in the axial direction. Then in the second term we replace v_z by the superficial velocity v_0 , because the latter is the effective fluid velocity in the reactor. Then Eq. 10.5-4 becomes

$$\rho \hat{C}_p v_0 \frac{dT}{dz} = \kappa_{\text{eff},zz} \frac{d^2 T}{dz^2} + S_c \quad (10.5-5)$$

This is the differential equation for the temperature in zone II. The same equation applies in zones I and III with the source term set equal to zero. The differential equations for the temperature are then

$$\text{Zone I} \quad (z < 0) \quad \rho \hat{C}_p v_0 \frac{dT^I}{dz} = \kappa_{\text{eff},zz} \frac{d^2 T^I}{dz^2} \quad (10.5-6)$$

$$\text{Zone II} \quad (0 < z < L) \quad \rho \hat{C}_p v_0 \frac{dT^{II}}{dz} = \kappa_{\text{eff},zz} \frac{d^2 T^{II}}{dz^2} + S_{c1} F(\Theta) \quad (10.5-7)$$

$$\text{Zone III} \quad (z > L) \quad \rho \hat{C}_p v_0 \frac{dT^{III}}{dz} = \kappa_{\text{eff},zz} \frac{d^2 T^{III}}{dz^2} \quad (10.5-8)$$

Here we have assumed that we can use the same value of the effective thermal conductivity in all three zones. These three second-order differential equations are subject to the following six boundary conditions:

$$\text{B.C. 1:} \quad \text{at } z = -\infty, \quad T^I = T_1 \quad (10.5-9)$$

$$\text{B.C. 2:} \quad \text{at } z = 0, \quad T^I = T^{II} \quad (10.5-10)$$

$$\text{B.C. 3:} \quad \text{at } z = 0, \quad \kappa_{\text{eff},zz} \frac{dT^I}{dz} = \kappa_{\text{eff},zz} \frac{dT^{II}}{dz} \quad (10.5-11)$$

$$\text{B.C. 4:} \quad \text{at } z = L, \quad T^{II} = T^{III} \quad (10.5-12)$$

$$\text{B.C. 5:} \quad \text{at } z = L, \quad \kappa_{\text{eff},zz} \frac{dT^{II}}{dz} = \kappa_{\text{eff},zz} \frac{dT^{III}}{dz} \quad (10.5-13)$$

$$\text{B.C. 6:} \quad \text{at } z = \infty, \quad T^{III} = \text{finite} \quad (10.5-14)$$

Equations 10.5-10 to 13 express the continuity of temperature and heat flux at the boundaries between the zones. Equations 10.5-9 and 14 specify requirements at the two ends of the system.

The solution of Eqs. 10.5-6 to 14 is considered here for arbitrary $F(\Theta)$. In many cases of practical interest, the convective heat transport is far more important than the axial conductive heat transport. Therefore, here we drop the conductive terms entirely (those containing $\kappa_{\text{eff},zz}$). This treatment of the problem still contains the salient features of the solution in the limit of large $\text{Pe} = \text{RePr}$ (see Problem 10B.18 for a fuller treatment).

If we introduce a dimensionless axial coordinate $Z = z/L$ and a dimensionless chemical heat source $N = S_{c1}L/\rho \hat{C}_p v_0(T_1 - T_0)$, then Eqs. 10.5-6 to 8 become

$$\text{Zone I} \quad (z < 0) \quad \frac{d\Theta^I}{dZ} = 0 \quad (10.5-15)$$

$$\text{Zone II} \quad (0 < z < L) \quad \frac{d\Theta^{II}}{dZ} = NF(\Theta) \quad (10.5-16)$$

$$\text{Zone III} \quad (z > L) \quad \frac{d\Theta^{III}}{dZ} = 0 \quad (10.5-17)$$

for which we need three boundary conditions:

$$\text{B.C. 1:} \quad \text{at } Z = -\infty, \quad \Theta^I = 1 \quad (10.5-18)$$

$$\text{B.C. 2:} \quad \text{at } Z = 0, \quad \Theta^I = \Theta^{II} \quad (10.5-19)$$

$$\text{B.C. 3:} \quad \text{at } Z = 1, \quad \Theta^{II} = \Theta^{III} \quad (10.5-20)$$

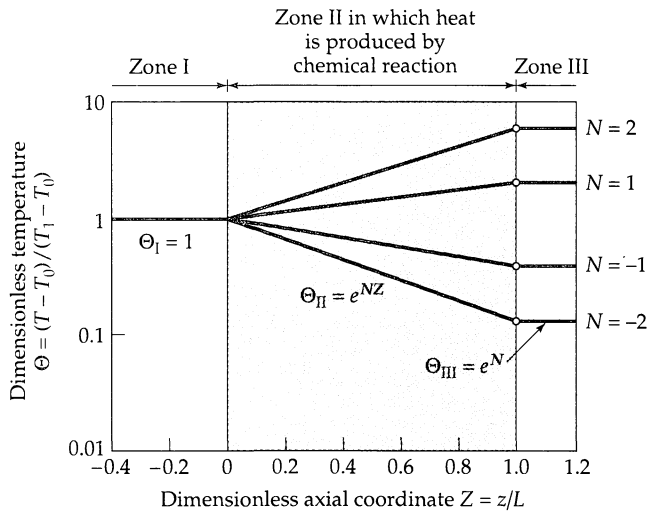


Fig. 10.5-2. Predicted temperature profiles in a fixed-bed axial-flow reactor when the heat production varies linearly with the temperature and when there is negligible axial diffusion.

The above first-order, separable differential equations, with boundary conditions, are easily solved to get

$$\text{Zone I} \quad \Theta^I = 1 \quad (10.5-21)$$

$$\text{Zone II} \quad \int_{\Theta^I}^{\Theta^{II}} \frac{1}{F(\Theta)} d\Theta = NZ \quad (10.5-22)$$

$$\text{Zone III} \quad \Theta^{III} = \Theta^{II}|_{Z=1} \quad (10.5-23)$$

These results are shown in Fig. 10.5-2 for a simple choice for the source function—namely, $F(\Theta) = \Theta$ —which is reasonable for small changes in temperature, if the reaction rate is insensitive to concentration.

Here in this section we ended up discarding the axial conduction terms. In Problem 10B.18, these terms are not discarded, and then the solution shows that there is some preheating (or precooling) in region I.

§10.6 HEAT CONDUCTION THROUGH COMPOSITE WALLS

In industrial heat transfer problems one is often concerned with conduction through walls made up of layers of various materials, each with its own characteristic thermal conductivity. In this section we show how the various resistances to heat transfer are combined into a total resistance.

In Fig. 10.6-1 we show a composite wall made up of three materials of different thicknesses, $x_1 - x_0$, $x_2 - x_1$, and $x_3 - x_2$, and different thermal conductivities k_{01} , k_{12} , and k_{23} . At $x = x_0$, substance 01 is in contact with a fluid with ambient temperature T_a , and at $x = x_3$, substance 23 is in contact with a fluid at temperature T_b . The heat transfer at the boundaries $x = x_0$ and $x = x_3$ is given by Newton's "law of cooling" with heat transfer

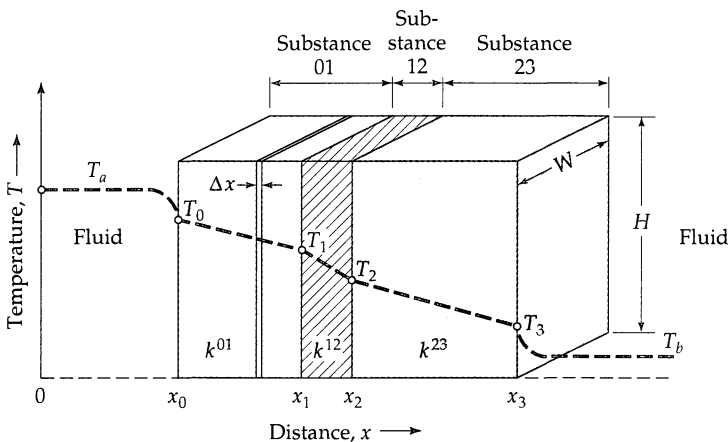


Fig. 10.6-1. Heat conduction through a composite wall, located between two fluid streams at temperatures T_a and T_b .

coefficients h_0 and h_3 , respectively. The anticipated temperature profile is sketched in Fig. 10.6-1.

First we set up the energy balance for the problem. Since we are dealing with heat conduction in a solid, the terms containing velocity in the \mathbf{e} vector can be discarded, and the only relevant contribution is the \mathbf{q} vector, describing heat conduction. We first write the energy balance for a slab of volume $WH \Delta x$

$$\text{Region 01:} \quad q_x|_x WH - q_x|_{x+\Delta x} WH = 0 \quad (10.6-1)$$

which states that the heat entering at x must be equal to the heat leaving at $x + \Delta x$, since no heat is produced within the region. After division by $WH \Delta x$ and taking the limit as $\Delta x \rightarrow 0$, we get

$$\text{Region 01:} \quad \frac{dq_x}{dx} = 0 \quad (10.6-2)$$

Integration of this equation gives

$$\text{Region 01:} \quad q_x = q_0 \quad (\text{a constant}) \quad (10.6-3)$$

The constant of integration, q_0 , is the heat flux at the plane $x = x_0$. The development in Eqs. 10.6-1, 2, and 3 can be repeated for regions 12 and 23 with continuity conditions on q_x at interfaces, so that the heat flux is constant and the same for all three slabs:

$$\text{Regions 01, 12, 23:} \quad q_x = q_0 \quad (10.6-4)$$

with the same constant for each of the regions. We may now introduce a Fourier's law for each of the three regions and get

$$\text{Region 01:} \quad -k_{01} \frac{dT}{dx} = q_0 \quad (10.6-5)$$

$$\text{Region 12:} \quad -k_{12} \frac{dT}{dx} = q_0 \quad (10.6-6)$$

$$\text{Region 23:} \quad -k_{23} \frac{dT}{dx} = q_0 \quad (10.6-7)$$

We now assume that k_{01} , k_{12} , and k_{23} are constants. Then we integrate each equation over the entire thickness of the relevant slab of material to get

$$\text{Region 01: } T_0 - T_1 = q_0 \left(\frac{x_1 - x_0}{k_{01}} \right) \quad (10.6-8)$$

$$\text{Region 12: } T_1 - T_2 = q_0 \left(\frac{x_2 - x_1}{k_{12}} \right) \quad (10.6-9)$$

$$\text{Region 23: } T_2 - T_3 = q_0 \left(\frac{x_3 - x_2}{k_{23}} \right) \quad (10.6-10)$$

In addition we have the two statements regarding the heat transfer at the surfaces according to Newton's law of cooling:

$$\text{At surface 0: } T_a - T_0 = \frac{q_0}{h_0} \quad (10.6-11)$$

$$\text{At surface 3: } T_3 - T_b = \frac{q_0}{h_3} \quad (10.6-12)$$

Addition of these last five equations then gives

$$T_a - T_b = q_0 \left(\frac{1}{h_0} + \frac{x_1 - x_0}{k_{01}} + \frac{x_2 - x_1}{k_{12}} + \frac{x_3 - x_2}{k_{23}} + \frac{1}{h_3} \right) \quad (10.6-13)$$

or

$$q_0 = \frac{T_a - T_b}{\left(\frac{1}{h_0} + \sum_{j=1}^3 \frac{x_j - x_{j-1}}{k_{j-1,j}} + \frac{1}{h_3} \right)} \quad (10.6-14)$$

Sometimes this result is rewritten in a form reminiscent of Newton's law of cooling, either in terms of the heat flux q_0 ($\text{J/m}^2 \cdot \text{s}$) or the heat flow Q_0 (J/s):

$$q_0 = U(T_a - T_b) \quad \text{or} \quad Q_0 = U(WH)(T_a - T_b) \quad (10.6-15)$$

The quantity U , called the "overall heat transfer coefficient," is given then by the following famous formula for the "additivity of resistances":

$$\frac{1}{U} = \frac{1}{h_0} + \sum_{j=1}^n \frac{x_j - x_{j-1}}{k_{j-1,j}} + \frac{1}{h_n} \quad (10.6-16)$$

Here we have generalized the formula to a system with n slabs of material. Equations 10.6-15 and 16 are useful for calculating the heat transfer rate through a composite wall separating two fluid streams, when the heat transfer coefficients and thermal conductivities are known. The estimation of heat transfer coefficients is discussed in Chapter 14.

In the above development it has been tacitly assumed that the solid slabs are contiguous with no intervening "air spaces." If the solid surfaces touch each other only at several points, the resistance to heat transfer will be appreciably increased.

EXAMPLE 10.6-1

Develop a formula for the overall heat transfer coefficient for the composite cylindrical pipe wall shown in Fig. 10.6-2.

Composite Cylindrical Walls

SOLUTION

An energy balance on a shell of volume $2\pi rL \Delta r$ for region 01 is

$$\text{Region 01: } q_r|_r \cdot 2\pi rL - q_r|_{r+\Delta r} \cdot 2\pi(r + \Delta r)L = 0 \quad (10.6-17)$$

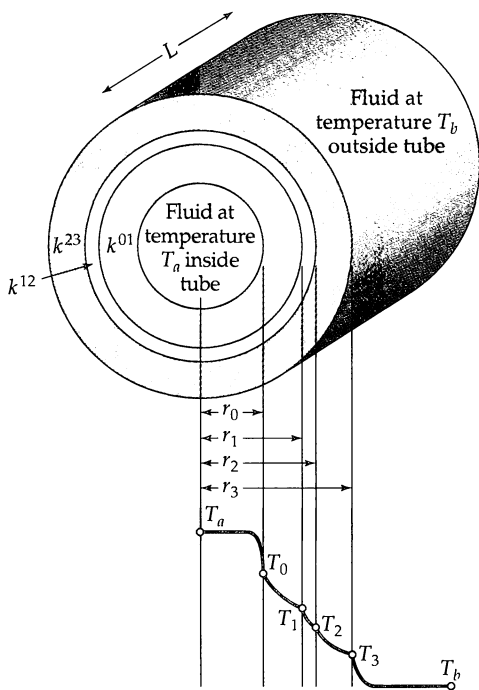


Fig. 10.6-2. Heat conduction through a laminated tube with a fluid at temperature T_a inside the tube and temperature T_b outside.

which can also be written as

$$\text{Region 01: } (2\pi r L q_r)|_r - (2\pi r L q_r)|_{r+\Delta r} = 0 \quad (10.6-18)$$

Dividing by $2\pi L \Delta r$ and taking the limit as Δr goes to zero gives

$$\text{Region 01: } \frac{d}{dr}(rq_r) = 0 \quad (10.6-19)$$

Integration of this equation gives

$$rq_r = r_0 q_0 \quad (10.6-20)$$

in which r_0 is the inner radius of region 01, and q_0 is the heat flux there. In regions 12 and 23, rq_r is equal to the same constant. Application of Fourier's law to the three regions gives

$$\text{Region 01: } -k_{01}r \frac{dT}{dr} = r_0 q_0 \quad (10.6-21)$$

$$\text{Region 12: } -k_{12}r \frac{dT}{dr} = r_0 q_0 \quad (10.6-22)$$

$$\text{Region 23: } -k_{23}r \frac{dT}{dr} = r_0 q_0 \quad (10.6-23)$$

If we assume that the thermal conductivities in the three annular regions are constants, then each of the above three equations can be integrated across its region to give

$$\text{Region 10: } T_0 - T_1 = r_0 q_0 \frac{\ln(r_1/r_0)}{k_{01}} \quad (10.6-24)$$

$$\text{Region 12: } T_1 - T_2 = r_0 q_0 \frac{\ln(r_2/r_1)}{k_{12}} \quad (10.6-25)$$

Region 23:

$$T_2 - T_3 = r_0 q_0 \frac{\ln(r_3/r_2)}{k_{23}} \quad (10.6-26)$$

At the two fluid-solid interfaces we can write Newton's law of cooling:

Surface 0:

$$T_a - T_0 = \frac{q_0}{h_0} \quad (10.6-27)$$

Surface 3:

$$T_3 - T_b = \frac{q_3}{h_3} = \frac{q_0}{h_3} \frac{r_0}{r_3} \quad (10.6-28)$$

Addition of the preceding five equations gives an equation for $T_a - T_b$. Then the equation is solved for q_0 to give

$$Q_0 = 2\pi L r_0 q_0 = \frac{2\pi L (T_a - T_b)}{\left(\frac{1}{r_0 h_0} + \frac{\ln(r_1/r_0)}{k_{01}} + \frac{\ln(r_2/r_1) \ln(r_3/r_2)}{k_{12} k_{23}} + \frac{1}{r_3 h_3} \right)} \quad (10.6-29)$$

We now define an "overall heat transfer coefficient based on the inner surface" U_0 by

$$Q_0 = 2\pi L r_0 q_0 = U_0 (2\pi L r_0) (T_a - T_b) \quad (10.6-30)$$

Combination of the last two equations gives, on generalizing to a system with n annular layers,

$$\frac{1}{r_0 U_0} = \left(\frac{1}{r_0 h_0} + \sum_{j=1}^n \frac{\ln(r_j/r_{j-1})}{k_{j-1,j}} + \frac{1}{r_n h_n} \right) \quad (10.6-31)$$

The subscript "0" on U_0 indicates that the overall heat transfer coefficient is referred to the radius r_0 .

§10.7 HEAT CONDUCTION IN A COOLING FIN¹

Another simple, but practical application of heat conduction is the calculation of the efficiency of a cooling fin. Fins are used to increase the area available for heat transfer between metal walls and poorly conducting fluids such as gases. A simple rectangular fin is shown in Fig. 10.7-1. The wall temperature is T_w and the ambient air temperature is T_a .

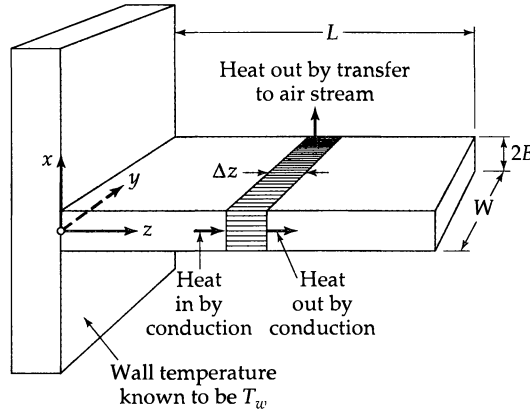


Fig. 10.7-1. A simple cooling fin with $B \ll L$ and $B \ll W$.

¹ For further information on fins, see M. Jakob, *Heat Transfer*, Vol. I, Wiley, New York (1949), Chapter 11; and H. D. Baehr and K. Stephan, *Heat and Mass Transfer*, Springer, Berlin (1998), §2.2.3.

A reasonably good description of the system may be obtained by approximating the true physical situation by a simplified model:

True situation	Model
1. T is a function of x , y , and z , but the dependence on z is most important.	1. T is a function of z alone.
2. A small quantity of heat is lost from the fin at the end (area $2BW$) and at the edges (area $(2BL + 2BL)$).	2. No heat is lost from the end or from the edges.
3. The heat transfer coefficient is a function of position.	3. The heat flux at the surface is given by $q_z = h(T - T_a)$, where h is constant and T depends on z .

The energy balance is made over a segment Δz of the bar. Since the bar is stationary, the terms containing \mathbf{v} in the combined energy flux vector \mathbf{e} may be discarded, and the only contribution to the energy flux is \mathbf{q} . Therefore the energy balance is

$$2BWq_z|_z - 2BWq_z|_{z+\Delta z} - h(2W\Delta z)(T - T_a) = 0 \quad (10.7-1)$$

Division by $2BW\Delta z$ and taking the limit as Δz approaches zero gives

$$-\frac{dq_z}{dz} = \frac{h}{B}(T - T_a) \quad (10.7-2)$$

We now insert Fourier's law ($q_z = -kdT/dz$), in which k is the thermal conductivity of the metal. If we assume that k is constant, we then get

$$\frac{d^2T}{dz^2} = \frac{h}{kB}(T - T_a) \quad (10.7-3)$$

This equation is to be solved with the boundary conditions

$$\text{B.C. 1:} \quad \text{at } z = 0, \quad T = T_w \quad (10.7-4)$$

$$\text{B.C. 2:} \quad \text{at } z = L, \quad \frac{dT}{dz} = 0 \quad (10.7-5)$$

We now introduce the following dimensionless quantities:

$$\Theta = \frac{T - T_a}{T_w - T_a} = \text{dimensionless temperature} \quad (10.7-6)$$

$$\zeta = \frac{z}{L} = \text{dimensionless distance} \quad (10.7-7)$$

$$N^2 = \frac{hL^2}{kB} = \text{dimensionless heat transfer coefficient}^2 \quad (10.7-8)$$

The problem then takes the form

$$\frac{d^2\Theta}{d\zeta^2} = N^2\Theta \quad \text{with } \Theta|_{\zeta=0} = 1 \quad \text{and} \quad \left. \frac{d\Theta}{d\zeta} \right|_{\zeta=1} = 0 \quad (10.7-9, 10, 11)$$

² The quantity N^2 may be rewritten as $N^2 = (hL/k)(L/B) = Bi(L/B)$, where Bi is called the *Biot number*, named after **Jean Baptiste Biot** (1774–1862) (pronounced “Bee-oh”). Professor of physics at the Collège de France, he received the Rumford Medal for his development of a simple, nondestructive test to determine sugar concentration.

Equation 10.7-9 may be integrated to give hyperbolic functions (see Eq. C.1-4 and §C.5). When the two integration constants have been determined, we get

$$\Theta = \cosh N\zeta - (\tanh N) \sinh N\zeta \quad (10.7-12)$$

This may be rearranged to give

$$\Theta = \frac{\cosh N(1 - \zeta)}{\cosh N} \quad (10.7-13)$$

This result is reasonable only if the heat lost at the end and at the edges is negligible.

The "effectiveness" of the fin surface is defined³ by

$$\eta = \frac{\text{actual rate of heat loss from the fin}}{\text{rate of heat loss from an isothermal fin at } T_w} \quad (10.7-14)$$

For the problem being considered here η is then

$$\eta = \frac{\int_0^W \int_0^L h(T - T_a) dz dy}{\int_0^W \int_0^L h(T_w - T_a) dz dy} = \frac{\int_0^1 \Theta d\zeta}{\int_0^1 d\zeta} \quad (10.7-15)$$

or

$$\eta = \frac{1}{\cosh N} \left(-\frac{1}{N} \sinh N(1 - \zeta) \right) \Big|_0^1 = \frac{\tanh N}{N} \quad (10.7-16)$$

in which N is the dimensionless quantity defined in Eq. 10.7-8.

EXAMPLE 10.7-1

Error in Thermocouple Measurement

In Fig. 10.7-2 a thermocouple is shown in a cylindrical well inserted into a gas stream. Estimate the true temperature of the gas stream if

$T_1 = 500^\circ\text{F}$ = temperature indicated by thermocouple

$T_w = 350^\circ\text{F}$ = wall temperature

$h = 120 \text{ Btu/hr} \cdot \text{ft}^2 \cdot \text{F}$ = heat transfer coefficient

$k = 60 \text{ Btu/hr} \cdot \text{ft}^3 \cdot \text{F}$ = thermal conductivity of well wall

$B = 0.08 \text{ in.}$ = thickness of well wall

$L = 0.2 \text{ ft}$ = length of well

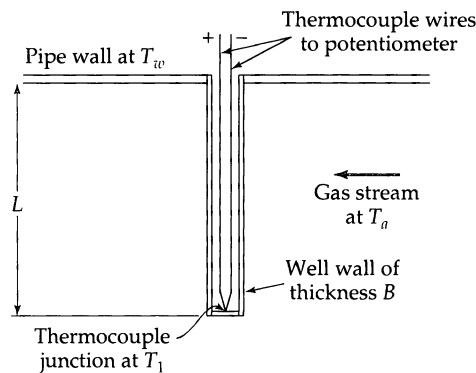


Fig. 10.7-2. A thermocouple in a cylindrical well.

³ M. Jakob, *Heat Transfer*, Vol. I, Wiley, New York (1949), p. 235.

SOLUTION

The thermocouple well wall of thickness B is in contact with the gas stream on one side only, and the tube thickness is small compared with the diameter. Hence the temperature distribution along this wall will be about the same as that along a bar of thickness $2B$, in contact with the gas stream on both sides. According to Eq. 10.7-13, the temperature at the end of the well (that registered by the thermocouple) satisfies

$$\begin{aligned}\frac{T_1 - T_a}{T_w - T_a} &= \frac{\cosh 0}{\cosh N} = \frac{1}{\cosh \sqrt{hL^2/kB}} \\ &= \frac{1}{\cosh \sqrt{(102)(0.2)^2/(60)(\frac{1}{12} \cdot 0.08)}} \\ &= \frac{1}{\cosh(2\sqrt{3})} = \frac{1}{16.0}\end{aligned}\quad (10.7-17)$$

Hence the actual ambient gas temperature is obtained by solving this equation for T_a :

$$\frac{500 - T_a}{350 - T_a} = \frac{1}{16.0} \quad (10.7-18)$$

and the result is

$$T_a = 510^\circ\text{F} \quad (10.7-19)$$

Therefore, the reading is 10°F too low.

This example has focused on one kind of error that can occur in thermometry. Frequently a simple analysis, such as the foregoing, can be used to estimate the measurement errors.⁴

§10.8 FORCED CONVECTION

In the preceding sections the emphasis has been placed on heat conduction in solids. In this and the following section we study two limiting types of heat transport in fluids: *forced convection* and *free convection* (also called *natural convection*). The main differences between these two modes of convection are shown in Fig. 10.8-1. Most industrial heat transfer problems are usually put into either one or the other of these two limiting categories. In some problems, however, both effects must be taken into account, and then we speak of *mixed convection* (see §14.6 for some empiricisms for handling this situation).

In this section we consider forced convection in a circular tube, a limiting case of which is simple enough to be solved analytically.^{1,2} A viscous fluid with physical properties (μ , k , ρ , C_p) assumed constant is in laminar flow in a circular tube of radius R . For $z < 0$ the fluid temperature is uniform at the inlet temperature T_1 . For $z > 0$ there is a constant radial heat flux $q_r = -q_0$ at the wall. Such a situation exists, for example, when a pipe is wrapped uniformly with an electrical heating coil, in which case q_0 is positive. If the pipe is being chilled, then q_0 has to be taken as negative.

As indicated in Fig. 10.8-1, the first step in solving a forced convection heat transfer problem is the calculation of the velocity profiles in the system. We have seen in §2.3

⁴ For further discussion, see M. Jakob, *Heat Transfer*, Vol. II, Wiley, New York (1949), Chapter 33, pp. 147–201.

¹ A. Eagle and R. M. Ferguson, *Proc. Roy. Soc. (London)*, A127, 540–566 (1930).

² S. Goldstein, *Modern Developments in Fluid Dynamics*, Oxford University Press (1938), Dover Edition (1965), Vol. II, p. 622.

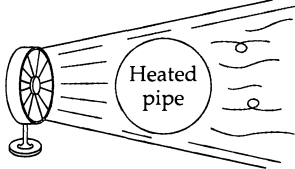
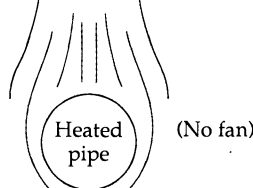
Forced Convection Heat Transfer	Free Convection Heat Transfer
	
Heat swept to right by forced stream of air	Heat transported upward by heated air that rises (No fan)
1. The flow patterns are determined primarily by some external force	1. The flow patterns are determined by the buoyant force on the heated fluid
2 First, the velocity profiles are found; then they are used to find the temperature profiles (usual procedure for fluids with constant physical properties)	2. The velocity profiles and temperature profiles are interdependent
3. The Nusselt number depends on the Reynolds and Prandtl numbers (see Chapter 14)	3. The Nusselt number depends on the Grashof and Prandtl numbers (see Chapter 14)

Fig. 10.8-1. A comparison of forced and free convection in non-isothermal systems.

how this may be done for tube flow by using the shell balance method. We know that the velocity distribution so obtained is $v_r = 0$, $v_\theta = 0$, and

$$v_z = \frac{(\mathcal{P}_0 - \mathcal{P}_L)R^2}{4\mu L} \left[1 - \left(\frac{r}{R} \right)^2 \right] = v_{z,\max} \left[1 - \left(\frac{r}{R} \right)^2 \right] \quad (10.8-1)$$

This parabolic distribution is valid sufficiently far downstream from the inlet that the entrance length has been exceeded.

In this problem, heat is being transported in both the r and the z directions. Therefore, for the energy balance we use a "washer-shaped" system, which is formed by the intersection of an annular region of thickness Δr with a slab of thickness Δz (see Fig. 10.8-2). In this problem, we are dealing with a flowing fluid, and therefore all terms in the \mathbf{e} vector will be retained. The various contributions to Eq. 10.1-1 are

$$\text{Total energy in at } r \quad e_r|_r \cdot 2\pi r \Delta z = (2\pi r e_r)|_r \Delta z \quad (10.8-2)$$

$$\text{Total energy out at } r + \Delta r \quad e_r|_{r+\Delta r} \cdot 2\pi(r + \Delta r) \Delta z = (2\pi r e_r)|_{r+\Delta r} \Delta z \quad (10.8-3)$$

$$\text{Total energy in at } z \quad e_z|_z \cdot 2\pi r \Delta r \quad (10.8-4)$$

$$\text{Total energy out at } z + \Delta z \quad e_z|_{z+\Delta z} \cdot 2\pi r \Delta r \quad (10.8-5)$$

$$\text{Work done on fluid by gravity} \quad \rho v_z g_z \cdot 2\pi r \Delta r \Delta z \quad (10.8-6)$$

The last contribution is the rate at which work is done on the fluid within the ring by gravity—that is, the force per unit volume ρg_z times the volume $2\pi r \Delta r \Delta z$ multiplied by the downward velocity of the fluid.

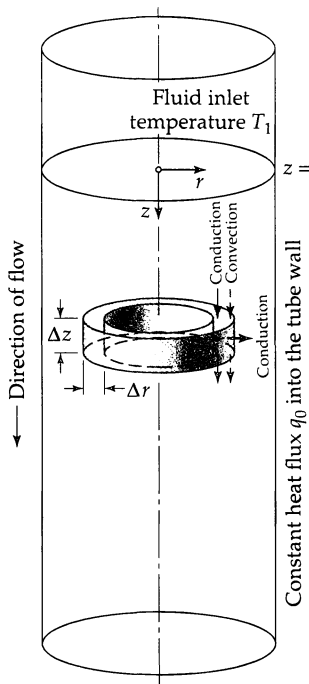


Fig. 10.8-2. Heating of a fluid in laminar flow through a circular tube, showing the annular ring over which the energy balance is made.

The energy balance is obtained by summing these contributions and equating the sum to zero. Then we divide by $2\pi \Delta r \Delta z$ to get

$$\frac{(re_r)|_r - (re_r)|_{r+\Delta r}}{\Delta r} + r \frac{e_z|_z - e_z|_{z+\Delta z}}{\Delta z} + \rho v_z g_z r = 0 \quad (10.8-7)$$

In the limit as Δr and Δz go to zero, we find

$$-\frac{1}{r} \frac{\partial}{\partial r} (re_r) - \frac{\partial e_z}{\partial z} + \rho v_z g = 0 \quad (10.8.8)$$

The subscript z in g_z has been omitted, since the gravity vector is acting in the $+z$ direction.

Next we use Eqs. 9.8-6 and 9.8-8 to write out the expressions for the r - and z -components of the combined energy flux vector, using the fact that the only nonzero component of \mathbf{v} is the axial component v_z :

$$e_r = \tau_{rz} v_z + q_r = -\left(\mu \frac{\partial v_z}{\partial r}\right) v_z - k \frac{\partial T}{\partial r} \quad (10.8-9)$$

$$\begin{aligned} e_z &= (\frac{1}{2} \rho v_z^2) v_z + \rho \hat{H} v_z + \tau_{zz} v_z + q_z \\ &= (\frac{1}{2} \rho v_z^2) v_z + (p - p^\circ) v_z + \rho \hat{C}_p (T - T^\circ) v_z - \left(2\mu \frac{\partial v_z}{\partial z}\right) v_z - k \frac{\partial T}{\partial z} \end{aligned} \quad (10.8-10)$$

Substituting these flux expressions into Eq. 10.8-8 and using the fact that v_z depends only on r gives, after some rearrangement,

$$\rho \hat{C}_p v_z \frac{\partial T}{\partial z} = k \left[\frac{1}{r} \frac{\partial}{\partial r} \left(r \frac{\partial T}{\partial r} \right) + \frac{\partial^2 T}{\partial z^2} \right] + \mu \left(\frac{\partial v_z}{\partial r} \right)^2 + v_z \left[-\frac{\partial p}{\partial z} + \mu \frac{1}{r} \frac{\partial}{\partial r} \left(r \frac{\partial v_z}{\partial r} \right) + \rho g \right] \quad (10.8-11)$$

The second bracket is exactly zero, as can be seen from Eq. 3.6-4, which is the z -component of the equation of motion for the Poiseuille flow in a circular tube (here $\mathcal{P} = p - \rho g z$). The

term containing the viscosity is the viscous heating, which we shall neglect in this discussion. The last term in the first bracket, corresponding to heat conduction in the axial direction, will be omitted, since we know from experience that it is usually small in comparison with the heat convection in the axial direction. Therefore, the equation that we want to solve here is

$$\rho \hat{C}_p v_{z,\max} \left[1 - \left(\frac{r}{R} \right)^2 \right] \frac{\partial T}{\partial z} = k \left[\frac{1}{r} \frac{\partial}{\partial r} \left(r \frac{\partial T}{\partial r} \right) \right] \quad (10.8-12)$$

This partial differential equation, when solved, describes the temperature in the fluid as a function of r and z . The boundary conditions are

$$\text{B.C. 1:} \quad \text{at } r = 0, \quad T = \text{finite} \quad (10.8-13)$$

$$\text{B.C. 2:} \quad \text{at } r = R, \quad k \frac{\partial T}{\partial r} = q_0 \text{ (constant)} \quad (10.8-14)$$

$$\text{B.C. 3:} \quad \text{at } z = 0, \quad T = T_1 \quad (10.8-15)$$

We now put the problem statement into dimensionless form. The choice of the dimensionless quantities is arbitrary. We choose

$$\Theta = \frac{T - T_1}{q_0 R / k} \quad \xi = \frac{r}{R} \quad \zeta = \frac{z}{\rho \hat{C}_p v_{z,\max} R^2 / k} \quad (10.8-16, 17, 18)$$

Generally one tries to select dimensionless quantities so as to minimize the number of parameters in the final problem formulation. In this problem the choice of $\xi = r/R$ is a natural one, because of the appearance of r/R in the differential equation. The choice for the dimensionless temperature is suggested by the second and third boundary conditions. Having specified these two dimensionless variables, the choice of dimensionless axial coordinate follows naturally.

The resulting problem statement, in dimensionless form, is now

$$(1 - \xi^2) \frac{\partial \Theta}{\partial \xi} = \frac{1}{\xi} \frac{\partial}{\partial \xi} \left(\xi \frac{\partial \Theta}{\partial \xi} \right) \quad (10.8-19)$$

with boundary conditions

$$\text{B.C. 1:} \quad \text{at } \xi = 0, \quad \Theta = \text{finite} \quad (10.8-20)$$

$$\text{B.C. 2:} \quad \text{at } \xi = 1, \quad \frac{\partial \Theta}{\partial \xi} = 1 \quad (10.8-21)$$

$$\text{B.C. 3:} \quad \text{at } \zeta = 0, \quad \Theta = 0 \quad (10.8-22)$$

The partial differential equation in Eq. 10.8-19 has been solved for these boundary conditions,³ but in this section we do not give the complete solution.

It is, however, instructive to obtain the asymptotic solution to Eq. 10.8-19 for large ζ . After the fluid is sufficiently far downstream from the beginning of the heated section, one expects that the constant heat flux through the wall will result in a rise of the fluid temperature that is linear in ζ . One further expects that the shape of the temperature profiles as a function of ξ will ultimately not undergo further change with increasing ζ (see Fig. 10.8-3). Hence a solution of the following form seems reasonable for large ζ :

$$\Theta(\xi, \zeta) = C_0 \zeta + \Psi(\xi) \quad (10.8-23)$$

in which C_0 is a constant to be determined presently.

³ R. Siegel, E. M. Sparrow, and T. M. Hallman, *Appl. Sci. Research*, A7, 386–392 (1958). See Example 12.2-1 for the complete solution and Example 12.2-2 for the asymptotic solution for small ζ .

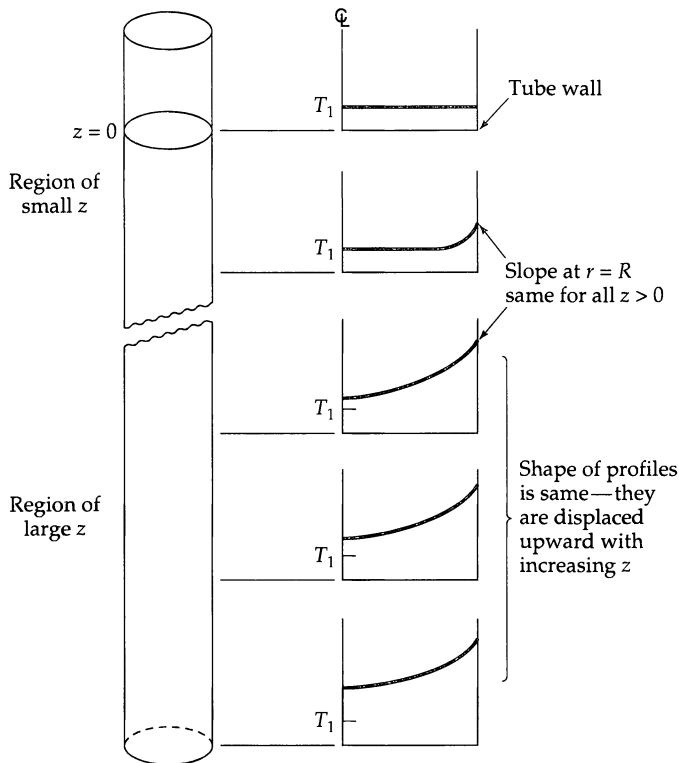


Fig. 10.8-3. Sketch showing how one expects the temperature $T(r, z)$ to look for the system shown in Fig. 10.8-2 when the fluid is heated by means of a heating coil wrapped uniformly around the tube (corresponding to q_0 positive).

The function in Eq. 10.8-23 is clearly not the complete solution to the problem; it does allow the partial differential equation and boundary conditions 1 and 2 to be satisfied, but clearly does not satisfy boundary condition 3. Hence we replace the latter by an integral condition (see Fig. 10.8-4),

$$\text{Condition 4: } 2\pi Rzq_0 = \int_0^{2\pi} \int_0^R \rho \hat{C}_p (T - T_1) v_z r dr d\theta \quad (10.8-24)$$

or, in dimensionless form,

$$\zeta = \int_0^1 \Theta(\xi, \zeta)(1 - \xi^2)\xi d\xi \quad (10.8-25)$$

This condition states that the energy entering through the walls over a distance ζ is the same as the difference between the energy leaving through the cross section at ζ and that entering at $\zeta = 0$.

Substitution of the postulated function of Eq. 10.8-23 into Eq. 10.8-19 leads to the following ordinary differential equation for Ψ (see Eq. C.1-11):

$$\frac{1}{\xi} \frac{d}{d\xi} \left(\xi \frac{d\Psi}{d\xi} \right) = C_0(1 - \xi^2) \quad (10.8-26)$$

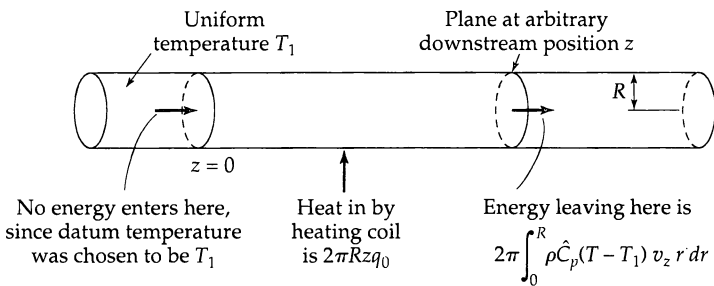


Fig. 10.8-4. Energy balance used for boundary condition 4 given in Eq. 10.8-24.

This equation may be integrated twice with respect to ξ and the result substituted into Eq. 10.8-23 to give

$$\Theta(\xi, \zeta) = C_0 \zeta + C_0 \left(\frac{\xi^2}{4} - \frac{\xi^4}{16} \right) + C_1 \ln \xi + C_2 \quad (10.8-27)$$

The three constants are determined from the conditions 1, 2, and 4 above:

$$\text{B.C. 1:} \quad C_1 = 0 \quad (10.8-28)$$

$$\text{B.C. 2:} \quad C_0 = 4 \quad (10.8-29)$$

$$\text{Condition 4:} \quad C_2 = -\frac{7}{24} \quad (10.8-30)$$

Substitution of these values into Eq. 10.8-27 gives finally

$$\boxed{\Theta(\xi, \zeta) = 4\zeta + \xi^2 - \frac{1}{4}\xi^4 - \frac{7}{24}} \quad (10.8-31)$$

This result gives the dimensionless temperature as a function of the dimensionless radial and axial coordinates. It is exact in the limit as $\zeta \rightarrow \infty$; for $\zeta > 0.1$, it predicts the local value of Θ to within about 2%.

Once the temperature distribution is known, one can get various derived quantities. There are two kinds of average temperatures commonly used in connection with the flow of fluids with constant ρ and \hat{C}_p :

$$\langle T \rangle = \frac{\int_0^{2\pi} \int_0^R T(r, z) r dr d\theta}{\int_0^{2\pi} \int_0^R r dr d\theta} = T_1 + (4\zeta + \frac{7}{24}) \frac{q_0 R}{k} \quad (10.8-32)$$

$$T_b = \frac{\langle v_z T \rangle}{\langle v_z \rangle} = \frac{\int_0^{2\pi} \int_0^R v_z(r) T(r, z) r dr d\theta}{\int_0^{2\pi} \int_0^R v_z(r) r dr d\theta} = T_1 + (4\zeta) \frac{q_0 R}{k} \quad (10.8-33)$$

Both averages are functions of z . The quantity $\langle T \rangle$ is the arithmetic average of the temperatures over the cross section at z . The "bulk temperature" T_b is the temperature one would obtain if the tube were chopped off at z and if the fluid issuing forth were collected in a container and thoroughly mixed. This average temperature is sometimes referred to as the "cup-mixing temperature" or the "flow-average temperature."

Now let us evaluate the local heat transfer driving force, $T_0 - T_b$, which is the difference between the wall and bulk temperatures at a distance z down the tube:

$$T_0 - T_b = \frac{11}{24} \frac{q_0 R}{k} = \frac{11}{48} \frac{q_0 D}{k} \quad (10.8-34)$$

where D is the tube diameter. We may now rearrange this result in the form of a dimensionless wall heat flux

$$\frac{q_0 D}{k(T_0 - T_b)} = \frac{48}{11} \quad (10.8-35)$$

which, in Chapter 14, will be identified as a *Nusselt number*.

Before leaving this section, we point out that the dimensionless axial coordinate ζ introduced above may be rewritten in the following way:

$$\zeta = \left[\frac{\mu}{D(v_z)\rho} \right] \left[\frac{k}{\hat{C}_p \mu} \right] \left[\frac{z}{R} \right] = \frac{1}{\text{RePr}} \left[\frac{z}{R} \right] = \frac{1}{\text{Pé}} \left[\frac{z}{R} \right] \quad (10.8-36)$$

Here D is the tube diameter, Re is the Reynolds number used in Part I, and Pr and Pé are the Prandtl and Péclet numbers introduced in Chapter 9. We shall find in Chapter 11 that the Reynolds and Prandtl numbers can be expected to appear in forced convection problems. This point will be reinforced in Chapter 14 in connection with correlations for heat transfer coefficients.

§10.9 FREE CONVECTION

In §10.8 we gave an example of forced convection. In this section we turn our attention to an elementary free convection problem—namely, the flow between two parallel walls maintained at different temperatures (see Fig. 10.9-1).

A fluid with density ρ and viscosity μ is located between two vertical walls a distance $2B$ apart. The heated wall at $y = -B$ is maintained at temperature T_2 , and the cooled wall at $y = +B$ is maintained at temperature T_1 . It is assumed that the temperature difference is sufficiently small that terms containing $(\Delta T)^2$ can be neglected.

Because of the temperature gradient in the system, the fluid near the hot wall rises and that near the cold wall descends. The system is closed at the top and bottom, so that the fluid is continuously circulating between the plates. The mass rate of flow of the

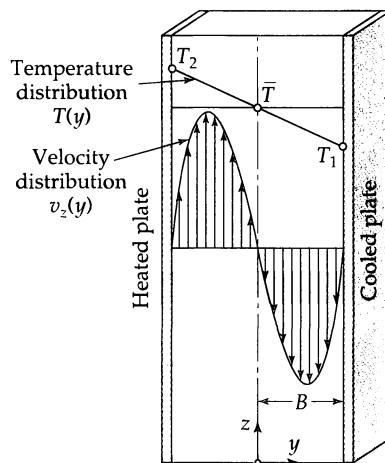


Fig. 10.9-1. Laminar free convection flow between two vertical plates at two different temperatures. The velocity is a cubic function of the coordinate y .

fluid in the upward-moving stream is the same as that in the downward-moving stream. The plates are presumed to be very tall, so that end effects near the top and bottom can be disregarded. Then for all practical purposes the temperature is a function of y alone.

An energy balance can now be made over a thin slab of fluid of thickness Δy , using the y -component of the combined energy flux vector \mathbf{e} as given in Eq. 9.8-6. The term containing the kinetic energy and enthalpy can be disregarded, since the y -component of the \mathbf{v} vector is zero. The y -component of the term $[\boldsymbol{\tau} \cdot \mathbf{v}]$ is $\tau_{yz}v_z = -\mu(dv_z/dy)v_z$, which would lead to the viscous heating contribution discussed in §10.4. However, in the very slow flows encountered in free convection, this term will be extremely small and can be neglected. The energy balance then leads to the equation

$$-\frac{dq_y}{dy} = 0 \quad \text{or} \quad k \frac{d^2T}{dy^2} = 0 \quad (10.9-1)$$

for constant k . The temperature equation is to be solved with the boundary conditions:

$$\text{B.C. 1:} \quad \text{at } y = -B, \quad T = T_2 \quad (10.9-2)$$

$$\text{B.C. 2:} \quad \text{at } y = +B, \quad T = T_1 \quad (10.9-3)$$

The solution to this problem is

$$T = \bar{T} - \frac{1}{2} \Delta T \frac{y}{B} \quad (10.9-4)$$

in which $\Delta T = T_2 - T_1$ is the difference of the wall temperatures, and $\bar{T} = \frac{1}{2}(T_1 + T_2)$ is their arithmetic mean.

By making a momentum balance over the same slab of thickness Δy , one arrives at a differential equation for the velocity distribution

$$\mu \frac{d^2v_z}{dy^2} = \frac{dp}{dz} + \rho g \quad (10.9-5)$$

Here the viscosity has been assumed constant (see Problem 10B.11) for a solution with temperature-dependent viscosity.

The phenomenon of free convection results from the fact that when the fluid is heated, the density (usually) decreases and the fluid rises. The mathematical description of the system must take this essential feature of the phenomenon into account. Because the temperature difference $\Delta T = T_2 - T_1$ is taken to be small in this problem, it can be expected that the density changes in the system will be small. This suggests that we should expand ρ in a Taylor series about the temperature $\bar{T} = \frac{1}{2}(T_1 + T_2)$ thus:

$$\begin{aligned} \rho &= \rho|_{T=\bar{T}} + \left. \frac{d\rho}{dT} \right|_{T=\bar{T}} (T - \bar{T}) + \dots \\ &= \bar{\rho} - \bar{\rho}\beta(T - \bar{T}) + \dots \end{aligned} \quad (10.9-6)$$

Here $\bar{\rho}$ and $\bar{\beta}$ are the density and coefficient of volume expansion evaluated at the temperature \bar{T} . The coefficient of volume expansion is defined as

$$\beta = \frac{1}{V} \left(\frac{\partial V}{\partial T} \right)_p = \frac{1}{(1/\rho)} \left(\frac{\partial(1/\rho)}{\partial T} \right)_p = -\frac{1}{\rho} \left(\frac{\partial \rho}{\partial T} \right)_p \quad (10.9-7)$$

We now introduce the "Taylor-made" equation of state of Eq. 10.9-6 (keeping two terms only) into the equation of motion in Eq. 10.9-5 to get

$$\mu \frac{d^2v_z}{dy^2} = \frac{dp}{dz} + \bar{\rho}g - \bar{\rho}g\bar{\beta}(T - \bar{T}) \quad (10.9-8)$$

This equation describes the balance among the viscous force, the pressure force, the gravity force, and the buoyant force $-\bar{\rho}g\beta(T - \bar{T})$ (all per unit volume). Into this we now substitute the temperature distribution given in Eq. 10.9-4 to get the differential equation

$$\mu \frac{d^2v_z}{dy^2} = \left(\frac{dp}{dz} + \bar{\rho}g \right) + \frac{1}{2}\bar{\rho}g\beta\Delta T \frac{y}{B} \quad (10.9-9)$$

which is to be solved with the boundary conditions

$$\text{B.C. 1:} \quad \text{at } y = -B, \quad v_z = 0 \quad (10.9-10)$$

$$\text{B.C. 2:} \quad \text{at } y = +B, \quad v_z = 0 \quad (10.9-11)$$

The solution is

$$v_z = \frac{(\bar{\rho}g\beta\Delta T)B^2}{12\mu} \left[\left(\frac{y}{B} \right)^3 - \left(\frac{y}{B} \right) \right] + \frac{B^2}{12\mu} \left(\frac{dp}{dz} + \bar{\rho}g \right) \left[\left(\frac{y}{B} \right)^2 - 1 \right] \quad (10.9-12)$$

We now require that the net mass flow in the z direction be zero, that is,

$$\int_{-B}^{+B} \rho v_z dy = 0 \quad (10.9-13)$$

Substitution of v_z from Eq. 10.9-12 and ρ from Eqs. 10.9-6 and 4 into this integral leads to the conclusion that

$$\frac{dp}{dz} = -\bar{\rho}g \quad (10.9-14)$$

when terms containing the square of the small quantity ΔT are neglected. Equation 10.9-14 states that the pressure gradient in the system is due solely to the weight of the fluid, and the usual hydrostatic pressure distribution prevails. Therefore the second term on the right side of Eq. 10.9-12 drops out and the final expression for the velocity distribution is

$$v_z = \frac{(\bar{\rho}g\beta\Delta T)B^2}{12\mu} \left[\left(\frac{y}{B} \right)^3 - \left(\frac{y}{B} \right) \right]$$

(10.9-15)

The average velocity in the upward-moving stream is

$$\langle v_z \rangle = \frac{(\bar{\rho}g\beta\Delta T)B^2}{48\mu} \quad (10.9-16)$$

The motion of the fluid is thus a direct result of the buoyant force term in Eq. 10.9-8, associated with the temperature gradient in the system. The velocity distribution of Eq. 10.9-15 is shown in Fig. 10.9-1. It is this sort of velocity distribution that occurs in the air space in a double-pane window or in double-wall panels in buildings. It is also this kind of flow that occurs in the operation of a Clusius–Dickel column used for separating isotopes or organic liquid mixtures by the combined effects of thermal diffusion and free convection.¹

¹ Thermal diffusion is the diffusion resulting from a temperature gradient. For a lucid discussion of the Clusius–Dickel column see K. E. Grew and T. L. Ibbs, *Thermal Diffusion in Gases*, Cambridge University Press (1952), pp. 94–106.

The velocity distribution in Eq. 10.9-15 may be rewritten using a dimensionless velocity $\check{v}_z = Bv_z\bar{\rho}/\mu$ and a dimensionless coordinate $\check{y} = y/B$ thus:

$$\check{v}_z = \frac{1}{2} \text{Gr}(\check{y}^3 - \check{y}) \quad (10.9-17)$$

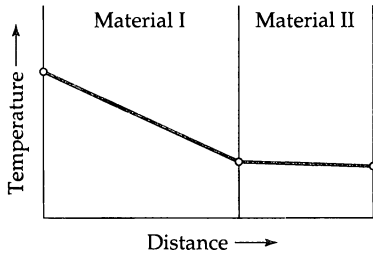
Here Gr is the dimensionless *Grashof number*,² defined by

$$\text{Gr} = \left[\frac{(\rho^2 g \beta \Delta T) B^3}{\mu^2} \right] = \left[\frac{\bar{\rho} g B^3 \Delta \rho}{\mu^2} \right] \quad (10.9-18)$$

where $\Delta \rho = \rho_1 - \rho_2$. The second form of the Grashof number is obtained from the first form by using Eq. 10.9-6. The Grashof number is the characteristic group occurring in analyses of free convection, as is shown by dimensional analysis in Chapter 11. It arises in heat transfer coefficient correlations in Chapter 14.

QUESTIONS FOR DISCUSSION

1. Verify that the Brinkman, Biot, Prandtl, and Grashof numbers are dimensionless.
2. To what problem in electrical circuits is the addition of thermal resistances analogous?
3. What is the coefficient of volume expansion for an ideal gas? What is the corresponding expression for the Grashof number?
4. What might be some consequences of large temperature gradients produced by viscous heating in viscometry, lubrication, and plastics extrusion?
5. In §10.8 would there be any advantage to choosing the dimensionless temperature and dimensionless axial coordinate to be $\Theta = (T - T_1)/T_1$ and $\xi = z/R$?
6. What would happen in §9.9 if the fluid were water and \bar{T} were 4°C?
7. Is there any advantage to solving Eq. 9.7-9 in terms of hyperbolic functions rather than exponential functions?
8. In going from Eq. 10.8-11 to Eq. 10.8-12 the axial conduction term was neglected with respect to the axial convection term. To justify this, put in some reasonable numerical values to estimate the relative sizes of the terms.
9. How serious is it to neglect the dependence of viscosity on temperature in solving forced convection problems? Viscous dissipation heating problems?
10. At steady state the temperature profiles in a laminated system appear thus:
Which material has the higher thermal conductivity?



11. Show that Eq. 10.6-4 can be obtained directly by rewriting Eq. 10.6-1 with $x + \Delta x$ replaced by x_0 . Similarly, one gets Eq. 10.6-20 from Eq. 10.6-17, with $r + \Delta r$ replaced by r_0 .

² Named for **Franz Grashof** (1826–1893) (pronounced “Grahss-hoff”). He was professor of applied mechanics in Karlsruhe and one of the founders of the Verein Deutscher Ingenieure in 1856.

PROBLEMS

- 10A.1. Heat loss from an insulated pipe.** A standard schedule 40, 2-in. steel pipe (inside diameter 2.067 in. and wall thickness 0.154 in.) carrying steam is insulated with 2 in. of 85% magnesia covered in turn with 2 in. of cork. Estimate the heat loss per hour per foot of pipe if the inner surface of the pipe is at 250°F and the outer surface of the cork is at 90°F. The thermal conductivities (in Btu/hr · ft · F) of the substances concerned are: steel, 26.1; 85% magnesia, 0.04; cork, 0.03.

Answer: 24 Btu/hr · ft

- 10A.2. Heat loss from a rectangular fin.** Calculate the heat loss from a rectangular fin (see Fig. 10.7-1) for the following conditions:

Air temperature	350°F
Wall temperature	500°F
Thermal conductivity of fin	60 Btu/hr · ft · F
Thermal conductivity of air	0.0022 Btu/hr · ft · F
Heat transfer coefficient	120 Btu/hr · ft ² · F
Length of fin	0.2 ft
Width of fin	1.0 ft
Thickness of fin	0.16 in.

Answer: 2080 Btu/hr

- 10A.3. Maximum temperature in a lubricant.** An oil is acting as a lubricant for a pair of cylindrical surfaces such as those shown in Fig. 10.4-1. The angular velocity of the outer cylinder is 7908 rpm. The outer cylinder has a radius of 5.06 cm, and the clearance between the cylinders is 0.027 cm. What is the maximum temperature in the oil if both wall temperatures are known to be 158°F? The physical properties of the oil are assumed constant at the following values:

Viscosity	92.3 cp
Density	1.22 g/cm ³
Thermal conductivity	0.055 cal/s · cm · C

Answer: 174°F

- 10A.4. Current-carrying capacity of wire.** A copper wire of 0.040 in. diameter is insulated uniformly with plastic to an outer diameter of 0.12 in. and is exposed to surroundings at 100°F. The heat transfer coefficient from the outer surface of the plastic to the surroundings is 1.5 Btu/hr · ft² · F. What is the maximum steady current, in amperes, that this wire can carry without heating any part of the plastic above its operating limit of 200°F? The thermal and electrical conductivities may be assumed constant at the values given here:

	k (Btu/hr · ft · F)	k_e (ohm ⁻¹ cm ⁻¹)
Copper	220	5.1×10^5
Plastic	0.20	0.0

Answer: 13.7 amp

- 10A.5. Free convection velocity.**

- (a) Verify the expression for the average velocity in the upward-moving stream in Eq. 10.9-16.
- (b) Evaluate $\bar{\beta}$ for the conditions given below.
- (c) What is the average velocity in the upward-moving stream in the system described in Fig. 10.9-1 for air flowing under these conditions?

Pressure	1 atm
Temperature of the heated wall	100°C
Temperature of the cooled wall	20°C
Spacing between the walls	0.6 cm

Answer: 2.3 cm/s

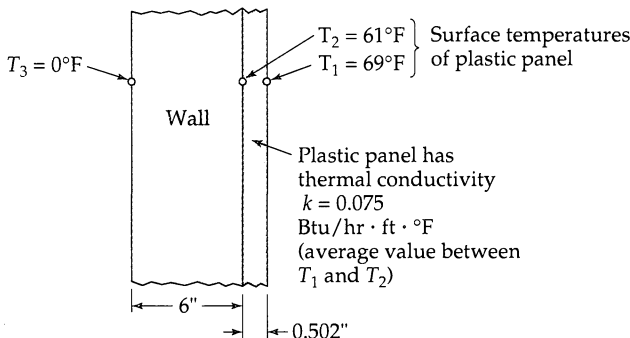


Fig. 10A.6. Determination of the thermal resistance of a wall.

- 10A.6. Insulating power of a wall** (Fig. 10A.6). The “insulating power” of a wall can be measured by means of the arrangement shown in the figure. One places a plastic panel against the wall. In the panel two thermocouples are mounted flush with the panel surfaces. The thermal conductivity and thickness of the plastic panel are known. From the measured steady-state temperatures shown in the figure, calculate:

- (a) The steady-state heat flux through the wall (and panel).
- (b) The “thermal resistance” (wall thickness divided by thermal conductivity).

Answers: (a) 14.4 Btu/hr · ft²; (b) 4.24 ft² · hr · F/Btu

- 10A.7. Viscous heating in a ball-point pen.** You are asked to decide whether the apparent decrease in viscosity in ball-point pen inks during writing results from “shear thinning” (decrease in viscosity because of non-Newtonian effects) or “temperature thinning” (decrease in viscosity because of temperature rise caused by viscous heating). If the temperature rise is less than 1K, then “temperature thinning” will not be important. Estimate the temperature rise using Eq. 10.4-9 and the following estimated data:

Clearance between ball and holding cavity	$5 \times 10^{-5} \text{ in.}$
Diameter of ball	1 mm
Viscosity of ink	10^4 cp
Speed of writing	100 in./min
Thermal conductivity of ink (rough guess)	$5 \times 10^{-4} \text{ cal/s} \cdot \text{cm} \cdot \text{C}$

- 10A.8. Temperature rise in an electrical wire.**

- (a) A copper wire, 5 mm in diameter and 15 ft long, has a voltage drop of 0.6 volts. Find the maximum temperature in the wire if the ambient air temperature is 25°C and the heat transfer coefficient h is $5.7 \text{ Btu/hr} \cdot \text{ft}^2 \cdot {}^\circ\text{F}$.
- (b) Compare the temperature drops across the wire and the surrounding air film.

- 10B.1. Heat conduction from a sphere to a stagnant fluid.** A heated sphere of radius R is suspended in a large, motionless body of fluid. It is desired to study the heat conduction in the fluid surrounding the sphere in the absence of convection.

- (a) Set up the differential equation describing the temperature T in the surrounding fluid as a function of r , the distance from the center of the sphere. The thermal conductivity k of the fluid is considered constant.
- (b) Integrate the differential equation and use these boundary conditions to determine the integration constants: at $r = R$, $T = T_R$; and at $r = \infty$, $T = T_\infty$.

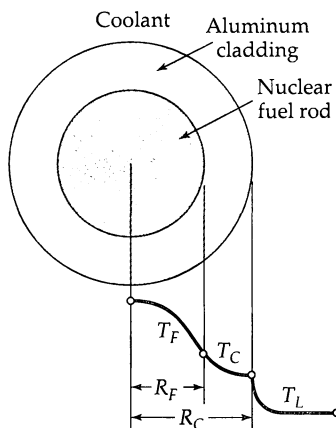


Fig. 10B.3. Temperature distribution in a cylindrical fuel-rod assembly.

(c) From the temperature profile, obtain an expression for the heat flux at the surface. Equate this result to the heat flux given by "Newton's law of cooling" and show that a dimensionless heat transfer coefficient (known as the *Nusselt number*) is given by

$$\text{Nu} = \frac{hD}{k} = 2 \quad (10B.1-1)$$

in which D is the sphere diameter. This well-known result provides the limiting value of Nu for heat transfer from spheres at low Reynolds and Grashof numbers (see §14.4).

(d) In what respect are the Biot number and the Nusselt number different?

- 10B.2. Viscous heating in slit flow.** Find the temperature profile for the viscous heating problem shown in Fig. 10.4-2, when given the following boundary conditions: at $x = 0$, $T = T_0$; at $x = b$, $q_x = 0$.

$$\text{Answer: } \frac{T - T_0}{\mu v_0/k} = \left(\frac{x}{b}\right) - \frac{1}{2} \left(\frac{x}{b}\right)^2$$

- 10B.3 Heat conduction in a nuclear fuel rod assembly** (Fig. 10B.3). Consider a long cylindrical nuclear fuel rod, surrounded by an annular layer of aluminum cladding. Within the fuel rod heat is produced by fission; this heat source depends on position approximately as

$$S_n = S_{n0} \left[1 + b \left(\frac{r}{R_F} \right)^2 \right] \quad (10B.3-1)$$

Here S_{n0} and b are known constants, and r is the radial coordinate measured from the axis of the cylindrical fuel rod. Calculate the maximum temperature in the fuel rod if the outer surface of the cladding is in contact with a liquid coolant at temperature T_L . The heat transfer coefficient at the cladding-coolant interface is h_L , and the thermal conductivities of the fuel rod and cladding are k_F and k_C .

$$\text{Answer: } T_{F,\max} - T_L = \frac{S_{n0}R_F^2}{4k_F} \left(1 + \frac{b}{4} \right) + \frac{S_{n0}R_F^2}{2k_C} \left(1 + \frac{b}{2} \right) \left(\frac{k_C}{R_C h_L} + \ln \frac{R_C}{R_F} \right)$$

- 10B.4. Heat conduction in an annulus** (Fig. 10B.4).

(a) Heat is flowing through an annular wall of inside radius r_0 and outside radius r_1 . The thermal conductivity varies linearly with temperature from k_0 at T_0 to k_1 at T_1 . Develop an expression for the heat flow through the wall.

(b) Show how the expression in (a) can be simplified when $(r_1 - r_0)/r_0$ is very small. Interpret the result physically.

$$\text{Answer: (a)} Q = 2\pi L(T_0 - T_1) \left(\frac{k_0 + k_1}{2} \right) \left(\ln \frac{r_1}{r_0} \right)^{-1}; \text{ (b)} Q = 2\pi r_0 L \left(\frac{k_0 + k_1}{2} \right) \left(\frac{T_0 - T_1}{r_1 - r_0} \right)$$

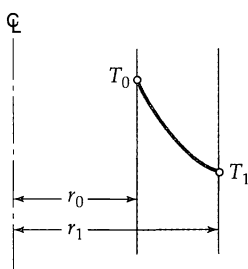


Fig. 10B.4. Temperature profile in an annular wall.

- 10B.5. Viscous heat generation in a polymer melt.** Rework the problem discussed in §10.4 for a molten polymer, whose viscosity can be adequately described by the power law model (see Chapter 8). Show that the temperature distribution is the same as that in Eq. 10.4-9 but with the Brinkman number replaced by

$$\text{Br}_n = \left[\frac{mv_b^{n+1}}{b^{n-1}kT_0} \right] \quad (10\text{B}.5-1)$$

- 10B.6. Insulation thickness for a furnace wall** (Fig. 10B.6). A furnace wall consists of three layers: (i) a layer of heat-resistant or refractory brick, (ii) a layer of insulating brick, and (iii) a steel plate, 0.25 in. thick, for mechanical protection. Calculate the thickness of each layer of brick to give minimum total wall thickness if the heat loss through the wall is to be 5000 Btu/ft² · hr, assuming that the layers are in excellent thermal contact. The following information is available:

Material	Maximum allowable temperature	Thermal conductivity (Btu/hr · ft · F)	
		at 100°F	at 2000°F
Refractory brick	2600°F	1.8	3.6
Insulating brick	2000°F	0.9	1.8
Steel	—	26.1	—

Answer: Refractory brick, 0.39 ft; insulating brick, 0.51 ft.

- 10B.7. Forced-convection heat transfer in flow between parallel plates** (Fig. 10B.7). A viscous fluid with temperature-independent physical properties is in fully developed laminar flow between two flat surfaces placed a distance $2B$ apart. For $z < 0$ the fluid temperature is uniform at $T = T_1$. For $z > 0$ heat is added at a constant, uniform flux q_0 at both walls. Find the temperature distribution $T(x, z)$ for large z .

- (a) Make a shell energy balance to obtain the differential equation for $T(x, z)$. Then discard the viscous dissipation term and the axial heat conduction term.

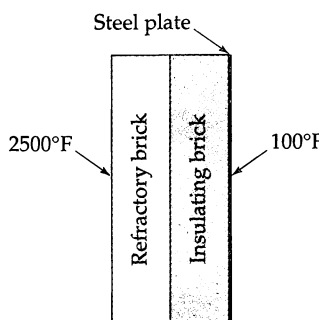


Fig. 10B.6. A composite furnace wall.

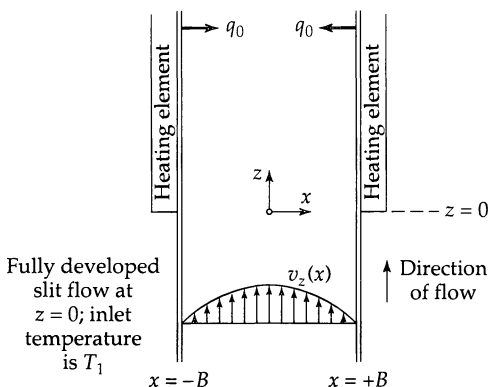


Fig. 10B.7. Laminar, incompressible flow between parallel plates, both of which are being heated by a uniform wall heat flux q_0 starting at $z = 0$.

(b) Recast the problem in terms of the dimensionless quantities

$$\Theta = \frac{T - T_1}{q_0 B / k} \quad \sigma = \frac{x}{B} \quad \zeta = \frac{kz}{\rho \hat{C}_p v_{z,\max} B^2} \quad (10B.7-1, 2, 3)$$

(c) Obtain the asymptotic solution for large z :

$$\Theta(\sigma, \zeta) = \frac{3}{2}\zeta + \frac{3}{4}\sigma^2 - \frac{1}{8}\sigma^4 - \frac{39}{280} \quad (10B.7-4)$$

10B.8. Electrical heating of a pipe (Fig. 10B.8). In the manufacture of glass-coated steel pipes, it is common practice first to heat the pipe to the melting range of glass and then to contact the hot pipe surface with glass granules. These granules melt and wet the pipe surface to form a tightly adhering nonporous coat. In one method of preheating the pipe, an electric current is passed along the pipe, with the result that the pipe is heated (as in §10.2). For the purpose of this problem make the following assumptions:

(i) The electrical conductivity of the pipe k is constant over the temperature range of interest. The local rate of electrical heat production S_r is then uniform throughout the pipe wall.

(ii) The top and bottom of the pipe are capped in such a way that heat losses through them are negligible.

(iii) Heat loss from the outer surface of the pipe to the surroundings is given by Newton's law of cooling: $q_r = h(T_k - T_a)$. Here h is a suitable heat transfer coefficient.

How much electrical power is needed to maintain the inner pipe surface at some desired temperature, T_k , for known k , T_a , h , and pipe dimensions?

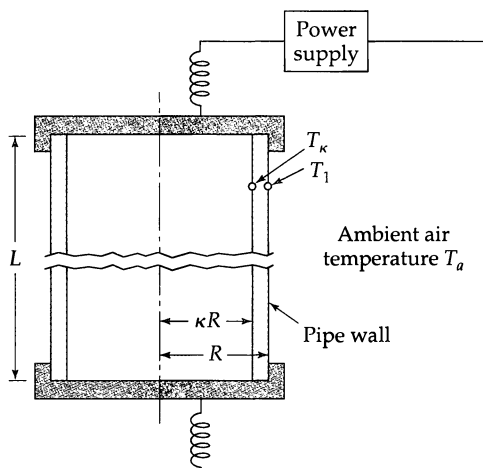


Fig. 10B.8. Electrical heating of a pipe.

$$\text{Answer: } P = \frac{\pi R^2 (1 - \kappa^2) L (T_1 - T_\kappa)}{\frac{(1 - \kappa^2)R}{2h} - \frac{(\kappa R)^2}{4k} \left[\left(1 - \frac{1}{\kappa^2}\right) - 2 \ln \kappa \right]}$$

- 10B.9.** **Plug flow with forced-convection heat transfer.** Very thick slurries and pastes sometimes move in channels almost as a solid plug. Thus, one can approximate the velocity by a constant value v_0 over the conduit cross section.

- (a) Rework the problem of §10.8 for plug flow in a *circular tube* of radius R . Show that the temperature distribution analogous to Eq. 10.8-31 is

$$\Theta(\xi, \zeta) = 2\xi + \frac{1}{2}\xi^2 - \frac{1}{4} \quad (10B.9-1)$$

in which $\zeta = kz/\rho \hat{C}_p v_0 R^2$, and Θ and ξ are defined as in §10.8.

- (b) Show that for plug flow in a *plane slit* of width $2B$ the temperature distribution analogous to Eq. 10B.7-4 is

$$\Theta(\xi, \zeta) = \zeta + \frac{1}{2}\sigma^2 - \frac{1}{6} \quad (10B.9-2)$$

in which $\zeta = kz/\rho \hat{C}_p v_0 B^2$, and Θ and σ are defined as in Problem 10B.7.

- 10B.10.** **Free convection in an annulus of finite height** (Fig. 10B.10). A fluid is contained in a vertical annulus closed at the top and bottom. The inner wall of radius κR is maintained at the temperature T_κ , and the outer wall of radius R is kept at temperature T_1 . Using the assumptions and approach of §10.9, obtain the velocity distribution produced by free convection.

- (a) First derive the temperature distribution

$$\frac{T_1 - T}{T_1 - T_\kappa} = \frac{\ln \xi}{\ln \kappa} \quad (10B.10-1)$$

in which $\xi = r/R$.

- (b) Then show that the equation of motion is

$$\frac{1}{\xi} \frac{d}{d\xi} \left(\xi \frac{dv_z}{d\xi} \right) = A + B \ln \xi \quad (10B.10-2)$$

in which $A = (R^2/\mu)(dp/dz + \rho_1 g)$ and $B = ((\rho_1 g \beta_1 \Delta T)R^2/\mu \ln \kappa)$ where $\Delta T = T_1 - T_\kappa$.

- (c) Integrate the equation of motion (see Eq. C.1-11) and apply the boundary conditions to evaluate the constants of integration. Then show that A can be evaluated by the requirement of no net mass flow through any plane $z = \text{constant}$, with the final result that

$$v_z = \frac{\rho_1 g \beta_1 \Delta T R^2}{16\mu} \left[\frac{(1 - \kappa^2)(1 - 3\kappa^2) - 4\kappa^4 \ln \kappa}{(1 - \kappa^2)^2 + (1 - \kappa^4) \ln \kappa} \left((1 - \xi^2) - (1 - \kappa^2) \frac{\ln \xi}{\ln \kappa} \right) + 4(\xi^2 - \kappa^2) \frac{\ln \xi}{\ln \kappa} \right] \quad (10B.10-3)$$

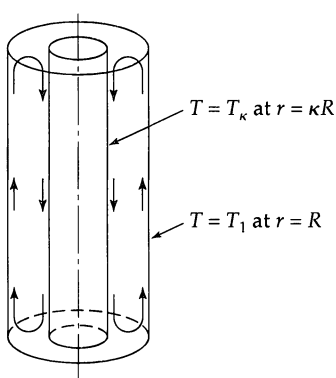


Fig. 10B.10. Free convection pattern in an annular space with $T_1 > T_\kappa$.

- 10B.11. Free convection with temperature-dependent viscosity.** Rework the problem in §10.9, taking into account the variation of viscosity with temperature. Assume that the “fluidity” (reciprocal of viscosity) is the following linear function of the temperature

$$\frac{1}{\mu} = \frac{1}{\bar{\mu}} [1 + \bar{\beta}_\mu (T - \bar{T})] \quad (10B.11-1)$$

Use the dimensionless quantities \check{y} , \check{v}_z , and Gr defined in §10.9 and in addition

$$b_\mu = \frac{1}{2} \bar{\beta}_\mu \Delta T \quad \text{and} \quad P = \frac{\bar{\rho} B^3}{\bar{\mu}^2} \left(\frac{dp}{dz} + \bar{\rho} g \right) \quad (10B.11-2, 3)$$

and show that the differential equation for the velocity distribution is

$$\frac{d}{d\check{y}} \left(\frac{1}{1 - b_\mu \check{y}} \frac{d\check{v}_z}{d\check{y}} \right) = P + Gr \check{y} \quad (10B.11-4)$$

Follow the procedure in §10.9, discarding terms containing the second and higher powers of b_μ . Show that this leads to $P = \frac{2}{15} Gr b_\mu$ and finally:

$$\check{v}_z = \frac{1}{6} Gr [(\check{y}^3 - \check{y}) - \frac{3}{20} b_\mu (\check{y}^2 - 1)(5\check{y}^2 - 1)] \quad (10B.11-5)$$

Sketch the result to show how the velocity profile becomes skewed because of the temperature-dependent viscosity.

- 10B.12. Heat conduction with temperature-dependent thermal conductivity** (Fig. 10B.12). The curved surfaces and the end surfaces (both shaded in the figure) of the solid in the shape of a half-cylindrical shell are insulated. The surface $\theta = 0$, of area $(r_2 - r_1)L$, is maintained at temperature T_0 , and the surface at $\theta = \pi$, also of area $(r_2 - r_1)L$, is kept at temperature T_π .

The thermal conductivity of the solid varies linearly with temperature from k_0 at $T = T_0$ to k_π at $T = T_\pi$.

(a) Find the steady-state temperature distribution.

(b) Find the total heat flow through the surface at $\theta = 0$.

- 10B.13. Flow reactor with exponentially temperature-dependent source.** Formulate the function $F(\Theta)$ of Eq. 10.5-1 for a zero-order reaction with the temperature dependence

$$S_c = K e^{-E/RT} \quad (10B.13-1)$$

in which K and E are constants, and R is the gas constant. Then insert $F(\Theta)$ into Eqs. 10.5-15 through 20 and solve for the dimensionless temperature profile with $k_{z,\text{eff}}$ neglected.

- 10B.14. Evaporation loss from an oxygen tank.**

(a) Liquefied gases are sometimes stored in well-insulated spherical containers vented to the atmosphere. Develop an expression for the steady-state heat transfer rate through the walls of such a container, with the radii of the inner and outer walls being r_0 and r_1 respectively and

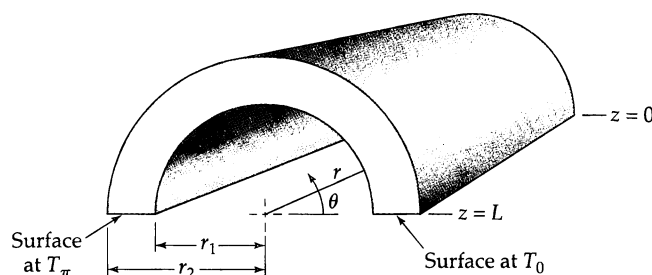


Fig. 10B.12. Tangential heat conduction in an annular shell.

the temperatures at the inner and outer walls being T_0 and T_1 . The thermal conductivity of the insulation varies linearly with temperature from k_0 at T_0 to k_1 at T_1 .

(b) Estimate the rate of evaporation of liquid oxygen from a spherical container of 6 ft inside diameter covered with a 1-ft-thick annular evacuated jacket filled with particulate insulation. The following information is available:

Temperature at inner surface of insulation	-183°C
Temperature at outer surface of insulation	0°C
Boiling point of O ₂	-183°C
Heat of vaporization of O ₂	1636 cal/g-mol
Thermal conductivity of insulation at 0°C	9.0×10^{-4} Btu/hr · ft · F
Thermal conductivity of insulation at -183°C	7.2×10^{-4} Btu/hr · ft · F

$$\text{Answers: (a)} Q_0 = 4\pi r_0 r_1 \left(\frac{k_0 + k_1}{2} \right) \left(\frac{T_1 - T_0}{r_1 - r_0} \right); \text{(b)} 0.198 \text{ kg/hr}$$

- 10B.15. Radial temperature gradients in an annular chemical reactor.** A catalytic reaction is being carried out at constant pressure in a packed bed between coaxial cylindrical walls with inner radius r_0 and outer radius r_1 . Such a configuration occurs when temperatures are measured with a centered thermowell, and is in addition useful for controlling temperature gradients if a thin annulus is used. The entire inner wall is at uniform temperature T_0 , and it can be assumed that there is no heat transfer through this surface. The reaction releases heat at a uniform volumetric rate S_c throughout the reactor. The effective thermal conductivity of the reactor contents is to be treated as a constant throughout.

(a) By a shell energy balance, derive a second-order differential equation that describes the temperature profiles, assuming that the temperature gradients in the axial direction can be neglected. What boundary conditions must be used?

(b) Rewrite the differential equation and boundary conditions in terms of the dimensionless radial coordinate and dimensionless temperature defined as

$$\xi = \frac{r}{r_0}; \quad \Theta = \frac{T - T_0}{S_c r_0^2 / 4k_{\text{eff}}} \quad (10B.15-1)$$

Explain why these are logical choices.

(c) Integrate the dimensionless differential equation to get the radial temperature profile. To what viscous flow problem is this conduction problem analogous?

(d) Develop expressions for the temperature at the outer wall and for the volumetric average temperature of the catalyst bed.

(e) Calculate the outer wall temperature when $r_0 = 0.45$ in., $r_1 = 0.50$ in., $k_{\text{eff}} = 0.3$ Btu/hr · ft · F, $T_0 = 900^\circ\text{F}$, and $S_c = 4800$ cal/hr · cm³.

(f) How would the results of part (e) be affected if the inner and outer radii were doubled?

Answer: (e) 888°F

- 10B.16. Temperature distribution in a hot-wire anemometer.** A hot-wire anemometer is essentially a fine wire, usually made of platinum, which is heated electrically and exposed to a flowing fluid. Its temperature, which is a function of the fluid temperature, fluid velocity, and the rate of heating, may be determined by measuring its electrical resistance. It is used for measuring velocities and velocity fluctuations in flow systems. In this problem we analyze the temperature distribution in the wire element.

We consider a wire of diameter D and length $2L$ supported at its ends ($z = -L$ and $z = +L$) and mounted perpendicular to an air stream. An electric current of density I amp/cm² flows through the wire, and the heat thus generated is partially lost by convection to the air stream (see Eq. 10.1-2) and partially by conduction toward the ends of the wire. Because of their size and their high electrical and thermal conductivity, the supports are not appreciably heated by the current, but remain at the temperature T_L , which is the same as that of the approaching air stream. Heat loss by radiation is to be neglected.

(a) Derive an equation for the steady-state temperature distribution in the wire, assuming that T depends on z alone; that is, the radial temperature variation in the wire is neglected. Further, assume uniform thermal and electrical conductivities in the wire, and a uniform heat transfer coefficient from the wire to the air stream.

(b) Sketch the temperature profile obtained in (a).

(c) Compute the current, in amperes, required to heat a platinum wire to a midpoint temperature of 50°C under the following conditions:

$$T_L = 20^\circ\text{C} \quad h = 100 \text{ Btu/hr} \cdot \text{ft}^2 \cdot \text{F}$$

$$D = 0.127 \text{ mm} \quad k = 40.2 \text{ Btu/hr} \cdot \text{ft} \cdot \text{F}$$

$$L = 0.5 \text{ cm} \quad k_e = 1.00 \times 10^5 \text{ ohm}^{-1} \text{ cm}^{-1}$$

$$\text{Answers: (a)} \quad T - T_L = \frac{D I^2}{4 h k_e} \left(1 - \frac{\cosh \sqrt{4h/D} z}{\cosh \sqrt{4h/D} L} \right); \quad \text{(b)} \quad 1.01 \text{ amp}$$

- 10B.17. Non-Newtonian flow with forced-convection heat transfer.**¹ For estimating the effect of non-Newtonian viscosity on heat transfer in ducts, the power law model of Chapter 8 gives velocity profiles that show rather well the deviation from parabolic shape.

(a) Rework the problem of §10.8 (heat transfer in a *circular tube*) for the power law model given in Eqs. 8.3-2, 3. Show that the final temperature profile is

$$\Theta = \frac{2(s+3)}{(s+1)} \zeta + \frac{(s+3)}{2(s+1)} \xi^2 - \frac{2}{(s+1)(s+3)} \xi^{s+3} - \frac{(s+3)^3 - 8}{4(s+1)(s+3)(s+5)} \quad (10B.17-1)$$

in which $s = 1/n$.

(b) Rework Problem 10B.7 (heat transfer in a *plane slit*) for the power law model. Obtain the dimensionless temperature profile:

$$\Theta = \frac{(s+2)}{(s+1)} \left[\zeta + \frac{1}{2} \sigma^2 - \frac{1}{(s+2)(s+3)} |\sigma|^{s+3} - \frac{(s+2)(s+3)(2s+5) - 6}{6(s+3)(s+4)(2s+5)} \right] \quad (10B.17-2)$$

Note that these results contain the Newtonian results ($s = 1$) and the plug flow results ($s = \infty$). See Problem 10D.2 for a generalization of this approach.

- 10B.18. Reactor temperature profiles with axial heat flux**² (Fig. 10B.18).

(a) Show that for a heat source that depends linearly on the temperature, Eqs. 10.5-6 to 14 have the solutions (for $m_+ \neq m_-$)

$$\Theta^I = 1 + \frac{m_+ m_- (\exp m_+ - \exp m_-)}{m_+^2 \exp m_+ - m_-^2 \exp m_-} \exp [(m_+ + m_-)Z] \quad (10B.18-1)$$

$$\Theta^{II} = \frac{m_+ (\exp m_+) (\exp m_- Z) - m_- (\exp m_-) (\exp m_+ Z)}{m_+^2 \exp m_+ - m_-^2 \exp m_-} (m_+ + m_-) \quad (10B.18-2)$$

$$\Theta^{III} = \frac{m_+^2 - m_-^2}{m_+^2 \exp m_+ - m_-^2 \exp m_-} \exp (m_+ + m_-) \quad (10B.18-3)$$

Here $m_{\pm} = \frac{1}{2}B(1 \pm \sqrt{1 - (4N/B)})$, in which $B = \rho v_0 \hat{C}_p L / \kappa_{\text{eff},zz}$. Some profiles calculated from these equations are shown in Fig. 10B.18.

¹ R. B. Bird, *Chem.-Ing. Technik*, **31**, 569–572 (1959).

² Taken from the corresponding results of G. Damköhler, *Z. Elektrochem.*, **43**, 1–8, 9–13 (1937), and J. F. Wehner and R. H. Wilhelm, *Chem. Engr. Sci.*, **6**, 89–93 (1956); **8**, 309 (1958), for isothermal flow reactors with longitudinal diffusion and first-order reaction. Gerhard Damköhler (1908–1944) achieved fame for his work on chemical reactions in flowing, diffusing systems; a key publication was in *Der Chemie-Ingenieur*, Leipzig (1937), pp. 359–485. Richard Herman Wilhelm (1909–1968), chairman of the Chemical Engineering Department at Princeton University, was well known for his work on fixed-bed catalytic reactors, fluidized transport, and the “parametric pumping” separation process.

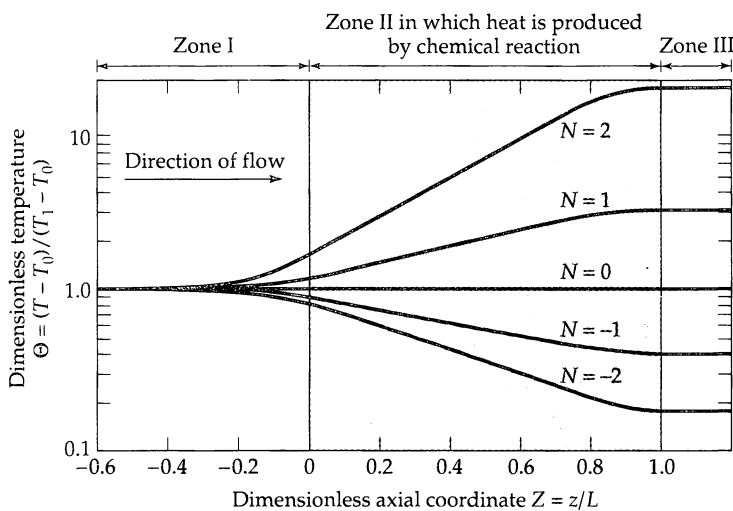


Fig. 10B.18. Predicted temperature profiles in a fixed-bed axial-flow reactor for $B = 8$ and various values of N .

- (b) Show that, in the limit as B goes to infinity, the above solution agrees with that in Eqs. 10.5-21, 22, and 23.
- (c) Make numerical comparisons of the results in Eq. 10.5-22 and Fig. 10B.18 for $N = 2$ at $Z = 0.0, 0.5, 0.9$, and 1.0 .
- (d) Assuming the applicability of Eq. 9.6-9, show that the results in Fig. 10B.18 correspond to a catalyst bed length L of 4 particle diameters. Since the ratio L/D_p is seldom less than 100 in industrial reactors, it follows that the neglect of $\kappa_{\text{eff},zz}$ is a reasonable assumption in steady-state design calculations.

10C.1. Heating of an electric wire with temperature-dependent electrical and thermal conductivity.³ Find the temperature distribution in an electrically heated wire when the thermal and electrical conductivities vary with temperature as follows:

$$\frac{k}{k_0} = 1 - \alpha_1 \Theta - \alpha_2 \Theta^2 + \dots \quad (10C.1-1)$$

$$\frac{k_e}{k_{e0}} = 1 - \beta_1 \Theta - \beta_2 \Theta^2 + \dots \quad (10C.1-2)$$

Here k_0 and k_{e0} are the values of the conductivities at temperature T_0 , and $\Theta = (T - T_0)/T_0$ is a dimensionless temperature rise. The coefficients α_i and β_i are constants. Such series expansions are useful over moderate temperature ranges.

- (a) Because of the temperature gradient in the wire, the electrical conductivity is a function of position, $k_e(r)$. Therefore, the current density is also a function of r : $I(r) = k_e(r) \cdot (E/L)$, and the electrical heat source also is position dependent: $S_e(r) = k_e(r) \cdot (E/L)^2$. The equation for the temperature distribution is then

$$-\frac{1}{r} \frac{d}{dr} \left(r k(r) \frac{dT}{dr} \right) = k_e(r) \left(\frac{E}{L} \right)^2 \quad (10C.1-3)$$

³ The solution given here was suggested by L. J. F. Broer (personal communication, 20 August 1958).

Now introduce the dimensionless quantities $\xi = r/R$ and $B = k_{e0}R^2E^2/k_0LT_0$ and show that Eq. 10C.1-3 then becomes

$$-\frac{1}{\xi} \frac{d}{d\xi} \left(\frac{k}{k_0} \xi \frac{d\Theta}{d\xi} \right) = B \frac{k_e}{k_{e0}} \quad (10C.1-4)$$

When the power series expressions for the conductivities are inserted into this equation we get

$$-\frac{1}{\xi} \frac{d}{d\xi} \left((1 - \alpha_1\Theta - \alpha_2\Theta^2 + \dots) \xi \frac{d\Theta}{d\xi} \right) = B(1 - \beta_1\Theta - \beta_2\Theta^2 + \dots) \quad (10C.1-5)$$

This is the equation that is to be solved for the dimensionless temperature distribution.

(b) Begin by noting that if all the α_i and β_i were zero (that is, both conductivities constant), then Eq. 10C.1-5 would simplify to

$$-\frac{1}{\xi} \frac{d}{d\xi} \left(\xi \frac{d\Theta}{d\xi} \right) = B \quad (10C.1-6)$$

When this is solved with the boundary conditions that $\Theta = \text{finite}$ at $\xi = 0$, and $\Theta = 0$ at $\xi = 1$, we get

$$\Theta = \frac{1}{4}B(1 - \xi^2) \quad (10C.1-7)$$

This is Eq. 10.2-13 in dimensionless notation.

Note that Eq. 10C.5 will have the solution in Eq. 10C.1-7 for small values of B —that is, for weak heat sources. For stronger heat sources, postulate that the temperature distribution can be expressed as a power series in the dimensionless heat source strength B :

$$\Theta = \frac{1}{4}B(1 - \xi^2)(1 + B\Theta_1 + B^2\Theta_2 + \dots) \quad (10C.1-8)$$

Here the Θ_n are functions of ξ but not of B . Substitute Eq. 10C.1-8 into Eq. 10C.1-5, and equate the coefficients of like powers of B to get a set of ordinary differential equations for the Θ_n , with $n = 1, 2, 3, \dots$. These may be solved with the boundary conditions that $\Theta_n = \text{finite}$ at $\xi = 0$ and $\Theta_n = 0$ at $\xi = 1$. In this way obtain

$$\Theta = \frac{1}{4}B(1 - \xi^2)[1 + B(\frac{1}{8}\alpha_1(1 - \xi^2) - \frac{1}{16}\beta_1(3 - \xi^2)) + O(B^2)] \quad (10C.1-9)$$

where $O(B^2)$ means “terms of the order of B^2 and higher.”

(c) For materials that are described by the Wiedemann–Franz–Lorenz law (see §9.5), the ratio k/k_eT is a constant (independent of temperature). Hence

$$\frac{k}{k_eT} = \frac{k_0}{k_{e0}T_0} \quad (10C.1-10)$$

Combine this with Eqs. 10C.1-1 and 2 to get

$$1 - \alpha_1\Theta - \alpha_2\Theta^2 + \dots = (1 - \beta_1\Theta - \beta_2\Theta^2 + \dots)(1 + \Theta) \quad (10C.1-11)$$

Equate coefficients of equal powers of the dimensionless temperature to get relations among the α_i and the β_i : $\alpha_1 = \beta_1 = 1$, $\alpha_2 = \beta_1 + \beta_2$, and so on. Use these relations to get

$$\Theta = \frac{1}{4}B(1 - \xi^2)[1 - \frac{1}{16}B((\beta_1 + 2) + ((\beta_1 - 2)\xi^2) + O(B^2))] \quad (10C.1-12)$$

10C.2. Viscous heating with temperature-dependent viscosity and thermal conductivity (Figs. 9.4-1 and 2). Consider the flow situation shown in Fig. 10.4-2. Both the stationary surface and the moving surface are maintained at a constant temperature T_0 . The temperature dependences of k and μ are given by

$$\frac{k}{k_0} = 1 + \alpha_1\Theta + \alpha_2\Theta^2 + \dots \quad (10C.2-1)$$

$$\frac{\mu_0}{\mu} = \frac{\varphi}{\varphi_0} = 1 + \beta_1\Theta + \beta_2\Theta^2 + \dots \quad (10C.2-2)$$

in which the α_i and β_i are constants, $\varphi = 1/\mu$ is the fluidity, and the subscript “0” means “evaluated at $T = T_0$.” The dimensionless temperature is defined as $\Theta = (T - T_0)/T_0$.

- (a) Show that the differential equations describing the viscous flow and heat conduction may be written in the forms

$$\frac{d}{d\xi} \left(\frac{\mu}{\mu_0} \frac{d\phi}{d\xi} \right) = 0 \quad (10C.2-3)$$

$$\frac{d}{d\xi} \left(\frac{k}{k_0} \frac{d\Theta}{d\xi} \right) + \text{Br} \frac{\mu}{\mu_0} \left(\frac{d\phi}{d\xi} \right)^2 = 0 \quad (10C.2-4)$$

in which $\phi = v_z/v_b$, $\xi = x/b$, and $\text{Br} = \mu_0 v_b^2/k_0 T_0$ (the Brinkman number).

- (b) The equation for the dimensionless velocity distribution may be integrated once to give $d\phi/d\xi = C_1 \cdot (\phi/\phi_0)$, in which C_1 is an integration constant. This expression is then substituted into the heat balance equation to get

$$\frac{d}{d\xi} \left((1 + \alpha_1 \Theta + \alpha_2 \Theta^2 + \dots) \frac{d\Theta}{d\xi} \right) + \text{Br} C_1^2 (1 + \beta_1 \Theta + \beta_2 \Theta^2 + \dots) = 0 \quad (10C.2-5)$$

Obtain the first two terms of a solution in the form

$$\Theta(\xi; \text{Br}) = \text{Br}\Theta_1(\xi) + \text{Br}^2\Theta_2(\xi) + \dots \quad (10C.2-6)$$

$$\phi(\xi; \text{Br}) = \phi_0 + \text{Br}\phi_1(\xi) + \text{Br}^2\phi_2(\xi) + \dots \quad (10C.2-7)$$

It is further suggested that the constant of integration C_1 also be expanded as a power series in the Brinkman number, thus

$$C_1(\text{Br}) = C_{10} + \text{Br}C_{11} + \text{Br}^2C_{12} + \dots \quad (10C.2-8)$$

- (c) Repeat the problem, changing the boundary condition at $y = b$ to $q_x = 0$ (instead of specifying the temperature).⁴

Answers: (b) $\phi = \xi - \frac{1}{12}\text{Br}\beta_1(\xi - 3\xi^2 + 2\xi^3) + \dots$

$$\Theta = \frac{1}{2}\text{Br}(\xi - \xi^2) - \frac{1}{8}\text{Br}^2\alpha_1(\xi^2 - 2\xi^3 + \xi^4) - \frac{1}{24}\text{Br}^2\beta_1(\xi - 2\xi^2 + 2\xi^3 - \xi^4) + \dots$$

(c) $\phi = \xi - \frac{1}{6}\text{Br}\beta_1(2\xi - 3\xi^2 + \xi^3) + \dots$

$$\Theta = \text{Br}(\xi - \frac{1}{2}\xi^2) - \frac{1}{8}\text{Br}^2\alpha_1(4\xi^2 - 4\xi^3 + \xi^4) + \frac{1}{24}\text{Br}^2\beta_1(-8\xi + 8\xi^2 - 4\xi^3 + \xi^4) + \dots$$

- 10C.3. Viscous heating in a cone-and-plate viscometer.**⁵ In Eq. 2B.11-3 there is an expression for the torque \mathcal{T} required to maintain an angular velocity Ω in a cone-and-plate viscometer with included angle ψ_0 (see Fig. 2B.11). It is desired to obtain a correction factor to account for the change in torque caused by the change in viscosity resulting from viscous heating. This effect can be a disturbing factor in viscometric measurements, causing errors as large as 20%.

- (a) Adapt the result of Problem 10C.2 to the cone-and-plate system as was done in Problem 2B.11(a). The boundary condition of zero heat flux at the cone surface seems to be more realistic than the assumption that the cone and plate temperatures are the same, inasmuch as the plate is thermostatted and the cone is not.

- (b) Show that this leads to the following modification of Eq. 2B.11-3:

$$T_z = \frac{2\pi\mu_0\Omega R^3}{3\psi_0} (1 - \frac{1}{5}\overline{\text{Br}}\beta_1 + \frac{1}{35}\overline{\text{Br}}^2(3\beta_1^2 + \alpha_1\beta_1 - 2\beta_2) + \dots) \quad (10C.3-1)$$

where $\overline{\text{Br}} = \mu_0\Omega^2R^2/k_0T_0$ is the Brinkman number. The symbol μ_0 stands for the viscosity at the temperature T_0 .

⁴ R. M. Turian and R. B. Bird, *Chem. Eng. Sci.*, **18**, 689–696 (1963).

⁵ R. M. Turian, *Chem. Eng. Sci.*, **20**, 771–781 (1965); the viscous heating correction for non-Newtonian fluids is discussed in this publication (see also R. B. Bird, R. C. Armstrong, and O. Hassager, *Dynamics of Polymeric Liquids*, Vol. 1, 2nd edition, Wiley-Interscience, New York (1987), pp. 223–227).

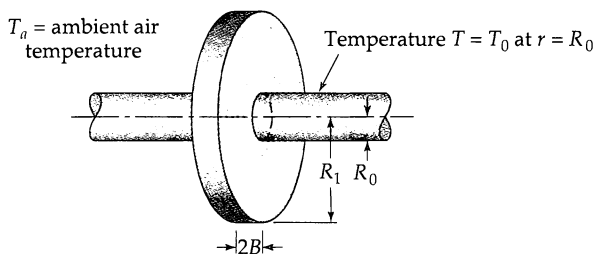


Fig. 10D.1. Circular fin on a heated pipe.

10D.1. Heat loss from a circular fin (Fig. 10D.1).

- Obtain the temperature profile $T(r)$ for a circular fin of thickness $2B$ on a pipe with outside wall temperature T_0 . Make the same assumptions that were made in the study of the rectangular fin in §10.7.
- Derive an expression for the total heat loss from the fin.

10D.2. Duct flow with constant wall heat flux and arbitrary velocity distribution.

- Rework the problem in §10.8 for an arbitrary fully developed, axisymmetric flow velocity distribution $v_z/v_{z,\max} = \phi(\xi)$, where $\xi = r/R$. Verify that the temperature distribution is given by

$$\Theta = C_0 \zeta + C_0 \int_0^{\xi} \frac{I(\bar{\xi})}{\bar{\xi}} d\bar{\xi} + C_1 \ln \xi + C_2 \quad (10D.2-1)$$

in which

$$I(\bar{\xi}) = \int_0^{\bar{\xi}} \phi \bar{\xi} d\bar{\xi} \quad (10D.2-2)$$

Show that $C_1 = 0$ and $C_0 = [I(1)]^{-1}$. Then show that the remaining constant is

$$C_2 = -[I(1)]^{-2} \int_0^1 \phi \xi \left[\int_0^{\xi} \xi^{-1} I(\bar{\xi}) d\bar{\xi} \right] d\xi \quad (10D.2-3)$$

Verify that the above equations lead to Eqs. 10.8-27 to 30 when the velocity profile is parabolic.

These results can be used to compute the temperature profiles for the fully developed tube flow of any kind of material as long as a reasonable estimation can be made for the velocity distribution. As special cases, one can get results for Newtonian flow, plug flow, non-Newtonian flow, and even, with some modifications, turbulent flow (see §13.4).⁶

- Show that the dimensionless temperature difference driving force $\Theta_0 - \Theta_b$ is

$$\Theta_0 - \Theta_b = [I(1)]^{-2} \int_0^1 \xi^{-1} [I(\xi)]^2 d\xi \quad (10D.2-4)$$

- Verify that the dimensionless wall heat flux is

$$\frac{q_w D}{k(T_0 - T_b)} = \frac{2}{\Theta_0 - \Theta_b} \quad (10D.2-5)$$

and that, for the laminar flow of Newtonian fluids, this quantity has the value $\frac{48}{11}$.

- What is the physical interpretation of $I(1)$?

⁶ R. N. Lyon, *Chem. Engr. Prog.*, **47**, 75–59 (1951); note that the definition of $\phi(\xi)$ used here is different from that in Tables 14.2-1 and 2.

Chapter 11

The Equations of Change for Nonisothermal Systems

§11.1 The energy equation

§11.2 Special forms of the energy equation

§11.3 The Boussinesq equation of motion for forced and free convection

§11.4 Use of the equations of change to solve steady-state problems

§11.5 Dimensional analysis of the equations of change for nonisothermal systems

In Chapter 10 we introduced the shell energy balance method for solving relatively simple, steady-state heat flow problems. We obtained the temperature profiles, as well as some derived properties such as average temperature and energy fluxes. In this chapter we generalize the shell energy balance and obtain the *equation of energy*, a partial differential equation that describes the transport of energy in a homogeneous fluid or solid.

This chapter is also closely related to Chapter 3, where we introduced the equation of continuity (conservation of mass) and the equation of motion (conservation of momentum). The addition of the equation of energy (conservation of energy) allows us to extend our problem-solving ability to include nonisothermal systems.

We begin in §11.1 by deriving the equation of change for the *total energy*. As in Chapter 10, we use the combined energy flux vector \mathbf{e} in applying the law of conservation of energy. In §11.2 we subtract the *mechanical energy* equation (given in §3.3) from the total energy equation to get an equation of change for the *internal energy*. From the latter we can get an equation of change for the *temperature*, and it is this kind of energy equation that is most commonly used.

Although our main concern in this chapter will be with the various energy equations just mentioned, we find it useful to discuss in §11.3 an approximate equation of motion that is convenient for solving problems involving free convection.

In §11.4 we summarize the equations of change encountered up to this point. Then we proceed to illustrate the use of these equations in a series of examples, in which we begin with the general equations and discard terms that are not needed. In this way we have a standard procedure for setting up and solving problems.

Finally, in §11.5 we extend the dimensional analysis discussion of §3.7 and show how additional dimensionless groups arise in heat transfer problems.

§11.1 THE ENERGY EQUATION

The equation of change for energy is obtained by applying the law of conservation of energy to a small element of volume $\Delta x \Delta y \Delta z$ (see Fig. 3.1-1) and then allowing the dimensions of the volume element to become vanishingly small. The law of conservation of

energy is an extension of the first law of classical thermodynamics, which concerns the difference in internal energies of two equilibrium states of a closed system because of the heat added to the system and the work done on the system (that is, the familiar $\Delta U = Q + W$).¹

Here we are interested in a stationary volume element, fixed in space, through which a fluid is flowing. Both kinetic energy and internal energy may be entering and leaving the system by convective transport. Heat may enter and leave the system by heat conduction as well. As we saw in Chapter 9, heat conduction is fundamentally a molecular process. Work may be done on the moving fluid by the stresses, and this, too, is a molecular process. This term includes the work done by pressure forces and by viscous forces. In addition, work may be done on the system by virtue of the external forces, such as gravity.

We can summarize the preceding paragraph by writing the conservation energy in words as follows:

$$\left\{ \begin{array}{l} \text{rate of} \\ \text{increase of} \\ \text{kinetic and} \\ \text{internal} \\ \text{energy} \end{array} \right\} = \left\{ \begin{array}{l} \text{net rate of kinetic} \\ \text{and internal} \\ \text{energy addition} \\ \text{by convective} \\ \text{transport} \end{array} \right\} + \left\{ \begin{array}{l} \text{net rate of heat} \\ \text{addition by} \\ \text{molecular} \\ \text{transport} \\ (\text{conduction}) \end{array} \right\} + \\ \left\{ \begin{array}{l} \text{rate of work} \\ \text{done on system} \\ \text{by molecular} \\ \text{mechanisms} \\ (\text{i.e., by stresses}) \end{array} \right\} + \left\{ \begin{array}{l} \text{rate of work} \\ \text{done on system} \\ \text{by external} \\ \text{forces} \\ (\text{e.g., by gravity}) \end{array} \right\} \quad (11.1-1)$$

In developing the energy equation we will use the \mathbf{e} vector of Eq. 9.8-5 or 6, which includes the first three brackets on the right side of Eq. 11.1-1. Several comments need to be made before proceeding:

- (i) By *kinetic energy* we mean that energy associated with the observable motion of the fluid, which is $\frac{1}{2}\rho\mathbf{v}^2 \equiv \frac{1}{2}\rho(\mathbf{v} \cdot \mathbf{v})$, per unit volume. Here \mathbf{v} is the fluid velocity vector.
- (ii) By *internal energy* we mean the kinetic energies of the constituent molecules calculated in a frame moving with the velocity \mathbf{v} , plus the energies associated with the vibrational and rotational motions of the molecules and also the energies of interaction among all the molecules. It is *assumed* that the internal energy U for a flowing fluid is the same function of temperature and density as that for a fluid at equilibrium. Keep in mind that a similar assumption is made for the thermodynamic pressure $p(\rho, T)$ for a flowing fluid.
- (iii) The *potential energy* does not appear in Eq. 11.1-1, since we prefer instead to consider the work done on the system by gravity. At the end of this section, however, we show how to express this work in terms of the potential energy.
- (iv) In Eq. 10.1-1 various *source terms* were included in the shell energy balance. In §10.4 the viscous heat source S_v appeared automatically, because the mechanical energy terms in \mathbf{e} were properly accounted for; the same situation prevails here, and the viscous heating term $-(\tau : \nabla \mathbf{v})$ will appear automatically in Eq. 11.2-1. The chemical, electrical, and nuclear source terms (S_c , S_e , and S_n) do not appear automatically, since chemical reactions, electrical effects, and nuclear

¹ R. J. Silbey and R. A. Alberty, *Physical Chemistry*, Wiley, New York, 3rd edition (2001), §2.3.

disintegrations have not been included in the energy balance. In Chapter 19, where the energy equation for mixtures with chemical reactions is considered, the chemical heat source S_c appears naturally, as does a “diffusive source term,” $\sum_\alpha (\mathbf{j}_\alpha \cdot \mathbf{g}_\alpha)$.

We now translate Eq. 11.1-1 into mathematical terms. The rate of increase of kinetic and internal energy within the volume element $\Delta x \Delta y \Delta z$ is

$$\Delta x \Delta y \Delta z \frac{\partial}{\partial t} \left(\frac{1}{2} \rho v^2 + \rho \hat{U} \right) . \quad (11.1-2)$$

Here \hat{U} is the internal energy per unit mass (sometimes called the “specific internal energy”). The product $\rho \hat{U}$ is the internal energy per unit volume, and $\frac{1}{2} \rho v^2 = \frac{1}{2} \rho (v_x^2 + v_y^2 + v_z^2)$ is the kinetic energy per unit volume.

Next we have to know how much energy enters and leaves across the faces of the volume element $\Delta x \Delta y \Delta z$.

$$\Delta y \Delta z (e_x|_x - e_x|_{x+\Delta x}) + \Delta x \Delta z (e_y|_y - e_y|_{y+\Delta y}) + \Delta x \Delta y (e_z|_z - e_z|_{z+\Delta z}) \quad (11.1-3)$$

Keep in mind that the \mathbf{e} vector includes the convective transport of kinetic and internal energy, the heat conduction, and the work associated with molecular processes.

The rate at which work is done on the fluid by the external force is the dot product of the fluid velocity \mathbf{v} and the force acting on the fluid ($\rho \Delta x \Delta y \Delta z \mathbf{g}$), or

$$\rho \Delta x \Delta y \Delta z (v_x g_x + v_y g_y + v_z g_z) \quad (11.1-4)$$

We now insert these various contributions into Eq. 11.1-1 and then divide by $\Delta x \Delta y \Delta z$. When Δx , Δy , and Δz are allowed to go to zero, we get

$$\frac{\partial}{\partial t} \left(\frac{1}{2} \rho v^2 + \rho \hat{U} \right) = - \left(\frac{\partial e_x}{\partial x} + \frac{\partial e_y}{\partial y} + \frac{\partial e_z}{\partial z} \right) + \rho (v_x g_x + v_y g_y + v_z g_z) \quad (11.1-5)$$

This equation may be written more compactly in vector notation as

$$\frac{\partial}{\partial t} \left(\frac{1}{2} \rho v^2 + \rho \hat{U} \right) = -(\nabla \cdot \mathbf{e}) + \rho(\mathbf{v} \cdot \mathbf{g}) \quad (11.1-6)$$

Next we insert the expression for the \mathbf{e} vector from Eq. 9.8-5 to get the *equation of energy*:

$\frac{\partial}{\partial t} \left(\frac{1}{2} \rho v^2 + \rho \hat{U} \right) = -(\nabla \cdot (\frac{1}{2} \rho v^2 + \rho \hat{U}) \mathbf{v}) - (\nabla \cdot \mathbf{q})$									
<table border="0" style="width: 100%; border-collapse: collapse;"> <tr> <td style="width: 33%;">rate of increase of energy per unit volume</td> <td style="width: 33%;">rate of energy addition per unit volume by convective transport</td> <td style="width: 33%;">rate of energy addition per unit volume by heat conduction</td> </tr> <tr> <td style="text-align: center;">- $(\nabla \cdot p \mathbf{v})$</td> <td style="text-align: center;">- $(\nabla \cdot [\tau \cdot \mathbf{v}])$</td> <td style="text-align: center;">+ $\rho(\mathbf{v} \cdot \mathbf{g})$</td> </tr> <tr> <td style="text-align: center;">rate of work done on fluid per unit volume by pressure forces</td> <td style="text-align: center;">rate of work done on fluid per unit volume by viscous forces</td> <td style="text-align: center;">rate of work done on fluid per unit volume by external forces</td> </tr> </table>	rate of increase of energy per unit volume	rate of energy addition per unit volume by convective transport	rate of energy addition per unit volume by heat conduction	- $(\nabla \cdot p \mathbf{v})$	- $(\nabla \cdot [\tau \cdot \mathbf{v}])$	+ $\rho(\mathbf{v} \cdot \mathbf{g})$	rate of work done on fluid per unit volume by pressure forces	rate of work done on fluid per unit volume by viscous forces	rate of work done on fluid per unit volume by external forces
rate of increase of energy per unit volume	rate of energy addition per unit volume by convective transport	rate of energy addition per unit volume by heat conduction							
- $(\nabla \cdot p \mathbf{v})$	- $(\nabla \cdot [\tau \cdot \mathbf{v}])$	+ $\rho(\mathbf{v} \cdot \mathbf{g})$							
rate of work done on fluid per unit volume by pressure forces	rate of work done on fluid per unit volume by viscous forces	rate of work done on fluid per unit volume by external forces							

(11.1-7)

This equation does not include nuclear, radiative, electromagnetic, or chemical forms of energy. For viscoelastic fluids, the next-to-last term has to be reinterpreted by replacing “viscous” by “viscoelastic.”

Equation 11.1-7 is the main result of this section, and it provides the basis for the remainder of the chapter. The equation can be written in another form to include the potential energy per unit mass, $\hat{\Phi}$, which has been defined earlier by $\mathbf{g} = -\nabla \hat{\Phi}$ (see §3.3). For moderate elevation changes, this gives $\hat{\Phi} = gh$, where h is a coordinate in the direction

opposed to the gravitational field. For terrestrial problems, where the gravitational field is independent of time, we can write

$$\begin{aligned}
 \rho(\mathbf{v} \cdot \mathbf{g}) &= -(\rho\mathbf{v} \cdot \nabla\hat{\Phi}) \\
 &= -(\nabla \cdot \rho\mathbf{v}\hat{\Phi}) + \hat{\Phi}(\nabla \cdot \rho\mathbf{v}) && \text{Use vector identity in Eq. A.4-19} \\
 &= -(\nabla \cdot \rho\mathbf{v}\hat{\Phi}) - \hat{\Phi}\frac{\partial\rho}{\partial t} && \text{Use Eq. 3.1-4} \\
 &= -(\nabla \cdot \rho\mathbf{v}\hat{\Phi}) - \frac{\partial}{\partial t}(\rho\hat{\Phi}) && \text{Use } \hat{\Phi} \text{ independent of } t
 \end{aligned} \tag{11.1-8}$$

When this result is inserted into Eq. 11.1-7 we get

$$\begin{aligned}
 \frac{\partial}{\partial t}(\frac{1}{2}\rho v^2 + \rho\hat{U} + \rho\hat{\Phi}) &= -(\nabla \cdot (\frac{1}{2}\rho v^2 + \rho\hat{U} + \rho\hat{\Phi})\mathbf{v}) \\
 &\quad - (\nabla \cdot \mathbf{q}) - (\nabla \cdot p\mathbf{v}) - (\nabla \cdot [\boldsymbol{\tau} \cdot \mathbf{v}])
 \end{aligned} \tag{11.1-9}$$

Sometimes it is convenient to have the energy equation in this form.

§11.2 SPECIAL FORMS OF THE ENERGY EQUATION

The most useful form of the energy equation is one in which the temperature appears. The object of this section is to arrive at such an equation, which can be used for prediction of temperature profiles.

First we subtract the mechanical energy equation in Eq. 3.3-1 from the energy equation in 11.1-7. This leads to the following *equation of change for internal energy*:

	$\frac{\partial}{\partial t}\rho\hat{U} =$	$-(\nabla \cdot \rho\hat{U}\mathbf{v}) - (\nabla \cdot \mathbf{q})$	
rate of increase in internal energy per unit volume	net rate of addition of internal energy by convective transport, per unit volume	rate of internal energy addition by heat conduction, per unit volume	
	$-p(\nabla \cdot \mathbf{v})$	$-(\boldsymbol{\tau} \cdot \nabla \mathbf{v})$	
reversible rate of internal energy increase per unit volume by compression	irreversible rate of internal energy increase per unit volume by viscous dissipation		

(11.2-1)

It is now of interest to compare the mechanical energy equation of Eq. 3.3-1 and the internal energy equation of Eq. 11.2-1. Note that the terms $p(\nabla \cdot \mathbf{v})$ and $(\boldsymbol{\tau} \cdot \nabla \mathbf{v})$ appear in both equations—but with opposite signs. Therefore, these terms describe the interconversion of mechanical and thermal energy. The term $p(\nabla \cdot \mathbf{v})$ can be either positive or negative, depending on whether the fluid is expanding or contracting; therefore it represents a *reversible* mode of interchange. On the other hand, for Newtonian fluids, the quantity $-(\boldsymbol{\tau} \cdot \nabla \mathbf{v})$ is always positive (see Eq. 3.3-3) and therefore represents an *irreversible* degradation of mechanical into internal energy. For viscoelastic fluids, discussed in Chapter 8, the quantity $-(\boldsymbol{\tau} \cdot \nabla \mathbf{v})$ does not have to be positive, since some energy may be stored as elastic energy.

We pointed out in §3.5 that the equations of change can be written somewhat more compactly by using the substantial derivative (see Table 3.5-1). Equation 11.2-1 can be

put in the substantial derivative form by using Eq. 3.5-4. This gives, with no further assumptions

$$\rho \frac{D\hat{U}}{Dt} = -(\nabla \cdot \mathbf{q}) - p(\nabla \cdot \mathbf{v}) - (\boldsymbol{\tau} : \nabla \mathbf{v}) \quad (11.2-2)$$

Next it is convenient to switch from internal energy to enthalpy, as we did at the very end of §9.8. That is, in Eq. 11.2-2 we set $\hat{U} = \hat{H} - p\hat{V} = \hat{H} - (p/\rho)$, making the standard assumption that thermodynamic formulas derived from equilibrium thermodynamics may be applied locally for nonequilibrium systems. When we substitute this formula into Eq. 11.2-2 and use the equation of continuity (Eq. A of Table 3.5-1), we get

$$\rho \frac{D\hat{H}}{Dt} = -(\nabla \cdot \mathbf{q}) - (\boldsymbol{\tau} : \nabla \mathbf{v}) + \frac{Dp}{Dt} \quad (11.2-3)$$

Next we may use Eq. 9.8-7, which presumes that the enthalpy is a function of p and T (this restricts the subsequent development to *Newtonian fluids*). Then we may get an expression for the change in the enthalpy in an element of fluid moving with the fluid velocity, which is

$$\begin{aligned} \rho \frac{D\hat{H}}{Dt} &= \rho \hat{C}_p \frac{DT}{Dt} + \rho \left[\hat{V} - T \left(\frac{\partial \hat{V}}{\partial T} \right)_p \right] \frac{Dp}{Dt} \\ &= \rho \hat{C}_p \frac{DT}{Dt} + \rho \left[\frac{1}{\rho} - T \left(\frac{\partial (1/\rho)}{\partial T} \right)_p \right] \frac{Dp}{Dt} \\ &= \rho \hat{C}_p \frac{DT}{Dt} + \left[1 + \left(\frac{\partial \ln \rho}{\partial \ln T} \right)_p \right] \frac{Dp}{Dt} \end{aligned} \quad (11.2-4)$$

Equating the right sides of Eqs. 11.2-3 and 11.2-4 gives

$$\rho \hat{C}_p \frac{DT}{Dt} = -(\nabla \cdot \mathbf{q}) - (\boldsymbol{\tau} : \nabla \mathbf{v}) - \left(\frac{\partial \ln \rho}{\partial \ln T} \right)_p \frac{Dp}{Dt}$$

(11.2-5)

This is the *equation of change for temperature*, in terms of the heat flux vector \mathbf{q} and the viscous momentum flux tensor $\boldsymbol{\tau}$. To use this equation we need expressions for these fluxes:

- (i) When Fourier's law of Eq. 9.1-4 is used, the term $-(\nabla \cdot \mathbf{q})$ becomes $+(\nabla \cdot k\nabla T)$, or, if the thermal conductivity is assumed constant, $+k\nabla^2 T$.
- (ii) When Newton's law of Eq. 1.2-7 is used, the term $-(\boldsymbol{\tau} : \nabla \mathbf{v})$ becomes $\mu\Phi_v + \kappa\Psi_v$, the quantity given explicitly in Eq. 3.3-3.

We do not perform the substitutions here, because the equation of change for temperature is almost never used in its complete generality.

We now discuss several special *restricted* versions of the equation of change for temperature. In all of these we use Fourier's law with constant k , and we omit the viscous dissipation term, since it is important only in flows with enormous velocity gradients:

- (i) For an *ideal gas*, $(\partial \ln \rho / \partial \ln T)_p = -1$, and

$$\rho \hat{C}_p \frac{DT}{Dt} = k\nabla^2 T + \frac{Dp}{Dt} \quad (11.2-6)$$

Or, if use is made of the relation $\tilde{C}_p - \tilde{C}_v = R$, the equation of state in the form $pM = \rho RT$, and the equation of continuity as written in Eq. A of Table 3.5-1, we get

$$\rho \hat{C}_v \frac{DT}{Dt} = k\nabla^2 T - p(\nabla \cdot \mathbf{v}) \quad (11.2-7)$$

(ii) For a *fluid flowing in a constant pressure system*, $Dp/Dt = 0$, and

$$\rho \hat{C}_p \frac{DT}{Dt} = k \nabla^2 T \quad (11.2-8)$$

(iii) For a *fluid with constant density*,¹ $(\partial \ln \rho / \partial \ln T)_p = 0$, and

$$\rho \hat{C}_p \frac{DT}{Dt} = k \nabla^2 T \quad (11.2-9)$$

(iv) For a *stationary solid*, \mathbf{v} is zero and

$$\rho \hat{C}_p \frac{\partial T}{\partial t} = k \nabla^2 T \quad (11.2-10)$$

These last five equations are the ones most frequently encountered in textbooks and research publications. Of course, one can always go back to Eq. 11.2-5 and develop less restrictive equations when needed. Also, one can add chemical, electrical, and nuclear source terms on an ad hoc basis, as was done in Chapter 10.

Equation 11.2-10 is the heat conduction equation for solids, and much has been written about this famous equation developed first by Fourier.² The famous reference work by Carslaw and Jaeger deserves special mention. It contains hundreds of solutions of this equation for a wide variety of boundary and initial conditions.³

§11.3 THE BOUSSINESQ EQUATION OF MOTION FOR FORCED AND FREE CONVECTION

The equation of motion given in Eq. 3.2-9 (or Eq. B of Table 3.5-1) is valid for both isothermal and nonisothermal flow. In nonisothermal flow, the fluid density and viscosity depend in general on temperature as well as on pressure. The variation in the density is particularly important because it gives rise to buoyant forces, and thus to free convection, as we have already seen in §10.9.

The buoyant force appears automatically when an equation of state is inserted into the equation of motion. For example, we can use the simplified equation of state introduced in Eq. 10.9-6 (this is called the *Boussinesq approximation*)¹

$$\rho(T) = \bar{\rho} - \bar{\rho}\bar{\beta}(T - \bar{T}) \quad (11.3-1)$$

in which $\bar{\beta}$ is $-(1/\rho)(\partial \rho / \partial T)_p$ evaluated at $T = \bar{T}$. This equation is obtained by writing the Taylor series for ρ as a function of T , considering the pressure p to be constant, and keeping only the first two terms of the series. When Eq. 11.3-1 is substituted into the ρg term (but not into the $\rho(D\mathbf{v}/Dt)$ term) of Eq. B of Table 3.5-1, we get the *Boussinesq equation*:

$$\rho \frac{D\mathbf{v}}{Dt} = (-\nabla p + \bar{\rho}\mathbf{g}) - [\nabla \cdot \boldsymbol{\tau}] - \bar{\rho}\mathbf{g}\bar{\beta}(T - \bar{T}) \quad (11.3-2)$$

¹ The assumption of constant density is made here, instead of the less stringent assumption that $(\partial \ln \rho / \partial \ln T)_p = 0$, since Eq. 11.2-9 is customarily used along with Eq. 3.1-5 (equation of continuity for constant density) and Eq. 3.5-6 (equation of motion for constant density and viscosity). Note that the hypothetical equation of state $\rho = \text{constant}$ has to be supplemented by the statement that $(\partial p / \partial T)_p = \text{finite}$, in order to permit the evaluation of certain thermodynamic derivatives. For example, the relation

$$\hat{C}_p - \hat{C}_V = -\frac{1}{\rho} \left(\frac{\partial \ln \rho}{\partial \ln T} \right)_p \left(\frac{\partial p}{\partial T} \right)_p \quad (11.2-9a)$$

leads to the result that $\hat{C}_p = \hat{C}_V$ for the “incompressible fluid” thus defined.

² J. B. Fourier, *Théorie analytique de la chaleur*, Œuvres de Fourier, Gauthier-Villars et Fils, Paris (1822).

³ H. S. Carslaw and J. C. Jaeger, *Conduction of Heat in Solids*, Oxford University Press, 2nd edition (1959).

¹ J. Boussinesq, *Théorie Analytique de Chaleur*, Vol. 2, Gauthier-Villars, Paris (1903).

This form of the equation of motion is very useful for heat transfer analyses. It describes the limiting cases of forced convection and free convection (see Fig. 10.8-1), and the region between these extremes as well. In *forced convection* the buoyancy term $-\bar{\rho}g\beta(T - \bar{T})$ is neglected. In *free convection* (or *natural convection*) the term $(-\nabla p + \bar{\rho}g)$ is small, and omitting it is usually appropriate, particularly for vertical, rectilinear flow and for the flow near submerged objects in large bodies of fluid. Setting $(-\nabla p + \bar{\rho}g)$ equal to zero is equivalent to assuming that the pressure distribution is just that for a fluid at rest.

It is also customary to replace ρ on the left side of Eq. 11.3-2 by $\bar{\rho}$. This substitution has been successful for free convection at moderate temperature differences. Under these conditions the fluid motion is slow, and the acceleration term Dv/Dt is small compared to g .

However, in systems where the acceleration term is large with respect to g , one must also use Eq. 11.3-1 for the density on the left side of the equation of motion. This is particularly true, for example, in gas turbines and near hypersonic missiles, where the term $(\rho - \bar{\rho})Dv/Dt$ may be at least as important as $\bar{\rho}g$.

§11.4 USE OF THE EQUATIONS OF CHANGE TO SOLVE STEADY-STATE PROBLEMS

In §§3.1 to 3.4 and in §§11.1 to 11.3 we have derived various equations of change for a pure fluid or solid. It seems appropriate here to present a summary of these equations for future reference. Such a summary is given in Table 11.4-1, with most of the equations given in both the $\partial/\partial t$ form and the D/Dt form. Reference is also made to the first place where each equation has been presented.

Although Table 11.4-1 is a useful summary, for problem solving we use the equations written out explicitly in the several commonly used coordinate systems. This has been done in Appendix B, and readers should thoroughly familiarize themselves with the tables there.

In general, to describe the nonisothermal flow of a Newtonian fluid one needs

- the equation of continuity
- the equation of motion (containing μ and κ)
- the equation of energy (containing μ , κ , and k)
- the thermal equation of state ($p = p(\rho, T)$)
- the caloric equation of state ($\hat{C}_p = \hat{C}_p(\rho, T)$)

as well as expressions for the density and temperature dependence of the viscosity, dilatational viscosity, and thermal conductivity. In addition one needs the boundary and initial conditions. The entire set of equations can then—in principle—be solved to get the pressure, density, velocity, and temperature as functions of position and time. If one wishes to solve such a detailed problem, numerical methods generally have to be used.

Often one may be content with a restricted solution, for making an order-of-magnitude analysis of a problem, or for investigating limiting cases prior to doing a complete numerical solution. This is done by making some standard assumptions:

- (i) *Assumption of constant physical properties.* If it can be assumed that all physical properties are constant, then the equations become considerably simpler, and in some cases analytical solutions can be found.
- (ii) *Assumption of zero fluxes.* Setting τ and q equal to zero may be useful for (a) adiabatic flow processes in systems designed to minimize frictional effects (such as Venturi meters and turbines), and (b) high-speed flows around streamlined objects. The solutions obtained would be of no use for describing the situation near fluid–solid boundaries, but may be adequate for analysis of phenomena far from the solid boundaries.

Table 11.4-1 Equations of Change for Pure Fluids in Terms of the Fluxes

Eq.	Special form	In terms of D/Dt	Comments	
Cont.	—	$\frac{D\rho}{Dt} = -\rho(\nabla \cdot \mathbf{v})$	Table 3.5-1 (A)	For $\rho = \text{constant}$, simplifies to $(\nabla \cdot \mathbf{v}) = 0$
Motion	General	$\rho \frac{D\mathbf{v}}{Dt} = -\nabla p - [\nabla \cdot \boldsymbol{\tau}] + \rho\mathbf{g}$	Table 3.5-1 (B)	For $\boldsymbol{\tau} = 0$ this becomes Euler's equation
	Approximate	$\rho \frac{D\mathbf{v}}{Dt} = -\nabla p - [\nabla \cdot \boldsymbol{\tau}] + \bar{\rho}\mathbf{g} - \bar{\rho}\mathbf{g}\beta(T - \bar{T})$	11.3-2 (C)	Displays buoyancy term
Energy	In terms of $\hat{K} + \hat{U} + \hat{\Phi}$	$\rho \frac{D(\hat{K} + \hat{U} + \hat{\Phi})}{Dt} = -(\nabla \cdot \mathbf{q}) - (\nabla \cdot p\mathbf{v}) - (\nabla \cdot [\boldsymbol{\tau} \cdot \mathbf{v}])$	— (D)	Exact only for Φ time independent
	In terms of $\hat{K} + \hat{U}$	$\rho \frac{D(\hat{K} + \hat{U})}{Dt} = -(\nabla \cdot \mathbf{q}) - (\nabla \cdot p\mathbf{v}) - (\nabla \cdot [\boldsymbol{\tau} \cdot \mathbf{v}]) + \rho(\mathbf{v} \cdot \mathbf{g})$	— (E)	
	In terms of $\hat{K} = \frac{1}{2}\mathbf{v}^2$	$\rho \frac{D\hat{K}}{Dt} = -(\mathbf{v} \cdot \nabla p) - (\mathbf{v} \cdot [\nabla \cdot \boldsymbol{\tau}]) + \rho(\mathbf{v} \cdot \mathbf{g})$	Table 3.5-1 (F)	From equation of motion
	In terms of \hat{U}	$\rho \frac{D\hat{U}}{Dt} = -(\nabla \cdot \mathbf{q}) - p(\nabla \cdot \mathbf{v}) - (\boldsymbol{\tau} : \nabla \mathbf{v})$	11.2-2 (G)	Term containing $(\nabla \cdot \mathbf{v})$ is zero for constant ρ
	In terms of \hat{H}	$\rho \frac{D\hat{H}}{Dt} = -(\nabla \cdot \mathbf{q}) - (\boldsymbol{\tau} : \nabla \mathbf{v}) + \frac{Dp}{Dt}$	11.2-3 (H)	$\hat{H} = \hat{U} + (p/\rho)$
	In terms of \hat{C}_v and T	$\rho \hat{C}_v \frac{DT}{Dt} = -(\nabla \cdot \mathbf{q}) - T \left(\frac{\partial p}{\partial T} \right)_\rho (\nabla \cdot \mathbf{v}) - (\boldsymbol{\tau} : \nabla \mathbf{v})$	— (I)	For an ideal gas $T(\partial p / \partial T)_p = p$
	In terms of \hat{C}_p and T	$\rho \hat{C}_p \frac{DT}{Dt} = -(\nabla \cdot \mathbf{q}) - \left(\frac{\partial \ln \rho}{\partial \ln T} \right)_p \frac{Dp}{Dt} - (\boldsymbol{\tau} : \nabla \mathbf{v})$	11.2-5 (J)	For an ideal gas $(\partial \ln \rho / \partial \ln T)_p = -1$

Cont.	—	$\frac{\partial}{\partial t} \rho = -(\nabla \cdot \rho \mathbf{v})$	3.1-4 (K)	For $\rho = \text{constant}$, simplifies to $(\nabla \cdot \mathbf{v}) = 0$
Motion	General	$\frac{\partial}{\partial t} \rho \mathbf{v} = -[\nabla \cdot \rho \mathbf{v} \mathbf{v}] - \nabla p - [\nabla \cdot \boldsymbol{\tau}] + \rho \mathbf{g}$	3.2-9 (L)	For $\boldsymbol{\tau} = 0$ this becomes Euler's equation
	Approximate	$\frac{\partial}{\partial t} \rho \mathbf{v} = -[\nabla \cdot \rho \mathbf{v} \mathbf{v}] - \nabla p - [\nabla \cdot \boldsymbol{\tau}] + \bar{\rho} \mathbf{g} - \bar{\rho} \mathbf{g} \beta(T - \bar{T})$	— (M)	Displays buoyancy term
Energy	In terms of $\hat{K} + \hat{U} + \hat{\Phi}$	$\frac{\partial}{\partial t} \rho (\hat{K} + \hat{U} + \hat{\Phi}) = -(\nabla \cdot \rho (\hat{K} + \hat{H} + \hat{\Phi}) \mathbf{v}) - (\nabla \cdot \mathbf{q}) - (\nabla \cdot [\boldsymbol{\tau} \cdot \mathbf{v}])$	11.1-9 (N)	Exact only for Φ time independent
	In terms of $\hat{K} + \hat{\Phi}$	$\frac{\partial}{\partial t} \rho (\hat{K} + \hat{\Phi}) = -(\nabla \cdot \rho (\hat{K} + \hat{\Phi}) \mathbf{v}) - (\mathbf{v} \cdot \nabla p) - (\mathbf{v} \cdot [\nabla \cdot \boldsymbol{\tau}])$	3.3-2 (O)	Exact only for Φ time independent From equation of motion
	In terms of $\hat{K} + \hat{U}$	$\frac{\partial}{\partial t} \rho (\hat{K} + \hat{U}) = -(\nabla \cdot \rho (\hat{K} + \hat{H}) \mathbf{v}) - (\nabla \cdot \mathbf{q}) - (\nabla \cdot [\boldsymbol{\tau} \cdot \mathbf{v}]) + \rho (\mathbf{v} \cdot \mathbf{g})$	11.1-7 (P)	
	In terms of $\hat{K} = \frac{1}{2} \mathbf{v}^2$	$\frac{\partial}{\partial t} \rho \hat{K} = -(\nabla \cdot \rho \hat{K} \mathbf{v}) - (\mathbf{v} \cdot \nabla p) - (\mathbf{v} \cdot [\nabla \cdot \boldsymbol{\tau}]) + \rho (\mathbf{v} \cdot \mathbf{g})$	3.3-1 (Q)	From equation of motion
	In terms of \hat{U}	$\frac{\partial}{\partial t} \rho \hat{U} = -(\nabla \cdot \rho \hat{U} \mathbf{v}) - (\nabla \cdot \mathbf{q}) - p (\nabla \cdot \mathbf{v}) - (\boldsymbol{\tau} : \nabla \mathbf{v})$	11.2-1 (R)	Term containing $(\nabla \cdot \mathbf{v})$ is zero for constant ρ
	In terms of \hat{H}	$\frac{\partial}{\partial t} \rho \hat{H} = -(\nabla \cdot \rho \hat{H} \mathbf{v}) - (\nabla \cdot \mathbf{q}) - (\boldsymbol{\tau} : \nabla \mathbf{v}) + \frac{Dp}{Dt}$	— (S)	$\hat{H} = \hat{U} + (p/\rho)$
Entropy	—	$\frac{\partial}{\partial t} \rho \hat{S} = -(\nabla \cdot \rho \hat{S} \mathbf{v}) - \left(\nabla \cdot \left(\frac{\mathbf{q}}{T} \right) \right) - \frac{1}{T^2} (\mathbf{q} \cdot \nabla T) - \frac{1}{T} (\boldsymbol{\tau} : \nabla \mathbf{v})$	11D.1-1 (T)	Last two terms describe entropy production

To illustrate the solution of problems in which the energy equation plays a significant role, we solve a series of (idealized) problems. We restrict ourselves here to steady-state flow problems and consider unsteady-state problems in Chapter 12. In each problem we start by listing the postulates that lead us to simplified versions of the equations of change.

EXAMPLE 11.4-1

Steady-State Forced-Convection Heat Transfer in Laminar Flow in a Circular Tube

Show how to set up the equations for the problem considered in §10.8—namely, that of finding the fluid temperature profiles for the fully developed laminar flow in a tube.

SOLUTION

We assume constant physical properties, and we postulate a solution of the following form: $\mathbf{v} = \delta_z v_z(r)$, $\mathcal{P} = \mathcal{P}(z)$, and $T = T(r, z)$. Then the equations of change, as given in Appendix B, may be simplified to

$$\text{Continuity:} \quad 0 = 0 \quad (11.4-1)$$

$$\text{Motion:} \quad 0 = -\frac{d\mathcal{P}}{dz} + \mu \left[\frac{1}{r} \frac{d}{dr} \left(r \frac{dv_z}{dr} \right) \right] \quad (11.4-2)$$

$$\text{Energy:} \quad \rho \hat{C}_p v_z \frac{\partial T}{\partial z} = k \left[\frac{1}{r} \frac{\partial}{\partial r} \left(r \frac{\partial T}{\partial r} \right) + \frac{\partial^2 T}{\partial z^2} \right] + \mu \left(\frac{dv_z}{dr} \right)^2 \quad (11.4-3)$$

The equation of continuity is automatically satisfied as a result of the postulates. The equation of motion, when solved as in Example 3.6-1, gives the velocity distribution (the parabolic velocity profile). This expression is then substituted into the convective heat transport term on the left side of Eq. 11.4-3 and into the viscous dissipation heating term on the right side.

Next, as in §10.8, we make two assumptions: (i) in the z direction, heat conduction is much smaller than heat convection, so that the term $\partial^2 T / \partial z^2$ can be neglected, and (ii) the flow is not sufficiently fast that viscous heating is significant, and hence the term $\mu(\partial v_z / \partial r)^2$ can be omitted. When these assumptions are made, Eq. 11.4-3 becomes the same as Eq. 10.8-12. From that point on, the asymptotic solution, valid for large z only, proceeds as in §10.8. Note that we have gone through three types of restrictive processes: (i) *postulates*, in which a tentative guess is made as to the form of the solution; (ii) *assumptions*, in which we eliminate some physical phenomena or effects by discarding terms or assuming physical properties to be constant; and (iii) an *asymptotic solution*, in which we obtain only a portion of the entire mathematical solution. It is important to distinguish among these various kinds of restrictions.

EXAMPLE 11.4-2

Tangential Flow in an Annulus with Viscous Heat Generation

Determine the temperature distribution in an incompressible liquid confined between two coaxial cylinders, the outer one of which is rotating at a steady angular velocity Ω_o (see §10.4 and Example 3.6-3). Use the nomenclature of Example 3.6-3, and consider the radius ratio κ to be fairly small so that the curvature of the fluid streamlines must be taken into account.

The temperatures of the inner and outer surfaces of the annular region are maintained at T_κ and T_1 , respectively, with $T_\kappa \neq T_1$. Assume steady laminar flow, and neglect the temperature dependence of the physical properties.

This is an example of a forced convection problem: The equations of continuity and motion are solved to get the velocity distribution, and then the energy equation is solved to get the temperature distribution. This problem is of interest in connection with heat effects in coaxial cylinder viscometers¹ and in lubrication systems.

¹J. R. Van Wazer, J. W. Lyons, K. Y. Kim, and R. E. Colwell, *Viscosity and Flow Measurement*, Wiley, New York (1963), pp. 82–85.

SOLUTION

We begin by postulating that $v = \delta_\theta v_\theta(r)$, that $\mathcal{P} = \mathcal{P}(r, z)$, and that $T = T(r)$. Then the simplification of the equations of change leads to Eqs. 3.6-20, 21, and 22 (the r -, θ -, and z -components of the equation of motion), and the energy equation

$$0 = k \frac{1}{r} \frac{d}{dr} \left(r \frac{dT}{dr} \right) + \mu \left[r \frac{d}{dr} \left(\frac{v_\theta}{r} \right) \right]^2 \quad (11.4-4)$$

When the solution to the θ -component of the equation of motion, given in Eq. 3.6-29, is substituted into the energy equation, we get

$$0 = k \frac{1}{r} \frac{d}{dr} \left(r \frac{dT}{dr} \right) + \frac{4\mu\Omega_o^2\kappa^4 R^4}{(1 - \kappa^2)^2} \frac{1}{r^4} \quad (11.4-5)$$

This is the differential equation for the temperature distribution. It may be rewritten in terms of dimensionless quantities by putting

$$\xi = \frac{r}{R} \quad \Theta = \frac{T - T_\kappa}{T_1 - T_\kappa} \quad N = \frac{\mu\Omega_o^2 R^2}{k(T_1 - T_\kappa)} \cdot \frac{\kappa^4}{(1 - \kappa^2)^2} \quad (11.4-6, 7, 8)$$

The parameter N is closely related to the Brinkman number of §10.4. Equation 11.4-5 now becomes

$$\frac{1}{\xi} \frac{d}{d\xi} \left(\xi \frac{d\Theta}{d\xi} \right) = -4N \frac{1}{\xi^4} \quad (11.4-9)$$

This is of the form of Eq. C.1-11 and has the solution

$$\Theta = -N \frac{1}{\xi^2} + C_1 \ln \xi + C_2 \quad (11.4-10)$$

The integration constants are found from the boundary conditions

$$\text{B.C. 1:} \quad \text{at } \xi = \kappa, \quad \Theta = 0 \quad (11.4-11)$$

$$\text{B.C. 2:} \quad \text{at } \xi = 1, \quad \Theta = 1 \quad (11.4-12)$$

Determination of the constants then leads to

$$\Theta = \left(1 - \frac{\ln \xi}{\ln \kappa} \right) + N \left[\left(1 - \frac{1}{\xi^2} \right) - \left(1 - \frac{1}{\kappa^2} \right) \frac{\ln \xi}{\ln \kappa} \right] \quad (11.4-13)$$

When $N = 0$, we obtain the temperature distribution for a motionless cylindrical shell of thickness $R(1 - \kappa)$ with inner and outer temperatures T_κ and T_1 . If N is large enough, there will be a maximum in the temperature distribution, located at

$$\xi = \sqrt{\frac{2 \ln(1/\kappa)}{(1/\kappa^2) - 1 + (1/N)}} \quad (11.4-14)$$

with the temperature at this point greater than either T_κ or T_1 .

Although this example provides an illustration of the use of the tabulated equations of change in cylindrical coordinates, in most viscometric and lubrication applications the clearance between the cylinders is so small that numerical values computed from Eq. 11.4-13 will not differ substantially from those computed from Eq. 10.4-9.

EXAMPLE 11.4-3***Steady Flow in a Nonisothermal Film***

A liquid is flowing downward in steady laminar flow along an inclined plane surface, as shown in Figs. 2.2-1 to 3. The free liquid surface is maintained at temperature T_0 , and the solid surface at $x = \delta$ is maintained at T_δ . At these temperatures the liquid viscosity has values μ_0 and μ_δ , respectively, and the liquid density and thermal conductivity may be assumed constant. Find the velocity distribution in this nonisothermal flow system, neglecting end effects

and recognizing that viscous heating is unimportant in this flow. Assume that the temperature dependence of viscosity may be expressed by an equation of the form $\mu = Ae^{B/T}$, with A and B being empirical constants; this is suggested by the Eyring theory given in §1.5.

We first solve the energy equation to get the temperature profile, and then use the latter to find the dependence of viscosity on position. Then the equation of motion can be solved to get the velocity profile.

SOLUTION

We postulate that $T = T(x)$ and that $\mathbf{v} = \delta_z v_z(x)$. Then the energy equation simplifies to

$$\frac{d^2T}{dx^2} = 0 \quad (11.4-15)$$

This can be integrated between the known terminal temperatures to give

$$\frac{T - T_0}{T_\delta - T_0} = \frac{x}{\delta} \quad (11.4-16)$$

The dependence of viscosity on temperature may be written as

$$\frac{\mu(T)}{\mu_0} = \exp\left[B\left(\frac{1}{T} - \frac{1}{T_0}\right)\right] \quad (11.4-17)$$

in which B is a constant, to be determined from experimental data for viscosity versus temperature. To get the dependence of viscosity on position, we combine the last two equations to get

$$\frac{\mu(x)}{\mu_0} = \exp\left[B \frac{T_0 - T}{T_0 T} \left(\frac{x}{\delta}\right)\right] \cong \exp\left[B \frac{T_0 - T}{T_0 T_\delta} \left(\frac{x}{\delta}\right)\right] \quad (11.4-18)$$

The second expression is a good approximation if the temperature does not change greatly through the film. When this equation is combined with Eq. 11.4-17, written for $T = T_\delta$, we then get

$$\frac{\mu(x)}{\mu_0} = \exp\left[\left(\ln \frac{\mu_\delta}{\mu_0}\right) \left(\frac{x}{\delta}\right)\right] = \left(\frac{\mu_\delta}{\mu_0}\right)^{x/\delta} \quad (11.4-19)$$

This is the same as the expression used in Example 2.2-2, if we set α equal to $-\ln(\mu_\delta/\mu_0)$. Therefore we may take over the result from Example 2.2-2 and write the velocity profile as

$$v_z = \left(\frac{\rho g \cos \beta}{\mu_0}\right) \left(\frac{\delta}{\ln(\mu_\delta/\mu_0)}\right)^2 \left[\frac{1 + (x/\delta) \ln(\mu_\delta/\mu_0)}{(\mu_\delta/\mu_0)^{x/\delta}} - \frac{1 + \ln(\mu_\delta/\mu_0)}{(\mu_\delta/\mu_0)} \right] \quad (11.4-20)$$

This completes the analysis of the problem begun in Example 2.2-2, by providing the appropriate value of the constant α .

EXAMPLE 11.4-4**Transpiration Cooling²**

A system with two concentric porous spherical shells of radii κR and R is shown in Fig. 11.4-1. The inner surface of the outer shell is at temperature T_1 , and the outer surface of the inner shell is at a lower temperature T_κ . Dry air at T_κ is blown outward radially from the inner shell into the intervening space and then through the outer shell. Develop an expression for the required rate of heat removal from the inner sphere as a function of the mass rate of flow of the gas. Assume steady laminar flow and low gas velocity.

In this example the equations of continuity and energy are solved to get the temperature distribution. The equation of motion gives information about the pressure distribution in the system.

² M. Jakob, *Heat Transfer*, Vol. 2, Wiley, New York (1957), pp. 394–415.

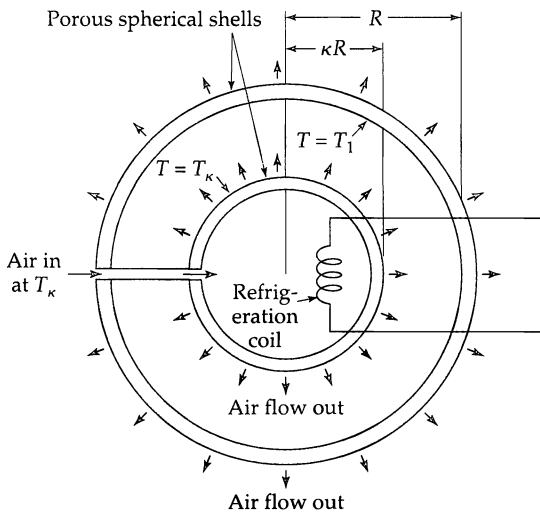


Fig. 11.4-1. Transpiration cooling. The inner sphere is being cooled by means of a refrigeration coil to maintain its temperature at T_k . When air is blown outward, as shown, less refrigeration is required.

SOLUTION

We postulate that for this system $\mathbf{v} = \delta_r v_r(r)$, $T = T(r)$, and $\mathcal{P} = \mathcal{P}(r)$. The *equation of continuity* in spherical coordinates then becomes

$$\frac{1}{r^2} \frac{d}{dr} (r^2 \rho v_r) = 0 \quad (11.4-21)$$

This equation can be integrated to give

$$r^2 \rho v_r = \text{const.} = \frac{w_r}{4\pi} \quad (11.4-22)$$

Here w_r is the radial mass flow rate of the gas.

The r -component of the *equation of motion* in spherical coordinates is, from Eq. B.6-7,

$$\rho v_r \frac{dv_r}{dr} = -\frac{d\mathcal{P}}{dr} + \mu \left[\frac{d}{dr} \left(\frac{1}{r^2} \frac{d}{dr} (r^2 v_r) \right) \right] \quad (11.4-23)$$

The viscosity term drops out because of Eq. 11.4-21. Integration of Eq. 11.4-23 then gives

$$\mathcal{P}(r) - \mathcal{P}(R) = \frac{w_r}{32\pi^2 \rho R^4} \left[1 - \left(\frac{R}{r} \right)^4 \right] \quad (11.4-24)$$

Hence the modified pressure \mathcal{P} increases with r , but only very slightly for the low gas velocity assumed here.

The *energy equation* in terms of the temperature, in spherical coordinates, is, according to Eq. B.9-3,

$$\rho \hat{C}_p v_r \frac{dT}{dr} = k \frac{1}{r^2} \frac{d}{dr} \left(r^2 \frac{dT}{dr} \right) \quad (11.4-25)$$

Here we have used Eq. 11.2-8, for which we assume that the thermal conductivity is constant, the pressure is constant, and there is no viscous dissipation—all reasonable assumptions for the problem at hand.

When Eq. 11.4-22 for the velocity distribution is used for v_r in Eq. 11.4-25, we obtain the following differential equation for the temperature distribution $T(r)$ in the gas between the two shells:

$$\frac{dT}{dr} = \frac{4\pi k}{w_r \hat{C}_p} \frac{d}{dr} \left(r^2 \frac{dT}{dr} \right) \quad (11.4-26)$$

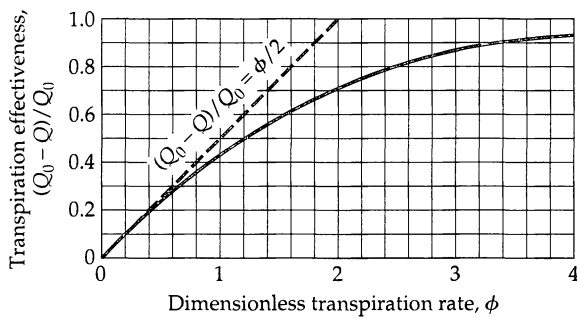


Fig. 11.4-2. The effect of transpiration cooling.

We make the change of variable $u = r^2(dT/dr)$ and obtain a first-order, separable differential equation for $u(r)$. This may be integrated, and when the boundary conditions are applied, we get

$$\frac{T - T_1}{T_\kappa - T_1} = \frac{e^{-R_0/r} - e^{-R_0/R}}{e^{-R_0/\kappa R} - e^{-R_0/R}} \quad (11.4-27)$$

in which $R_0 = w\hat{C}_p/4\pi k$ is a constant with units of length.

The rate of heat flow toward the inner sphere is

$$Q = -4\pi\kappa^2 R^2 q_r \Big|_{r=\kappa R} \quad (11.4-28)$$

and this is the required rate of heat removal by the refrigerant. Insertion of Fourier's law for the r -component of the heat flux gives

$$Q = +4\pi\kappa^2 R^2 k \frac{dT}{dr} \Big|_{r=\kappa R} \quad (11.4-29)$$

Next we evaluate the temperature gradient at the surface with the aid of Eq. 11.4-27 to obtain the expression for the heat removal rate.

$$Q = \frac{4\pi R_0 k(T_1 - T_\kappa)}{\exp[(R_0/\kappa R)(1-\kappa)] - 1} \quad (11.4-30)$$

In the limit that the mass flow rate of the gas is zero, so that $R_0 = 0$, the heat removal rate becomes

$$Q_0 = \frac{4\pi\kappa R k(T_1 - T_\kappa)}{1 - \kappa} \quad (11.4-31)$$

The fractional reduction in heat removal as a result of the transpiration of the gas is then

$$\frac{Q_0 - Q}{Q_0} = 1 - \frac{\phi}{e^\phi - 1} \quad (11.4-32)$$

Here $\phi = R_0(1 - \kappa)/\kappa R = w\hat{C}_p(1 - \kappa)/4\pi\kappa R k$ is the "dimensionless transpiration rate." Equation 11.4-32 is shown graphically in Fig. 11.4-2. For small values of ϕ , the quantity $(Q_0 - Q)/Q_0$ approaches the asymptote $\frac{1}{2}\phi$.

EXAMPLE 11.4-5

Free-Convection Heat Transfer from a Vertical Plate

A flat plate of height H and width W (with $W \gg H$) heated to a temperature T_0 is suspended in a large body of fluid, which is at ambient temperature T_1 . In the neighborhood of the heated plate the fluid rises because of the buoyant force (see Fig. 11.4-3). From the equations of change, deduce the dependence of the heat loss on the system variables. The physical properties of the fluid are considered constant, except that the change in density with temperature will be accounted for by the Boussinesq approximation.

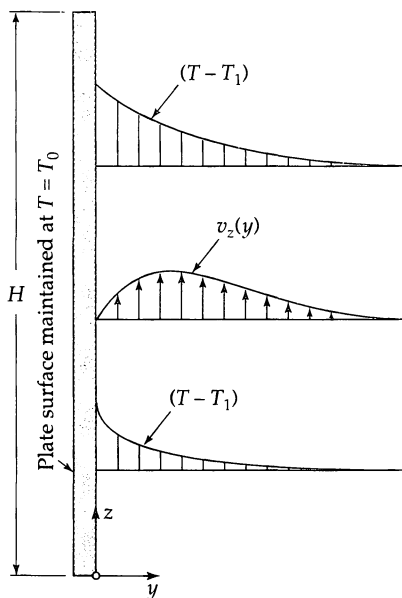


Fig. 11.4-3. The temperature and velocity profiles in the neighborhood of a vertical heated plate.

SOLUTION

We postulate that $\mathbf{v} = \delta_y v_y(y, z) + \delta_z v_z(y, z)$ and that $T = T(y, z)$. We assume that the heated fluid moves almost directly upward, so that $v_y \ll v_z$. Then the x - and y -components of Eq. 11.3-2 give $p = p(z)$, so that the pressure is given to a very good approximation by $-dp/dz - \bar{\rho}g = 0$, which is the hydrostatic pressure distribution. The remaining equations of change are

$$\text{Continuity} \quad \frac{\partial v_y}{\partial y} + \frac{\partial v_z}{\partial z} = 0 \quad (11.4-33)$$

$$\text{Motion} \quad \bar{\rho} \left(v_y \frac{\partial}{\partial y} + v_z \frac{\partial}{\partial z} \right) v_z = \mu \left(\frac{\partial^2}{\partial y^2} + \frac{\partial^2}{\partial z^2} \right) v_z + \bar{\rho} g \bar{\beta} (T - T_1) \quad (11.4-34)$$

$$\text{Energy} \quad \bar{\rho} \hat{C}_p \left(v_y \frac{\partial}{\partial y} + v_z \frac{\partial}{\partial z} \right) (T - T_1) = k \left(\frac{\partial^2}{\partial y^2} + \frac{\partial^2}{\partial z^2} \right) (T - T_1) \quad (11.4-35)$$

in which $\bar{\rho}$ and $\bar{\beta}$ are evaluated at the ambient temperature T_1 . The dashed-underlined terms will be omitted on the ground that momentum and energy transport by molecular processes in the z direction is small compared with the corresponding convective terms on the left side of the equations. These omissions should give a satisfactory description of the system except for a small region around the bottom of the plate. With this simplification, the following boundary conditions suffice to analyze the system up to $z = H$:

$$\text{B.C. 1:} \quad \text{at } y = 0, \quad v_y = v_z = 0 \quad \text{and} \quad T = T_0 \quad (11.4-36)$$

$$\text{B.C. 2:} \quad \text{as } y \rightarrow \pm\infty, \quad v_z \rightarrow 0 \quad \text{and} \quad T \rightarrow T_1 \quad (11.4-37)$$

$$\text{B.C. 3:} \quad \text{at } z = 0, \quad v_z = 0 \quad (11.4-38)$$

Note that the temperature rise appears in the equation of motion and that the velocity distribution appears in the energy equation. Thus these equations are "coupled." Analytic solutions of such coupled, nonlinear differential equations are very difficult, and we content ourselves here with a dimensional analysis approach.

To do this we introduce the following dimensionless variables:

$$\Theta = \frac{T - T_1}{T_0 - T_1} = \text{dimensionless temperature} \quad (11.4-39)$$

$$\zeta = \frac{z}{H} = \text{dimensionless vertical coordinate} \quad (11.4-40)$$

$$\eta = \left(\frac{B}{\mu \alpha H} \right)^{1/4} y \quad \text{dimensionless horizontal coordinate} \quad (11.4-41)$$

$$\phi_z = \left(\frac{\mu}{\alpha B H} \right)^{1/2} v_z \quad \text{dimensionless vertical velocity} \quad (11.4-42)$$

$$\phi_y = \left(\frac{\mu H}{\alpha^3 B} \right)^{1/4} v_y \quad \text{dimensionless horizontal velocity} \quad (11.4-43)$$

in which $\alpha = k/\rho \hat{C}_p$ and $B = \bar{\rho} g \bar{\beta}(T_0 - T_1)$.

When the equations of change, without the dashed-underlined terms, are written in terms of these dimensionless variables, we get

$$\text{Continuity} \quad \frac{\partial \phi_y}{\partial \eta} + \frac{\partial \phi_z}{\partial \zeta} = 0 \quad (11.4-44)$$

$$\text{Motion} \quad \frac{1}{\text{Pr}} \left(\phi_y \frac{\partial}{\partial \eta} + \phi_z \frac{\partial}{\partial \zeta} \right) \phi_z = \frac{\partial^2 \phi_z}{\partial \eta^2} + \Theta \quad (11.4-45)$$

$$\text{Energy} \quad \left(\phi_y \frac{\partial}{\partial \eta} + \phi_z \frac{\partial}{\partial \zeta} \right) \Theta = \frac{\partial^2 \Theta}{\partial \eta^2} \quad (11.4-46)$$

The preceding boundary conditions then become

$$\text{B.C. 1:} \quad \text{at } \eta = 0, \quad \phi_y = \phi_z = 0, \quad \Theta = 1 \quad (11.4-47)$$

$$\text{B.C. 2:} \quad \text{as } \eta \rightarrow \infty, \quad \phi_z \rightarrow 0, \quad \Theta \rightarrow 0 \quad (11.4-48)$$

$$\text{B.C. 3:} \quad \text{at } \zeta = 0, \quad \phi_z = 0 \quad (11.4-49)$$

One can see immediately from these equations and boundary conditions that the dimensionless velocity components ϕ_y and ϕ_z and the dimensionless temperature Θ will depend on η and ζ and also on the Prandtl number, Pr . Since the flow is usually very slow in free convection, the terms in which Pr appears will generally be rather small; setting them equal to zero would correspond to the "creeping flow assumption." Hence we expect that the dependence of the solution on the Prandtl number will be weak.

The average heat flux from one side of the plate may be written as

$$q_{\text{avg}} = \frac{1}{H} \int_0^H \left(-k \frac{\partial T}{\partial y} \right) \Big|_{y=0} dz \quad (11.4-50)$$

The integral may now be written in terms of the dimensionless quantities

$$\begin{aligned} q_{\text{avg}} &= k(T_0 - T_1) \left(\frac{B}{\mu \alpha H} \right)^{1/4} \cdot \int_0^1 \left(-\frac{\partial \Theta}{\partial \eta} \right) \Big|_{\eta=0} d\zeta \\ &= k(T_0 - T_1) \left(\frac{B}{\mu \alpha H} \right)^{1/4} \cdot C \\ &= C \cdot \frac{k}{H} (T_0 - T_1) \left(\left(\frac{\hat{C}_p \mu}{k} \right) \left(\frac{\bar{\rho}^2 g \bar{\beta} (T_0 - T_1) H^3}{\mu^2} \right) \right)^{1/4} \\ &= C \cdot \frac{k}{H} (T_0 - T_1) (\text{GrPr})^{1/4} \end{aligned} \quad (11.4-51)$$

in which the grouping $\text{Ra} = \text{GrPr}$ is referred to as the *Rayleigh number*. Because Θ is a function of η , ζ , and Pr , the derivative $\partial \Theta / \partial \eta$ is also a function of η , ζ , and Pr . Then $\partial \Theta / \partial \eta$, evaluated at $\eta = 0$, depends only on ζ and Pr . The definite integral over ζ is thus a function of Pr . From the remarks made earlier, we can infer that this function, called C , will be only a weak function of the Prandtl number—that is, nearly a constant.

The preceding analysis shows that, even without solving the partial differential equations, we can predict that the average heat flux is proportional to the $\frac{5}{4}$ -power of the temperature difference $(T_0 - T_1)$ and inversely proportional to the $\frac{1}{4}$ -power of H . Both predictions have been confirmed by experiment. The only thing we could not do was to find C as a function of Pr .

To determine that function, we have to make experimental measurements or solve Eqs. 11.4-44 to 4. In 1881, Lorenz³ obtained an approximate solution to these equations and found $C = 0.548$. Later, more refined calculations⁴ gave the following dependence of C on Pr :

Pr	0.73 (air)	1	10	100	1000	∞
C	0.518	0.535	0.620	0.653	0.665	0.670

These values of C are nearly in exact agreement with the best experimental measurements in the laminar flow range (i.e., for $\text{GrPr} < 10^9$).⁵

EXAMPLE 11.4-6

Adiabatic Frictionless Processes in an Ideal Gas

Develop equations for the relationship of local pressure to density or temperature in a stream of ideal gas in which the momentum flux τ and the heat flux q are negligible.

SOLUTION

With τ and q neglected, the equation of energy [Eq. (J) in Table 11.4-1] may be rewritten as

$$\rho \hat{C}_p \frac{DT}{Dt} = \left(\frac{\partial \ln \hat{V}}{\partial \ln T} \right)_p \frac{Dp}{Dt} \quad (11.4-52)$$

For an ideal gas, $p\hat{V} = RT/M$, where M is the molecular weight of the gas, and Eq. 11.4-52 becomes

$$\rho \hat{C}_p \frac{DT}{Dt} = \frac{Dp}{Dt} \quad (11.4-53)$$

Dividing this equation by p and assuming the molar heat capacity $\tilde{C}_p = M\hat{C}_p$ to be constant, we can again use the ideal gas law to get

$$\frac{D}{Dt} \left(\frac{\tilde{C}_p}{R} \ln T - \ln p \right) = 0 \quad (11.4-54)$$

Hence the quantity in parentheses is a constant along the path of a fluid element, as is its antilogarithm, so that we have

$$T^{\tilde{C}_p/R} p^{-1} = \text{constant} \quad (11.4-55)$$

This relation applies to all thermodynamic states p, T that a fluid element encounters as it moves along with the fluid.

Introducing the definition $\gamma = \hat{C}_p/\hat{C}_V$ and the ideal gas relations $\tilde{C}_p - \tilde{C}_V = R$ and $p = \rho RT/M$, one obtains the related expressions

$$p^{(\gamma-1)/\gamma} T^{-1} = \text{constant} \quad (11.4-56)$$

and

$$\rho p^{-\gamma} = \text{constant} \quad (11.4-57)$$

These last three equations find frequent use in the study of frictionless adiabatic processes in ideal gas dynamics. Equation 11.4-57 is a famous relation well worth remembering.

³ L. Lorenz, *Wiedemann's Ann. der Physik u. Chemie*, **13**, 422–447, 582–606 (1881). See also U. Grigull, *Die Grundgesetze der Wärmeübertragung*, Springer-Verlag, Berlin, 3rd edition (1955), pp. 263–269.

⁴ See S. Whitaker, *Fundamental Principles of Heat Transfer*, Krieger, Malabar Fla. (1977), §5.11. The limiting case of $\text{Pr} \rightarrow \infty$ has been worked out numerically by E. J. LeFevre [Heat Div. Paper 113, Dept. Sci. and Ind. Res., Mech. Engr. Lab. (Great Britain), Aug. 1956] and it was found that

$$\left. \frac{\partial \Theta}{\partial \eta} \right|_{\eta=0} = \frac{0.5028}{\zeta^{1/4}} \quad \left. \frac{\partial \phi_i}{\partial \eta} \right|_{\eta=0} = \frac{1.16}{\zeta^{1/4}} \quad (11.4-51a, b)$$

Equation 11.4-51a corresponds to the value $C = 0.670$ above. This result has been verified experimentally by C. R. Wilke, C. W. Tobias, and M. Eisenberg, *J. Electrochem. Soc.*, **100**, 513–523 (1953), for the analogous mass transfer problem.

⁵ For an analysis of free convection in three-dimensional creeping flow, see W. E. Stewart, *Int. J. Heat and Mass Transfer*, **14**, 1013–1031 (1971).

When the momentum flux τ and the heat flux q are zero, there is no change in entropy following an element of fluid (see Eq. 11D.1-3). Hence the derivative $d \ln p / d \ln T = \gamma / (\gamma - 1)$ following the fluid motion has to be understood to mean $(\partial \ln p / \partial \ln T)_S = \gamma / (\gamma - 1)$. This equation is a standard formula from equilibrium thermodynamics.

EXAMPLE 11.4-7

One-Dimensional Compressible Flow: Velocity, Temperature, and Pressure Profiles in a Stationary Shock Wave

We consider here the adiabatic expansion⁶⁻¹⁰ of an ideal gas through a convergent-divergent nozzle under such conditions that a stationary shock wave is formed. The gas enters the nozzle from a reservoir, where the pressure is p_0 , and discharges to the atmosphere, where the pressure is p_a . In the absence of a shock wave, the flow through a well-designed nozzle is virtually frictionless (hence *isentropic* for the adiabatic situation being considered). If, in addition, p_a/p_0 is sufficiently small, it is known that the flow is essentially sonic at the throat (the region of minimum cross section) and is supersonic in the divergent portion of the nozzle. Under these conditions the pressure will continually decrease, and the velocity will increase in the direction of the flow, as indicated by the curves in Fig. 11.4-4.

However, for any nozzle design there is a range of p_a/p_0 for which such an isentropic flow produces a pressure less than p_a at the exit. Then the isentropic flow becomes unstable. The simplest of many possibilities is a stationary normal shock wave, shown schematically in the Fig. 11.4-4 as a pair of closely spaced parallel lines. Here the velocity falls off very rapidly

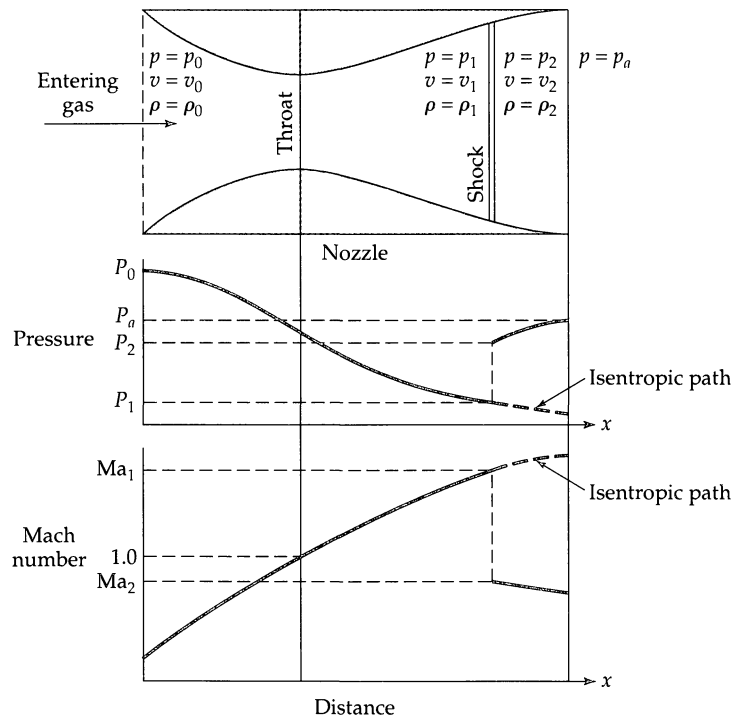


Fig. 11.4-4. Formation of a shock wave in a nozzle.

⁶ H. W. Liepmann and A. Roshko, *Elements of Gas Dynamics*, Wiley, New York (1957), §§5.4 and 13.13.

⁷ J. O. Hirschfelder, C. F. Curtiss, and R. B. Bird, *Molecular Theory of Gases and Liquids*, Wiley, New York, 2nd corrected printing (1964), pp. 791-797.

⁸ M. Morduchow and P. A. Libby, *J. Aeronautical Sci.*, **16**, 674-684 (1948).

⁹ R. von Mises, *J. Aeronautical Sci.*, **17**, 551-554 (1950).

¹⁰ G. S. S. Ludford, *J. Aeronautical Sci.*, **18**, 830-834 (1951).

to a subsonic value, while both the pressure and the density rise. These changes take place in an extremely thin region, which may therefore be considered locally one-dimensional and laminar, and they are accompanied by a very substantial dissipation of mechanical energy. Viscous dissipation and heat conduction effects are thus concentrated in an extremely small region of the nozzle, and it is the purpose of the example to explore the fluid behavior there. For simplicity the shock wave will be considered normal to the fluid streamlines; in practice, much more complicated shapes are often observed. The velocity, pressure, and temperature just upstream of the shock can be calculated and will be considered as known for the purposes of this example.

Use the three equations of change to determine the conditions under which a shock wave is possible and to find the velocity, temperature, and pressure distributions in such a shock wave. Assume steady, one-dimensional flow of an ideal gas, neglect the dilatational viscosity κ , and ignore changes of μ , k , and \hat{C}_p with temperature and pressure.

SOLUTION

The equations of change in the neighborhood of the stationary shock wave may be simplified to

$$\text{Continuity: } \frac{d}{dx} \rho v_x = 0 \quad (11.4-58)$$

$$\text{Motion: } \rho v_x \frac{dv_x}{dx} = -\frac{dp}{dx} + \frac{4}{3} \frac{d}{dx} \left(\mu \frac{dv_x}{dx} \right) \quad (11.4-59)$$

$$\text{Energy: } \rho \hat{C}_p v_x \frac{dT}{dx} = \frac{d}{dx} \left(k \frac{dT}{dx} \right) + v_x \frac{dp}{dx} + \frac{4}{3} \mu \left(\frac{dv_x}{dx} \right)^2 \quad (11.4-60)$$

The energy equation is in the form of Eq. J of Table 11.4-1, written for an ideal gas in a steady-state situation.

The equation of *continuity* may be integrated to give

$$\rho v_x = \rho_1 v_1 \quad (11.4-61)$$

in which ρ_1 and v_1 are quantities evaluated a short distance upstream from the shock.

In the *energy* equation we eliminate ρv_x by use of Eq. 11.4-61 and dp/dx by using the equation of motion to get (after some rearrangement)

$$\rho_1 \hat{C}_p v_1 \frac{dT}{dx} = \frac{d}{dx} \left(k \frac{dT}{dx} \right) - \rho_1 v_1 \frac{d}{dx} \left(\frac{1}{2} v_x^2 \right) + \frac{4}{3} \mu \frac{d}{dx} \left(v_x \frac{dv_x}{dx} \right) \quad (11.4-62)$$

We next move the second term on the right side over to the left side and divide the entire equation by $\rho_1 v_1$. Then each term is integrated with respect to x to give

$$\hat{C}_p T + \frac{1}{2} v_x^2 = \frac{k}{\rho_1 \hat{C}_p v_1} \frac{d}{dx} (\hat{C}_p T + (\frac{4}{3} \text{Pr}) \frac{1}{2} v_x^2) + C_1 \quad (11.4-63)$$

in which C_1 is a constant of integration and $\text{Pr} = \hat{C}_p \mu / k$. For most gases Pr is between 0.65 and 0.85, with an average value close to 0.75. Therefore, to simplify the problem we set Pr equal to $\frac{3}{4}$. Then Eq. 11.4-63 becomes a first-order, linear ordinary differential equation, for which the solution is

$$\hat{C}_p T + \frac{1}{2} v_x^2 = C_1 + C_{11} \exp[(\rho_1 \hat{C}_p v_1 / k)x] \quad (11.4-64)$$

Since $\hat{C}_p T + \frac{1}{2} v_x^2$ cannot increase without limit in the positive x direction, the second integration constant C_{11} must be zero. The first integration constant is evaluated from the upstream conditions, so that

$$\hat{C}_p T + \frac{1}{2} v_x^2 = \hat{C}_p T_1 + \frac{1}{2} v_1^2 \quad (11.4-65)$$

Of course, if we had not chosen Pr to be $\frac{3}{4}$, a numerical integration of Eq. 11.4-63 would have been required.

Next we substitute the integrated continuity equation into the equation of motion and integrate once to obtain

$$\rho_1 v_1 v_x = -p + \frac{4}{3} \mu \frac{dv_x}{dx} + C_{III} \quad (11.4-66)$$

Evaluation of the constant C_{III} from upstream conditions, where $dv_x/dx = 0$, gives $C_{III} = \rho_1 v_1^2 + p_1 = \rho_1 [v_1^2 + (RT_1/M)]$. We now multiply both sides by v_x and divide by $\rho_1 v_1$. Then, with the help of the ideal gas law, $p = \rho RT/M$, and Eqs. 11.4-61 and 65, we may eliminate p from Eq. 11.4-60 to obtain a relation containing only v_x and x as variables:

$$\frac{4}{3} \frac{\mu}{\rho_1 v_1} v_x \frac{dv_x}{dx} = \frac{\gamma + 1}{2\gamma} v_x^2 + \frac{\gamma - 1}{\gamma} C_1 - \frac{C_{III}}{\rho_1 v_1} v_x \quad (11.4-67)$$

This equation can, after considerable rearrangement, be rewritten in terms of dimensionless variables:

$$\phi \frac{d\phi}{d\xi} = \beta Ma_1(\phi - 1)(\phi - \alpha) \quad (11.4-68)$$

The relevant dimensionless quantities are

$$\phi = \frac{v_x}{v_1} = \text{dimensionless velocity} \quad (11.4-69)$$

$$\xi = \frac{x}{\lambda} = \text{dimensionless coordinate} \quad (11.4-70)$$

$$Ma_1 = \frac{v_1}{\sqrt{\gamma RT_1/M}} = \text{Mach number at the upstream condition} \quad (11.4-71)$$

$$\alpha = \frac{\gamma - 1}{\gamma + 1} + \frac{2}{\gamma + 1} \frac{1}{Ma_1^2} \quad (11.4-72)$$

$$\beta = \frac{9}{8}(\gamma + 1)\sqrt{\pi/8\gamma} \quad (11.4-73)$$

The reference length λ is the mean free path defined in Eq. 1.4-3 (with d^2 eliminated by use of Eq. 1.4-9):

$$\lambda = \frac{3\mu_1}{\rho_1} \sqrt{\frac{\pi M}{8RT_1}} \quad (11.4-74)$$

We may integrate Eq. 11.4-68 to obtain

$$\frac{1 - \phi}{(\phi - \alpha)^\alpha} = \exp[\beta Ma_1(1 - \alpha)(\xi - \xi_0)] \quad (\alpha < \phi < 1) \quad (11.4-75)$$

This equation describes the dimensionless velocity distribution $\phi(\xi)$ containing an integration constant $\xi_0 = x_0/\lambda$, which specifies the position of the shock wave in the nozzle; here ξ_0 is considered to be known. It can be seen from the plot of Eq. 11.4-85 in Fig. 11.4-5 that shock waves

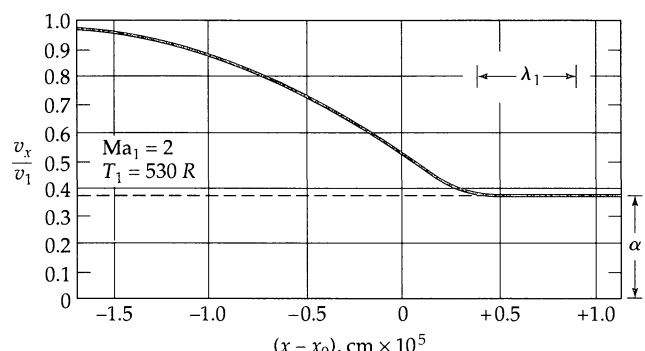


Fig. 11.4-5. Velocity distribution in a stationary shock wave.

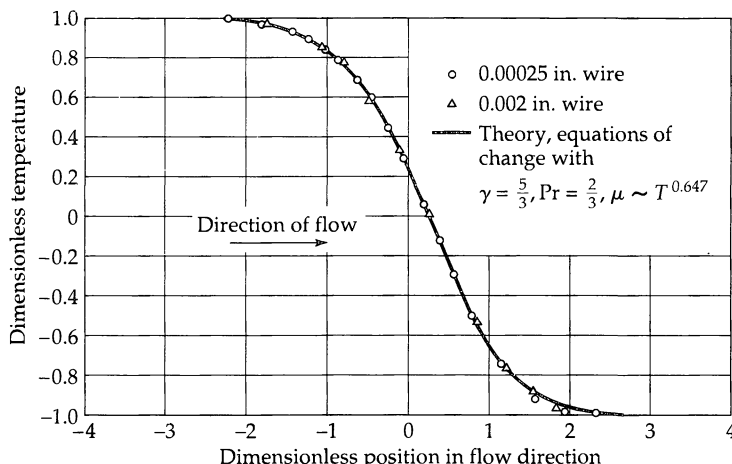


Fig. 11.4-6. Semi-log plot of the temperature profile through a shock wave, for helium with $\text{Ma}_1 = 1.82$. The experimental values were measured with a resistance-wire thermometer. [Adapted from H. W. Liepmann and A. Roshko, *Elements of Gas Dynamics*, Wiley, New York (1957), p. 333]

are indeed very thin. The temperature and pressure distributions may be determined from Eq. 11.4-75 and Eqs. 11.4-65 and 66. Since ϕ must approach unity as $\xi \rightarrow -\infty$, the constant α is less than 1. This can be true only if $\text{Ma}_1 > 1$ —that is, if the upstream flow is supersonic. It can also be seen that for very large positive ξ , the dimensionless velocity ϕ approaches α . The Mach number Ma_1 is defined as the ratio of v_1 to the velocity of sound at T_1 (see Problem 11C.1).

In the above development we chose the Prandtl number Pr to be $\frac{3}{4}$, but the solution has been extended⁸ to include other values of Pr as well as the temperature variation of the viscosity.

The tendency of a gas in supersonic flow to revert spontaneously to subsonic flow is important in wind tunnels and in the design of high-velocity systems—for example, in turbines and rocket engines. Note that the changes taking place in shock waves are irreversible and that, since the velocity gradients are so very steep, a considerable amount of mechanical energy is dissipated.

In view of the thinness of the predicted shock wave, one may question the applicability of the analysis given here, based on the continuum equations of change. Therefore it is desirable to compare the theory with experiment. In Fig. 11.4-6 experimental temperature measurements for a shock wave in helium are compared with the theory for $\gamma = \frac{5}{3}$, $\text{Pr} = \frac{2}{3}$, and $\mu \sim T^{0.647}$. We can see that the agreement is excellent. Nevertheless we should recognize that this is a simple system, inasmuch as helium is monatomic, and therefore internal degrees of freedom are not involved. The corresponding analysis for a diatomic or polyatomic gas would need to consider the exchange of energy between translational and internal degrees of freedom, which typically requires hundreds of collisions, broadening the shock wave considerably. Further discussion of this matter can be found in Chapter 11 of Ref. 7.

§11.5 DIMENSIONAL ANALYSIS OF THE EQUATIONS OF CHANGE FOR NONISOTHERMAL SYSTEMS

Now that we have shown how to use the equations of change for nonisothermal systems to solve some representative heat transport problems, we discuss the dimensional analysis of these equations.

Just as the dimensional analysis discussion in §3.7 provided an introduction for the discussion of friction factors in Chapter 6, the material in this section provides the background needed for the discussion of heat transfer coefficient correlations in Chapter 14. As in Chapter 3, we write the equations of change and boundary conditions in dimensionless form. In this way we find some dimensionless parameters that can be used to characterize nonisothermal flow systems.

We shall see, however, that the analysis of nonisothermal systems leads us to a larger number of dimensionless groups than we had in Chapter 3. As a result, greater reliance has to be placed on judicious simplifications of the equations of change and on carefully chosen physical models. Examples of the latter are the Boussinesq equation of motion for free convection (§11.3) and the laminar boundary layer equations (§12.4).

As in §3.7, for the sake of simplicity we restrict ourselves to a fluid with constant μ , k , and \hat{C}_p . The density is taken to be $\rho = \bar{\rho} - \bar{\rho}\beta(T - \bar{T})$ in the ρg term in the equation of motion, and $\rho = \bar{\rho}$ everywhere else (the “Boussinesq approximation”). The equations of change then become with $p + \rho gh$ expressed as \mathcal{P} ,

$$\text{Continuity:} \quad (\nabla \cdot \mathbf{v}) = 0 \quad (11.5-1)$$

$$\text{Motion:} \quad \bar{\rho} \frac{D\mathbf{v}}{Dt} = -\nabla \mathcal{P} + \mu \nabla^2 \mathbf{v} + \bar{\rho} g \bar{\beta}(T - \bar{T}) \quad (11.5-2)$$

$$\text{Energy:} \quad \bar{\rho} \hat{C}_p \frac{DT}{Dt} = k \nabla^2 T + \mu \Phi_v \quad (11.5-3)$$

We now introduce quantities made dimensionless with the characteristic quantities (subscript 0 or 1) as follows:

$$\check{x} = \frac{x}{l_0} \quad \check{y} = \frac{y}{l_0} \quad \check{z} = \frac{z}{l_0} \quad \check{t} = \frac{v_0 t}{l_0} \quad (11.5-4)$$

$$\check{\mathbf{v}} = \frac{\mathbf{v}}{v_0} \quad \check{\mathcal{P}} = \frac{\mathcal{P} - \mathcal{P}_0}{\bar{\rho} v_0^2} \quad \check{T} = \frac{T - T_0}{T_1 - T_0} \quad (11.5-5)$$

$$\check{\Phi}_v = \left(\frac{l_0}{v_0}\right)^2 \Phi_v \quad \check{\nabla} = l_0 \nabla \quad \frac{D}{Dt} = \left(\frac{l_0}{v_0}\right) \frac{D}{Dt} \quad (11.5-6)$$

Here l_0 , v_0 , and \mathcal{P}_0 are the reference quantities introduced in §3.7, and T_0 and T_1 are temperatures appearing in the boundary conditions. In Eq. 11.5-2 the value \bar{T} is the temperature around which the density ρ was expanded.

In terms of these dimensionless variables, the equations of change in Eqs. 11.5-1 to 3 take the forms

$$\text{Continuity:} \quad (\check{\nabla} \cdot \check{\mathbf{v}}) = 0 \quad (11.5-7)$$

$$\text{Motion:} \quad \frac{D\check{\mathbf{v}}}{Dt} = -\check{\nabla} \check{\mathcal{P}} + \left[\frac{\mu}{l_0 v_0 \bar{\rho}} \right] \check{\nabla}^2 \check{\mathbf{v}} - \left[\frac{g l_0 \bar{\beta} (T_1 - T_0)}{v_0^2} \right] \left(\frac{\mathbf{g}}{g} \right) (\check{T} - \check{T}) \quad (11.5-8)$$

$$\text{Energy:} \quad \frac{D\check{T}}{Dt} = \left[\frac{k}{l_0 v_0 \bar{\rho} \hat{C}_p} \right] \check{\nabla}^2 \check{T} + \left[\frac{\mu v_0}{l_0 \bar{\rho} \hat{C}_p (T_1 - T_0)} \right] \check{\Phi}_v \quad (11.5-9)$$

The characteristic velocity can be chosen in several ways, and the consequences of the choices are summarized in Table 11.5-1. The dimensionless groups appearing in Eqs. 11.5-8 and 9, along with some combinations of these groups, are summarized in Table 11.5-2. Further dimensionless groups may arise in the boundary conditions or in the equation of state. The Froude and Weber numbers have already been introduced in §3.7, and the Mach number in Ex. 11.4-7.

We already saw in Chapter 10 how several dimensionless groups appeared in the solution of nonisothermal problems. Here we have seen that the same groupings appear naturally when the equations of change are made dimensionless. These dimensionless groups are used widely in correlations of heat transfer coefficients.

Table 11.5-1 Dimensionless Groups in Equations 11.5-7, 8, and 9

Special cases →	Forced convection	Intermediate	Free convection (A)	Free convection (B)
Choice for $v_0 \rightarrow$	v_0	v_0	ν/l_0	α/l_0
$\left[\frac{\mu}{l_0 v_0 \rho} \right]$	$\frac{1}{\text{Re}}$	$\frac{1}{\text{Re}}$	1	Pr
$\left[\frac{g l_0 \beta (T_1 - T_0)}{v_0^2} \right]$	Neglect	$\frac{\text{Gr}}{\text{Re}^2}$	Gr	GrPr^2
$\left[\frac{k}{l_0 v_0 \rho \hat{C}_p} \right]$	$\frac{1}{\text{RePr}}$	$\frac{1}{\text{RePr}}$	$\frac{1}{\text{Pr}}$	1
$\left[\frac{\mu v_0}{l_0 \rho \hat{C}_p (T_1 - T_0)} \right]$	$\frac{\text{Br}}{\text{RePr}}$	$\frac{\text{Br}}{\text{RePr}}$	Neglect	Neglect

Notes:

^a For forced convection and forced-plus-free (“intermediate”) convection, v_0 is generally taken to be the approach velocity (for flow around submerged objects) or an average velocity in the system (for flow in conduits).

^b For free convection there are two standard choices for v_0 , labeled as A and B. In §10.9, Case A arises naturally. Case B proves convenient if the assumption of creeping flow is appropriate, so that $D\vec{v}/Dt$ can be neglected (see Example 11.5-2). Then a new dimensionless pressure difference $\hat{P} = \text{Pr}\check{P}$, different from \check{P} in Eq. 3.7-4, can be introduced, so that when the equation of motion is divided by Pr , the only dimensionless group appearing in the equation is GrPr . Note that in Case B, no dimensionless groups appear in the equation of energy.

It is sometimes useful to think of the dimensionless groups as ratios of various forces or effects in the system, as shown in Table 11.5-3. For example, the inertial term in the equation of motion is $\rho[\mathbf{v} \cdot \nabla \mathbf{v}]$ and the viscous term is $\mu \nabla^2 \mathbf{v}$. To get “typical” values of these terms, replace the variables by the characteristic “yardsticks” used in constructing dimensionless variables. Hence replace $\rho[\mathbf{v} \cdot \nabla \mathbf{v}]$ by $\rho v_0^2/l_0$, and replace $\mu \nabla^2 \mathbf{v}$ by $\mu v_0/l_0^2$ to get rough orders of magnitude. The ratio of these two terms then gives the Reynolds number, as shown in the table. The other dimensionless groups are obtained in similar fashion.

Table 11.5-2 Dimensionless Groups Used in Nonisothermal Systems

$\text{Re} = [l_0 v_0 \rho / \mu] = [l_0 v_0 / \nu]$	= Reynolds number
$\text{Pr} = [\hat{C}_p \mu / k] = [\nu / \alpha]$	= Prandtl number
$\text{Gr} = [g \beta (T_1 - T_0) l_0^3 / \nu^2]$	= Grashof number
$\text{Br} = [\mu v_0^2 / k(T_1 - T_0)]$	= Brinkman number
$\text{Pé} = \text{RePr}$	= Péclet number
$\text{Ra} = \text{GrPr}$	= Rayleigh number
$\text{Ec} = \text{Br/Pr}$	= Eckert number

Table 11.5-3 Physical Interpretation of Dimensionless Groups

$\text{Re} = \frac{\rho v_0^2 / l_0}{\mu v_0 / l_0^2} = \frac{\text{inertial force}}{\text{viscous force}}$
$\text{Fr} = \frac{\rho v_0^2 / l_0}{\rho g} = \frac{\text{inertial force}}{\text{gravity force}}$
$\frac{\text{Gr}}{\text{Re}^2} = \frac{\rho g \beta (T_1 - T_0)}{\rho v_0^2 / l_0} = \frac{\text{buoyant force}}{\text{inertial force}}$
$\hat{\text{Pe}} = \text{RePr} = \frac{\rho \hat{C}_p v_0 (T_1 - T_0) / l_0}{k (T_1 - T_0) / l_0^2} = \frac{\text{heat transport by convection}}{\text{heat transport by conduction}}$
$\text{Br} = \frac{\mu (v_0 / l_0)^2}{k (T_1 - T_0) / l_0^2} = \frac{\text{heat production by viscous dissipation}}{\text{heat transport by conduction}}$

A low value for the Reynolds number means that viscous forces are large in comparison with inertial forces. A low value of the Brinkman number indicates that the heat produced by viscous dissipation can be transported away quickly by heat conduction. When Gr/Re^2 is large, the buoyant force is important in determining the flow pattern.

Since dimensional analysis is an art requiring judgment and experience, we give three illustrative examples. In the first two we analyze forced and free convection in simple geometries. In the third we discuss scale-up problems in a relatively complex piece of equipment.

EXAMPLE 11.5-1

Temperature Distribution about a Long Cylinder

It is desired to predict the temperature distribution in a gas flowing about a long, internally cooled cylinder (system I) from experimental measurements on a one-quarter scale model (system II). If possible the same fluid should be used in the model as in the full-scale system. The system, shown in Fig. 11.5-1, is the same as that in Example 3.7-1 except that it is now nonisothermal. The fluid approaching the cylinder has a speed v_∞ and a temperature T_∞ , and the cylinder surface is maintained at T_0 , for example, by the boiling of a refrigerant contained within it.

Show by means of dimensional analysis how suitable experimental conditions can be chosen for the model studies. Perform the dimensional analysis for the "intermediate case" in Table 11.5-1.

SOLUTION

The two systems, I and II, are geometrically similar. To ensure dynamical similarity, as pointed out in §3.7, the dimensionless differential equations and boundary conditions must be the same, and the dimensionless groups appearing in them must have the same numerical values.

Here we choose the characteristic length to be the diameter D of the cylinder, the characteristic velocity to be the approach velocity v_∞ of the fluid, the characteristic pressure to be the pressure at $x = -\infty$ and $y = 0$, and the characteristic temperatures to be the temperature T_∞ of the approaching fluid and the temperature T_0 of the cylinder wall. These characteristic quantities will carry a label I or II corresponding to the system being described.

Both systems are described by the dimensionless differential equations given in Eqs. 11.5-7 to 9, and by boundary conditions

$$\text{B.C. 1} \quad \text{as } \check{x}^2 + \check{y}^2 \rightarrow \infty, \quad \check{v} \rightarrow \check{0}_x, \quad \check{T} \rightarrow 1 \quad (11.5-10)$$

$$\text{B.C. 2} \quad \text{at } \check{x}^2 + \check{y}^2 = \frac{1}{4}, \quad \check{v} = 0, \quad \check{T} = 0 \quad (11.5-11)$$

$$\text{B.C. 3} \quad \text{at } \check{x} \rightarrow -\infty \text{ and } \check{y} = 0, \quad \check{P} \rightarrow 0 \quad (11.5-12)$$

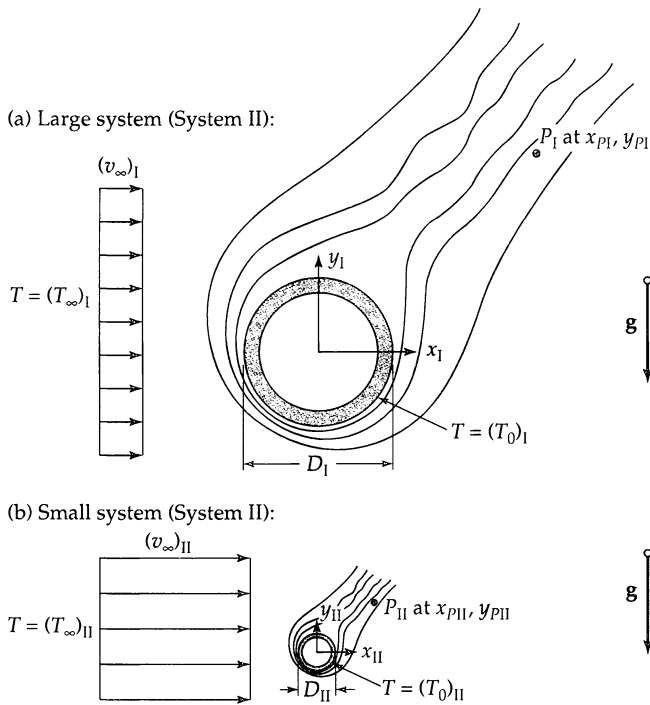


Fig. 11.5-1. Temperature profiles about long heated cylinders. The contour lines in the two figures represent surfaces of constant temperature.

in which $\check{T} = (T - T_0)/(T_\infty - T_0)$. For this simple geometry, the boundary conditions contain no dimensionless groups. Therefore, the requirement that the differential equations and boundary conditions in dimensionless form be identical is that the following dimensionless groups be equal in the two systems: $Re = Dv_\infty \rho / \mu$, $Pr = \hat{C}_p \mu / k$, $Br = \mu v_\infty^2 / k(T_\infty - T_0)$, and $Gr = \rho^2 g \beta (T_\infty - T_0) D^3 / \mu^2$. In the latter group we use the ideal gas expression $\beta = 1/T$.

To obtain the necessary equality for the four governing dimensionless groups, we may use different values of the four disposable parameters in the two systems: the approach velocity v_∞ , the fluid temperature T_∞ , the approach pressure P_∞ , and the cylinder temperature T_0 .

The similarity requirements are then (for $D_I = 4D_{II}$):

$$\text{Equality of Pr} \quad \frac{\nu_I}{\nu_{II}} = \frac{\alpha_I}{\alpha_{II}} \quad (11.5-13)$$

$$\text{Equality of Re} \quad \frac{\nu_I}{\nu_{II}} = 4 \frac{v_{\infty I}}{v_{\infty II}} \quad (11.5-14)$$

$$\text{Equality of Gr} \quad \left(\frac{\nu_I}{\nu_{II}} \right)^2 = 64 \frac{T_{\infty II}}{T_{\infty I}} \frac{(T_\infty - T_0)_I}{(T_\infty - T_0)_{II}} \quad (11.5-15)$$

$$\text{Equality of Br} \quad \left(\frac{Pr_I}{Pr_{II}} \right) \left(\frac{v_{\infty I}}{v_{\infty II}} \right)^2 = \frac{\hat{C}_{pI}}{\hat{C}_{pII}} \frac{(T_\infty - T_0)_I}{(T_\infty - T_0)_{II}} \quad (11.5-16)$$

Here $\nu = \mu/\rho$ is the kinematic viscosity and $\alpha = k/\rho \hat{C}_p$ is the thermal diffusivity.

The simplest way to satisfy Eq. 11.5-13 is to use the same fluid at the same approach pressure P_∞ and temperature T_∞ in the two systems. If that is done, Eq. 11.5-14 requires that the approach velocity in the small model (II) be four times that used in the full-scale system (I). If the fluid velocity is moderately large and the temperature differences small, the equality of Pr

and Re in the two systems provides a sufficient approximation to dynamic similarity. This is the limiting case of forced convection with negligible viscous dissipation.

If, however, the temperature differences $T_\infty - T_0$ are large, free-convection effects may be appreciable. Under these conditions, according to Eq. 11.5-15, temperature differences in the model must be 64 times those in the large system to ensure similarity.

From Eq. 11.5-16 it may be seen that such a ratio of temperature differences will not permit equality of the Brinkman number. For the latter a ratio of 16 would be needed. This conflict will not normally arise, however, as free-convection and viscous heating effects are seldom important simultaneously. Free-convection effects arise in low-velocity systems, whereas viscous heating occurs to a significant degree only when velocity gradients are very large.

EXAMPLE 11.5-2

Free Convection in a Horizontal Fluid Layer; Formation of Bénard Cells

We wish to investigate the free-convection motion in the system shown in Fig. 11.5-2. It consists of a thin layer of fluid between two horizontal parallel plates, the lower one at temperature T_0 , and the upper one at T_1 , with $T_1 < T_0$. In the absence of fluid motion, the conductive heat flux will be the same for all z , and a nearly uniform temperature gradient will be established at steady state. This temperature gradient will in turn cause a density gradient. If the density decreases with increasing z , the system will clearly be stable, but if it increases a potentially unstable situation occurs. It appears possible in this latter case that any chance disturbance may cause the more dense fluid to move downward and displace the lighter fluid beneath it. If the temperatures of the top and bottom surfaces are maintained constant, the result may be a continuing free-convection motion. This motion will, however, be opposed by viscous forces and may, therefore, occur only if the temperature difference tending to cause it is greater than some critical minimum value.

Determine by means of dimensional analysis the functional dependence of this fluid motion and the conditions under which it may be expected to arise.

SOLUTION

The system is described by Eqs. 11.5-1 to 3 along with the following boundary conditions:

$$\text{B.C. 1:} \quad \text{at } z = 0, \quad \mathbf{v} = 0 \quad T = T_0 \quad (11.5-17)$$

$$\text{B.C. 2:} \quad \text{at } z = h, \quad \mathbf{v} = 0 \quad T = T_1 \quad (11.5-18)$$

$$\text{B.C. 3:} \quad \text{at } r = R, \quad \mathbf{v} = 0 \quad \partial T / \partial r = 0 \quad (11.5-19)$$

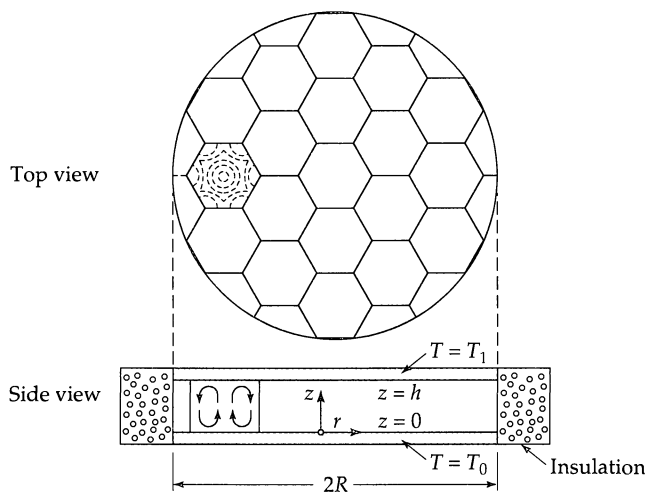


Fig. 11.5-2. Bénard cells formed in the region between two horizontal parallel plates, with the bottom plate at a higher temperature than the upper one. If the Rayleigh number exceeds a certain critical value, the system becomes unstable and hexagonal Bénard cells are produced.

We now restate the problem in dimensionless form, using $l_0 = h$. We use the dimensionless quantities listed under Case B in Table 11.5-1, and we select the reference temperature \bar{T} to be $\frac{1}{2}(T_0 + T_1)$, so that

$$\text{Continuity:} \quad (\check{\nabla} \cdot \check{\mathbf{v}}) = 0 \quad (11.5-20)$$

$$\text{Motion:} \quad \frac{D\check{\mathbf{v}}}{Dt} = -\check{\nabla}\check{P} + \text{Pr}\check{\nabla}^2\check{\mathbf{v}} - \text{GrPr}^2\left(\frac{\mathbf{g}}{g}\right)(\check{T} - \frac{1}{2}) \quad (11.5-21)$$

$$\text{Energy:} \quad \frac{D\check{T}}{Dt} = \check{\nabla}^2\check{T} \quad (11.5-22)$$

with dimensionless boundary conditions

$$\text{B.C. 1:} \quad \text{at } \check{z} = 0, \quad \check{\mathbf{v}} = 0 \quad \check{T} = 0 \quad (11.5-23)$$

$$\text{B.C. 2:} \quad \text{at } \check{z} = 1, \quad \check{\mathbf{v}} = 0 \quad \check{T} = 1 \quad (11.5-24)$$

$$\text{B.C. 3:} \quad \text{at } \check{r} = R/h, \quad \check{\mathbf{v}} = 0 \quad \partial\check{T}/\partial\check{r} = 0 \quad (11.5-25)$$

If the above dimensionless equations could be solved along with the dimensionless boundary conditions, we would find that the velocity and temperature profiles would depend only on Gr , Pr , and R/h . Furthermore, the larger the ratio R/h is, the less prominent its effect will be, and in the limit of extremely large horizontal plates, the system behavior will depend solely on Gr and Pr .

If we consider only steady creeping flows, then the term $D\check{\mathbf{v}}/Dt$ may be set equal to zero. Then we define a new dimensionless pressure difference as $\check{P} = \text{Pr}\check{P}$. With the left side of Eq. 11.5-21 equal to zero, we may now divide by Pr and the resulting equation contains only one dimensionless group, namely the Rayleigh number¹ $\text{Ra} = \text{GrPr} = \rho^2 g \beta (T_1 - T_0) l_0^3 C_p / \mu k$, whose value will determine the behavior of the system. This illustrates how one may reduce the number of dimensionless groups that are needed to describe a nonisothermal flow system.

The preceding analysis suggests that there may be a critical value of the Rayleigh number, and when this critical value is exceeded, fluid motion will occur. This suggestion has been amply confirmed experimentally^{2,3} and the critical Rayleigh number has been found to be 1700 ± 51 for $R/h >> 1$. For Rayleigh numbers below the critical value, the fluid is stationary, as evidenced by the observation that the heat flux across the liquid layer is the same as that predicted for conduction through a static fluid: $q_z = k(T_0 - T_1)/h$. As soon as the critical Rayleigh number is exceeded, however, the heat flux rises sharply, because of convective energy transport. An increase of the thermal conductivity reduces the Rayleigh number, thus moving Ra toward its stable range.

The assumption of creeping flow is a reasonable one for this system and is asymptotically correct when $\text{Pr} \rightarrow \infty$. It is also very convenient, inasmuch as it allows analytic solutions of the relevant equations of change.⁴ One such solution, which agrees well with experiment, is sketched qualitatively in Fig. 11.5-2. This flow pattern is cellular and hexagonal, with upflow at the center of each hexagon and downflow at the periphery. The units of this fascinating pattern are called *Bénard cells*.⁵ The analytic solution also confirms the existence of a critical Rayleigh number. For the boundary conditions of this problem and very large R/h it has been calculated⁴ to be 1708, which is in excellent agreement with the experimental result cited above.

¹ The Rayleigh number is named after Lord Rayleigh (J. W. Strutt), *Phil. Mag.*, (6) **32**, 529–546 (1916).

² P. L. Silveston, *Forsch. Ingenieur-Wesen*, **24**, 29–32, 59–69 (1958).

³ S. Chandrasekhar, *Hydrodynamic and Hydromagnetic Instability*, Oxford University Press (1961); T. E. Faber, *Fluid Dynamics for Physicists*, Cambridge University Press (1995), §8.7.

⁴ A. Pellew and R. V. Southwell, *Proc. Roy. Soc.*, **A176**, 312–343 (1940).

⁵ H. Bénard, *Revue générale des sciences pures et appliquées*, **11**, 1261–1271, 1309–1328 (1900); *Annales de Chimie et de Physique*, **23**, 62–144 (1901).

Similar behavior is observed for other boundary conditions. If the upper plate of Fig. 11.5-2 is replaced by a liquid–gas interface, so that the surface shear stress in the liquid is negligible, cellular convection is predicted theoretically³ for Rayleigh numbers above about 1101. A spectacular example of this type of instability occurs in the occasional spring “turnover” of water in northern lakes. If the lake water is cooled to near freezing during the winter, an adverse density gradient will occur as the surface waters warm toward 4°C, the temperature of maximum density for water.

In shallow liquid layers with free surfaces, instabilities can also arise from surface-tension gradients. The resulting surface stresses produce cellular convection superficially similar to that resulting from temperature gradients, and the two effects may be easily confused. Indeed, it appears that the steady flows first seen by Bénard, and ascribed to buoyancy effects, may actually have been produced by surface-tension gradients.⁶

EXAMPLE 11.5-3

Surface Temperature of an Electrical Heating Coil

An electrical heating coil of diameter D is being designed to keep a large tank of liquid above its freezing point. It is desired to predict the temperature that will be reached at the coil surface as a function of the heating rate Q and the tank surface temperature T_0 . This prediction is to be made on the basis of experiments with a smaller, geometrically similar apparatus filled with the same liquid.

Outline a suitable experimental procedure for making the desired prediction. Temperature dependence of the physical properties, other than the density, may be neglected. The entire heating coil surface may be assumed to be at a uniform temperature T_1 .

SOLUTION

This is a free-convection problem, and we use the column labeled A in Table 11.5-1 for the dimensionless groups. From the equations of change and the boundary conditions, we know that the dimensionless temperature $\check{T} = (T - T_0)/(T_1 - T_0)$ must be a function of the dimensionless coordinates and depend on the dimensionless groups Pr and Gr .

The total energy input rate through the coil surface is

$$Q = -k \int_S \frac{\partial T}{\partial r} \Big|_S dS \quad (11.5-26)$$

Here r is the coordinate measured outward from and normal to the coil surface, S is the surface area of the coil, and the temperature gradient is that of the fluid immediately adjacent to the coil surface. In dimensionless form this relation is

$$\frac{Q}{k(T_1 - T_0)D} = - \int_{\check{S}} \frac{\partial \check{T}}{\partial \check{r}} \Big|_{\check{S}} d\check{S} = \psi(\text{Pr}, \text{Gr}) \quad (11.5-27)$$

in which ψ is a function of $\text{Pr} = \hat{C}_p \mu / k$ and $\text{Gr} = \rho^2 g \beta (T_1 - T_0) D^3 / \mu^2$. Since the large-scale and small-scale systems are geometrically similar, the dimensionless function \check{S} describing the surface of integration will be the same for both systems and hence does not need to be included in the function ψ . Similarly, if we write the boundary conditions for temperature, velocity, and pressure at the coil and tank surfaces, we will obtain only size ratios that will be identical in the two systems.

We now note that the desired quantity $(T_1 - T_0)$ appears on both sides of Eq. 11.5-27. If we multiply both sides of the equation by the Grashof number, then $(T_1 - T_0)$ appears only on the right side:

$$\frac{Q \rho^2 g \beta D^2}{k \mu^2} = \text{Gr} \cdot \psi(\text{Pr}, \text{Gr}) \quad (11.5-28)$$

⁶ C. V. Sternling and L. E. Scriven, *AIChE Journal*, **5**, 514–523 (1959); L. E. Scriven and C. V. Sternling, *J. Fluid Mech.*, **19**, 321–340 (1964).

In principle, we may solve Eq. 11.5-28 for Gr and obtain an expression for $(T_1 - T_0)$. Since we are neglecting the temperature dependence of physical properties, we may consider the Prandtl number constant for the given fluid and write

$$T_1 - T_0 = \frac{\mu^2}{\rho^2 g \beta D^3} \cdot \phi \left(\frac{Q \rho^2 g \beta D^2}{k \mu^2} \right) \quad (11.5-29)$$

Here ϕ is an experimentally determinable function of the group $Q \rho^2 g \beta D^2 / k \mu^2$. We may then construct a plot of Eq. 11.5-29 from the experimental measurements of T_1 , T_0 , and D for the small-scale system, and the known physical properties of the fluid. This plot may then be used to predict the behavior of the large-scale system.

Since we have neglected the temperature dependence of the fluid properties, we may go even further. If we maintain the ratio of the Q values in the two systems equal to the inverse square of the ratio of the diameters, then the corresponding ratio of the values of $(T_1 - T_0)$ will be equal to the inverse cube of the ratio of the diameters.

QUESTIONS FOR DISCUSSION

1. Define energy, potential energy, kinetic energy, and internal energy. What common units are used for these?
2. How does one assign the physical meaning to the individual terms in Eqs. 11.1-7 and 11.2-1?
3. In getting Eq. 11.2-7 we used the relation $\bar{C}_p - \bar{C}_V = R$, which is valid for ideal gases. What is the corresponding equation for nonideal gases and liquids?
4. Summarize all the steps required in obtaining the equation of change for the temperature.
5. Compare and contrast forced convection and free convection, with regard to methods of problem solving, dimensional analysis, and occurrence in industrial and meteorological problems.
6. If a rocket nose cone were made of a porous material and a volatile liquid were forced slowly through the pores during reentry into the atmosphere, how would the cone surface temperature be affected and why?
7. What is Archimedes' principle, and how is it related to the term $\bar{\rho}g\beta(T - \bar{T})$ in Eq. 11.3-2?
8. Would you expect to see Bénard cells while heating a shallow pan of water on a stove?
9. When, if ever, can the equation of energy be completely and exactly solved without detailed knowledge of the velocity profiles of the system?
10. When, if ever, can the equation of motion be completely solved for a nonisothermal system without detailed knowledge of the temperature profiles of the system?

PROBLEMS

- 11A.1. Temperature in a friction bearing.** Calculate the maximum temperature in the friction bearing of Problem 3A.1, assuming the thermal conductivity of the lubricant to be $4.0 \times 10^{-4} \text{ cal/s} \cdot \text{cm} \cdot ^\circ\text{C}$, the metal temperature 200°C , and the rate of rotation 4000 rpm.

Answer: About 225°C

- 11A.2. Viscosity variation and velocity gradients in a nonisothermal film.** Water is falling down a vertical wall in a film 0.1 mm thick. The water temperature is 100°C at the free liquid surface and 80°C at the wall surface.

(a) Show that the maximum fractional deviation between viscosities predicted by Eqs. 11.4-17 and 18 occurs when $T = \sqrt{T_0 T_\delta}$.

(b) Calculate the maximum fractional deviation for the conditions given.

Answer: (b) 0.5%

11A.3. Transpiration cooling.

- (a) Calculate the temperature distribution between the two shells of Example 11.4-4 for radial mass flow rates of zero and 10^{-5} g/s for the following conditions:

$$\begin{aligned} R &= 500 \text{ microns} & T_R &= 300^\circ\text{C} \\ \kappa R &= 100 \text{ microns} & T_\kappa &= 100^\circ\text{C} \\ k &= 6.13 \times 10^{-5} \text{ cal/cm} \cdot \text{s} \cdot \text{C} \\ \hat{C}_p &= 0.25 \text{ cal/g} \cdot \text{C} \end{aligned}$$

- (b) Compare the rates of heat conduction to the surface at κR in the presence and absence of convection.

- 11A.4. Free-convection heat loss from a vertical surface.** A small heating panel consists essentially of a flat, vertical, rectangular surface 30 cm high and 50 cm wide. Estimate the total rate of heat loss from one side of this panel by free convection, if the panel surface is at 150°F , and the surrounding air is at 70°F and 1 atm. Use the value $C = 0.548$ of Lorenz in Eq. 11.4-51 and the value of C recommended by Whitaker, and compare the results of the two calculations.

Answer: 8.1 cal/sec by Lorenz expression

- 11A.5. Velocity, temperature, and pressure changes in a shock wave.** Air at 1 atm and 70°F is flowing at an upstream Mach number of 2 across a stationary shock wave. Calculate the following quantities, assuming that γ is constant at 1.4 and that $\hat{C}_p = 0.24 \text{ Btu/lb}_m \cdot \text{F}$:

- (a) The initial velocity of the air.
 (b) The velocity, temperature, and pressure downstream from the shock wave.
 (c) The changes of internal and kinetic energy across the shock wave.

Answer: (a) 2250 ft/s

(b) 844 ft/s; 888 R; 4.48 atm

(c) $\Delta\hat{U} = +61.4 \text{ Btu/lb}_m$; $\Delta\hat{K} = 86.9 \text{ Btu/lb}_m$

- 11A.6. Adiabatic frictionless compression of an ideal gas.** Calculate the temperature attained by compressing air, initially at 100°F and 1 atm, to 0.1 of its initial volume. It is assumed that $\gamma = 1.40$ and that the compression is frictionless and adiabatic. Discuss the result in relation to the operation of an internal combustion engine.

Answer: 950°F

- 11A.7. Effect of free convection on the insulating value of a horizontal air space.** Two large parallel horizontal metal plates are separated by a 2.5 cm air gap, with the air at an average temperature of 100°C . How much hotter may the lower plate be (than the upper plate) without causing the onset of the cellular free convection discussed in Example 11.5-2? How much may this temperature difference be increased if a very thin metal sheet is placed midway between the two plates?
Answers: Approximately 3 and 48°C , respectively.

11B.1. Adiabatic frictionless processes in an ideal gas.

- (a) Note that a gas that obeys the ideal gas law may deviate appreciably from $\tilde{C}_p = \text{constant}$. Hence, rework Example 11.4-6 using a molar heat capacity expression of the form

$$\tilde{C}_p = a + bT + cT^2 \quad (11B.1-1)$$

- (b) Determine the final pressure, p_2 , required if methane (CH_4) is to be heated from 300K and 1 atm to 800K by adiabatic frictionless compression. The recommended empirical constants¹

¹ O. A. Hougen, K. M. Watson, and R. A. Ragatz, *Chemical Process Principles*, Part I, 2nd edition, Wiley, New York (1958), p. 255. See also Part II, pp. 646–653, for a fuller discussion of isentropic process calculations.

for methane are: $a = 2.322 \text{ cal/g-mole} \cdot \text{K}$, $b = 38.04 \times 10^{-3} \text{ cal/g-mole} \cdot \text{K}^2$, and $c = -10.97 \times 10^{-6} \text{ cal/g-mole} \cdot \text{K}^3$.

Answers: (a) $pT^{-a/R} \exp[-(b/R)T - (c/2R)T^2] = \text{constant}$;

(b) 270 atm

11B.2. Viscous heating in laminar tube flow (asymptotic solutions).

(a) Show that for fully developed laminar Newtonian flow in a circular tube of radius R , the energy equation becomes

$$\rho \hat{C}_p v_{z,\max} \left[1 - \left(\frac{r}{R} \right)^2 \right] \frac{\partial T}{\partial z} = k \frac{1}{r} \frac{\partial}{\partial r} \left(r \frac{\partial T}{\partial r} \right) + \frac{4\mu v_{z,\max}^2}{R^2} \left(\frac{r}{R} \right)^2 \quad (11B.2-1)$$

if the viscous dissipation terms are not neglected. Here $v_{z,\max}$ is the maximum velocity in the tube. What restrictions have to be placed on any solutions of Eq. 11B.2-1?

(b) For the *isothermal wall* problem ($T = T_0$ at $r = R$ for $z > 0$ and at $z = 0$ for all r), find the asymptotic expression for $T(r)$ at large z . Do this by recognizing that $\partial T / \partial z$ will be zero at large z . Solve Eq. 11B.2-1 and obtain

$$T - T_0 = \frac{\mu v_{z,\max}^2}{4k} \left[1 - \left(\frac{r}{R} \right)^4 \right] \quad (11B.2-2)$$

(c) For the *adiabatic wall* problem ($q_r = 0$ at $r = R$ for all z) an asymptotic expression for large z may be found as follows: Omit the heat conduction term in Eq. 11B.2-1, and then average the remaining terms over the tube cross section, by multiplying by rdr and then integrating from $r = 0$ to $r = R$. Then integrate the resulting equation over z to get

$$\langle T \rangle - T_1 = (4\mu v_{z,\max} / \rho \hat{C}_p R^2) z \quad (11B.2-3)$$

in which T_1 is the inlet temperature at $z = 0$. Postulate now that an asymptotic temperature profile at large z is of the form

$$T - T_1 = (4\mu v_{z,\max} / \rho \hat{C}_p R^2) z + f(r) \quad (11B.2-4)$$

Substitute this into Eq. 11B.2-1 and integrate the resulting equation for $f(r)$ to obtain

$$T - T_1 = \frac{4\mu v_{z,\max}}{\rho \hat{C}_p R^2} z + \frac{\mu v_{z,\max}^2}{k} \left[\left(\frac{r}{R} \right)^2 - \frac{1}{2} \left(\frac{r}{R} \right)^4 \right] \quad (11B.2-5)$$

Keep in mind that the solutions in Eqs. 11B.2-2 and 5 are valid solutions only for large z . The complete solution for small z is discussed in Problem 11D.2.

11B.3. Velocity distribution in a nonisothermal film.

Show that Eq. 11.4-20 meets the following requirements:

(a) At $x = \delta$, $v_z = 0$.

(b) At $x = 0$, $\partial v_z / \partial x = 0$.

(c) $\lim_{\mu_0 \rightarrow \mu_0} v_z(x) = (\rho g \delta^2 \cos \beta / 2\mu_0) [1 - (x/\delta)^2]$

11B.4. Heat conduction in a spherical shell

(Fig. 11B.4). A spherical shell has inner and outer radii R_1 and R_2 . A hole is made in the shell at the north pole by cutting out the conical segment in the region $0 \leq \theta \leq \theta_1$. A similar hole is made at the south pole by removing the portion $(\pi - \theta_1) \leq \theta \leq \pi$. The surface $\theta = \theta_1$ is kept at temperature $T = T_1$, and the surface at $\theta = \pi - \theta_1$ is held at $T = T_2$. Find the steady-state temperature distribution, using the heat conduction equation.

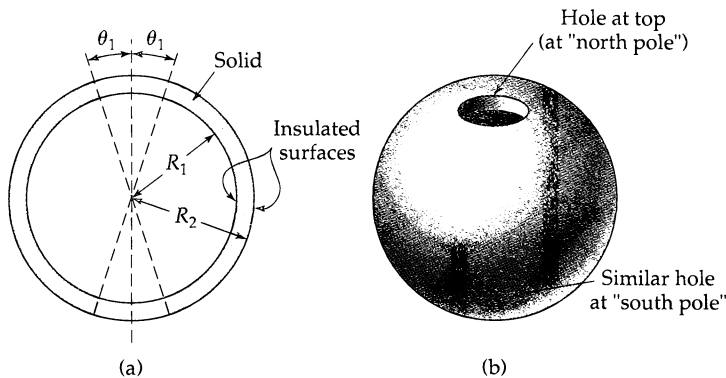


Fig. 11B.4. Heat conduction in a spherical shell: (a) cross section containing the z -axis; (b) view of the sphere from above.

11B.5. Axial heat conduction in a wire² (Fig. 11B.5). A wire of constant density ρ moves downward with uniform speed v into a liquid metal bath at temperature T_0 . It is desired to find the temperature profile $T(z)$. Assume that $T = T_\infty$ at $z = \infty$, and that resistance to radial heat conduction is negligible. Assume further that the wire temperature is $T = T_0$ at $z = 0$.

(a) First solve the problem for constant physical properties \hat{C}_p and k . Obtain

$$\Theta = \frac{T - T_\infty}{T_0 - T_\infty} = \exp\left(-\frac{\rho \hat{C}_p v z}{k}\right) \quad (11B.5-1)$$

(b) Next solve the problem when \hat{C}_p and k are known functions of the dimensionless temperature Θ : $k = k_\infty K(\Theta)$ and $\hat{C}_p = \hat{C}_{p\infty} L(\Theta)$. Obtain the temperature profile,

$$-\left(\frac{\rho \hat{C}_{p\infty} v z}{k_\infty}\right) = \int_1^\Theta \frac{K(\bar{\Theta}) d\bar{\Theta}}{\int_0^{\bar{\Theta}} L(\bar{\Theta}) d\bar{\Theta}} \quad (11B.5-2)$$

(c) Verify that the solution in (b) satisfies the differential equation from which it was derived.

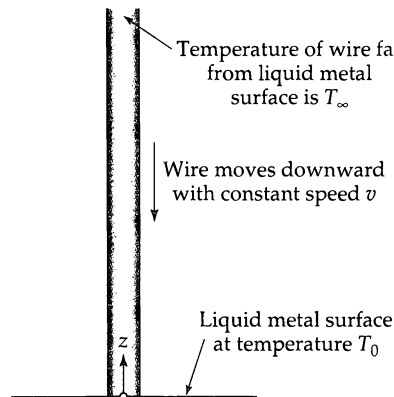


Fig. 11B.5. Wire moving into a liquid metal bath.

² Suggested by Prof. G. L. Borman, Mechanical Engineering Department, University of Wisconsin.

- 11B.6. Transpiration cooling in a planar system.** Two large flat porous horizontal plates are separated by a relatively small distance L . The upper plate at $y = L$ is at temperature T_L , and the lower one at $y = 0$ is to be maintained at a lower temperature T_0 . To reduce the amount of heat that must be removed from the lower plate, an ideal gas at T_0 is blown upward through both plates at a steady rate. Develop an expression for the temperature distribution and the amount of heat q_0 that must be removed from the cold plate per unit area as a function of the fluid properties and gas flow rate. Use the abbreviation $\phi = \rho \hat{C}_p v_y L / k$.

$$\text{Answer: } \frac{T - T_L}{T_0 - T_L} = \frac{e^{\phi y/L} - e^\phi}{1 - e^\phi}; q_0 = \frac{k(T_L - T_0)}{L} \left(\frac{\phi}{e^\phi - 1} \right)$$

- 11B.7. Reduction of evaporation losses by transpiration** (Fig. 11B.7). It is proposed to reduce the rate of evaporation of liquefied oxygen in small containers by taking advantage of transpiration. To do this, the liquid is to be stored in a spherical container surrounded by a spherical shell of a porous insulating material as shown in the figure. A thin space is to be left between the container and insulation, and the opening in the insulation is to be stoppered. In operation, the evaporating oxygen is to leave the container proper, move through the gas space, and then flow uniformly out through the porous insulation.

Calculate the rate of heat gain and evaporation loss from a tank 1 ft in diameter covered with a shell of insulation 6 in. thick under the following conditions with and without transpiration.

Temperature of liquid oxygen	-297°F
Temperature of outer surface of insulation	30°F
Effective thermal conductivity of insulation	0.02 Btu/hr · ft · F
Heat of evaporation of oxygen	91.7 Btu/lb
Average \hat{C}_p of O_2 flowing through insulation	0.22 Btu/lb · F

Neglect the thermal resistance of the liquid oxygen, container wall, and gas space, and neglect heat losses through the stopper. Assume the particles of insulation to be in local thermal equilibrium with the gas.

Answers: 82 Btu/hr without transpiration; 61 Btu/hr with transpiration

- 11B.8. Temperature distribution in an embedded sphere.** A sphere of radius R and thermal conductivity k_1 is embedded in an infinite solid of thermal conductivity k_0 . The center of the sphere is located at the origin of coordinates, and there is a constant temperature gradient A in the positive z direction far from the sphere. The temperature at the center of the sphere is T° .

The steady-state temperature distributions in the sphere T_1 and in the surrounding medium T_0 have been shown to be:³

$$T_1(r, \theta) - T^\circ = \left[\frac{3k_0}{k_1 + 2k_0} \right] Ar \cos \theta \quad r \leq R \quad (11B.8-1)$$

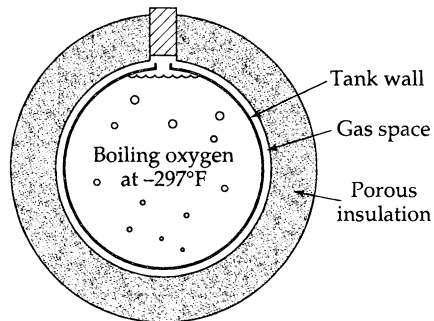


Fig. 11B.7. Use of transpiration to reduce the evaporation rate.

³ L. D. Landau and E. M. Lifshitz, *Fluid Mechanics*, 2nd edition, Pergamon Press, Oxford (1987), p. 199.

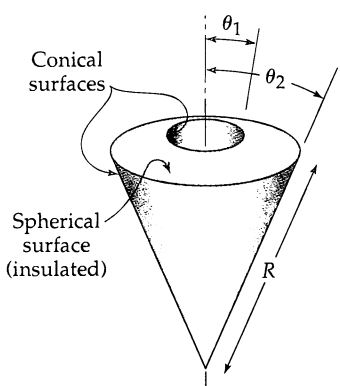


Fig. 11B.9. Body formed from the intersection of two cones and a sphere.

$$T_0(r, \theta) - T^\circ = \left[1 - \frac{k_1 - k_0}{k_1 + 2k_0} \left(\frac{R}{r} \right)^3 \right] Ar \cos \theta \quad r \geq R \quad (11B.8-2)$$

- (a) What are the partial differential equations that must be satisfied by Eqs. 11B.8-1 and 2?
 - (b) Write down the boundary conditions that apply at $r = R$.
 - (c) Show that T_1 and T_0 satisfy their respective partial differential equations in (a).
 - (d) Show that Eqs. 11B.8-1 and 2 satisfy the boundary conditions in (b).
- 11B.9. Heat flow in a solid bounded by two conical surfaces** (Fig. 11B.9). A solid object has the shape depicted in the figure. The conical surfaces $\theta_1 = \text{constant}$ and $\theta_2 = \text{constant}$ are held at temperatures T_1 and T_2 , respectively. The spherical surface at $r = R$ is insulated. For steady-state heat conduction, find
- (a) The partial differential equation that $T(\theta)$ must satisfy.
 - (b) The solution to the differential equation in (a) containing two constants of integration.
 - (c) Expressions for the constants of integration.
 - (d) The expression for the θ -component of the heat flux vector.
 - (e) The total heat flow (cal/sec) across the conical surface at $\theta = \theta_1$.
- Answer: (e) $Q = \frac{2\pi R k(T_1 - T_2)}{\ln\left(\frac{\tan \frac{1}{2}\theta_2}{\tan \frac{1}{2}\theta_1}\right)}$*
- 11B.10. Freezing of a spherical drop** (Fig. 11B.10). To evaluate the performance of an atomizing nozzle, it is proposed to atomize a nonvolatile liquid wax into a stream of cool air. The atomized wax particles are expected to solidify in the air, from which they may later be collected and

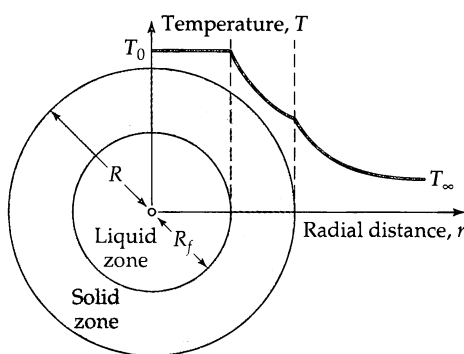


Fig. 11B.10. Temperature profile in the freezing of a spherical drop.

examined. The wax droplets leave the atomizer only slightly above their melting point. Estimate the time t_f required for a drop of radius R to freeze completely, if the drop is initially at its melting point T_0 and the surrounding air is at T_∞ . Heat is lost from the drop to the surrounding air according to Newton's law of cooling, with a constant heat-transfer coefficient h . Assume that there is no volume change in the solidification process. Solve the problem by using a quasi-steady-state method.

(a) First solve the steady-state heat conduction problem in the solid phase in the region between $r = R_f$ (the liquid-solid interface) and $r = R$ (the solid-air interface). Let k be the thermal conductivity of the solid phase. Then find the radial heat flow Q across the spherical surface at $r = R$.

(b) Then write an unsteady-state energy balance, by equating the heat liberation at $r = R_f(t)$ resulting from the freezing of the solid to the heat flow Q across the spherical surface at $r = R$. Integrate the resulting separable, first-order differential equation between the limits 0 and R , to obtain the time that it takes for the drop to solidify. Let $\Delta\hat{H}_f$ be the latent heat of freezing (per unit mass).

$$\text{Answers: (a)} Q = \frac{h \cdot 4\pi R^2 (T_0 - T_\infty)}{[1 - (hR/k)] + (hR^2/kR)}; \quad \text{(b)} t_f = \frac{\rho \Delta\hat{H}_f R}{h(T_0 - T_\infty)} \left[\frac{1}{3} + \frac{1}{6} \frac{hR}{k} \right]$$

- 11B.11. Temperature rise in a spherical catalyst pellet** (Fig. 11B.11). A catalyst pellet has a radius R and a thermal conductivity k (which may be assumed constant). Because of the chemical reaction occurring within the porous pellet, heat is generated at a rate of $S_c \text{ cal/cm}^3 \cdot \text{s}$. Heat is lost at the outer surface of the pellet to a gas stream at constant temperature T_g by convective heat transfer with heat transfer coefficient h . Find the steady-state temperature profile, assuming that S_c is constant throughout.

- (a) Set up the differential equation by making a shell energy balance.
- (b) Set up the differential equation by simplifying the appropriate form of the energy equation.
- (c) Integrate the differential equation to get the temperature profile. Sketch the function $T(r)$.
- (d) What is the limiting form of $T(r)$ when $h \rightarrow \infty$?
- (e) What is the maximum temperature in the system?
- (f) Where in the derivation would one modify the procedure to account for variable k and variable S_c ?

- 11B.12. Stability of an exothermic reaction system.³** Consider a porous slab of thickness $2B$, width W , and length L , with $B \ll W$ and $B \ll L$. Within the slab an exothermic reaction occurs, with a temperature-dependent rate of heat production $S_c(T) = S_{c0} \exp A(T - T_0)$.

- (a) Use the energy equation to obtain a differential equation for the temperature in the slab. Assume constant physical properties, and postulate a steady-state solution $T(x)$.
- (b) Write the differential equation and boundary conditions in terms of these dimensionless quantities: $\xi = x/B$, $\Theta = A(T - T_0)$, and $\lambda = S_{c0}AB^2/k$.
- (c) Integrate the differential equation (*hint:* first multiply by $2d\Theta/d\xi$) to obtain

$$\left(\frac{d\Theta}{d\xi} \right)^2 = 2\lambda(\exp \Theta_0 - \exp \Theta) \quad (11B.12-1)$$

in which Θ_0 is an auxiliary constant representing the value of Θ at $\xi = 0$.

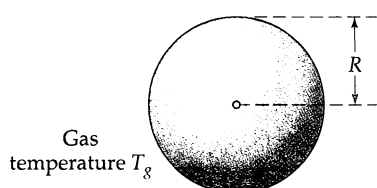


Fig. 11B.11. Sphere with internal heat generation.

- (d) Integrate the result of (c) and make use of the boundary conditions to obtain the relation between the slab thickness and midplane temperature

$$\exp(-\frac{1}{2}\Theta_0) \operatorname{arccosh}(\exp(\frac{1}{2}\Theta_0)) = \sqrt{\frac{1}{2}\lambda} \quad (11B.12-2)$$

- (e) Calculate λ at $\Theta_0 = 0.5, 1.0, 1.2, 1.4$, and 2.0 ; graph these results to find the maximum value of λ for steady-state conditions. If this value of λ is exceeded, the system will explode.

- 11B.13. Laminar annular flow with constant wall heat flux.** Repeat the development of §10.8 for flow in an annulus of inner and outer radii κR and R , respectively, starting with the equations of change. Heat is added to the fluid through the inner cylinder wall at a rate q_0 (heat per unit time), and the outer cylinder wall is thermally insulated.

- 11B.14. Unsteady-state heating of a sphere.** A sphere of radius R and thermal diffusivity α is initially at a uniform temperature T_0 . For $t > 0$ the sphere is immersed in a well-stirred water bath maintained at a temperature $T_1 > T_0$. The temperature within the sphere is then a function of the radial coordinate r and the time t . The solution to the heat conduction equation is given by:⁴

$$\frac{T - T_0}{T_1 - T_0} = 1 + 2 \sum_{n=1}^{\infty} (-1)^n \left(\frac{R}{n\pi r} \right) \sin \left(\frac{n\pi r}{R} \right) \exp(-\alpha n^2 \pi^2 t / R^2) \quad (11B.14-1)$$

It is desired to verify that this equation satisfies the differential equation, the boundary conditions, and the initial condition.

- (a) Write down the differential equation describing the problem.
- (b) Show that Eq. 11B.14-1 for $T(r, t)$ satisfies the differential equation in (a).
- (c) Show that the boundary condition at $r = R$ is satisfied.
- (d) Show that T is finite at $r = 0$.
- (e) To show that Eq. 11B.14-1 satisfies the initial condition, set $t = 0$ and $T = T_0$ and obtain the following:

$$-1 = 2 \sum_{n=1}^{\infty} (-1)^n \left(\frac{R}{n\pi r} \right) \sin \left(\frac{n\pi r}{R} \right) \quad (11B.14-2)$$

To show that this is true, multiply both sides by $\sin(m\pi r/R)$, where m is any integer from 1 to ∞ , and integrate from $r = 0$ to $r = R$. In the integration all terms with $m \neq n$ vanish on the right side. The term with $m = n$, when integrated, equals the integral on the left side.

- 11B.15. Dimensionless variables for free convection.**⁵ The dimensionless variables in Eqs. 11.4-39 to 43 can be obtained by simple arguments. The form of Θ is dictated by the boundary conditions and that of ζ is suggested by the geometry. The remaining dimensionless variables may be found as follows:

- (a) Set $\eta = y/y_0$, $\phi_z = v_z/v_{z0}$, and $\phi_y = v_y/v_{y0}$, the subscript-zero quantities being constants. Then the differential equations in Eqs. 11.4-33 to 35 become

$$\phi_y \frac{\partial \phi_y}{\partial \eta} + \left[\frac{v_{z0}y_0}{v_{y0}H} \right] \frac{\partial \phi_z}{\partial \zeta} = 0 \quad (11B.15-1)$$

$$\phi_y \frac{\partial \phi_y}{\partial \eta} + \left[\frac{v_{z0}y_0}{v_{y0}H} \right] \phi_z \frac{\partial \phi_z}{\partial \zeta} = \left[\frac{\mu}{\rho y_0 v_{y0}} \right] \frac{\partial^2 \phi_z}{\partial \eta^2} + \left[\frac{y_0 g \beta (T_0 - T_1)}{v_{y0} v_{z0}} \right] \Theta \quad (11B.15-2)$$

$$\phi_y \frac{\partial \Theta}{\partial \eta} + \left[\frac{v_{z0}y_0}{v_{y0}H} \right] \phi_z \frac{\partial \Theta}{\partial \zeta} = \left[\frac{k}{\rho \hat{C}_p y_0 v_{y0}} \right] \frac{\partial^2 \Theta}{\partial \eta^2} \quad (11B.15-3)$$

with the boundary conditions given in Eqs. 11.4-47 to 49.

⁴ H. S. Carslaw and J. C. Jaeger, *Conduction of Heat in Solids*, 2nd edition, Oxford University Press (1959), p. 233, Eq. (4).

⁵ The procedure used here is similar to that suggested by J. D. Hellums and S. W. Churchill, *AIChE Journal*, **10**, 110–114 (1964).

- (b) Choose appropriate values of v_{z0} , v_{y0} , and y_0 to convert the equations in (a) into Eqs. 11.4-44 to 46, and show that the definitions in Eqs. 11.4-41 to 43 follow directly.
- (c) Why is the choice of variables developed in (b) preferable to that obtained by setting the three dimensionless groups in Eqs. 11B.15-1 and 2 equal to unity?

- 11C.1. The speed of propagation of sound waves.** Sound waves are harmonic compression waves of very small amplitude traveling through a compressible fluid. The velocity of propagation of such waves may be estimated by assuming that the momentum flux tensor τ and the heat flux vector q are zero and that the velocity v of the fluid is small.⁶ The neglect of τ and q is equivalent to assuming that the entropy is constant following the motion of a given fluid element (see Problem 11D.1).

- (a) Use equilibrium thermodynamics to show that

$$\left(\frac{\partial p}{\partial \rho}\right)_S = \gamma \left(\frac{\partial p}{\partial \rho}\right)_T \quad (11C.1-1)$$

in which $\gamma = C_p/C_V$.

- (b) When sound is being propagated through a fluid, there are slight perturbations in the pressure, density, and velocity from the rest state: $p = p_0 + p'$, $\rho = \rho_0 + \rho'$, and $v = v_0 + v'$, the subscript-zero quantities being constants associated with the rest state (with v_0 being zero), and the primed quantities being very small. Show that when these quantities are substituted into the equation of continuity and the equation of motion (with the τ and g terms omitted) and products of the small primed quantities are omitted, we get

$$\text{Equation of continuity} \quad \frac{\partial \rho}{\partial t} = -\rho_0 (\nabla \cdot v) \quad (11C.1-2)$$

$$\text{Equation of motion} \quad \rho_0 \frac{\partial v}{\partial t} = -\nabla p \quad (11C.1-3)$$

- (c) Next use the result in (a) to rewrite the equation of motion as

$$\rho_0 \frac{\partial v}{\partial t} = -v_s^2 \nabla \rho \quad (11C.1-4)$$

in which $v_s^2 = \gamma(\partial p / \partial \rho)_T$.

- (d) Show how Eqs. 11C.1-2 and 4 can be combined to give

$$\frac{\partial^2 \rho}{\partial t^2} = v_s^2 \nabla^2 \rho \quad (11C.1-5)$$

- (e) Show that a solution of Eq. 11C.1-5 is

$$\rho = \rho_0 \left[1 + A \sin \left(\frac{2\pi}{\lambda} (z - v_s t) \right) \right] \quad (11C.1-6)$$

This solution represents a harmonic wave of wavelength λ and amplitude $\rho_0 A$ traveling in the z direction at a speed v_s . More general solutions may be constructed by a superposition of waves of different wavelengths and directions.

- 11C.2. Free convection in a slot.** A fluid of constant viscosity, with density given by Eq. 11.3-1, is confined in a rectangular slot. The slot has vertical walls at $x = \pm B$, $y = \pm W$, and a top and bottom at $z = \pm H$, with $H \gg W \gg B$. The walls are nonisothermal, with temperature distribution $T_w = T + Ay$, so that the fluid circulates by free convection. The velocity profiles are to be predicted, for steady laminar flow conditions and small deviations from the mean density $\bar{\rho}$.

⁶ See L. Landau and E. M. Lifshitz, *Fluid Mechanics*, 2nd edition, Pergamon, Oxford (1987), Chapter VIII; R. J. Silbey and R. A. Alberty, *Physical Chemistry*, 3rd edition, Wiley, New York (2001), §17.4.

- (a) Simplify the equations of continuity, motion, and energy according to the postulates: $v = \delta_z v_z(x, y)$, $\partial^2 v_z / \partial y^2 \ll \partial^2 v_z / \partial x^2$, and $T = T(y)$. These postulates are reasonable for slow flow, except near the edges $y = \pm W$ and $z = \pm H$.
- (b) List the boundary conditions to be used with the problem as simplified in (a).
- (c) Solve for the temperature, pressure, and velocity profiles.
- (d) When making diffusion measurements in closed chambers, free convection can be a serious source of error, and temperature gradients must be avoided. By way of illustration, compute the maximum tolerable temperature gradient, A , for an experiment with water at 20°C in a chamber with $B = 0.1$ mm, $W = 2.0$ mm, and $H = 2$ cm, if the maximum permissible convective movement is 0.1% of H in a one-hour experiment.

Answers: (c) $v_z(x, y) = \frac{\bar{\rho}g\beta A}{2\mu} (x^2 - B^2)y$; (d) 2.7×10^{-3} K/cm

- 11C.3. Tangential annular flow of a highly viscous liquid.** Show that Eq. 11.4-13 for flow in an annular region reduces to Eq. 10.4-9 for plane slit flow in the limit as κ approaches unity. Comparisons of this kind are often useful for checking results.

The right side of Eq. 11.4-13 is indeterminate at $\kappa = 1$, but its limit as $\kappa \rightarrow 1$ can be obtained by expanding in powers of $\varepsilon = 1 - \kappa$. To do this, set $\kappa = 1 - \varepsilon$ and $\xi = 1 - \varepsilon[1 - (x/b)]$; then the range $\kappa \leq \xi \leq 1$ in Problem 11.4-2 corresponds to the range $0 \leq x \leq b$ in §10.4. After making the substitutions, expand the right side of Eq. 11.4-13 in powers of ε (neglecting terms beyond ε^2) and show that Eq. 10.4-9 is obtained.

- 11C.4. Heat conduction with variable thermal conductivity.**

(a) For steady-state heat conduction in solids, Eq. 11.2-5 becomes $(\nabla \cdot \mathbf{q}) = 0$, and insertion of Fourier's law gives $(\nabla \cdot k\nabla T) = 0$. Show that the function $F = \int k dT + \text{const.}$ satisfies the Laplace equation $\nabla^2 F = 0$, provided that k depends only on T .

(b) Use the result in (a) to solve Problem 10B.12 (part a), using an arbitrary function $k(T)$.

- 11C.5. Effective thermal conductivity of a solid with spherical inclusions** (Fig. 11C.5). Derive Eq. 9.6-1 for the effective thermal conductivity of a two-phase system by starting with Eqs. 11B.8-1 and 2. We construct two systems both contained within a spherical region of radius R' : (a) the "true" system, a medium with thermal conductivity k_0 , in which there are embedded n tiny spheres of thermal conductivity k_1 and radius R ; and (b) an "equivalent" system, which is a continuum, with an effective thermal conductivity k_{eff} . Both of these systems are placed in a temperature gradient A , and both are surrounded by a medium with thermal conductivity k_0 .

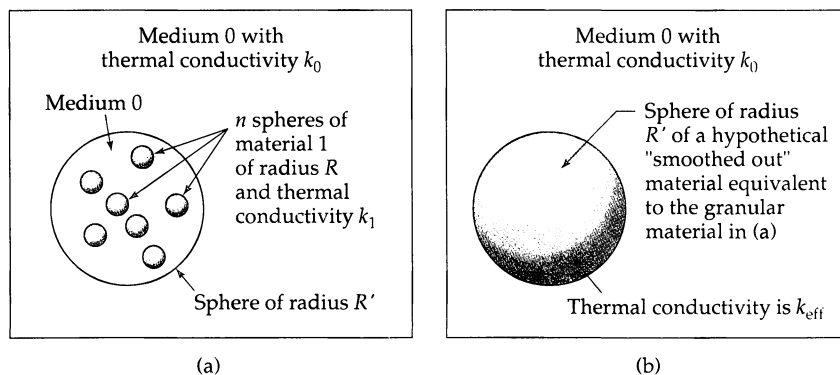


Fig. 11C.5. Thought experiment used by Maxwell to get the thermal conductivity of a composite solid: (a) the "true" discrete system, and (b) the "equivalent" continuum system.

- (a) For the “true” system we know that at a large distance L from the system (i.e., $L \gg R'$), the temperature field will be given by a slight modification of Eq. 11B.8-2, provided that the tiny occluded spheres are very “dilute” in the true system:

$$T_0(r, \theta) - T^\circ = \left[1 - n \frac{k_1 - k_0}{k_1 + 2k_0} \left(\frac{R'}{r} \right)^3 \right] Ar \cos \theta \quad (11C.5-1)$$

Explain carefully how this result is obtained.

- (b) Next, for the “equivalent system,” we can write from Eq. 11B.8-2

$$T_0(r, \theta) - T^\circ = \left[1 - \frac{k_{\text{eff}} - k_0}{k_{\text{eff}} + 2k_0} \left(\frac{R'}{r} \right)^3 \right] Ar \cos \theta \quad (11C.5-2)$$

- (c) Next derive the relation $nR^3 = \phi R'^3$, in which ϕ is the volume fraction of the occlusions in the “true system.”

- (d) Equate the right sides of Eqs. 11C.5-1 and 2 to get Maxwell’s equation⁷ in Eq. 9.6-1.

- 11C.6. Interfacial boundary conditions.** Consider a nonisothermal interfacial surface $S(t)$ between pure phases I and II in a nonisothermal system. The phases may consist of two immiscible fluids (so that no material crosses $S(t)$), or two different pure phases of a single substance (between which mass may be interchanged by condensation, evaporation, freezing, or melting). Let \mathbf{n}^I be the local unit normal to $S(t)$ directed into phase I. A superscript I or II will be used for values along S in each phase, and a superscript s for values in the interface itself. The usual interfacial boundary conditions on tangential velocity v_t and temperature T on S are

$$v_t^I = v_t^{II} \quad (\text{no slip}) \quad (11C.6-1)$$

$$T^I = T^{II} \quad (\text{continuity of temperature}) \quad (11C.6-2)$$

In addition, the following simplified conservation equations are suggested⁸ for surfactant-free interfaces:

Interfacial mass balance

$$(\mathbf{n}^I \cdot \{\rho^I(\mathbf{v}^I - \mathbf{v}^s) - \rho^{II}(\mathbf{v}^{II} - \mathbf{v}^s)\}) = 0 \quad (11C.6-3)$$

Interfacial momentum balance

$$\mathbf{n}^I \left[(p^I - p^{II}) + (\rho^I v^{I2} - \rho^{II} v^{II2}) + \sigma \left(\frac{1}{R_1} + \frac{1}{R_2} \right) \right] + [\mathbf{n}^I \cdot \{\boldsymbol{\tau}^I - \boldsymbol{\tau}^{II}\}] = -\nabla^s \sigma \quad (11C.6-4)$$

Interfacial internal energy balance

$$(\mathbf{n}^I \cdot \rho^I(\mathbf{v}^I - \mathbf{v}^s))[(\hat{H}^I - \hat{H}^{II}) + \frac{1}{2}(v^{I2} - v^{II2})] + (\mathbf{n}^I \cdot \{\mathbf{q}^I - \mathbf{q}^{II}\}) = \sigma(\nabla^s \cdot \mathbf{v}^s) \quad (11C.6-5)$$

The momentum balance of Eq. 3C.5-1 has been extended here to include the surface gradient $\nabla^s \sigma$ of the interfacial tension; the resulting tangential force gives rise to a variety of interfacial flow phenomena, known as *Marangoni effects*.^{9,10} Equation 11C.6-5 is obtained in the manner of §11.2, from total and mechanical energy balances on S , neglecting interfacial excess energy \hat{U}^s , heat flux \mathbf{q}^s , and viscous dissipation ($\boldsymbol{\tau}^s : \nabla^s \mathbf{v}^s$); fuller results are given elsewhere.⁸

⁷ J. C. Maxwell, *A Treatise on Electricity and Magnetism*, Vol. 1, Oxford University Press (1891, reprinted 1998), §314.

⁸ J. C. Slattery, *Advanced Transport Phenomena*, Cambridge University Press (1999), pp. 58, 435; more complete conditions are given in Ref. 8.

⁹ C. G. M. Marangoni, *Ann. Phys. (Poggendorff)*, **3**, 337–354 (1871); C. V. Sternling and L. E. Scriven, *AIChE Journal*, **5**, 514–523 (1959).

¹⁰ D. A. Edwards, H. Brenner, and D. T. Wasan, *Interfacial Transport Processes and Rheology*, Butterworth-Heinemann, Stoneham, Mass. (1991).

- (a) Verify the dimensional consistency of each interfacial balance equation.
- (b) Under what conditions are \mathbf{v}^l and \mathbf{v}^u equal?
- (c) Show how the balance equations simplify when phases I and II are two pure immiscible liquids.
- (d) Show how the balance equations simplify when one phase is a solid.

11C.7. Effect of surface-tension gradients on a falling film.

- (a) Repeat the determination of the shear-stress and velocity distributions of Example 2.1-1 in the presence of a small temperature gradient dT/dz in the direction of flow. Assume that this temperature gradient produces a constant surface-tension gradient $d\sigma/dz = A$ but has no other effect on system physical properties. Note that this surface-tension gradient will produce a shear stress at the free surface of the film (see Problem 11C.6) and, hence, will require a nonzero velocity gradient there. Once again, postulate a stable, nonrippling, laminar film.
- (b) Calculate the film thickness as a function of the net downward flow rate and discuss the physical significance of the result.

$$\text{Answer: (a)} \tau_{xz} = \rho g x \cos \beta + A; v_z = \frac{\rho g \delta^2 \cos \beta}{2\mu} \left[1 - \left(\frac{x}{\delta} \right)^2 \right] + \frac{A\delta}{\mu} \left(1 - \frac{x}{\delta} \right)$$

11D.1. Equation of change for entropy. This problem is an introduction to the thermodynamics of irreversible processes. A treatment of multicomponent mixtures is given in §§24.1 and 2.

- (a) Write an entropy balance for the fixed volume element $\Delta x \Delta y \Delta z$. Let \mathbf{s} be the *entropy flux vector*, measured with respect to the fluid velocity vector \mathbf{v} . Further, let the *rate of entropy production* per unit volume be designated by g_s . Show that when the volume element $\Delta x \Delta y \Delta z$ is allowed to become vanishingly small, one finally obtains an *equation of change for entropy* in either of the following two forms:¹¹

$$\frac{\partial}{\partial t} \rho \hat{S} = -(\nabla \cdot \rho \hat{S} \mathbf{v}) - (\nabla \cdot \mathbf{s}) + g_s \quad (11D.1-1)$$

$$\rho \frac{D\hat{S}}{Dt} = -(\nabla \cdot \mathbf{s}) + g_s \quad (11D.1-2)$$

in which \hat{S} is the entropy per unit mass.

- (b) If one assumes that the thermodynamic quantities can be defined locally in a nonequilibrium situation, then \hat{U} can be related to \hat{S} and \hat{V} according to the thermodynamic relation $d\hat{U} = T d\hat{S} - p d\hat{V}$. Combine this relation with Eq. 11.2-2 to get

$$\rho \frac{D\hat{S}}{Dt} = -\frac{1}{T} (\nabla \cdot \mathbf{q}) - \frac{1}{T} (\boldsymbol{\tau} : \nabla \mathbf{v}) \quad (11D.1-3)$$

- (c) The local entropy flux is equal to the local energy flux divided by the local temperature¹²⁻¹⁵; that is, $\mathbf{s} = \mathbf{q}/T$. Once this relation between \mathbf{s} and \mathbf{q} is recognized, we can compare Eqs. 11D.1-2 and 3 to get the following expression for the rate of entropy production per unit volume:

$$g_s = -\frac{1}{T^2} (\mathbf{q} \cdot \nabla T) - \frac{1}{T} (\boldsymbol{\tau} : \nabla \mathbf{v}) \quad (11D.1-4)$$

¹¹ G. A. J. Jaumann, *Sitzungsber. der Math.-Naturwiss. Klasse der Kaiserlichen Akad. der Wissenschaften (Wien)*, **102**, Abt. IIa, 385–530 (1911).

¹² Carl Henry Eckart (1902–1973), vice-chancellor of the University of California at San Diego (1965–1969), made fundamental contributions to quantum mechanics, geophysical hydrodynamics, and the thermodynamics of irreversible processes; his key contributions to transport phenomena are in C. H. Eckart, *Phys. Rev.*, **58**, 267–268, 269–275 (1940).

¹³ C. F. Curtiss and J. O. Hirschfelder, *J. Chem. Phys.*, **18**, 171–173 (1950).

¹⁴ J. G. Kirkwood and B. L. Crawford, Jr., *J. Phys. Chem.* **56**, 1048–1051 (1952).

¹⁵ S. R. de Groot and P. Mazur, *Non-Equilibrium Thermodynamics*, North-Holland, Amsterdam (1962).

The first term on the right side is the rate of entropy production associated with heat transport, and the second is the rate of entropy production resulting from momentum transport. Equation 11D.1-4 is the starting point for the thermodynamic study of the irreversible processes in a pure fluid.

(d) What conclusions can be drawn when Newton's law of viscosity and Fourier's law of heat conduction are inserted into Eq. 11D.1-4?

11D.2. Viscous heating in laminar tube flow.

(a) Continue the analysis begun in Problem 11B.2—namely, that of finding the temperature profiles in a Newtonian fluid flowing in a circular tube at a speed sufficiently high that viscous heating effects are important. Assume that the velocity profile at the inlet ($z = 0$) is fully developed, and that the inlet temperature is uniform over the cross section. Assume all physical properties to be constant.

(b) Repeat the analysis for a power law non-Newtonian viscosity.¹⁶

11D.3. Derivation of the energy equation using integral theorems. In §11.1 the energy equation is derived by accounting for the energy changes occurring in a small rectangular volume element $\Delta x \Delta y \Delta z$.

(a) Repeat the derivation using an arbitrary volume element V with a fixed boundary S by following the procedure outlined in Problem 3D.1. Begin by writing the law of conservation of energy as

$$\frac{d}{dt} \int_V (\rho \hat{U} + \frac{1}{2} \rho v^2) dV = - \int_S (\mathbf{n} \cdot \mathbf{e}) dS + \int_V (\mathbf{v} \cdot \mathbf{g}) dV \quad (11D.3-1)$$

Then use the Gauss divergence theorem to convert the surface integral into a volume integral, and obtain Eq. 11.1-6.

(b) Do the analogous derivation for a moving “blob” of fluid.

¹⁶ R. B. Bird, *Soc. Plastics Engrs. Journal*, **11**, 35–40 (1955).

Temperature Distributions with More Than One Independent Variable

- §12.1 Unsteady heat conduction in solids
- §12.2^O Steady heat conduction in laminar, incompressible flow
- §12.3^O Steady potential flow of heat in solids
- §12.4^O Boundary layer theory for nonisothermal flow

In Chapter 10 we saw how simple heat flow problems can be solved by means of shell energy balances. In Chapter 11 we developed the energy equation for flow systems, which describes the heat transport processes in more complex situations. To illustrate the usefulness of the energy equation, we gave in §11.4 a series of examples, most of which required no knowledge of solving partial differential equations.

In this chapter we turn to several classes of heat transport problems that involve more than one dependent variable, either two spatial variables, or one space variable and the time variable. The types of problems and the mathematical methods parallel those given in Chapter 4.

§12.1 UNSTEADY HEAT CONDUCTION IN SOLIDS

For solids, the energy equation of Eq. 11.2-5, when combined with Fourier's law of heat conduction, becomes

$$\rho \hat{C}_p \frac{\partial T}{\partial t} = (\nabla \cdot k \nabla T) \quad (12.1-1)$$

If the thermal conductivity can be assumed to be independent of the temperature and position, then Eq. 12.1-1 becomes

$$\frac{\partial T}{\partial t} = \alpha \nabla^2 T \quad (12.1-2)$$

in which $\alpha = k / \rho \hat{C}_p$ is the thermal diffusivity of the solid. Many solutions to this equation have been worked out. The treatise of Carslaw and Jaeger¹ contains a thorough dis-

¹ H. S. Carslaw and J. C. Jaeger, *Conduction of Heat in Solids*, 2nd edition, Oxford University Press (1959).

cussion of solution methods as well as a very comprehensive tabulation of solutions for a wide variety of boundary and initial conditions. Many frequently encountered heat conduction problems may be solved just by looking up the solution in this impressive reference work.

In this section we illustrate four important methods for solving unsteady heat conduction problems: the method of combination of variables, the method of separation of variables, the method of sinusoidal response, and the method of Laplace transform. The first three of these were also used in §4.1.

EXAMPLE 12.1-1

Heating a Semi-Infinite Slab

A solid material occupying the space from $y = 0$ to $y = \infty$ is initially at temperature T_0 . At time $t = 0$, the surface at $y = 0$ is suddenly raised to temperature T_1 and maintained at that temperature for $t > 0$. Find the time-dependent temperature profiles $T(y, t)$.

SOLUTION

For this problem, Eq. 12.1-2 becomes

$$\frac{\partial \Theta}{\partial t} = \alpha \frac{\partial^2 \Theta}{\partial y^2} \quad (12.1-3)$$

Here a dimensionless temperature difference $\Theta = (T - T_0)/(T_1 - T_0)$ has been introduced. The initial and boundary conditions are then

$$\text{I.C.:} \quad \text{at } t \leq 0, \quad \Theta = 0 \quad \text{for all } y \quad (12.1-4)$$

$$\text{B.C. 1:} \quad \text{at } y = 0, \quad \Theta = 1 \quad \text{for all } t > 0 \quad (12.1-5)$$

$$\text{B.C. 2:} \quad \text{at } y = \infty, \quad \Theta = 0 \quad \text{for all } t > 0 \quad (12.1-6)$$

This problem is mathematically analogous to that formulated in Eqs. 4.1-1 to 4. Hence the solution in Eq. 4.1-15 can be taken over directly by appropriate changes in notation:

$$\Theta = 1 - \frac{2}{\sqrt{\pi}} \int_0^{y/\sqrt{4\alpha t}} \exp(-\eta^2) d\eta \quad (12.1-7)$$

or

$$\frac{T - T_0}{T_1 - T_0} = 1 - \operatorname{erf} \frac{y}{\sqrt{4\alpha t}} \quad (12.1-8)$$

The solution shown in Fig. 4.1-2 describes the temperature profiles when the ordinate is labeled $(T - T_0)/(T_1 - T_0)$ and the abscissa $y/\sqrt{4\alpha t}$.

Since the error function reaches a value of 0.99 when the argument is about 2, the *thermal penetration thickness* δ_T is

$$\delta_T = 4\sqrt{\alpha t} \quad (12.1-9)$$

That is, for distances $y > \delta_T$, the temperature has changed by less than 1% of the difference $T_1 - T_0$. If it is necessary to calculate the temperature in a slab of finite thickness, the solution in Eq. 12.1-8 will be a good approximation when δ_T is small with respect to the slab thickness. However, when δ_T is of the order of magnitude of the slab thickness or greater, then the series solution of Example 12.1-2 has to be used.

The wall heat flux can be calculated from Eq. 12.1-8 as follows:

$$q_y|_{y=0} = -k \frac{\partial T}{\partial y} \Big|_{y=0} = \frac{k}{\sqrt{\pi \alpha t}} (T_1 - T_0) \quad (12.1-10)$$

Hence, the wall heat flux varies as $t^{-1/2}$, whereas the penetration thickness varies as $t^{1/2}$.

EXAMPLE 12.1-2 A solid slab occupying the space between $y = -b$ and $y = +b$ is initially at temperature T_0 . At time $t = 0$ the surfaces at $y = \pm b$ are suddenly raised to T_1 and maintained there. Find $T(y, t)$.

Heating of a Finite Slab

SOLUTION

For this problem we define the following dimensionless variables:

$$\text{Dimensionless temperature} \quad \Theta = \frac{T_1 - T}{T_1 - T_0} \quad (12.1-11)$$

$$\text{Dimensionless coordinate} \quad \eta = \frac{y}{b} \quad (12.1-12)$$

$$\text{Dimensionless time} \quad \tau = \frac{\alpha t}{b^2} \quad (12.1-13)$$

With these dimensionless variables, the differential equation and boundary conditions are

$$\frac{\partial \Theta}{\partial \tau} = \frac{\partial^2 \Theta}{\partial \eta^2} \quad (12.1-14)$$

$$\text{I.C.:} \quad \text{at } \tau = 0, \quad \Theta = 1 \quad (12.1-15)$$

$$\text{B.C. 1 and 2:} \quad \text{at } \eta = \pm 1, \quad \Theta = 0 \quad \text{for } \tau > 0 \quad (12.1-16)$$

Note that no parameters appear when the problem is restated thus.

We can solve this problem by the method of separation of variables. We start by postulating that a solution of the following product form can be obtained:

$$\Theta(\eta, \tau) = f(\eta)g(\tau) \quad (12.1-17)$$

Substitution of this trial function into Eq. 12.1-14 and subsequent division by the product $f(\eta)g(\tau)$ gives

$$\frac{1}{g} \frac{dg}{d\tau} = \frac{1}{f} \frac{d^2f}{d\eta^2} \quad (12.1-18)$$

The left side is a function of τ alone, and the right side is a function of η alone. This can be true only if both sides equal a constant, which we call $-c^2$. If the constant is called $+c^2$, $+c$, or $-c$, the same final result is obtained, but the solution is a bit messier. Equation 12.1-18 can then be separated into two ordinary differential equations

$$\frac{dg}{d\tau} = -c^2 g \quad (12.1-19)$$

$$\frac{d^2f}{d\eta^2} = -c^2 f \quad (12.1-20)$$

These equations are of the form of Eq. C.1-1 and 3 and may be integrated to give

$$g = A \exp(-c^2 \tau) \quad (12.1-21)$$

$$f = B \sin c\eta + C \cos c\eta \quad (12.1-22)$$

in which A , B , and C are constants of integration.

Because of the symmetry about the xz -plane, we must have $\Theta(\eta, \tau) = \Theta(-\eta, \tau)$, and thus $f(\eta) = f(-\eta)$. Since the sine function does not have this kind of behavior, we have to require that B be zero. Use of either of the two boundary conditions gives

$$C \cos c = 0 \quad (12.1-23)$$

Clearly C cannot be zero, because that choice leads to a physically inadmissible solution. However, the equality can be satisfied by many different choices of c , which we call c_n :

$$c_n = (n + \frac{1}{2})\pi \quad n = 0, \pm 1, \pm 2, \pm 3, \dots, \pm \infty \quad (12.1-24)$$

Hence Eq. 12.1-14 can be satisfied by

$$\Theta_n = A_n C_n \exp[(n + \frac{1}{2})^2 \pi^2 \tau] \cos(n + \frac{1}{2})\pi\eta \quad (12.1-25)$$

The subscripts n remind us that A and C may be different for each value of n . Because of the linearity of the differential equation, we may now superpose all the solutions of the form of Eq. 12.1-25. In doing this we note that the exponentials and cosines for n have the same values as those for $-(n + 1)$, so that the terms with negative indices combine with those with positive indices. The superposition then gives

$$\Theta = \sum_{n=0}^{\infty} D_n \exp[-(n + \frac{1}{2})^2 \pi^2 \tau] \cos(n + \frac{1}{2})\pi\eta \quad (12.1-26)$$

in which $D_n = A_n C_n + A_{-(n+1)} C_{-(n+1)}$.

The D_n are now determined by using the initial condition, which gives

$$1 = \sum_{n=0}^{\infty} D_n \cos(n + \frac{1}{2})\pi\eta \quad (12.1-27)$$

Multiplication by $\cos(m + \frac{1}{2})\pi\eta$ and integration from $\eta = -1$ to $\eta = +1$ gives

$$\int_{-1}^{+1} \cos(m + \frac{1}{2})\pi\eta d\eta = \sum_{n=0}^{\infty} D_n \int_{-1}^{+1} \cos(m + \frac{1}{2})\pi\eta \cos(n + \frac{1}{2})\pi\eta d\eta \quad (12.1-28)$$

When the integrations are performed, all integrals on the right side are identically zero, except for the term in which $n = m$. Hence we get

$$\frac{\sin(m + \frac{1}{2})\pi\eta}{(m + \frac{1}{2})\pi} \Big|_{\eta=-1}^{\eta=+1} = D_m \frac{\frac{1}{2}(m + \frac{1}{2})\pi\eta + \frac{1}{4} \sin 2(m + \frac{1}{2})\pi\eta}{(m + \frac{1}{2})\pi} \Big|_{\eta=-1}^{\eta=+1} \quad (12.1-29)$$

After inserting the limits, we may solve for D_m to get

$$D_m = \frac{2(-1)^m}{(m + \frac{1}{2})\pi} \quad (12.1-30)$$

Substitution of this expression into Eq. 12.1-26 gives the temperature profiles, which we now rewrite in terms of the original variables²

$$\frac{T_1 - T}{T_1 - T_0} = 2 \sum_{n=0}^{\infty} \frac{(-1)^n}{(n + \frac{1}{2})\pi} \exp[-(n + \frac{1}{2})^2 \pi^2 \alpha t / b^2] \cos(n + \frac{1}{2})\pi y / b \quad (12.1-31)$$

The solutions to many unsteady-state heat conduction problems come out as infinite series, such as that just obtained here. These series converge rapidly for large values² of the dimensionless time, $\alpha t / b^2$. For very short times the convergence is very slow, and in the limit as $\alpha t / b^2$ approaches zero, the solution in Eq. 12.1-31 may be shown to approach that given in Eq. 12.1-8 (see Problem 12D.1). Although Eq. 12.1-31 is unwieldy for some practical calculations, a graphical presentation, such as that in Fig. 12.1-1, is easy to use (see Problem 12A.3). From the figure it is clear that when the dimensionless time $\tau = \alpha t / b^2$ is 0.1, the heat has "penetrated" measurably to the center plane of the slab, and that at $\tau = 1.0$ the heating is 90% complete at the center plane.

Results analogous to Fig. 12.1-1 are given for infinite cylinders and for spheres in Figs. 12.1-2 and 3. These charts can also be used to build up the solutions for the analogous heat conduction problems in rectangular parallelepipeds and cylinders of finite length (see Prob. 12C.1).

² H. S. Carslaw and J. C. Jaeger, *Conduction of Heat in Solids*, 2nd edition, Oxford University Press (1959), p. 97, Eq. (8); the alternate solution in Eq. (9) converges rapidly for small times.

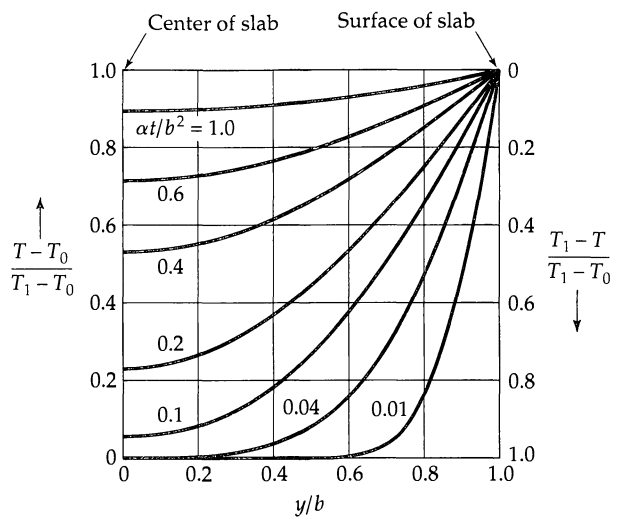


Fig. 12.1-1. Temperature profiles for unsteady-state heat conduction in a slab of finite thickness $2b$. The initial temperature of the slab is T_0 , and T_1 is the temperature imposed at the slab surfaces for time $t > 0$.
[H. S. Carslaw and J. C. Jaeger, *Conduction of Heat in Solids*, 2nd edition, Oxford University Press (1959), p. 101.]

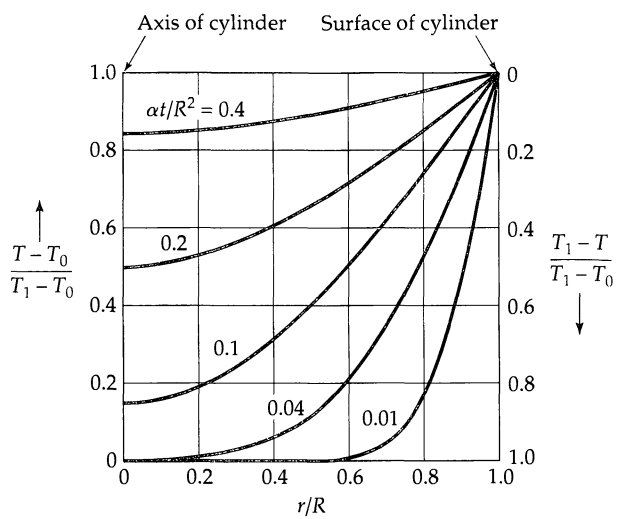


Fig. 12.1-2. Temperature profiles for unsteady-state heat conduction in a cylinder of radius R . The initial temperature of the cylinder is T_0 , and T_1 is the temperature imposed at the cylinder surface for time $t > 0$.
[H. S. Carslaw and J. C. Jaeger, *Conduction of Heat in Solids*, 2nd edition, Oxford University Press (1959), p. 200.]

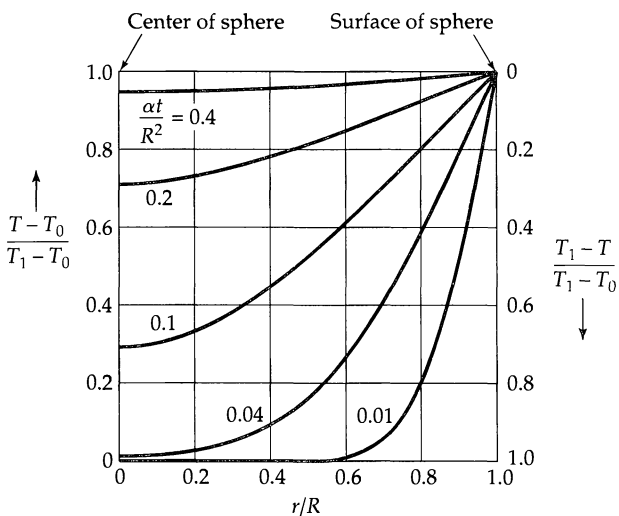


Fig. 12.1-3. Temperature profiles for unsteady-state heat conduction in a sphere of radius R . The initial temperature of the sphere is T_0 , and T_1 is the temperature imposed at the sphere surface for time $t > 0$.
[H. S. Carslaw and J. C. Jaeger, *Conduction of Heat in Solids*, 2nd edition, Oxford University Press (1959), p. 234.]

EXAMPLE 12.1-3

Unsteady Heat Conduction near a Wall with Sinusoidal Heat Flux

SOLUTION

A solid body occupying the space from $y = 0$ to $y = \infty$ is initially at temperature T_0 . Beginning at time $t = 0$, a periodic heat flux given by

$$q_y = q_0 \cos \omega t = q_0 \Re\{e^{i\omega t}\} \quad (12.1-32)$$

is imposed at $y = 0$. Here q_0 is the amplitude of the heat flux oscillations, and ω is the (circular) frequency. It is desired to find the temperature in this system, $T(y, t)$, in the "periodic steady state" (see Problem 4.1-3).

For one-dimensional heat conduction, Eq. 12.1-2 is

$$\frac{\partial T}{\partial t} = \alpha \frac{\partial^2 T}{\partial y^2} \quad (12.1-33)$$

Multiplying by $-k$ and operating on the entire equation with $\partial/\partial y$ gives

$$\frac{\partial}{\partial t} \left(-k \frac{\partial T}{\partial y} \right) = \alpha \frac{\partial^2}{\partial y^2} \left(-k \frac{\partial T}{\partial y} \right) \quad (12.2-34)$$

or, by making use of $q_y = -k(\partial T / \partial y)$,

$$\frac{\partial q_y}{\partial t} = \alpha \frac{\partial^2 q_y}{\partial y^2} \quad (12.1-35)$$

Hence q_y satisfies the same differential equation as T . The boundary conditions are

$$\text{B.C. 1:} \quad \text{at } y = 0, \quad q_y = q_0 \Re\{e^{i\omega t}\} \quad (12.1-36)$$

$$\text{B.C. 2:} \quad \text{at } y = \infty, \quad q_y = 0 \quad (12.1-37)$$

This problem is formally exactly the same as that given in Eqs. 4.1-44, 46, and 47. Hence the solution in Eq. 4.1-57 may be taken over with appropriate notational changes:

$$q_y(y, t) = q_0 e^{-\sqrt{\omega/2\alpha}y} \cos \left(\omega t - \sqrt{\frac{\omega}{2\alpha}} y \right) \quad (12.1-38)$$

Then by integrating Fourier's law

$$-k \int_T^{T_0} dT = \int_y^\infty q_y(y, t) dy \quad (12.1-39)$$

Substitution of the heat flux distribution into the right side of this equation gives after integration

$$T - T_0 = \frac{q_0}{k} \sqrt{\frac{\alpha}{\omega}} e^{-\sqrt{\omega/2\alpha}y} \cos \left(\omega t - \sqrt{\frac{\omega}{2\alpha}} y - \frac{\pi}{4} \right) \quad (12.1-40)$$

Thus, at the surface $y = 0$, the temperature oscillations lag behind the heat flux oscillations by $\pi/4$.

This problem illustrates a standard procedure for obtaining the "periodic steady state" in heat conduction systems. It also shows how one can use the heat conduction equation in terms of the heat flux, when boundary conditions on the heat flux are known.

EXAMPLE 12.1-4

Cooling of a Sphere in Contact with a Well-Stirred Fluid

A homogeneous solid sphere of radius R , initially at a uniform temperature T_1 , is suddenly immersed at time $t = 0$ in a volume V_f of well-stirred fluid of temperature T_0 in an insulated tank. It is desired to find the thermal diffusivity $\alpha_s = k_s / \rho_s C_{ps}$ of the solid by observing the change of the fluid temperature T_f with time. We use the following dimensionless variables:

$$\Theta_s(\xi, \tau) = \frac{T_1 - T_s}{T_1 - T_0} = \text{dimensionless solid temperature} \quad (12.1-41)$$

$$\Theta_f(\tau) = \frac{T_1 - T_f}{T_1 - T_0} = \text{dimensionless fluid temperature} \quad (12.1-42)$$

$$\xi = \frac{r}{R} = \text{dimensionless radial coordinate} \quad (12.1-43)$$

$$\tau = \frac{\alpha_s t}{R^2} = \text{dimensionless time} \quad (12.1-44)$$

SOLUTION

The reader may verify that the problem stated in dimensionless variables is

Solid	Fluid
$\frac{\partial \Theta_s}{\partial \tau} = \frac{1}{\xi^2} \frac{\partial}{\partial \xi} \left(\xi^2 \frac{\partial \Theta_s}{\partial \xi} \right) \quad (12.1-45)$	$\frac{d \Theta_f}{d \tau} = -\frac{3}{B} \frac{\partial \Theta_s}{\partial \xi} \Big _{\xi=1} \quad (12.1-49)$
At $\tau = 0, \Theta_s = 0 \quad (12.1-46)$	At $\tau = 0, \Theta_f = 1 \quad (12.1-50)$
At $\xi = 1, \Theta_s = \Theta_f \quad (12.1-47)$	
At $\xi = 0, \Theta_s = \text{finite} \quad (12.1-48)$	

in which $B = \rho_f \hat{C}_{pj} V_f / \rho_s \hat{C}_{ps} V_s$, the V 's representing the volume of the fluid and of the solid.

Linear problems with complicated boundary conditions and/or coupling between equations are often solved readily by the Laplace transform method. We now take the Laplace transform of the preceding equations and their boundary conditions to get:

Solid	Fluid
$p \bar{\Theta}_s = \frac{1}{\xi^2} \frac{d}{d \xi} \left(\xi^2 \frac{d \bar{\Theta}_s}{d \xi} \right) \quad (12.1-51)$	$p \bar{\Theta}_f - 1 = -\frac{3}{B} \frac{d \bar{\Theta}_s}{d \xi} \Big _{\xi=1} \quad (12.1-54)$
At $\xi = 1, \bar{\Theta}_s = \bar{\Theta}_f \quad (12.1-52)$	
At $\xi = 0, \bar{\Theta}_s = \text{finite} \quad (12.1-53)$	

Here p is the transform variable.³ The solution to Eq. 12.1-51 is

$$\bar{\Theta}_s = \frac{C_1}{\xi} \sinh \sqrt{p} \xi + \frac{C_2}{\xi} \cosh \sqrt{p} \xi \quad (12.1-55)$$

Because of the boundary condition at $\xi = 0$, we must set C_2 equal to zero. Substitution of this result into Eq. 12.1-54 then gives

$$\bar{\Theta}_f = \frac{1}{p} + 3 \frac{C_1}{Bp} (\sinh \sqrt{p} - \sqrt{p} \cosh \sqrt{p}) \quad (12.1-56)$$

Next, we insert these last two results into the boundary condition at $\xi = 1$, in order to determine C_1 . This gives us for $\bar{\Theta}_f$:

$$\bar{\Theta}_f = \frac{1}{p} + 3 \left(\frac{1 - (1/\sqrt{p}) \tanh \sqrt{p}}{(3 - Bp)\sqrt{p} \tanh \sqrt{p} - 3p} \right) \quad (12.1-57)$$

We now divide the numerator and denominator within the parentheses by p , and take the inverse Laplace transform to get

$$\Theta_f = 1 + 3 \mathcal{L}^{-1} \left\{ \frac{(1/p) - (1/p^{3/2}) \tanh \sqrt{p}}{(3 - Bp)(1/\sqrt{p}) \tanh \sqrt{p} - 3} \right\} \equiv 1 + 3 \mathcal{L}^{-1} \left\{ \frac{N(p)}{D(p)} \right\} \quad (12.1-58)$$

³ We use the definition $\mathcal{L}\{f(t)\} = \tilde{f}(p) = \int_0^\infty f(t)e^{-pt} dt$.

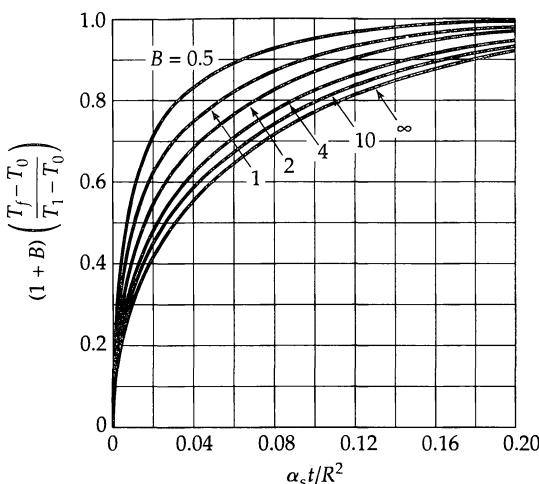


Fig. 12.1-4. Variation of the fluid temperature with time after a sphere of radius R at temperature T_1 is placed in a well-stirred fluid initially at a temperature T_0 . The dimensionless parameter B is defined in the text following Eq. 12.1-50. [H. S. Carslaw and J. C. Jaeger, *Conduction of Heat in Solids*, 2nd edition, Oxford University Press (1959), p. 241.]

It can be shown that $D(p)$ has a single root at $p = 0$, and roots at $\sqrt{p_k} = ib_k$ (with $k = 1, 2, \dots, \infty$), where the b_k are the nonzero roots of $\tan b_k = 3b_k/(3 + Bb_k^2)$. The Heaviside partial fractions expansion theorem⁴ may now be used with

$$\frac{N(0)}{D'(0)} = -\frac{1/3}{1+B} \quad \frac{N(p_k)}{D'(p_k)} = \frac{2B}{9(1+B) + B^2b_k^2} \quad (12.1-59, 60)$$

to get

$$\Theta_f = \frac{B}{1+B} + 6B \sum_{k=1}^{\infty} \frac{\exp(-b_k^2 \tau)}{9(1+B) + B^2b_k^2} \quad (12.1-61)$$

Equation 12.1-61 is shown graphically in Fig. 12.1-4. In this result the only place where the thermal diffusivity of the solid α_s appears is in the dimensionless time $\tau = \alpha_s t / R^2$, so that the temperature rise of the fluid can be used to determine experimentally the thermal diffusivity of the solid. Note that the Laplace transform technique allows us to get the temperature history of the fluid without obtaining the temperature profiles in the solid.

§12.2 STEADY HEAT CONDUCTION IN LAMINAR, INCOMPRESSIBLE FLOW

In the preceding discussion of heat conduction in solids, we needed to use only the energy equation. For problems involving flowing fluids, however, all three equations of change are needed. Here we restrict the discussion to steady flow of incompressible, Newtonian fluids with constant fluid properties, for which the relevant equations of change are:

$$\text{Continuity} \quad (\nabla \cdot \mathbf{v}) = 0 \quad (12.2-1)$$

$$\text{Motion} \quad \rho[\mathbf{v} \cdot \nabla \mathbf{v}] = \mu \nabla^2 \mathbf{v} - \nabla \mathcal{P} \quad (12.2-2)$$

$$\text{Energy} \quad \rho \hat{C}_p (\mathbf{v} \cdot \nabla T) = k \nabla^2 T + \mu \Phi_v \quad (12.2-3)$$

⁴ A. Erdélyi, W. Magnus, F. Oberhettinger, and F. G. Tricomi, *Tables of Integral Transforms*, Vol. 1, McGraw-Hill, New York (1954), p. 232, Eq. 20; see also C. R. Wylie and L. C. Barrett, *Advanced Engineering Mathematics*, McGraw-Hill, New York, 6th Edition (1995), §10.9.

In Eq. 12.2-3, Φ_v is the dissipation function given in Eq. 3.3-3. To get the temperature profiles for forced convection, a two-step procedure is used: first Eqs. 12.2-1 and 2 are solved to obtain the velocity distribution $v(r, t)$; then the expression for v is substituted into Eq. 12.2-3, which may in turn be solved to get the temperature distribution $T(r, t)$.

Many analytical solutions of Eqs. 12.2-1 to 3 are available for commonly encountered situations.¹⁻⁷ One of the oldest forced-convection problems is the *Graetz–Nusselt problem*,⁸ describing the temperature profiles in tube flow where the wall temperature undergoes a sudden step change at some position along the tube (see Problems 12D.2, 3, and 4). Analogous solutions have been obtained for arbitrary variations of wall temperature and wall flux.⁹ The Graetz–Nusselt problem has also been extended to non-Newtonian fluids.¹⁰ Solutions have also been developed for a large class of laminar heat exchanger problems,¹¹ in which the wall boundary condition is provided by the continuity of heat flux across the surfaces separating the two streams. A further problem of interest is duct flow with significant viscous heating effects (the *Brinkman problem*).¹²

In this section we extend the discussion of the problem treated in §10.8—namely, the determination of temperature profiles for laminar flow of an incompressible fluid in a circular tube. In that section we set up the problem and found the asymptotic solution for distances far downstream from the beginning of the heated zone. Here, we give the complete solution to the partial differential equation as well as the asymptotic solution for short distances. That is, the system shown in Fig. 10.8-2 is discussed from three viewpoints in this book:

- a. Complete solution of the partial differential equation by the method of separation of variables (Example 12.2-1).
- b. Asymptotic solution for short distances down the tube by the method of combination of variables (Example 12.2-2).
- c. Asymptotic solution for large distances down the tube (§10.8).

¹ M. Jakob, *Heat Transfer*, Vol. I, Wiley, New York (1949), pp. 451–464.

² H. Gröber, S. Erk, and U. Grigull, *Die Grundgesetze der Wärmeübertragung*, Springer, Berlin (1961), Part II.

³ R. K. Shah and A. L. London, *Laminar Flow Forced Convection in Ducts*, Academic Press, New York (1978).

⁴ L. C. Burmeister, *Convective Heat Transfer*, Wiley-Interscience, New York (1983).

⁵ L. D. Landau and E. M. Lifshitz, *Fluid Mechanics*, Pergamon, Oxford (1987), Chapter 5.

⁶ L. G. Leal, *Laminar Flow and Convective Transport Processes*, Butterworth-Heinemann (1992), Chapters 8 and 9.

⁷ W. M. Deen, *Analysis of Transport Phenomena*, Oxford University Press (1998), Chapters 9 and 10.

⁸ L. Graetz, *Ann. Phys. (N.F.)*, **18**, 79–94 (1883), **25**, 337–357 (1885); W. Nusselt, *Zeits. Ver. deutsch. Ing.*, **54**, 1154–1158 (1910). For the “extended Graetz problem,” which includes axial conduction, see E. Papoutsakis, D. Ramkrishna, and H. C. Lim, *Appl. Sci. Res.*, **36**, 13–34 (1980).

⁹ E. N. Lightfoot, C. Massot, and F. Irani, *Chem. Eng. Progress Symp. Series*, Vol. 61, No. 58 (1965), pp. 28–60.

¹⁰ R. B. Bird, R. C. Armstrong, and O. Hassager, *Dynamics of Polymeric Liquids*, Wiley-Interscience (1987), 2nd edition, Vol. 1, §4.4.

¹¹ R. J. Nunge and W. N. Gill, *AIChE Journal*, **12**, 279–289 (1966).

¹² H. C. Brinkman, *Appl. Sci. Research*, **A2**, 120–124 (1951); R. B. Bird, *SPE Journal*, **11**, 35–40 (1955); H. L. Toor, *Ind. Eng. Chem.*, **48**, 922–926 (1956).

EXAMPLE 12.2-1

*Laminar Tube Flow
with Constant Heat
Flux at the Wall*

Solve Eq. 10.8-19 with the boundary conditions given in Eqs. 10.8-20, 21, and 22.

SOLUTION

The complete solution for the temperature is postulated to be of the following form:

$$\Theta(\xi, \zeta) = \Theta_\infty(\xi, \zeta) - \Theta_d(\xi, \zeta) \quad (12.2-4)$$

in which $\Theta_\infty(\xi, \zeta)$ is the asymptotic solution given in Eq. 10.3-31, and $\Theta_d(\xi, \zeta)$ is a function that will be damped out exponentially with time. By substituting the expression for $\Theta(\xi, \zeta)$ in Eq. 12.2-4 into Eq. 10.8-19, it may be shown that the function $\Theta_d(\xi, \zeta)$ must satisfy Eq. 10.8-19 and also the following boundary conditions:

$$\text{B.C. 1:} \quad \text{at } \xi = 0, \quad \frac{\partial \Theta_d}{\partial \xi} = 0 \quad (12.2-5)$$

$$\text{B.C. 2:} \quad \text{at } \xi = 1, \quad \frac{\partial \Theta_d}{\partial \xi} = 0 \quad (12.2-6)$$

$$\text{B.C. 3:} \quad \text{at } \zeta = 0, \quad \Theta_d = \Theta_\infty(\xi, 0) \quad (12.2-7)$$

We anticipate that a solution to the equation for $\Theta_d(\xi, \zeta)$ will be factorable,

$$\Theta_d(\xi, \zeta) = X(\xi)Z(\zeta) \quad (12.2-8)$$

Then Eq. 10.8-19 can be separated into two ordinary differential equations

$$\frac{dZ}{d\zeta} = -c^2 Z \quad (12.2-9)$$

$$\frac{1}{\xi} \frac{d}{d\xi} \left(\xi \frac{dX}{d\xi} \right) + c^2(1 - \xi^2)X = 0 \quad (12.2-10)$$

in which $-c^2$ is the separation constant. Since the boundary conditions on X are $dX/d\xi = 0$ at $\xi = 0, 1$, we have a Sturm-Liouville problem.¹³ Therefore we know there will be an infinite number of eigenvalues c_k and eigenfunctions X_k , and that the final solution must be of the form:

$$\Theta(\xi, \zeta) = \Theta_\infty(\xi, \zeta) - \sum_{k=1}^{\infty} B_k \exp(-c_k^2 \zeta) X_k(\xi) \quad (12.2-11)$$

where

$$B_k = \frac{\int_0^1 \Theta_\infty(\xi, 0) [X_k(\xi)] (1 - \xi^2) \xi \, d\xi}{\int_0^1 [X_k(\xi)]^2 (1 - \xi^2) \xi \, d\xi} \quad (12.2-12)$$

The problem is thus reduced to finding the eigenfunctions $X_k(\xi)$ by solving Eq. 12.2-10, and then getting the eigenvalues c_k by applying the boundary condition at $\xi = 1$. This has been done for k up to 7 for this problem.¹⁴

¹³ M. D. Greenberg, *Advanced Engineering Mathematics*, Prentice-Hall, Upper Saddle River, N.J., Second Edition (1998), §17.7.

¹⁴ R. Siegel, E. M. Sparrow, and T. M. Hallman, *Appl. Sci. Research*, **A7**, 386–392 (1958).

EXAMPLE 12.2-2

Laminar Tube Flow with Constant Heat Flux at the Wall:

Asymptotic Solution for the Entrance Region

Note that the sum in Eq. 12.2-11 converges rapidly for large z but slowly for small z . Develop an expression for $T(r, z)$ that is useful for small values.

SOLUTION

For small z the heat addition affects only a very thin region near the wall, so that the following three approximations lead to results that are accurate in the limit as $z \rightarrow 0$:

- Curvature effects may be neglected and the problem treated as though the wall were flat; call the distance from the wall $y = R - r$.
- The fluid may be regarded as extending from the (flat) heat transfer surface ($y = 0$) to $y = \infty$.
- The velocity profile may be regarded as linear, with a slope given by the slope of the parabolic velocity profile at the wall: $v_z(y) = v_0 y / R$, in which $v_0 = (\mathcal{P}_0 - \mathcal{P}_L)R^2 / 2\mu L$.

This is the way the system would appear to a tiny “observer” who is located within the very thin shell of heated fluid. To this observer, the wall would seem flat, the fluid would appear to be of infinite extent, and the velocity profile would seem to be linear.

The energy equation then becomes, in the region just slightly beyond $z = 0$,

$$v_0 \frac{y}{R} \frac{\partial T}{\partial z} = \alpha \frac{\partial^2 T}{\partial y^2} \quad (12.2-13)$$

Actually it is easier to work with the corresponding equation for the heat flux in the y direction ($q_y = -k \partial T / \partial y$). This equation is obtained by dividing Eq. 12.2-13 by y and differentiating with respect to y :

$$v_0 \frac{1}{R} \frac{\partial q_y}{\partial z} = \alpha \frac{\partial}{\partial y} \left(\frac{1}{y} \frac{\partial q_y}{\partial y} \right) \quad (12.2-14)$$

It is more convenient to work with dimensionless variables defined as

$$\psi = \frac{q_s}{q_0} \quad \eta = \frac{y}{R} \quad \lambda = \frac{\alpha z}{v_0 R^2} \quad (12.2-15)$$

Then Eq. 12.2-14 becomes

$$\frac{\partial \psi}{\partial \lambda} = \frac{\partial}{\partial \eta} \left(\frac{1}{\eta} \frac{\partial \psi}{\partial \eta} \right) \quad (12.2-16)$$

with these boundary conditions:

$$\text{B.C. 1:} \quad \text{at } \lambda = 0, \quad \psi = 0 \quad (12.2-17)$$

$$\text{B.C. 2:} \quad \text{at } \eta = 0, \quad \psi = 1 \quad (12.2-18)$$

$$\text{B.C. 3:} \quad \text{as } \eta \rightarrow \infty, \quad \psi \rightarrow 0 \quad (12.2-19)$$

This problem can be solved by the method of combination of variables (see Examples 4.1-1 and 12.1-1) by using the new independent variable $\chi = \eta / \sqrt[3]{9\lambda}$. Then Eq. 12.2-16 becomes

$$\chi \frac{d^2 \psi}{d\chi^2} + (3\chi^3 - 1) \frac{d\psi}{d\chi} = 0 \quad (12.2-20)$$

The boundary conditions are: at $\chi = 0$, $\psi = 1$, and as $\chi \rightarrow \infty$, $\psi \rightarrow 0$. The solution of Eq. 12.2-20 is found by first letting $d\psi/d\chi = p$, and getting a first-order equation for p . The equation for p can be solved and then ψ is obtained as

$$\psi(\chi) = \frac{\int_{\chi}^{\infty} \bar{\chi} \exp(-\bar{\chi}^3) d\bar{\chi}}{\int_0^{\infty} \bar{\chi} \exp(-\bar{\chi}^3) d\bar{\chi}} = \frac{3}{\Gamma(2/3)} \int_{\chi}^{\infty} \bar{\chi} \exp(-\bar{\chi}^3) d\bar{\chi} \quad (12.2-21)$$

The temperature profile may then be obtained by integrating the heat flux:

$$\int_{T_1}^{T_2} dT = -\frac{1}{k} \int_y^{\infty} q_y dy \quad (12.2-22)$$

or, in dimensionless form,

$$\Theta(\eta, \lambda) = \frac{T - T_1}{q_0 R / k} = \sqrt[3]{9\lambda} \int_{\chi}^{\infty} \psi d\chi \quad (12.2-23)$$

Then the expression for ψ is inserted into the integral, and the order of integration in the double integral can be reversed (see Problem 12D.7). The result is

$$\Theta(\eta, \lambda) = \sqrt[3]{9\lambda} \left[\frac{\exp(-\chi^3)}{\Gamma(\frac{2}{3})} - \chi \left(1 - \frac{\Gamma(\frac{2}{3}, \chi^3)}{\Gamma(\frac{2}{3})} \right) \right] \quad (12.2-24)$$

Here $\Gamma(\frac{2}{3})$ is the (complete) gamma function, and $\Gamma(\frac{2}{3}, \chi^3)$ is an incomplete gamma function.¹⁵ To compare this result with that in Example 12.2-1, we note that $\eta = 1 - \xi$ and $\lambda = \frac{1}{2}\zeta$. The dimensionless temperature is defined identically in §10.8, in Example 12.2-1, and here.

§12.3 STEADY POTENTIAL FLOW OF HEAT IN SOLIDS

The steady flow of heat in solids of constant thermal conductivity is described by

$$\text{Fourier's law} \quad \mathbf{q} = -k\nabla T \quad (12.3-1)$$

$$\text{Heat conduction equation} \quad \nabla^2 T = 0 \quad (12.3-2)$$

These equations are exactly analogous to the expression for the velocity in terms of the velocity potential ($\mathbf{v} = -\nabla\phi$), and the Laplace equation for the velocity potential ($\nabla^2\phi = 0$), which we encountered in §4.3. Steady heat conduction problems can therefore be solved by application of potential theory.

For two-dimensional heat conduction in solids with constant thermal conductivity, the temperature satisfies the two-dimensional Laplace equation:

$$\frac{\partial^2 T}{\partial x^2} + \frac{\partial^2 T}{\partial y^2} = 0 \quad (12.3-3)$$

We now use the fact that *any* analytic function $w(z) = f(x, y) + ig(x, y)$ provides two scalar functions f and g , which are solutions of Eq. 12.3-3. Curves of $f = \text{constant}$ may be interpreted as lines of heat flow, and curves of $g = \text{constant}$ are the corresponding isotherms for *some* heat flow problems. These two sets of curves are orthogonal—that is, they intersect at right angles. Furthermore, the components of the heat flux vector at any point are given by

$$ik \frac{dw}{dz} = q_x - iq_y \quad (12.3-4)$$

Given an analytic function, it is easy to find heat flow problems that are described by it. But the inverse process of finding an analytic function suitable for a given heat flow problem is generally very difficult. Some methods for this are available, but they are outside the scope of this textbook.^{1,2}

¹⁵ M. Abramowitz and I. A. Stegun, eds., *Handbook of Mathematical Functions*, Dover, New York, 9th Printing (1973), pp. 255 et seq.

¹ H. S. Carslaw and J. C. Jaeger, *Conduction of Heat in Solids*, 2nd edition, Oxford University Press (1959), Chapter XVI.

² M. D. Greenberg, *Advanced Engineering Mathematics*, Prentice-Hall, Upper Saddle River, N.J., 2nd Edition (1998), Chapter 22.

For every complex function $w(z)$, two heat flow nets are obtained by interchanging the lines of constant f and the lines of constant g . Furthermore, two additional nets are obtained by working with the inverse function $z(w)$ as illustrated in Chapter 4 for ideal fluid flow.

Note that potential fluid flow and potential heat flow are mathematically similar, the two-dimensional flow nets in both cases being described by analytic functions. Physically, however, there are certain important differences. The fluid flow nets described in §4.3 are for a fluid with no viscosity (a fictitious fluid!), and therefore one cannot use them to calculate the drag forces at surfaces. On the other hand, the heat flow nets described here are for solids that have a finite thermal conductivity, and therefore the results can be used to calculate the heat flow at all surfaces. Moreover, in §4.3 the velocity profiles do *not* satisfy the Laplace equation, whereas in this section the temperature profiles *do* satisfy the Laplace equation. Further information about analogous physical processes described by the Laplace equation is available in books on partial differential equations.³

Here we give just one example to provide a glimpse of the use of analytic functions; further examples may be found in the references cited.

EXAMPLE 12.3-1

Temperature Distribution in a Wall

Consider a wall of thickness b extending from 0 to ∞ in the y direction, and from $-\infty$ to $+\infty$ in the direction perpendicular to the x and y directions (see Fig. 12.3-1). The surfaces at $x = \pm\frac{1}{2}b$ are held at temperature T_0 , whereas the bottom of the wall at the surface $y = 0$ is maintained at temperature T_1 . Show that the imaginary part of the function⁴

$$w(z) = \frac{1}{\pi} \ln \left(\frac{(\sin \pi z/b) - 1}{(\sin \pi z/b) + 1} \right) \quad (12.3-5)$$

gives the steady temperature distribution $\Theta(x, y) = (T - T_0)/(T_1 - T_0)$.

SOLUTION

The imaginary part of $w(z)$ in Eq. 12.3-5 is

$$\Theta(x, y) = \frac{2}{\pi} \arctan \left(\frac{\cos \pi x/b}{\sinh \pi y/b} \right) \quad (12.3-6)$$

in which the arctangent is in the range from 0 to $\frac{\pi}{2}$. When $x = \pm\frac{1}{2}b$, Eq. 12.3-6 gives $\Theta = 0$, and when $y = 0$, it gives $\Theta = (2/\pi) \arctan \infty = 1$.

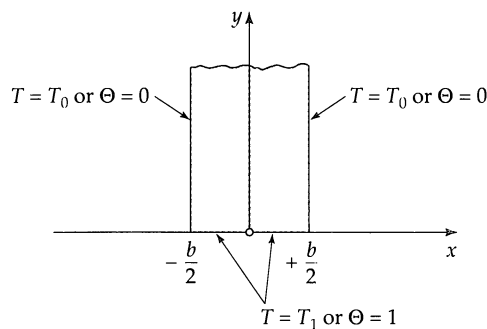


Fig. 12.3-1. Steady two-dimensional temperature distribution in a wall.

³ I. N. Sneddon, *Elements of Partial Differential Equations*, Dover, New York (1996), Chapter 4.

⁴ R. V. Churchill, *Introduction to Complex Variables and Applications*, McGraw-Hill, New York (1948), Chapter IX. See also C. R. Wylie and L. C. Barrett, *Advanced Engineering Mathematics*, McGraw-Hill, New York, 6th Edition (1995), Chapter 20.

From Eq. 12.3-6 the heat flux through the base of the wall may be obtained:

$$q_y|_{y=0} = -k \frac{\partial T}{\partial y} \Big|_{y=0} = \frac{2k \sec \pi x/b}{b} (T_1 - T_0) \quad (12.3-7)$$

§12.4 BOUNDARY LAYER THEORY FOR NONISOTHERMAL FLOW^{1,2,3}

In §4.4 the use of boundary layer approximations for steady, laminar flow of incompressible fluids at constant temperature was discussed. We saw that, in the neighborhood of a solid surface, the equations of continuity and motion could be simplified, and that these equations may be solved to get “exact boundary layer solutions” and that an integrated form of these equations (the von Kármán momentum balance) enables one to get “approximate boundary layer solutions.” In this section we extend the previous development by including the boundary layer equation for energy transport, so that the temperature profiles near solid surfaces can be obtained.

As in §4.4 we consider the steady two-dimensional flow around a submerged object such as that shown in Fig. 4.4-1. In the vicinity of the solid surface the equations of change may be written (omitting the bars over ρ and β) as:

$$\text{Continuity} \quad \frac{\partial v_x}{\partial x} + \frac{\partial v_y}{\partial y} = 0 \quad (12.4-1)$$

$$\text{Motion} \quad \rho \left(v_x \frac{\partial v_x}{\partial x} + v_y \frac{\partial v_x}{\partial y} \right) = \rho v_e \frac{dv_e}{dx} + \mu \frac{\partial^2 v_x}{\partial y^2} + \rho g_x \beta (T - T_\infty) \quad (12.4-2)$$

$$\text{Energy} \quad \rho \hat{C}_p \left(v_x \frac{\partial T}{\partial x} + v_y \frac{\partial T}{\partial y} \right) = k \frac{\partial^2 T}{\partial y^2} + \mu \left(\frac{\partial v_x}{\partial y} \right)^2 \quad (12.4-3)$$

Here ρ , μ , k , and \hat{C}_p are regarded as constants, and $\mu(\partial v_x / \partial y)^2$ is the viscous heating effect, which is henceforth disregarded. Solutions of these equations are asymptotically accurate for small momentum diffusivity $\nu = \mu/\rho$ in Eq. 12.4-2, and for small thermal diffusivity $\alpha = k/\rho \hat{C}_p$ in Eq. 12.4-3.

Equation 12.4-1 is the same as Eq. 4.4-1. Equation 12.4-2 differs from Eq. 4.4-2 because of the inclusion of the buoyant force term (see §11.3), which can be significant even when fractional changes in density are small. Equation 12.4-3 is obtained from Eq. 11.2-9 by neglecting the heat conduction in the x direction. More complete forms of the boundary layer equations may be found elsewhere.^{2,3}

The usual boundary conditions for Eqs. 12.4-1 and 2 are that $v_x = v_y = 0$ at the solid surface, and that the velocity merges into the potential flow at the outer edge of the *velocity boundary layer*, so that $v_x \rightarrow v_e(x)$. For Eq. 12.4-3 the temperature T is specified to be T_0 at the solid surface and T_∞ at the outer edge of the *thermal boundary layer*. That is, the velocity and temperature are different from $v_e(x)$ and T_∞ only in thin layers near the solid surface. However, the velocity and temperature boundary layers will be of different thicknesses corresponding to the relative ease of the diffusion of momentum and heat. Since $\text{Pr} = \nu/\alpha$, for $\text{Pr} > 1$ the temperature boundary layer usually lies inside the veloc-

¹ H. Schlichting, *Boundary-Layer Theory*, 7th edition, McGraw-Hill, New York (1979), Chapter 12.

² K. Stewartson, *The Theory of Laminar Boundary Layers in Compressible Fluids*, Oxford University Press (1964).

³ E. R. G. Eckert and R. M. Drake, Jr., *Analysis of Heat and Mass Transfer*, McGraw-Hill, New York, (1972), Chapters 6 and 7.

ity boundary layer, whereas for $\text{Pr} < 1$ the relative thicknesses are just reversed (keep in mind that for gases Pr is about $\frac{3}{4}$, whereas for ordinary liquids $\text{Pr} > 1$ and for liquid metals $\text{Pr} \ll 1$).

In §4.4 we showed that the boundary layer equation of motion could be integrated formally from $y = 0$ to $y = \infty$, if use is made of the equation of continuity. In a similar fashion the integration of Eqs. 12.4-1 to 3 can be performed to give

$$\begin{aligned} \text{Momentum} \quad \mu \frac{\partial v_x}{\partial y} \Big|_{y=0} &= \frac{d}{dx} \int_0^\infty \rho v_x (v_e - v_x) dy + \frac{dv_e}{dx} \int_0^\infty \rho (v_e - v_x) dy \\ &+ \int_0^\infty \rho g_s \beta (T - T_\infty) dy \end{aligned} \quad (12.4-4)$$

$$\text{Energy} \quad k \frac{\partial T}{\partial y} \Big|_{y=0} = \frac{d}{dx} \int_0^\infty \rho \hat{C}_p v_x (T_\infty - T) dy \quad (12.4-5)$$

Equations 12.4-4 and 5 are the *von Kármán momentum and energy balances*, valid for forced-convection and free-convection systems. The no-slip condition $v_y = 0$ at $y = 0$ has been used here, as in Eq. 4.4-4; nonzero velocities at $y = 0$ occur in mass transfer systems and will be considered in Chapter 20.

As mentioned in §4.4, there are two approaches for solving boundary layer problems: analytical or numerical solutions of Equations 12.4-1 to 3 are called "exact boundary layer solutions," whereas solutions obtained from Eqs. 12.4-4 and 5, with reasonable guesses for the velocity and temperature profiles, are called "approximate boundary layer solutions." Often considerable physical insight can be obtained by the second method, and with relatively little effort. Example 12.4-1 illustrates this method.

Extensive use has been made of the boundary layer equations to establish correlations of momentum- and heat-transfer rates, as we shall see in Chapter 14. Although in this section we do not treat free convection, in Chapter 14 many useful results are given along with the appropriate literature citations.

EXAMPLE 12.4-1

Heat Transfer in Laminar Forced Convection along a Heated Flat Plate (von Kármán Integral Method)

Obtain the temperature profiles near a flat plate, along which a Newtonian fluid is flowing, as shown in Fig. 12.4-1. The wetted surface of the plate is maintained at temperature T_0 and the temperature of the approaching fluid is T_∞ .

SOLUTION

In order to use the von Kármán balances we first postulate reasonable forms for the velocity and temperature profiles. The following polynomial form gives 0 at the wall and 1 at the outer limit of the boundary layer, with a slope of zero at the outer limit:

$$\begin{cases} \frac{v_x}{v_\infty} = 2\left(\frac{y}{\delta}\right) - 2\left(\frac{y}{\delta}\right)^3 + \left(\frac{y}{\delta}\right)^4 & y \leq \delta(x) \\ \frac{v_x}{v_\infty} = 1 & y \geq \delta(x) \end{cases} \quad (12.4-6, 7)$$

$$\begin{cases} \frac{T_0 - T}{T_0 - T_\infty} = 2\left(\frac{y}{\delta_T}\right) - 2\left(\frac{y}{\delta_T}\right)^3 + \left(\frac{y}{\delta_T}\right)^4 & y \leq \delta_T(x) \\ \frac{T_0 - T}{T_0 - T_\infty} = 1 & y \geq \delta_T(x) \end{cases} \quad (12.4-8, 9)$$

That is, we assume that the dimensionless velocity and temperature profiles have the same form within their respective boundary layers. We further *assume* that the boundary layer thicknesses $\delta(x)$ and $\delta_T(x)$ have a constant ratio, so that $\Delta = \delta_T(x)/\delta(x)$ is independent of x . Two possibilities have to be considered: $\Delta \leq 1$ and $\Delta \geq 1$. We consider here $\Delta \leq 1$ and relegate the other case to Problem 12D.8.

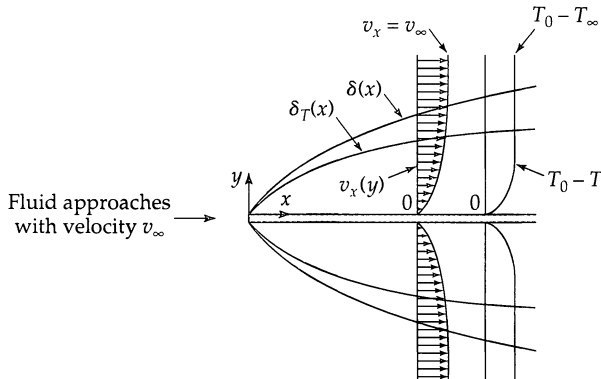


Fig. 12.4-1. Boundary layer development for the flow along a heated flat plate, showing the thermal boundary layer for $\Delta = \delta_T(x)/\delta(x) < 1$. The surface of the plate is at temperature T_0 , and the approaching fluid is at T_∞ .

The use of Eqs. 12.4-4 and 5 is now straightforward but tedious. Substitution of Eqs. 12.4-6 through 9 into the integrals gives (with v_c set equal to v_∞ here)

$$\int_0^\infty \rho v_x(v_\infty - v_x) dy = \rho v_\infty^2 \delta(x) \int_0^1 (2\eta - 2\eta^3 + \eta^4)(1 - 2\eta + 2\eta^3 - \eta^4) d\eta = \frac{37}{315} \rho v_\infty^2 \delta(x) \quad (12.4-10)$$

$$\begin{aligned} \int_0^\infty \rho \hat{C}_p v_x(T_\infty - T) dy &= \rho \hat{C}_p v_\infty (T_\infty - T_0) \delta_T(x) \int_0^\infty (2\eta_T \Delta - 2\eta_T^3 \Delta^3 + \eta_T^4 \Delta^4) \\ &\quad \cdot (1 - 2\eta_T + 2\eta_T^3 - \eta_T^4) d\eta_T \\ &= (\frac{2}{15}\Delta - \frac{3}{140}\Delta^3 + \frac{1}{180}\Delta^4) \rho \hat{C}_p v_\infty (T_\infty - T_0) \delta_T(x) \end{aligned} \quad (12.4-11)$$

In these integrals $\eta = y/\delta(x)$ and $\eta_T = y/\delta_T(x) = y/\Delta\delta(x)$. Next, substitution of these integrals into Eqs. 12.4-4 and 5 gives differential equations for the boundary layer thicknesses. These first-order separable differential equations are easily integrated, and we get

$$\delta(x) = \sqrt{\frac{1260}{37} \left(\frac{vx}{v_\infty} \right)} \quad (12.4-12)$$

$$\delta_T(x) = \sqrt{\frac{4}{\frac{2}{15}\Delta - \frac{3}{140}\Delta^3 + \frac{1}{180}\Delta^4} \left(\frac{\alpha x}{v_\infty} \right)} \quad (12.4-13)$$

The boundary layer thicknesses are now determined, except for the evaluation of Δ in Eq. 12.4-13. The ratio of Eq. 12.4-12 to Eq. 12.4-13 gives an equation for Δ as a function of the Prandtl number:

$$\frac{2}{15}\Delta^3 - \frac{3}{140}\Delta^5 + \frac{1}{180}\Delta^6 = \frac{37}{315}\text{Pr}^{-1} \quad \Delta \leq 1 \quad (12.4-14)$$

When this sixth-order algebraic equation is solved for Δ as a function of Pr , it is found that the solution may be curve-fitted by the simple relation⁴

$$\Delta = \text{Pr}^{-1/3} \quad \Delta < 1 \quad (12.4-15)$$

within about 5%.

⁴ H. Schlichting, *Boundary-Layer Theory*, 7th edition, McGraw-Hill, New York (1979), pp. 292–308.

Table 12.4-1 Comparison of Boundary Layer Heat Transfer Calculations for Flow along a Flat Plate

Method	Value of numerical coefficient in expression for heat transfer rate in Eq. 12.4-17
Von Kármán method with profiles of Eqs. 12.4-9 to 12	$\sqrt{148/315} = 0.685$
Exact solution of Eqs. 12.4-1 to 3 by Pohlhausen	0.657 at $\text{Pr} = 0.6$ 0.664 at $\text{Pr} = 1.0$ 0.670 at $\text{Pr} = 2.0$
Curve fit of exact calculations (Pohlhausen)	0.664
Asymptotic solution of Eqs. 12.4-1 to 3 for $\text{Pr} \gg 1$	0.677

The temperature profile is then finally given (for $\Delta \leq 1$) by

$$\frac{T_0 - T}{T_0 - T_\infty} = 2\left(\frac{y}{\Delta\delta}\right) - 2\left(\frac{y}{\Delta\delta}\right)^3 + \left(\frac{y}{\Delta\delta}\right)^4 \quad (12.4-16)$$

in which $\Delta \approx \text{Pr}^{-1/3}$ and $\delta(x) = \sqrt{(1260/37)(\nu x/v_\infty)}$. The assumption of laminar flow made here is valid for $x < x_{crit}$, where $x_{crit}v_\infty\rho/\mu$ is usually greater than 10^5 .

Finally, the rate of heat loss from both sides of a heated plate of width W and length L can be obtained from Eqs. 12.4-5, 11, 12, 15, and 16:

$$\begin{aligned} Q &= 2 \int_0^W \int_0^L q_y|_{y=0} dx dz \\ &= 2 \int_0^W \int_0^\infty \rho \hat{C}_p v_x (T - T_\infty)|_{x=L} dy dz \\ &= 2 W \rho \hat{C}_p v_\infty (T_0 - T_\infty) \left(\frac{2}{15} \Delta - \frac{3}{140} \Delta^3 + \frac{1}{180} \Delta^4 \right) \delta_T(L) \\ &\approx \sqrt{\frac{148}{315}} (2WL)(T_0 - T_\infty) \left(\frac{k}{L} \right) \text{Pr}^{1/3} \text{Re}_L^{1/2} \end{aligned} \quad (12.4-17)$$

in which $\text{Re}_L = Lv_\infty\rho/\mu$. Thus the boundary layer approach allows one to obtain the dependence of the rate of heat loss Q on the dimensions of the plate, the flow conditions, and the thermal properties of the fluid.

Eq. 12.4-17 is in good agreement with more detailed solutions based on Eqs. 12.4-1 to 3. The asymptotic solution for Q at large Prandtl numbers, given in the next example,⁵ has the same form except that the numerical coefficient $\sqrt{148/315} = 0.685$ is replaced by 0.677. The exact solution for Q at finite Prandtl numbers, obtained numerically,⁶ has the same form except that the coefficient is replaced by a slowly varying function $C(\text{Pr})$, shown in Table 12.4-1. The value $C = 0.664$ is exact at $\text{Pr} = 1$ and good within $\pm 2\%$ for $\text{Pr} > 0.6$.

The proportionality of Q to $\text{Pr}^{1/3}$, found here, is asymptotically correct in the limit as $\text{Pr} \rightarrow \infty$, not only for the flat plate but also for all geometries that permit a laminar, nonseparating boundary layer, as illustrated in the next example. Deviations from $Q \sim \text{Pr}^{1/3}$ occur at finite Prandtl numbers for flow along a flat plate and even more so for flows near other-shaped objects and near rotating surfaces. These deviations arise from nonlinearity of the velocity profiles within the thermal boundary layer. Asymptotic expansions for the Pr dependence of Q have been presented by Merk and others.⁷

⁵ M. J. Lighthill, *Proc. Roy. Soc., A* **202**, 359–377 (1950).

⁶ E. Pohlhausen, *Zeits. f. angew. Math. u. Mech.*, **1**, 115–121 (1921).

⁷ H. J. Merk, *J. Fluid Mech.*, **5**, 460–480 (1959).

EXAMPLE 12.4-2

Heat Transfer in Laminar Forced Convection along a Heated Flat Plate (Asymptotic Solution for Large Prandtl Numbers)⁵

In the preceding example we used the von Kármán boundary layer integral expressions. Now we repeat the same problem but obtain an exact solution of the boundary layer equations in the limit that the Prandtl number is large—that is, for liquids (see §9.1). In this limit, the outer edge of the thermal boundary layer is well inside the velocity boundary layer. Therefore it can safely be assumed that v_x varies linearly with y throughout the entire thermal boundary layer.

SOLUTION

By combining the boundary layer equations of continuity and energy (Eqs. 12.4-1 and 3) we get

$$v_x \frac{\partial T}{\partial x} + \left(- \int_0^y \frac{\partial v_x}{\partial x} dy \right) \frac{\partial T}{\partial y} = \alpha \frac{\partial^2 T}{\partial y^2} \quad (12.4-18)$$

in which $\alpha = k/\rho C_p$. The leading term of a Taylor expansion for the velocity distribution near the wall is

$$\frac{v_x}{v_\infty} = c \frac{y}{\sqrt{\nu x/v_\infty}} \quad (12.4-19)$$

in which the constant $c = 0.4696/\sqrt{2} = 0.332$ can be inferred from Eq. 4.4-30.

Substitution of this velocity expression into Eq. 12.4-18 gives

$$\left(c \frac{y v_\infty}{\sqrt{\nu x/v_\infty}} \right) \frac{\partial T}{\partial x} + \left(\frac{c}{4} \frac{y^2 v_\infty / x}{\sqrt{\nu x/v_\infty}} \right) \frac{\partial T}{\partial y} = \alpha \frac{\partial^2 T}{\partial y^2} \quad (12.4-20)$$

This has to be solved with the boundary conditions that $T = T_0$ at $y = 0$, and $T = T_\infty$ at $x = 0$.

This equation can be solved by the method of combination of variables. The choice of the dimensionless variables

$$\Pi(\eta) = \frac{T_0 - T}{T_0 - T_\infty} \quad \text{and} \quad \eta = \left(\frac{c v_\infty^{3/2}}{12 \alpha \nu^{1/2}} \right)^{1/3} \frac{y}{x^{1/2}} \quad (12.4-21, 22)$$

makes it possible to rewrite Eq. 12.4-20 (see Eq. C.1-9) as

$$\frac{d^2 \Pi}{d\eta^2} + 3\eta^2 \frac{d\Pi}{d\eta} = 0 \quad (12.4-23)$$

Integration of this equation with the boundary conditions that $\Pi = 0$ at $\eta = 0$ and $\Pi \rightarrow 1$ as $\eta \rightarrow \infty$ gives

$$\Pi(\eta) = \frac{\int_0^\eta \exp(-\bar{\eta}^3) d\bar{\eta}}{\int_0^\infty \exp(-\bar{\eta}^3) d\bar{\eta}} = \frac{\int_0^\eta \exp(-\bar{\eta}^3) d\bar{\eta}}{\Gamma(\frac{4}{3})} \quad (12.4-24)$$

for the dimensionless temperature distribution. See §C.4 for a discussion of the gamma function $\Gamma(n)$.

For the rate of heat loss from both sides of a heated plate of width W and length L , we get

$$\begin{aligned} Q &= 2 \int_0^W \int_0^L q_y|_{y=0} dx dz \\ &= 2W \int_0^L \left(-k \frac{\partial T}{\partial y} \right) \Big|_{y=0} dx \\ &= (2WL)(T_0 - T_\infty) \left(\frac{k}{L} \right) \int_0^L \left(+k \frac{d\Pi}{d\eta} \right) \Big|_{\eta=0} \left(\frac{cv_\infty^{3/2}}{12\alpha\nu^{1/2}} \right)^{1/3} \frac{dx}{x^{1/2}} \\ &= (2WL)(T_0 - T_\infty) \left(\frac{k}{L} \right) \left[\frac{2}{\Gamma(\frac{4}{3})} \left(\frac{c}{12} \right)^{1/3} \right] \text{Pr}^{1/3} \text{Re}_L^{1/2} \end{aligned} \quad (12.4-25)$$

which is the same result as that in Eq. 12.4-17 aside from a numerical constant. The quantity within brackets equals 0.677, the asymptotic value that appears in Table 12.4-1.

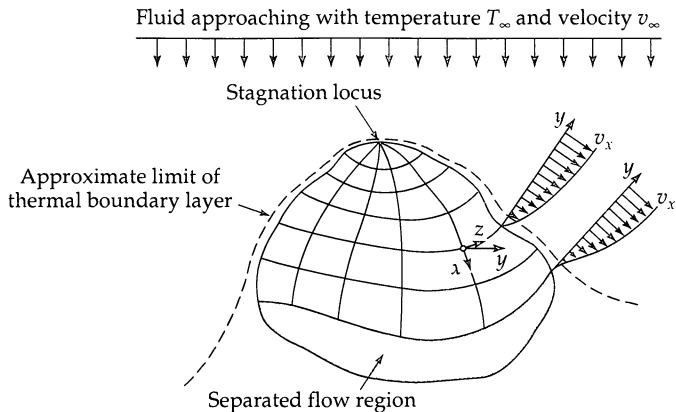


Fig. 12.4-2. Heat transfer from a three-dimensional surface. The asymptotic analysis applies upstream of the separated and turbulent flow regions. These regions are illustrated for cylinders in Fig. 3.7-2.

EXAMPLE 12.4-3

Forced Convection in Steady Three-Dimensional Flow at High Prandtl Numbers^{8,9}

The technique introduced in the preceding example has been extended to flow around objects of arbitrary shape. Consider the steady flow of a fluid over a stationary object as shown in Fig. 12.4-2. The fluid approaches at a uniform temperature T_∞ , and the solid surface is maintained at a uniform temperature T_0 . The temperature distribution and heat transfer rate are to be found for the region of laminar flow, which extends downstream from the stagnation locus to the place where turbulence or flow separation begins. The velocity profiles are considered to be known.

The thermal boundary layer is considered to be very thin. This implies that the isotherms nearly coincide with the solid surface, so that the heat flux \mathbf{q} is nearly normal to the surface. It also implies that the complete velocity profiles are not needed here. We need to know the state of the motion only near the solid surface.

To capitalize on these simplifications, we choose the coordinates in a special way (see Fig. 12.4-2). We define y as the distance from the surface into the fluid just as in Fig. 12.4-1. We further define x and z as the coordinates of the nearest point on the surface, measured parallel and perpendicular to the tangential motion next to the surface. We express elements of arc in the x and z directions as $h_x dx$ and $h_z dz$, where h_x and h_z are position-dependent "scale factors" discussed in §A.7. Since we are interested here in the region of small y , the scale factors are treated as functions only of x and z .

With this choice of coordinates, the velocity components for small y become

$$v_x = \beta(x, z)y \quad (12.4-26)$$

$$v_y = \left(-\frac{1}{2h_x h_z} \frac{\partial}{\partial x} (h_z \beta) \right) y^2 \quad (12.4-27)$$

$$v_z = 0 \quad (12.4-28)$$

Here $\beta(x, z)$ is the local value of $\partial v_x / \partial y$ on the surface; it is positive in the nonseparated region, but may vanish at points of stagnation or separation. These equations are obtained by writing Taylor series for v_x and v_z , retaining terms through the first degree in y , and then inte-

⁸ W. E. Stewart, *AIChE Journal*, **9**, 528–535 (1963).

⁹ For related two-dimensional analyses, see M. J. Lighthill, *Proc. Roy. Soc., A* **202**, 359–377 (1950); V. G. Levich, *Physico-Chemical Hydrodynamics*, Chapter 2, Prentice-Hall, Englewood Cliffs, N.J. (1962); A. Acrivos, *Physics of Fluids*, **3**, 657–658 (1960).

grating the continuity equation with the boundary condition $v_y = 0$ at the surface to obtain v_y . These results are valid for Newtonian or non-Newtonian flow with temperature-independent density and viscosity.¹⁰

By a procedure analogous to that used in Example 12.4-2, one obtains a result similar to that given in Eq. 12.4-24. The only difference is that η is defined more generally as $\eta = y/\delta_T$, where δ_T is the thermal boundary layer thickness given by

$$\delta_T = \frac{1}{\sqrt{h_z \beta}} \left(9\alpha \int_{x_1(z)}^x \sqrt{h_z \beta} h_x h_z d\bar{x} \right)^{1/3} \quad (12.4-29)$$

and $x_1(z)$ is the upstream limit of the heat transfer region. From Eqs. 12.4-24 and 25 the local surface heat flux q_0 and the total heat flow for a heated region of the form $x_1(z) < x < x_2(z)$, $z_1 < z < z_2$ are

$$q_0 = \frac{k(T_0 - T_\infty)}{\Gamma(\frac{4}{3}) \delta_T} \quad (12.4-30)$$

$$Q = \frac{3^{1/3} k(T_0 - T_\infty)}{2\alpha^{1/3} \Gamma(\frac{4}{3})} \int_{z_1}^{z_2} \left(\int_{x_1(z)}^{x_2(z)} \sqrt{h_z \beta} h_x h_z d\bar{x} \right)^{2/3} dz \quad (12.4-31)$$

This last result shows how Q depends on the fluid properties, the velocity profiles, and the geometry of the system. We see that Q is proportional to the temperature difference, to $k/\alpha^{1/3} = k^{2/3} \rho^{1/3} C_p^{1/3}$, and to the $\frac{1}{3}$ -power of a mean velocity gradient over the surface.

Show how the above results can be used to obtain the heat transfer rate from a heated sphere of radius R with a viscous fluid streaming past it in creeping flow¹¹ (see Example 4.2-1 and Fig. 2.6-1).

SOLUTION

The boundary-layer coordinates x , y , and z may be identified here with $\pi - \theta$, $r - R$, and ϕ of Fig. 2.6-1. Then stagnation occurs at $\theta = \pi$, and separation occurs at $\theta = 0$. The scale factors are $h_x = R$, and $h_z = R \sin \theta$. The interfacial velocity gradient β is

$$\beta = -\left. \frac{\partial v_\theta}{\partial r} \right|_{r=R} = \frac{3}{2} \frac{v_\infty}{R} \sin \theta \quad (12.4-32)$$

Insertion of the above into Eqs. 12.4-29 and 31 gives the following results for forced convection heat transfer from an isothermal sphere of diameter D :

$$\begin{aligned} \delta_T &= \frac{1}{\sqrt{\frac{3}{2} v_\infty \sin^2 \theta}} \left(-9\alpha \int_\pi^0 \sqrt{\frac{3}{2} v_\infty \sin^2 \theta} R^2 \sin \theta d\theta \right)^{1/3} \\ &= (\frac{3}{4})^{1/3} D (\text{Re Pr})^{-1/3} \frac{(\pi - \theta + \frac{1}{2} \sin 2\theta)^{1/3}}{\sin \theta} \end{aligned} \quad (12.4-33)$$

$$\begin{aligned} Q &= \frac{3^{1/3} k(T_0 - T_\infty)}{2\alpha^{1/3} \Gamma(\frac{4}{3})} \int_0^{2\pi} \left(- \int_\pi^0 \sqrt{\frac{3}{2} v_\infty \sin^2 \theta} R^2 \sin \theta d\theta \right)^{2/3} d\phi \\ &= (\pi D^2)(T_0 - T_\infty) \left(\frac{k}{D} \right) \left[\frac{(3\pi)^{2/3}}{2^{7/3} \Gamma(\frac{4}{3})} \right] (\text{Re Pr})^{1/3} \end{aligned} \quad (12.4-34)$$

The constant in brackets is 0.991.

The behavior predicted by Eq. 12.4-33 is sketched in Fig. 12.4-3. The boundary layer thickness increases steadily from a small value at the stagnation point to an infinite value at separation, where the boundary layer becomes a wake extending downstream. The analysis here is most accurate for the forward part of the sphere, where δ_T is small; fortunately, that is

¹⁰ Temperature-dependent properties have been included by Acrivos, *loc. cit.*

¹¹ The solution to this problem was first obtained by V. G. Levich, *loc. cit.* It has been extended to somewhat higher Reynolds numbers by A. Acrivos and T. D. Taylor, *Phys. Fluids*, **5**, 387–394 (1962).

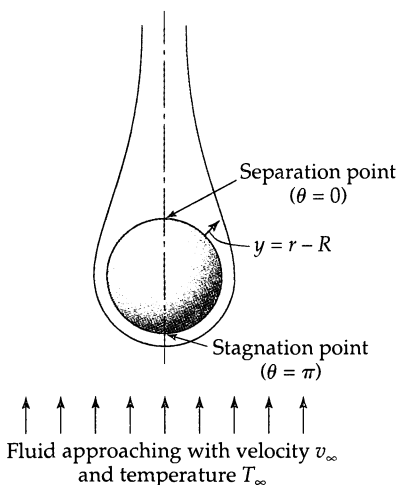


Fig. 12.4-3. Forced-convection heat transfer from a sphere in creeping flow. The shaded region shows the thermal boundary layer (defined by $\Pi_T \leq 0.99$ or $y \leq 1.5\delta_T$) for $\text{Pe} = \text{RePr} \approx 200$.

also the region where most of the heat transfer occurs. The result for Q is good within about 5% for $\text{RePr} > 100$; this limits its use primarily to fluids with $\text{Pr} > 100$, since creeping flow is obtained only at Re of the order of 1 or less.¹²

Results of the same form as Eq. 12.4-34 are obtained for creeping flow in other geometries, including packed beds.^{8,13}

It should be emphasized that the asymptotic solutions are particularly important: they are relatively easy to obtain, and for many applications they are sufficiently accurate. We will see in Chapter 14 that some of the standard heat transfer correlations are based on asymptotic solutions of the type discussed here.

QUESTIONS FOR DISCUSSION

1. How does Eq. 12.1-2 have to be modified if there is a heat source within the solid?
2. Show how Eq. 12.1-10 is obtained from Eq. 12.1-8. What is the viscous flow analog of this equation?
3. What kinds of heat conduction problems can be solved by Laplace transform and which cannot?
4. In Example 12.1-3 the heat flux and the temperature both satisfy the "heat conduction equation." Is this always true?
5. Draw a carefully labeled sketch of the results in Eqs. 12.1-38 and 40 showing what is meant by the statement that the "temperature oscillations lag behind the heat flux oscillations by $\pi/4$."
6. Verify that Eq. 12.1-40 satisfies the boundary conditions. Does it have to satisfy an initial condition? If so, what is it?
7. In Ex. 12.2-1, would the method of separation of variables work if applied directly to the function $\Theta(\xi, \zeta)$ rather than to $\Theta_d(\xi, \zeta)$?
8. In Example 12.2-2, how does the wall temperature depend on the downstream coordinate z ?
9. By means of a carefully labeled diagram, show what is meant by the two cases $\Delta \leq 1$ and $\Delta \geq 1$ in §12.4. Which case applies to dilute polyatomic gases? Organic liquids? Molten metals?
10. Summarize the situations in which the four mathematical methods in §12.1 are applicable.

¹² A review of analyses for a wide range of $\text{Pe} = \text{RePr}$ is given by S. K. Friedlander, *AIChE Journal*, **7**, 347–348 (1961).

¹³ J. P. Sørensen and W. E. Stewart, *Chem. Eng. Sci.*, **29**, 833–837 (1974).

PROBLEMS

- 12A.1. Unsteady-state heat conduction in an iron sphere.** An iron sphere of 1-in. diameter has the following physical properties: $k = 30 \text{ Btu/hr} \cdot \text{ft} \cdot \text{F}$, $\hat{C}_p = 0.12 \text{ Btu/lb}_m \cdot \text{F}$, and $\rho = 436 \text{ lb}_m/\text{ft}^3$. Initially the sphere is at a temperature of 70°F.

- (a) What is the thermal diffusivity of the sphere?
 (b) If the sphere is suddenly plunged into a large body of fluid of temperature 270°F, how much time is needed for the center of the sphere to attain a temperature of 128°F?
 (c) A sphere of the same size and same initial temperature, but made of another material, requires twice as long for its center to reach 128°F. What is its thermal diffusivity?
 (d) The chart used in the solution of (b) and (c) was prepared from the solution to a partial differential equation. What is that differential equation?

Answers: (a) $0.574 \text{ ft}^2/\text{hr}$; (b) 1.1 sec; (c) $0.287 \text{ ft}^2/\text{hr}$

- 12A.2 Comparison of the two slab solutions for short times.** What error is made by using Eq. 12.1-8 (based on the semi-infinite slab) instead of Eq. 12.1-31 (based on the slab of finite thickness), when $at/b^2 = 0.01$ and for a position 0.9 of the way from the midplane to the slab surface? Use the graphically presented solutions for making the comparison.

Answer: 4%

- 12A.3 Bonding with a thermosetting adhesive¹** (Fig. 12A.3). It is desired to bond together two sheets of a solid material, each of thickness 0.77 cm. This is done by using a thin layer of thermosetting material, which fuses and forms a good bond at 160°C. The two plates are inserted in a press, with both platens of the press maintained at a constant temperature of 220°C. How long will the sheets have to be held in the press, if they are initially at 20°C? The solid sheets have a thermal diffusivity of $4.2 \times 10^{-3} \text{ cm}^2/\text{s}$.

Answer: 85 s

- 12A.4. Quenching of a steel billet.** A cylindrical steel billet 1 ft in diameter and 3 ft long, initially at 1000°F, is quenched in oil. Assume that the surface of the billet is at 200°F during the quenching process. The steel has the following properties, which may be assumed to be independent of the temperature: $k = 25 \text{ Btu/hr} \cdot \text{ft} \cdot \text{F}$, $\rho = 7.7 \text{ g/cm}^3$, and $C_p = 0.12 \text{ cal/g} \cdot \text{C}$.

Estimate the temperature of the hottest point in the billet after five minutes of quenching. Neglect end effects; that is, make the calculation for a cylinder of the given diameter but of infinite length. See Problem 12C.1 for the method for taking end effects into account.

Answer: 750°F

- 12A.5. Measurement of thermal diffusivity from amplitude of temperature oscillations.**

- (a) It is desired to use the results of Example 12.1-3 to measure the thermal diffusivity $\alpha = k/\rho\hat{C}_p$ of a solid material. This may be done by measuring the amplitudes A_1 and A_2 at two

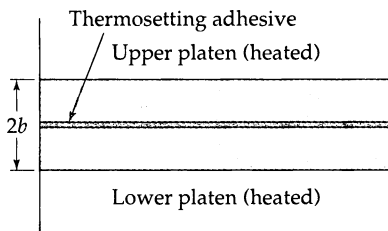


Fig. 12A.3. Two sheets of solid material with a thin layer of adhesive in between.

¹ This problem is based on Example 10 of J. M. McKelvey, Chapter 2 of *Processing of Thermoplastic Materials* (E. C. Bernhardt, ed.), Reinhold, New York (1959), p. 93.

points at distances y_1 and y_2 from the periodically heated surface. Show that the thermal diffusivity may then be estimated from the formula

$$\alpha = \frac{\omega}{2} \left(\frac{y_2 - y_1}{\ln(A_1/A_2)} \right)^2 \quad (12A.4-1)$$

(b) Calculate the thermal diffusivity α when the sinusoidal surface heat flux has a frequency 0.0030 cycles/s, if $y_2 - y_1 = 6.19$ cm and the amplitude ratio A_1/A_2 is 6.05.

Answer: $\alpha = 0.111$

- 12A.6. Forced convection from a sphere in creeping flow.** A sphere of diameter D , whose surface is maintained at a temperature T_0 , is located in a fluid stream approaching with a velocity v_∞ and temperature T_∞ . The flow around the sphere is in the "creeping flow" regime—that is, with the Reynolds number less than about 0.1. The heat loss from the sphere is described by Eq. 12.4-34.

(a) Verify that the equation is dimensionally correct.

(b) Estimate the rate of heat transfer, Q , for the flow around a sphere of diameter 1 mm. The fluid is an oil at $T_\infty = 50^\circ\text{C}$ moving at a velocity 1.0 cm/sec with respect to the sphere, the surface of which is at a temperature of 100°C . The oil has the following properties: $\rho = 0.9 \text{ g/cm}^3$, $\hat{C}_p = 0.45 \text{ cal/g}\cdot\text{K}$, $k = 3.0 \times 10^{-4} \text{ cal/s}\cdot\text{cm}\cdot\text{K}$, and $\mu = 150 \text{ cp}$.

- 12B.1. Measurement of thermal diffusivity in an unsteady-state experiment.** A solid slab, 1.90 cm thick, is brought to thermal equilibrium in a constant-temperature bath at 20.0°C . At a given instant ($t = 0$) the slab is clamped tightly between two thermostatted copper plates, the surfaces of which are carefully maintained at 40.0°C . The midplane temperature of the slab is sensed as a function of time by means of a thermocouple. The experimental data are:

t (sec)	0	120	240	360	480	600
T (C)	20.0	24.4	30.5	34.2	36.5	37.8

Determine the thermal diffusivity and thermal conductivity of the slab, given that $\rho = 1.50 \text{ g/cm}^3$ and $\hat{C}_p = 0.365 \text{ cal/g}\cdot\text{C}$.

Answer: $\alpha = 1.50 \times 10^{-3} \text{ cm}^2/\text{s}$; $k = 7.9 \times 10^{-4} \text{ cal/s}\cdot\text{cm}\cdot\text{C}$ or $0.19 \text{ Btu/hr}\cdot\text{ft}\cdot\text{F}$

- 12B.2. Two-dimensional forced convection with a line heat source.** A fluid at temperature T_∞ flows in the x direction across a long, infinitesimally thin wire, which is heated electrically at a rate Q/L (energy per unit time per unit length). The wire thus acts as a line heat source. It is assumed that the wire does not disturb the flow appreciably. The fluid properties (density, thermal conductivity, and heat capacity) are assumed constant and the flow is assumed uniform. Furthermore, radiant heat transfer from the wire is neglected.

(a) Simplify the energy equation to the appropriate form, by neglecting the heat conduction in the x direction with respect to the heat transport by convection. Verify that the following conditions on the temperature are reasonable:

$$T \rightarrow T_\infty \quad \text{as } y \rightarrow \infty \quad \text{for all } x \quad (12B.2-1)$$

$$T = T_\infty \quad \text{at } x < 0 \quad \text{for all } y \quad (12B.2-2)$$

$$\int_{-\infty}^{+\infty} \rho \hat{C}_p (T - T_\infty) |_x v_x dy = Q/L \quad \text{for all } x > 0 \quad (12B.2-3)$$

(b) Postulate a solution of the form (for $x > 0$)

$$T(x, y) - T_\infty = f(x)g(\eta) \quad \text{where } \eta = y/\delta(x) \quad (12B.2-4)$$

Show by means of Eq. 12B.2-3 that $f(x) = C_1/\delta(x)$. Then insert Eq. 12B.2-4 into the energy equation and obtain

$$-\left[\frac{v_x \delta}{\alpha} \frac{d\delta}{dx} \right] \frac{d}{d\eta} (\eta g) = \frac{d^2 g}{d\eta^2} \quad (12B.2-5)$$

(c) Set the quantity in brackets in Eq. 12B.2-5 equal to 2 (why?), and then solve to get $\delta(x)$.

- (d) Then solve the equation for $g(\eta)$.
 (e) Finally, evaluate the constant C_1 , and thereby complete the derivation of the temperature distribution.

12B.3. Heating of a wall (constant wall heat flux). A very thick solid wall is initially at the temperature T_0 . At time $t = 0$, a constant heat flux q_0 is applied to one surface of the wall (at $y = 0$), and this heat flux is maintained. Find the time-dependent temperature profiles $T(y, t)$ for small times. Since the wall is very thick it can be safely assumed that the two wall surfaces are an infinite distance apart in obtaining the temperature profiles.

- (a) Follow the procedure used in going from Eq. 12.1-33 to Eq. 12.1-35, and then write the appropriate boundary and initial conditions. Show that the analytical solution of the problem is

$$T(y, t) - T_0 = \frac{q_0}{k} \left(\sqrt{\frac{4\alpha t}{\pi}} \exp(-y^2/4\alpha t) - \frac{2y}{\sqrt{\pi}} \int_{y/\sqrt{4\alpha t}}^{\infty} \exp(-u^2) du \right) \quad (12B.3-1)$$

- (b) Verify that the solution is correct by substituting it into the one-dimensional heat conduction equation for the temperature (see Eq. 12.1-33). Also show that the boundary and initial conditions are satisfied.

12B.4. Heat transfer from a wall to a falling film (short contact time limit)² (Fig. 12B.4). A cold liquid film flowing down a vertical solid wall, as shown in the figure, has a considerable cooling effect on the solid surface. Estimate the rate of heat transfer from the wall to the fluid for such short contact times that the fluid temperature changes appreciably only in the immediate vicinity of the wall.

- (a) Show that the velocity distribution in the falling film, given in §2.2, may be written as $v_z = v_{z,\max}[2(y/\delta) - (y/\delta)^2]$, in which $v_{z,\max} = \rho g \delta^2 / 2\mu$. Then show that in the vicinity of the wall the velocity is a linear function of y given by

$$v_z \approx \frac{\rho g \delta}{\mu} y \quad (12B.4-1)$$

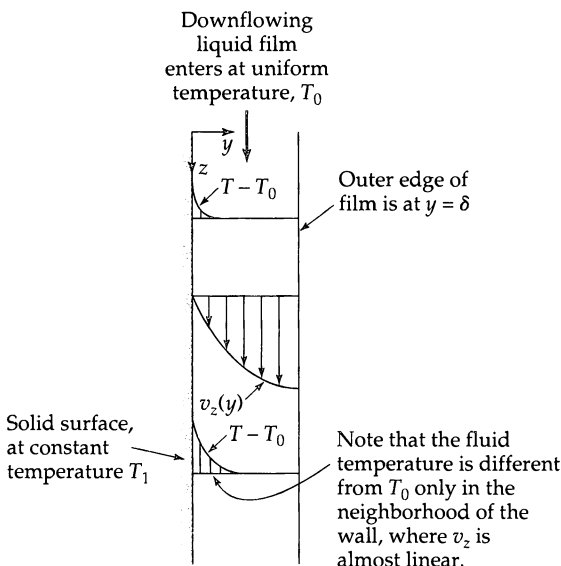


Fig. 12B.4. Heat transfer to a film falling down a vertical wall.

² R. L. Pigford, *Chemical Engineering Progress Symposium Series*, 51, No. 17, 79–92 (1955). Robert Lamar Pigford (1917–1988), who taught at both the University of Delaware and the University of California in Berkeley, researched many aspects of diffusion and mass transfer; he was the founding editor of *Industrial and Engineering Chemistry Fundamentals*.

(b) Show that the energy equation for this situation reduces to

$$\rho \hat{C}_p v_z \frac{\partial T}{\partial z} = k \frac{\partial^2 T}{\partial y^2} \quad (12B.4-2)$$

List all the simplifying assumptions needed to get this result. Combine the preceding two equations to obtain

$$y \frac{\partial T}{\partial z} = \beta \frac{\partial^2 T}{\partial y^2} \quad (12B.4-3)$$

in which $\beta = \mu k / \rho^2 \hat{C}_p g \delta$.

(c) Show that for short contact times we may write as boundary conditions

$$\text{B.C. 1: } T = T_0 \quad \text{for } z = 0 \quad \text{and } y > 0 \quad (12B.4-4)$$

$$\text{B.C. 2: } T = T_0 \quad \text{for } y = \infty \quad \text{and } z \text{ finite} \quad (12B.4-5)$$

$$\text{B.C. 3: } T = T_1 \quad \text{for } y = 0 \quad \text{and } z > 0 \quad (12B.4-6)$$

Note that the true boundary condition at $y = \delta$ is replaced by a fictitious boundary condition at $y = \infty$. This is possible because the heat is penetrating just a very short distance into the fluid.

(d) Use the dimensionless variables $\Theta(\eta) = (T - T_0)/(T_1 - T_0)$ and $\eta = y/\sqrt[3]{9\beta z}$ to rewrite the differential equation as (see Eq. C.1-9):

$$\frac{d^2\Theta}{d\eta^2} + 3\eta^2 \frac{d\Theta}{d\eta} = 0 \quad (12B.4-7)$$

Show that the boundary conditions are $\Theta = 0$ for $\eta = \infty$ and $\Theta = 1$ at $\eta = 0$.

(e) In Eq. 12B.4-7, set $d\Theta/d\eta = p$ and obtain an equation for $p(\eta)$. Solve that equation to get $d\Theta/d\eta = p(\eta) = C_1 \exp(-\eta^3)$. Show that a second integration and application of the boundary conditions give

$$\Theta = \frac{\int_{\eta}^{\infty} \exp(-\bar{\eta}^3) d\bar{\eta}}{\int_0^{\infty} \exp(-\bar{\eta}^3) d\bar{\eta}} = \frac{1}{\Gamma(\frac{4}{3})} \int_{\eta}^{\infty} \exp(-\bar{\eta}^3) d\bar{\eta} \quad (12B.4-8)$$

(f) Show that the average heat flux to the fluid is

$$q_{\text{avg}}|_{y=0} = \frac{3}{2} \frac{(9\beta L)^{-1/3}}{\Gamma(\frac{4}{3})} k(T_1 - T_0) \quad (12B.4-9)$$

where use is made of the Leibniz formula in §C.3.

12B.5. Temperature in a slab with heat production. The slab of thermal conductivity k in Example 12.1-2 is initially at a temperature T_0 . For time $t > 0$ there is a uniform volume production of heat S_0 within the slab.

(a) Obtain an expression for the dimensionless temperature $k(T - T_0)/S_0 b^2$ as a function of the dimensionless coordinate $\eta = y/b$ and the dimensionless time by looking up the solution in the book by Carslaw and Jaeger.

(b) What is the maximum temperature reached at the center of the slab?

(c) How much time elapses before 90% of the temperature rise occurs?

Answer: (c) $t \approx b^2/\alpha$

12B.6. Forced convection in slow flow across a cylinder (Fig. 12B.6). A long cylinder of radius R is suspended in an infinite fluid of constant properties ρ, μ, \hat{C}_p , and k . The fluid approaches with

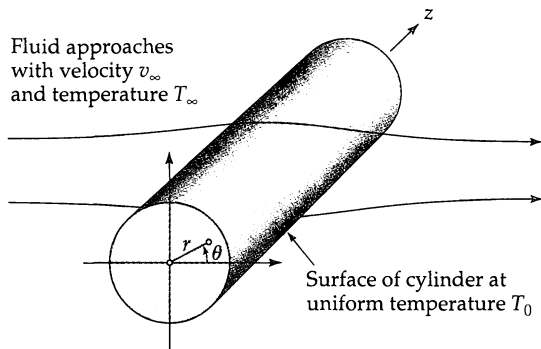


Fig. 12B.6. Heat transfer from a long cylinder of radius R .

temperature T_∞ and velocity v_∞ . The cylindrical surface is maintained at temperature T_0 . For this system the velocity distribution has been determined by Lamb³ in the limit of $\text{Re} \ll 1$. His result for the region close to the cylinder is

$$\psi = -\frac{v_\infty R \sin \theta}{2S} \left[\frac{r}{R} \left(2 \ln \frac{r}{R} - 1 \right) + \frac{R}{r} \right] \quad (12B.6-1)$$

in which ψ is the first polar-coordinate stream function in Table 4.2-1. The dimensionless quantity S is given by $S = \frac{1}{2} - \gamma + \ln(8/\text{Re})$, where $\gamma = 0.5772 \dots$ is "Euler's constant," and $\text{Re} = Dv_\infty \rho / \mu$.

- (a) For this system, determine the interfacial velocity gradient β defined in Example 12.4-3.
- (b) Determine the rate of heat loss Q from a length L of the cylinder using the method of Example 12.4-3. Note that

$$\int_0^\pi \sqrt{\sin \theta} d\theta = B(\frac{3}{4}, \frac{1}{2}) = 2.3963 \dots \quad (12B.6-2)$$

where $B(m, n) = \Gamma(m)\Gamma(n)/\Gamma(m+n)$ is the "beta function."

- (c) Determine δ_T/R at $\theta = 0, \frac{1}{2}\pi$, and π .

Answers: (a) $\beta = \frac{2v_\infty \sin \theta}{RS}$

(b) $Q = C(\pi DL)(T_0 - T_\infty) \left(\frac{k}{D} \right) \left(\frac{\text{Re Pr}}{S} \right)^{1/3}$ (Evaluate the constant C)

(c) $\frac{\delta_T}{R} = \left(\frac{9S}{\text{Re Pr}} \right)^{1/3} f(\theta); f = \infty, 1.1982, (\frac{2}{3})^{1/3}$

12B.7. Timetable for roasting turkey

- (a) A homogeneous solid body of arbitrary shape is initially at temperature T_0 throughout. At $t = 0$ it is immersed in a fluid medium of temperature T_1 . Let L be a characteristic length in the solid. Show that dimensional analysis predicts that

$$\Theta = \Theta(\xi, \eta, \zeta, \tau, \text{and geometrical ratios}) \quad (12B.7-1)$$

where $\Theta = (T - T_0)/(T_1 - T_0)$, $\xi = x/L$, $\eta = y/L$, $\zeta = z/L$, and $\tau = at/L^2$. Relate this result to the graphs given in §12.1.

³ H. Lamb, *Phil. Mag.*, (6) 21, 112–110 (1911). For a survey of more detailed analyses, see L. Rosenhead (ed.), *Laminar Boundary Layers*, Oxford University Press, London (1963), Chapter 4.

(b) A typical timetable for roasting turkey at 350°F is⁴

Mass of turkey (lb _m)	Time required per unit mass (min/lb _m)
6–10	20–25
10–16	18–20
18–25	15–18

Compare this empirically determined cooking schedule with the results of part (a), for geometrically similar turkeys at an initial temperature T_0 , cooked with a given surface temperature T_1 to the same dimensionless temperature distribution $\Theta = \Theta(\xi, \eta, \zeta)$.

12B.8. Use of asymptotic boundary layer solution. Use the results of Ex. 12.4-2 to obtain δ_T and q_0 for the system in Problem 12D.4. By comparing δ_T with D , estimate the range of applicability of the solution obtained in Problem 12D.4.

12B.9. Non-Newtonian heat transfer with constant wall heat flux (asymptotic solution for small axial distances). Rework Example 12.2-2 for a fluid whose non-Newtonian behavior is described adequately by the power law model. Show that the solution given in Eq. 12.2-2 may be taken over for the power law model simply by an appropriate modification in the definition of v_0 .

12C.1. Product solutions for unsteady heat conduction in solids.

(a) In Example 12.1-2 the unsteady state heat conduction equation is solved for a slab of thickness $2b$. Show that the solution to Eq. 12.1-2 for the analogous problem for a rectangular block of finite dimensions $2a$, $2b$, and $2c$ may be written as the product of the solutions for three slabs of corresponding dimensions:

$$\frac{T_1 - T(x, y, z, t)}{T_1 - T_0} = \Theta\left(\frac{x}{a}, \frac{\alpha t}{a^2}\right)\Theta\left(\frac{y}{b}, \frac{\alpha t}{b^2}\right)\Theta\left(\frac{z}{c}, \frac{\alpha t}{c^2}\right) \quad (12C.1-1)$$

in which $\Theta(y/b, \alpha t/b^2)$ is the right side of Eq. 12.1-31.

(b) Prove a similar result for cylinders of finite length; then rework Problem 12A.4 without the assumption that the cylinder is infinitely long.

12C.2. Heating of a semi-infinite slab with variable thermal conductivity. Rework Example 12.1-1 for a solid whose thermal conductivity varies with temperature as follows:

$$\frac{k}{k_0} = 1 + \beta\left(\frac{T - T_0}{T_1 - T_0}\right) \quad (12C.2-1)$$

in which k_0 is the thermal conductivity at temperature T_0 , and β is a constant. Use the following approximate procedure:

(a) Let $\Theta = (T - T_0)/(T_1 - T_0)$ and $\eta = y/\delta(t)$, where $\delta(t)$ is a boundary layer thickness that changes with time. Then assume that

$$\Theta(y, t) = \Phi(\eta) \quad (12C.2-2)$$

in which the function $\Phi(\eta)$ gives the shapes of the “similar” profiles. This is tantamount to assuming that the temperature profiles have the same shape for all values of β , which, of course, is not really true.

(b) Substitute the above approximate profiles into the heat conduction equation and obtain the following differential equation for the boundary layer thickness:

$$M\delta \frac{d\delta}{dt} = \alpha_0 N \quad (12C.2-3)$$

⁴ *Woman's Home Companion Cook Book*, Garden City Publishing Co., (1946), courtesy of Jean Stewart.

in which $\alpha_0 = k_0/\rho\hat{C}_p$ and

$$M = \int_0^1 \Phi(\eta) d\eta \text{ and } N = (1 + \beta\Phi)(d\Phi/d\eta)|_0^1 \quad (12C.2-4, 5)$$

Then solve for the function $\delta(t)$.

(c) Now let $\Phi(\eta) = 1 - \frac{3}{2}\eta + \frac{1}{2}\eta^3$. Why is this a felicitous choice? Then find the time-dependent temperature distribution $T(y, t)$ as well as the heat flux at $y = 0$.

- 12C.3.** Heat conduction with phase change (the *Neumann–Stefan problem*) (Fig. 12C.3)⁵. A liquid, contained in a long cylinder, is initially at temperature T_1 . For time $t \geq 0$, the bottom of the container is maintained at a temperature T_0 , which is below the melting point T_m . We want to estimate the movement of the solid–liquid interface, $Z(t)$, during the freezing process.

For the sake of simplicity, we assume here that the physical properties ρ , k , and \hat{C}_p are constants and the same in both the solid and liquid phases. Let $\Delta\dot{H}_f$ be the heat of fusion per gram, and use the abbreviation $\Lambda = \Delta\dot{H}_f/\hat{C}_p(T_1 - T_0)$.

(a) Write the equation for heat conduction for the liquid (L) and solid (S) regions; state the boundary and initial conditions.

(b) Assume solutions of the form:

$$\Theta_S \equiv \frac{T_S - T_0}{T_1 - T_0} = C_1 + C_2 \operatorname{erf} \frac{z}{\sqrt{4\alpha t}} \quad (12C.3-1)$$

$$\Theta_L \equiv \frac{T_L - T_0}{T_1 - T_0} = C_3 + C_4 \operatorname{erf} \frac{z}{\sqrt{4\alpha t}} \quad (12C.3-2)$$

(c) Use the boundary condition at $z = 0$ to show that $C_1 = 0$, and the condition at $z = \infty$ to show that $C_3 = 1 - C_4$. Then use the fact that $T_S = T_L = T_m$ at $z = Z(t)$ to conclude that $Z(t) = \lambda\sqrt{4\alpha t}$, where λ is some (as yet undetermined) constant. Then get C_3 and C_4 in terms of λ . Use the remaining boundary condition to get λ in terms of Λ and $\Theta_m = (T_m - T_0)/(T_1 - T_0)$:

$$\sqrt{\pi}\Lambda\lambda \exp \lambda^2 = \frac{\Theta_m}{\operatorname{erf} \lambda} - \frac{1 - \Theta_m}{1 - \operatorname{erf} \lambda} \quad (12C.3-3)$$

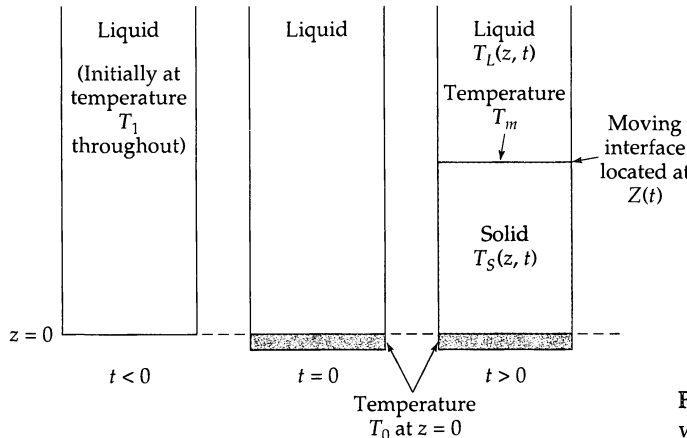


Fig. 12C.3. Heat conduction with solidification.

⁵ For literature references and related problems, see H. S. Carslaw and J. C. Jaeger, *Conduction of Heat in Solids*, 2nd edition, Oxford University Press (1959), Chapter XI; on pp. 283–286 the problem considered here is worked out for the situation that the physical properties of the liquid and solid phases are different. See also S. G. Bankoff, *Advances in Chemical Engineering*, Vol. 5, Academic Press, New York (1964), pp. 75–150; J. Crank, *Free and Moving Boundary Problems*, Oxford University Press (1984); J. M. Hill, *One-Dimensional Stefan Problems*, Longmans (1987).

What is the final expression for $Z(t)$? (Note: In this problem it has been assumed that a phase change occurs instantaneously and that no supercooling of the liquid phase occurs. It turns out that in the freezing of many liquids, this assumption is untenable. That is, to describe the solidification process correctly, one has to take into account the kinetics of the crystallization process.⁶⁾

- 12C.4.** **Viscous heating in oscillatory flow.**⁷ Viscous heating can be a disturbing factor in viscosity measurements. Here we see how viscous heating can affect the measurement of viscosity in an oscillating-plate system.

A Newtonian fluid is located in the region between two parallel plates separated by a distance b . Both plates are maintained at a temperature T_0 . The lower plate (at $z = 0$) is made to oscillate sinusoidally in the z direction with a velocity amplitude v_0 and a circular frequency ω . Estimate the temperature rise resulting from viscous heating. Consider only the high-frequency limit.

- (a) Show that the velocity distribution is given by

$$\frac{v_z(x, t)}{v_0} = \frac{\left[\begin{array}{l} \left(\sinh a(1 - \xi) \cos a(1 - \xi) \sinh a \cos a \right) \cos \omega t \\ + \left(\sin a(1 - \xi) \cosh a(1 - \xi) \sin a \cosh a \right) \sin \omega t \\ + \left(-\sin a(1 - \xi) \cosh a(1 - \xi) \sinh a \cos a \right) \sin \omega t \\ + \left(\sinh a(1 - \xi) \cos a(1 - \xi) \sin a \cosh a \right) \cos \omega t \end{array} \right]}{\sinh^2 a \cos^2 a + \cosh^2 a \sin^2 a} \quad (12C.4-1)$$

where $a = \sqrt{\rho \omega b^2 / 2\mu}$ and $\xi = x/b$.

- (b) Next calculate the dissipation function Φ_v for the velocity profile in Eq. 12C.4-1. Then obtain a time-averaged dissipation function $\bar{\Phi}_v$, by averaging over one cycle. Use the formulas

$$\overline{\cos^2 \omega t} = \overline{\sin^2 \omega t} = \frac{1}{2} \quad \text{and} \quad \overline{\sin \omega t \cos \omega t} = 0 \quad (12C.4-2)$$

which may be verified. Then simplify the result for high frequencies (i.e., for large values of a) to obtain

$$\bar{\Phi}_v (\text{large } \omega) = a^2 \left(\frac{v_0}{b} \right)^2 e^{-2a\xi} \quad (12C.4-3)$$

- (c) Next take a time average of the heat conduction equation to obtain

$$0 = k \frac{d^2 \bar{T}}{dx^2} + \mu \bar{\Phi}_v \quad (12C.4-4)$$

in which \bar{T} is the temperature averaged over one cycle. Solve this to get

$$\bar{T} - T_0 = \left(\frac{\mu v_0^2}{4k} \right) [(1 - e^{-2a\xi}) - (1 - e^{-2a})\xi] \quad (12C.4-5)$$

This shows how the temperature in the slit depends on position. From this function, the maximum temperature rise can be calculated. For reasonably high frequencies, $\bar{T} - T_0 \approx \mu v_0^2 / 4k$.

- 12C.5. Solar heat penetration.** Many desert animals protect themselves from excessive diurnal temperature fluctuations by burrowing sufficiently far underground that they can maintain

⁶ H. Janeschitz-Kriegl, *Plastics and Rubber Processing and Applications*, 4, 145–158 (1984); H. Janeschitz-Kriegl, in *One-Hundred Years of Chemical Engineering* (N. A. Peppas, ed.), Kluwer Academic Publishers, Dordrecht (Netherlands) (1989), pp. 111–124; H. Janeschitz-Kriegl, E. Ratajski, and G. Eder, *Ind. Eng. Chem. Res.*, 34, 3481–3487 (1995); G. Astarita and J. M. Kenny, *Chem. Eng. Comm.*, 53, 69–84 (1987).

⁷ R. B. Bird, *Chem. Eng. Prog. Symposium Series*, Vol. 61, No. 58 (1965), pp. 13–14; see also F. Ding, A. J. Giacomin, R. B. Bird, and C-B Kweon, *J. Non-Newtonian Fluid Mech.*, 86, 359–374 (1999).

themselves at a reasonably steady temperature. Let the temperature in the ground be $T(y, t)$, where y is the depth below the surface of the earth and t is the time, measured from the time of maximum temperature T_0 . Further, let the temperature far beneath the surface be T_∞ , and let the surface temperature be given by

$$\begin{aligned} T(0, t) - T_\infty &= 0 && \text{for } t < 0 \\ T(0, t) - T_\infty &= (T_0 - T_\infty) \cos \omega t && \text{for } t \geq 0 \end{aligned} \quad (12C.5-1)$$

Here $\omega = 2\pi/t_{\text{per}}$, in which t_{per} is the time for one full cycle of the oscillating temperature—namely, 24 hours. Then it can be shown that the temperature at any depth is given by

$$\begin{aligned} \frac{T(y, t) - T_\infty}{T_0 - T_\infty} &= e^{-\sqrt{\omega/2\alpha}y} \cos(\omega t - \sqrt{\omega/2\alpha}y) \\ &\quad - \frac{1}{\pi} \int_0^\infty e^{-\bar{\omega}t} (\sin \sqrt{\bar{\omega}/\alpha}y) \frac{\bar{\omega}}{\omega^2 + \bar{\omega}^2} d\bar{\omega} \end{aligned} \quad (12C.5-2)$$

This equation is the heat conduction analog of Eq. 4D.1-1, which describes the response of the velocity profiles near an oscillating plate. The first term describes the “periodic steady state” and the second the “transient” behavior. Assume the following properties for the soil:⁸ $\rho = 1515 \text{ kg/m}^3$, $k = 0.027 \text{ W/m}\cdot\text{K}$, and $\hat{C}_p = 800 \text{ J/kg}\cdot\text{K}$.

- (a) Assume that the heating of the earth’s surface is exactly sinusoidal, and find the amplitude of the temperature variation beneath the surface at a distance y . To do this, use only the periodic steady state term in Eq. 12C.5-2. Show that at a depth of 10 cm, this amplitude has the value of 0.0172.
- (b) Discuss the importance of the transient term in Eq. 12C.5-2. Estimate the size of this contribution.
- (c) Next consider an arbitrary formal expression for the daily surface temperature, given as a Fourier series of the form

$$\frac{T(0, t) - T_\infty}{T_0 - T_\infty} = \sum_{n=0}^{\infty} (a_n \cos n\omega t + b_n \sin n\omega t) \quad (12C.5-3)$$

How many terms in this series are used to solve part (a)?

- 12C.6. Heat transfer in a falling non-Newtonian film.** Repeat Problem 12B.4 for a polymeric fluid that is reasonably well described by the power law model of Eq. 8.3-3.

12D.1. Unsteady-state heating of a slab (Laplace transform method).

- (a) Re-solve the problem in Example 12.1-2 by using the Laplace transform, and obtain the result in Eq. 12.1-31.
- (b) Note that the series in Eq. 12.1-31 does not converge rapidly at short times. By inverting the Laplace transform in a way different from that in (a), obtain a different series that is rapidly convergent for small times.⁹
- (c) Show how the first term in the series in (b) is related to the “short contact time” solution of Example 12.1-1.

12D.2. The Graetz-Nusselt problem (Table 12D.2).

- (a) A fluid (Newtonian or generalized Newtonian) is in laminar flow in a circular tube of radius R . In the inlet region $z < 0$, the fluid temperature is uniform at T_1 . In the region $z > 0$, the wall temperature is maintained at T_0 . Assume that all physical properties are constant and

⁸ W. M. Rohsenow, J. P. Hartnett, and Y. I. Cho, eds., *Handbook of Heat Transfer*, 3rd edition, McGraw-Hill (1998), p. 2.68.

⁹ H. S. Carslaw and J. C. Jaeger, *Conduction of Heat in Solids*, 2nd edition, Oxford University Press (1959), pp. 308–310.

that viscous dissipation and axial heat conduction effects are negligible. Use the following dimensionless variables:

$$\Theta = \frac{T - T_0}{T_1 - T_0} \quad \phi = \frac{v_z}{\langle v_z \rangle} \quad \xi = \frac{r}{R} \quad \zeta = \frac{\alpha z}{\langle v_z \rangle R^2} \quad (12D.2-1)$$

Show that the temperature profiles in this system are

$$\Theta = \sum_{i=1}^{\infty} A_i X_i(\xi) \exp(-\beta_i^2 \zeta) \quad (12D.2-2)$$

in which X_i and β_i are the eigenfunctions and eigenvalues obtained from the solution to the following equation:

$$\frac{1}{\xi} \frac{d}{d\xi} \left(\xi \frac{dX_i}{d\xi} \right) + \beta_i^2 \phi X_i = 0 \quad (12D.2-3)$$

with boundary conditions $X = \text{finite}$ at $\xi = 0$ and $X = 0$ at $\xi = 1$. Show further that

$$A_i = \frac{\int_0^1 X_i \phi \xi \, d\xi}{\int_0^1 X_i^2 \xi \, d\xi} \quad (12D.2-4)$$

(b) Solve Eq. 12D.2-3 for the Newtonian fluid by obtaining a power series solution for X_i . Calculate the lowest eigenvalue by solving an algebraic equation. Check your result against that given in Table 12D.2.

(c) From the work involved in (b) in computing β_i^2 it can be inferred that the computation of the higher eigenvalues is quite tedious. For eigenvalues higher than the second or third the Wenzel-Kramers-Brillouin (WKB) method¹⁰ can be used; the higher the eigenvalue, the more accurate the WKB method is. Read about this method, and verify that for the Newtonian fluid

$$\beta_i^2 = \frac{1}{2}(4i - \frac{4}{3})^2 \quad (12D.2-5)$$

A similar formula has been derived for the power law model.¹¹

Table 12D.2 Eigenvalues β_i^2 for the Graetz-Nusselt Problem for Newtonian Fluids^a

<i>i</i>	By direct calculation ^b	By WKB method ^c	By Stodola and Vianello method ^d
1	3.67	3.56	3.661 ^c
2	22.30	22.22	—
3	56.95	56.88	—
4	107.6	107.55	—

^a The β_i^2 here correspond to $\frac{1}{2}\lambda_i^2$ in W. M. Rohsenow, J. P. Hartnett, and Y. I. Cho, *Handbook of Heat Transfer*, McGraw-Hill (New York), Table 5.3 on p. 510.

^b Values taken from K. Yamagata, *Memoirs of the Faculty of Engineering, Kyushu University*, Volume VIII, No. 6, Fukuoka, Japan (1940).

^c Computed from Eq. 12D.2-5.

^d For the particular trial function in part (d) of the problem.

¹⁰ J. Heading, *An Introduction to Phase-Integral Methods*, Wiley, New York (1962); J. R. Sellars, M. Tribus, and J. S. Klein, *Trans. ASME*, **78**, 441–448 (1956).

¹¹ I. R. Whiteman and W. B. Drake, *Trans. ASME*, **80**, 728–732 (1958).

(d) Obtain the lowest eigenvalue by the method of Stodola and Vianello. Use Eqs. 71a and 72b on p. 203 of Hildebrand's book,¹² with $\phi = 2(1 - \xi^2)$ for Newtonian flow and $X_1 = 1 - \xi^2$ as a simple, but suitable, trial function. Show that this leads quickly to the value $\beta_1^2 = 3.661$.

- 12D.3. The Graetz-Nusselt problem (asymptotic solution for large z).** Note that, in the limit of very large z , only one term ($i = 1$) is needed in Eq. 12D.2-2. It is desired to use this result to compute the heat flux at the wall, q_0 , at large z and to express the result as

$$q_0 = (\text{a function of system and fluid properties}) \times (T_b - T_0) \quad (12D.3-1)$$

where T_b is the "bulk fluid temperature" defined in Eq. 10.8-33.

(a) First verify that

$$q_0 = -\frac{k}{R} \frac{\partial \Theta / \partial \xi|_{\xi=1}}{\Theta_b} (T_b - T_0) \quad (12D.3-2)$$

Here Θ is the same as in Problem 12D.2, and $\Theta_b = (T_b - T_0)/(T_1 - T_0)$.

(b) Show that for large z , Eq. 12D.3-2 and Eq. 12D.2-2 both give

$$q_0 = \frac{k}{2R} \beta_1^2 (T_b - T_0) \quad (12D.3-3)$$

Hence for large z , all one needs to know is the first eigenvalue; the eigenfunctions need not be calculated. This shows how useful the method of Stodola and Vianello¹² is for computing the limiting value of a heat flux.

- 12D.4. The Graetz-Nusselt problem (asymptotic solution for small z).**

(a) Apply the method of Example 12.2-2 to the solution of the problem discussed in Problem 12D.2. Consider a Newtonian fluid and use the following dimensionless quantities:

$$\Theta = \frac{T_1 - T}{T_1 - T_0} \quad \zeta = \frac{z}{R} \quad \sigma = \frac{R - r}{R} = \frac{s}{R} \quad N = \frac{4\langle v_z \rangle R}{\alpha} \quad (12D.4-1)$$

Show that the method of combination of variables gives

$$\Theta = \frac{1}{\Gamma(\frac{4}{3})} \int_{\eta}^{\infty} \exp(-\bar{\eta}^3) d\bar{\eta} \quad (12D.4-2)$$

in which $\eta = (N\sigma^3/9\zeta)^{1/3}$.

(b) Show that the wall flux is

$$q_r|_{r=R} = \frac{k}{R} \left[\frac{1}{9^{1/3} \Gamma(\frac{4}{3})} \left(\text{Re Pr} \frac{D}{z} \right)^{1/3} \right] (T_1 - T_0) \quad (12D.4-3)$$

The quantity $(\text{Re Pr} D/z) = (4/\pi)(w\hat{C}_p/kz)$ appears frequently; the grouping $Gz = (w\hat{C}_p/kz)$ is called the *Graetz number*. Compare this result with that in Eq. 12D.3-3, with regard to the dependence on the dimensionless groups.

(c) How may the results be written so that they are valid for any generalized Newtonian model?

- 12D.5. The Graetz problem for flow between parallel plates.** Work through Problems 12D.2, 3, and 4 for flow between parallel plates (or flow in a thin rectangular duct).

- 12D.6. The constant wall heat flux problem for parallel plates.** Apply the methods used in §10.8, Example 12.2-1, and Ex. 12.2-2 to the flow between parallel plates.

¹² F. B. Hildebrand, *Advanced Calculus for Applications*, Prentice-Hall, Englewood Cliffs, N.J. (1963), §5.5.

- 12D.7. Asymptotic solution for small z for laminar tube flow with constant heat flux.** Fill in the missing steps between Eq. 12.2-23 and Eq. 12.2-24. Insertion of the expression for ψ into Eq. 12.2-23 gives

$$\Theta = \sqrt[3]{9\lambda} \int_x^\infty \left[\frac{3}{\Gamma(\frac{2}{3})} \int_{\bar{x}}^\infty \bar{\chi} \exp(-\bar{\chi}^3) d\bar{\chi} \right] d\bar{\chi} \quad (12D.7-1)$$

Why do we introduce the symbols \bar{x} and $\bar{\chi}$? Next, exchange the order of integration to get

$$\Theta = \sqrt[3]{9\lambda} \int_x^\infty \left[\frac{3}{\Gamma(\frac{2}{3})} \int_x^{\bar{x}} \bar{\chi} \exp(-\bar{\chi}^3) d\bar{\chi} \right] d\bar{\chi} \quad (12D.7-2)$$

Then perform the integration over $\bar{\chi}$ and obtain

$$\Theta(\eta, \lambda) = \frac{\sqrt[3]{9\lambda}}{\Gamma(\frac{2}{3})} \left[\exp(-\chi^3) - 3\chi \left(\int_0^\infty \chi \exp(-\chi^3) d\chi - \int_0^\chi \bar{\chi} \exp(-\bar{\chi}^3) d\bar{\chi} \right) \right] \quad (12D.7-3)$$

Then use the definitions $\Gamma(a) = \int_0^\infty t^{a-1} e^{-t} dt$ and $\Gamma(a, x) = \int_x^\infty t^{a-1} e^{-t} dt$ for the complete and incomplete gamma functions.

- 12D.8. Forced conduction heat transfer from a flat plate (thermal boundary layer extends beyond the momentum boundary layer).** Show that the result analogous to Eq. 12.4-14 for $\Delta > 1$ is¹³

$$\frac{3}{10} \Delta^2 - \frac{3}{10} \Delta + \frac{2}{15} - \frac{3}{140} \frac{1}{\Delta^2} + \frac{1}{180\Delta^3} = \frac{37}{315} \frac{1}{\text{Pr}} \quad (12D.8-1)$$

¹³ H. Schlichting, *Boundary-Layer Theory*, 7th edition, McGraw-Hill, New York (1979), p. 306.

Temperature Distributions in Turbulent Flow

- §13.1 Time-smoothed equations of change for incompressible nonisothermal flow
- §13.2 The time-smoothed temperature profile near a wall
- §13.3 Empirical expressions for the turbulent heat flux
- §13.4° Temperature distribution for turbulent flow in tubes
- §13.5° Temperature distribution for turbulent flow in jets
- §13.6° Fourier analysis of energy transport in tube flow at large Prandtl numbers

In Chapters 10 to 12 we have shown how to obtain temperature distributions in solids and in fluids in laminar motion. The procedure has involved solving the equations of change with appropriate boundary and initial conditions.

We now turn to the problem of finding temperature profiles in turbulent flow. This discussion is quite similar to that given in Chapter 5. We begin by time-smoothing the equations of change. In the time-smoothed energy equation there appears a turbulent heat flux $\bar{q}^{(t)}$, which is expressed in terms of the correlation of velocity and temperature fluctuations. There are several rather useful empiricisms for $\bar{q}^{(t)}$, which enable one to predict time-smoothed temperature distributions in wall turbulence and in free turbulence. We use heat transfer in tube flow to illustrate the method.

The most apparent influence of turbulence on heat transport is the enhanced transport perpendicular to the main flow. If heat is injected into a fluid flowing in *laminar* flow in the z direction, then the movement of heat in the x and y directions is solely by conduction and proceeds very slowly. On the other hand, if the flow is *turbulent*, the heat "spreads out" in the x and y directions extremely rapidly. This rapid dispersion of heat is a characteristic feature of turbulent flow. This mixing process is worked out in some detail here for flow in tubes and in circular jets.

Although it has been conventional to study turbulent heat transport via the time-smoothed energy equation, it is also possible to analyze the heat flux at a wall by use of a Fourier transform technique without time-smoothing. This is set forth in the last section.

§13.1 TIME-SMOOTHED EQUATIONS OF CHANGE FOR INCOMPRESSIBLE NONISOTHERMAL FLOW

In §5.2 we introduced the notions of time-smoothed quantities and turbulent fluctuations. In this chapter we shall be primarily concerned with the temperature profiles. We introduce the time-smoothed temperature \bar{T} and temperature fluctuation T' , and write analogously to Eq. 5.2-1

$$T = \bar{T} + T' \quad (13.1-1)$$

Clearly T' averages to zero so that $\bar{T}' = 0$, but quantities like $\bar{v}_x' \bar{T}'$, $\bar{v}_y' \bar{T}'$, and $\bar{v}_z' \bar{T}'$ will not be zero because of the “correlation” between the velocity and temperature fluctuations at any point.

For a nonisothermal pure fluid we need three equations of change, and we want to discuss here their time-smoothed forms. The time-smoothed equations of continuity and motion for a fluid with constant density and viscosity were given in Eqs. 5.2-10 and 12, and need not be repeated here. For a fluid with constant μ , ρ , \hat{C}_p , and k , Eq. 11.2-5, when put in the $\partial/\partial t$ form by using Eq. 3.5-4, and with Newton’s and Fourier’s law included, becomes

$$\begin{aligned} \frac{\partial}{\partial t} \rho \hat{C}_p T = & - \left(\frac{\partial}{\partial x} \rho \hat{C}_p v_x T + \frac{\partial}{\partial y} \rho \hat{C}_p v_y T + \frac{\partial}{\partial z} \rho \hat{C}_p v_z T \right) + k \left(\frac{\partial^2 T}{\partial x^2} + \frac{\partial^2 T}{\partial y^2} + \frac{\partial^2 T}{\partial z^2} \right) \\ & + \mu \left[2 \left(\frac{\partial v_x}{\partial x} \right)^2 + \left(\frac{\partial v_x}{\partial y} \right)^2 + 2 \left(\frac{\partial v_x}{\partial y} \right) \left(\frac{\partial v_y}{\partial x} \right) + \dots \right] \end{aligned} \quad (13.1-2)$$

in which only a few sample terms in the viscous dissipation term $-(\tau : \nabla \mathbf{v}) = \mu \Phi_v$ have been written (see Eq. B.7-1 for the complete expression).

In Eq. 13.1-2 we replace T by $T = \bar{T} + T'$, v_x by $\bar{v}_x + v'_x$, and so on. Then the equation is time-smoothed to give

$$\begin{aligned} \frac{\partial}{\partial t} \rho \hat{C}_p \bar{T} = & - \left(\frac{\partial}{\partial x} \rho \hat{C}_p \bar{v}_x \bar{T} + \frac{\partial}{\partial y} \rho \hat{C}_p \bar{v}_y \bar{T} + \frac{\partial}{\partial z} \rho \hat{C}_p \bar{v}_z \bar{T} \right) \\ & - \left(\frac{\partial}{\partial x} \rho \hat{C}_p \bar{v}_x' \bar{T}' + \frac{\partial}{\partial y} \rho \hat{C}_p \bar{v}_y' \bar{T}' + \frac{\partial}{\partial z} \rho \hat{C}_p \bar{v}_z' \bar{T}' \right) \\ & + k \left(\frac{\partial^2 \bar{T}}{\partial x^2} + \frac{\partial^2 \bar{T}}{\partial y^2} + \frac{\partial^2 \bar{T}}{\partial z^2} \right) \\ & + \mu \left[2 \left(\frac{\partial \bar{v}_x}{\partial x} \right)^2 + \left(\frac{\partial \bar{v}_x}{\partial y} \right)^2 + 2 \left(\frac{\partial \bar{v}_x}{\partial y} \right) \left(\frac{\partial \bar{v}_y}{\partial x} \right) + \dots \right] \\ & + \mu \left[2 \overline{\left(\frac{\partial v'_x}{\partial x} \right) \left(\frac{\partial v'_x}{\partial x} \right)} + \overline{\left(\frac{\partial v'_x}{\partial y} \right) \left(\frac{\partial v'_x}{\partial y} \right)} + 2 \overline{\left(\frac{\partial v'_x}{\partial y} \right) \left(\frac{\partial v'_y}{\partial x} \right)} + \dots \right] \end{aligned} \quad (13.1-3)$$

Comparison of this equation with the preceding one shows that the time-smoothed equation has the same form as the original equation, except for the appearance of the terms indicated by dashed underlines, which are concerned with the turbulent fluctuations. We are thus led to the definition of the turbulent heat flux $\bar{\mathbf{q}}^{(t)}$ with components

$$\bar{q}_x^{(t)} = \rho \hat{C}_p \bar{v}_x' \bar{T}' \quad \bar{q}_y^{(t)} = \rho \hat{C}_p \bar{v}_y' \bar{T}' \quad \bar{q}_z^{(t)} = \rho \hat{C}_p \bar{v}_z' \bar{T}' \quad (13.1-4)$$

and the turbulent energy dissipation function $\bar{\Phi}_v^{(t)}$:

$$\bar{\Phi}_v^{(t)} = \sum_{i=1}^3 \sum_{j=1}^3 \left(\overline{\left(\frac{\partial v'_i}{\partial x_j} \right) \left(\frac{\partial v'_i}{\partial x_j} \right)} + \overline{\left(\frac{\partial v'_i}{\partial x_j} \right) \left(\frac{\partial v'_j}{\partial x_i} \right)} \right) \quad (13.1-5)$$

The similarity between the components of $\bar{\mathbf{q}}^{(t)}$ in Eq. 13.1-4 and those of $\bar{\tau}^{(t)}$ in Eq. 5.2-8 should be noted. In Eq. 13.1-5, v'_1 , v'_2 , and v'_3 are synonymous with v'_x , v'_y , and v'_z , and x_1 , x_2 , and x_3 have the same meaning as x , y , and z .

To summarize, we list all three time-smoothed equations of change for turbulent flows of pure fluids with constant μ , ρ , \hat{C}_p , and k in their D/Dt form (the first two were given in Eqs. 5.2-10 and 12):

$$\text{Continuity} \quad (\nabla \cdot \bar{\mathbf{v}}) = 0 \quad (13.1-6)$$

$$\text{Motion} \quad \rho \frac{D \bar{\mathbf{v}}}{Dt} = -\nabla \bar{p} - [\nabla \cdot (\bar{\tau}^{(v)} + \bar{\tau}^{(t)})] + \rho \mathbf{g} \quad (13.1-7)$$

$$\text{Energy} \quad \rho \hat{C}_p \frac{DT}{Dt} = -(\nabla \cdot (\bar{\mathbf{q}}^{(v)} + \bar{\mathbf{q}}^{(t)})) + \mu (\bar{\Phi}_v^{(v)} + \bar{\Phi}_v^{(t)}) \quad (13.1-8)$$

in which it is understood that $D/Dt = \partial/\partial t + \bar{\mathbf{v}} \cdot \nabla$. Here $\bar{\mathbf{q}}^{(v)} = -k\nabla\bar{T}$, and $\bar{\Phi}_v^{(v)}$ is the viscous dissipation function of Eq. B.7-1, but with all the v_i replaced by \bar{v}_i .

In discussing turbulent heat flow problems, it has been customary to drop the viscous dissipation terms. Then, one sets up a turbulent heat transfer problem as for laminar flow, except that τ and q are replaced by $\bar{\tau}^{(v)} + \bar{\tau}^{(t)}$ and $\bar{\mathbf{q}}^{(v)} + \bar{\mathbf{q}}^{(t)}$, respectively, and time-smoothed \bar{p} , $\bar{\mathbf{v}}$, and \bar{T} are used in the remaining terms.

§13.2 THE TIME-SMOOTHED TEMPERATURE PROFILE NEAR A WALL¹

Before giving empiricisms for $\bar{\mathbf{q}}^{(t)}$ in the next section, we present a short discussion of some results that do not depend on any empiricism.

We consider the turbulent flow along a flat wall as shown in Fig. 13.2-1, and we inquire as to the temperature in the inertial sublayer. We pattern the development after that for Eq. 5.3-1. We let the heat flux into the fluid at $y = 0$ be $q_0 = \bar{q}_y|_{y=0}$ and we postulate that the heat flux in the inertial sublayer will not be very different from that at the wall.

We seek to relate q_0 to the time-smoothed temperature gradient in the inertial sublayer. Because transport in this region is dominated by turbulent convection, the viscosity μ and the thermal conductivity k will not play an important role. Therefore the only parameters on which $d\bar{T}/dy$ can depend are q_0 , $v_* = \sqrt{\tau_0/\rho}$, ρ , \hat{C}_p , and y . We must further use the fact that the linearity of the energy equation implies that $d\bar{T}/dy$ must be proportional to q_0 . The only combination that satisfies these requirements is

$$-\frac{d\bar{T}}{dy} = \frac{\beta q_0}{\kappa \rho \hat{C}_p v_* y} \quad (13.2-1)$$

in which κ is the dimensionless constant in Eq. 5.3-1, and β is an additional constant (which turns out¹ to be the turbulent Prandtl number $\text{Pr}^{(t)} = v^{(t)}/\alpha^{(t)}$).

When Eq. 13.2-1 is integrated we get

$$T_0 - \bar{T} = \frac{\beta q_0}{\kappa \rho \hat{C}_p v_*} \ln y + C \quad (13.2-2)$$

where T_0 is the wall temperature and C is a constant of integration. The constant is to be determined by matching the logarithmic expression with the expression for $\bar{T}(y)$ that

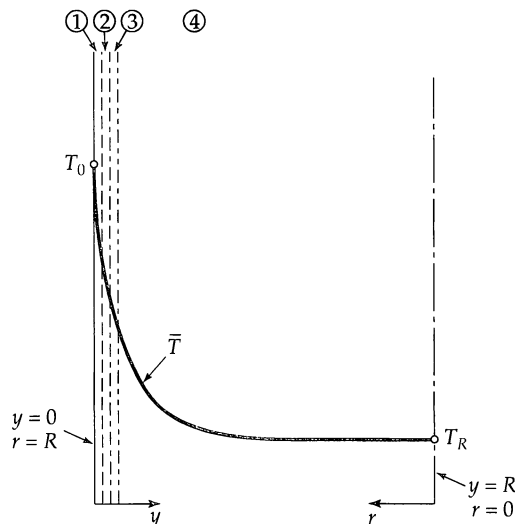


Fig. 13.2-1. Temperature profile in a tube with turbulent flow. The regions are (1) viscous sublayer, (2) buffer layer, (3) inertial sublayer, and (4) main turbulent stream.

¹ L. Landau and E. M. Lifshitz, *Fluid Mechanics*, 2nd edition, Pergamon Press, New York (1987), §54.

holds at the junction with the viscous sublayer. The latter expression will involve both μ and k ; hence C will necessarily contain μ and k , and will therefore include the dimensionless group $\text{Pr} = \hat{C}_p \mu / k$. If, in addition, we introduce the dimensionless coordinate yv_* / ν , then Eq. 13.2-2 can be rewritten as

$$T_0 - \bar{T} = \frac{\beta q_0}{\kappa p \hat{C}_p v_*} \left[\ln \left(\frac{yv_*}{\nu} \right) + f(\text{Pr}) \right] \quad \text{for } \frac{yv_*}{\nu} > 1 \quad (13.2-3)$$

in which $f(\text{Pr})$ is a function representing the thermal resistance between the wall and the inertial sublayer. Landau and Lifshitz (see Ref. 1 on page 409) estimate, from a mixing-length argument (see Eq. 13.3-3), that, for large Prandtl numbers, $f(\text{Pr}) = \text{constant} \cdot \text{Pr}^{3/4}$; however, Example 13.3-1 implies that the function $f(\text{Pr}) = \text{constant} \cdot \text{Pr}^{2/3}$ is better. Keep in mind that Eq. 13.2-3 can be expected to be valid only in the inertial sublayer and that it should not be used in the immediate neighborhood of the wall.

§13.3 EMPIRICAL EXPRESSIONS FOR THE TURBULENT HEAT FLUX

In §13.1 we saw that the time-smoothing of the energy equation gives rise to a turbulent heat flux $\bar{q}^{(t)}$. In order to solve the energy equation for the time-smoothed temperature profiles, it is customary to postulate a relation between $\bar{q}^{(t)}$ and the time-smoothed temperature gradient. We summarize here two of the most popular empirical expressions; more of these can be found in the heat transfer literature.

Eddy Thermal Conductivity

By analogy with the Fourier law of heat conduction we may write

$$\bar{q}_y^{(t)} = -k^{(t)} \frac{d\bar{T}}{dy} \quad (13.3-1)$$

in which the quantity $k^{(t)}$ is called the *turbulent thermal conductivity* or the *eddy thermal conductivity*. This quantity is not a physical property of the fluid, but depends on position, direction, and the nature of the turbulent flow.

The eddy kinematic viscosity $\nu^{(t)} = \mu^{(t)} / \rho$ and the eddy thermal diffusivity $\alpha^{(t)} = k^{(t)} / \rho \hat{C}_p$ have the same dimensions. Their ratio is a dimensionless group

$$\text{Pr}^{(t)} = \frac{\nu^{(t)}}{\alpha^{(t)}} \quad (13.3-2)$$

called the *turbulent Prandtl number*. This dimensionless quantity is of the order of unity, values in the literature varying from 0.5 to 1.0. For gas flow in conduits, $\text{Pr}^{(t)}$ ranges from 0.7 to 0.9 (for circular tubes the value 0.85 has been recommended¹), whereas for flow in jets and wakes the value is more nearly 0.5. The assumption that $\text{Pr}^{(t)} = 1$ is called the *Reynolds analogy*.

The Mixing-Length Expression of Prandtl and Taylor

According to Prandtl's mixing-length theory, momentum and energy are transferred in turbulent flow by the same mechanism. Hence, by analogy with Eq. 5.4-4, one obtains

$$\bar{q}_y^{(t)} = -\rho \hat{C}_p l^2 \left| \frac{d\bar{v}_x}{dy} \right| \frac{d\bar{T}}{dy} \quad (13.3-3)$$

¹ W. M. Kays and M. E. Crawford, *Convective Heat and Mass Transfer*, 3rd edition, McGraw-Hill, New York (1993), pp. 259–266.

where l is the Prandtl mixing length introduced in Eq. 5.4-4. Note that this expression predicts that $\text{Pr}^{(t)} = 1$. The Taylor vorticity transport theory² gives $\text{Pr}^{(t)} = \frac{1}{2}$.

EXAMPLE 13.3-1

An Approximate Relation for the Wall Heat Flux for Turbulent Flow in a Tube

Use the Reynolds analogy ($\nu^{(t)} = \alpha^{(t)}$), along with Eq. 5.4-2 for the eddy viscosity, to estimate the wall heat flux q_0 for the turbulent flow in a tube of diameter $D = 2R$. Express the result in terms of the temperature-difference driving force $T_0 - \bar{T}_R$, where T_0 is the temperature at the wall ($y = 0$) and \bar{T}_R is the time-smoothed temperature at the tube axis ($y = R$).

SOLUTION

The time-smoothed radial heat flux in a tube is given by the sum of $\bar{q}_r^{(v)}$ and $\bar{q}_r^{(t)}$:

$$\begin{aligned}\bar{q}_r &= -(k + k^{(t)}) \frac{d\bar{T}}{dr} = -(1 + \frac{\alpha^{(t)}}{\alpha}) k \frac{d\bar{T}}{dr} \\ &= +(1 + \frac{\nu^{(t)}}{\alpha}) k \frac{d\bar{T}}{dy} \quad (13.3-4)\end{aligned}$$

Here we have used Eq. 13.3-1 and the Reynolds analogy, and we have switched to the coordinate y , which is the distance from the wall. We now use the empirical expression of Eq. 5.4-2, which applies across the viscous sublayer next to the wall:

$$\bar{q}_y = - \left[1 + \text{Pr} \left(\frac{y v_*}{14.5 \nu} \right)^3 \right] k \frac{d\bar{T}}{dy} \quad \text{for } \frac{y v_*}{\nu} < 5 \quad (13.3-5)$$

where $\bar{q}_r = -\bar{q}_y$ has been used.

If now we approximate the heat flux \bar{q}_y in Eq. 13.3-5 by its wall value q_0 , then integration from $y = 0$ to $y = R$ gives

$$q_0 \int_0^R \frac{dy}{1 + \text{Pr}(y v_* / 14.5 \nu)^3} = k(T_0 - \bar{T}_R) \quad (13.3-6)$$

For very large Prandtl numbers, the upper limit R in the integral can be replaced by ∞ , since the integrand is decreasing rapidly with increasing y . Then when the integration on the left side is performed and the result is put into dimensionless form, we get

$$\frac{q_0 D}{k(T_0 - \bar{T}_R)} = \frac{3\sqrt{3}}{2\pi(14.5)} \left(\frac{v_*}{\langle v_z \rangle} \right) \text{Re} \text{Pr}^{1/3} = \frac{1}{17.5} \sqrt{\frac{f}{2}} \text{Re} \text{Pr}^{1/3} \quad (13.3-7)$$

in which Eq. 6.1-4a has been used to eliminate v_* in favor of the friction factor.

The above development is only approximate. We have not taken into account the change of the bulk temperature as the fluid moves axially through the tube, nor have we taken into account the change in the heat flux throughout the tube. Furthermore, the result is restricted to very high Pr , because of the extension of the integration to $y = \infty$. Another derivation is given in the next section, which is free from these assumptions. However, we will see that at large Prandtl numbers the result in Eq. 13.4-20 simplifies to that in Eq. 13.3-7 but with a different numerical constant.

§13.4 TEMPERATURE DISTRIBUTION FOR TURBULENT FLOW IN TUBES

In §10.8 we showed how to get the asymptotic behavior of the temperature profiles for large z in a fluid in laminar flow in a circular tube. We repeat that problem here, but for a fluid in fully developed turbulent flow. The fluid enters the tube of radius R at an inlet temperature T_1 . For $z > 0$ the fluid is heated because of a uniform radial heat flux q_0 at the wall (see Fig. 13.4-1).

² G. I. Taylor, *Proc. Roy. Soc. (London)*, A135, 685–702 (1932); *Phil. Trans.*, A215, 1–26 (1915).

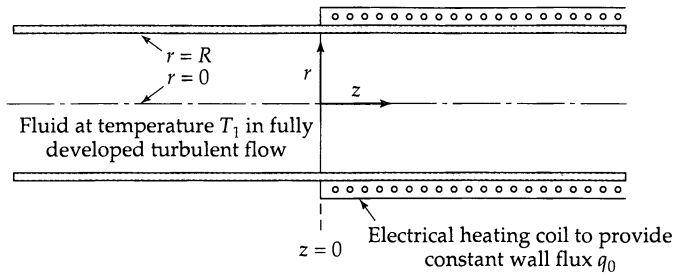


Fig. 13.4-1. System used for heating a liquid in fully developed turbulent flow with constant heat flux for $z > 0$.

We start from the energy equation, Eq. 13.1-8, written in cylindrical coordinates

$$\rho \hat{C}_p \bar{v}_z \frac{\partial \bar{T}}{\partial z} = -\frac{1}{r} \frac{\partial}{\partial r} (r(\bar{q}_r^{(v)} + \bar{q}_r^{(t)})) \quad (13.4-1)$$

Then insertion of the expression for the radial heat flux from Eq. 13.3-4 gives

$$\bar{v}_z \frac{\partial \bar{T}}{\partial z} = \frac{1}{r} \frac{\partial}{\partial r} \left(r(\alpha + \alpha^{(t)}) \frac{\partial \bar{T}}{\partial r} \right) \quad (13.4-2)$$

This is to be solved with the boundary conditions

$$\text{B.C. 1:} \quad \text{at } r = 0, \quad \bar{T} = \text{finite} \quad (13.4-3)$$

$$\text{B.C. 2:} \quad \text{at } r = R, \quad +k \frac{\partial \bar{T}}{\partial r} = q_0 \quad (\text{a constant}) \quad (13.4-4)$$

$$\text{B.C. 3:} \quad \text{at } z = 0, \quad \bar{T} = T_1 \quad (13.4-5)$$

We now use the same dimensionless variables as already given in Eqs. 10.8-16 to 18 (with \bar{T} in place of T in the definition of the dimensionless temperature). Then Eq. 13.4-2 in dimensionless form is

$$\phi \frac{\partial \Theta}{\partial \xi} = \frac{1}{\xi} \frac{\partial}{\partial \xi} \left(\xi \left(1 + \frac{\alpha^{(t)}}{\alpha} \right) \frac{\partial \Theta}{\partial \xi} \right) \quad (13.4-6)$$

in which $\phi(\xi) = \bar{v}_z/v_{\max}$ is the dimensionless turbulent velocity profile. This equation is to be solved with the dimensionless boundary conditions

$$\text{B.C. 1:} \quad \text{at } \xi = 0, \quad \Theta = \text{finite} \quad (13.4-7)$$

$$\text{B.C. 2:} \quad \text{at } \xi = 1, \quad +\frac{\partial \Theta}{\partial \xi} = 1 \quad (13.4-8)$$

$$\text{B.C. 3:} \quad \text{at } \zeta = 0, \quad \Theta = 0 \quad (13.4-9)$$

The complete solution to this problem has been given,¹ but we content ourselves here with the solution for large z .

We begin by assuming an asymptotic solution of the form of Eq. 10.8-23

$$\Theta(\xi, \zeta) = C_0 \zeta + \Psi(\xi) \quad (13.4-10)$$

which must satisfy the differential equation, together with B.C. 1 and 2 and Condition 4 in Eq. 10.8-24 (with T and $v_z = v_{\max}(1 - \xi^2)$ replaced by \bar{T} and $v_z = v_{\max}\phi(\xi)$). The resulting equation for Ψ is

$$\frac{1}{\xi} \frac{d}{d\xi} \left(\xi \left(1 + \frac{\alpha^{(t)}}{\alpha} \right) \frac{d\Psi}{d\xi} \right) = C_0 \phi \quad (13.4-11)$$

¹ R. H. Notter and C. A. Sleicher, *Chem. Eng. Sci.*, **27**, 2073–2093 (1972).

Integrating this equation twice and then constructing the function Θ using Eq. 13.4-10, we get

$$\Theta = C_0 \xi + C_1 \int_0^\xi \frac{I(\bar{\xi})}{\bar{\xi}[1 + (\alpha^{(t)} / \alpha)]} d\bar{\xi} + C_2 \int_0^\xi \frac{1}{\bar{\xi}[1 + (\alpha^{(t)} / \alpha)]} d\bar{\xi} + C_3 \quad (13.4-12)$$

in which it is understood that $\alpha^{(t)}$ is a function of $\bar{\xi}$, and $I(\bar{\xi})$ is shorthand for the integral

$$I(\bar{\xi}) = \int_0^{\bar{\xi}} \phi \bar{\xi} d\bar{\xi} \quad (13.4-13)$$

The constant of integration C_1 is set equal to zero in order to satisfy B.C. 1. The constant C_0 is found by applying B.C. 2, which gives

$$C_0 = \left(\int_0^1 \phi \xi d\xi \right)^{-1} = [I(1)]^{-1} \quad (13.4-14)$$

The remaining constant, C_2 , can, if desired, be obtained from Condition 4, but we shall not need it here (see Problem 13D.1).

We next get an expression for the dimensionless temperature difference $\Theta_0 - \Theta_b$, the “driving force” for the heat transfer at the tube wall:

$$\begin{aligned} \Theta_0 - \Theta_b &= C_0 \int_0^1 \frac{I(\xi)}{\xi[1 + (\alpha^{(t)} / \alpha)]} d\xi - \frac{C_0}{I(1)} \int_0^1 \phi \xi \left[\int_0^\xi \frac{I(\bar{\xi})}{\bar{\xi}[1 + (\alpha^{(t)} / \alpha)]} d\bar{\xi} \right] d\xi \\ &= C_0 \int_0^1 \frac{I(\xi)}{\xi[1 + (\alpha^{(t)} / \alpha)]} d\xi - \frac{C_0}{I(1)} \int_0^1 \frac{I(\bar{\xi})}{\bar{\xi}[1 + (\alpha^{(t)} / \alpha)]} \left[\int_{\bar{\xi}}^1 \phi \xi d\xi \right] d\bar{\xi} \end{aligned} \quad (13.4-15)$$

In the second line, the order of integration of the double integral has been reversed. The inner integral in the second term on the right is just $I(1) - I(\bar{\xi})$, and the portion containing $I(1)$ exactly cancels the first term in Eq. 13.4-15. Hence when Eq. 13.4-14 is used, we get

$$\Theta_0 - \Theta_b = \int_0^1 \frac{[I(\xi)/I(1)]^2}{\xi[1 + (\alpha^{(t)} / \alpha)]} d\xi \quad (13.4-16)$$

But the quantity $I(1)$ appearing in Eq. 13.4-16 has a simple interpretation:

$$I(1) = \int_0^1 \phi \xi d\xi = \left(\int_0^R \bar{v}_z r dr \right) \frac{1}{\bar{v}_{z,\max} R^2} = \frac{1}{2} \frac{\langle \bar{v}_z \rangle}{\bar{v}_{z,\max}} \quad (13.4-17)$$

Finally, we want to get the dimensionless wall heat flux,

$$\frac{q_0 D}{k(T_0 - T_b)} = \frac{2}{\Theta_0 - \Theta_b} \quad (13.4-18)$$

the reciprocal of which is²

$$\frac{k(T_0 - T_b)}{q_0 D} = 2 \left(\frac{\bar{v}_{z,\max}}{\langle \bar{v}_z \rangle} \right)^2 \int_0^1 \frac{[I(\xi)]^2}{\xi[1 + (\nu^{(t)} / \nu)(\text{Pr} / \text{Pr}^{(t)})]} d\xi \quad (13.4-19)$$

To use this result, it is necessary to have an expression for the time-smoothed velocity distribution \bar{v}_z (which appears in $I(\xi)$), the turbulent kinematic viscosity $\nu^{(t)}$ as a function of position, and a postulate for the turbulent Prandtl number $\text{Pr}^{(t)}$.

² Equation 13.4-19 was first developed by R. N. Lyon, *Chem. Eng. Prog.*, **47**, 75–79 (1950) in a paper on liquid–metal heat transfer. The left side of Eq. 13.4-19 is the reciprocal of the Nusselt number, $\text{Nu} = hD/k$, which is a dimensionless heat transfer coefficient. This nomenclature is discussed in the next chapter.

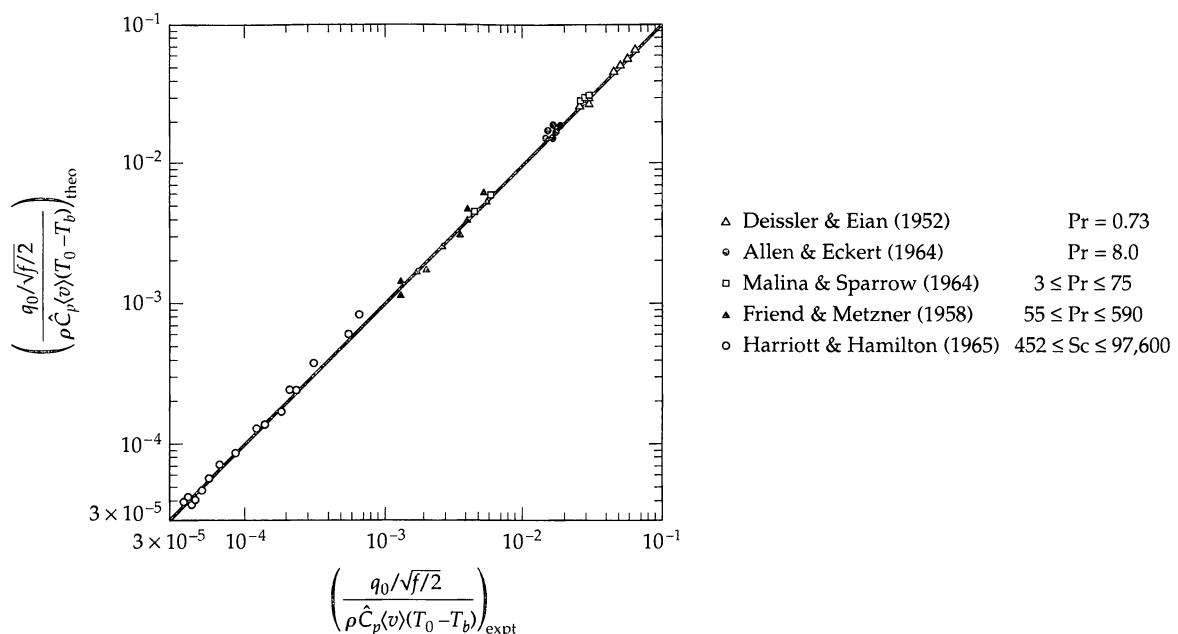


Fig. 13.4-2. Comparison of the expression in Eq. 13.4-20 for the wall heat flux in fully developed turbulent flow with the experimental data of R. G. Deissler and C. S. Eian, *NACA Tech. Note #2629* (1952); R. W. Allen and E. R. G. Eckert, *J. Heat Transfer, Trans. ASME, Ser. C*, **86**, 301–310 (1964); J. A. Malina and E. M. Sparrow, *Chem. Eng. Sci.*, **19**, 953–962 (1964); W. L. Friend and A. B. Metzner, *AICHE Journal*, **4**, 393–402 (1958); P. Harriott and R. M. Hamilton, *Chem. Eng. Sci.*, **20**, 1073–1078 (1965). The data of Harriott and Hamilton are for the analogous mass transfer experiment, for which Eq. 13.4-20 also applies.

Extensive calculations based on Eq. 13.4-19 were performed by Sandall, Hanna, and Mazet.³ These authors took the turbulent Prandtl number to be unity. They divided the region of integration into two parts, one near the wall and the other for the turbulent core. In the “wall region” they used the modified van Driest equation of Eq. 5.4-7 for the mixing length, and in the “core region” they used a logarithmic velocity distribution. Their final result³ is given as

$$\frac{q_0 D}{k(T_0 - T_b)} = \frac{\text{Re} \Pr \sqrt{f/2}}{12.48 \Pr^{2/3} - 7.853 \Pr^{1/3} + 3.613 \ln \Pr + 5.8 + 2.78 \ln(\frac{1}{45} \text{Re} \sqrt{f/8})} \quad (13.4-20)$$

In obtaining this result, Eq. 6.1-4a has been used.

Equation 13.4-20 agrees with the available data on heat transfer (and mass transfer) within 3.6 and 8.1% over the range $0.73 < \Pr < 590$, depending on the sets of data studied. The analogous mass transfer expression, containing $\text{Sc} = \mu / \rho D_{AB}$ instead of \Pr , was reported³ to agree with the mass transfer data within 8% over the range $452 < \text{Sc} < 97600$. The agreement of the theory with the heat transfer and mass transfer data, shown in Fig. 13.4-2, is quite convincing.

³ O. C. Sandall, O. T. Hanna, and P. R. Mazet, *Canad. J. Chem. Eng.*, **58**, 443–447 (1980). See also O. T. Hanna and O. C. Sandall, *AICHE Journal*, **18**, 527–533 (1972).

§13.5 TEMPERATURE DISTRIBUTION FOR TURBULENT FLOW IN JETS¹

In §5.6 we derived an expression for the velocity distribution in a circular fluid jet discharging into an infinite expanse of the same fluid (see Fig. 5.6-1). Here we wish to extend this problem by considering an incoming jet with temperature T_0 higher than that of the surrounding fluid T_1 . The problem then is to find the time-smoothed temperature distribution $\bar{T}(r, z)$ in a steadily driven jet. We expect that this distribution will be monotone decreasing in both the r and z directions.

We start by assuming that viscous dissipation is negligible, and we neglect the contribution $\bar{q}^{(v)}$ to the heat flux as well as the axial contribution to $\bar{q}^{(t)}$. Then Eq. 13.1-8 takes the time-averaged form

$$\hat{\rho}\hat{C}_p\left(\bar{v}_r \frac{\partial \bar{T}}{\partial r} + \bar{v}_z \frac{\partial \bar{T}}{\partial z}\right) = -\frac{1}{r} \frac{\partial}{\partial r} (r\bar{q}_r^{(t)}) \quad (13.5-1)$$

Then we express the turbulent heat flux in terms of the turbulent thermal conductivity introduced in Eq. 13.3-1:

$$\bar{q}_r^{(t)} = -k^{(t)} \frac{\partial \bar{T}}{\partial r} = -\rho \hat{C}_p \alpha^{(t)} \frac{\partial \bar{T}}{\partial r} = \rho \hat{C}_p \frac{\nu^{(t)}}{\text{Pr}^{(t)}} \frac{\partial \bar{T}}{\partial r} \quad (13.5-2)$$

When Eq. 13.5-1 is written in terms of a dimensionless temperature function

$$\Theta(\xi, \zeta) = \frac{\bar{T} - T_1}{T_0 - T_1} \quad (13.5-3)$$

it becomes

$$\left(\bar{v}_r \frac{\partial \Theta}{\partial r} + \bar{v}_z \frac{\partial \Theta}{\partial z}\right) = \frac{\nu^{(t)}}{\text{Pr}^{(t)}} \frac{1}{r} \frac{\partial}{\partial r} \left(r \frac{\partial \Theta}{\partial r}\right) \quad (13.5-4)$$

Here it has been assumed that the turbulent Prandtl number and the turbulent kinematic viscosity are constants (see the discussion after Eq. 5.6-3). This equation is to be solved with the boundary conditions:

$$\text{B.C. 1:} \quad \text{at } z = 0, \quad \Theta = 1 \quad (13.5-5)$$

$$\text{B.C. 2:} \quad \text{at } r = 0, \quad \Theta \text{ is finite} \quad (13.5-6)$$

$$\text{B.C. 3:} \quad \text{at } r = \infty, \quad \Theta = 0 \quad (13.5-7)$$

Next we introduce the expressions for the time-smoothed velocity components \bar{v}_r and \bar{v}_z in terms of a stream function $F(\xi)$, as given in Eqs. 5.6-12 and 13, and a trial expression for the dimensionless time-smoothed temperature function:

$$\Theta(\xi, \zeta) = \frac{1}{\zeta} f(\xi) \quad (13.5-8)$$

Here $\xi = r/z$ and $\zeta = (\rho\nu^{(t)}/w)z$, where w is the total mass flow rate in the jet. The proposal in Eq. 13.5-8 is motivated by the expression for \bar{v}_z that was found in Eq. 5.6-21.

When these expressions for the velocity components and the dimensionless temperature are substituted into Eq. 13.5-1, some terms cancel and others can be combined, and as a result, the following rather simple equation is obtained:

$$\text{Pr}^{(t)} \frac{1}{\xi} \frac{d}{d\xi} (Ff) = \frac{1}{\xi} \frac{d}{d\xi} \left(\xi \frac{df}{d\xi} \right) \quad (13.5-9)$$

¹ J. O. Hinze, *Turbulence*, 2nd edition, McGraw-Hill, New York (1975), pp. 531–546.

This equation can be integrated once to give

$$\text{Pr}^{(t)} F f = \xi \frac{df}{d\xi} + C \quad (13.5-10)$$

The constant of integration may be set equal to zero, since, according to Eq. 5.6-20, $F = 0$ at $\xi = 0$. A second integration from 0 to ξ then gives

$$\begin{aligned} \ln \frac{f(\xi)}{f(0)} &= \text{Pr}^{(t)} \int_0^\xi \frac{F}{\xi} d\xi = -\text{Pr}^{(t)} \int_0^\xi \frac{C_3^2 \xi}{1 + \frac{1}{4}(C_3 \xi)^2} d\xi \\ &= -\text{Pr}^{(t)} \ln (1 + \frac{1}{4}(C_3 \xi)^2)^2 \end{aligned} \quad (13.5-11)$$

or

$$\frac{f(\xi)}{f(0)} = (1 + \frac{1}{4}(C_3 \xi)^2)^{-2\text{Pr}^{(t)}} \quad (13.5-12)$$

Finally, comparison of Eqs. 13.5-12 and 13.5-8 with Eq. 5.6-21 shows that the shapes of the time-smoothed temperature and axial velocity profiles are closely related,

$$\frac{\Theta}{\Theta_{\max}} = \left(\frac{\bar{v}_z}{\bar{v}_{z,\max}} \right)^{\text{Pr}^{(t)}} \quad (13.5-13)$$

an equation attributed to Reichardt.² This theory provides a moderately satisfactory explanation for the shapes of the temperature profiles.¹ The turbulent Prandtl (or Schmidt) number deduced from temperature (or concentration) measurements in circular jets is about 0.7.

The quantity C_3 appearing in Eq. 13.5-12 was given explicitly in Eq. 5.6-23 as $C_3 = \sqrt{3/16\pi}\sqrt{J/\rho}(1/\nu^{(t)})$, where J is the rate of momentum flow in the jet, defined in Eq. 5.6-2. Similarly, an expression for the quantity $f(0)$ in Eq. 13.5-12 can be found by equating the energy in the incoming jet to the energy crossing any plane downstream:

$$w\hat{C}_p(T_0 - T_1) = \int_0^{2\pi} \int_0^\infty \rho\hat{C}_p v_z (\bar{T} - T_1) r dr d\theta \quad (13.5-14)$$

Insertion of the expressions for the velocity and temperature profiles and integrating then gives

$$\frac{1}{f(0)} = 4\pi C_3^2 \int_0^\infty (1 + \frac{1}{4}(C_3 \xi)^2)^{-(2+2\text{Pr}^{(t)})} \xi d\xi = \frac{8}{C_3} \frac{1}{1 + 2\text{Pr}^{(t)}} \quad (13.5-15)$$

Combining Eqs. 13.5-3, 13.5-8, 5.6-23, 13.5-12, and 13.5-15 then gives the complete expression for the temperature profiles $\bar{T}(r, z)$ in the circular turbulent jet, in terms of the total momentum of the jet, the turbulent viscosity, the turbulent Prandtl number, and the fluid density.

13.6 FOURIER ANALYSIS OF ENERGY TRANSPORT IN TUBE FLOW AT LARGE PRANDTL NUMBERS

In the preceding two sections we analyzed energy transport in turbulent systems by use of time-smoothed equations of change. Empirical expressions were then required to describe the turbulent fluxes in terms of time-smoothed profiles, using eddy transport coef-

² H. Reichardt, *Zeits. f. angew. Math. u. Mech.*, **24**, 268–272 (1944).

ficients estimated from experiments. In this section we analyze a turbulent energy transport problem without time-smoothing—that is, by direct use of the energy equation with fluctuating velocity and temperature fields. The Fourier transform¹ is well suited for such problems, and the “method of dominant balance”² gives useful information without detailed computations.

The specific question considered here is the influence of the thermal diffusivity, $\alpha = k/\rho\hat{C}_p$, on the expected distribution and fluctuations of the fluid temperature in turbulent forced convection near a wall.³ This topic was discussed in Example 13.3-1 by an approximate procedure.

Let us consider a fluid with constant ρ , \hat{C}_p , and k in turbulent flow through a tube of inner radius $R = \frac{1}{2}D$. The flow enters at $z = -\infty$ with uniform temperature T_1 and exits at $z = L$. The tube wall is adiabatic for $z < 0$, and isothermal at T_0 for $0 \leq z \leq L$. Heat conduction in the z direction is neglected. The temperature distribution $T(r, \theta, z, t)$ is to be analyzed in the long-time limit, in the thin thermal boundary layer that forms for $z > 0$ when the *molecular* thermal diffusivity α is small (as in a Newtonian fluid when the Prandtl number, $\text{Pr} = \hat{C}_p\mu/k = \mu/\rho\alpha$, is large). A stretching function $\kappa(\alpha)$ will be derived for the average thickness of the thermal boundary layer without introducing an *eddy* thermal diffusivity $\alpha^{(l)}$.

In the limit as $\alpha \rightarrow 0$, the thermal boundary layer lies entirely within the viscous sublayer, where the velocity components are given by truncated Taylor expansions in the distance $y = R - r$ from the wall (compare these expansions with those in Eqs. 5.4-8 to 10)

$$v_\theta = \beta_\theta y + O(y^2) \quad (13.6-1)$$

$$v_z = \beta_z y + O(y^2) \quad (13.6-2)$$

$$v_r = -\left(\frac{1}{R} \frac{\partial \beta_\theta}{\partial \theta} + \frac{\partial \beta_z}{\partial z}\right) \frac{y^2}{2} + O(y^3) \quad (13.6-3)$$

Here the coefficients β_θ and β_z are treated as given functions of θ , z , and t . These velocity expressions satisfy the no-slip conditions and the wall-impermeability condition at $y = 0$ and the continuity equation at small y , and are consistent with the equation of motion to the indicated orders in y . The energy equation can then be written as

$$\frac{\partial T}{\partial t} + \left(\beta_\theta \frac{\partial T}{\partial \theta} + \beta_z \frac{\partial T}{\partial z}\right)y - \left(\frac{1}{R} \frac{\partial \beta_\theta}{\partial \theta} + \frac{\partial \beta_z}{\partial z}\right) \frac{y^2}{2} \frac{\partial T}{\partial y} = \alpha \frac{\partial^2 T}{\partial y^2} \quad (13.6-4)$$

with the usual boundary layer approximation for $\nabla^2 T$, and with the following boundary conditions on $T(y, \theta, z, t)$:

$$\text{Inlet condition:} \quad \text{at } z = 0, \quad T(y, \theta, 0, t) = T_1 \quad \text{for } 0 < y \leq R \quad (13.6-5)$$

$$\text{Wall condition:} \quad \text{at } y = 0, \quad T(0, \theta, z, t) = T_0 \quad \text{for } 0 \leq z \leq L \quad (13.6-6)$$

The initial temperature distribution $T(y, \theta, z, 0)$ is not needed, since its effect disappears in the long-time limit.

To obtain results asymptotically valid for $\alpha \rightarrow 0$, we introduce a stretched coordinate $Y = y/\kappa(\alpha)$, which is the distance from the wall relative to the average boundary layer thickness $\kappa(\alpha)$. The range of Y is from 0 at $y = 0$ to ∞ at $y = R$ in the limit as $\alpha \rightarrow 0$.

¹ R. N. Bracewell, *The Fourier Transform and its Applications*, 2nd edition, McGraw-Hill, New York (1978).

² This method is well presented in C. M. Bender and S. A. Orzag, *Advanced Mathematical Methods for Scientists and Engineers*, McGraw-Hill, New York (1978), pp. 435–437.

³ W. E. Stewart, *AIChE Journal*, **33**, 2008–2016 (1987); errata, *ibid.*, **34**, 1030 (1988); W. E. Stewart and D. G. O’Sullivan, *AIChE Journal* (to be submitted).

Use of κY in place of y , and introduction of the dimensionless temperature function $\Theta(Y, \theta, z, t) = (T - T_1)/(T_0 - T_1)$, enable us to rewrite Eq. 13.6-4 as

$$\frac{\partial \Theta}{\partial t} + \left(\frac{\beta_\theta}{R} \frac{\partial \Theta}{\partial \theta} + \beta_z \frac{\partial \Theta}{\partial z} \right) \kappa Y - \left(\frac{1}{R} \frac{\partial \beta_\theta}{\partial \theta} + \frac{\partial \beta_z}{\partial z} \right) \frac{\kappa Y^2}{2} \frac{\partial \Theta}{\partial y} = \frac{\alpha}{\kappa^2} \frac{\partial^2 \Theta}{\partial Y^2} \quad (13.6-7)$$

with boundary conditions as follows:

$$\text{Inlet condition:} \quad \text{at } z = 0, \quad \Theta(Y, \theta, 0, t) = 0 \quad \text{for } Y > 0 \quad (13.6-8)$$

$$\text{Wall condition:} \quad \text{at } Y = 0, \quad \Theta(0, \theta, z, t) = 1 \quad \text{for } 0 \leq z \leq L \quad (13.6-9)$$

Equation 13.6-7 contains an unbounded derivative $\partial \Theta / \partial t$ with a coefficient 1 independent of α . Thus a change of variables is needed to analyze the influence of the parameter α in this problem. For this purpose we turn to the Fourier transform, a standard tool for analyzing noisy processes.

We choose the following definition¹ for the Fourier transform of a function $g(t)$ into the domain of frequency ν at a particular position Y, θ, z :

$$\mathcal{F}[g(t)] = \int_{-\infty}^{\infty} e^{-2\pi i \nu t} g(t) dt = \tilde{g}(\nu) \quad (13.6-10)$$

The corresponding transforms for the t -derivative and for products of functions of t are

$$\int_{-\infty}^{\infty} e^{-2\pi i \nu t} \frac{\partial}{\partial t} g(t) dt = 2\pi i \nu \tilde{g}(\nu) \quad (13.6-11)$$

$$\int_{-\infty}^{\infty} e^{-2\pi i \nu t} g(t) h(t) dt = \int_{-\infty}^{\infty} \tilde{g}(\nu) \tilde{h}(\nu - \nu_1) d\nu_1 = \tilde{g} * \tilde{h} \quad (13.6-12)$$

and the latter integral is known as the *convolution* of the transforms \tilde{g} and \tilde{h} .

Before taking the Fourier transforms of Eqs. 13.6-7 to 9, we express each included function $g(t)$ as a time average \bar{g} plus a fluctuating function $g'(t)$ and expand each product of such functions. The resulting expressions have the following Fourier transforms:

$$\mathcal{F}[\bar{g} + g'] = \delta(\nu) \bar{g} + \tilde{g}'(\nu) \quad (13.6-13)$$

$$\begin{aligned} \mathcal{F}[(\bar{g} + g')(\bar{h} + h')] &= \mathcal{F}[\bar{g}\bar{h} + \bar{g}\bar{h}' + g'\bar{h} + g'h'] \\ &= \delta(\nu) \bar{g}\bar{h} + \bar{g}\tilde{h}' + \tilde{g}'\bar{h} + \tilde{g}'*\tilde{h}' \end{aligned} \quad (13.6-14)$$

Here $\delta(\nu)$ is the Dirac delta function, obtained as the Fourier transform of the function $g(t) = 1$ in the long-duration limit. The leading term in the last line is a real-valued impulse at $\nu = 0$, coming from the time-independent product $\bar{g}\bar{h}$. The next two terms are complex-valued functions of the frequency ν . The convolution term $\tilde{g}'*\tilde{h}'$ may contain complex-valued functions of ν , along with a real-valued impulse $\delta(\nu)g'h'$ coming from time-independent products of simple harmonic oscillations present in g' and h' .

Taking the Fourier transform of Eq. 13.6-7 by the method just given and noting that $\bar{\Theta}/\partial t$ is identically zero, we obtain the differential equation

$$\begin{aligned} 2\pi i \nu \tilde{\Theta}' &+ \left(\delta(\nu) \frac{\bar{\beta}_\theta}{R} \frac{\partial \bar{\Theta}}{\partial \theta} + \frac{\bar{\beta}_\theta}{R} \frac{\partial \tilde{\Theta}'}{\partial \theta} + \frac{\tilde{\beta}_\theta'}{R} \frac{\partial \bar{\Theta}}{\partial \theta} + \frac{\tilde{\beta}_\theta'}{R} * \frac{\partial \tilde{\Theta}'}{\partial \theta} \right) \kappa Y \\ &+ \left(\delta(\nu) \bar{\beta}_z \frac{\partial \bar{\Theta}}{\partial z} + \bar{\beta}_z \frac{\partial \tilde{\Theta}'}{\partial z} + \tilde{\beta}_z' \frac{\partial \bar{\Theta}}{\partial z} + \tilde{\beta}_z' * \frac{\partial \tilde{\Theta}'}{\partial z} \right) \kappa Y \\ &- \left(\frac{\delta(\nu)}{R} \frac{\partial \beta_\theta}{\partial \theta} \frac{\partial \bar{\Theta}}{\partial Y} + \frac{1}{R} \frac{\partial \beta_\theta}{\partial \theta} \frac{\partial \tilde{\Theta}'}{\partial Y} + \frac{1}{R} \frac{\partial \beta_\theta'}{\partial \theta} \frac{\partial \bar{\Theta}}{\partial Y} + \frac{1}{R} \frac{\partial \beta_\theta'}{\partial \theta} * \frac{\partial \tilde{\Theta}'}{\partial Y} \right) \frac{\kappa Y^2}{2} \\ &- \left(\delta(\nu) \frac{\partial \bar{\beta}_z}{\partial z} \frac{\partial \bar{\Theta}}{\partial Y} + \frac{\partial \bar{\beta}_z}{\partial z} \frac{\partial \tilde{\Theta}'}{\partial Y} + \frac{\partial \tilde{\beta}_z'}{\partial z} \frac{\partial \bar{\Theta}}{\partial Y} + \frac{\partial \tilde{\beta}_z'}{\partial z} * \frac{\partial \tilde{\Theta}'}{\partial Y} \right) \frac{\kappa Y^2}{2} \\ &= \left(\delta(\nu) \frac{\partial^2 \bar{\Theta}}{\partial Y^2} + \frac{\partial^2 \tilde{\Theta}'}{\partial Y^2} \right) \frac{\alpha}{\kappa^2} \end{aligned} \quad (13.6-15)$$

for the Fourier-transformed temperature $\tilde{\Theta}(Y, \theta, z, \nu)$. The transformed boundary conditions are

$$\text{Inlet condition:} \quad \text{at } z = 0, \quad \tilde{\Theta}(Y, \theta, z, \nu) = 0 \quad \text{for } Y > 0 \quad (13.6-16)$$

$$\text{Wall condition:} \quad \text{at } Y = 0, \quad \tilde{\Theta}(Y, \theta, z, \nu) = \delta(\nu) \quad \text{for } 0 \leq z \leq L \quad (13.6-17)$$

Here again, the unit impulse function $\delta(\nu)$ appears as the Fourier transform of the function $g(t) = 1$ in the long-duration limit.

Two types of contributions appear in Eq. 13.6-15: real-valued zero-frequency impulses $\delta(\nu)$ from functions and products independent of t , and complex-valued functions of ν from time-dependent product terms. We consider these two types of contributions separately here, thus decoupling Eq. 13.6-15 into two equations.

We begin with the zero-frequency impulse terms. In addition to the explicit $\delta(\nu)$ terms of Eq. 13.6-15, implicit impulses arise in the convolution terms from synchronous oscillations of velocity and temperature, giving rise to the turbulent energy flux $\bar{q}^{(t)} = \rho C_p v' T'$ discussed in §13.2. The coefficients of all the impulse terms must be proportional functions of α , in order that the dominant terms at each point remain balanced (i.e., of comparable size) as $\alpha \rightarrow 0$. Therefore, the coefficient κ of the convective impulse terms, including those from synchronous fluctuations, must be proportional to the coefficient α/κ^2 of the conductive impulse term, giving $\kappa \propto \alpha^{1/3}$, or

$$\kappa = \text{Pr}^{-1/3} D \quad (13.6-18)$$

for the dependence of the average thermal boundary layer thickness on the Prandtl number.

The remaining terms in Eq. 13.6-15 describe the turbulent temperature fluctuations. They include the accumulation term $2\pi i\nu \tilde{\Theta}'$ and the remaining convection and conduction terms. The coefficients of all these terms (including $2\pi i\nu$ in the leading term) must be proportional functions of α in order that these terms likewise remain balanced as $\alpha \rightarrow 0$. This reasoning confirms Eq. 13.6-18 and gives the further relation $\nu \propto \kappa$, or

$$\frac{D\Delta\nu}{\langle v_z \rangle} \propto \kappa = \text{Pr}^{-1/3} D \quad (13.6-19)$$

for the frequency bandwidth $\Delta\nu$ of the temperature fluctuations. Consequently, the stretched frequency $\text{Pr}^{1/3}\nu$ and stretched time $\text{Pr}^{-1/3}t$ are natural variables for reporting Fourier analyses of turbulent forced convection. Shaw and Hanratty⁴ reported turbulence spectra for their mass transfer experiments analogously, in terms of a stretched frequency variable proportional to $\text{Sc}^{1/3}\nu$ (here $\text{Sc} = \mu/\rho\mathcal{D}_{AB}$ is the Schmidt number, the mass transfer analog of the Prandtl number, which contains the binary diffusivity \mathcal{D}_{AB} , to be introduced in Chapter 16).

Thus far we have considered only the leading term of a Taylor expansion in κ for each term in the energy equations. More accurate results are obtainable by continuing the Taylor expansions to higher powers of κ , and thus of $\text{Pr}^{-1/3}D$. The resulting formal solution is a perturbation expansion

$$\tilde{\Theta} = \tilde{\Theta}_0(Y, \theta, z, \text{Pr}^{1/3}\nu) + \kappa \tilde{\Theta}_1(Y, \theta, z, \text{Pr}^{1/3}\nu) + \dots \quad (13.6-20)$$

for the distribution of the fluctuating temperature over position and frequency in a given velocity field.

The expansion for \bar{T} (the long-time average of the temperature) corresponding to Eq. 13.6-20 is obtained from the zero-frequency part of $\tilde{\Theta}$,

$$\bar{\Theta} = \bar{\Theta}_0(Y, \theta, z) + \kappa \bar{\Theta}_1(Y, \theta, z) + \dots \quad (13.6-21)$$

⁴ D. A. Shaw and T. J. Hanratty, *AICHE Journal*, 23, 160–169 (1977); D. A. Shaw and T. J. Hanratty, *AICHE Journal*, 23, 28–37 (1977).

From this we can calculate the local time-averaged heat flux at the wall:

$$q_0 = -k \frac{\partial \bar{T}}{\partial y} \Big|_{y=0} = -\frac{k(T_0 - T_1)}{\text{Pr}^{-1/3} D} \frac{\partial \bar{\Theta}}{\partial Y} \Big|_{Y=0} \quad (13.6-22)$$

and the local Nusselt number is then

$$\text{Nu}_{\text{loc}} = \frac{q_0 D}{k(T_0 - T_1)} = \text{Pr}^{1/3} \left(-\frac{\partial \bar{\Theta}}{\partial Y} \right) \Big|_{Y=0} \quad (13.6-23)$$

Then the mean Nusselt number over the wall surface for heat transfer, and the analogous quantity for mass transfer, are

$$\text{Nu}_m = \text{Pr}^{1/3} \left\langle \left(-\frac{\partial \bar{\Theta}}{\partial Y} \right) \Big|_{Y=0} \right\rangle = a_1 \text{Pr}^{1/3} + a_2 \text{Pr}^0 + \dots \quad (13.6-24)$$

$$\text{Sh}_m = \text{Sc}^{1/3} \left\langle \left(-\frac{\partial \bar{\Theta}_A}{\partial Y} \right) \Big|_{Y=0} \right\rangle = a_1 \text{Sc}^{1/3} + a_2 \text{Sc}^0 + \dots \quad (13.6-25)$$

In this last equation Sh_m , $\bar{\Theta}_A$, and Sc are the mass transfer analogs of Nu_m , $\bar{\Theta}$, and Pr . We give the mass transfer expression here (rather than wait until Part III) because electrochemical mass transfer experiments give better precision than heat transfer experiments and the available range of Schmidt numbers is much greater than that of Prandtl numbers.

If the expansions in Eq. 13.6-24 and 25 are truncated to one term, we are led to $\text{Nu}_m \propto \text{Pr}^{1/3}$ and $\text{Sh}_m \propto \text{Sc}^{1/3}$. These expressions are essential ingredients in the famous Chilton–Colburn relations⁵ (see Eqs. 14.3-18 and 19, and Eqs. 22.3-22 to 24). The first term in Eq. 13.6-24 or 25 also corresponds to the high Prandtl (or Schmidt) number asymptote of Eq. 13.4-20.⁶

With the development of electrochemical methods of measuring mass transfer at surfaces, it has become possible to investigate the second term in Eq. 13.6-25. In Fig. 13.6-1 are shown the data of Shaw and Hanratty, who measured the diffusion-limited current to a wall electrode for values of the Schmidt number $\text{Sc} = \mu/\rho D_{AB}$ from 693 to 37,200. These data are fitted³ very well by the expression

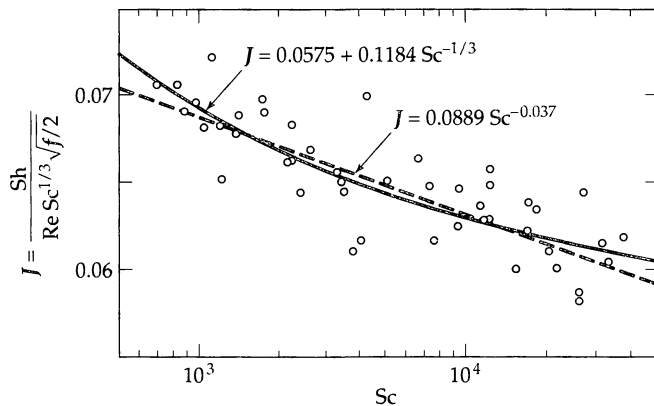


Fig. 13.6-1. Turbulent mass-transfer data of D. A. Shaw and T. J. Hanratty [AIChE Journal, 28, 23–37, 160–169 (1977)] compared to a curve based on Eq. 13.6-25 (solid curve). Shown also is a simple power law function obtained by Shaw and Hanratty.

⁵ T. H. Chilton and A. P. Colburn, *Ind. Eng. Chem.*, **26**, 1183–1187 (1934). Thomas Hamilton Chilton (1899–1972) had his entire professional career at the E. I. du Pont de Nemours Company, Inc., in Wilmington, Delaware; he was President of AIChE in 1951. After “retiring” he was a guest professor at a dozen or so universities.

⁶ See also O. C. Sandall and O. T. Hanna, *AIChE Journal*, **25**, 290–192 (1979).

$$\frac{Sh}{ReSc^{1/3}\sqrt{f/2}} = 0.0575 + 0.1184Sc^{-1/3} \quad (13.6-26)$$

in which $f(Re)$ is the friction factor defined in Chapter 6. Equation 13.6-26 combines the observed Re number dependence of the Sherwood number with the two leading terms of Eq. 13.6-25 (that is, the coefficients a_1, a_2, \dots are proportional to $Re\sqrt{f/2}$). Equation 13.6-26 lends itself to clear physical interpretation: The leading term corresponds to a diffusional boundary layer so thin that the tangential velocity is linear in y and the wall curvature can be neglected, whereas the second term accounts for wall curvature and the y^2 terms in the tangential velocity expansions of Eqs. 13.6-1 and 2). In higher approximations, special terms can be expected to arise from edge effects as noted by Newman⁷ and Stewart.³

QUESTIONS FOR DISCUSSION

1. Compare turbulent thermal conductivity and turbulent viscosity as to definition, order of magnitude, and dependence on physical properties and the nature of the flow.
2. What is the “Reynolds analogy,” and what is its significance?
3. Is there any connection between Eq. 13.2-3 and Eq. 13.4-12, after the integration constants in the latter have been evaluated?
4. Is the analogy between Fourier’s law of heat conduction and Eq. 13.3-1 a valid one?
5. What is the physical significance of the fact that the turbulent Prandtl number is of the order of unity?

PROBLEMS

13B.1. Wall heat flux for turbulent flow in tubes (approximate). Work through Example 13.3-1, and fill in the missing steps. In particular, verify the integration in going from Eq. 13.3-6 to Eq. 13.3-7.

13B.2. Wall heat flux for turbulent flow in tubes.

(a) Summarize the assumptions in §13.4.

(b) Work through the mathematical details of that section, taking particular care with the steps connecting Eq. 13.4-12 and Eq. 13.4-16.

(c) When is it not necessary to find the constant C_2 in Eq. 13.4-12?

13C.1. Wall heat flux for turbulent flow between two parallel plates.

(a) Work through the development in §13.4, and then perform a similar derivation for turbulent flow in a thin slit shown in Fig. 2B.3. Show that the analog of Eq. 13.4-19 is

$$\frac{k(T_0 - T_b)}{q_0 B} = \left(\frac{\bar{v}_{z,\max}}{\langle \bar{v}_z \rangle} \right)^2 \int_0^1 \frac{[J(\xi)]^2}{[1 + (\nu^{(l)} / \nu)(Pr/Pr^{(l)})]} d\xi \quad (13C.1-1)$$

in which $\xi = x/B$ and $J(\xi) = \int_0^\xi \phi(\bar{\xi}) d\bar{\xi}$.

(b) Show how the result in (a) simplifies for laminar flow of Newtonian fluids, and for “plug flow” (flat velocity profiles).

Answer: (b) $\frac{35}{17}, 3$

13D.1. The temperature profile for turbulent flow in tubes. To calculate the temperature distribution for turbulent flow in circular tubes from Eq. 13.4-12, it is necessary to know C_2 .

(a) Show how to get C_2 by applying B.C. 4 as was done in §10.8. The result is

$$C_2 = \int_0^1 \frac{[I(\xi)/I(1)]^2 - [I(\xi)/I(1)]}{\xi[1 + (\alpha^{(l)}/\alpha)]} d\xi \quad (13D.1-1)$$

(b) Verify that Eq. 13D.1-1 gives $C_2 = \frac{7}{24}$ for a Newtonian fluid.

⁷ J. S. Newman, *Electroanalytical Chemistry*, 6, 187–352 (1973).

Interphase Transport in Nonisothermal Systems

- §14.1 Definitions of heat transfer coefficients
- §14.2 Analytical calculations of heat transfer coefficients for forced convection through tubes and slits
- §14.3 Heat transfer coefficients for forced convection in tubes
- §14.4 Heat transfer coefficients for forced convection around submerged objects
- §14.5 Heat transfer coefficients for forced convection through packed beds
- §14.6^O Heat transfer coefficients for free and mixed convection
- §14.7^O Heat transfer coefficients for condensation of pure vapors on solid surfaces

In Chapter 10 we saw how shell energy balances may be set up for various simple problems and how these balances lead to differential equations from which the temperature profiles may be calculated. We also saw in Chapter 11 that the energy balance over an arbitrary differential fluid element leads to a partial differential equation—the energy equation—which may be used to set up more complex problems. Then in Chapter 13 we saw that the time-smoothed energy equation, together with empirical expressions for the turbulent heat flux, provides a useful basis for summarizing and extrapolating temperature profile measurements in turbulent systems. Hence, at this point the reader should have a fairly good appreciation for the meaning of the equations of change for nonisothermal flow and their range of applicability.

It should be apparent that all of the problems discussed have pertained to systems of rather simple geometry and furthermore that most of these problems have contained assumptions, such as temperature-independent viscosity and constant fluid density. For some purposes, these solutions may be adequate, especially for order-of-magnitude estimates. Furthermore, the study of simple systems provides the stepping stones to the discussion of more complex problems.

In this chapter we turn to some of the problems in which it is convenient or necessary to use a less detailed analysis. In such problems the usual engineering approach is to formulate energy balances over pieces of equipment, or parts thereof, as described in Chapter 15. In the macroscopic energy balance thus obtained, there are usually terms that require estimating the heat that is transferred through the system boundaries. This requires knowing the *heat transfer coefficient* for describing the interphase transport. Usually the heat transfer coefficient is given, for the flow system of interest, as an empirical correlation of

the *Nusselt number*¹ (a dimensionless wall heat flux or heat transfer coefficient) as a function of the relevant dimensionless quantities, such as the Reynolds and Prandtl numbers.

This situation is not unlike that in Chapter 6, where we learned how to use dimensionless correlations of the friction factor to solve momentum transfer problems. However, for nonisothermal problems the number of dimensionless groups is larger, the types of boundary conditions are more numerous, and the temperature dependence of the physical properties is often important. In addition, the phenomena of free convection, condensation, and boiling are encountered in nonisothermal systems.

We have purposely limited ourselves here to a small number of heat transfer formulas and correlations—just enough to introduce the reader to the subject without attempting to be encyclopedic. Many treatises and handbooks treat the subject in much greater depth.^{2,3,4,5,6}

§14.1 DEFINITIONS OF HEAT TRANSFER COEFFICIENTS

Let us consider a flow system with the fluid flowing either in a conduit or around a solid object. Suppose that the solid surface is warmer than the fluid, so that heat is being transferred from the solid to the fluid. Then the rate of heat flow across the solid–fluid interface would be expected to depend on the area of the interface and on the temperature drop between the fluid and the solid. It is customary to define a proportionality factor h (the *heat transfer coefficient*) by

$$Q = hA \Delta T \quad (14.1-1)$$

in which Q is the heat flow into the fluid (J/hr or Btu/hr), A is a characteristic area, and ΔT is a characteristic temperature difference. Equation 14.1-1 can also be used when the fluid is cooled. Equation 14.1-1, in slightly different form, has been encountered in Eq. 10.1-2. Note that h is not defined until the area A and the temperature difference ΔT have been specified. We now consider the usual definitions for h for two types of flow geometry.

As an example of *flow in conduits*, we consider a fluid flowing through a circular tube of diameter D (see Fig. 14.1-1), in which there is a heated wall section of length L and varying inside surface temperature $T_0(z)$, going from T_{01} to T_{02} . Suppose that the bulk temperature T_b of the fluid (defined in Eq. 10.8-33 for fluids with constant ρ and C_p) increases from T_{b1} to T_{b2} in the heated section. Then there are three conventional definitions of heat transfer coefficients for the fluid in the heated section:

$$Q = h_1(\pi DL)(T_{01} - T_{b1}) \equiv h_1(\pi DL)\Delta T_1 \quad (14.1-2)$$

$$Q = h_a(\pi DL) \left(\frac{(T_{01} - T_{b1}) + (T_{02} - T_{b2})}{2} \right) \equiv h_a(\pi DL)\Delta T_a \quad (14.1-3)$$

$$Q = h_{\ln}(\pi DL) \left(\frac{(T_{01} - T_{b1}) - (T_{02} - T_{b2})}{\ln(T_{01} - T_{b1}) - \ln(T_{02} - T_{b2})} \right) \equiv h_{\ln}(\pi DL)\Delta T_{\ln} \quad (14.1-4)$$

¹ This dimensionless group is named for **Ernst Kraft Wilhelm Nusselt** (1882–1957), the German engineer who was the first major figure in the field of convective heat and mass transfer. See, for example, W. Nusselt, *Zeits. d. Ver. deutsch. Ing.*, **53**, 1750–1755 (1909), *Forschungsarb. a. d. Geb. d. Ingenieurwes.*, No. 80, 1–38, Berlin (1910), and *Gesundheits-Ing.*, **38**, 477–482, 490–496 (1915).

² M. Jakob, *Heat Transfer*, Vol. 1 (1949) and Vol. 2 (1957), Wiley, New York.

³ W. M. Kays and M. E. Crawford, *Convective Heat and Mass Transfer*, 3rd edition, McGraw-Hill, New York (1993).

⁴ H. D. Baehr and K. Stephan, *Heat and Mass Transfer*, Springer, Berlin (1998).

⁵ W. M. Rohsenow, J. P. Hartnett, and Y. I. Cho (eds.), *Handbook of Heat Transfer*, McGraw-Hill, New York (1998).

⁶ H. Gröber, S. Erk, and U. Grigull, *Die Grundgesetze der Wärmeübertragung*, Springer, Berlin, 3rd edition (1961).

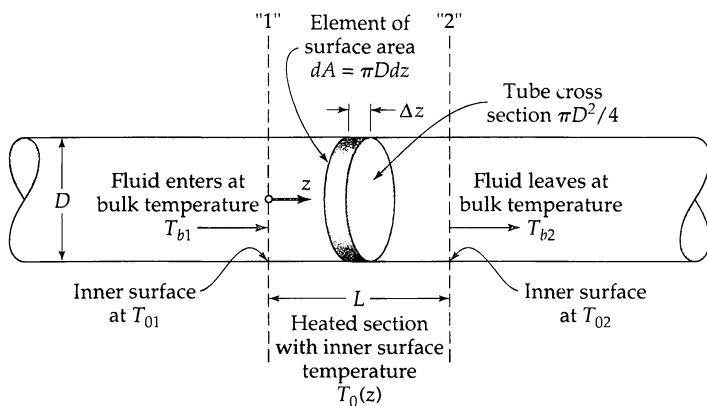


Fig. 14.1-1. Heat transfer in a circular tube.

That is, h_1 is based on the temperature difference ΔT_1 at the inlet, h_a is based on the *arithmetic mean* ΔT_a of the terminal temperature differences, and h_{ln} is based on the corresponding *logarithmic mean* temperature difference ΔT_{ln} . For most calculations h_{ln} is preferable, because it is less dependent on L/D than the other two, although it is not always used.¹ In using heat transfer correlations from treatises and handbooks, one must be careful to note the definitions of the heat transfer coefficients.

If the wall temperature distribution is initially unknown, or if the fluid properties change appreciably along the pipe, it is difficult to predict the heat transfer coefficients defined above. Under these conditions, it is customary to rewrite Eq. 14.1-2 in the differential form:

$$dQ = h_{loc}(\pi D dz)(T_0 - T_b) \equiv h_{loc}(\pi D dz)\Delta T_{loc} \quad (14.1-5)$$

Here dQ is the heat added to the fluid over a distance dz along the pipe, ΔT_{loc} is the local temperature difference (at position z), and h_{loc} is the *local heat transfer coefficient*. This equation is widely used in engineering design. Actually, the definition of h_{loc} and ΔT_{loc} is not complete without specifying the shape of the element of area. In Eq. 14.1-5 we have set $dA = \pi D dz$, which means that h_{loc} and ΔT_{loc} are the mean values for the shaded area dA in Fig. 14.1-1.

As an example of *flow around submerged objects*, consider a fluid flowing around a sphere of radius R , whose surface temperature is maintained at a uniform value T_0 . Suppose that the fluid approaches the sphere with a uniform temperature T_∞ . Then we may define a *mean heat transfer coefficient*, h_m , for the entire surface of the sphere by the relation

$$Q = h_m(4\pi R^2)(T_0 - T_\infty) \quad (14.1-6)$$

The characteristic area is here taken to be the heat transfer surface (as in Eqs. 14.1-2 to 5), whereas in Eq. 6.1-5 we used the sphere cross section.

A local coefficient can also be defined for submerged objects by analogy with Eq. 14.1-5:

$$dQ = h_{loc}(dA)(T_0 - T_\infty) \quad (14.1-7)$$

This coefficient is more informative than h_m because it predicts how the heat flux is distributed over the surface. However, most experimentalists report only h_m , which is easier to measure.

¹ If $\Delta T_2/\Delta T_1$ is between 0.5 and 2.0, then ΔT_a may be substituted for ΔT_{ln} , and h_a for h_{ln} , with a maximum error of 4%. This degree of accuracy is acceptable in most heat transfer calculations.

Table 14.1-1 Typical Orders of Magnitude for Heat Transfer Coefficients^a

System	h (W/m ² · K) or (kcal/m ² · hr · C)	h (Btu/ft ² · hr · F)
<i>Free convection</i>		
Gases	3–20	1–4
Liquids	100–600	20–120
Boiling water	1000–20,000	200–4000
<i>Forced convection</i>		
Gases	10–100	2–20
Liquids	50–500	10–100
Water	500–10,000	100–2000
<i>Condensing vapors</i>	1000–100,000	200–20,000

^a Taken from H. Gröber, S. Erk, and U. Grigull, *Wärmeübertragung*, Springer, Berlin, 3rd edition (1955), p. 158. When given h in kcal/m² · hr · C, multiply by 0.204 to get h in Btu/ft² · hr · F, and by 1.162 to get h in W/m² · K. For additional conversion factors, see Appendix F.

Let us emphasize that the definitions of A and ΔT must be made clear before h is defined. Keep in mind, also, that h is not a constant characteristic of the fluid medium. On the contrary, the heat transfer coefficient depends in a complicated way on many variables, including the fluid properties (k , μ , ρ , C_p), the system geometry, and the flow velocity. The remainder of this chapter is devoted to predicting the dependence of h on these quantities. Usually this is done by using experimental data and dimensional analysis to develop correlations. It is also possible, for some very simple systems, to calculate the heat transfer coefficient directly from the equations of change. Some typical ranges of h are given in Table 14.1-1.

We saw in §10.6 that, in the calculation of heat transfer rates between two fluid streams separated by one or more solid layers, it is convenient to use an *overall heat transfer coefficient*, U_0 , which expresses the combined effect of the series of resistances through which the heat flows. We give here a definition of U_0 and show how to calculate it in the special case of heat exchange between two coaxial streams with bulk temperatures T_h ("hot") and T_c ("cold"), separated by a cylindrical tube of inside diameter D_0 and outside diameter D_1 :

$$dQ = U_0(\pi D_0 dz)(T_h - T_c) \quad (14.1-8)$$

$$\frac{1}{D_0 U_0} = \left(\frac{1}{D_0 h_0} + \frac{\ln(D_1/D_0)}{2k^{01}} + \frac{1}{D_1 h_1} \right)_{\text{loc}} \quad (14.1-9)$$

Note that U_0 is defined as a local coefficient. This is the definition implied in most design procedures (see Example 15.4-1).

Equations 14.1-8 and 9 are, of course, restricted to thermal resistances connected in *series*. In some situations there may be appreciable *parallel* heat flux at one or both surfaces by radiation, and Eqs. 14.1-8 and 9 will require special modification (see Example 16.5-2).

To illustrate the physical significance of heat transfer coefficients and illustrate one method of measuring them, we conclude this section with an analysis of a hypothetical set of heat transfer data.

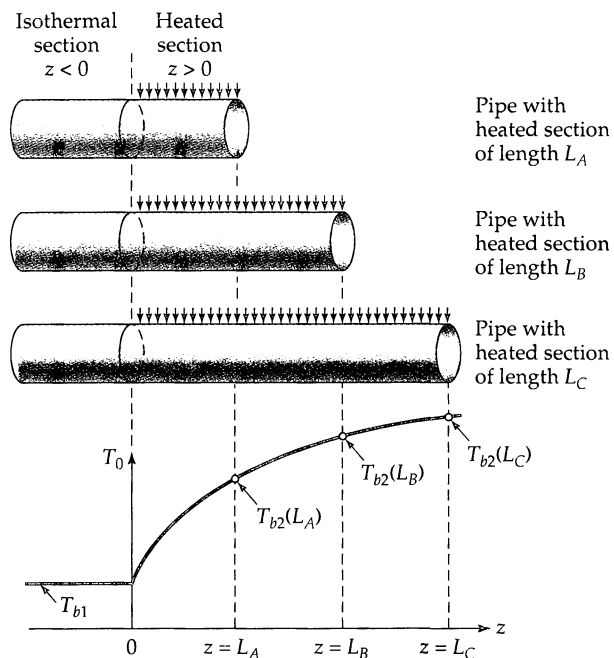


Fig. 14.1-2. Series of experiments for measuring heat transfer coefficients.

EXAMPLE 14.1-1

Calculation of Heat Transfer Coefficients from Experimental Data

A series of simulated steady-state experiments on the heating of air in tubes is shown in Fig. 14.1-2. In the first experiment, air at $T_{b1} = 200.0^\circ\text{F}$ is flowing in a 0.5-in. i.d. tube with fully developed laminar velocity profile in the isothermal pipe section for $z < 0$. At $z = 0$ the wall temperature is suddenly increased to $T_0 = 212.0^\circ\text{F}$ and maintained at that value for the remaining tube length L_A . At $z = L_A$ the fluid flows into a mixing chamber in which the cup-mixing (or "bulk") temperature T_{b2} is measured. Similar experiments are done with tubes of different lengths, L_B , L_C , and so on, with the following results:

Experiment	A	B	C	D	E	F	G
L (in.)	1.5	3.0	6.0	12.0	24.0	48.0	96.0
T_{b2} ($^\circ\text{F}$)	201.4	202.2	203.1	204.6	206.6	209.0	211.0

In all experiments, the air flow rate w is 3.0 lb_{in}/hr. Calculate h_1 , h_a , h_{inv} , and the exit value of h_{loc} as functions of the L/D ratio.

SOLUTION

First we make a steady-state energy balance over a length L of the tube, by stating that the heat in through the walls plus the energy entering at $z = 0$ by convection equals the energy leaving the tube at $z = L$. The axial energy flux at the tube entry and exit may be calculated from Eq. 9.8-6. For fully developed flow, changes in the kinetic energy flux $\frac{1}{2}\rho v^2 \mathbf{v}$ and the work term $[\tau \cdot \mathbf{v}]$ will be negligible relative to changes in the enthalpy flux. We also assume that $q_z \ll \rho H v_z$, so that the axial heat conduction term may be neglected. Hence the only contribution to the energy flux entering and leaving with the flow will be the term containing the enthalpy, which can be computed with the help of Eq. 9.8-8 and the assumptions that the heat capacity and density of the fluid are constant throughout. Therefore the steady-state energy balance becomes simply "rate of energy flow in = rate of energy flow out," or

$$Q + w\hat{C}_p T_{b1} = w\hat{C}_p T_{b2} \quad (14.1-10)$$

Using Eq. 14.1-2 to evaluate Q and rearranging gives

$$w\hat{C}_p(T_{b2} - T_{b1}) = h_1(\pi D L)(T_0 - T_{b1}) \quad (14.1-11)$$

from which

$$h_1 = \frac{w\hat{C}_p}{\pi D^2} \frac{(T_{b2} - T_{b1})}{(T_0 - T_{b1})} \left(\frac{D}{L} \right) \quad (14.1-12)$$

This gives us the formula for calculating h_1 from the data given above.

Analogously, use of Eqs. 14.1-3 and 14.1-4 gives

$$h_a = \frac{w\hat{C}_p}{\pi D^2} \frac{(T_{b2} - T_{b1})}{(T_0 - T_b)_a} \left(\frac{D}{L} \right) \quad (14.1-13)$$

$$h_{ln} = \frac{w\hat{C}_p}{\pi D^2} \frac{(T_{b2} - T_{b1})}{(T_0 - T_b)_{ln}} \left(\frac{D}{L} \right) \quad (14.1-14)$$

for obtaining h_a and h_{ln} from the data.

To evaluate h_{loc} , we have to use the preceding data to construct a continuous curve $T_b(z)$, as in Fig. 14.1-2, to represent the change in bulk temperature with z in the longest (96-in.) tube. Then Eq. 14.1-10 becomes

$$Q(z) + w\hat{C}_p T_{b1} = w\hat{C}_p T_b(z) \quad (14.1-15)$$

By differentiating this expression with respect to z and combining the result with Eq. 14.1-5, we get

$$w\hat{C}_p \frac{dT_b}{dz} = h_{loc} \pi D (T_0 - T_b) \quad (14.1-16)$$

or

$$h_{loc} = \frac{w\hat{C}_p}{\pi D} \frac{1}{(T_0 - T_b)} \frac{dT_b}{dz} \quad (14.1-17)$$

Since T_0 is constant, this becomes

$$h_{loc} = -\frac{w\hat{C}_p}{\pi D^2} \frac{d \ln(T_0 - T_b)}{d(z/L)} \left(\frac{D}{L} \right) \quad (14.1-18)$$

The derivative in this equation is conveniently determined from a plot of $\ln(T_0 - T_b)$ versus z/L . Because a differentiation is involved, it is difficult to determine h_{loc} precisely.

The calculated results are shown in Fig. 14.1-3. Note that all of the coefficients decrease with increasing L/D , but that h_{loc} and h_{ln} vary less than the others. They approach a common asymptote (see Problem 14B.5 and Fig. 14.1-3). Somewhat similar behavior is observed in turbulent flow with constant wall temperature, except that h_{loc} approaches the asymptote much more rapidly (see Fig. 14.3-2).

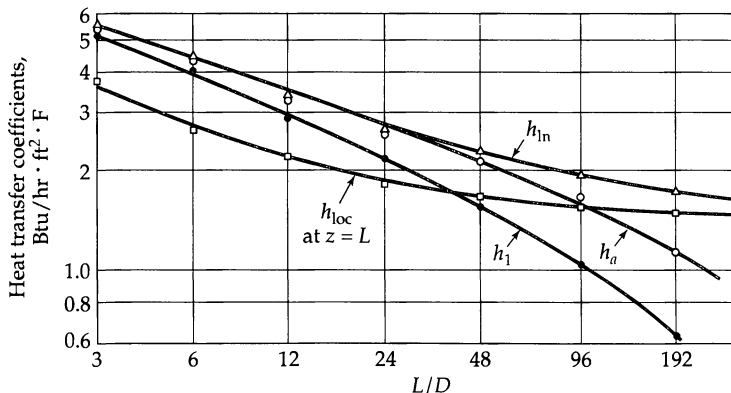


Fig. 14.1-3. Heat transfer coefficients calculated in Example 14.1-1.

§14.2 ANALYTICAL CALCULATIONS OF HEAT TRANSFER COEFFICIENTS FOR FORCED CONVECTION THROUGH TUBES AND SLITS

Recall from Chapter 6, where we defined and discussed friction factors, that for some very simple laminar flow systems we could obtain analytical formulas for the (dimensionless) friction factor as a function of the (dimensionless) Reynolds number. We would like to do the same for the heat transfer coefficient, h , which, however, is not dimensionless. Nonetheless we can construct with it a dimensionless quantity, $\text{Nu} = hD/k$, the *Nusselt number*, using the fluid thermal conductivity k and a characteristic length D that must be specified for each flow system. Two other related dimensionless groups are commonly used: the *Stanton number*, $\text{St} = \text{Nu}/\text{RePr}$, and the *Chilton-Colburn j-factor* for heat transfer, $j_H = \text{Nu}/\text{RePr}^{1/3}$. Each of these dimensionless groups may be “decorated” with subscript 1, a , \ln , or m , corresponding to the subscript on the Nusselt number.

By way of illustration, let us return to §10.8 where we discussed the heating of a fluid in laminar flow in a tube, with all the fluid properties being considered constant. From Eq. 10.8-33 and Eq. 10.8-31 we can get the difference between the wall temperature and the bulk temperature:

$$\begin{aligned} T_0 - T_b &= \left(4\zeta + \frac{11}{24}\right)\left(\frac{q_0 R}{k}\right) - 4\zeta\left(\frac{q_0 R}{k}\right) \\ &= \frac{11}{24}\left(\frac{q_0 R}{k}\right) = \frac{11}{48}\left(\frac{q_0 D}{k}\right) \end{aligned} \quad (14.2-1)$$

in which R and D are the radius and diameter of the tube. Solving for the wall flux we get

$$q_0 = \frac{48}{11}\left(\frac{k}{D}\right)(T_0 - T_b) \quad (14.2-2)$$

Then making use of the definition of the local heat transfer coefficient h_{loc} —namely, that $q_0 = h_{\text{loc}}(T_0 - T_b)$ —we find that

$$h_{\text{loc}} = \frac{48}{11}\left(\frac{k}{D}\right) \quad \text{or} \quad \text{Nu}_{\text{loc}} = \frac{hD}{k} = \frac{48}{11} \quad (14.2-3)$$

This result is the entry in Eq. (L) of Table 14.2-1—namely, for the laminar flow of a constant-property fluid with a constant wall heat flux, for very large z . The other entries in Table 14.2-1 and 2 may be obtained in a similar way.¹ Some Nusselt numbers for Newtonian fluids with constant physical properties are shown in Fig. 14.2-1.²

¹ These tables are taken from R. B. Bird, R. C. Armstrong, and O. Hassager, *Dynamics of Polymeric Liquids*, Vol. 1, *Fluid Mechanics*, 1st edition, Wiley, New York, (1987), pp. 212–213. They are based, in turn, on W. J. Beek and R. Eggink, *De Ingenieur*, **74**, (35) Ch. 81–Ch. 89 (1962) and J. M. Valstar and W. J. Beek, *De Ingenieur*, **75**, (1), Ch. 1–Ch. 7 (1963).

² The correspondence between the entries of Tables 14.2-1 and 2 and problems in this book is as follows (\odot = circular tube, \parallel = plane slit):

Eq. (C)	Problem 12D.4 \odot ; 12D.5 \parallel	Laminar Newtonian
Eq. (F)	Problem 12D.3 \odot ; 12D.5 \parallel	Laminar Newtonian
Eq. (G)	Problem 10B.9(a) \odot ; 10B.9(b) \parallel	Plug flow
Eq. (I)	Problem 12D.7 \odot ; 12D.6 \parallel	Laminar Newtonian
Eq. (K)	Problem 10D.2 \odot	Laminar non-Newtonian
Eq. (L)	Problem 12D.6 \parallel	Laminar Newtonian

Equations analogous to Eqs. (K) in Tables 14.2-1 and 2 are given for turbulent flow in Eqs. 13.4-19 and 13C.1-1.

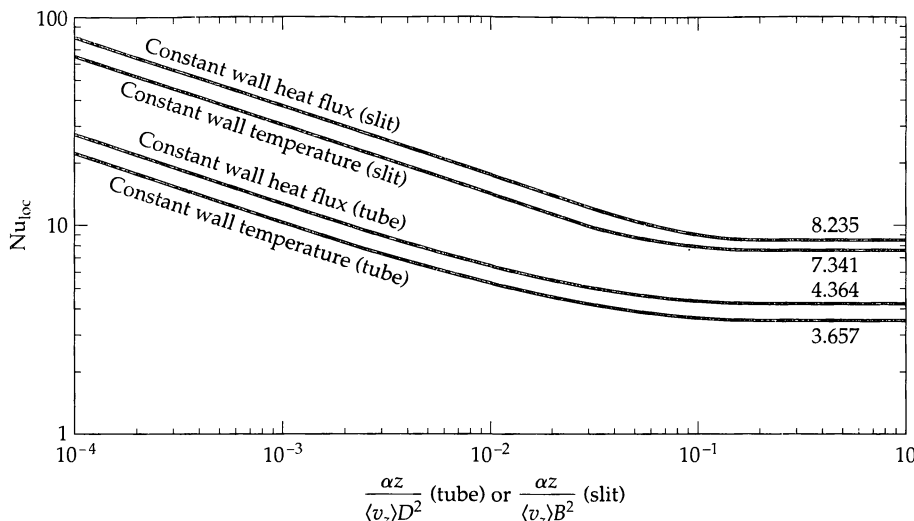


Fig. 14.2-1. The Nusselt number for fully developed, laminar flow of Newtonian fluids with constant physical properties: $\text{Nu}_{\text{loc}} = h_{\text{loc}}D/k$ for circular tubes of diameter D , and $\text{Nu}_{\text{loc}} = 4h_{\text{loc}}B/k$ for slits of half-width B . The limiting expressions are given in Tables 14.2-1 and 14.2-2.

For *turbulent flow* in a circular tube with constant heat flux, the Nusselt number can be obtained from Eq. 13.4-20 (which in turn originated with Eq. (K) of Table 14.2-1):³

$$\text{Nu}_{\text{loc}} = \frac{\text{RePr}\sqrt{f}/2}{12.48\text{Pr}^{2/3} - 7.853\text{Pr}^{1/3} + 3.613 \ln \text{Pr} + 5.8 + 2.78 \ln(\frac{1}{45}\text{Re}\sqrt{f}/8)} \quad (14.2-4)$$

This is valid only for $\alpha z / \langle v_z \rangle D^2 \gg 1$, for fluids with constant physical properties, and for tubes with no roughness. It has been applied successfully over the Prandtl-number range $0.7 < \text{Pr} < 590$. Note that, for very large Prandtl numbers, Eq. 14.2-4 gives

$$\text{Nu}_{\text{loc}} = 0.0566 \text{ RePr}^{1/3} \sqrt{f} \quad (14.2-5)$$

The $\text{Pr}^{1/3}$ dependence agrees exactly with the large Pr limit in §13.6 and Eq. 13.3-7. For turbulent flow there is little difference between Nu for constant wall temperature and for constant wall heat flux.

For the turbulent flow of *liquid metals*, for which the Prandtl numbers are generally much less than unity, there are two results of importance. Notter and Sleicher⁴ solved the energy equation numerically, using a realistic turbulent velocity profile, and obtained the rates of heat transfer through the wall. The final results were curve-fitted to simple analytical expressions for two cases:

$$\text{Constant wall temperature:} \quad \text{Nu}_{\text{loc}} = 4.8 + 0.0156 \text{ Re}^{0.85} \text{ Pr}^{0.93} \quad (14.2-6)$$

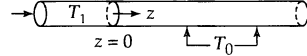
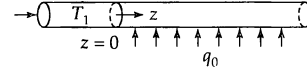
$$\text{Constant wall heat flux:} \quad \text{Nu}_{\text{loc}} = 6.3 + 0.0167 \text{ Re}^{0.85} \text{ Pr}^{0.93} \quad (14.2-7)$$

These equations are limited to $L/D > 60$ and constant physical properties. Equation 14.2-7 is displayed in Fig. 14.2-2.

³ O. C. Sandall, O. T. Hanna, and P. R. Mazet, *Canad. J. Chem. Eng.*, **58**, 443–447 (1980).

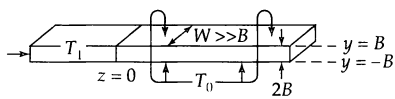
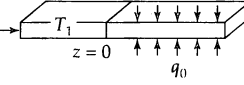
⁴ R. H. Notter and C. A. Sleicher, *Chem. Eng. Sci.*, **27**, 2073–2093 (1972).

Table 14.2-1 Asymptotic Results for Local Nusselt Numbers (Tube Flow)^{a,b}; $Nu_{loc} = h_{loc}D/k$

All values are local Nu numbers	Constant wall temperature 		Constant wall heat flux 	
	Thermal entrance region ^c	Plug flow	Laminar non-Newtonian flow	Laminar Newtonian flow
$\frac{\langle v_z \rangle D^2}{\alpha z} \gg 1$	Plug flow	$Nu = \frac{1}{\sqrt{\pi}} \left(\frac{\langle v_z \rangle D^2}{\alpha z} \right)^{1/2}$ (A)	Plug flow	$Nu = \frac{\sqrt{\pi}}{2} \left(\frac{\langle v_z \rangle D^2}{\alpha z} \right)^{1/2}$ (G)
	Laminar non-Newtonian flow	$Nu = \frac{2}{9^{1/3} \Gamma(\frac{2}{3})} \left[\frac{\langle v_z \rangle D^2}{\alpha z} \left(-\frac{1}{4} \frac{d\phi}{d\xi} \Big _{\xi=1} \right) \right]^{1/3}$ (B)	Laminar non-Newtonian flow	$Nu = \frac{2\Gamma(\frac{2}{3})}{9^{1/3}} \left[\frac{\langle v_z \rangle D^2}{\alpha z} \left(-\frac{1}{4} \frac{d\phi}{d\xi} \Big _{\xi=1} \right) \right]^{1/3}$ (H)
	Laminar Newtonian flow	$Nu = \frac{2}{9^{1/3} \Gamma(\frac{4}{3})} \left(\frac{\langle v_z \rangle D^2}{\alpha z} \right)^{1/3}$ (C)	Laminar Newtonian flow	$Nu = \frac{2\Gamma(\frac{2}{3})}{9^{1/3}} \left(\frac{\langle v_z \rangle D^2}{\alpha z} \right)^{1/3}$ (I)
Thermally fully developed flow $\frac{\langle v_z \rangle D^2}{\alpha z} \ll 1$	Plug flow	$Nu = 5.772$ (D)	Plug flow	$Nu = 8$ (J)
	Laminar non-Newtonian flow	$Nu = \beta_1^2$, where β_1 is the lowest eigenvalue of $\frac{1}{\xi} \frac{d}{d\xi} \left(\xi \frac{dX_n}{d\xi} \right) + \beta_n^2 \phi(\xi) X_n = 0;$ $X'_n(0) = 0, X_n(1) = 0$ (E)	Laminar non-Newtonian flow	$Nu = \left[2 \int_0^1 \frac{1}{\xi} \left[\int_0^\xi \xi' \phi(\xi') d\xi' \right]^2 d\xi \right]^{-1}$ (K)
	Laminar Newtonian flow	$Nu = 3.657$ (F)	Laminar Newtonian flow	$Nu = \frac{48}{11} = 4.364$ (L)

^a Note: $\phi(\xi) = v_z / \langle v_z \rangle$, where $\xi = r/R$ and $R = D/2$; for Newtonian fluids $\langle v_z \rangle D^2 / \alpha z = Re Pr(D/z)$ with $Re = D \langle v_z \rangle \rho / \mu$. Here $\alpha = k / \rho \hat{C}_p$.^b W. J. Beek and R. Eggink, *De Ingenieur*, **74**, No. 35, Ch. 81–89 (1962); erratum, **75**, No. 1, Ch. 7 (1963).^c The grouping $\langle v_z \rangle D^2 / \alpha z$ is sometimes written as $Gz \cdot (L/z)$ where $Gz = \langle v_z \rangle D^2 / \alpha L$ is called the Graetz number; here L is the length of the pipe past $z = 0$. Thus the thermal entry region corresponds to large Graetz number.

Table 14.2-2 Asymptotic Results for Local Nusselt Numbers (Thin-Slit Flow)^{a,b}; $\text{Nu}_{\text{loc}} = 4h_{\text{loc}}B/k$

All values are local Nu numbers	Constant wall temperature		Constant wall heat flux	
		$\text{Nu} = \frac{4}{\sqrt{\pi}} \left(\frac{\langle v_z \rangle B^2}{\alpha z} \right)^{1/2}$ (A)		$\text{Nu} = 2\sqrt{\pi} \left(\frac{\langle v_z \rangle B^2}{\alpha z} \right)^{1/2}$ (G)
Thermal entrance region^c	Plug flow	$\text{Nu} = \frac{4}{\sqrt{\pi}} \left(\frac{\langle v_z \rangle B^2}{\alpha z} \right)^{1/2}$ (A)	Plug flow	$\text{Nu} = 2\sqrt{\pi} \left(\frac{\langle v_z \rangle B^2}{\alpha z} \right)^{1/2}$ (G)
	Laminar non- Newtonian flow	$\text{Nu} = \frac{4}{9^{1/3}\Gamma(\frac{4}{3})} \left[\frac{\langle v_z \rangle B^2}{\alpha z} \left(-\frac{d\phi}{d\sigma} \Big _{\sigma=1} \right) \right]^{1/3}$ (B)	Laminar non- Newtonian flow	$\text{Nu} = \frac{4\Gamma(\frac{2}{3})}{9^{1/3}} \left[\frac{\langle v_z \rangle B^2}{\alpha z} \left(-\frac{d\phi}{d\sigma} \Big _{\sigma=1} \right) \right]^{1/3}$ (H)
	Laminar Newtonian flow	$\text{Nu} = \frac{4}{3^{1/3}\Gamma(\frac{4}{3})} \left(\frac{\langle v_z \rangle B^2}{\alpha z} \right)^{1/3}$ (C)	Laminar Newtonian flow	$\text{Nu} = \frac{4\Gamma(\frac{2}{3})}{3^{1/3}} \left(\frac{\langle v_z \rangle B^2}{\alpha z} \right)^{1/3}$ (I)
Thermally fully developed flow	Plug flow	$\text{Nu} = \pi^2 = 9.870$ (D)	Plug flow	$\text{Nu} = 12$ (J)
	Laminar non- Newtonian flow	$\text{Nu} = 4\beta_1^2$, where β_1 is the lowest eigenvalue of $\frac{d^2 X_n}{d\sigma^2} + \beta_n^2 \phi(\sigma) X_n = 0; \quad X_n(\pm 1) = 0$ (E)	Laminar non- Newtonian flow	$\text{Nu} = \left[\frac{1}{4} \int_0^1 \left[\int_0^\sigma \phi(\sigma') d\sigma' \right]^2 d\sigma \right]^{-1}$ (K)
	Laminar Newtonian flow	$\text{Nu} = 7.541$ (F)	Laminar Newtonian flow	$\text{Nu} = \frac{140}{17} = 8.235$ (L)

^a Note: $\phi(\sigma) = v_z/\langle v_z \rangle$, where $\sigma = y/B$; for Newtonian fluids $\langle v_z \rangle D^2/\alpha z = 4 \text{RePr}(B/z)$ with $\text{Re} = 4B\langle v_z \rangle p/\mu$. Here $\alpha = k/p\hat{C}_p$.

^b J. M. Valstar and W. J. Beek, *De Ingenieur*, 75, No. 1, Ch. 1-7 (1963).

^c The grouping $\langle v_z \rangle B^2/\alpha z$ is sometimes written as $Gz \cdot (L/z)$ where $Gz = \langle v_z \rangle B^2/\alpha L$ is called the Graetz number; here L is the length of the slit past $z = 0$. Thus the thermal entry region corresponds to large Graetz number.

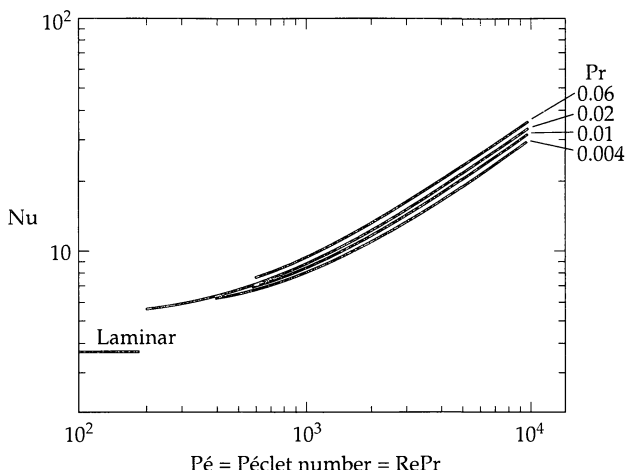


Fig. 14.2-2. Nusselt numbers for turbulent flow of liquid metals in circular tubes, based on the theoretical calculations of R. H. Notter and C. A. Sleicher, *Chem. Eng. Sci.*, 27, 2073–2093 (1972).

It has been emphasized that all the results of this section are limited to fluids with constant physical properties. When there are large temperature differences in the system, it is necessary to take into account the temperature dependence of the viscosity, density, heat capacity, and thermal conductivity. Usually this is done by means of an empiricism—namely, by evaluating the physical properties at some appropriate average temperature. Throughout this chapter, unless explicitly stated otherwise, it is understood that all physical properties are to be calculated at the film temperature T_f defined as follows:⁵

- For tubes, slits, and other ducts,

$$T_f = \frac{1}{2}(T_{0a} + T_{ba}) \quad (14.2-8)$$

in which T_{0a} is the arithmetic average of the surface temperatures at the two ends, $T_{0a} = \frac{1}{2}(T_{01} + T_{02})$, and T_{ba} is the arithmetic average of the inlet and outlet bulk temperatures, $T_{ba} = \frac{1}{2}(T_{b1} + T_{b2})$.

It is also recommended that the Reynolds number be written as $\text{Re} = D(\rho v)/\mu = Dw/S\mu$, in order to account for viscosity, velocity, and density changes over the cross section of area S .

- For submerged objects with uniform surface temperature T_0 in a stream of liquid approaching with uniform temperature T_∞ ,

$$T_f = \frac{1}{2}(T_0 + T_\infty) \quad (14.2-9)$$

For flow systems involving more complicated geometries, it is preferable to use experimental correlations of the heat transfer coefficients. In the following sections we show how such correlations can be established by a combination of dimensional analysis and experimental data.

⁵ W. J. M. Douglas and S. W. Churchill, *Chem. Eng. Prog. Symposium Series*, No. 18, 52, 23–28 (1956); E. R. G. Eckert, *Recent Advances in Heat and Mass Transfer*, McGraw-Hill, New York (1961), pp. 51–81, Eq. (20); more detailed reference states have been proposed by W. E. Stewart, R. Kilgour, and K.-T. Liu, University of Wisconsin–Madison Mathematics Research Center Report #1310 (June 1973).

§14.3 HEAT TRANSFER COEFFICIENTS FOR FORCED CONVECTION IN TUBES

In the previous section we have shown that Nusselt numbers for some laminar flows can be computed from first principles. In this section we show how dimensional analysis leads us to a general form for the dependence of the Nusselt number on various dimensionless groups, and that this form includes not only the results of the preceding section, but turbulent flows as well. Then we present a dimensionless plot of Nusselt numbers that was obtained by correlating experimental data.

First we extend the dimensional analysis given in §11.5 to obtain a general form for correlations of heat transfer coefficients in forced convection. Consider the steadily driven laminar or turbulent flow of a Newtonian fluid through a straight tube of inner radius R , as shown in Fig. 14.3-1. The fluid enters the tube at $z = 0$ with velocity uniform out to very near the wall, and with a uniform inlet temperature T_1 ($= T_{b1}$). The tube wall is insulated except in the region $0 \leq z \leq L$, where a uniform inner-surface temperature T_0 is maintained by heat from vapor condensing on the outer surface. For the moment, we assume constant physical properties ρ , μ , k , and C_p . Later we will extend the empiricism given in §14.2 to provide a fuller allowance for the temperature dependence of these properties.

We follow the same procedure used in §6.2 for friction factors. We start by writing the expression for the instantaneous heat flow from the tube wall into the fluid in the system described above,

$$Q(t) = \int_0^L \int_0^{2\pi} \left(+k \frac{\partial T}{\partial r} \right) \Big|_{r=R} R d\theta dz \quad (14.3-1)$$

which is valid for laminar or turbulent flow (in laminar flow, Q would, of course, be independent of time). The + sign appears here because the heat is added to the system in the negative r direction.

Equating the expressions for Q given in Eqs. 14.1-2 and 14.3-1 and solving for h_1 , we get

$$h_1(t) = \frac{1}{\pi D L (T_0 - T_{b1})} \int_0^L \int_0^{2\pi} \left(+k \frac{\partial T}{\partial r} \right) \Big|_{r=R} R d\theta dz \quad (14.3-2)$$

Next we introduce the dimensionless quantities $\check{r} = r/D$, $\check{z} = z/D$, and $\check{T} = (T - T_0)/(T_{b1} - T_0)$, and multiply by D/k to get an expression for the Nusselt number $Nu_1 = h_1 D/k$:

$$Nu_1(t) = \frac{1}{2\pi L/D} \int_0^{L/D} \int_0^{2\pi} \left(-\frac{\partial \check{T}}{\partial \check{r}} \right) \Big|_{\check{r}=1/2} d\theta d\check{z} \quad (14.3-3)$$

Thus the (instantaneous) Nusselt number is basically a *dimensionless temperature gradient averaged over the heat transfer surface*.

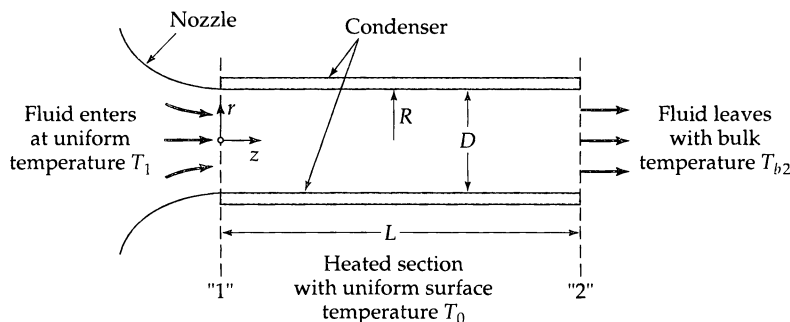


Fig. 14.3-1. Heat transfer in the entrance region of a tube.

The dimensionless temperature gradient appearing in Eq. 14.3-3 could, in principle, be evaluated by differentiating the expression for \check{T} obtained by solving Eqs. 11.5-7, 8, and 9 with the boundary conditions

$$\text{at } \check{z} = 0, \quad \check{v} = \delta_z \quad \text{for } 0 \leq \check{r} < \frac{1}{2} \quad (14.3-4)$$

$$\text{at } \check{r} = \frac{1}{2}, \quad \check{v} = 0 \quad \text{for } \check{z} \geq 0 \quad (14.3-5)$$

$$\text{at } \check{r} = 0 \text{ and } \check{z} = 0, \quad \check{\mathcal{P}} = 0 \quad (14.3-6)$$

$$\text{at } \check{z} = 0, \quad \check{T} = 1 \quad \text{for } 0 \leq \check{r} \leq \frac{1}{2} \quad (14.3-7)$$

$$\text{at } \check{r} = \frac{1}{2} \quad \check{T} = 0 \quad \text{for } 0 \leq \check{z} \leq L/D \quad (14.3-8)$$

where $\check{v} = v/\langle v_z \rangle_1$ and $\check{\mathcal{P}} = (\mathcal{P} - \mathcal{P}_1)/\rho \langle v_z \rangle_1^2$. As in §6.2, we have neglected the $\partial^2/\partial \check{z}^2$ terms of the equations of change on the basis of order-of-magnitude reasoning similar to that in §4.4. With those terms suppressed, upstream transport of heat and momentum are excluded, so that the solutions upstream of plane 2 in Fig. 14.3-1 do not depend on L/D .

From Eqs. 11.5-7, 8, and 9 and these boundary conditions, we conclude that the dimensionless instantaneous temperature distribution must be of the following form:

$$\check{T} = \check{T}(\check{r}, \theta, \check{z}, \check{t}; \text{Re, Pr, Br}) \quad \text{for } 0 \leq \check{z} \leq L/D \quad (14.3-9)$$

Substitution of this relation into Eq. 14.3-3 leads to the conclusion that $\text{Nu}_1(\check{t}) = \text{Nu}_1(\text{Re}, \text{Pr}, \text{Br}, L/D, \check{t})$. When time-averaged over an interval long enough to include all the turbulent disturbances, this becomes

$$\text{Nu}_1 = \text{Nu}_1(\text{Re, Pr, Br, } L/D) \quad (14.3-10)$$

A similar relation is valid when the flow at plane 1 is fully developed.

If, as is often the case, the viscous dissipation heating is small, the Brinkman number can be omitted. Then Eq. 14.3-10 simplifies to

$$\text{Nu}_1 = \text{Nu}_1(\text{Re, Pr, } L/D) \quad (14.3-11)$$

Therefore, dimensional analysis tells us that, for forced-convection heat transfer in circular tubes with constant wall temperature, experimental values of the heat transfer coefficient h_1 can be correlated by giving Nu_1 as a function of the Reynolds number, the Prandtl number, and the geometric ratio L/D . This should be compared with the similar, but simpler, situation with the friction factor (Eqs. 6.2-9 and 10).

The same reasoning leads us to similar expressions for the other heat transfer coefficients we have defined. It can be shown (see Problem 14.B-4) that

$$\text{Nu}_a = \text{Nu}_a(\text{Re, Pr, } L/D) \quad (14.3-12)$$

$$\text{Nu}_{ln} = \text{Nu}_{ln}(\text{Re, Pr, } L/D) \quad (14.3-13)$$

$$\text{Nu}_{loc} = \text{Nu}_{loc}(\text{Re, Pr, } L/D) \quad (14.3-14)$$

in which $\text{Nu}_a = h_a D/k$, $\text{Nu}_{ln} = h_{ln} D/k$, and $\text{Nu}_{loc} = h_{loc} D/k$. That is, to each of the heat transfer coefficients, there is a corresponding Nusselt number. These Nusselt numbers are, of course, interrelated (see Problem 14.B-5). These general functional forms for the Nusselt numbers have a firm scientific basis, since they involve only the dimensional analysis of the equations of change and boundary conditions.

Thus far we have assumed that the physical properties are constants over the temperature range encountered in the flow system. At the end of §14.2 we indicated that evaluating the physical properties at the film temperature is a suitable empiricism. However, for very large temperature differences, the viscosity variations may result in such a large distortion of the velocity profiles that it is necessary to account for this by introducing an additional dimensionless group, μ_b/μ_0 , where μ_b is the viscosity at the arithmetic

average bulk temperature and μ_0 is the viscosity at the arithmetic average wall temperature.¹ Then we may write

$$\text{Nu} = \text{Nu}(\text{Re}, \text{Pr}, L/D, \mu_b/\mu_0) \quad (14.3-15)$$

This type of correlation seems to have first been presented by Sieder and Tate.² If, in addition, the density varies significantly, then some free convection may occur. This effect can be accounted for in correlations by including the Grashof number along with the other dimensionless groups. This point is pursued further in §14.6.

Let us now pause to reflect on the significance of the above discussion for constructing heat transfer correlations. The heat transfer coefficient h depends on *eight* physical quantities (D , $\langle v \rangle$, ρ , μ_0 , μ_b , C_p , k , L). However, Eq. 14.3-15 tells us that this dependence can be expressed more concisely by giving Nu as a function of only *four* dimensionless groups (Re , Pr , L/D , μ_b/μ_0). Thus, instead of taking data on h for 5 values of each of the eight individual physical quantities (5^8 tests), we can measure h for 5 values of the dimensionless groups (5^4 tests)—a rather dramatic saving of time and effort.

A good global view of heat transfer in circular tubes with nearly constant wall temperature can be obtained from the Sieder and Tate² correlation shown in Fig. 14.3-2. This is of the form of Eq. 14.3-15. It has been found empirically^{2,3} that transition to turbulence usually begins at about $\text{Re} = 2100$, even when the viscosity varies appreciably in the radial direction.

For *highly turbulent flow*, the curves for $L/D > 10$ converge to a single curve. For $\text{Re}_b > 20,000$ this curve is described by the equation

$$\text{Nu}_{\text{In}} = 0.026 \text{ Re}^{0.8} \text{ Pr}^{1/3} \left(\frac{\mu_b}{\mu_0} \right)^{0.14} \quad (14.3-16)$$

This equation reproduces available experimental data within about $\pm 20\%$ in the ranges $10^4 < \text{Re}_b < 10^5$ and $0.6 < \text{Pr} < 100$.

For *laminar flow*, the descending lines at the left are given by the equation

$$\text{Nu}_{\text{In}} = 1.86 \left(\text{Re} \text{Pr} \frac{D}{L} \right)^{1/3} \left(\frac{\mu_b}{\mu_0} \right)^{0.14} \quad (14.3-17)$$

¹ One can arrive at the viscosity ratio by inserting into the equations of change a temperature-dependent viscosity, described, for example, by a Taylor expansion about the wall temperature:

$$\mu = \mu_0 + \frac{\partial \mu}{\partial T} \Bigg|_{T=T_0} (T - T_0) + \dots \quad (14.3-15a)$$

When the series is truncated and the differential quotient is approximated by a difference quotient, we get

$$\mu \approx \mu_0 + \left(\frac{\mu_b - \mu_0}{T_b - T_0} \right) (T - T_0) \quad (14.3-15b)$$

or, with some rearrangement,

$$\frac{\mu}{\mu_0} \approx 1 + \left(\frac{\mu_b}{\mu_0} - 1 \right) \left(\frac{T - T_0}{T_b - T_0} \right) \quad (14.3-15c)$$

Thus, the viscosity ratio appears in the equation of motion and hence in the dimensionless correlation.

² E. N. Sieder and G. E. Tate, *Ind. Eng. Chem.*, **28**, 1429–1435 (1936).

³ A. P. Colburn, *Trans. AIChE*, **29**, 174–210 (1933). Alan Philip Colburn (1904–1955), provost at the University of Delaware (1950–1955), made important contributions to the fields of heat and mass transfer, including the “Chilton–Colburn relations.”